Volume 71A
Number 6
Nov.–Dec. 1967

A Memorial Issue

WILLIAM FREDERICK MEGGERS

July 13, 1888—November 19, 1966

Physics and Chemistry

U.S. DEPARTMENT OF COMMERCE

SECTION A

JOURNAL OF RESEARCH

NATIONAL BUREAU OF STANDARDS

Journal of Research

of the

National Bureau of Standards

A. Physics and Chemistry

Nov.–Dec. • 1967

VOLUME • 71A

NUMBER • 6

Editor: C. W. Beckett

Associate Editors: D. D. Wagman
J. M. Richardson

Publication dates:
Feb. 1, Apr. 1, June 1, Aug. 1, Oct. 1, Dec. 1, 1967

JOURNAL OF RESEARCH

The National Bureau of Standards Journal of Research reports research and development in the fields of activity shown at right. Also included from time to time are survey articles on topics closely related to the Bureau's scientific and technical program.

The Journal is published in three separate sections as follows:

A. Physics and Chemistry

Contains papers of interest primarily to scientists working in these fields. Issued six times a year. Annual subscription: domestic, $5.00; foreign, $6.00. Single copy, $1.00.

B. Mathematics and Mathematical Physics

Presents studies and compilations designed mainly for the mathematician and the theoretical physicist. Issued quarterly. Annual subscription: domestic, $2.25; foreign, $2.75. Single copy, 75c.

C. Engineering and Instrumentation

Reports research and development results of interest chiefly to the engineer and the applied scientist. Issued quarterly. Annual subscription: domestic, $2.75; foreign, $3.50. Single copy, 75c.

The National Bureau of Standards is a principal focal point in the Federal Government for assuring maximum application of the physical and engineering sciences to the advancement of technology in industry and commerce. Its responsibilities include development and maintenance of the national standards of measurement, and the provision of means for making measurements consistent with those standards; determination of physical constants and properties of materials; development of methods for testing materials, mechanisms, and structures, and making such tests as may be necessary, particularly for government agencies; cooperation in the establishment of standard practices for incorporation in codes and specifications; advisory service to government agencies on scientific and technical problems; invention and development of devices to serve special needs of the Government; assistance to industry, business and consumers in the development and acceptance of commercial standards and simplified trade practice recommendations; administration of programs in cooperation with United States business groups and standards organizations for the development of international standards of practice; and maintenance of a clearinghouse for the collection and dissemination of scientific, technical and engineering information. The scope of the Bureau's activities is suggested in the following listing of its three Institutes and their organizational units.

Institute for Basic Standards. Applied Mathematics. Electricity. Metrology. Mechanics. Heat. Atomic Physics. Physical Chemistry. Radiation Physics. Laboratory Astrophysics.* Radio Standards Laboratory.* Radio Standards Physics & Radio Standards Engineering. Office of Standard Reference Data.

Institute for Materials Research. Analytical Chemistry. Metallurgy. Reactor Radiations. Polymers. Inorganic Materials. Cryogenics.* Office of Standard Reference Materials.

Institute for Applied Technology. Building Research. Electronic Instrumentation. Technical Analysis. Center for Computer Sciences and Technology. Textile and Apparel Technology Center. Office of Weights and Measures. Office of Engineering Standards Services. Office of Invention and Innovation. Office of Vehicle Systems Research. Clearinghouse for Federal Scientific and Technical Information.** Materials Evaluation Laboratory. NBS/GSA Testing Laboratory.

*Located at Boulder, Colo. 80302.
**Located at 5285 Port Royal Road, Springfield, Va. 22151.

U.S. DEPARTMENT OF COMMERCE
Alexander B. Trowbridge, Secretary
NATIONAL BUREAU OF STANDARDS
A. V. Astin, Director

Order all publications from the Superintendent of Documents
U.S. Government Printing Office, Washington, D.C. 20402

Use of funds for printing this publication approved by the Director of the Bureau of the Budget (June 22, 1966).

Contents

Guest Editor: Charles H. Corliss

	Page
William Frederick Meggers, A Tribute. Karl G. Kessler.	II
The second spectrum of ytterbium (Yb II). W. F. Meggers. (Edited by Charlotte E. Moore.)	396
An improved description of technetium spectra (Tc I and Tc II), 2000 to 9000 Å. W. R. Bozman, W. F. Meggers, and C. H. Corliss.	547
Lifetimes of energy levels in neutral iron. C. H. Corliss and J. L. Tech.	567
Transition probabilities in argon I. C. H. Corliss and J. B. Shumaker, Jr.	575
The fifth spectrum of praseodymium. Victor Kaufman and Jack Sugar.	583
Fundamental energy levels of neutral promethium (Pm I). Joseph Reader and Sumner P. Davis.	587
Publications of the National Bureau of Standards.	601
Index to volume 71A, January to December 1967.	613

William F. Meggers

(Informal photos by Jack Tech)

Foreword

When Dr. William F. Meggers came to NBS in 1914, the Bohr theory was only a year old. When he died in 1966, extensive analyses were available for the spectra of most neutral and singly ionized atoms; only one or two stable atoms remained for which some spectral regularities were not known. More than any other man, Dr. Meggers came to be identified with this voluminous increase in our knowledge of atomic structure.

During the early years of atomic spectroscopy, the analysis of spectra engaged the efforts of many of the world's physicists. When, during the early 1930's, the glamour in this field passed on to nuclear physics, most physicists followed. Though much was known about atomic structure, the available information was frequently fragmentary and unreliable, and virtually nothing was known about the complex rare earths.

Working with his colleague, Dr. Carl C. Kiess, and a handful of others, Dr. Meggers turned to ever more complex atoms and gave us, through his 178 published papers, one of the most extensive, significant, and reliable collections of data available to science.

In this issue we pay tribute to Dr. Meggers' distinguished career. These papers on spectroscopy were contributed by some of his students who are now working in the Spectroscopy Section at NBS—the section he directed during most of his professional career. Though officially retired since 1958, Dr. Meggers continued to make significant contributions to spectroscopy. At the time of his death, he was working on the analyses of four rare earth spectra. One of these is published in this issue. The importance of this paper is well brought out by its editor, Charlotte E. Moore, who has generously spent much time preparing this analysis for publication.

On December 16, 1966, a number of Dr. Meggers' colleagues and friends gathered at NBS to commemorate his distinguished career in spectroscopy. A. V. Astin, Paul D. Foote, George R. Harrison, and Carl C. Kiess spoke in tribute to Dr. Meggers. A pamphlet containing their remarks is available upon request.

We at NBS are deeply grateful for having had the privilege of working with Dr. Meggers. He was a great person and an outstanding scientist. His work will continue to influence the progress of atomic spectroscopy for years to come.

KARL G. KESSLER, Chief
Atomic Physics Division, NBS.

JOURNAL OF RESEARCH of the National Bureau of Standards—A. Physics and Chemistry
Vol. 71A, No. 6, November–December 1967

The Second Spectrum of Ytterbium (Yb II)

William F. Meggers

(Edited by Charlotte E. Moore)

(May 26, 1967)

The analysis of Yb II provides the most complete interpretation of a complex rare-earth spectrum known to date. The total number of energy levels is 315; 141 even levels and 174 odd levels. Three coupling schemes are represented: LS-coupling for the terms $4f^{14}ns\ ^2S(n=6,\ 7,\ 8)$; $4f^{14}nd\ ^2D(n=5, 6, 7)$ and $4f^{13}6s^2\ ^2F^\circ$: J_lJ_{ll}-coupling for the levels from the configurations $4f^{13}6s\,6p$ and $4f^{13}5d\,6p$; and J_lJ_{ll}-coupling for those from the $4f^{13}5d\,6s$ and $4f^{13}5d^2$ configurations.

More than 5000 Yb II lines are listed, of which about 80 percent have been classified, and 95 percent of the total intensity is accounted for. Observed Zeeman patterns for over 1000 lines have yielded g-values for 258 levels. The agreement between observation and theory is excellent as regards both the positions of the energy levels and the g-values. The theoretical work was done in collaboration with Racah and his associates over more than a decade.

A limit, 98150 K, giving an ionization potential of 12.17 eV, has been derived from the three-member ^2S series.

Key Words: Analysis of Yb II. Atomic energy levels of Yb II. Classified lines of Yb II. Spectrum, Yb II. Ytterbium, second spectrum. Zeeman effect in Yb II.

1. Introduction

In November 1966 death claimed the eminent spectroscopist, William F. Meggers, the author of the present paper. It was characteristic of this author to leave a rich heritage for his colleagues. Part of this heritage is the analysis of Yb II. His interest in this rare-earth spectrum dates back at least to 1932 when the first regularities were known. In 1937 he and Scribner "provided the first useful description of conventional arc and spark spectra of this element" [1].[1] Some 1250 Yb II lines in the range 2000 to 11000 Å were reported. The resonance lines of Yb II were interpreted "with considerable certainty" as due to the transition from the ground state $4f^{14}6s\ ^2S$ to $4f^{14}6p\ ^2P^\circ$, giving rise to the strong lines at 3694.190 and 3289.370 Å. The second series member $4f^{14}7s\ ^2S$ was also reported at this time.

Although this work was handicapped by the use of impure materials and conventional light sources, Meggers succeeded, in 1939, in photographing the first Zeeman patterns of ytterbium lines with the Bitter magnet and concave gratings of the Massachusetts Institute of Technology. With these Zeeman data and further observations of spark spectra he was able to extend the quantum interpretation of the spectrum. In 1947 he had measured 400 Zeeman patterns, reobserved and measured the spectrum from 2000 to 9000 Å, and classified about 700 Yb II lines "as combinations between 38 odd and 76 even levels." Additional configurations were detected. The configurations $4f^{13}5d\,6s$, $4f^{13}5d^2$, and $4f^{13}6s\,6d$ give rise to many odd levels whose combinations with larger families of even levels from $4f^{13}6s\,6p$ and $4f^{13}5d\,6p$ give Yb II "its rare earth characteristics" [2].

"When pure ytterbium metal and new light sources became available in 1950, Meggers and Corliss decided to make a new description of ytterbium spectra" [3]. In the new list some 5100 Yb II lines are recorded together with the Zeeman Effect Type for more than 1000 lines. "The spectra of microwave and ring discharges of ytterbium were photographed side-by-side together with short images of superimposed standards from iron arcs or from thorium-iodide tubes. To disperse and focus the spectra, four concave gratings of 6.5 m radius, in Wadsworth-type mountings, were used." The "region from 2000 Å to 2500 Å was photographed in the first order of two (30,000 lines per inch) gratings with a plate factor of 2.4 Å/mm." From "2500 Å to 4500 Å, the spectra were recorded in the second order of either grating with a plate factor of 0.87 Å/mm, and the same setting served to record the range 5000 Å to 9000 Å in the first order with a plate factor of 1.74 Å/mm." From 7000 to 10000 Å a third grating having 15,000 lines per inch was used, the plate factor being 5 Å/mm.

In 1962 Sugar developed a light source "for producing self-reversed lines in both first and second spectra of rare-earth elements" [4]. He made the first observations with this source with ytterbium electrodes, covering the range 2400 to 7000 Å. "These spectrograms were evaluated by Meggers . . . who found that 50 lines of Yb II were absorbed or self-reversed."

In 1963 N. Spector photographed ytterbium spectra from 6600 to 11600 Å by means of a sliding spark, a source described in a paper by Sugar [5]. Longer than 9000 Å Meggers found several hundred additional lines on these spectrograms, "many of which have been explained as transitions between previously established Yb II energy levels."

[1] Figures in brackets indicate the literature references at the end of this paper.

There are four classified Yb II lines longer than 11600 Å: these were observed by Humphreys and Paul with a lead sulfide cell as detector, and electrodeless lamps as source [6].

In the 1966 reference, Meggers gives a clearly written history of other observations and work on ytterbium spectra, which need not be repeated here. It was his intention to prepare a Monograph on this spectrum that would serve as an inspiration to others who were engaged in the difficult task of interpreting complex rare-earth spectra. Although the material was not in final form for publication, the analysis was essentially completed at the time of his death. The details of publication have been carried out with his general idea in mind, insofar as it could be anticipated.

2. Interpretation of the Spectrum

The first recollection of the writer (C. E. M.) regarding Yb II is connected with the concern of both Meggers and H. N. Russell over the failure to find the elusive $4f^{14}\,5d\,^2D$ term in spite of an exhaustive search made with the earlier line lists. The late G. Racah became interested in this problem and in December 1952 pointed out that this term was not a rare-earth term, and could, therefore, be extrapolated from the spectra Hf II to W II. His predicted position placed the two respective levels surprisingly high i.e., near 23500 and 25000 K, thus explaining why the earlier searches had been fruitless. Earlier, however (1951) with the aid of Meggers' data, Racah had detected an unusual kind of coupling (J_IJ_{II}) in the configuration $4f^{13}\,6s\,6p$ of Yb II, which is described below. Thus started the long and fruitful collaboration between these eminent spectroscopists, which has resulted in the present analysis. From this date to the present time, with the aid of digital computers in both the experimental and theoretical aspects of the work, this complex spectrum has been unraveled slowly, by using the observed levels to obtain parameters for predicting missing levels, and repeating the process. The early correspondence reveals the painstaking care used in this step-by-step method to push the search for new levels to its present state. The collaboration for nearly 15 years has contributed results of far-reaching importance in the realm of complex rare-earth spectra.

To date there are 141 known even energy levels of Yb II. These are tabulated in table 1: the odd levels, 174 in all, are given in table 2. The level values are accurate "to about ±0.02 K." The tables are arranged similarly. Each table contains eight columns, headed, respectively: Configuration, Designation, J, Level, Interval, Observed g, Calculated g, and the number of observed combinations on which the level is based.

Three types of coupling-schemes are needed to describe the energy levels of Yb II.[2] The only entries in the "Interval" column are those for the regular terms having LS-coupling. These terms result from the configurations having the completed shell of f-electrons: $4f^{14}\,ns\,^2S(n=6, 7, 8)$, $4f^{14}\,nd\,^2D(n=5, 6, 7)$, $4f^{14}\,6p\,^2P^\circ$, and from the configuration $4f^{13}\,6s^2\,^2F^\circ$. All other assigned levels belong to the configurations $4f^{13}\,6s\,6p$, $4f^{13}\,5d\,6p$, $4f^{13}\,5d\,6s$, and $4f^{13}\,5d^2$.

The key to the interpretation of the spectrum was given by the configuration $4f^{13}\,6s\,6p$ [8]. The coupling is a J_IJ_{II}-coupling, a type first noted by Shenstone in the $3d^9\,4s\,4p$ configuration of Cu I, who described it as $3d^9\,^2D + 4s\,4p\,^3P, {}^1P$ [9]. In Yb II "the low levels are given by the three states of $sp\,^3P_{J_{II}}$; each of these states may assume different orientations in the quadrupole field of $f^{13}\,^2F_{3\frac{1}{2}}$, and thus splits into 1, 3, or 5 levels depending on the J_{II} value. The three levels of $^1P_1$ lie somewhat higher, and the whole distribution is repeated 10000 cm^{-1} higher, in the field of $f^{13}\,^2F_{2\frac{1}{2}}$." The interval of the ground term of the grandparent, $4f^{13}\,^2F^\circ$ in Yb IV, 10090 K [10] is clearly reflected in Yb II and "the J-value of the grandparent is very well defined" [8]. The complete J_IJ_{II}-coupling notation is given in column one of table 1, and the corresponding groups of levels are given in column four. All of the 24 predicted levels of the $4f^{13}\,6s\,6p$ configuration have been found.

Similar notation is used for the levels from the $4f^{13}\,5d\,6p$ configuration (table 1). Of the 113 predicted levels, 108 are known.

Except for the regular terms mentioned above, the identified odd levels (table 2) have the configurations $4f^{13}\,5d\,6s$ or $4f^{13}\,5d^2$. Racah [8] has noted that "the orbital momentum of $sd\,^3D$ in the former group is orientated in the electrostatic field of the core before it is coupled with its own spin. The resulting coupling scheme is a J_IL_{II}-coupling." This "is the natural generalization of the jl coupling for configurations with two electrons outside the core." Instead of pairs, there are mostly groups of three levels or isolated levels according to the resultant spin of the outer electrons, and the multiplicity is indicated by the superscript at the left of the brackets in column two. The complete J_IL_{II}-coupling notation is given in column one of table 2. All 39 predicted levels from $4f^{13}\,5d\,6s$ are known. Of the 81 predicted levels from $4f^{13}\,5d^2$, 73 have been found.

The two coupling schemes described above are illustrated in figures 1 and 2, which are self-explanatory [8]. Racah noted that the present work on Yb II provides the first example of J_IL_{II}-coupling in a complex spectrum. It has already served as a "model" for Tm II, as reported by Spector [11]. Both types of coupling may well be expected in other complex rare-earth spectra.

After tables 1 and 2 had been completed, a final machine search was made by J. Tech for the five missing levels from the $4f^{13}\,5d\,6p$ configuration and for the nine missing levels from $4f^{13}\,5d^2$. The range covered in this search was ±300 K from the predicted values. He succeeded in finding the level $59632.21^\circ_{6\frac{1}{2}}$, which has been included in the tables with a question, since the total number of combinations on which it is based, is five, and one of these may be a blend.

[2] A summary of coupling schemes for one-electron spectra may be found in a paper by Gutman and Levinson [7], which has been translated by J. Tech. This may serve, also, as a useful general guide for the interpretation of spectra having more than one electron outside the core.

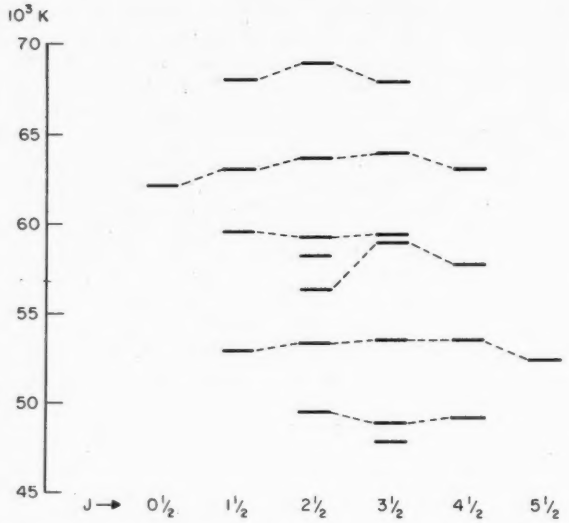

FIGURE 1. *The configuration* $4f^{13}(^2F^o_{31/2,\ 21/2})6s\ 6p$ *in* Yb II: J_1J_{II}*-coupling.*

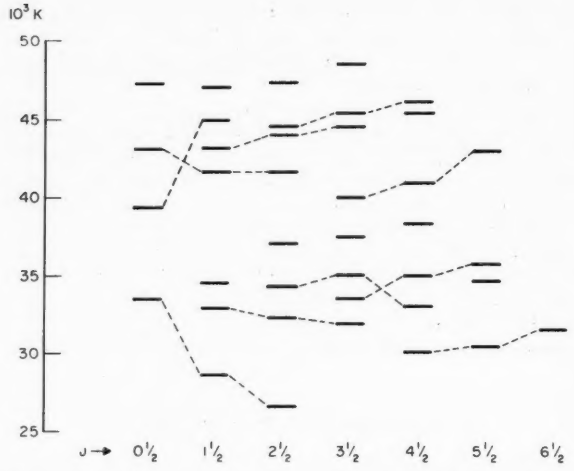

FIGURE 2. *The configuration* $4f^{13}(^2F^o_{31/2,\ 21/2})5d\ 6s$ *in* Yb II: J_1L_{II}*-coupling.*

The arrays of observed levels as described in the various coupling schemes are presented in table 3, which shows the relation of the various groups to the atomic structure.

In addition there are 58 miscellaneous high odd levels, above 84000 K, in table 2, which have not yet been assigned configurations.

The calculations of the energy matrices for Yb II have been carried out at The Hebrew University in Jerusalem. New diagonalizations including interaction were reported by Racah in August 1965 [12]. After his untimely death a few weeks later, the work was continued by Z. Goldschmidt and others. In fact, the $4f^{13}\,5d\,6p(^1P_1)$ configuration was interpreted by Mrs. Goldschmidt after introducing configuration interaction. She has kindly furnished the final data on the coupling schemes, and on the calculated positions and *g*-values for the individual levels. The observed and calculated values for both levels and *g*-values are in remarkably good agreement. The mean error (o-c) in the level values is 103 K for the even levels, and 144 K for the odd levels. A separate publication on the theoretical interpretation of the spectrum, the exact composition of the levels, and the agreement between observation and theory is in the hands of Mrs. Goldschmidt, who is familiar with the details of the work on Yb II carried on by Racah and his associates over the years.

3. Observations of Zeeman Effect

In a letter to Racah dated July 16, 1965, Meggers writes "I have spent many months of dreary drudgery deriving *g*-factors and classified lines from 98 pages of square array." As stated above, the first Zeeman observations were made at the Massachusetts Institute of Technology in 1939. At this time, Zeeman patterns for 400 Yb lines were obtained by accident, when they appeared as impurities in Tm spectra. "In favorable cases the resolution reached 0.05 Lorentz unit." Further Zeeman observations in the range 2000 to 9000 Å were made in 1959 at the National Bureau of Standards, where a Weiss magnet was used. "The highest resolution achieved was about 0.1 Lorentz unit."

"These investigations extending intermittently over a quarter century" have resulted in observed Zeeman patterns for more than 1000 lines of Yb II. Observed *g*-values have been derived for 136 even levels (column six, table 1) and for 122 odd levels (column six, table 2).

Details of the Zeeman observations are included in the last five columns of table 6. The standard Zeeman Types 4, 5, 6 for even multiplicity, and Type 7, which has "a single undisplaced parallel (*p*) component and two symmetrically displaced normal (*n*) components," are indicated in column seven, labeled "Type." Excellent illustrations of these types may be found in the paper by Meggers and Corliss on an "Improved Description of Hafnium Spectra" [13].

The next two columns, eight and nine, contain the *g*-values of the respective levels of the transition giving rise to the line. The "1st" *g*-value is that of the low level involved, i.e., the first entry in column six of table 6. The "2nd" *g*-value is that of the high level, i.e., the second entry in column six of this table. For example, 8781.96Å is designated as $37516^o_{31/2}$—$48900_{31/2}$. The *g*-value for 37516^o is 1.114; that for 48900 is 1.034. The last two columns of table 6, ten and eleven, give the strongest *p*-component, and the strongest *n*-component, respectively.

All entries in parentheses have been assumed in making the calculations to derive observed *g*-values. For some lines the strongest *p*-component is in parentheses. If Δg is small, it has been assumed that the measurement refers to the weakest *p*-component. The

entry in parentheses is, therefore, the appropriate fraction of the observed value.

The observed *g*-values in tables 1 and 2 were obtained by averaging the separate values. Many are based on resolved patterns. The average value can generally be used as an assumed value for one level, to derive the *g*-value for the other level in cases of unresolved patterns. When this has been done, the assumed *g*-value is in parentheses.

For resolved patterns, an excellent value of Δg can often be determined, which may differ slightly from the one indicated by the strongest *p*-component. The best value has been used in the calculations, which explains small differences between the value of Δg from the observed *g*-values and that from column ten.

Most of the final *g*-values were assigned by Meggers, who had completed the reductions of all Zeeman observations and interpreted practically all of the resolved patterns. A number of *g*-values from unresolved patterns have been derived by C. E. M. as described above. They have been added in table 6, and used only to supplement the averages adopted by Meggers.

Most of the lines for which the Zeeman Effect has been observed, are classified. The remaining unclassified lines having a known Zeeman Effect, are listed in table 4, which gives in successive columns the wavelength, spark intensity, wave number Type, strongest *p*-, and strongest *n*-components. As in table 5 which contains the strongest unclassified lines, the entries are from table 6.

The overall consistency of the individual *g*-values reveals the painstaking skill and care of the author in making the observations, in reducing them, and in interpreting them.

TABLE 1. *Even levels of* Yb II

Configuration	Desig.	*J*	Level	Interval	Obs. *g*	Calc. *g*	No. Comb.
$4f^{14}(^1S)6s$	$6s\ ^2S$	0½	0.00		1.998	2.000	14
$4f^{14}(^1S)5d$	$5d\ ^2D$	1½	22960.80	1371.89	1.802	0.800	37
		2½	24332.69		1.202	1.200	39
$4f^{13}(^2F^\circ_{3½})6s\ 6p(^3P_0)$		3½	47912.31		1.280	1.284	26
$4f^{13}(^2F^\circ_{3½})6s\ 6p(^3P_1)$		4½	49301.16		1.187	1.196	27
		3½	48900.41		1.044	1.051	26
		2½	49498.04		1.145	1.140	24
$4f^{13}(^2F^\circ_{3½})6s\ 6p(^3P_2)$		5½	52517.35		1.27	1.272	19
		4½	53720.71		1.26	1.270	30
		3½	53715.26		1.181	1.190	26
		2½	53404.96		1.033	1.043	35
		1½	52938.01		0.877	0.879	17
$4f^{14}(^1S)7s$	$7s\ ^2S$	0½	54304.30		2.001	2.000	12
$4f^{13}(^2F^\circ_{3½})6s\ 6p(^1P_1)$		2½	56375.91		1.226	1.233	34
		3½	59090.13		1.122	1.112	39
		4½	57765.32		1.12	1.112	36
$4f^{13}(^2F^\circ_{2½})6s\ 6p(^3P_0)$		2½	58283.91		0.77	0.761	25
$4f^{13}(^2F^\circ_{2½})6s\ 6p(^3P_1)$		3½	59618.90		1.00	1.020	23
		2½	59259.24		1.105	1.114	31
		1½	59710.65		0.82	0.777	22
$4f^{13}(^2F^\circ_{2½})6s\ 6p(^3P_2)$		0½	62136.94		0.08	0.113	11
		1½	63011.85		0.79	0.812	21
		2½	63702.32		1.07	1.040	29
		3½	63957.80		1.148	1.144	23
		4½	63163.79		1.12	1.138	22

TABLE 1. *Even levels of* Yb II—Continued

Configuration	Desig.	J	Level	Interval	Obs. g	Calc. g	No. Comb.
$4f^{13}(^2F^\circ_{2\frac{1}{2}})6s\,6p(^1P_1)$		$3\frac{1}{2}$	67938.68		0.960	0.954	42
		$2\frac{1}{2}$	69079.88		0.89	0.907	29
		$1\frac{1}{2}$	68150.57		0.928	0.927	42
$4f^{13}(^2F^\circ_{3\frac{1}{2}})5d\,6p(^3F_2)$		$1\frac{1}{2}$	55702.07		1.693	1.700	17
		$2\frac{1}{2}$	58823.58		1.266	1.278	39
		$3\frac{1}{2}$	61051.06		1.18	1.176	35
		$4\frac{1}{2}$	61214.66		1.07	1.054	44
		$5\frac{1}{2}$	58961.37		0.974	0.985	21
$4f^{13}(^2F^\circ_{3\frac{1}{2}})5d\,6p(^3F_3)$		$0\frac{1}{2}$	61120.49		1.661	1.661	13
		$1\frac{1}{2}$	60586.46		1.323	1.339	26
		$2\frac{1}{2}$	64055.82		1.108	1.062	42
		$3\frac{1}{2}$	65093.14		0.973	1.006	37
		$4\frac{1}{2}$	64923.11		1.10	1.125	49
		$5\frac{1}{2}$	66082.25		1.141	1.147	29
		$6\frac{1}{2}$	61873.40		1.10	1.114	16
$4f^{13}(^2F^\circ_{3\frac{1}{2}})5d\,6p(^3F_4)$		$7\frac{1}{2}$	64891.30		1.19	1.200	8
		$6\frac{1}{2}$	68720.44		1.157	1.155	23
		$5\frac{1}{2}$	68148.88		1.20	1.207	29
		$4\frac{1}{2}$	68549.23		1.157	1.147	49
		$3\frac{1}{2}$	68450.11		1.08	1.100	39
		$2\frac{1}{2}$	66395.72		1.235	1.249	37
		$1\frac{1}{2}$	65888.46		1.206	1.212	30
		$0\frac{1}{2}$	66462.86		1.11	1.084	16
$4f^{13}(^2F^\circ_{3\frac{1}{2}})5d\,6p(^3D_1)$		$2\frac{1}{2}$	61374.49		1.299	1.298	34
		$3\frac{1}{2}$	64598.28		1.223	1.217	48
		$4\frac{1}{2}$	63726.83		1.005	1.009	47
$4f^{13}(^2F^\circ_{3\frac{1}{2}})5d\,6p(^3D_2)$		$5\frac{1}{2}$	63944.18		1.115	1.102	33
		$4\frac{1}{2}$	65950.95		1.09	1.074	46
		$3\frac{1}{2}$	66558.00		1.100	1.105	47
		$2\frac{1}{2}$	66351.21		1.125	1.106	41
		$1\frac{1}{2}$	64461.08		1.176	1.164	25
$4f^{13}(^2F^\circ_{3\frac{1}{2}})5d\,6p(^3D_3)$		$6\frac{1}{2}$	65875.77		1.205	1.198	26
		$5\frac{1}{2}$	66571.58		1.189	1.189	44
		$4\frac{1}{2}$	67416.03		1.26	1.262	50
		$3\frac{1}{2}$	68756.04		1.32	1.343	48
		$2\frac{1}{2}$	68135.00		1.087	1.087	39
		$1\frac{1}{2}$	67204.97		1.04	1.064	29
		$0\frac{1}{2}$	67955.23		0.895	0.880	18
$4f^{13}(^2F^\circ_{3\frac{1}{2}})5d\,6p(^3P_0)$		$3\frac{1}{2}$	69395.20		0.94	0.944	43
$4f^{13}(^2F^\circ_{3\frac{1}{2}})5d\,6p(^3P_1)$		$2\frac{1}{2}$	69607.54		1.210	1.202	45
		$3\frac{1}{2}$	61822.58		1.327	1.338	39
		$4\frac{1}{2}$	69957.49		1.112	1.115	53
$4f^{13}(^2F^\circ_{3\frac{1}{2}})5d\,6p(^3P_2)$		$5\frac{1}{2}$	70793.96		1.20	1.214	39
		$4\frac{1}{2}$	70858.18		1.28	1.284	46
		$3\frac{1}{2}$	71222.36		1.15	1.149	43
		$2\frac{1}{2}$	70954.27		1.014	1.017	43
		$1\frac{1}{2}$	71113.84		0.967	0.955	33

TABLE 1. *Even levels of* Yb II—Continued

Configuration	Desig.	J	Level	Interval	Obs. g	Calc. g	No. Comb.
$4f^{14}(^1S)6d$	$6d\,^2D$	$1\frac{1}{2}$	62174.10	384.92	0.80	0.800	17
		$2\frac{1}{2}$	62559.02		1.22	1.200	19
$4f^{13}(^2F^\circ_{3\frac{1}{2}})5d\,6p(^1D_2)$		$5\frac{1}{2}$	62861.27		1.140	1.139	30
		$4\frac{1}{2}$	65199.54		1.08	1.078	42
		$3\frac{1}{2}$	65577.11		1.055	1.050	44
		$2\frac{1}{2}$	63234.11		1.208	1.282	37
		$1\frac{1}{2}$	63647.73		1.149	1.133	31
$4f^{13}(^2F^\circ_{3\frac{1}{2}})5d\,6p(^1F_3)$		$0\frac{1}{2}$	65566.72		1.43	1.460	20
		$1\frac{1}{2}$	69443.52		1.15	1.175	35
		$2\frac{1}{2}$	71468.70		1.02	0.996	34
		$3\frac{1}{2}$	72779.99		1.10	1.105	41
		$4\frac{1}{2}$	73283.35		1.04	1.011	43
		$5\frac{1}{2}$	73291.95		1.09	1.084	38
		$6\frac{1}{2}$	70136.24		1.12	1.150	26
$4f^{13}(^2F^\circ_{3\frac{1}{2}})5d\,6p(^1P_1)$		$2\frac{1}{2}$	77606.58		1.14	1.169	30
		$3\frac{1}{2}$	79628.71		1.11	1.126	29
		$4\frac{1}{2}$	78070.19		1.10	1.114	33
$4f^{13}(^2F^\circ_{2\frac{1}{2}})5d\,6p(^3F_2)$		$4\frac{1}{2}$	68943.65		0.89	0.881	23
		$3\frac{1}{2}$	72202.03		0.86	0.864	29
		$2\frac{1}{2}$	71270.01		0.91	0.912	39
		$1\frac{1}{2}$	71763.67		1.11	1.101	31
		$0\frac{1}{2}$	75905.77		1.28	1.308	15
$4f^{13}(^2F^\circ_{2\frac{1}{2}})5d\,6p(^3F_3)$		$5\frac{1}{2}$	72615.74		0.99	0.996	24
		$4\frac{1}{2}$	76516.11		1.01	0.999	24
		$3\frac{1}{2}$	75640.06		0.81	0.830	29
		$2\frac{1}{2}$	74270.48		0.92	0.910	32
		$1\frac{1}{2}$	73657.29		1.04	1.071	22
		$0\frac{1}{2}$	73636.83		0.70	0.692	17
$4f^{13}(^2F^\circ_{2\frac{1}{2}})5d\,6p(^3F_4)$		$6\frac{1}{2}$	76233.60		1.07	1.108	10
		$5\frac{1}{2}$					
		$4\frac{1}{2}$	79126.83		1.15?	1.140	17
		$3\frac{1}{2}$	77882.04		1.13	1.142	28
		$2\frac{1}{2}$	76170.25		1.12	1.093	31
		$1\frac{1}{2}$	76517.21		0.85	0.792	14
$4f^{13}(^2F^\circ_{2\frac{1}{2}})5d\,6p(^1D_2)$		$0\frac{1}{2}$	70029.04		0.68	0.670	16
		$1\frac{1}{2}$	73116.71		0.863	0.797	21
		$2\frac{1}{2}$	75550.94		0.91	0.945	38
		$3\frac{1}{2}$	74973.41		1.07	1.040	26
		$4\frac{1}{2}$	73750.90		1.07	1.007	37
$4f^{14}\,8s$	$8s\,^2S$	$0\frac{1}{2}$	73039.61			2.000	7
$4f^{13}(^2F^\circ_{2\frac{1}{2}})5d\,6p(^3D_1)$		$3\frac{1}{2}$	73966.81		0.763	0.765	23
		$2\frac{1}{2}$	76676.31		1.10	1.048	39
		$1\frac{1}{2}$	77284.02		0.90	0.964	23

TABLE 1. *Even levels of* Yb II – Continued

Configuration	Desig.	J	Level	Interval	Obs. g	Calc. g	No. Comb.
$4f^{13}(^2F^\circ_{2\frac{1}{2}})5d\,6p(^3D_2)$		$4\frac{1}{2}$	74568.58		1.04	1.032	22
		$3\frac{1}{2}$	76323.49		1.00	0.960	37
		$2\frac{1}{2}$	79583.11		0.68	0.671	15
		$1\frac{1}{2}$	74991.36		1.05	1.060	30
		$0\frac{1}{2}$	74989.49		0.52	0.511	15
$4f^{13}(^2F^\circ_{2\frac{1}{2}})5d\,6p(^3D_3)$		$5\frac{1}{2}$	76649.80		1.08	1.083	14
		$4\frac{1}{2}$	77747.40		1.07	1.087	25
		$3\frac{1}{2}$	77449.32		1.16	1.161	29
		$2\frac{1}{2}$	78814.86		1.22	1.210	22
		$1\frac{1}{2}$	79605.95		1.16	1.129	24
		$0\frac{1}{2}$	77887.30		2.20	2.170	12
$4f^{14}(^1S)7d$	$7d\,^2D$	$1\frac{1}{2}$	76799.07	39.93	0.84	0.800	15
		$2\frac{1}{2}$	76839.00		1.11	1.200	35
$4f^{13}(^2F^\circ_{2\frac{1}{2}})5d\,6p(^3P_0)$		$2\frac{1}{2}$	81657.13			1.051	26
$4f^{13}(^2F^\circ_{2\frac{1}{2}})5d\,6p(^3P_1)$		$3\frac{1}{2}$	80457.71		0.99	0.984	23
		$2\frac{1}{2}$	75058.11		0.76	0.732	29
		$1\frac{1}{2}$	81512.62		0.48	0.502	12
$4f^{13}(^2F^\circ_{2\frac{1}{2}})5d\,6p(^3P_2)$		$0\frac{1}{2}$					
		$1\frac{1}{2}$	78464.76		1.18	1.193	22
		$2\frac{1}{2}$	81312.65		1.11?	1.049	29
		$3\frac{1}{2}$	81692.92		1.16	1.164	18
		$4\frac{1}{2}$	81205.27		1.09	1.115	17
$4f^{13}(^2F^\circ_{2\frac{1}{2}})5d\,6p(^1F_3)$		$5\frac{1}{2}$	80679.18		1.00?	1.019	13
		$4\frac{1}{2}$					
		$3\frac{1}{2}$	83363.88		0.97	0.956	21
		$2\frac{1}{2}$	82891.80		1.03?	1.066	27
		$1\frac{1}{2}$	82398.98		1.042	1.061	18
		$0\frac{1}{2}$	82091.32			1.223	7
$4f^{13}(^2F^\circ_{2\frac{1}{2}})5d\,6p(^1P_1)$		$1\frac{1}{2}$					
		$2\frac{1}{2}$	89713.17			0.869	14
		$3\frac{1}{2}$					

TABLE 2. *Odd levels of* Yb II

Configuration	Desig.	J	Level	Interval	Obs. g	Calc. g	No. Comb.
$4f^{13}\,6s^2$	$6s^2\,^2F^\circ$	$3\frac{1}{2}$	*21418.75*	−10149.33	1.145	1.143	30
		$2\frac{1}{2}$	*31568.08*		0.862	0.866	50
$4f^{14}(^1S)6p$	$6p\ ^2P^\circ$	$0\frac{1}{2}$	*27061.82*	3330.41	0.667	0.667	13
		$1\frac{1}{2}$	*30392.23*		1.333	1.333	28
$4f^{13}(^2F^\circ_{3\frac{1}{2}})5d\,6s(^3D^\circ)$	$^3[1\frac{1}{2}]^\circ$	$2\frac{1}{2}$	*26759.02*		1.570	1.576	27
		$1\frac{1}{2}$	*28757.98*		1.440	1.447	30
		$0\frac{1}{2}$	*33653.86*		1.320	1.318	22

TABLE 2. *Odd levels of* Yb II—Continued

Configuration	Desig.	J	Level	Interval	Obs. g	Calc. g	No. Comb.
$4f^{13}(^2F^\circ_{3/2})5d\,6s(^3D^\circ)$ *Continued*	$^3[5\frac{1}{2}]^\circ$	$4\frac{1}{2}$	*30224.33*		0.935	0.936	31
		$5\frac{1}{2}$	*30562.79*		1.112	1.124	25
		$6\frac{1}{2}$	*31631.59*		1.230	1.231	12
	$^3[2\frac{1}{2}]^\circ$	$3\frac{1}{2}$	*31979.90*		1.331	1.336	43
		$2\frac{1}{2}$	*32371.10*		1.170	1.157	44
		$1\frac{1}{2}$	*32981.59*		0.866	0.908	40
	$^3[3\frac{1}{2}]^\circ$	$4\frac{1}{2}$	*33052.29*		1.264	1.267	36
		$3\frac{1}{2}$	*35059.00*		1.124	1.112	51
		$2\frac{1}{2}$	*34389.76*		1.007	1.017	47
	$^3[4\frac{1}{2}]^\circ$	$3\frac{1}{2}$	*33494.68*		0.991	1.003	48
		$4\frac{1}{2}$	*35019.13*		1.158	1.159	38
		$5\frac{1}{2}$	*35831.68*		1.214	1.219	29
$4f^{13}(^2F^\circ_{3/2})5d\,6s(^1D^\circ)$	$^1[1\frac{1}{2}]^\circ$	$1\frac{1}{2}$	*34575.37*		1.434	1.395	41
	$^1[5\frac{1}{2}]^\circ$	$5\frac{1}{2}$	*34784.95*		1.119	1.120	29
	$^1[2\frac{1}{2}]^\circ$	$2\frac{1}{2}$	*37077.59*		1.113	1.113	52
	$^1[3\frac{1}{2}]^\circ$	$3\frac{1}{2}$	*37516.59*		1.119	1.126	59
	$^1[4\frac{1}{2}]^\circ$	$4\frac{1}{2}$	*38342.02*		1.093	1.090	42
$4f^{13}(^2F^\circ_{2/2})5d\,6s(^3D^\circ)$	$^3[0\frac{1}{2}]^\circ$	$0\frac{1}{2}$	*39378.89*		1.850	1.859	21
		$1\frac{1}{2}$	*44940.61*		1.244	1.248	53
	$^3[4\frac{1}{2}]^\circ$	$3\frac{1}{2}$	*40035.82*		0.720	0.714	53
		$4\frac{1}{2}$	*40917.91*		0.967	0.978	40
		$5\frac{1}{2}$	*42915.13*		1.115	1.125	20
	$^3[1\frac{1}{2}]^\circ$	$2\frac{1}{2}$	*41678.73*		1.193	1.182	43
		$1\frac{1}{2}$	*41688.45*		0.784	0.784	39
		$0\frac{1}{2}$	*43007.79*		0.15	0.148	21
	$^3[2\frac{1}{2}]^\circ$	$1\frac{1}{2}$	*43075.09*		0.96	0.928	49
		$2\frac{1}{2}$	*43956.41*		0.99	0.967	47
		$3\frac{1}{2}$	*44438.03*		1.10	1.091	55
	$^3[3\frac{1}{2}]^\circ$	$2\frac{1}{2}$	*44497.51*		0.734	0.770	45
		$3\frac{1}{2}$	*45429.82*		1.150	1.128	51
		$4\frac{1}{2}$	*46169.78*		1.10	1.104	45
$4f^{13}(^2F^\circ_{2/2})5d\,6s(^1D^\circ)$	$^1[4\frac{1}{2}]^\circ$	$4\frac{1}{2}$	*45335.03*		1.01	0.981	39
	$^1[1\frac{1}{2}]^\circ$	$1\frac{1}{2}$	*47005.46*		0.990	0.971	45
	$^1[0\frac{1}{2}]^\circ$	$0\frac{1}{2}$	*47228.96*		0.74	0.806	26
	$^1[2\frac{1}{2}]^\circ$	$2\frac{1}{2}$	*47329.44*		0.990	0.974	56
	$^1[3\frac{1}{2}]^\circ$	$3\frac{1}{2}$	*48556.57*		0.941	0.921	50

TABLE 2. *Odd levels of* Yb II — Continued

Configuration	Desig.	J	Level	Interval	Obs. g	Calc. g	No. Comb.
$4f^{13}(^2F^\circ_{3/2})5d^2(^3F^\circ)$	$^3[2\frac{1}{2}]^\circ$	$3\frac{1}{2}$	*47758.54*		1.08	1.123	43
		$2\frac{1}{2}$	*45012.79*		1.281	1.298	38
		$1\frac{1}{2}$	*50832.65*		0.956	0.977	22
	$^3[3\frac{1}{2}]^\circ$	$4\frac{1}{2}$	*46354.55*		1.29	1.284	32
		$3\frac{1}{2}$	*45273.02*		1.18	1.209	56
		$2\frac{1}{2}$	*51248.86*		1.034	1.052	44
	$^3[1\frac{1}{2}]^\circ$	$0\frac{1}{2}$	*46902.71*		1.30	1.201	20
		$1\frac{1}{2}$	*45737.29*		1.333	1.384	50
		$2\frac{1}{2}$	*48272.77*		1.14	1.147	55
	$^3[6\frac{1}{2}]^\circ$	$5\frac{1}{2}$	*46547.72*		0.97	0.971	21
		$6\frac{1}{2}$	*47680.40*		1.12	1.118	13
		$7\frac{1}{2}$	*48923.30*		1.20	1.195	6
	$^3[5\frac{1}{2}]^\circ$	$4\frac{1}{2}$	*47663.52*		0.98	1.011	38
		$5\frac{1}{2}$	*48503.82*		1.10	1.129	25
		$6\frac{1}{2}$	*49727.19*		1.20	1.200	12
	$^3[0\frac{1}{2}]^\circ$	$1\frac{1}{2}$	*48024.70*		1.38	1.354	30
		$0\frac{1}{2}$	*49419.13*		1.41	1.432	16
	$^3[4\frac{1}{2}]^\circ$	$3\frac{1}{2}$	*49008.93*		1.03	1.046	43
		$4\frac{1}{2}$	*49916.50*		1.090	1.062	27
		$5\frac{1}{2}$	*50468.05*		1.213	1.198	22
$4f^{13}(^2F^\circ_{3/2})5d^2(^1G^\circ)$	$^1[0\frac{1}{2}]^\circ$	$0\frac{1}{2}$	*52067.87*		0.54	0.530	21
	$^1[1\frac{1}{2}]^\circ$	$1\frac{1}{2}$	*52987.76*		1.131	1.116	28
	$^1[7\frac{1}{2}]^\circ$	$7\frac{1}{2}$	*53322.89*		1.04	1.072	5
	$^1[2\frac{1}{2}]^\circ$	$2\frac{1}{2}$	*53716.38*		1.183	1.154	42
	$^1[3\frac{1}{2}]^\circ$	$3\frac{1}{2}$	*57103.02*		1.10	1.078	25
	$^1[6\frac{1}{2}]^\circ$	$6\frac{1}{2}$	*57561.62*		1.04	1.042	7
	$^1[4\frac{1}{2}]^\circ$	$4\frac{1}{2}$	*58484.54*		1.02	1.061	17
	$^1[5\frac{1}{2}]^\circ$	$5\frac{1}{2}$	*59753.84*		1.11	1.082	11
$4f^{13}(^2F^\circ_{3/2})5d^2(^3P^\circ)$	$^3[3\frac{1}{2}]^\circ$	$4\frac{1}{2}$	*52880.75*		1.26	1.268	26
		$3\frac{1}{2}$	*52921.62*		1.15	1.173	35
		$2\frac{1}{2}$	*53120.58*		0.944	0.950	34
	$^3[4\frac{1}{2}]^\circ$	$3\frac{1}{2}$	*55462.68*		0.878	0.874	28
		$4\frac{1}{2}$	*56088.39*		1.11	1.100	20
		$5\frac{1}{2}$	*56621.15*		1.16	1.215	15
	$^3[2\frac{1}{2}]^\circ$	$3\frac{1}{2}$	*56500.64*		1.352	1.360	20
		$2\frac{1}{2}$	*57798.51*		1.151	1.152	30
		$1\frac{1}{2}$	*58162.75*		0.94	0.930	17

TABLE 2. *Odd levels of* Yb II – Continued

Configuration	Desig.	J	Level	Interval	Obs. g	Calc. g	No. Comb.
$4f^{13}(^2F^\circ_{3/2})5d^2(^1D^\circ)$	$^1[3\frac{1}{2}]^\circ$	$3\frac{1}{2}$	*53644.89*		1.18	1.181	38
	$^1[5\frac{1}{2}]^\circ$	$5\frac{1}{2}$	*54192.51*		1.11	1.110	19
	$^1[4\frac{1}{2}]^\circ$	$4\frac{1}{2}$	*54640.82*		1.13	1.128	30
	$^1[1\frac{1}{2}]^\circ$	$1\frac{1}{2}$	*55221.46*		1.11	1.069	27
	$^1[2\frac{1}{2}]^\circ$	$2\frac{1}{2}$	*56056.91*		1.12	1.131	22
$4f^{13}(^2F^\circ_{3/2})5d^2(^1S^\circ)$	$^1[3\frac{1}{2}]^\circ$	$3\frac{1}{2}$					
$4f^{13}(^2F^\circ_{2/2})5d^2(^3F^\circ)$	$^3[5\frac{1}{2}]^\circ$	$4\frac{1}{2}$	*56480.77*		0.76	0.767	23
		$5\frac{1}{2}$	*58051.51*		0.95	0.966	10
		$6\frac{1}{2}$	*59632.21?*			1.087	5
	$^3[2\frac{1}{2}]^\circ$	$1\frac{1}{2}$	*56840.04*		0.90	0.930	20
		$2\frac{1}{2}$	*62163.92*			1.082	24
		$3\frac{1}{2}$	*62046.07*		1.14	1.134	17
	$^3[0\frac{1}{2}]^\circ$	$0\frac{1}{2}$	*56977.71*		2.19	2.174	11
		$1\frac{1}{2}$	*59777.07*		1.63	1.623	12
	$^3[4\frac{1}{2}]^\circ$	$3\frac{1}{2}$	*57534.45*		0.87	0.837	27
		$4\frac{1}{2}$	*59046.89*		1.08	1.051	14
		$5\frac{1}{2}$	*61442.82*		1.11	1.134	12
	$^3[3\frac{1}{2}]^\circ$	$2\frac{1}{2}$	*58661.13*		0.86	0.821	25
		$3\frac{1}{2}$	*59624.66*			0.964	19
		$4\frac{1}{2}$	*60649.86*		1.10	1.123	13
	$^3[1\frac{1}{2}]^\circ$	$0\frac{1}{2}$	*58672.53*		0.538	0.522	13
		$1\frac{1}{2}$	*60910.14*		1.00	1.095	17
		$2\frac{1}{2}$	*59439.08*		0.994	1.054	22
$4f^{13}(^2F^\circ_{2/2})5d^2(^3P^\circ)$	$^3[2\frac{1}{2}]^\circ$	$1\frac{1}{2}$	*63028.26*		0.51	0.531	11
		$2\frac{1}{2}$	*63417.03*		1.01	1.019	16
		$3\frac{1}{2}$	*64169.39*			1.078	17
	$^3[3\frac{1}{2}]^\circ$	$2\frac{1}{2}$?	*65594.06*		1.19?	0.809	8
		$3\frac{1}{2}$	*66796.03*			0.970	7
		$4\frac{1}{2}$					
	$^3[1\frac{1}{2}]^\circ$	$2\frac{1}{2}$	*67933.51*		1.17	1.203	8
		$1\frac{1}{2}$	*67789.60?*			1.051	5
		$0\frac{1}{2}$					
$4f^{13}(^2F^\circ_{2/2})5d^2(^1G^\circ)$	$^1[6\frac{1}{2}]^\circ$	$6\frac{1}{2}$					
	$^1[1\frac{1}{2}]^\circ$	$1\frac{1}{2}$	*64191.97*		1.193	1.105	8
	$^1[2\frac{1}{2}]^\circ$	$2\frac{1}{2}$	*65739.47*		0.879	0.896	11

TABLE 2. *Odd levels of* Yb II – Continued

Configuration	Desig.	J	Level	Interval	Obs. g	Calc. g	No. Comb.
$4f^{13}(^2F^\circ_{2\frac{1}{2}})5d^2(^1G^\circ)$ *Continued*	$^1[3\frac{1}{2}]^\circ$	$3\frac{1}{2}$					
	$^1[5\frac{1}{2}]^\circ$	$5\frac{1}{2}$					
	$^1[4\frac{1}{2}]^\circ$	$4\frac{1}{2}$					
$4f^{13}(^2F^\circ_{2\frac{1}{2}})5d^2(^1D^\circ)$	$^1[4\frac{1}{2}]^\circ$	$4\frac{1}{2}$	*64365.00*			0.959	11
	$^1[3\frac{1}{2}]^\circ$	$3\frac{1}{2}$	*64970.74*			1.051	11
	$^1[0\frac{1}{2}]^\circ$	$0\frac{1}{2}$	*65149.31*			0.484	4
	$^1[2\frac{1}{2}]^\circ$	$2\frac{1}{2}$	*66205.87*			0.924	9
	$^1[1\frac{1}{2}]^\circ$	$1\frac{1}{2}$	*66189.00*		0.91	0.888	8
$4f^{13}(^2F^\circ_{2\frac{1}{2}})5d^2(^1S^\circ)$	$^1[2\frac{1}{2}]^\circ$	$2\frac{1}{2}$					
		$4\frac{1}{2}$	*84?17.85*		1.19		14
		$3\frac{1}{2}$	*84444.07*				15
		$2\frac{1}{2}$	*84632.71*				9
		$2\frac{1}{2}$	*86148.67*		1.575		14
		$1\frac{1}{2}$	*86226.31*		1.35		16
		$3\frac{1}{2}$	*87385.74*		1.14		17
		$5\frac{1}{2}$	*88702.97*		1.08?		16
		$3\frac{1}{2}$	*88721.12*		1.17		19
		$4\frac{1}{2}$	*89605.80*		0.94?		13
		$2\frac{1}{2}$	*89615.59*				19
		$1\frac{1}{2}$	*89897.55*		1.01		20
		$3\frac{1}{2}$	*90142.74*				20
		$4\frac{1}{2}$	*90209.67*				21
		$5\frac{1}{2}$	*90279.08*		1.12		17
		$4\frac{1}{2}$	*90717.54*				25
		$2\frac{1}{2}$	*90859.07*				19
		$3\frac{1}{2}$	*91237.94*				17
		$6\frac{1}{2}$	*91301.57*		1.22		8

TABLE 2. *Odd levels of* Yb II —Continued

Configuration	Desig.	J	Level	Interval	Obs. g	Calc. g	No. Comb.
		3½	*91536.40*		1.13?		16
		2½	*91602.54*		1.17		16
		4½	*92015.76*				20
		1½	*92278.27*		1.49?		10
		3½	*92303.24*				17
		5½	*92647.34*				14
		4½	*92914.15*				15
		3½	*92919.10*				17
		3½	*92976.50*				13
		5½	*93096.30*		1.23		14
		3½	*93195.03*				13
		5½	*93242.39*				15
		6½	*93246.19*		1.21?		8
		3½	*93463.01*				15
		4½	*93503.89*				16
		2½	*93546.00*				16
		2½	*93864.57*				11
		4½	*93867.22*				16
		1½	*93998.52*				17
		3½	*94008.96*				22
		3½	*94303.58*		1.12		23
		5½	*94335.70*				18
		4½	*94360.00*				12
		1½	*94428.80*				6
		1½	*94823.18*				11
		4½	*95550.55*				14
		3½	*95691.32*				19
		5½	*95754.30*		0.89?		8

TABLE 2. *Odd levels of* Yb II – Continued

Configuration	Desig.	J	Level	Interval	Obs. g	Calc. g	No. Comb.
		$5\frac{1}{2}$	*96382.06*		1.23		10
		$4\frac{1}{2}$	*96482.44*				13
		$5\frac{1}{2}$	*96898.03*				12
		$6\frac{1}{2}$	*97043.28*				7
		$4\frac{1}{2}$	*97086.51*				14
		$4\frac{1}{2}$	*98521.73*				15
		$6\frac{1}{2}$	*98620.02*				8
		$5\frac{1}{2}$	*98802.66*				15
		$6\frac{1}{2}$	*98829.49*				6
		$5\frac{1}{2}$	*99246.37*				7
		$4\frac{1}{2}$	*99414.42*				12
		$5\frac{1}{2}$	*100025.57*				11

4. Ionization Potential

In the 1937 paper [1] Meggers refers to the collaboration with H. N. Russell on the interpretation of Yb spectra. As early as 1932 [14], Russell derived an ionization potential of 12.1 eV for Yb II from the three-member series $ns^2S(n=6, 7, 8)$, reported in 1947 by Meggers [2]. Since then the third member of the series has been corrected. From a modified Ritz formula the revised limit 98150 has been determined, giving an ionization potential 12.17 eV [15] from multiplication by the present conversion factor (cm^{-1} to eV) 0.000123981.

A semi-empirical method of deriving ionization potentials by a smooth run of Δn^* was suggested by Russell and Meggers in their analyses of La spectra [16]. Sugar and Reader [15] discuss the details of the method and the general run of ionization potentials for second spectra of the lanthanon group of rare earths.

5. Classified Lines

All observed lines of Yb II in the 1966 description of the spectrum [3] are listed in table 6. Column one contains the wavelength. With the exception of the first four entries, which are from Humphreys and Paul [6], practically all wavelengths are from [3], although a few additions and corrections to the published list noted by Meggers, have been included.

Columns two and three contain, respectively, estimated intensities of the lines as observed with the Meggers lamp and with the Thomson lamp. These sources are described in detail in [3]. "Literal symbols following intensity numbers have the following meanings:

A = nearly all absorbed in the pulsed arc.
R = wide reversal in the pulsed arc.
r = narrow reversal in the pulsed arc.
d = double but not resolved.
e = enhanced near wall of Thomson tube.
h = hazy as distinguished from sharp.
H = very hazy.
l = shaded or displaced to longer waves.
s = shaded or displaced to shorter waves."

The wave number is in column four. The next column, "o-c," gives the difference between the observed wave number and that calculated from the energy levels listed in tables 1 and 2. The levels giving rise to the transitions producing the lines are designated numerically in column six. They are the whole numbers of the levels tabulated in tables 1 and 2. The respective J-values are entered as subscripts. Odd levels are printed in italics. The last five columns contain Zeeman data, as explained in detail in section 3.

The total number of known Yb II lines is 5129. Of these, 3907 have been classified. There are 145 lines entered as blends, i.e., having more than one classifi-

TABLE 3. Yb II *Observed Levels*

Configuration	Observed Terms		
$1s^2\ 2s^2\ 2p^6\ 3s^2\ 3p^6\ 3d^{10}\ 4s^2\ 4p^6\ 4d^{10}\ 5s^2\ 5p^6$+			
$4f^{13}\ 6s^2$	$6s^2\ {}^2F^\circ$		
	$ns(n \geq 6)$	$np(n \geq 6)$	$nd(n \geq 5)$
$4f^{14}({}^1S)nl$	6, 7, $8s\ {}^2S$	$6p\ {}^2P^\circ$	5, 6, $7d\ {}^2D$

J_1J_{11}—Coupling Notation

$4f^{13}({}^2F^\circ_{3/2})6s\ 6p({}^3P_0)$			3½				
$({}^3P_1)$		2½	3½	4½			
$({}^3P_2)$	1½	2½	3½	4½	5½		
$({}^1P_1)$		2½	3½	4½			
$4f^{13}({}^2F^\circ_{2/2})6s\ 6p({}^3P_0)$			2½				
$({}^3P_1)$		1½	2½	3½			
$({}^3P_2)$	0½	1½	2½	3½	4½		
$({}^1P_1)$		1½	2½	3½			
$4f^{13}({}^2F^\circ_{3/2})5d\ 6p({}^3F_2)$		1½	2½	3½	4½	5½	
$({}^3F_3)$	0½	1½	2½	3½	4½	5½	6½
$({}^3F_4)$	0½	1½	2½	3½	4½	5½	6½ 7½
$({}^1F_3)$	0½	1½	2½	3½	4½	5½	6½
$({}^3D_1)$		2½	3½	4½			
$({}^3D_2)$		1½	2½	3½	4½	5½	
$({}^3D_3)$	0½	1½	2½	3½	4½	5½	6½
$({}^1D_2)$		1½	2½	3½	4½	5½	
$({}^3P_0)$			3½				
$({}^3P_1)$		2½	3½	4½			
$({}^3P_2)$	1½	2½	3½	4½	5½		
$({}^1P_1)$		2½	3½	4½			
$4f^{13}({}^2F^\circ_{2/2})5d\ 6p({}^3F_2)$	0½	1½	2½	3½	4½		
$({}^3F_3)$	0½	1½	2½	3½	4½	5½	
$({}^3F_4)$		1½	2½	3½	4½		6½
$({}^1F_3)$	0½	1½	2½	3½		5½	
$({}^3D_1)$		1½	2½	3½			
$({}^3D_2)$	0½	1½	2½	3½	4½		
$({}^3D_3)$	0½	1½	2½	3½	4½	5½	
$({}^1D_2)$	0½	1½	2½	3½	4½		
$4f^{13}({}^2F^\circ_{2/2})5d\ 6p({}^3P_0)$			2½				
$({}^3P_1)$		1½	2½	3½			
$({}^3P_2)$	1½	2½	3½	4½			
$({}^1P_1)$			2½				

J_1L_{11}—Coupling Notation

$4f^{13}({}^2F^\circ_{3/2})5d\ 6s({}^3D^\circ)$	${}^3[1½]^\circ$	${}^3[2½]^\circ$	${}^3[3½]^\circ$	${}^3[4½]^\circ$	${}^3[5½]^\circ$		
$({}^1D^\circ)$	${}^1[1½]^\circ$	${}^1[2½]^\circ$	${}^1[3½]^\circ$	${}^1[4½]^\circ$	${}^1[5½]^\circ$		
$4f^{13}({}^2F^\circ_{2/2})5d\ 6s({}^3D^\circ)$	${}^3[0½]^\circ$	${}^3[1½]^\circ$	${}^3[2½]^\circ$	${}^3[3½]^\circ$	${}^3[4½]^\circ$		
$({}^1D^\circ)$	${}^1[0½]^\circ$	${}^1[1½]^\circ$	${}^1[2½]^\circ$	${}^1[3½]^\circ$	${}^1[4½]^\circ$		
$4f^{13}({}^2F^\circ_{3/2})5d^2\ ({}^3F^\circ)$	${}^3[0½]^\circ$	${}^3[1½]^\circ$	${}^3[2½]^\circ$	${}^3[3½]^\circ$	${}^3[4½]^\circ$	${}^3[5½]^\circ$	${}^3[6½]^\circ$
$({}^3P^\circ)$			${}^3[2½]^\circ$	${}^3[3½]^\circ$	${}^3[4½]^\circ$		
$({}^1G^\circ)$	${}^1[0½]^\circ$	${}^1[1½]^\circ$	${}^1[2½]^\circ$	${}^1[3½]^\circ$	${}^1[4½]^\circ$	${}^1[5½]^\circ$	${}^1[6½]^\circ$ ${}^1[7½]^\circ$
$({}^1D^\circ)$		${}^1[1½]^\circ$	${}^1[2½]^\circ$	${}^1[3½]^\circ$	${}^1[4½]^\circ$	${}^1[5½]^\circ$	
$4f^{13}({}^2F^\circ_{2/2})5d^2\ ({}^3F^\circ)$	${}^3[0½]^\circ$	${}^3[1½]^\circ$	${}^3[2½]^\circ$	${}^3[3½]^\circ$	${}^3[4½]^\circ$	${}^3[5½]^\circ$	
$({}^3P^\circ)$		${}^3[1½]^\circ$	${}^3[2½]^\circ$	${}^3[3½]^\circ$			
$({}^1G^\circ)$		${}^1[1½]^\circ$	${}^1[2½]^\circ$				
$({}^1D^\circ)$	${}^1[0½]^\circ$	${}^1[1½]^\circ$	${}^1[2½]^\circ$	${}^1[3½]^\circ$	${}^1[4½]^\circ$		

cation, thus bringing the total number of classifications to 4054. In addition, 49 classifications which are considered to be masked, are entered in parentheses in table 6; these have not been included in the counts. In most cases the Zeeman pattern has been used as the deciding factor regarding masked lines. The number of computed combinations in the square array totals 10360. These numbers are, however, somewhat misleading. Nearly all of the strong lines are classified and "95 percent of the total intensity is accounted for." The strongest unclassified lines are listed in table 5, which includes all remaining lines having an estimated spark intensity of 15 or greater. The wavelengths and intensities are from table 6.

The present Monograph brings to a conclusion an accomplishment that is a lasting tribute to W. F. Meggers. In this work an ambition of more than 30 years of his distinguished career is realized. It is characteristic that he collaborated with the late Professor Racah and his associates for over 15 years on the interpretation of this complex rare-earth spectrum. The writer is deeply indebted to these eminent spectroscopists for their unfailing and expert work. The success of that part of the project of the "Atomic Energy Levels" program concerned with rare-earth spectra depends entirely on such contributions. Difficult ground-breaking research is required for this success.

277-259 O - 68 - 2

TABLE 4. *Unclassified lines of* Yb II *having an observed Zeeman effect*

Wavelength Air	Intensity		Wave Number	Zeeman Type	Zeeman Components	
	Meggers lamp	Thomson lamp			Strongest *p*	Strongest *n*
Å			*K*			
8263.640	4	150	12097.88	4	0.16*w*	1.03
8192.400		30	12203.08	4	*w*	1.03
8171.820	1	30	12233.81	5	*w*	1.40
8149.080		15	12267.95	6	1.150	1.20
8093.030		8	12352.91	6	0.512	1.478
7803.650	20	300	12810.99	6?	0.938	0.938
7362.920	2	15	13577.83	5?	0.11	0.99
7339.800		60	13620.60	7?	0	1.12
7317.740		30	13661.66	7?	0	0.963
7306.630	1	100	13682.43	5?		
7086.080		20	14108.29	4	*w*	0.96
6582.790	2	250	15186.93	7	0	0.97
5042.982	3	20	19824.01	7	0	1.20
3573.750	1	10	27973.82	7	0	1.013
3443.587	30	20	29031.17	?	0	1.18
3337.171	30	100	29956.89	7	0	1.019
3014.526	10	60	33163.05	7	0	1.12
2963.460	40	300	33734.49	6	0.16	1.08
2940.517	25	150	33997.68	5	*w*	1.44
2881.930	7	60	34688.79	5	*w*	1.24
2864.725	4	40	34897.12	4	*w*	0.94
2830.880	4	30	35314.32	7	0	0.99
2594.200	3	15	38536.01	6	0.22	
2516.820	50	300	39720.72	7	0	1.348
2515.600	2	7	39739.99	7	0	0.91

In Israel, warmest thanks are due Mrs. Z. B. Goldschmidt and her associates for their collaboration in providing the theoretical calculations of the configurations and matrices. The theses by S. Aberbach and D. Sperber in 1953 were useful contributions to earlier calculations for Yb II. At this Bureau, the cooperation of the Spectroscopy Section is appreciated. Special thanks are due W. C. Martin, J. Sugar, C. H. Corliss, N. Spector, and J. Tech.

The writer is deeply indebted to Mrs. Isabel D. Murray for her extreme competence and painstaking care in preparing for publication the enormous amount of tabular data on Yb II.

It is most regrettable that the author did not live to see his Monograph on Yb II thru publication, after his long years of labor. The writer has attempted to present the material as accurately as possible, with the aid of his beautifully kept records of work. In spite of her inability to do justice to the description of his accomplishment, she hopes that this monumental contribution will serve as the model he had in mind over the years.

Washington, D.C.
May 26, 1967

6. References

[1] W. F. Meggers and B. F. Scribner, J. Res. NBS **19,** 651 to 664 (1937) RP1053.
[2] W. F. Meggers, J. Opt. Soc. Am. **37,** 988, 989(A) (1947).
[3] W. F. Meggers and C. H. Corliss, J. Res. NBS **70A** (Phys. and Chem.) No. 1, 63 to 106 (1966).
[4] J. Sugar, J. Res. NBS **66A** (Phys. and Chem.) No. 4, 321 to 324 (1962).
[5] J. Sugar, J. Opt. Soc. Am. **53,** 831 to 839 (1963).
[6] C. J. Humphreys and E. Paul, Jr., Quarterly Report Foundational Research Projects, NAVORD Report 5970, NOLC Report 473, 57 to 67 (1959).
[7] A. M. Gutman and I. B. Levinsón; Translated by J. Tech., Smithsonian Inst. Astroph. Obs., Astron. Translations Ser. No. 8, 20 to 25 (1967).
[8] G. Racah, Proc. Rydberg Centennial Conference on Atomic Spectroscopy, Lunds Univ. Årsskrift. N. F. Avd. 2, **50,** No. 21; Kungl. Fys. Sällsk. Handl. N.F. **65,** No. 21, 31 to 42 (1954). See also, J. Opt. Soc. Am. **50,** 408 to 411 (1960).
[9] A. G. Shenstone, Phil. Trans. Roy. Soc. London **A241,** No. 832, 301 (1948).
[10] B. W. Bryant, J. Opt. Soc. Am. **55,** 771 to 779 (1965).
[11] N. Spector, J. Opt. Soc. Am. **57,** 312 to 317 (1967).
[12] G. Racah, letter, August 15 (1965).
[13] C. H. Corliss and W. F. Meggers, J. Res. NBS **61,** 270, 271 (1958) RP2904.
[14] H. N. Russell, private communication, February (1932).
[15] J. Sugar and J. Reader, J. Opt. Soc. Am. **55,** 1286 to 1290 (1965).
[16] H. N. Russell and W. F. Meggers, J. Res. NBS **9,** 625 to 668 (1932) RP497.

TABLE 5. *Strongest unclassified lines of* Yb II

Wavelength Air	Intensity		Wave number	Wavelength Air	Intensity		Wave number
	Meggers Lamp	Thomson Lamp			Meggers Lamp	Thomson Lamp	
Å			K	Å			K
10830.36		100	9230.77	5042.982	3	20	19824.01
10829.11		40	9231.84	4965.43	3	15	20133.62
10711.60		80*h*	9333.12	4837.045	500	1000	20668.00
10516.65		40	9506.13	4350.801		15	22977.81
9893.90		100*H*	10104.47	4281.972	20	50	23347.16
9693.72		50	10313.13	4215.519	6	20	23715.19
9664.23		20	10344.60	4202.44	15	30*hl*	23789.00
9482.44		20	10542.92	4177.40	2	50	23931.59
9428.10		30	10603.68	4119.25	20	30	24269.42
9380.18		15	10657.85	4077.713	10	20	24516.63
9325.68		20*h*	10720.14	3857.586	10	20	25915.60
9314.88	2	40	10732.57	3807.574	50	500	26255.99
9272.68	3	30	10781.41	3779.184	1	15	26453.22
9253.57	7	70	10803.68	3743.138		15*h*	26707.96
9196.50		20*H*	10870.72	3716.139	10	40	26902.00
9167.06	3	40	10905.63	3574.58		30*h*	27967.33
9163.69		15	10909.64	3482.564	5	30*h*	28706.26
9105.95		15*h*	10978.82	3477.022	20	30	28752.01
9096.88		20	10989.76	3472.324	5	20	28790.91
9080.35	1	60	11009.77	3390.421	1*h*	30*h*	29486.40
8985.71	8	60	11125.73	3390.246	1*h*	40*h*	29487.92
8980.74		20	11131.88	3376.623	3	30	29606.89
8855.12	50	300	11289.80	3363.645	10	20	29721.11
8291.01		20	12057.94	3362.438	10	70	29731.78
8263.64	4	150	12097.88	3352.491	10	30	29820.00
8192.40		30	12203.08	3342.93	20*h*	100*h*	29905.28
8171.82	1	30	12233.81	3337.171	30	100	29956.89
8149.08		15	12267.95	3315.101	1*h*	15*h*	30156.31
8124.50		15	12305.07	3179.344	30	70	31443.93
8023.46	1	20	12460.02	3166.727	2	20	31569.21
7803.65	20	300	12810.99	3114.905	3	20	32094.40
7362.92	2	15	13577.83	3014.526	10	60	33163.05
7339.80		60	13620.60	3007.923	5	30	33235.85
7317.74		30	13661.66	3004.642	1	15	33272.14
7306.63	1	100	13682.43	2963.46	40	300	33734.49
7086.08		20	14108.29	2950.52	2	20	33882.43
6829.80	1	70	14637.68	2940.517	25	150	33997.68
6670.18		50	14987.96	2881.93	7	60	34688.79
6616.40	2	40	15109.79	2864.725	4	40	34897.12
6582.79	2	250	15186.93	2830.880	4	30	35314.32
6485.55	10	200*h*	15414.63	2594.20	3	15	38536.01
6453.11	10	150	15492.12	2516.82	50	300	39720.72
6150.62		70*h*	16254.03	2369.42		50	42191.53
6120.30	5	250	16334.55	2284.99		30	43750.37
5833.99	5*h*	200*h*	17136.18	2161.60	10	40	46247.50
5581.05	2	40	17912.80	2155.50		30	46378.37
5331.536		20	18751.10	2102.73	5	20	47542.14
5256.85		20	19017.51				
5074.609		80	19700.46				

TABLE 6. Yb II—*Observed and classified lines*

1	2	3	4	5	6	7	8	9	10	11
Wavelength air	Intensity		Wave number	o–c	Classification	Zeeman type	1st g	2nd g	Zeeman components	
	Meggers lamp	Thomson lamp							Strong p	Strong n
Å			K	K						
24377.26	250		4101.06	+0.04	$22960_{1\frac{1}{2}} - 27061^{\circ}_{0\frac{1}{2}}$					
16498.42	1500		6059.53	−0.01	$24332_{2\frac{1}{2}} - 30392^{\circ}_{1\frac{1}{2}}$					
13452.62	300		7431.46	+0.03	$22960_{1\frac{1}{2}} - 30392^{\circ}_{1\frac{1}{2}}$					
12692.48	450		7876.53	+0.04	$40035^{\circ}_{3\frac{1}{2}} - 47912_{3\frac{1}{2}}$					
11559.05		5	8648.86	−0.04	$24332_{2\frac{1}{2}} - 32981^{\circ}_{1\frac{1}{2}}$					
11442.70		1	8736.80							
11299.78		5*h*	8847.31							
11277.83		1	8864.53	−0.06	$40035^{\circ}_{3\frac{1}{2}} - 48900_{3\frac{1}{2}}$					
11060.25		2*h*	9038.91							
11051.05		2	9046.44	−0.03	$47329^{\circ}_{2\frac{1}{2}} - 56375_{2\frac{1}{2}}$					
11035.15		1*h*	9059.47							
11023.37		1*h*	9069.15							
11002.95		4	9085.98	−0.03	$54640^{\circ}_{4\frac{1}{2}} - 63726_{4\frac{1}{2}}$					
10980.47		3*h*	9104.58							
10959.94		1*h*	9121.64							
10943.17		1	9135.62	+0.02	$55462^{\circ}_{3\frac{1}{2}} - 64598_{3\frac{1}{2}}$					
10882.92		1*h*	9186.19							
10856.25		1	9208.76	+0.01	$48556^{\circ}_{3\frac{1}{2}} - 57765_{4\frac{1}{2}}$					
10845.53		3*h*	9217.86							
10830.36		100	9230.77							
10829.11		40	9231.84							
10810.82		5*h*	9247.46							
10802.47		4	9254.61	−0.01	$56621^{\circ}_{5\frac{1}{2}} - 65875_{6\frac{1}{2}}$					
10776.11		1	9277.25	+0.02	$44438^{\circ}_{3\frac{1}{2}} - 53715_{3\frac{1}{2}}$					
10774.38		1	9278.73							
10754.99		1	9295.46	−0.01	$53716^{\circ}_{2\frac{1}{2}} - 63011_{1\frac{1}{2}}$					
10745.87		3	9303.35	−0.01	$54640^{\circ}_{4\frac{1}{2}} - 63944_{5\frac{1}{2}}$					
10731.94		3	9315.43							
10721.68		3*h*	9324.34							
10717.07		2	9328.35							
10711.60		80*h*	9333.12							
10691.02		1*h*	9351.08	−0.06	$61442^{\circ}_{5\frac{1}{2}} - 70793_{5\frac{1}{2}}$					
10689.20		2*h*	9352.67							
10678.64		1	9361.92	−0.02	$66189^{\circ}_{1\frac{1}{2}} - 75550_{2\frac{1}{2}}$					
10676.73		30	9363.60	−0.09 +0.04	$44940^{\circ}_{1\frac{1}{2}} - 54304_{0\frac{1}{2}}$ $56375_{2\frac{1}{2}} - 65739^{\circ}_{2\frac{1}{2}}$					
10666.30		2*h*	9372.75							
10651.36		5	9385.90	0.00 −0.06	$64365^{\circ}_{4\frac{1}{2}} - 73750_{4\frac{1}{2}}$ $75058_{2\frac{1}{2}} - 84444^{c}_{3\frac{1}{2}}$					
10638.35		1	9397.38	+0.08	$65594^{\circ}_{2\frac{1}{2}} - 74991_{1\frac{1}{2}}$					

See footnotes at end of table.

TABLE 6. Yb II—*Observed and classified lines*—Continued

1	2	3	4	5	6	7	8	9	10	11
Wave-length air	Intensity		Wave number	o–c	Classification	Zeeman type	1st g	2nd g	Zeeman components	
	Meggers lamp	Thomson lamp							Strong p	Strong n
Å			K	K						
10628.11		4	9406.43	−0.03	$57798^{\circ}_{2\frac{1}{2}} - 67204_{1\frac{1}{2}}$					
10602.75		2*h*	9428.93							
10584.87		1	9444.86	0.00	$64191^{\circ}_{1\frac{1}{2}} - 73636_{0\frac{1}{2}}$					
10580.74		1	9448.55	0.00	$43956^{\circ}_{2\frac{1}{2}} - 53404_{2\frac{1}{2}}$					
10574.50		2*h*	9454.12	−0.02	$58484^{\circ}_{4\frac{1}{2}} - 67938_{3\frac{1}{2}}$					
10570.51		1	9457.69							
10567.42		3	9460.46	+0.03	$55462^{\circ}_{3\frac{1}{2}} - 64923_{4\frac{1}{2}}$					
10565.46		4	9462.21	−0.01	$40035^{\circ}_{3\frac{1}{2}} - 49498_{2\frac{1}{2}}$					
10556.48		2*h*	9470.26	+0.08	$56480^{\circ}_{4\frac{1}{2}} - 65950_{4\frac{1}{2}}$					
10547.78		4	9478.07	+0.03	$58672^{\circ}_{0\frac{1}{2}} - 68150_{1\frac{1}{2}}$					
10546.24		1	9479.46							
10516.65		40	9506.13							
10502.56		1	9518.88	−0.02	$53644^{\circ}_{3\frac{1}{2}} - 63163_{4\frac{1}{2}}$					
10501.08		4	9520.22	+0.02	$56056^{\circ}_{2\frac{1}{2}} - 65577_{3\frac{1}{2}}$					
10490.03		1	9530.25							
10485.56		2	9534.31	−0.01	$54192^{\circ}_{5\frac{1}{2}} - 63726_{4\frac{1}{2}}$					
10477.15		1*h*	9541.97							
10456.88		1	9560.46							
10455.88		2	9561.38							
10446.15		1	9570.28	−0.01	$38342^{\circ}_{4\frac{1}{2}} - 47912_{3\frac{1}{2}}$					
10445.27		4*h*	9571.09							
10425.42		2	9589.31	+0.09	$58644^{\circ}_{3\frac{1}{2}} - 63234_{2\frac{1}{2}}$					
10416.16		5	9597.84	0.00	$64970^{\circ}_{3\frac{1}{2}} - 74568_{4\frac{1}{2}}$					
10414.15		1	9599.69	−0.06	$62163^{\circ}_{2\frac{1}{2}} - 71763_{1\frac{1}{2}}$					
10411.40		10	9602.23	+0.01	$42915^{\circ}_{5\frac{1}{2}} - 52517_{5\frac{1}{2}}$					
10397.98		3	9614.62							
10391.64		1*h*	9620.48							
10388.85		2*h*	9623.07							
10363.89		3	9646.24							
10345.62		1*h*	9663.28							
10343.99		4*h*	9664.80							
10339.49		2*h*	9669.01							
10337.35		1*h*	9671.01							
10328.74		2*h*	9679.07							
10327.33		1	9680.39							
10293.40		2*h*	9712.30							
10283.38		2	9721.76							
10275.82		1	9728.92							
10259.93		3*h*	9743.98							
10257.97		1*h*	9745.85							

TABLE 6. Yb II—*Observed and classified lines*—Continued

1	2	3	4	5	6	7	8	9	10	11
Wave-length air	Intensity		Wave number	o–c	Classification	Zeeman type	1st g	2nd g	Zeeman components	
	Meggers lamp	Thomson lamp							Strong p	Strong n
Å			K	K						
10251.85		10	9751.66	−0.01	$54192^{\circ}_{5\frac{1}{2}} - 63944_{5\frac{1}{2}}$					
10242.30		1*h*	9760.76	+0.04	$48900_{3\frac{1}{2}} - 58661^{\circ}_{2\frac{1}{2}}$					
10222.98		2*h*	9779.20	+0.04	$77606_{2\frac{1}{2}} - 87385^{\circ}_{3\frac{1}{2}}$					
10212.34		1*h*	9789.39							
10198.92		1*h*	9802.27	+0.07	$51248^{\circ}_{2\frac{1}{2}} - 61051_{3\frac{1}{2}}$					
10189.53		10*h*	9811.31							
10186.03		5	9814.68	+0.03	$49008^{\circ}_{3\frac{1}{2}} - 58823_{2\frac{1}{2}}$					
10172.39		2	9827.84							
10168.71		1*h*	9831.39							
10167.42		1*h*	9832.64							
10157.63		1	9842.12	+0.07	$65149^{\circ}_{0\frac{1}{2}} - 74991_{1\frac{1}{2}}$?					
10148.91		3	9850.57	0.00	$56500^{\circ}_{3\frac{1}{2}} - 66351_{2\frac{1}{2}}$					
10145.30		4*h*	9854.08							
10136.34		3*h*	9862.79							
10107.09		1	9891.33	+0.06	$53120^{\circ}_{2\frac{1}{2}} - 63011_{1\frac{1}{2}}$					
10103.24		3	9895.10	+0.02	$56500^{\circ}_{3\frac{1}{2}} - 66395_{2\frac{1}{2}}$					
10100.39		1*h*	9897.89							
10086.67		1	9911.36							
10068.79		2*h*	9928.96							
10067.47		1	9930.26	+0.04	$43007^{\circ}_{0\frac{1}{2}} - 52938_{1\frac{1}{2}}$					
10066.30		5	9931.41	+0.06	$53716^{\circ}_{2\frac{1}{2}} - 63647_{1\frac{1}{2}}$					
10063.22		2*h*	9934.45							
10046.95		2	9950.54							
10039.90		1	9957.53	+0.07	$54640^{\circ}_{4\frac{1}{2}} - 64598_{3\frac{1}{2}}$					
10032.55		50	9964.82	+0.04	$45737^{\circ}_{1\frac{1}{2}} - 55702_{1\frac{1}{2}}$					
10020.70		1	9976.61							
10016.78		15	9980.51	−0.01	$52880^{\circ}_{4\frac{1}{2}} - 62861_{5\frac{1}{2}}$					
10007.96		3	9989.31							
10003.38		4	9993.88	+0.02	$56088^{\circ}_{3\frac{1}{2}} - 66082_{5\frac{1}{2}}$					
9994.64		1	10002.62	−0.05	$64970^{\circ}_{3\frac{1}{2}} - 74973_{3\frac{1}{2}}$					
9992.75		1	10004.51	+0.07	$59439^{\circ}_{2\frac{1}{2}} - 69443_{1\frac{1}{2}}$					
9990.47		6	10006.80	+0.02	$47758^{\circ}_{3\frac{1}{2}} - 57765_{4\frac{1}{2}}$					
9984.66		1	10012.62							
9976.50	2	30	10020.81	+0.02	$22960_{1\frac{1}{2}} - 32981^{\circ}_{1\frac{1}{2}}$					
9970.10		200*H*	10027.24	−0.06	$82891_{2\frac{1}{2}} - 92919^{\circ}_{3\frac{1}{2}}$					
9959.25		2	10038.16	+0.05	$62163^{\circ}_{2\frac{1}{2}} - 72202_{3\frac{1}{2}}$					
9953.32		4	10044.15	+0.02	$60910^{\circ}_{1\frac{1}{2}} - 70954_{2\frac{1}{2}}$					
9945.98		4	10051.56							

TABLE 6. Yb II—*Observed and classified lines*—Continued

1	2	3	4	5	6	7	8	9	10	11
Wave-length air	Intensity		Wave number	o–c	Classification	Zeeman type	1st g	2nd g	Zeeman components	
	Meggers lamp	Thomson lamp							Strong p	Strong n
Å			K	K						
9940.23		3	10057.37	$\begin{cases}-0.06\\+0.01\end{cases}$	$53644^{\circ}_{3\frac{1}{2}} - 63702_{2\frac{1}{2}}$ $56500^{\circ}_{3\frac{1}{2}} - 66558_{3\frac{1}{2}}$					
9932.98		1	10064.71	+0.02	$58484^{\circ}_{4\frac{1}{2}} - 68549_{4\frac{1}{2}}$					
9915.99		6	10081.96	+0.02	$53644^{\circ}_{3\frac{1}{2}} - 63726_{4\frac{1}{2}}$					
9914.02		2	10083.96							
9904.50		3	10093.65							
9896.50		20	10101.81	+0.01	$47663^{\circ}_{4\frac{1}{2}} - 57765_{4\frac{1}{2}}$					
9893.90		100*H*	10104.47							
9892.20		4*h*	10106.20	−0.03	$52067^{\circ}_{0\frac{1}{2}} - 62174_{1\frac{1}{2}}$					
9885.02		1	10113.54	+0.01	$53120^{\circ}_{2\frac{1}{2}} - 63234_{2\frac{1}{2}}$					
9884.09		3	10114.50	+0.07	$55462^{\circ}_{3\frac{1}{2}} - 65577_{3\frac{1}{2}}$					
9881.04		1	10117.62	0.00	$66205^{\circ}_{2\frac{1}{2}} - 76323_{3\frac{1}{2}}$					
9849.25		2*h*	10150.27							
9837.89		2*h*	10161.99							
9830.09		2	10170.06							
9826.25		2	10174.03							
9818.33		6*h*	10182.24							
9816.25		2*h*	10184.40							
9800.41		1	10200.86							
9797.67		6	10203.71	$\begin{cases}+0.06\\+0.01\end{cases}$	$59753^{\circ}_{5\frac{1}{2}} - 69957_{4\frac{1}{2}}$ $60910^{\circ}_{1\frac{1}{2}} - 71113_{1\frac{1}{2}}$					
9770.61		2*h*	10231.97							
9760.38	200	1000	10242.69	+0.01	$24332_{2\frac{1}{2}} - 34575^{\circ}_{1\frac{1}{2}}$					
9745.39		7	10258.45							
9735.10		1	10269.29							
9717.58		2	10287.81	−0.03	$50832^{\circ}_{1\frac{1}{2}} - 61120_{0\frac{1}{2}}$					
9716.88		8	10288.55							
9711.44		5	10294.31	+0.01	$56056^{\circ}_{2\frac{1}{2}} - 66351_{2\frac{1}{2}}$					
9706.65		10	10299.39							
9705.60		3*h*	10300.51							
9700.26		2*h*	10306.18							
9694.33		2	10312.48	−0.01	$52921^{\circ}_{3\frac{1}{2}} - 63234_{2\frac{1}{2}}$					
9693.72		50	10313.13							
9678.00	1	5	10329.88	+0.01	$43075^{\circ}_{1\frac{1}{2}} - 53404_{2\frac{1}{2}}$					
9677.56		1	10330.35							
9671.78		1	10336.52	+0.03	$57798^{\circ}_{2\frac{1}{2}} - 68135_{2\frac{1}{2}}$					
9669.62		1	10338.83	+0.02	$56056^{\circ}_{2\frac{1}{2}} - 66395_{2\frac{1}{2}}$					
9669.03		2	10339.46	+0.02	$53716^{\circ}_{2\frac{1}{2}} - 64055_{2\frac{1}{2}}$					
9664.23		20	10344.60							
9663.60		1	10345.27	+0.01	$55221^{\circ}_{1\frac{1}{2}} - 65566_{0\frac{1}{2}}$					
9663.09		2	10345.82							

TABLE 6. Yb II—*Observed and classified lines*—Continued

1	2	3	4	5	6	7	8	9	10	11
Wave-length air	Intensity		Wave number	o–c	Classification	Zeeman type	1st g	2nd g	Zeeman components	
	Meggers lamp	Thomson lamp							Strong p	Strong n
Å			K	K						
9661.01		6*h*	10348.05							
9657.25		3	10352.08	+0.02	$57798^{\circ}_{2\frac{1}{2}} - 68150_{1\frac{1}{2}}$					
9648.86		3	10361.08							
9644.92		2*h*	10365.31							
9637.59		3*h*	10373.19							
9630.97		5	10380.32							
9629.04		2	10382.40	0.00	$59753^{\circ}_{5\frac{1}{2}} - 70136_{6\frac{1}{2}}$					
9623.60		9*h*	10388.27							
9619.82		3*h*	10392.35							
9613.49		1	10399.20	+0.01	$64169^{\circ}_{3\frac{1}{2}} - 74568_{4\frac{1}{2}}$					
9611.30		2	10401.57							
9610.77		2	10402.14							
9608.81		2	10404.26	+0.03	$57534^{\circ}_{3\frac{1}{2}} - 67938_{3\frac{1}{2}}$					
9602.64		20	10410.95	+0.02	$53644^{\circ}_{3\frac{1}{2}} - 64055_{2\frac{1}{2}}$					
9600.55		2*h*	10413.21							
9595.60		2*h*	10418.59							
9594.26		2*h*	10420.04	−0.08	$56375_{2\frac{1}{2}} - 66796^{\circ}_{3\frac{1}{2}}$					
9589.14		7*h*	10425.60							
9578.21		1	10437.50							
9577.45		3	10438.33							
9564.64		3	10452.31	−0.01	$54640^{\circ}_{4\frac{1}{2}} - 65093_{3\frac{1}{2}}$					
9559.83		5	10457.57	+0.02	$48503^{\circ}_{5\frac{1}{2}} - 58961_{5\frac{1}{2}}$					
9555.55		5	10462.25							
9536.43		3	10483.23	+0.04	$56088^{\circ}_{4\frac{1}{2}} - 66571_{5\frac{1}{2}}$					
9532.71		8*h*	10487.32	+0.01	$66189^{\circ}_{1\frac{1}{2}} - 76676_{2\frac{1}{2}}$					
9531.83		20	10488.29	+0.02	$55462^{\circ}_{3\frac{1}{2}} - 65950_{4\frac{1}{2}}$					
9527.91		3*h*	10492.60							
9522.68		4*h*	10498.37							
9520.19		3	10501.11	+0.02	$56056^{\circ}_{2\frac{1}{2}} - 66558_{3\frac{1}{2}}$					
9511.61		3	10510.58							
9504.03		1	10518.97							
9498.90		3	10524.65							
9496.63		10	10527.16	+0.01	$53120^{\circ}_{2\frac{1}{2}} - 63647_{1\frac{1}{2}}$					
9490.85		2	10533.57	+0.01	$48556^{\circ}_{3\frac{1}{2}} - 59090_{3\frac{1}{2}}$					
9482.44		20	10542.92							
9475.35		1	10550.81	0.00	$48272^{\circ}_{2\frac{1}{2}} - 58823_{2\frac{1}{2}}$					
9474.20		2*h*	10552.09							
9468.54[a]	2	3	10558.39							
9468.20		10*h*	10558.77	+0.05	$54640^{\circ}_{4\frac{1}{2}} - 65199_{4\frac{1}{2}}$					
9464.03		4*h*	10563.43							

TABLE 6. Yb II—*Observed and classified lines*—Continued

1	2	3	4	5	6	7	8	9	10	11
Wave-length air	Intensity		Wave number	o–c	Classification	Zeeman type	1st g	2nd g	Zeeman components	
	Meggers lamp	Thomson lamp							Strong p	Strong n
Å			K	K						
9457.07		6h	10571.20	−0.01	$82891_{2\frac{1}{2}} - 93463^{\circ}_{3\frac{1}{2}}$					
9445.45		6h	10584.20							
9442.75		7	10587.23	−0.03	$57561^{\circ}_{6\frac{1}{2}} - 68148_{5\frac{1}{2}}$					
9428.10		30	10603.68							
9423.79		3d	10608.53	−0.04	$63028^{\circ}_{1\frac{1}{2}} - 73636_{0\frac{1}{2}}$					
9417.09		5	10616.08	+0.01	$62163^{\circ}_{2\frac{1}{2}} - 72779_{3\frac{1}{2}}$					
9408.11		4	10626.21							
9405.75		3	10628.88							
9404.73		10	10630.03							
9397.79		2h	10637.88							
9390.61		8h	10646.01							
9388.32		2	10648.61							
9380.18		15	10657.85							
9378.29		3	10660.00	+0.03	$52987^{\circ}_{1\frac{1}{2}} - 63647_{1\frac{1}{2}}$					
9372.12		3	10667.02	+0.02	$55221^{\circ}_{1\frac{1}{2}} - 65888_{1\frac{1}{2}}$					
9367.86		1	10671.87							
9367.21		2	10672.61							
9352.58	8	80	10689.30	+0.02	$45012^{\circ}_{2\frac{1}{2}} - 55702_{1\frac{1}{2}}$					
9349.25	80	300	10693.11	+0.05	$22960_{1\frac{1}{2}} - 33653^{\circ}_{0\frac{1}{2}}$					
9341.89		4h	10701.54							
9334.67		3	10709.81							
9328.56		3h	10716.83							
9325.68		20h	10720.14							
9324.60		2h	10721.38							
9321.14		2h	10725.36							
9320.30		1	10726.33	+0.02	$24332_{2\frac{1}{2}} - 35059^{\circ}_{3\frac{1}{2}}$					
9316.58		1	10730.61	+0.01	$54192^{\circ}_{5\frac{1}{2}} - 64923_{4\frac{1}{2}}$					
9314.88	2	40	10732.57							
9302.74		2	10746.57	−0.04	$50468^{\circ}_{5\frac{1}{2}} - 61214_{4\frac{1}{2}}$					
9301.33		3	10748.20							
9299.67		1	10750.12							
9298.74		6	10751.20							
9289.87	4	100	10761.46	0.00	$44940^{\circ}_{1\frac{1}{2}} - 55702_{1\frac{1}{2}}$					
9287.36		1	10764.37	−0.06	$53404_{2\frac{1}{2}} - 64169^{\circ}_{3\frac{1}{2}}$					
9272.68	3	30	10781.41							
9271.84		2	10782.39	0.00	$58661^{\circ}_{2\frac{1}{2}} - 69443_{1\frac{1}{2}}$					
9263.73		4h	10791.83							
9261.11		4h	10794.88	0.00	$56621^{\circ}_{5\frac{1}{2}} - 67416_{4\frac{1}{2}}$					
9257.70		8	10798.86	−0.02	$48024^{\circ}_{1\frac{1}{2}} - 58823_{2\frac{1}{2}}$					
9253.57	7	70	10803.68							

TABLE 6. Yb II—*Observed and classified lines*—Continued

1	2	3	4	5	6	7	8	9	10	11
Wave-length air	Intensity		Wave number	o–c	Classification	Zeeman type	1st g	2nd g	Zeeman components	
	Meggers lamp	Thomson lamp							Strong p	Strong n
Å			K	K						
9252.27		3	10805.19	−0.02	$52921^{\circ}_{3\frac{1}{2}} - 63726_{4\frac{1}{2}}$					
9251.95	1	5	10805.57	−0.01	$42915^{\circ}_{5\frac{1}{2}} - 53720_{4\frac{1}{2}}$					
9245.69		2*h*	10812.88							
9241.86		2	10817.36	0.00	$48272^{\circ}_{2\frac{1}{2}} - 59090_{3\frac{1}{2}}$					
9226.17		6*h*	10835.76	+0.10	$57103^{\circ}_{3\frac{1}{2}} - 67938_{3\frac{1}{2}}$					
9220.77		7*h*	10842.11							
9218.26		1	10845.06	+0.05	$54304_{0\frac{1}{2}} - 65149^{\circ}_{0\frac{1}{2}}$?					
9217.40		6	10846.07	−0.01	$52880^{\circ}_{4\frac{1}{2}} - 63726_{4\frac{1}{2}}$					
9215.28		5	10848.57							
9211.07		2	10853.52	−0.01 +0.07	$60910^{\circ}_{1\frac{1}{2}} - 71763_{1\frac{1}{2}}$ $63417^{\circ}_{2\frac{1}{2}} - 74270_{2\frac{1}{2}}$					
9207.65		7*h*	10857.56							
9196.50		20*H*	10870.72							
9192.40		3*h*	10875.57							
9191.41		3	10876.74							
9190.18		5*h*	10878.19							
9187.53		4	10881.33	−0.02	$67933^{\circ}_{2\frac{1}{2}} - 78814_{2\frac{1}{2}}$					
9187.01		1	10881.95	+0.05	$53716^{\circ}_{2\frac{1}{2}} - 64598_{3\frac{1}{2}}$					
9182.32		5*h*	10887.51							
9178.52		5	10892.01							
9175.76		2*h*	10895.29							
9172.59		2*h*	10899.06							
9170.70		3*h*	10901.30							
9168.70		2*h*	10903.68							
9167.06	3	40	10905.63							
9163.69		15	10909.64							
9162.85		2	10910.64	−0.02 +0.04	$58484^{\circ}_{4\frac{1}{2}} - 69395_{3\frac{1}{2}}$ $59046^{\circ}_{4\frac{1}{2}} - 69957_{4\frac{1}{2}}$					
9158.62		15	10915.68	+0.02	$57534^{\circ}_{3\frac{1}{2}} - 68450_{3\frac{1}{2}}$					
9152.45		8*H*	10923.04	−0.11	$65594^{\circ}_{2\frac{1}{2}} - 76517_{1\frac{1}{2}}$?					
9150.60		1*h*	10925.25	+0.01	$51248^{\circ}_{2\frac{1}{2}} - 62174_{1\frac{1}{2}}$					
9149.57		2*h*	10926.48							
9142.22		7	10935.26	+0.02 0.00	$53120^{\circ}_{2\frac{1}{2}} - 64055_{2\frac{1}{2}}$ $56480^{\circ}_{4\frac{1}{2}} - 67416_{4\frac{1}{2}}$					
9141.37		15	10936.28	−0.01	$54640^{\circ}_{4\frac{1}{2}} - 65577_{3\frac{1}{2}}$					
9133.17	3	60	10946.10	+0.01	$45429^{\circ}_{3\frac{1}{2}} - 56375_{2\frac{1}{2}}$					
9127.08		1	10953.40	+0.01	$53644^{\circ}_{3\frac{1}{2}} - 64598_{3\frac{1}{2}}$					
9126.00		7*h*	10954.70							
9123.62		2	10957.55	+0.02	$57798^{\circ}_{2\frac{1}{2}} - 68756_{3\frac{1}{2}}$					
9122.30		15	10959.14	0.00	$38342^{\circ}_{4\frac{1}{2}} - 49301_{4\frac{1}{2}}$					
9120.52		5*h*	10961.28							

TABLE 6. Yb II—*Observed and classified lines*—Continued

1	2	3	4	5	6	7	8	9	10	11
Wavelength air	Intensity		Wave number	o–c	Classification	Zeeman type	1st g	2nd g	Zeeman components	
	Meggers lamp	Thomson lamp							Strong p	Strong n
Å			K	K						
9113.24		7h	10970.03							
9105.95		15h	10978.82							
9096.88		20	10989.76							
9094.57		4	10992.55							
9083.98		3h	11005.37							
9082.61		7	11007.03	0.00	$54192^{\circ}_{5\frac{1}{2}} - 65199_{4\frac{1}{2}}$					
9080.35	1	60	11009.77							
9077.91		4	11012.73							
9076.21		2	11014.79	+0.01	$57534^{\circ}_{3\frac{1}{2}} - 68549_{4\frac{1}{2}}$					
9066.47		1	11026.62							
9062.06		15	11031.99	+0.01	$57103^{\circ}_{3\frac{1}{2}} - 68135_{2\frac{1}{2}}$					
9057.08		3h	11038.06							
9055.35		2	11040.17	+0.05	$59753^{\circ}_{5\frac{1}{2}} - 70793_{5\frac{1}{2}}$					
9040.38		3h	11058.45							
9035.02	2	20	11065.01	−0.03	$47758^{\circ}_{3\frac{1}{2}} - 58823_{2\frac{1}{2}}$					
9029.62		2	11071.62							
9021.00		100hl	11082.20	−0.05	$65594^{\circ}_{2\frac{1}{2}} - 76676_{2\frac{1}{2}}$					
9017.02		5h	11087.09							
9014.27		2	11090.48	−0.08	$75058_{2\frac{1}{2}} - 86148^{\circ}_{2\frac{1}{2}}$					
9004.83		3	11102.10							
9004.21	10	150	11102.87	−0.02	$45273^{\circ}_{3\frac{1}{2}} - 56375_{2\frac{1}{2}}$					
8985.71	8	60	11125.73							
8982.45		2	11129.76	+0.01	$55221^{\circ}_{1\frac{1}{2}} - 66351_{2\frac{1}{2}}$					
8980.74		20	11131.88							
8978.58		6	11134.56	−0.02 0.00	$47912_{3\frac{1}{2}} - 59046^{\circ}_{4\frac{1}{2}}$ $49916^{\circ}_{4\frac{1}{2}} - 61051_{3\frac{1}{2}}$					
8971.65		3h	11143.16							
8967.71		5	11148.06	0.00	$56056^{\circ}_{2\frac{1}{2}} - 67204_{1\frac{1}{2}}$					
8959.06	2	70	11158.82	0.00	$57561^{\circ}_{6\frac{1}{2}} - 68720_{6\frac{1}{2}}$					
8956.72		9	11161.74	−0.01	$59632^{\circ}_{6\frac{1}{2}} - 70793_{5\frac{1}{2}}$?					
8952.23		6	11167.34	+0.01	$49419^{\circ}_{6\frac{1}{2}} - 60586_{1\frac{1}{2}}$					
8947.78		6	11172.89	+0.03 −0.03	$56977^{\circ}_{6\frac{1}{2}} - 68150_{1\frac{1}{2}}$ $61442^{\circ}_{5\frac{1}{2}} - 72615_{5\frac{1}{2}}$					
8946.66		5	11174.29	+0.03	$55221^{\circ}_{1\frac{1}{2}} - 66395_{2\frac{1}{2}}$					
8942.87		3	11179.02							
8930.12		1	11194.98							
8927.38		4	11198.42							
8922.56		100	11204.47	−0.09	$44497^{\circ}_{2\frac{1}{2}} - 55702_{1\frac{1}{2}}$?					
8912.14	4	60	11217.57	−0.03	$46547^{\circ}_{5\frac{1}{2}} - 57765_{4\frac{1}{2}}$					
8907.81		2h	11223.02							

TABLE 6. Yb II – *Observed and classified lines* – Continued

1	2	3	4	5	6	7	8	9	10	11
Wavelength air	Intensity		Wave number	o–c	Classification	Zeeman type	1st g	2nd g	Zeeman components	
	Meggers lamp	Thomson lamp							Strong p	Strong n
Å			K	K						
8902.92		7*h*	11229.19	−0.02	$43075^{\circ}_{1\frac{1}{2}} - 54304_{0\frac{1}{2}}$					
8897.61		1	11235.89							
8896.50		4	11237.29	+0.01	$62046^{\circ}_{3\frac{1}{2}} - 73283_{4\frac{1}{2}}$					
8890.45	5	50	11244.94	0.00	$65594^{\circ}_{2\frac{1}{2}} - 76839_{2\frac{1}{2}}$					
8874.53		9	11265.11							
8873.33		4	11266.63							
8867.40		1	11274.17							
8865.65		1	11276.39							
8864.18		1	11278.26	+0.04	$53644^{\circ}_{3\frac{1}{2}} - 64923_{4\frac{1}{2}}$					
8863.98		4	11278.52	+0.07	$47005^{\circ}_{1\frac{1}{2}} - 58283_{2\frac{1}{2}}$					
8862.12		3	11280.88	−0.09	$47680^{\circ}_{6\frac{1}{2}} - 58961_{5\frac{1}{2}}$					
8861.70		1	11281.42	+0.05	$57798^{\circ}_{2\frac{1}{2}} - 69079_{2\frac{1}{2}}$					
8855.12	50	300	11289.80							
8851.05		1	11294.99	+0.03	$56840^{\circ}_{1\frac{1}{2}} - 68135_{2\frac{1}{2}}$					
8849.52		1	11296.95							
8848.83	4	60	11297.83	−0.02	$47663^{\circ}_{4\frac{1}{2}} - 58961_{5\frac{1}{2}}$					
8842.64		2	11305.74							
8839.24		10	11310.08	−0.08 −0.05	$51248^{\circ}_{2\frac{1}{2}} - 62559_{2\frac{1}{2}}$ $54640^{\circ}_{4\frac{1}{2}} - 65950_{4\frac{1}{2}}$					
8825.52		2	11327.67	+0.03	$56088^{\circ}_{4\frac{1}{2}} - 67416_{4\frac{1}{2}}$					
8822.45		7	11331.61	+0.02	$47758^{\circ}_{3\frac{1}{2}} - 59090_{3\frac{1}{2}}$					
8815.52		9	11340.52	+0.02	$53120^{\circ}_{2\frac{1}{2}} - 64461_{1\frac{1}{2}}$					
8806.05		2	11352.71	−0.04	$64970^{\circ}_{3\frac{1}{2}} - 76323_{3\frac{1}{2}}$					
8800.32		2*h*	11360.10							
8797.99	5	100	11363.11	−0.01	$45012^{\circ}_{2\frac{1}{2}} - 56375_{2\frac{1}{2}}$					
8783.76		2	11381.52	−0.03	$64169^{\circ}_{3\frac{1}{2}} - 75550_{2\frac{1}{2}}$					
8781.96	1	10	11383.85	+0.03	$37516^{\circ}_{3\frac{1}{2}} - 48900_{3\frac{1}{2}}$	6	1.114	1.034	0.28	1.074
8762.42		5	11409.24	+0.04	$57534^{\circ}_{3\frac{1}{2}} - 68943_{4\frac{1}{2}}$	5	0.874	0.904	(0.015)	1.007
8761.26		2	11410.75	−0.02	$46354^{\circ}_{4\frac{1}{2}} - 57765_{4\frac{1}{2}}$					
8750.88		1*h*	11424.28							
8749.10		40	11426.61	0.00	$47663^{\circ}_{4\frac{1}{2}} - 59090_{3\frac{1}{2}}$	4	0.970	1.100	0.065	0.514
8744.27		1	11432.92							
8742.84		7	11434.79							
8742.45		10	11435.30	0.00	$44940^{\circ}_{1\frac{1}{2}} - 56375_{2\frac{1}{2}}$	7	1.23	(1.226)	0	1.226
8740.48		5	11437.88	0.00 +0.02	$48272^{\circ}_{2\frac{1}{2}} - 59710_{1\frac{1}{2}}$ $72779_{3\frac{1}{2}} - 84217^{\circ}_{4\frac{1}{2}}$					
8737.78		10	11441.41	−0.02	$54640^{\circ}_{4\frac{1}{2}} - 66082_{5\frac{1}{2}}$	7	1.14	(1.141)	0	1.165
8735.23		1	11444.75	−0.04	$58162^{\circ}_{1\frac{1}{2}} - 69607_{2\frac{1}{2}}$					
8725.19		10	11457.92	+0.01	$56480^{\circ}_{4\frac{1}{2}} - 67938_{3\frac{1}{2}}$					

TABLE 6. Yb II—*Observed and classified lines*—Continued

1	2	3	4	5	6	7	8	9	10	11
Wave-length air	Intensity		Wave number	o–c	Classification	Zeeman type	1st g	2nd g	Zeeman components	
	Meggers lamp	Thomson lamp							Strong p	Strong n
Å			K	K						
8723.33		1	11460.36							
8710.15		4	11477.71	+0.01	$53120^{\circ}_{2\frac{1}{2}} - 64598_{3\frac{1}{2}}$	4	(0.944)	1.224	0.140	?
8699.84		1	11491.31							
8697.67		1	11494.18	+0.04	$47329^{\circ}_{2\frac{1}{2}} - 58823_{2\frac{1}{2}}$					
8691.24		1	11502.68							
8672.34		20	11527.75	+0.02	$56621^{\circ}_{5\frac{1}{2}} - 68148_{5\frac{1}{2}}$	7	1.20	1.20	0	1.205
8671.53		1	11528.82							
8659.04		15	11545.45	+0.02 +0.08	$57534^{\circ}_{3\frac{1}{2}} - 69079_{2\frac{1}{2}}$ $(64970^{\circ}_{3\frac{1}{2}} - 76516_{4\frac{1}{2}})^{b}$	4	0.80?	0.86	(0.03)	0.65
8641.86		15	11568.41	0.00	$53322^{\circ}_{7\frac{1}{2}} - 64891_{7\frac{1}{2}}$					
8633.25		1	11579.94	+0.08	$52067^{\circ}_{0\frac{1}{2}} - 63647_{1\frac{1}{2}}$					
8621.62		2	11595.56	+0.02	$46169^{\circ}_{4\frac{1}{2}} - 57765_{4\frac{1}{2}}$	6	1.179	1.205	0.12	1.192
8620.75		1	11596.73	+0.04	$57798^{\circ}_{2\frac{1}{2}} - 69395_{3\frac{1}{2}}$					
8607.49	200	400	11614.60	+0.03	$22960_{1\frac{1}{2}} - 34575^{\circ}_{1\frac{1}{2}}$	6	0.801	1.433	0.948	1.118
8594.57		8	11632.06							
8592.85		10	11634.39	+0.03	$56500^{\circ}_{3\frac{1}{2}} - 68135_{2\frac{1}{2}}$	5	1.348	1.091	0.128	1.994
8587.89		1	11641.11	+0.03	$63417^{\circ}_{2\frac{1}{2}} - 75058_{2\frac{1}{2}}$					
8585.00		1	11645.02	+0.01	$57798^{\circ}_{2\frac{1}{2}} - 69443_{1\frac{1}{2}}$					
8579.08		7	11653.06	+0.04	$57103^{\circ}_{3\frac{1}{2}} - 68756_{3\frac{1}{2}}$	6	1.21?	1.41?	0.74	1.31
8566.83		2	11669.72							
8561.74		20	11676.66	0.00	$52921^{\circ}_{3\frac{1}{2}} - 64598_{3\frac{1}{2}}$	6	1.135	1.215	0.28	1.175
8556.90		4	11683.27	+0.01	$54192^{\circ}_{5\frac{1}{2}} - 65875_{6\frac{1}{2}}$					
8554.92		2	11685.97	+0.02	$48024^{\circ}_{1\frac{1}{2}} - 59710_{1\frac{1}{2}}$	6	(1.38)	0.81	0.86	?
8548.15		1	11695.22	+0.02	$67933^{\circ}_{2\frac{1}{2}} - 79628_{3\frac{1}{2}}$					
8543.66		5	11701.37	+0.01	$49419^{\circ}_{0\frac{1}{2}} - 61120_{0\frac{1}{2}}$					
8532.59		1	11716.55	+0.04	$41688^{\circ}_{1\frac{1}{2}} - 53404_{2\frac{1}{2}}$					
8527.65		1	11723.34							
8525.54		1	11726.24	+0.01	$41678^{\circ}_{2\frac{1}{2}} - 53404_{2\frac{1}{2}}$					
8517.54		2*h*	11737.25							
8503.56		1*h*	11756.55							
8502.18		3	11758.46	+0.02	$54192^{\circ}_{5\frac{1}{2}} - 65950_{4\frac{1}{2}}$	4	1.10	(1.08)	*w*	1.15
8500.55		2	11760.71	+0.02	$47329^{\circ}_{2\frac{1}{2}} - 59090_{3\frac{1}{2}}$					
8483.31		2	11784.61	+0.04	$37516^{\circ}_{3\frac{1}{2}} - 49301_{4\frac{1}{2}}$					
8481.03		2	11787.78							
8480.27		2*h*	11788.84							
8477.79		2*h*	11792.29							
8473.35		2	11798.47							
8465.75		15	11809.06	+0.03	$57798^{\circ}_{2\frac{1}{2}} - 69607_{2\frac{1}{2}}$	6	1.155	1.215	0.15	1.185
8460.54		2	11816.33	−0.02	$67789^{\circ}_{1\frac{1}{2}} - 79605_{1\frac{1}{2}}$?					

TABLE 6. Yb II—*Observed and classified lines*—Continued

1	2	3	4	5	6	7	8	9	10	11
Wave-length air	Intensity		Wave number	o–c	Classification	Zeeman type	1st g	2nd g	Zeeman components	
	Meggers lamp	Thomson lamp							Strong p	Strong n
Å			K	K						
8458.72		1	11818.87							
8455.87	4	30	11822.86	+0.04	$37077^{\circ}_{2\frac{1}{2}} - 48900_{3\frac{1}{2}}$	4	1.09	1.04	(0.025)	0.91
8446.32		6	11836.22							
8438.92		1	11846.60							
8438.42		2	11847.30							
8437.07		3	11849.20	+0.07	$61442^{\circ}_{5\frac{1}{2}} - 73291_{5\frac{1}{2}}$					
8435.61		3	11851.25							
8428.83		15	11860.78	+0.05 +0.03	$53716^{\circ}_{2\frac{1}{2}} - 65577_{3\frac{1}{2}}$ $(57534^{\circ}_{3\frac{1}{2}} - 69395_{3\frac{1}{2}})$	4	1.192	1.068	0.062	0.758
8427.26		3	11862.99							
8424.89		1	11866.33	+0.04	$58162^{\circ}_{1\frac{1}{2}} - 70029_{0\frac{1}{2}}$	4	1.992	0.908	0.542	0.366
8411.84	1	100	11884.74	+0.04	$54304_{0\frac{1}{2}} - 66189^{\circ}_{1\frac{1}{2}}$					
8408.89		3	11888.91	+0.04	$81657_{2\frac{1}{2}} - 93546^{\circ}_{2\frac{1}{2}}$					
8403.58		2	11896.42							
8400.61		1	11900.63							
8396.79		8	11906.04	−0.04 +0.06	$49916^{\circ}_{4\frac{1}{2}} - 61822_{3\frac{1}{2}}$ $(58051^{\circ}_{5\frac{1}{2}} - 69957_{4\frac{1}{2}})$	4	(1.09)	1.35	0.13	?
8381.26		20	11928.10	+0.02	$56621^{\circ}_{5\frac{1}{2}} - 68549_{4\frac{1}{2}}$					
8380.03		3	11929.85	+0.05	$47329^{\circ}_{2\frac{1}{2}} - 59259_{2\frac{1}{2}}$					
8379.39		8	11930.76	0.00	$54640^{\circ}_{4\frac{1}{2}} - 66571_{5\frac{1}{2}}$					
8378.34		3	11932.26	+0.04	$53644^{\circ}_{3\frac{1}{2}} - 65577_{3\frac{1}{2}}$					
8374.40		15	11937.87	−0.01	$44438^{\circ}_{3\frac{1}{2}} - 56375_{2\frac{1}{2}}$	4	1.080	1.20	0.060	0.780
8371.77		2*h*	11941.62							
8356.75*		5	11963.09	−0.01	$63028^{\circ}_{1\frac{1}{2}} - 74991_{1\frac{1}{2}}$					
8352.37		4	11969.36	+0.02	$56480^{\circ}_{4\frac{1}{2}} - 68450_{3\frac{1}{2}}$					
8350.15		9	11972.54	−0.02	$53120^{\circ}_{2\frac{1}{2}} - 65093_{3\frac{1}{2}}$					
8347.14		2*h*	11976.86	0.00	$57103^{\circ}_{3\frac{1}{2}} - 69079_{2\frac{1}{2}}$					
8343.49		2	11982.10							
8342.51		8	11983.51	0.00	$55221^{\circ}_{1\frac{1}{2}} - 67204_{1\frac{1}{2}}$					
8341.30		2	11985.25	0.00	$51248^{\circ}_{2\frac{1}{2}} - 63234_{2\frac{1}{2}}$					
8336.34		5	11992.38							
8334.43		10	11995.12							
8331.71		2*h*	11999.04							
8318.01		1	12018.80	−0.03	$66796^{\circ}_{3\frac{1}{2}} - 78814_{2\frac{1}{2}}$					
8310.53		2	12029.62	0.00	$59439^{\circ}_{2\frac{1}{2}} - 71468_{2\frac{1}{2}}$	7	0.98?	(1.02)	0	1.00
8310.38		2	12029.84	−0.01 +0.02	$63028^{\circ}_{1\frac{1}{2}} - 75058_{2\frac{1}{2}}$ $82398_{1\frac{1}{2}} - 94428^{\circ}_{1\frac{1}{2}}$					
8308.40		1	12032.70							
8307.67		2	12033.76							
8301.74		15	12042.36	0.00	$52880^{\circ}_{4\frac{1}{2}} - 64923_{4\frac{1}{2}}$	6	1.262	1.110	0.688	1.186
8291.01		20	12057.94							

TABLE 6. Yb II—*Observed and classified lines*—Continued

1	2	3	4	5	6	7	8	9	10	11
Wavelength air	Intensity		Wave number	o–c	Classification	Zeeman type	1st g	2nd g	Zeeman components	
	Meggers lamp	Thomson lamp							Strong p	Strong n
Å			K	K						
8289.25		3	12060.50	+0.01	$56088^{\circ}_{4\frac{1}{2}} - 68148_{5\frac{1}{2}}$					
8283.78		15	12068.47	+0.01	$56480^{\circ}_{4\frac{1}{2}} - 68549_{4\frac{1}{2}}$	6	0.758?	1.160	1.815	(0.959?)
8282.14		2	12070.86							
8280.60		2	12073.10	+0.01	$57534^{\circ}_{3\frac{1}{2}} - 69607_{2\frac{1}{2}}$					
8276.29		2*h*	12079.39							
8267.90		2	12091.65							
8266.52		7	12093.66	0.00	$56056^{\circ}_{2\frac{1}{2}} - 68150_{1\frac{1}{2}}$					
8263.64	4	150	12097.88			4			0.16*w*	1.03
8261.70		1	12100.72							
8246.48		1*h*	12123.05							
8241.66		5	12130.14	+0.01	$60649^{\circ}_{4\frac{1}{2}} - 72779_{3\frac{1}{2}}$					
8240.01		1	12132.57							
8237.20		2	12136.71							
8230.78		1	12146.18	−0.03	$49727^{\circ}_{6\frac{1}{2}} - 61873_{6\frac{1}{2}}$					
8227.41		1	12151.15	+0.04	$64365^{\circ}_{4\frac{1}{2}} - 76516_{4\frac{1}{2}}$					
8225.41		5	12154.11	+0.01	$64169^{\circ}_{3\frac{1}{2}} - 76323_{3\frac{1}{2}}$	6			0.35	
8213.64		30	12171.52	0.00	$52921^{\circ}_{3\frac{1}{2}} - 65093_{3\frac{1}{2}}$	6	1.150	0.972	0.625	1.060
8213.24		10	12172.12	+0.04	$53716^{\circ}_{2\frac{1}{2}} - 65888_{1\frac{1}{2}}$	6?	1.16	(1.206)	*d*?	1.10
8206.55		3	12182.04							
8199.08		1	12193.14							
8194.83		2	12199.46							
8192.40		30	12203.08			4			*w*	1.03
8190.61		10	12205.75	+0.02	$49008^{\circ}_{3\frac{1}{2}} - 61214_{4\frac{1}{2}}$	7			0	1.050
8189.53		2	12207.36							
8183.28		1	12216.68							
8180.34		2*h*	12221.07							
8179.01		4	12223.06	+0.03	$63417^{\circ}_{2\frac{1}{2}} - 75640_{3\frac{1}{2}}$					
8178.46		4	12223.88							
8178.14		3	12224.36	−0.05	$62046^{\circ}_{3\frac{1}{2}} - 74270_{2\frac{1}{2}}$					
8173.60		3*h*	12231.15							
8171.82	1	30	12233.81			5			*w*	1.40
8169.69		1*h*	12237.00							
8169.29		2*h*	12237.60							
8166.73		4*h*	12241.44							
8166.05		1	12242.46							
8162.00		2*h*	12248.53							
8158.49	5	80	12253.80	+0.02	$47005^{\circ}_{1\frac{1}{2}} - 59259_{2\frac{1}{2}}$	5	0.982	1.100	0.059	1.276
8157.40		150	12255.44	+0.04	$56500^{\circ}_{3\frac{1}{2}} - 68756_{3\frac{1}{2}}$	6	(1.352)	1.316	*w*	1.334
8155.12		3	12258.86	−0.03	$66205^{\circ}_{2\frac{1}{2}} - 78464_{1\frac{1}{2}}$					
8149.08		15	12267.95			6			0.150	1.20

TABLE 6. Yb II—*Observed and classified lines*—Continued

1	2	3	4	5	6	7	8	9	10	11
Wave-length air	Intensity		Wave number	o–c	Classification	Zeeman type	1st g	2nd g	Zeeman components	
	Meggers lamp	Thomson lamp							Strong p	Strong n
Å			K	K						
8148.83		3	12268.33							
8146.64		1	12271.63							
8143.81		2*h*	12275.89							
8142.47		20	12277.91	−0.01	$52921^{\circ}_{3\frac{1}{2}} - 65199_{4\frac{1}{2}}$	4	1.11	1.05	(0.032)	0.82
8137.92		2	12284.77	−0.03	$64365^{\circ}_{4\frac{1}{2}} - 76649_{5\frac{1}{2}}$					
8133.01		8	12292.19	+0.01	$57103^{\circ}_{3\frac{1}{2}} - 69395_{3\frac{1}{2}}$					
8131.92		2	12293.84							
8124.50		15	12305.07							
8123.85		9	12306.05	−0.01	$53644^{\circ}_{3\frac{1}{2}} - 65950_{4\frac{1}{2}}$					
8122.49		5	12308.11	+0.03	$61442^{\circ}_{5\frac{1}{2}} - 73750_{4\frac{1}{2}}$	5?	1.13	(1.02)	0.057	?
8121.35		3*h*	12309.84							
8121.12		2	12310.19							
8118.80	5	150	12313.71	+0.02	$48272^{\circ}_{2\frac{1}{2}} - 60586_{1\frac{1}{2}}$	4	1.127	1.313	0.093	0.848
8115.46		6	12318.77	−0.02	$52880^{\circ}_{4\frac{1}{2}} - 65199_{4\frac{1}{2}}$					
8111.61		9	12324.62	+0.03	$59439^{\circ}_{2\frac{1}{2}} - 71763_{1\frac{1}{2}}$					
8111.19	2	10	12325.26	+0.02	$64191^{\circ}_{1\frac{1}{2}} - 76517_{1\frac{1}{2}}$	6	1.198	0.838	0.538	1.018
8104.44		5	12335.52	+0.02	$45429^{\circ}_{3\frac{1}{2}} - 57765_{4\frac{1}{2}}$	4	(1.15)	1.13	*w*	1.05
8103.22		1	12337.38							
8101.64		1	12339.79							
8100.20		3*h*	12341.98							
8097.06		1	12346.77	+0.05	$64169^{\circ}_{3\frac{1}{2}} - 76516_{4\frac{1}{2}}$					
8093.03		8	12352.91			6[c]	1.990	0.966	0.512	1.478
8084.74		9	12365.58	+0.02	$49008^{\circ}_{3\frac{1}{2}} - 61374_{2\frac{1}{2}}$	4	1.045	1.295	0.125	0.420
8079.47		5	12373.65	+0.01	$58484^{\circ}_{4\frac{1}{2}} - 70858_{4\frac{1}{2}}$	6	(1.02)	1.25	1.025	?
8078.10		2	12375.75							
8076.95		1	12377.51							
8075.92	2	40	12379.09	+0.02	$54192^{\circ}_{5\frac{1}{2}} - 66571_{5\frac{1}{2}}$	6	1.10	1.18	0.44	1.14
8074.53		7	12381.22	+0.01	$47329^{\circ}_{2\frac{1}{2}} - 59710_{1\frac{1}{2}}$	5	0.991	0.815	0.088	1.255
8066.72	2	50	12393.20	−0.02	$50468^{\circ}_{5\frac{1}{2}} - 62861_{5\frac{1}{2}}$	6	1.212	1.140	0.40	1.176
				−0.01	$(52067^{\circ}_{0\frac{1}{2}} - 64461_{1\frac{1}{2}})$					
				0.00	$(56056^{\circ}_{2\frac{1}{2}} - 68450_{3\frac{1}{2}})$					
8063.02	2	60	12398.89	+0.02	$51248^{\circ}_{2\frac{1}{2}} - 63647_{1\frac{1}{2}}$	4	1.028	1.144	0.058	0.854
8053.43	50	500	12413.66	+0.01	$46547^{\circ}_{5\frac{1}{2}} - 58961_{5\frac{1}{2}}$	6	0.952	0.972	0.104	0.962
8049.03	5	30	12420.44	−0.01	$37077^{\circ}_{2\frac{1}{2}} - 49498_{2\frac{1}{2}}$	6	(1.113)	1.145	0.08	
8042.63		5	12430.33	+0.04	$45335^{\circ}_{4\frac{1}{2}} - 57765_{4\frac{1}{2}}$					
8038.16		10	12437.24							
8035.53		4	12441.31	0.00	$58672^{\circ}_{0\frac{1}{2}} - 71113_{1\frac{1}{2}}$	5	0.536	0.966	0.215	1.181
8034.43		1	12443.01	0.00	$56500^{\circ}_{3\frac{1}{2}} - 68943_{4\frac{1}{2}}$					
8023.46	1	20	12460.02							
8022.93		10	12460.85	+0.01	$56088^{\circ}_{4\frac{1}{2}} - 68549_{4\frac{1}{2}}$					

TABLE 6. Yb II—*Observed and classified lines*—Continued

1	2	3	4	5	6	7	8	9	10	11
Wavelength air	Intensity		Wave number	o–c	Classification	Zeeman type	1st g	2nd g	Zeeman components	
	Meggers lamp	Thomson lamp							Strong p	Strong n
Å			K	K						
8021.62	3	150	12462.88	0.00	$56480^{\circ}_{4\frac{1}{2}} - 68943_{4\frac{1}{2}}$	6	0.747	0.859	0.508	0.803
8013.17		15	12476.02	+0.02	$55462^{\circ}_{3\frac{1}{2}} - 67938_{3\frac{1}{2}}$	6	0.878	0.954	0.263	0.916
8009.53	4	50	12481.69	0.00	$47228^{\circ}_{0\frac{1}{2}} - 59710_{1\frac{1}{2}}$	4	1.035	0.917	0.059	0.858?
8007.83	15	300	12484.34	0.00	$64191^{\circ}_{1\frac{1}{2}} - 76676_{2\frac{1}{2}}$	4	1.190	1.088	0.051	0.935
8002.73	1	20	12492.30	0.00	$45273^{\circ}_{3\frac{1}{2}} - 57765_{4\frac{1}{2}}$	4	1.053?	1.001?	(0.026)	0.818?
8001.30		2*h*	12494.53	+0.04	$48556^{\circ}_{3\frac{1}{2}} - 61051_{3\frac{1}{2}}$					
7994.90		30	12504.53	+0.01	$57103^{\circ}_{3\frac{1}{2}} - 69607_{2\frac{1}{2}}$	4	1.084	1.208	0.062	0.774
7984.31		4	12521.12							
7968.09	1	6	12546.61	−0.01	$45737^{\circ}_{1\frac{1}{2}} - 58283_{2\frac{1}{2}}$					
7964.12	2	80	12552.86	−0.02	$53322^{\circ}_{7\frac{1}{2}} - 65875_{6\frac{1}{2}}$	4	1.090	1.222	0.066	0.232
7958.80		3	12561.25	+0.02	$58661^{\circ}_{2\frac{1}{2}} - 71222_{3\frac{1}{2}}$					
7958.48	2	40	12561.76	0.00	$48024^{\circ}_{1\frac{1}{2}} - 60586_{1\frac{1}{2}}$	6	1.35	1.31	0.070	1.33
7950.35	2	60	12574.60	−0.02	$57561^{\circ}_{6\frac{1}{2}} - 70136_{6\frac{1}{2}}$	6				
7950.01		2	12575.14							
7947.60	1	40	12578.95	−0.01	$52987^{\circ}_{1\frac{1}{2}} - 65566_{0\frac{1}{2}}$	4	1.129	1.423	0.147	0.982
7930.04		8	12606.81	−0.01	$46354^{\circ}_{4\frac{1}{2}} - 58961_{5\frac{1}{2}}$	4	1.28	0.98	0.146	0.37
7928.71		7	12608.92	+0.04 −0.07	$58661^{\circ}_{2\frac{1}{2}} - 71270_{2\frac{1}{2}}$ $(66205^{\circ}_{2\frac{1}{2}} - 78814_{2\frac{1}{2}})$					
7913.30		6	12633.48	−0.01	$60649^{\circ}_{4\frac{1}{2}} - 73283_{4\frac{1}{2}}$					
7912.46		10	12634.82	−0.01	$53716^{\circ}_{2\frac{1}{2}} - 66351_{2\frac{1}{2}}$					
7906.25		2*h*	12644.74							
7904.82	10	200	12647.03	0.00	$64191^{\circ}_{1\frac{1}{2}} - 76839_{2\frac{1}{2}}$	4	1.200	1.108	0.046	0.970
7899.54		5	12655.48	−0.01	$52921^{\circ}_{3\frac{1}{2}} - 65577_{3\frac{1}{2}}$	6	1.17	(1.055)	0.407	?
7897.90		2	12658.11	+0.02	$48556^{\circ}_{3\frac{1}{2}} - 61214_{4\frac{1}{2}}$					
7891.93		1	12667.69	+0.04	$56088^{\circ}_{4\frac{1}{2}} - 68756_{3\frac{1}{2}}$					
7874.10	1	20	12696.37	+0.01	$52880^{\circ}_{4\frac{1}{2}} - 65577_{3\frac{1}{2}}$	5	1.261	1.049	0.106	2.003
7865.13		7	12710.85	+0.01	$48503^{\circ}_{5\frac{1}{2}} - 61214_{4\frac{1}{2}}$	5	1.151	1.093	(0.029)	1.414
7856.20		4	12725.30	+0.01	$65739^{\circ}_{2\frac{1}{2}} - 78464_{1\frac{1}{2}}$	4	0.880	1.176	0.148	0.436
7849.85		6	12735.59	+0.01	$46354^{\circ}_{4\frac{1}{2}} - 59090_{3\frac{1}{2}}$					
7848.49		15	12737.80	−0.02	$58484^{\circ}_{4\frac{1}{2}} - 71222_{3\frac{1}{2}}$	4	1.040	1.122	(0.041)	0.751
7840.45	1	40	12750.86	+0.03	$53644^{\circ}_{3\frac{1}{2}} - 66395_{2\frac{1}{2}}$	4	1.179	1.231	(0.026)	1.048
7839.17		1*h*	12752.94							
7833.02		9	12762.96	+0.01	$59439^{\circ}_{2\frac{1}{2}} - 72202_{3\frac{1}{2}}$	4	0.991	0.855	0.068	0.515
7825.52	1	50	12775.19	−0.02	$54640^{\circ}_{4\frac{1}{2}} - 67416_{4\frac{1}{2}}$	6	1.132	1.260	0.582	1.195
7824.64		3	12776.63	−0.03 +0.04	$64970^{\circ}_{3\frac{1}{2}} - 77747_{4\frac{1}{2}}$ $76839_{2\frac{1}{2}} - 89615^{\circ}_{2\frac{1}{2}}$					
7815.52		5	12791.53	+0.01 −0.06	$58162^{\circ}_{1\frac{1}{2}} - 70954_{2\frac{1}{2}}$ $(46169^{\circ}_{4\frac{1}{2}} - 58961_{5\frac{1}{2}})$	5	0.95	(1.014)	*w*	1.107
7811.96	1	8	12797.36	+0.01	$40917^{\circ}_{4\frac{1}{2}} - 53715_{3\frac{1}{2}}$	4	0.965	1.175	0.105	0.230
7808.64		4	12802.80	0.00	$40917^{\circ}_{4\frac{1}{2}} - 53720_{4\frac{1}{2}}$	6	(0.967)	1.265	1.338	?

277-259 O - 68 - 3

TABLE 6. Yb II—*Observed and classified lines*—Continued

1	2	3	4	5	6	7	8	9	10	11
Wavelength air	Intensity		Wave number	o–c	Classification	Zeeman type	1st g	2nd g	Zeeman components	
	Meggers lamp	Thomson lamp							Strong p	Strong n
Å			K	K						
7806.11		3	12806.95	−0.01	$51248^{\circ}_{2\frac{1}{2}} - 64055_{2\frac{1}{2}}$					
7804.57		6	12809.48	−0.01	$62163^{\circ}_{2\frac{1}{2}} - 74973_{3\frac{1}{2}}$					
7803.65	20	300	12810.99			6?			0.938	0.938
7802.01		9	12813.68	+0.03	$49008^{\circ}_{3\frac{1}{2}} - 61822_{3\frac{1}{2}}$					
7801.17		8	12815.06	−0.02	$50832^{\circ}_{1\frac{1}{2}} - 63647_{1\frac{1}{2}}$					
7799.44		3	12817.91	−0.01	$48556^{\circ}_{3\frac{1}{2}} - 61374_{2\frac{1}{2}}$					
7785.02		3	12841.65	+0.03	$53716^{\circ}_{2\frac{1}{2}} - 66558_{3\frac{1}{2}}$	4	(1.18)	1.11	w	0.95
7777.96	1	7	12853.30	−0.01	$35059^{\circ}_{3\frac{1}{2}} - 47912_{3\frac{1}{2}}$	6	(1.12)	1.28	0.57	?
7777.49		6	12854.08	−0.01	$45429^{\circ}_{3\frac{1}{2}} - 58283_{2\frac{1}{2}}$	5	1.140	0.774	0.183	2.055
7772.78		2	12861.87	−0.03	$59753^{\circ}_{5\frac{1}{2}} - 72615_{5\frac{1}{2}}$					
7767.43		2	12870.73	+0.03	$65594^{\circ}_{2\frac{1}{2}} - 78464_{1\frac{1}{2}}$	?	1.19?	(1.18)	d	1.21
7766.02		2	12873.07							
7753.91	2	5	12893.17	−0.01	$35019^{\circ}_{4\frac{1}{2}} - 47912_{3\frac{1}{2}}$					
7753.29		6	12894.20	+0.01	$62163^{\circ}_{2\frac{1}{2}} - 75058_{2\frac{1}{2}}$					
7749.38		1	12900.71	+0.01	$52987^{\circ}_{1\frac{1}{2}} - 65888_{1\frac{1}{2}}$					
7745.93		5	12906.45	−0.01	$63417^{\circ}_{2\frac{1}{2}} - 76323_{3\frac{1}{2}}$	5?	1.06?	(1.02)	w	0.93
7741.94		3	12913.11	0.00	$53644^{\circ}_{3\frac{1}{2}} - 66558_{3\frac{1}{2}}$					
7741.66		2	12913.57	+0.03	$55221^{\circ}_{1\frac{1}{2}} - 68135_{2\frac{1}{2}}$	7	1.10?	(1.087)	0	1.07
7741.15		2	12914.42	−0.01	$56480^{\circ}_{4\frac{1}{2}} - 69395_{3\frac{1}{2}}$					
7737.59	1	8	12920.37	+0.02	$46169^{\circ}_{4\frac{1}{2}} - 59090_{3\frac{1}{2}}$	4	1.040	1.066	(0.013)	0.950
7732.46		4*h*	12928.94							
7732.35		6	12929.12	+0.01	$55221^{\circ}_{1\frac{1}{2}} - 68150_{1\frac{1}{2}}$	6	1.110	0.922	0.284	1.016
7719.82		15	12950.11	+0.01	$48923^{\circ}_{7\frac{1}{2}} - 61873_{6\frac{1}{2}}$					
7719.23		40	12951.10	+0.01	$58162^{\circ}_{1\frac{1}{2}} - 71113_{1\frac{1}{2}}$	6	0.93	0.97	0.062	0.952
7697.62		5	12987.45	+0.02	$55462^{\circ}_{3\frac{1}{2}} - 68450_{3\frac{1}{2}}$					
7683.77		9	13010.86	−0.03	$45273^{\circ}_{3\frac{1}{2}} - 58283_{2\frac{1}{2}}$	5	1.187	0.761	0.213	2.252
7678.20		1	13020.30							
7676.62		8	13022.98	+0.01	$56056^{\circ}_{2\frac{1}{2}} - 69079_{2\frac{1}{2}}$	6	1.120	0.890	0.575	1.005
7666.57		1	13040.05							
7655.71		5	13058.55	0.00	$76839_{2\frac{1}{2}} - 89897^{\circ}_{1\frac{1}{2}}$	4	0.89	1.01	0.06	0.713
7648.88		4	13070.21	+0.01	$52880^{\circ}_{4\frac{1}{2}} - 65950_{4\frac{1}{2}}$	6	1.25	(1.08)	0.76	?
7645.84		8	13075.41	+0.02 +0.09	$65739^{\circ}_{2\frac{1}{2}} - 78814_{2\frac{1}{2}}$ $(53720_{4\frac{1}{2}} - 66796^{\circ}_{3\frac{1}{2}})$	6	0.878	1.222	0.866	1.150
7640.63		1	13084.32	0.00	$64365^{\circ}_{4\frac{1}{2}} - 77449_{3\frac{1}{2}}$					
7639.47		4	13086.31	+0.02	$45737^{\circ}_{1\frac{1}{2}} - 58823_{2\frac{1}{2}}$	4	(1.33)	1.27	w	1.18
7636.65		3	13091.14	0.00	$58672^{\circ}_{0\frac{1}{2}} - 71763_{1\frac{1}{2}}$					
7634.62		6	13094.62							
7633.95	6	100	13095.77	−0.02	$48024^{\circ}_{1\frac{1}{2}} - 61120_{0\frac{1}{2}}$	4	1.371	1.659	0.144	1.227
7631.81		4	13099.45	0.00	$64970^{\circ}_{3\frac{1}{2}} - 78070_{4\frac{1}{2}}$					

TABLE 6. Yb II—*Observed and classified lines*—Continued

1	2	3	4	5	6	7	8	9	10	11
Wave-length air	Intensity		Wave number	o–c	Classification	Zeeman type	1st g	2nd g	Zeeman components	
	Meggers lamp	Thomson lamp							Strong p	Strong n
Å			K	K						
7630.87		1	13101.06	+0.02	$60649^{\circ}_{4\frac{1}{2}} - 73750_{4\frac{1}{2}}$					
7630.48		9	13101.73	+0.01	$48272^{\circ}_{2\frac{1}{2}} - 61374_{2\frac{1}{2}}$					
7630.00		8	13102.55	+0.01	$58661^{\circ}_{2\frac{1}{2}} - 71763_{1\frac{1}{2}}$					
7627.45	1	50	13106.93	+0.03	$56500^{\circ}_{3\frac{1}{2}} - 69607_{2\frac{1}{2}}$	5	1.355	1.221	0.067	1.690
7627.24	1	70	13107.29	+0.03	$58162^{\circ}_{1\frac{1}{2}} - 71270_{2\frac{1}{2}}$	7	0.93	(0.91)	0	0.88
7616.50		2	13125.78	+0.02	$61442^{\circ}_{5\frac{1}{2}} - 74568_{4\frac{1}{2}}$					
7611.69		15	13134.07	−0.01	$49727^{\circ}_{6\frac{1}{2}} - 62861_{5\frac{1}{2}}$	5	1.200	(1.140)	?	1.530
7607.09		2	13142.01	+0.02	$63028^{\circ}_{1\frac{1}{2}} - 76170_{2\frac{1}{2}}$					
7599.13		20	13155.78	+0.02	$57798^{\circ}_{2\frac{1}{2}} - 70954_{2\frac{1}{2}}$	6	1.148	1.000	0.368	1.074
7582.93		40	13183.88	−0.02	$24332_{2\frac{1}{2}} - 37516^{\circ}_{3\frac{1}{2}}$	4	1.184	1.120	(0.032)	0.960
7579.97	1	60	13189.03	+0.03	$56840^{\circ}_{1\frac{1}{2}} - 70029_{0\frac{1}{2}}$	5	0.910	0.682	0.115	1.024
7572.81		5	13201.50	0.00	$52880^{\circ}_{4\frac{1}{2}} - 66082_{5\frac{1}{2}}$					
7566.65		15	13212.25	+0.03	$51248^{\circ}_{2\frac{1}{2}} - 64461_{1\frac{1}{2}}$	4	1.034	1.178	0.072	0.818
7560.18		1	13223.56	+0.04	$54192^{\circ}_{5\frac{1}{2}} - 67416_{4\frac{1}{2}}$					
7556.13	1	40	13230.65	+0.02	$53120^{\circ}_{2\frac{1}{2}} - 66351_{2\frac{1}{2}}$	6	0.819?	0.645?	0.438	0.732?
7555.14	1	60	13232.38	+0.04	$57561^{\circ}_{6\frac{1}{2}} - 70793_{5\frac{1}{2}}$	4	1.032	1.204	0.086	0.086?
7541.10	5	80	13257.01	−0.01	$47329^{\circ}_{2\frac{1}{2}} - 60586_{1\frac{1}{2}}$	4	0.980	1.314	0.167	0.480
7537.40		1	13263.52	+0.01	$48900_{3\frac{1}{2}} - 62163^{\circ}_{2\frac{1}{2}}$					
7533.09		3	13271.11	−0.01	$45012^{\circ}_{2\frac{1}{2}} - 58283_{2\frac{1}{2}}$					
7530.78		3	13275.18	+0.04	$53120^{\circ}_{2\frac{1}{2}} - 66395_{2\frac{1}{2}}$					
7528.07		8	13279.96	+0.03	$64169^{\circ}_{3\frac{1}{2}} - 77449_{3\frac{1}{2}}$					
7520.94		4	13292.55	+0.03	$47758^{\circ}_{3\frac{1}{2}} - 61051_{3\frac{1}{2}}$					
7520.46		15	13293.40	+0.04	$55462^{\circ}_{3\frac{1}{2}} - 68756_{3\frac{1}{2}}$	6	0.88	1.32	1.560	1.10
7517.94		2	13297.85	−0.01	$54640^{\circ}_{4\frac{1}{2}} - 67938_{3\frac{1}{2}}$					
7516.24		2	13300.86	+0.04	$43075^{\circ}_{1\frac{1}{2}} - 56375_{2\frac{1}{2}}$					
7512.86		15	13306.85	+0.04	$56088^{\circ}_{4\frac{1}{2}} - 69395_{3\frac{1}{2}}$					
7508.07		8	13315.34	+0.01	$57798^{\circ}_{2\frac{1}{2}} - 71113_{1\frac{1}{2}}$	5	1.150	0.970	0.090	1.420
7503.32		1*h*	13323.76	+0.03	$57534^{\circ}_{3\frac{1}{2}} - 70858_{4\frac{1}{2}}$					
7501.33		1*h*	13327.30	+0.01	$44438^{\circ}_{3\frac{1}{2}} - 57765_{4\frac{1}{2}}$					
7500.09		3*h*	13329.50							
7496.24		20	13336.35	+0.01	$56621^{\circ}_{5\frac{1}{2}} - 69957_{4\frac{1}{2}}$					
7495.15		2	13338.29	0.00	$56056^{\circ}_{2\frac{1}{2}} - 69395_{3\frac{1}{2}}$					
7494.37		3	13339.68	+0.04	$59777^{\circ}_{1\frac{1}{2}} - 73116_{1\frac{1}{2}}$					
7492.34	1	6	13343.29	−0.01	$44940^{\circ}_{1\frac{1}{2}} - 58283_{2\frac{1}{2}}$	4	1.237	0.767	0.235	0.062
7483.19		2	13359.61	−0.06	$70858_{4\frac{1}{2}} - 84217^{\circ}_{4\frac{1}{2}}$					
7482.80		1	13360.30	−0.04	$60910^{\circ}_{1\frac{1}{2}} - 74270_{2\frac{1}{2}}$					
7481.04		6	13363.45	0.00	$52987^{\circ}_{1\frac{1}{2}} - 66351_{2\frac{1}{2}}$	7	1.13?	(1.125)	0	1.12
7477.86	1	5	13369.13	−0.01	$40035^{\circ}_{3\frac{1}{2}} - 53404_{2\frac{1}{2}}$					
7477.61	7	200	13369.58	0.00	$48503^{\circ}_{5\frac{1}{2}} - 61873_{6\frac{1}{2}}$	7	(1.10)	1.10	0	1.08

TABLE 6. Yb II—*Observed and classified lines*—Continued

1	2	3	4	5	6	7	8	9	10	11
Wave-length air	Intensity		Wave number	o–c	Classification	Zeeman type	1st g	2nd g	Zeeman components	
	Meggers lamp	Thomson lamp							Strong p	Strong n
Å			K	K						
7475.24		2	13373.81							
7473.32		5	13377.25	+0.01	$66205^{\circ}_{2\frac{1}{2}} - 79583_{2\frac{1}{2}}$					
7468.09		8	13386.62	+0.01	$56056^{\circ}_{2\frac{1}{2}} - 69443_{1\frac{1}{2}}$					
7467.58[a]	40	30	13387.53							
7464.10	5	60	13393.77	+0.01	$45429^{\circ}_{3\frac{1}{2}} - 58823_{2\frac{1}{2}}$	4	1.149	1.275	0.063	0.834
7456.20		2	13407.96	0.00	$52987^{\circ}_{1\frac{1}{2}} - 66395_{2\frac{1}{2}}$					
7451.21		1	13416.94	−0.01	$66189^{\circ}_{1\frac{1}{2}} - 79605_{1\frac{1}{2}}$					
7449.60		1	13419.84	+0.02	$57534^{\circ}_{3\frac{1}{2}} - 70954_{2\frac{1}{2}}$					
7447.37	1	60	13423.86	+0.01 −0.03	$57798^{\circ}_{2\frac{1}{2}} - 71222_{3\frac{1}{2}}$ $(70793_{5\frac{1}{2}} - 84217^{\circ}_{4\frac{1}{2}})$	7	1.16	(1.15)	0	1.136
7444.20		2	13429.58	−0.01	$52921^{\circ}_{3\frac{1}{2}} - 66351_{2\frac{1}{2}}$					
7439.84	1	80	13437.45	+0.03	$53120^{\circ}_{2\frac{1}{2}} - 66558_{3\frac{1}{2}}$	5	0.943	1.098	0.078	1.485
7433.39	4	30	13449.11	−0.01	$46169^{\circ}_{4\frac{1}{2}} - 59618_{3\frac{1}{2}}$	5	1.115	1.057	(0.028)	1.315
7429.51	2	40	13456.13	+0.01	$47758^{\circ}_{3\frac{1}{2}} - 61214_{4\frac{1}{2}}$	4	1.067	1.029	(0.019)	0.896
7429.10		2	13456.87	+0.02	$56500^{\circ}_{3\frac{1}{2}} - 69957_{4\frac{1}{2}}$					
7422.15	40	200	13469.48	0.00	$35831^{\circ}_{5\frac{1}{2}} - 49301_{4\frac{1}{2}}$	5	(1.214)	1.20	w	1.295
7421.04		2	13471.49	−0.01	$57798^{\circ}_{2\frac{1}{2}} - 71270_{2\frac{1}{2}}$					
7419.60	1	40	13474.10	0.00	$52921^{\circ}_{3\frac{1}{2}} - 66395_{2\frac{1}{2}}$	4	1.155	1.233	(0.039)	0.96
7419.06		8	13475.09	−0.01	$52987^{\circ}_{1\frac{1}{2}} - 66462_{0\frac{1}{2}}$					
7418.49		4	13476.12	−0.01 −0.02	$50468^{\circ}_{3\frac{1}{2}} - 63944_{5\frac{1}{2}}$ $62163^{\circ}_{2\frac{1}{2}} - 75640_{3\frac{1}{2}}$					
7418.15		3	13476.74	+0.02	$56480^{\circ}_{4\frac{1}{2}} - 69957_{4\frac{1}{2}}$					
7411.63		4	13488.59	0.00	$53716^{\circ}_{2\frac{1}{2}} - 67204_{1\frac{1}{2}}$	5	1.17	1.05	0.061	1.35
7406.00	10	150	13498.85	0.00	$52067^{\circ}_{0\frac{1}{2}} - 65566_{0\frac{1}{2}}$	6	0.51	1.41	0.45	0.96
7402.70		2	13504.86	−0.01	$62046^{\circ}_{3\frac{1}{2}} - 73550_{2\frac{1}{2}}$					
7402.45		1	13505.32							
7400.97		5	13508.02	−0.04	$54640^{\circ}_{4\frac{1}{2}} - 68148_{5\frac{1}{2}}$					
7397.10	1	40	13515.09	0.00	$56621^{\circ}_{5\frac{1}{2}} - 70136_{6\frac{1}{2}}$	4	1.126	1.076	(0.025)	0.800
7396.04		1	13517.03	−0.01	$64365^{\circ}_{4\frac{1}{2}} - 77882_{3\frac{1}{2}}$					
7393.34	4	30	13521.96	+0.01	$45737^{\circ}_{1\frac{1}{2}} - 59259_{2\frac{1}{2}}$	4	1.333	1.099	0.117	0.748
7393.03		1	13522.53	−0.02	$34389^{\circ}_{2\frac{1}{2}} - 47912_{3\frac{1}{2}}$					
7389.22	6	150	13529.50	−0.01	$59753^{\circ}_{5\frac{1}{2}} - 73283_{4\frac{1}{2}}$	5	1.112	1.050	(0.031)	1.395
7384.50	7	150	13538.15	+0.04	$59753^{\circ}_{5\frac{1}{2}} - 73291_{5\frac{1}{2}}$	6	(1.08)	1.08?	0	1.08
7383.00		2	13540.90	0.00	$58661^{\circ}_{2\frac{1}{2}} - 72202_{3\frac{1}{2}}$					
7377.73	20	400	13550.57	+0.01 −0.06	$45273^{\circ}_{3\frac{1}{2}} - 58823_{2\frac{1}{2}}$ $56056^{\circ}_{2\frac{1}{2}} - 69607_{2\frac{1}{2}}$					
7377.43	10	300	13551.12	−0.02	$47663^{\circ}_{4\frac{1}{2}} - 61214_{4\frac{1}{2}}$					
7373.06	3	15	13559.15	+0.03	$39378^{\circ}_{0\frac{1}{2}} - 52938_{1\frac{1}{2}}$	4	1.833	0.873	0.48	0.393
7367.78		20	13568.87	+0.02	$59046^{\circ}_{4\frac{1}{2}} - 72615_{5\frac{1}{2}}$	4	(1.08)	1.01?	?	0.70
7362.92	2	15	13577.83			5	0.88[e]	0.66[e]	0.11	0.99

TABLE 6. Yb II—*Observed and classified lines*—Continued

1	2	3	4	5	6	7	8	9	10	11
Wavelength air	Intensity		Wave number	o–c	Classification	Zeeman type	1st g	2nd g	Zeeman components	
	Meggers lamp	Thomson lamp							Strong p	Strong n
Å			K	K						
7362.83		60	13577.99	−0.02	$64169^{\circ}_{3\frac{1}{2}} - 77747_{4\frac{1}{2}}$					
7354.17		4	13593.98	−0.01	$62046^{\circ}_{3\frac{1}{2}} - 75640_{3\frac{1}{2}}$	6	1.14	(0.81)	1.16	?
7350.42		15	13600.92	0.00	$58162^{\circ}_{1\frac{1}{2}} - 71763_{1\frac{1}{2}}$					
7342.30	10	400	13615.96	+0.01	$47758^{\circ}_{3\frac{1}{2}} - 61374_{2\frac{1}{2}}$	4	1.098	1.294	0.098	0.608
7341.64		4	13617.18	−0.02	$55462^{\circ}_{3\frac{1}{2}} - 69079_{2\frac{1}{2}}$					
7339.80		60	13620.60			7			0	1.12
7331.31	1	80	13636.37	−0.01	$52921^{\circ}_{3\frac{1}{2}} - 66558_{3\frac{1}{2}}$	6	1.15	1.09	0.21	1.12
7329.29		2	13640.13							
7323.05		2	13651.75							
7318.77		1	13659.73	−0.01	$59632^{\circ}_{6\frac{1}{2}} - 73291_{5\frac{1}{2}}$					
7317.74		30	13661.66			7			0	0.963
7313.18		15	13670.18	−0.01	$57798^{\circ}_{2\frac{1}{2}} - 71468_{2\frac{1}{2}}$					
7309.19		40	13677.64	+0.01	$59439^{\circ}_{2\frac{1}{2}} - 73116_{1\frac{1}{2}}$	5	0.998	0.862	0.068	1.202
7306.63	1	100	13682.43			5?				
7305.92		8	13683.76	+0.01	$46902^{\circ}_{0\frac{1}{2}} - 60586_{1\frac{1}{2}}$					
7302.15		15	13690.82	−0.01	$52880^{\circ}_{4\frac{1}{2}} - 66571_{5\frac{1}{2}}$	4	1.244	1.188	(0.028)	0.934
7294.50		1	13705.18	−0.01	$64365^{\circ}_{4\frac{1}{2}} - 78070_{4\frac{1}{2}}$					
7290.56		3	13712.59	−0.06	$64169^{\circ}_{3\frac{1}{2}} - 77882_{3\frac{1}{2}}$					
7287.96		2	13717.48	−0.01	$58484^{\circ}_{4\frac{1}{2}} - 72202_{3\frac{1}{2}}$					
7285.02		1	13723.02	0.00	$67789^{\circ}_{1\frac{1}{2}} - 81512_{1\frac{1}{2}}$?					
7284.70		1	13723.62	0.00	$67933^{\circ}_{2\frac{1}{2}} - 81657_{2\frac{1}{2}}$					
7279.67		5	13733.10	0.00	$59046^{\circ}_{4\frac{1}{2}} - 72779_{3\frac{1}{2}}$					
7278.37		30	13735.56	0.00	$57534^{\circ}_{3\frac{1}{2}} - 71270_{2\frac{1}{2}}$	4	0.86?	(0.91)	(0.027)	0.638?
7268.03		4	13755.10	0.00	$45335^{\circ}_{4\frac{1}{2}} - 59090_{3\frac{1}{2}}$					
				−0.06	$57103^{\circ}_{3\frac{1}{2}} - 70858_{4\frac{1}{2}}$					
7265.76		10	13759.39	−0.02	$67933^{\circ}_{2\frac{1}{2}} - 81692_{3\frac{1}{2}}$	7	1.16	(1.16)	0	1.15
7259.76		6	13770.77	−0.04	$63028^{\circ}_{1\frac{1}{2}} - 76799_{1\frac{1}{2}}$					
7259.56		3	13771.14	0.00	$53644^{\circ}_{3\frac{1}{2}} - 67416_{4\frac{1}{2}}$					
7251.55	30	200	13786.36	−0.04	$44497^{\circ}_{2\frac{1}{2}} - 58283_{2\frac{1}{2}}$	6	0.730	0.764	0.084	0.747
7238.95	1	80	13810.35	+0.02	$49916^{\circ}_{4\frac{1}{2}} - 63726_{4\frac{1}{2}}$					
7238.73	4	80	13810.77	−0.02	$45012^{\circ}_{2\frac{1}{2}} - 58823_{2\frac{1}{2}}$					
				+0.03	$63028^{\circ}_{1\frac{1}{2}} - 76839_{2\frac{1}{2}}$					
7235.42	1	40	13817.09	−0.02	$45273^{\circ}_{3\frac{1}{2}} - 59090_{3\frac{1}{2}}$	6	1.19	1.13	0.218	1.16
7228.98		2	13829.40	−0.02	$45429^{\circ}_{3\frac{1}{2}} - 59259_{2\frac{1}{2}}$	5	1.14	(1.105)	*w*	1.22
7222.72	20	150	13841.39	−0.02	$35059^{\circ}_{3\frac{1}{2}} - 48900_{3\frac{1}{2}}$	6	1.10	1.03	0.245	1.065
7221.50		10	13843.72	+0.08	$65739^{\circ}_{2\frac{1}{2}} - 79583_{2\frac{1}{2}}$					
7221.21	1	60	13844.28	0.00	$51248^{\circ}_{2\frac{1}{2}} - 65093_{3\frac{1}{2}}$	7	(1.034)	0.99	0	0.90
7220.38	2	50	13845.87	−0.01	$44438^{\circ}_{3\frac{1}{2}} - 58283_{2\frac{1}{2}}$	5	1.10	0.76	0.168	1.94
				0.00	$(80457_{3\frac{1}{2}} - 94303^{\circ}_{3\frac{1}{2}})$					
7217.57		60	13851.26	+0.01	$57103^{\circ}_{3\frac{1}{2}} - 70954_{2\frac{1}{2}}$	5	1.11	1.05	(0.03)	1.265

TABLE 6. Yb II—*Observed and classified lines*—Continued

1	2	3	4	5	6	7	8	9	10	11
Wave-length air	Intensity		Wave number	o–c	Classification	Zeeman type	1st g	2nd g	Zeeman components	
	Meggers lamp	Thomson lamp							Strong p	Strong n
Å			K	K						
7209.65		1	13866.48	0.00	$65739^{\circ}_{2\frac{1}{2}} - 79605_{1\frac{1}{2}}$					
7209.38		2	13867.00	+0.01	$63417^{\circ}_{2\frac{1}{2}} - 77284_{1\frac{1}{2}}$					
7209.10		8	13867.54	+0.01	$67789^{\circ}_{1\frac{1}{2}} - 81657_{2\frac{1}{2}}$?					
7208.29	4	200	13869.09	−0.01	$56088^{\circ}_{4\frac{1}{2}} - 69957_{4\frac{1}{2}}$	7	1.09?	(1.11)	0	1.10
7201.09		20	13882.96	−0.01	$44940^{\circ}_{1\frac{1}{2}} - 58823_{2\frac{1}{2}}$	7	(1.244)	1.260	0	1.285
7191.87		1	13900.76	−0.04	$64169^{\circ}_{3\frac{1}{2}} - 78070_{4\frac{1}{2}}$					
7182.60		2	13918.70	−0.02	$60649^{\circ}_{4\frac{1}{2}} - 74568_{4\frac{1}{2}}$					
7175.48		300	13932.51	−0.01	$55462^{\circ}_{3\frac{1}{2}} - 69395_{3\frac{1}{2}}$	6	0.878	0.924	0.165	0.90
7174.60		8	13934.22	−0.03	$57534^{\circ}_{3\frac{1}{2}} - 71468_{2\frac{1}{2}}$					
7154.52		5	13973.33	−0.03	$45737^{\circ}_{1\frac{1}{2}} - 59710_{1\frac{1}{2}}$	6	1.32	0.80	0.800	1.060
7148.16		2	13985.76							
7147.94		8	13986.19	−0.03	$45273^{\circ}_{3\frac{1}{2}} - 59259_{2\frac{1}{2}}$					
7145.15		4	13991.69	−0.09	$75905_{0\frac{1}{2}} - 89897^{\circ}_{1\frac{1}{2}}$	7			0	0.86
7142.39	1	120	13997.06	0.00	$59753^{\circ}_{5\frac{1}{2}} - 73750_{4\frac{1}{2}}$	5	1.145	1.077	(0.034)	1.450
7137.67		2	14006.31	−0.02	$62163^{\circ}_{2\frac{1}{2}} - 76170_{2\frac{1}{2}}$					
7134.83		2	14011.89	0.00	$65594^{\circ}_{2\frac{1}{2}} - 79605_{1\frac{1}{2}}$					
7128.94		2	14023.47	+0.13	$41678^{\circ}_{2\frac{1}{2}} - 55702_{1\frac{1}{2}}$					
7126.81	2	100	14027.66	−0.02	$49916^{\circ}_{4\frac{1}{2}} - 63944_{5\frac{1}{2}}$	5	1.087	1.113	(0.013)	1.230
7124.46		5	14032.28	−0.01	$63417^{\circ}_{2\frac{1}{2}} - 77449_{3\frac{1}{2}}$	5	1.011	1.161	0.075	1.536
7117.99		10	14045.04	−0.01	$47329^{\circ}_{2\frac{1}{2}} - 61374_{2\frac{1}{2}}$	6	0.986	1.298	0.780	1.142
7108.37		6	14064.05	+0.01	$47758^{\circ}_{3\frac{1}{2}} - 61822_{3\frac{1}{2}}$	6	1.104	1.326	0.774	1.215
7101.66		10	14077.33	−0.01	$45012^{\circ}_{2\frac{1}{2}} - 59090_{3\frac{1}{2}}$	4	1.279	1.102	0.088	0.662
7099.70		2	14081.22	0.00	$60910^{\circ}_{1\frac{1}{2}} - 74991_{1\frac{1}{2}}$					
7098.11		6	14084.37	−0.02	$53120^{\circ}_{2\frac{1}{2}} - 67204_{1\frac{1}{2}}$	4	0.95	1.04	(0.045)	0.815
7089.40		1	14101.68							
7086.08		20	14108.29			4			w	0.96
7082.61		80	14115.20	−0.02	$54640^{\circ}_{4\frac{1}{2}} - 68756_{3\frac{1}{2}}$	4	1.129	1.325	0.098	0.443
7081.81		4	14116.79	0.00	$22960_{1\frac{1}{2}} - 37077^{\circ}_{2\frac{1}{2}}$					
7080.77		1	14118.87	+0.01	$58661^{\circ}_{2\frac{1}{2}} - 72779_{3\frac{1}{2}}$					
7080.53		40	14119.34	0.00	$57103^{\circ}_{3\frac{1}{2}} - 71222_{3\frac{1}{2}}$	6	1.10	1.16	0.212	1.127
7078.11		5	14124.17	−0.01	$62046^{\circ}_{3\frac{1}{2}} - 76170_{2\frac{1}{2}}$	7	(1.14)	1.13?	0	1.170
7077.07		1	14126.25	+0.01	$59624^{\circ}_{3\frac{1}{2}} - 73750_{4\frac{1}{2}}$					
7074.60		2	14131.18	−0.02	$58484^{\circ}_{4\frac{1}{2}} - 72615_{5\frac{1}{2}}$					
7072.12		4	14136.13	0.00	$56977^{\circ}_{0\frac{1}{2}} - 71113_{1\frac{1}{2}}$	4	2.188	0.968	0.611	0.358
7066.20		10	14147.98	+0.01	$60910^{\circ}_{1\frac{1}{2}} - 75058_{2\frac{1}{2}}$					
7060.67		60	14159.06	0.00	$47663^{\circ}_{4\frac{1}{2}} - 61822_{3\frac{1}{2}}$	4	0.99	1.32	0.165	−0.165?
7060.41		2	14159.58	+0.01	$62163^{\circ}_{2\frac{1}{2}} - 76323_{3\frac{1}{2}}$					
7056.72		4	14166.98	−0.01	$57103^{\circ}_{3\frac{1}{2}} - 71270_{2\frac{1}{2}}$	5	1.115	0.937	0.089	1.560
7053.80	1	200	14172.85	+0.04	$56621^{\circ}_{5\frac{1}{2}} - 70793_{5\frac{1}{2}}$	7	1.20	1.20	0	1.203
7052.58		10	14175.30	−0.03	$38342^{\circ}_{4\frac{1}{2}} - 52517_{5\frac{1}{2}}$	5	1.088	1.273	0.093	2.110

TABLE 6. Yb II—*Observed and classified lines*—Continued

1	2	3	4	5	6	7	8	9	10	11
Wave-length air	Intensity		Wave number	o–c	Classification	Zeeman type	1st g	2nd g	Zeeman components	
	Meggers lamp	Thomson lamp							Strong p	Strong n
Å			K	K						
7045.75		15	14189.04	−0.04	$45429^{\circ}_{3\frac{1}{2}} - 59618_{3\frac{1}{2}}$					
7045.51		20	14189.52	−0.03	$63417^{\circ}_{2\frac{1}{2}} - 77606_{2\frac{1}{2}}$					
7043.78	30	700	14193.01	+0.01	$47680^{\circ}_{6\frac{1}{2}} - 61873_{6\frac{1}{2}}$	7	1.11	(1.11)	0	1.112
7031.52		30	14217.76	−0.02	$46902^{\circ}_{0\frac{1}{2}} - 61120_{0\frac{1}{2}}$	6	1.30	1.66	0.179	1.482
7029.38		3	14222.08	+0.02	$55221^{\circ}_{1\frac{1}{2}} - 69443_{1\frac{1}{2}}$					
7029.27		2	14222.31	+0.01	$53716^{\circ}_{2\frac{1}{2}} - 67938_{3\frac{1}{2}}$					
7027.84	10	150	14225.20	+0.02	$49008^{\circ}_{3\frac{1}{2}} - 63234_{2\frac{1}{2}}$					
7023.97		6	14233.04	−0.01	$78070_{4\frac{1}{2}} - 92303^{\circ}_{3\frac{1}{2}}$					
7022.27		6	14236.48	+0.02	$59046^{\circ}_{4\frac{1}{2}} - 73283_{4\frac{1}{2}}$					
7022.00	2	200	14237.03	0.00	$56621^{\circ}_{5\frac{1}{2}} - 70858_{4\frac{1}{2}}$	4	1.099	1.144	(0.022)	0.898
7019.48	2	20	14242.14	−0.02	$35059^{\circ}_{3\frac{1}{2}} - 49301_{4\frac{1}{2}}$	5	1.16	1.20	(0.021)	1.35
7012.75		5	14255.81	+0.05	$63028^{\circ}_{1\frac{1}{2}} - 77284_{1\frac{1}{2}}$	6	0.510	0.854	0.507	0.682
7003.90		1	14273.82	+0.02	$56840^{\circ}_{1\frac{1}{2}} - 71113_{1\frac{1}{2}}$					
7002.14		1	14277.41	−0.01	$62046^{\circ}_{3\frac{1}{2}} - 76323_{3\frac{1}{2}}$					
6999.88	50	800	14282.02	−0.01	$35019^{\circ}_{4\frac{1}{2}} - 49301_{4\frac{1}{2}}$	6	1.144	1.170	0.118	1.157
6998.98		2	14283.86	−0.01	$45335^{\circ}_{4\frac{1}{2}} - 59618_{3\frac{1}{2}}$					
6993.31	5	250	14295.44	−0.01	$58484^{\circ}_{4\frac{1}{2}} - 72779_{3\frac{1}{2}}$	4	1.06	(1.10)	w	0.92
6981.99	20	300	14318.61	−0.02	$44940^{\circ}_{1\frac{1}{2}} - 59259_{2\frac{1}{2}}$	4	1.23	1.09	0.07	0.88
6978.36		5	14326.06	−0.01	$44497^{\circ}_{2\frac{1}{2}} - 58823_{2\frac{1}{2}}$					
6977.67	20	150	14327.48	−0.02	$43956^{\circ}_{2\frac{1}{2}} - 58283_{2\frac{1}{2}}$	6	0.989	0.763	0.571	0.876
6977.30		1	14328.24	−0.01	$51248^{\circ}_{2\frac{1}{2}} - 65577_{3\frac{1}{2}}$					
6970.54		7	14342.14	−0.01	$59624^{\circ}_{3\frac{1}{2}} - 73966_{3\frac{1}{2}}$					
6968-73	1	30	14345.86	−0.02	$45273^{\circ}_{3\frac{1}{2}} - 59618_{3\frac{1}{2}}$	6	1.194	1.004	0.670	1.099
6964.47		3	14354.64							
6963.47		10	14356.70	−0.02	$54192^{\circ}_{5\frac{1}{2}} - 68549_{4\frac{1}{2}}$					
6963.10	5	300	14357.46	+0.01 −0.08	$48503^{\circ}_{5\frac{1}{2}} - 62861_{5\frac{1}{2}}$ $(56500^{\circ}_{3\frac{1}{2}} - 70858_{4\frac{1}{2}})$	6	1.08	1.10	0.11	1.09
6959.11	1	60	14365.69	+0.01	$57103^{\circ}_{3\frac{1}{2}} - 71468_{2\frac{1}{2}}$	5	1.10	1.03	(0.034)	1.27
6952.14		4	14380.09							
6949.50		10	14385.56	+0.01	$44438^{\circ}_{3\frac{1}{2}} - 58823_{2\frac{1}{2}}$	4	1.12	1.29	0.083	0.70
6944.95		30	14394.98	−0.01	$52067^{\circ}_{0\frac{1}{2}} - 66462_{0\frac{1}{2}}$	6	0.531	1.097	0.283	0.814
6934.05	100	600	14417.61	−0.02	$33494^{\circ}_{3\frac{1}{2}} - 47912_{3\frac{1}{2}}$	6	0.980	1.271	1.032	1.125
6926.08	1	30	14434.20	+0.01	$53716^{\circ}_{2\frac{1}{2}} - 68150_{1\frac{1}{2}}$	5	1.177	0.935	0.121	1.540
6923.78		2	14438.99	−0.05	$35059^{\circ}_{3\frac{1}{2}} - 49498_{2\frac{1}{2}}$					
6921.30		5	14444.17	−0.01	$58672^{\circ}_{0\frac{1}{2}} - 73116_{1\frac{1}{2}}$	5	0.53	0.85	0.16	1.01
6916.78		1	14453.61	−0.02	$56500^{\circ}_{3\frac{1}{2}} - 70954_{2\frac{1}{2}}$					
6916.10		3	14455.03	−0.03	$50468^{\circ}_{5\frac{1}{2}} - 64923_{4\frac{1}{2}}$					
6915.84		4	14455.57	−0.01	$58661^{\circ}_{2\frac{1}{2}} - 73116_{1\frac{1}{2}}$	7	0.86	(0.86)	0	0.868
6911.34		1	14464.98	−0.03	$63417^{\circ}_{2\frac{1}{2}} - 77882_{3\frac{1}{2}}$					
6911.11	1	20	14465.47	0.00	$67933^{\circ}_{2\frac{1}{2}} - 82398_{1\frac{1}{2}}$	5	1.168	1.042	0.063	1.357
6908.92		2	14470.05	+0.01	$62046^{\circ}_{3\frac{1}{2}} - 76516_{4\frac{1}{2}}$					

TABLE 6. Yb II—*Observed and classified lines*—Continued

1	2	3	4	5	6	7	8	9	10	11
Wavelength air	Intensity		Wave number	o–c	Classification	Zeeman type	1st g	2nd g	Zeeman components	
	Meggers lamp	Thomson lamp							Strong p	Strong n
Å			K	K						
6901.06		2	14486.53	−0.05	$69957_{4\frac{1}{2}} - 84444^{\circ}_{3\frac{1}{2}}$					
6897.78		1	14493.42	+0.01	$59777^{\circ}_{1\frac{1}{2}} - 74270_{2\frac{1}{2}}$					
6897.31	1	40	14494.41	0.00	$52921^{\circ}_{3\frac{1}{2}} - 67416_{4\frac{1}{2}}$	5	1.227	1.305	(0.039)	1.577
6889.59	10	100	14510.65	0.00	$34389^{\circ}_{2\frac{1}{2}} - 48900_{3\frac{1}{2}}$	5	(1.007)	1.038	*w*	1.117
6888.76		2	14512.40	+0.01	$62163^{\circ}_{2\frac{1}{2}} - 76676_{2\frac{1}{2}}$					
6886.95		8	14516.21	0.00	$34784^{\circ}_{5\frac{1}{2}} - 49301_{4\frac{1}{2}}$	4	1.11	1.16	(0.026)	0.87
6886.77		5	14516.59	−0.03	$48900_{3\frac{1}{2}} - 63417^{\circ}_{2\frac{1}{2}}$					
				−0.03	$66796^{\circ}_{3\frac{1}{2}} - 81312_{2\frac{1}{2}}$					
6881.40	1	100	14527.92	−0.01	$54192^{\circ}_{5\frac{1}{2}} - 68720_{6\frac{1}{2}}$	5	1.123	1.159	(0.018)	1.357
6877.93	2	250	14535.25	−0.03	$52880^{\circ}_{4\frac{1}{2}} - 67416_{4\frac{1}{2}}$	6	1.26	1.26	0	1.26
6871.51		3	14548.83							
6864.27	2	300	14564.17	−0.06	$58051^{\circ}_{5\frac{1}{2}} - 72615_{5\frac{1}{2}}$	6	0.949	0.971	0.117	0.960
6857.64		2	14578.25	−0.07	$63028^{\circ}_{1\frac{1}{2}} - 77606_{2\frac{1}{2}}$					
6844.05		1	14607.20	−0.02	$48556^{\circ}_{3\frac{1}{2}} - 63163_{4\frac{1}{2}}$					
6843.02		2	14609.40	+0.02	$67789^{\circ}_{1\frac{1}{2}} - 82398_{1\frac{1}{2}}$?					
6830.99		2	14635.13	−0.02	$62163^{\circ}_{2\frac{1}{2}} - 76799_{1\frac{1}{2}}$					
6829.80	1	70	14637.68							
6828.90	2	200	14639.61	+0.01	$51248^{\circ}_{2\frac{1}{2}} - 65888_{1\frac{1}{2}}$	4	1.03	1.20	0.090	0.75
6828.35		2	14640.79	−0.01	$60910^{\circ}_{1\frac{1}{2}} - 75550_{2\frac{1}{2}}$					
6826.18		5	14645.44	−0.03	$64169^{\circ}_{3\frac{1}{2}} - 78814_{2\frac{1}{2}}$					
6826.02		10	14645.78	−0.04	$59624^{\circ}_{3\frac{1}{2}} - 74270_{2\frac{1}{2}}$					
6819.41		2	14659.98	+0.01	$48503^{\circ}_{5\frac{1}{2}} - 63163_{4\frac{1}{2}}$					
6816.18		40	14666.93	−0.01	$46547^{\circ}_{5\frac{1}{2}} - 61214_{4\frac{1}{2}}$					
6815.88	1	100	14667.57	−0.01	$57534^{\circ}_{3\frac{1}{2}} - 72202_{3\frac{1}{2}}$	6	0.865	0.831	0.12	0.848
6812.42		2	14675.02	−0.06	$62163^{\circ}_{2\frac{1}{2}} - 76839_{2\frac{1}{2}}$					
6809.30		5	14681.75	−0.03	$49916^{\circ}_{4\frac{1}{2}} - 64598_{3\frac{1}{2}}$	4				
6803.91		20	14693.38	−0.01	$49008^{\circ}_{3\frac{1}{2}} - 63702_{2\frac{1}{2}}$					
6802.47	2	400	14696.49	−0.02	$46354^{\circ}_{4\frac{1}{2}} - 61051_{3\frac{1}{2}}$	5	1.28	1.18	(0.050)	1.63
6798.29		2*h*	14705.52	−0.05	$56088^{\circ}_{4\frac{1}{2}} - 70793_{5\frac{1}{2}}$					
6796.80		2*h*	14708.75							
6792.58		30	14717.88	−0.02	$49008^{\circ}_{3\frac{1}{2}} - 63726_{4\frac{1}{2}}$					
6790.82		20	14721.70	−0.02	$56500^{\circ}_{3\frac{1}{2}} - 71222_{3\frac{1}{2}}$	6	1.35	(1.15)	0.69	
6786.32		1	14731.46	−0.03	$50468^{\circ}_{5\frac{1}{2}} - 65199_{4\frac{1}{2}}$					
6785.14	1	150	14734.02	−0.05	$50832^{\circ}_{1\frac{1}{2}} - 65566_{0\frac{1}{2}}$	4	0.94	1.42	0.24	0.70
6775.79		2	14754.35	−0.03	$54640^{\circ}_{4\frac{1}{2}} - 69395_{3\frac{1}{2}}$					
				+0.04	$73966_{3\frac{1}{2}} - 88721^{c}_{3\frac{1}{2}}$					
6772.42	1	50	14761.70	−0.03	$44497^{\circ}_{2\frac{1}{2}} - 59259_{2\frac{1}{2}}$	6	0.729	1.095	0.920	0.912
6761.31		4	14785.95	−0.01	$56977^{\circ}_{0\frac{1}{2}} - 71763_{1\frac{1}{2}}$	4	2.20	1.10	0.55	0.55
6759.10		15	14790.79	+0.01	$61442^{\circ}_{5\frac{1}{2}} - 76233_{6\frac{1}{2}}$	4	(1.11)	1.10?	*w*	1.01
6755.44	1	150	14798.80	−0.01	$58484^{\circ}_{4\frac{1}{2}} - 73283^{d}_{4\frac{1}{2}}$	6	0.58	0.62	0.18	0.60?

TABLE 6. Yb II—*Observed and classified lines*—Continued

1	2	3	4	5	6	7	8	9	10	11
Wavelength air	Intensity		Wave number	o–c	Classification	Zeeman type	1st g	2nd g	Zeeman components	
	Meggers lamp	Thomson lamp							Strong p	Strong n
Å			K	K						
6754.69		3	14800.44	−0.04	$47758^{\circ}_{3\frac{1}{2}} - 62559_{2\frac{1}{2}}$					
6751.45		10	14807.55	−0.03	$55221^{\circ}_{1\frac{1}{2}} - 70029_{0\frac{1}{2}}$					
6746.64		6	14818.10	0.00	$53120^{\circ}_{2\frac{1}{2}} - 67938_{3\frac{1}{2}}$					
6745.23	30	600	14821.20	−0.01	$44438^{\circ}_{3\frac{1}{2}} - 59259_{2\frac{1}{2}}$	7	1.10	1.10	0	1.10
6740.59		8	14831.40	0.00	$59439^{\circ}_{2\frac{1}{2}} - 74270_{2\frac{1}{2}}$					
6738.24		2	14836.57	+0.04	$69607_{2\frac{1}{2}} - 84444^{\circ}_{3\frac{1}{2}}$					
6734.56		1	14844.68	+0.02	$47329^{\circ}_{2\frac{1}{2}} - 62174_{1\frac{1}{2}}$					
6732.53		15	14849.16	−0.01	$45737^{\circ}_{1\frac{1}{2}} - 60586_{1\frac{1}{2}}$	7	1.33	(1.323)	0	1.34
6728.37		1	14858.34							
6727.61	400	2000	14860.02	0.00	$33052^{\circ}_{4\frac{1}{2}} - 47912_{3\frac{1}{2}}$	7	(1.264)	1.27	0	1.24
6727.12		20	14861.10	0.00	$66796^{\circ}_{3\frac{1}{2}} - 81657_{2\frac{1}{2}}$					
6724.36	1	30	14867.20	+0.03	$43956^{\circ}_{2\frac{1}{2}} - 58823_{2\frac{1}{2}}$	6	0.99	1.25	0.67	1.12
6724.19		1	14867.58							
6723.90		1	14868.22	−0.01	$49301_{4\frac{1}{2}} - 64169^{\circ}_{3\frac{1}{2}}$					
6718.00	1	30	14881.27	−0.01	$46169^{\circ}_{4\frac{1}{2}} - 61051_{3\frac{1}{2}}$					
6710.95		1	14896.91	+0.02	$66796^{\circ}_{3\frac{1}{2}} - 81692_{3\frac{1}{2}}$					
6710.73		3	14897.40	+0.04	$56056^{\circ}_{2\frac{1}{2}} - 70954_{2\frac{1}{2}}$					
6707.61		15	14904.33	−0.01	$53644^{\circ}_{3\frac{1}{2}} - 68549_{4\frac{1}{2}}$					
6699.36	100	1000	14922.68	+0.01	$34575^{\circ}_{1\frac{1}{2}} - 49498_{2\frac{1}{2}}$	4	1.430	1.142	0.144	0.710
6698.93		5	14923.64	+0.01	$56840_{1\frac{1}{2}} - 71763_{1\frac{1}{2}}$					
6698.13		3	14925.42	+0.01	$39378^{\circ}_{0\frac{1}{2}} - 54304_{0\frac{1}{2}}$					
6689.84		15	14943.92	0.00	$59624^{\circ}_{3\frac{1}{2}} - 74568_{4\frac{1}{2}}$					
6689.28	10	150	14945.17	+0.03	$47228^{\circ}_{0\frac{1}{2}} - 62174_{1\frac{1}{2}}$	5	0.74	(0.80)	w	0.83
6687.64		1	14948.83	−0.04	$49008^{\circ}_{3\frac{1}{2}} - 63957_{3\frac{1}{2}}$					
6685.34		1	14953.97	+0.01	$58162^{\circ}_{1\frac{1}{2}} - 73116_{1\frac{1}{2}}$					
6683.41		10	14958.29	0.00	$67933^{\circ}_{2\frac{1}{2}} - 82891_{2\frac{1}{2}}$					
6682.06		15	14961.31	−0.03	$48272^{\circ}_{2\frac{1}{2}} - 63234_{2\frac{1}{2}}$					
6680.74		4	14964.27	−0.03	$58672^{\circ}_{0\frac{1}{2}} - 73636_{0\frac{1}{2}}$					
6679.30	1	100	14967.50	+0.03	$52987^{\circ}_{1\frac{1}{2}} - 67955_{0\frac{1}{2}}$					
6673.08		10	14981.45	−0.03	$57798^{\circ}_{2\frac{1}{2}} - 72779_{3\frac{1}{2}}$	4	1.14	(1.10)	w	1.005
6670.57		1	14987.08	−0.07	$48024^{\circ}_{1\frac{1}{2}} - 63011_{1\frac{1}{2}}$					
6670.18		50	14987.96							
6666.78		20	14995.60	−0.03	$60910^{\circ}_{1\frac{1}{2}} - 75905_{0\frac{1}{2}}$					
6666.55		40	14996.12	−0.04	$58661^{\circ}_{2\frac{1}{2}} - 73657_{1\frac{1}{2}}$	4	0.865	1.033	0.084	0.613
6665.08		1	14999.43							
6661.90	2	200	15006.59	−0.02	$49916^{\circ}_{4\frac{1}{2}} - 64923_{4\frac{1}{2}}$	6	1.092	1.054	0.170	1.073
6658.43		60	15014.41	−0.01	$53120^{\circ}_{2\frac{1}{2}} - 68135_{2\frac{1}{2}}$	6	0.944	1.088	0.341	1.016
6657.26		25	15017.05	−0.01	$52921^{\circ}_{3\frac{1}{2}} - 67938_{3\frac{1}{2}}$					
6651.52		4	15030.01	+0.02	$53120^{\circ}_{2\frac{1}{2}} - 68150_{1\frac{1}{2}}$					
6647.25		1	15039.66	0.00	$53716^{\circ}_{2\frac{1}{2}} - 68756_{3\frac{1}{2}}$					

TABLE 6. Yb II—*Observed and classified lines*—Continued

1	2	3	4	5	6	7	8	9	10	11
Wave-length air	Intensity		Wave number	o–c	Classification	Zeeman type	1st g	2nd g	Zeeman components	
	Meggers lamp	Thomson lamp							Strong p	Strong n
Å			K	K						
6644.94		6	15044.89	+0.01	$46169^{\circ}_{4\frac{1}{2}} - 61214_{4\frac{1}{2}}$					
6644.06	2	200	15046.88	−0.01	$49008^{\circ}_{3\frac{1}{2}} - 64055_{2\frac{1}{2}}$	4	1.02	1.07	(0.024)	0.90
6640.88		15	15054.09	−0.03	$57561^{\circ}_{6\frac{1}{2}} - 72615_{5\frac{1}{2}}$					
6639.62		3	15056.94	+0.01	$56056^{\circ}_{2\frac{1}{2}} - 71113_{1\frac{1}{2}}$					
6639.19		5	15057.92	−0.01	$52880^{\circ}_{4\frac{1}{2}} - 67938_{3\frac{1}{2}}$					
6636.54		2	15063.93	+0.09	$49301_{4\frac{1}{2}} - 64365^{\circ}_{4\frac{1}{2}}$					
6632.40		2	15073.34	+0.05	$61442^{\circ}_{5\frac{1}{2}} - 76516_{4\frac{1}{2}}$					
6619.66		40	15102.35	0.00	$51248^{\circ}_{2\frac{1}{2}} - 66351_{2\frac{1}{2}}$					
6617.72		4	15106.77	−0.01	$66205^{\circ}_{2\frac{1}{2}} - 81312_{2\frac{1}{2}}$					
6617.06	100	1000	15108.28	0.00	$34389^{\circ}_{2\frac{1}{2}} - 49498_{2\frac{1}{2}}$	6	1.00	1.14	0.35	1.07
6616.40	2	40	15109.79							
6615.80	1	80	15111.16	+0.01	$53644^{\circ}_{3\frac{1}{2}} - 68756_{3\frac{1}{2}}$					
6611.87		4	15120.14	+0.04	$62163^{\circ}_{2\frac{1}{2}} - 77284_{1\frac{1}{2}}$					
6611.32		5	15121.40	+0.01	$44497^{\circ}_{2\frac{1}{2}} - 59618_{3\frac{1}{2}}$					
6610.31		1	15123.71	+0.06	$66189^{\circ}_{1\frac{1}{2}} - 81312_{2\frac{1}{2}}$					
6608.68		1	15127.44							
6605.82	4	250	15133.99	+0.02	$56088^{\circ}_{4\frac{1}{2}} - 71222_{3\frac{1}{2}}$	7	1.12	(1.15)	0	1.01
6604.45		50	15137.13	+0.03	$52067^{\circ}_{0\frac{1}{2}} - 67204_{1\frac{1}{2}}$					
6600.68		7	15145.77	+0.02	$48556^{\circ}_{3\frac{1}{2}} - 63702_{2\frac{1}{2}}$					
6600.03		2	15147.26	+0.02	$52987^{\circ}_{1\frac{1}{2}} - 68135_{2\frac{1}{2}}$					
6593.25		50	15162.84	+0.03	$52987^{\circ}_{1\frac{1}{2}} - 68150_{1\frac{1}{2}}$					
6592.69	2	150	15164.13	+0.02	$49727^{\circ}_{6\frac{1}{2}} - 64891_{7\frac{1}{2}}$	7	(1.18)	1.18	0	1.18
6592.12		30	15165.44	−0.01	$56056^{\circ}_{2\frac{1}{2}} - 71222_{3\frac{1}{2}}$					
6590.72	1	15	15168.66	+0.02	$47005^{\circ}_{1\frac{1}{2}} - 62174_{1\frac{1}{2}}$					
6587.26		1	15176.63	−0.01	$49916^{\circ}_{4\frac{1}{2}} - 65093_{3\frac{1}{2}}$					
6585.41	100	1000	15180.89	+0.02 +0.02	$44438^{\circ}_{3\frac{1}{2}} - 59618_{3\frac{1}{2}}$ $(47680^{\circ}_{6\frac{1}{2}} - 62861_{5\frac{1}{2}})$	6	1.079	0.991	0.32	1.035
6582.79	2	250	15186.93			7			0	0.97
6578.10		20	15197.76	+0.01	$47663^{\circ}_{4\frac{1}{2}} - 62861_{5\frac{1}{2}}$					
6574.10	2	200	15207.01	+0.03	$61442^{\circ}_{5\frac{1}{2}} - 76649_{5\frac{1}{2}}$	6	1.10	1.08	0.20	1.08
6573.31		10	15208.83	+0.01 −0.04	$43075^{\circ}_{1\frac{1}{2}} - 58283_{2\frac{1}{2}}$ $79126_{4\frac{1}{2}} - 94335^{\circ}_{5\frac{1}{2}}$					
6571.44	10	400	15213.16	+0.02 +0.06	$44497^{\circ}_{2\frac{1}{2}} - 59710_{1\frac{1}{2}}$ $(56056^{\circ}_{2\frac{1}{2}} - 71270_{2\frac{1}{2}})$	4	(0.734)	0.80	w	0.63
6570.94		9	15214.32	+0.03	$59777^{\circ}_{1\frac{1}{2}} - 74991_{1\frac{1}{2}}$					
6567.60		9	15222.06							
6563.38		2	15231.84	0.00	$58051^{\circ}_{5\frac{1}{2}} - 73283_{4\frac{1}{2}}$					
6562.35		5*h*	15234.24	+0.01	$46902^{\circ}_{0\frac{1}{2}} - 62136_{0\frac{1}{2}}$					
6560.94		1*h*	15237.51	0.00	$69395_{3\frac{1}{2}} - 84632^{\circ}_{2\frac{1}{2}}$					
6559.65		2	15240.51	+0.07	$58051^{\circ}_{5\frac{1}{2}} - 73291_{5\frac{1}{2}}$					

TABLE 6. Yb II—*Observed and classified lines*—Continued

1	2	3	4	5	6	7	8	9	10	11
Wave-length air	Intensity		Wave number	o–c	Classification	Zeeman type	1st g	2nd g	Zeeman components	
	Meggers lamp	Thomson lamp							Strong p	Strong n
Å			K	K						
6557.46		4	15245.60	+0.06	$57534^{\circ}_{3\frac{1}{2}} - 72779_{3\frac{1}{2}}$					
6552.61		2	15256.88							
6548.53	2	200	15266.39	+0.03	$58484^{\circ}_{4\frac{1}{2}} - 73750_{4\frac{1}{2}}$	6	0.96	1.01	0.22	0.99
6547.77		9	15268.16	+0.03	$52880^{\circ}_{4\frac{1}{2}} - 68148_{5\frac{1}{2}}$					
6546.35		2	15271.47	+0.08	$46902^{\circ}_{0\frac{1}{2}} - 62174_{1\frac{1}{2}}$					
6541.38	3	400	15283.07	+0.03	$49916^{\circ}_{4\frac{1}{2}} - 65199_{4\frac{1}{2}}$	6	(1.090)	1.05?	d	1.07
6540.36		1	15285.46	+0.06	$62163^{\circ}_{2\frac{1}{2}} - 77449_{3\frac{1}{2}}$					
6531.71		5	15305.70	+0.02	$58661^{\circ}_{2\frac{1}{2}} - 73966_{3\frac{1}{2}}$					
6531.26		4	15306.75	0.00	$66205^{\circ}_{2\frac{1}{2}} - 81512_{1\frac{1}{2}}$					
6527.01		25	15316.72	+0.05	$54640^{\circ}_{4\frac{1}{2}} - 69957_{4\frac{1}{2}}$					
6526.36		3	15318.24	+0.04	$57798^{\circ}_{2\frac{1}{2}} - 73116_{1\frac{1}{2}}$					
6523.19	2	250	15325.69	+0.01	$46547^{\circ}_{5\frac{1}{2}} - 61873_{6\frac{1}{2}}$					
6521.52		25	15329.61	+0.08	$53120^{\circ}_{2\frac{1}{2}} - 68450_{3\frac{1}{2}}$					
6507.15		1	15363.47	−0.03	$53716^{\circ}_{2\frac{1}{2}} - 69079_{2\frac{1}{2}}$					
6503.01	50	500	15373.25	+0.01	$38342^{\circ}_{4\frac{1}{2}} - 53715_{3\frac{1}{2}}$	4	1.00	1.08	(0.038)	0.734
6502.28		20	15374.97	+0.01	$48272^{\circ}_{2\frac{1}{2}} - 63647_{1\frac{1}{2}}$					
6500.70	2	30	15378.71	+0.02	$38342^{\circ}_{4\frac{1}{2}} - 53720_{4\frac{1}{2}}$					
6498.79	1	20	15383.23	+0.03	$45737^{\circ}_{1\frac{1}{2}} - 61120_{0\frac{1}{2}}$					
6493.58		5	15395.57	+0.07	$55462^{\circ}_{3\frac{1}{2}} - 70858_{4\frac{1}{2}}$					
6492.73	10	700	15397.59	+0.04	$53322^{\circ}_{7\frac{1}{2}} - 68720_{6\frac{1}{2}}$	4	0.98	1.04	(0.032)	0.57
6491.18		5	15401.26	+0.03	$48556^{\circ}_{3\frac{1}{2}} - 63957_{3\frac{1}{2}}$					
6490.32		20	15403.30	+0.05	$62046^{\circ}_{3\frac{1}{2}} - 77449_{3\frac{1}{2}}$					
6488.47		200	15407.70	−0.02	$50468^{\circ}_{5\frac{1}{2}} - 65875_{6\frac{1}{2}}$					
6487.08		10	15411.00	−0.02	$73291^{\circ}_{5\frac{1}{2}} - 88702^{\circ}_{5\frac{1}{2}}$					
6486.74		50	15411.81	+0.02	$56056^{\circ}_{2\frac{1}{2}} - 71468_{2\frac{1}{2}}$					
6485.55	10	200*h*	15414.63							
6477.63		6	15433.48	+0.03	$59624^{\circ}_{3\frac{1}{2}} - 75058_{2\frac{1}{2}}$					
6476.36		1	15436.51	+0.01	$63028^{\circ}_{1\frac{1}{2}} - 78464_{1\frac{1}{2}}$					
6474.74	30	1500	15440.37	+0.01	$48503^{\circ}_{5\frac{1}{2}} - 63944_{5\frac{1}{2}}$	6	1.10	1.12	0.09	1.11
6470.17		1	15451.27	+0.01	$66205^{\circ}_{2\frac{1}{2}} - 81657_{2\frac{1}{2}}$					
6466.79		7	15459.35	+0.03	$64169^{\circ}_{3\frac{1}{2}} - 79628_{3\frac{1}{2}}$					
6465.78		3*h*	15461.77	−0.04	$68756_{3\frac{1}{2}} - 84217^{\circ}_{4\frac{1}{2}}$					
6463.15	50	2000	15468.06	+0.03	$46354^{\circ}_{4\frac{1}{2}} - 61822_{3\frac{1}{2}}$	7	1.30	(1.327)	0	1.21
6456.95	2	150	15482.91	+0.01	$50468^{\circ}_{5\frac{1}{2}} - 65950_{4\frac{1}{2}}$					
6455.23		4	15487.03	+0.06 −0.02	$64970^{\circ}_{3\frac{1}{2}} - 80457_{3\frac{1}{2}}$ $66205^{\circ}_{2\frac{1}{2}} - 81692_{3\frac{1}{2}}$					
6453.30	1	150	15491.67	+0.08	$55462^{\circ}_{3\frac{1}{2}} - 70954_{2\frac{1}{2}}$					
6453.11	10	150	15492.12							
6452.10		15	15494.55	+0.01	$58162^{\circ}_{1\frac{1}{2}} - 73657_{1\frac{1}{2}}$					
6442.10		9	15518.60	+0.04	$50832^{\circ}_{1\frac{1}{2}} - 66351_{2\frac{1}{2}}$					

TABLE 6. Yb II—*Observed and classified lines*—Continued

1	2	3	4	5	6	7	8	9	10	11
Wave-length air	Intensity		Wave number	o–c	Classification	Zeeman type	1st g	2nd g	Zeeman components	
	Meggers lamp	Thomson lamp							Strong p	Strong n
Å			K	K						
6440.79	5	400	15521.76	+0.07	$59046^{\circ}_{4\frac{1}{2}} - 74568_{4\frac{1}{2}}$	6	1.08	1.05	0.12	1.07w
6437.98	1	150	15528.53	+0.04	$52921^{\circ}_{3\frac{1}{2}} - 68450_{3\frac{1}{2}}$					
6432.73	1000	3000	15541.20	−0.01	$32371^{\circ}_{2\frac{1}{2}} - 47912_{3\frac{1}{2}}$	5	1.172	1.280	0.054	1.550
6427.60	20	400	15553.61	+0.05	$47005^{\circ}_{1\frac{1}{2}} - 62559_{2\frac{1}{2}}$	5	0.98	1.22	0.11	1.53
6423.67		5	15563.12	+0.05	$50832^{\circ}_{1\frac{1}{2}} - 66395_{2\frac{1}{2}}$					
6416.98		7	15579.35							
6412.85		30	15589.38	+0.03	$49008^{\circ}_{3\frac{1}{2}} - 64598_{3\frac{1}{2}}$					
6402.64		50	15614.24	+0.04	$50468^{\circ}_{5\frac{1}{2}} - 66082_{5\frac{1}{2}}$					
6397.15		2	15627.64	+0.03	$52921^{\circ}_{3\frac{1}{2}} - 68549_{4\frac{1}{2}}$					
6396.68		1	15628.79							
6396.09		7	15630.23	+0.02	$50832^{\circ}_{1\frac{1}{2}} - 66462_{0\frac{1}{2}}$					
6393.91		3	15635.56	+0.10	$53120^{\circ}_{2\frac{1}{2}} - 68756_{3\frac{1}{2}}$					
6393.59		8	15636.34							
6393.23	4	150	15637.22	+0.02	$45737^{\circ}_{1\frac{1}{2}} - 61374_{2\frac{1}{2}}$	4	(1.33)	1.30	0	1.26
6389.69		10	15645.89	+0.04	$44940^{\circ}_{1\frac{1}{2}} - 60586_{1\frac{1}{2}}$					
6386.84		25	15652.87	+0.07	$46169^{\circ}_{4\frac{1}{2}} - 61822_{3\frac{1}{2}}$					
6382.92	20	200	15662.48	−0.01	$43956^{\circ}_{2\frac{1}{2}} - 59618_{3\frac{1}{2}}$	7	1.00	(1.00)	0	0.99
6380.47		3	15668.50	+0.02	$52880^{\circ}_{4\frac{1}{2}} - 68549_{4\frac{1}{2}}$					
6377.01	6	400	15677.00	+0.03	$57103^{\circ}_{3\frac{1}{2}} - 72779_{3\frac{1}{2}}$	7	(1.10)	1.10	0	1.09
6376.74	1	20	15677.66	+0.04	$48024^{\circ}_{1\frac{1}{2}} - 63702_{2\frac{1}{2}}$					
6374.81	4	80	15682.41	0.00	$47329^{\circ}_{2\frac{1}{2}} - 63011_{1\frac{1}{2}}$	5	1.01	0.81	0.10	1.31
6367.91		4	15699.40	+0.01	$58051^{\circ}_{5\frac{1}{2}} - 73750_{4\frac{1}{2}}$					
6364.92		3	15706.77	+0.01	$56056^{\circ}_{2\frac{1}{2}} - 71763_{1\frac{1}{2}}$					
6360.33		4	15718.11	−0.01	$62163^{\circ}_{2\frac{1}{2}} - 77882_{3\frac{1}{2}}$					
6356.67	2	200	15727.16	+0.02	$53716^{\circ}_{2\frac{1}{2}} - 69443_{1\frac{1}{2}}$	5	(1.183)	1.16	0	1.22
6355.38	20	1000	15730.35	+0.02	$57561^{\circ}_{6\frac{1}{2}} - 73291_{5\frac{1}{2}}$	5	1.06?	(1.09)	w	0.92?
6354.39		20	15732.80	−0.01	$55221^{\circ}_{1\frac{1}{2}} - 70954_{2\frac{1}{2}}$					
6348.05		10	15748.51	+0.02	$43075^{\circ}_{1\frac{1}{2}} - 58823_{2\frac{1}{2}}$					
6347.32		20	15750.33	+0.02	$53644^{\circ}_{3\frac{1}{2}} - 69395_{3\frac{1}{2}}$					
6345.74	40	400	15754.25	+0.01	$43956^{\circ}_{2\frac{1}{2}} - 59710_{1\frac{1}{2}}$					
6343.54		7	15759.71	+0.03	$55462^{\circ}_{3\frac{1}{2}} - 71222_{3\frac{1}{2}}$					
6342.65		1	15761.92							
6341.41		6	15765.00	+0.02	$54192^{\circ}_{5\frac{1}{2}} - 69957_{4\frac{1}{2}}$					
6340.93		15	15766.20	+0.03	$60910^{\circ}_{1\frac{1}{2}} - 76676_{2\frac{1}{2}}$	7	1.10	(1.10)	0	1.10
6338.10		7	15773.24	+0.09	$65739^{\circ}_{2\frac{1}{2}} - 81512_{1\frac{1}{2}}$					
6334.20		5	15782.95	+0.06 −0.10	$47228^{\circ}_{0\frac{1}{2}} - 63011_{1\frac{1}{2}}$ $48272^{\circ}_{2\frac{1}{2}} - 64055_{2\frac{1}{2}}$					
6333.45	1	70	15784.82	−0.02	$45429^{\circ}_{3\frac{1}{2}} - 61214_{4\frac{1}{2}}$					
6324.77	40	400	15806.48	0.00	$33494^{\circ}_{3\frac{1}{2}} - 49301_{4\frac{1}{2}}$	5	0.995	1.195	0.10	1.895

TABLE 6. Yb II—*Observed and classified lines*—Continued

1	2	3	4	5	6	7	8	9	10	11
Wave-length air	Intensity		Wave number	o–c	Classification	Zeeman type	1st g	2nd g	Zeeman components	
	Meggers lamp	Thomson lamp							Strong p	Strong n
Å			K	K						
6324.43	1	90	15807.33	0.00	$55462^{\circ}_{3\frac{1}{2}} - 71270_{2\frac{1}{2}}$	4	(0.878)	0.89	0	0.85
6313.61		1	15834.42	0.00	$52921^{\circ}_{3\frac{1}{2}} - 68756_{3\frac{1}{2}}$					
6312.99		20	15835.98	+0.01	$62046^{\circ}_{3\frac{1}{2}} - 77882_{3\frac{1}{2}}$	7	1.14	(1.12)	0	1.13
6308.15	400	2000	15848.13	+0.01	$33052^{\circ}_{4\frac{1}{2}} - 48900_{3\frac{1}{2}}$	5	1.260	1.030	0.115	2.07
6303.91		5	15858.79	+0.01	$57798^{\circ}_{2\frac{1}{2}} - 73657_{1\frac{1}{2}}$					
6303.27	50	400	15860.40	−0.02	$37077^{\circ}_{2\frac{1}{2}} - 52938_{1\frac{1}{2}}$	5	1.12	0.90	0.11	1.45
6300.94		8	15866.26	+0.01	$60649^{\circ}_{4\frac{1}{2}} - 76516_{4\frac{1}{2}}$					
6297.35	5	400	15875.31	+0.02	$52880^{\circ}_{4\frac{1}{2}} - 68756_{3\frac{1}{2}}$					
6292.56		2	15887.39	+0.03	$52067^{\circ}_{0\frac{1}{2}} - 67955_{0\frac{1}{2}}$					
6292.17	2	20	15888.37	0.00	$37516^{\circ}_{3\frac{1}{2}} - 53404_{2\frac{1}{2}}$					
6291.06		5	15891.18	+0.02	$53716^{\circ}_{2\frac{1}{2}} - 69607_{2\frac{1}{2}}$					
6285.72		3	15904.68	+0.01	$47329^{\circ}_{2\frac{1}{2}} - 63234_{2\frac{1}{2}}$					
6281.96		4	15914.20	+0.02	$49008^{\circ}_{3\frac{1}{2}} - 64923_{4\frac{1}{2}}$					
6280.60		2	15917.64	−0.02	$65739^{\circ}_{2\frac{1}{2}} - 81657_{2\frac{1}{2}}$					
6277.08	2	150	15926.57	+0.05	$59046^{\circ}_{4\frac{1}{2}} - 74973_{3\frac{1}{2}}$	7	1.08	1.07	0	1.07
6274.78	2000	10000	15932.41	0.00	$31979^{\circ}_{3\frac{1}{2}} - 47912_{3\frac{1}{2}}$	6	1.326	1.280	0.16	1.303
6271.15	6	250	15941.63	−0.01	$45273^{\circ}_{3\frac{1}{2}} - 61214_{4\frac{1}{2}}$	4	(1.18)	1.04	w	0.57
6270.31	3	100	15943.77	−0.01 +0.04	$47758^{\circ}_{3\frac{1}{2}} - 63702_{2\frac{1}{2}}$ $(54192^{\circ}_{5\frac{1}{2}} - 70136_{6\frac{1}{2}})$	5	(1.08)	1.01	w	1.26
6269.95	1	40	15944.68	+0.01	$45429^{\circ}_{3\frac{1}{2}} - 61374_{2\frac{1}{2}}$					
6265.45	1	80	15956.13	+0.02	$51248^{\circ}_{2\frac{1}{2}} - 67204_{1\frac{1}{2}}$	7	(1.034)	1.04	0	1.02
6262.89		15	15962.65	0.00	$53644^{\circ}_{3\frac{1}{2}} - 69607_{2\frac{1}{2}}$					
6260.79	30	1500	15968.01	+0.01	$48923^{\circ}_{7\frac{1}{2}} - 64891_{7\frac{1}{2}}$	6?	1.20	1.20	0	1.20
6250.39		1	15994.58	−0.01	$56621^{\circ}_{5\frac{1}{2}} - 72615_{5\frac{1}{2}}$					
6249.54		1	15996.75							
6248.29		20	15999.95	+0.01	$60649^{\circ}_{4\frac{1}{2}} - 76649_{5\frac{1}{2}}$					
6246.97	500	4000	16003.33	−0.03	$33494^{\circ}_{3\frac{1}{2}} - 49498_{2\frac{1}{2}}$	4	0.990	1.140	(0.08)	0.60
6245.93		6	16006.00	−0.02	$55462^{\circ}_{3\frac{1}{2}} - 71468_{2\frac{1}{2}}$					
6244.39		1	16009.95							
6242.25	1	30	16015.43	+0.03	$59624^{\circ}_{3\frac{1}{2}} - 75640_{3\frac{1}{2}}$					
6239.67		3	16022.06	+0.03	$52921^{\circ}_{3\frac{1}{2}} - 68943_{4\frac{1}{2}}$					
6236.13	3	150	16031.15	+0.03	$48024^{\circ}_{1\frac{1}{2}} - 64055_{2\frac{1}{2}}$	4	1.36	1.12	0.12	0.76
6234.85	3	250	16034.44	−0.01	$49916^{\circ}_{4\frac{1}{2}} - 65950_{4\frac{1}{2}}$	6	1.08	1.06	0.11	1.07
6233.37	5	250	16038.25	−0.02	$45012^{\circ}_{2\frac{1}{2}} - 61051_{3\frac{1}{2}}$	4	1.20	1.12	(0.042)	0.91
6232.02		2	16041.72	+0.01	$48556^{\circ}_{3\frac{1}{2}} - 64598_{3\frac{1}{2}}$					
6229.36		10	16048.57	+0.02	$55221^{\circ}_{1\frac{1}{2}} - 71270_{2\frac{1}{2}}$					
6223.63	15	500	16063.35	+0.04	$47663^{\circ}_{4\frac{1}{2}} - 63726_{4\frac{1}{2}}$	7	1.00	(1.005)	0	1.000
6216.14		9	16082.70	0.00	$52067^{\circ}_{0\frac{1}{2}} - 68150_{1\frac{1}{2}}$					
6215.56	6	200	16084.20	−0.01	$49008^{\circ}_{3\frac{1}{2}} - 65093_{3\frac{1}{2}}$	6	1.01	0.96	0.19	0.99
6213.74		3	16088.92	−0.03	$44497^{\circ}_{2\frac{1}{2}} - 60586_{1\frac{1}{2}}$					

TABLE 6. Yb II—*Observed and classified lines*—Continued

1	2	3	4	5	6	7	8	9	10	11
Wave-length air	Intensity		Wave number	o–c	Classification	Zeeman type	1st g	2nd g	Zeeman components	
	Meggers lamp	Thomson lamp							Strong p	Strong n
Å			K	K						
6212.28		2	16092.70	−0.01	$64365^{\circ}_{4\frac{1}{2}} - 80457_{3\frac{1}{2}}$					
6211.10		1	16095.75	−0.02	$66796^{\circ}_{3\frac{1}{2}} - 82891_{2\frac{1}{2}}$					
6208.89	3	70	16101.48	+0.01	$45273^{\circ}_{3\frac{1}{2}} - 61374_{2\frac{1}{2}}$					
6208.10	10	500	16103.53	0.00	$50468^{\circ}_{5\frac{1}{2}} - 66571_{5\frac{1}{2}}$	6	1.22	1.20	0.09	1.21
6206.49		3	16107.71	−0.02	$58162^{\circ}_{1\frac{1}{2}} - 74270_{2\frac{1}{2}}$					
6204.88		4	16111.89	+0.03	$59439^{\circ}_{2\frac{1}{2}} - 75550_{2\frac{1}{2}}$					
6204.20		4	16113.66	+0.02	$56088^{\circ}_{4\frac{1}{2}} - 72202_{3\frac{1}{2}}$					
6196.01		6	16134.95	−0.02	$56480^{\circ}_{4\frac{1}{2}} - 72615_{5\frac{1}{2}}$					
6191.14		7*h*	16147.65	+0.06	$49419^{\circ}_{0\frac{1}{2}} - 65566_{0\frac{1}{2}}$					
6190.78	15	1000	16148.59	+0.01	$49727^{\circ}_{6\frac{1}{2}} - 65875_{6\frac{1}{2}}$	7	1.21	(1.205)	0	1.206
6189.03	1	90	16153.15	+0.01	$54640^{\circ}_{4\frac{1}{2}} - 70793_{5\frac{1}{2}}$					
6187.08		20	16158.24	−0.02	$52921^{\circ}_{3\frac{1}{2}} - 69079_{2\frac{1}{2}}$					
6185.43		2	16162.55							
6184.05		1	16166.16	+0.08	$63417^{\circ}_{2\frac{1}{2}} - 79583_{2\frac{1}{2}}$					
6178.81	1	20	16179.87	−0.01 +0.04	$44940^{\circ}_{1\frac{1}{2}} - 61120_{0\frac{1}{2}}$ $75058_{2\frac{1}{2}} - 91237^{\circ}_{3\frac{1}{2}}$					
6178.63		3	16180.34	+0.01	$57103^{\circ}_{3\frac{1}{2}} - 73283_{4\frac{1}{2}}$					
6175.58		90	16188.33	+0.02	$48272^{\circ}_{2\frac{1}{2}} - 64461_{1\frac{1}{2}}$	4	1.15	(1.176)	0	1.11
6175.36		9	16188.91	−0.01	$63417^{\circ}_{2\frac{1}{2}} - 79605_{1\frac{1}{2}}$					
6174.70	1	60	16190.64	+0.03	$49008^{\circ}_{3\frac{1}{2}} - 65199_{4\frac{1}{2}}$					
6173.76		7	16193.10	−0.01	$66205^{\circ}_{2\frac{1}{2}} - 82398_{1\frac{1}{2}}$					
6171.63	30	300	16198.69	+0.02	$37516^{\circ}_{3\frac{1}{2}} - 53715_{3\frac{1}{2}}$	6	1.13	1.18	0.17	1.16
6169.55	100	200	16204.15	+0.03	$37516^{\circ}_{3\frac{1}{2}} - 53720_{4\frac{1}{2}}$					
6164.53		2	16217.35	−0.01	$54640^{\circ}_{4\frac{1}{2}} - 70858_{4\frac{1}{2}}$					
6152.57	800	4000	16248.87	0.00	$33052^{\circ}_{4\frac{1}{2}} - 49301_{4\frac{1}{2}}$	6	1.262	1.190	0.336	1.23
6150.62		70*h*	16254.03							
6149.44		1	16257.14	+0.06	$47912_{3\frac{1}{2}} - 64169^{\circ}_{3\frac{1}{2}}$					
6146.91	10	400	16263.84	+0.06	$47680^{\circ}_{6\frac{1}{2}} - 63944_{5\frac{1}{2}}$	7	1.12	(1.115)	0	1.14
6146.29		3	16265.48	−0.03	$78070_{4\frac{1}{2}} - 94335^{\circ}_{5\frac{1}{2}}$					
6142.83	1	60	16274.64	+0.02	$53120^{\circ}_{2\frac{1}{2}} - 69395_{3\frac{1}{2}}$	7	(0.944)	0.94	0	0.95
6141.70		1	16277.63							
6141.05		3	16279.35	0.00	$56500^{\circ}_{3\frac{1}{2}} - 72779_{3\frac{1}{2}}$					
6140.55		2	16280.68	+0.02	$47663^{\circ}_{4\frac{1}{2}} - 63944_{5\frac{1}{2}}$					
6135.41		2	16294.32	+0.04	$47663^{\circ}_{4\frac{1}{2}} - 63957_{3\frac{1}{2}}$					
6134.28	7	200	16297.32	+0.04	$47758^{\circ}_{3\frac{1}{2}} - 64055_{2\frac{1}{2}}$	7	1.10	(1.108)	0	1.09
6133.55		3	16299.26	+0.04	$56480^{\circ}_{4\frac{1}{2}} - 72779_{3\frac{1}{2}}$					
6132.94		25	16300.88	+0.04	$62163^{\circ}_{2\frac{1}{2}} - 78464_{1\frac{1}{2}}$					
6131.53	1	80	16304.63	+0.05	$61442^{\circ}_{5\frac{1}{2}} - 77747_{4\frac{1}{2}}$	5	1.11	(1.07)	*w*	1.30
6128.51		5	16312.67	+0.07	$53644^{\circ}_{3\frac{1}{2}} - 69957_{4\frac{1}{2}}$					
6128.18	10	300	16313.54	−0.01	$46547^{\circ}_{5\frac{1}{2}} - 62861_{5\frac{1}{2}}$					

TABLE 6. Yb II—*Observed and classified lines*—Continued

1	2	3	4	5	6	7	8	9	10	11
Wave-length air	Intensity		Wave number	o–c	Classification	Zeeman type	1st g	2nd g	Zeeman components	
	Meggers lamp	Thomson lamp							Strong p	Strong n
Å			K	K						
6127.92		10	16314.24	+0.06	$64365^{\circ}_{4\frac{1}{2}} - 80679_{5\frac{1}{2}}$					
6126.89		1	16316.98	+0.02	$58672^{\circ}_{0\frac{1}{2}} - 74989_{0\frac{1}{2}}$					
6126.39	3	100	16318.31	+0.02	$47329^{\circ}_{2\frac{1}{2}} - 63647_{1\frac{1}{2}}$					
6124.63		3	16323.00	+0.06	$53120^{\circ}_{2\frac{1}{2}} - 69443_{1\frac{1}{2}}$					
6123.67	1	30	16325.56	+0.05	$48272^{\circ}_{2\frac{1}{2}} - 64598_{3\frac{1}{2}}$					
6122.98	40	250	16327.40	+0.03	$37077^{\circ}_{2\frac{1}{2}} - 53404_{2\frac{1}{2}}$	6	1.118	1.052	0.164	1.085
6121.91		9	16330.25	+0.02	$58661^{\circ}_{2\frac{1}{2}} - 74991_{1\frac{1}{2}}$					
6120.30	5	250	16334.55							
6117.54	2	10	16341.92	+0.01	$64970^{\circ}_{3\frac{1}{2}} - 81312_{2\frac{1}{2}}$					
6116.67	10	70	16344.24	+0.01	$31568^{\circ}_{2\frac{1}{2}} - 47912_{3\frac{1}{2}}$					
6110.13	6	200	16361.74	+0.04	$45012^{\circ}_{2\frac{1}{2}} - 61374_{2\frac{1}{2}}$	7	1.30	(1.299)	0	1.30
6108.32		2	16366.58	+0.04	$48556^{\circ}_{3\frac{1}{2}} - 64923_{4\frac{1}{2}}$					
6106.18	5	200	16372.32	0.00	$50832^{\circ}_{1\frac{1}{2}} - 67204_{1\frac{1}{2}}$	6	0.957	1.043	0.129	1.000
6105.58	1	10	16373.93	+0.05	$60910^{\circ}_{1\frac{1}{2}} - 77284_{1\frac{1}{2}}$					
6098.89		7	16391.89	+0.05	$73750_{4\frac{1}{2}} - 90142^{\circ}_{3\frac{1}{2}}$					
				−0.05	$77606_{2\frac{1}{2}} - 93998^{\circ}_{1\frac{1}{2}}$					
6098.54	3	250	16392.83	+0.07	$45429^{\circ}_{3\frac{1}{2}} - 61822_{3\frac{1}{2}}$					
6096.98	1	30	16397.02	+0.04	$58661^{\circ}_{2\frac{1}{2}} - 75058_{2\frac{1}{2}}$					
6095.98		3	16399.71	+0.06	$45737^{\circ}_{1\frac{1}{2}} - 62136_{0\frac{1}{2}}$					
6089.14	20	100	16418.14	+0.05	$22960_{1\frac{1}{2}} - 39378^{\circ}_{0\frac{1}{2}}$					
6088.70	3	200	16419.32	+0.03	$48503^{\circ}_{5\frac{1}{2}} - 64923_{4\frac{1}{2}}$	7	1.11	(1.10)	0	1.16
6083.86	1	30	16432.38	+0.02	$57534^{\circ}_{3\frac{1}{2}} - 73966_{3\frac{1}{2}}$					
6083.29	5	200	16433.92	+0.04	$44940^{\circ}_{1\frac{1}{2}} - 61374_{2\frac{1}{2}}$	5	1.26	(1.299)	w	1.36
6082.37	6	500	16436.41	+0.03	$48024^{\circ}_{1\frac{1}{2}} - 64461_{1\frac{1}{2}}$	6	1.39	1.19	0.30	1.28
6082.21		10	16436.84	+0.03	$45737^{\circ}_{1\frac{1}{2}} - 62174_{1\frac{1}{2}}$					
6075.21	3	200	16455.78	+0.02	$52987^{\circ}_{1\frac{1}{2}} - 69443_{1\frac{1}{2}}$	7	1.14	(1.145)	0	1.14
6074.10		1	16458.79	+0.02	$73750_{4\frac{1}{2}} - 90209^{\circ}_{4\frac{1}{2}}$					
6070.19		20	16469.39	+0.06	$49419^{\circ}_{0\frac{1}{2}} - 65888_{1\frac{1}{2}}$					
6068.64	1	60	16473.60	+0.02	$52921^{\circ}_{3\frac{1}{2}} - 69395_{3\frac{1}{2}}$					
6063.01		4	16488.89	+0.02	$58484^{\circ}_{4\frac{1}{2}} - 74973_{3\frac{1}{2}}$					
6059.93		3	16497.27							
6056.46	10	500	16506.72	0.00	$46354^{\circ}_{4\frac{1}{2}} - 62861_{5\frac{1}{2}}$	4	1.288	(1.140)	w	0.475
6053.61		3	16514.50	+0.05	$52880^{\circ}_{4\frac{1}{2}} - 69395_{3\frac{1}{2}}$					
6052.88	100	900	16516.49	+0.04	$32981^{\circ}_{1\frac{1}{2}} - 49498_{2\frac{1}{2}}$	5	0.87	1.15	0.14	1.57
6052.66		250	16517.09	+0.02	$58051^{\circ}_{5\frac{1}{2}} - 74568_{4\frac{1}{2}}$					
6048.87		2	16527.44	+0.09	$56088^{\circ}_{4\frac{1}{2}} - 72615_{5\frac{1}{2}}$					
6048.18	5	50	16529.32	+0.01	$32371^{\circ}_{2\frac{1}{2}} - 48900_{3\frac{1}{2}}$					
6045.52		6	16536.60	+0.03	$48556^{\circ}_{3\frac{1}{2}} - 65093_{3\frac{1}{2}}$					
6043.45		1	16542.26	+0.05	$55221^{\circ}_{1\frac{1}{2}} - 71763_{1\frac{1}{2}}$					
6042.22	2	100	16545.63	+0.04	$59624^{\circ}_{3\frac{1}{2}} - 76170_{2\frac{1}{2}}$					
6040.77	15	500	16549.60	+0.04	$45273^{\circ}_{3\frac{1}{2}} - 61822_{3\frac{1}{2}}$	6	1.19	1.31	0.43	1.25

TABLE 6. Yb II—*Observed and classified lines*—Continued

1	2	3	4	5	6	7	8	9	10	11
Wavelength air	Intensity		Wave number	o–c	Classification	Zeeman type	1st g	2nd g	Zeeman components	
	Meggers lamp	Thomson lamp							Strong p	Strong n
Å			K	K						
6038.82		9	16554.94	+0.09	$63028°_{1\frac{1}{2}} - 79583_{2\frac{1}{2}}$					
6029.76		1	16579.82							
6024.08	40	400	16595.45	−0.01	$41688°_{1\frac{1}{2}} - 58283_{2\frac{1}{2}}$	7	(0.784)	0.77	0	0.76
6021.92	10	400	16601.40	−0.05	$54192°_{5\frac{1}{2}} - 70793_{5\frac{1}{2}}$					
				+0.01	$59632°_{6\frac{1}{2}} - 76233_{6\frac{1}{2}}$	6	1.08	1.10	0.11	1.09
6020.55	40	400	16605.18	0.00	$41678°_{2\frac{1}{2}} - 58283_{2\frac{1}{2}}$					
6017.70		2	16613.04	+0.01	$44438°_{3\frac{1}{2}} - 61051_{3\frac{1}{2}}$					
6016.62	5	50	16616.03	−0.04	$46547°_{5\frac{1}{2}} - 63163_{4\frac{1}{2}}$					
6012.51		9	16627.38	+0.01	$61442°_{5\frac{1}{2}} - 78070_{4\frac{1}{2}}$					
6012.16	1	15	16628.35	−0.01	$47329°_{2\frac{1}{2}} - 63957_{3\frac{1}{2}}$					
6011.55		8	16630.04	−0.01	$43956°_{2\frac{1}{2}} - 60586_{1\frac{1}{2}}$					
6009.56	1	10	16635.55	−0.01	$43075°_{1\frac{1}{2}} - 59710_{1\frac{1}{2}}$					
6008.80	5	50	16637.65	−0.02	$37077°_{2\frac{1}{2}} - 53715_{3\frac{1}{2}}$					
6007.41	20	1000	16641.50	0.00	$49916°_{4\frac{1}{2}} - 66558_{3\frac{1}{2}}$	4	1.08	(1.100)	w	0.99
6004.015		10	16650.91	−0.03	$62163°_{2\frac{1}{2}} - 78814_{2\frac{1}{2}}$					
6002.52	3	90	16655.06	−0.02	$49916°_{4\frac{1}{2}} - 66571_{5\frac{1}{2}}$					
6001.05	1	30	16659.14	+0.02	$56977°_{0\frac{1}{2}} - 73636_{0\frac{1}{2}}$	6	2.20	0.71	0.745	1.45
6000.91		8	16659.53	+0.02	$65739°_{2\frac{1}{2}} - 82398_{1\frac{1}{2}}$					
5999.95	1	30	16662.19	−0.01	$56621°_{5\frac{1}{2}} - 73283_{4\frac{1}{2}}$					
5998.71		25	16665.64	−0.03	$54192°_{5\frac{1}{2}} - 70858_{4\frac{1}{2}}$					
5996.84		1	16670.83	+0.03	$56621°_{5\frac{1}{2}} - 73291_{5\frac{1}{2}}$					
5993.95		1	16678.87	−0.05	$76516_{4\frac{1}{2}} - 93195°_{3\frac{1}{2}}$					
5993.704		15	16679.55	−0.03	$56977°_{0\frac{1}{2}} - 73657_{1\frac{1}{2}}$					
5991.51	2000	6000	16685.66	−0.01	$35831°_{5\frac{1}{2}} - 52517_{5\frac{1}{2}}$	6	1.213	1.260	0.26	1.236
5990.01		10	16689.84	+0.02	$51248°_{2\frac{1}{2}} - 67938_{3\frac{1}{2}}$					
5987.91	15	500	16695.69	−0.03	$48503°_{5\frac{1}{2}} - 65199_{4\frac{1}{2}}$					
5986.78	1	40	16698.84	+0.01	$59624°_{3\frac{1}{2}} - 76323_{3\frac{1}{2}}$					
5985.35	20	300	16702.83	−0.03	$43007°_{0\frac{1}{2}} - 59710_{1\frac{1}{2}}$	5	0.16	0.82	0.32	1.15
				+0.03	$(66189°_{1\frac{1}{2}} - 82891_{2\frac{1}{2}})$					
5978.11		10	16723.06	−0.02	$56056°_{2\frac{1}{2}} - 72779_{3\frac{1}{2}}$					
5976.93		2	16726.36	−0.02	$47329°_{2\frac{1}{2}} - 64055_{2\frac{1}{2}}$					
5973.49	2	20	16736.00	−0.03	$57534°_{3\frac{1}{2}} - 74270_{2\frac{1}{2}}$					
5972.29		1	16739.36	+0.01	$55462°_{3\frac{1}{2}} - 72202_{3\frac{1}{2}}$					
5972.02		2	16740.12	−0.02	$59777°_{1\frac{1}{2}} - 76517_{1\frac{1}{2}}$					
5970.26		5	16745.05	+0.03	$46902°_{0\frac{1}{2}} - 63647_{1\frac{1}{2}}$					
5964.12		1	16762.29	+0.02	$59753°_{5\frac{1}{2}} - 76516_{4\frac{1}{2}}$					
5961.83	1	60	16768.73	−0.06	$62046°_{3\frac{1}{2}} - 78814_{2\frac{1}{2}}$	4	1.15	(1.22)	w	0.99
5959.03		7	16776.61	−0.02	$44438°_{3\frac{1}{2}} - 61214_{4\frac{1}{2}}$					
5956.86		7	16782.72	−0.07	$69443_{1\frac{1}{2}} - 86226°_{1\frac{1}{2}}$					
				+0.01	$56500°_{3\frac{1}{2}} - 73283_{4\frac{1}{2}}$					

TABLE 6. Yb II—*Observed and classified lines*—Continued

1	2	3	4	5	6	7	8	9	10	11
Wavelength air	Intensity		Wave number	o–c	Classification	Zeeman type	1st g	2nd g	Zeeman components	
	Meggers lamp	Thomson lamp							Strong p	Strong n
Å			K	K						
5950.93	5	250	16799.44	−0.02	$60649^{\circ}_{4\frac{1}{2}} - 77449_{3\frac{1}{2}}$	7?	1.13	(1.16)	w	1.03
5949.83		20	16802.55	−0.03	$56480^{\circ}_{4\frac{1}{2}} - 73283_{4\frac{1}{2}}$					
5948.98		5	16804.95	+0.03	$65594^{\circ}_{2\frac{1}{2}} - 82398_{1\frac{1}{2}}$					
5947.26	15	500	16809.81	+0.02	$45012^{\circ}_{2\frac{1}{2}} - 61822_{3\frac{1}{2}}$	5	1.32	(1.327)	0	1.34
5946.00	40	2000	16813.37	+0.02	$53322^{\circ}_{7\frac{1}{2}} - 70136_{6\frac{1}{2}}$	4	1.01	1.07	(0.03)	0.61
5944.63	1	10	16817.25	0.00	$56840^{\circ}_{1\frac{1}{2}} - 73657_{1\frac{1}{2}}$					
5943.55	5	200	16820.30	−0.07	$48272^{\circ}_{2\frac{1}{2}} - 65093_{3\frac{1}{2}}$					
5943.05	20	250	16821.72	−0.01	$45737^{\circ}_{1\frac{1}{2}} - 62559_{2\frac{1}{2}}$					
5941.29		2	16826.70	−0.04	$58162^{\circ}_{1\frac{1}{2}} - 74989_{0\frac{1}{2}}$					
5940.63		1	16828.57	−0.04	$58162^{\circ}_{1\frac{1}{2}} - 74991_{1\frac{1}{2}}$					
5939.35	2	8	16832.20							
5938.15	1	10	16835.60	0.00	$72779_{3\frac{1}{2}} - 89615^{\circ}_{2\frac{1}{2}}$					
5936.68		20	16839.77	+0.03	$47758^{\circ}_{3\frac{1}{2}} - 64598_{3\frac{1}{2}}$					
5935.05	20	1000	16844.39	0.00	$49727^{\circ}_{6\frac{1}{2}} - 66571_{5\frac{1}{2}}$	5	1.20	(1.19)	0	1.24
5934.01		1	16847.34	−0.07	$40917^{\circ}_{4\frac{1}{2}} - 57765_{4\frac{1}{2}}$					
5929.77		10	16859.39	0.00	$73283_{4\frac{1}{2}} - 90142^{\circ}_{3\frac{1}{2}}$					
5928.24		2	16863.74	−0.05	$57103^{\circ}_{3\frac{1}{2}} - 73966_{3\frac{1}{2}}$					
5920.98		2	16884.42	+0.01	$59439^{\circ}_{2\frac{1}{2}} - 76323_{3\frac{1}{2}}$					
5920.38	5	300	16886.13	−0.01	$51248^{\circ}_{2\frac{1}{2}} - 68135_{2\frac{1}{2}}$	6	1.029	1.081	(0.128)	1.06
5919.10		7	16889.78	−0.03	$58661^{\circ}_{2\frac{1}{2}} - 75550_{2\frac{1}{2}}$					
5916.95		2	16895.92	−0.04	$59753^{\circ}_{5\frac{1}{2}} - 76649_{5\frac{1}{2}}$					
5914.912	2	20	16901.74	+0.03	$51248^{\circ}_{2\frac{1}{2}} - 68150_{1\frac{1}{2}}$					
5909.33	2	10	16917.70	−0.02	$73291_{5\frac{1}{2}} - 90209^{\circ}_{4\frac{1}{2}}$					
5908.36	400	1500	16920.48	−0.03	$31979^{\circ}_{3\frac{1}{2}} - 48900_{3\frac{1}{2}}$	6	1.335	1.045	1.015	1.190
5906.33		2	16926.30	−0.02	$73283_{4\frac{1}{2}} - 90209^{\circ}_{4\frac{1}{2}}$					
5903.38	3	90	16934.76	0.00	$47663^{\circ}_{4\frac{1}{2}} - 64598_{3\frac{1}{2}}$					
5902.80		3	16936.42	−0.04	$44438^{\circ}_{3\frac{1}{2}} - 61374_{2\frac{1}{2}}$					
5900.85		20	16942.02	0.00 +0.01	$49008^{\circ}_{3\frac{1}{2}} - 65950_{4\frac{1}{2}}$ $65149^{\circ}_{0\frac{1}{2}} - 82091_{0\frac{1}{2}}$					
5898.77	15	800	16947.99	+0.01	$50468^{\circ}_{5\frac{1}{2}} - 67416_{4\frac{1}{2}}$	4	1.21	1.25	(0.021)	1.02
5897.21	50	2500	16952.47	0.00	$48923^{\circ}_{7\frac{1}{2}} - 65875_{6\frac{1}{2}}$	7	1.20	(1.205)	0	1.174
5896.63		6*d*	16954.14							
5892.30		2	16966.60	−0.04	$73750_{4\frac{1}{2}} - 90717^{\circ}_{4\frac{1}{2}}$					
5888.02		4	16978.93	0.00	$58661^{\circ}_{2\frac{1}{2}} - 75640_{3\frac{1}{2}}$					
5882.80	100	600	16994.00	−0.01	$46169^{\circ}_{4\frac{1}{2}} - 63163_{4\frac{1}{2}}$					
5874.67	2	200	17017.52	−0.07	$59632^{\circ}_{6\frac{1}{2}} - 76649_{5\frac{1}{2}}$	7			0	1.08
5873.12		10	17022.01	+0.01	$59777^{\circ}_{1\frac{1}{2}} - 76799_{1\frac{1}{2}}$					
5872.15		1	17024.82	+0.04	$76170_{2\frac{1}{2}} - 93195^{\circ}_{3\frac{1}{2}}$					
5868.94		7	17034.13	0.00	$57534^{\circ}_{3\frac{1}{2}} - 74568_{4\frac{1}{2}}$					

277-259 O - 68 - 4

TABLE 6. Yb II—*Observed and classified lines*—Continued

1	2	3	4	5	6	7	8	9	10	11
Wave-length air	Intensity		Wave number	o–c	Classification	Zeeman type	1st g	2nd g	Zeeman components	
	Meggers lamp	Thomson lamp							Strong p	Strong n
Å			K	K						
5868.34	2	100	17035.87	0.00 −0.01	$52921^{\circ}_{3\frac{1}{2}} - 69957_{4\frac{1}{2}}$ $(64169^{\circ}_{3\frac{1}{2}} - 81205_{4\frac{1}{2}})$	4	1.14	(1.112)	w	1.00
5866.69		6	17040.66	−0.02	$63417^{\circ}_{2\frac{1}{2}} - 80457_{3\frac{1}{2}}$					
5866.48		1	17041.27	−0.01	$52987^{\circ}_{1\frac{1}{2}} - 70029_{0\frac{1}{2}}$					
5865.63	1	70	17043.74	+0.01	$49419^{\circ}_{0\frac{1}{2}} - 66462_{0\frac{1}{2}}$	6	1.42	1.12	0.15	1.27
5863.86		3	17048.89							
5863.37		1	17050.31	−0.05	$47005^{\circ}_{1\frac{1}{2}} - 64055_{2\frac{1}{2}}$					
5862.90	1	15	17051.68	+0.03	$59624^{\circ}_{3\frac{1}{2}} - 76676_{2\frac{1}{2}}$					
5854.89		3	17075.01							
5854.30	5	70	17076.73	−0.01	$52880^{\circ}_{3\frac{1}{2}} - 69957_{4\frac{1}{2}}$					
5853.84		3	17078.07	−0.06	$59439^{\circ}_{2\frac{1}{2}} - 76517_{1\frac{1}{2}}$					
5852.92		5	17080.75	−0.01	$62046^{\circ}_{3\frac{1}{2}} - 79126_{4\frac{1}{2}}$					
5847.18	1	40	17097.52	−0.02	$60649^{\circ}_{4\frac{1}{2}} - 77747_{4\frac{1}{2}}$	6	1.10	1.08	0.08	1.09
5839.56		1	17119.83							
5838.62	2	70	17122.59	+0.01	$50832^{\circ}_{1\frac{1}{2}} - 67955_{0\frac{1}{2}}$	5	(0.956)	0.90	0	0.98
5837.14	600	4000	17126.93	−0.01	$32371^{\circ}_{2\frac{1}{2}} - 49498_{2\frac{1}{2}}$	6	1.172	1.148	0.06	1.160
5836.18	1	50	17129.75	0.00	$56621^{\circ}_{5\frac{1}{2}} - 73750_{4\frac{1}{2}}$					
5835.53	1	30	17131.65	+0.01	$47329^{\circ}_{2\frac{1}{2}} - 64461_{1\frac{1}{2}}$					
5833.99	5*h*	200*h*	17136.18							
5831.58		5	17143.26	0.00	$64169^{\circ}_{3\frac{1}{2}} - 81312_{2\frac{1}{2}}$					
5831.04		15	17144.85	0.00	$41678^{\circ}_{2\frac{1}{2}} - 58823_{2\frac{1}{2}}$					
5828.49		1	17152.35	+0.02	$65739^{\circ}_{2\frac{1}{2}} - 82891_{2\frac{1}{2}}$					
5824.33	2	50	17164.60	+0.03	$47758^{\circ}_{3\frac{1}{2}} - 64923_{4\frac{1}{2}}$	7	1.09	(1.10)	0	1.14
5823.36		2	17167.46	0.00	$57103^{\circ}_{3\frac{1}{2}} - 74270_{2\frac{1}{2}}$					
5819.99		3	17177.40							
5819.41	50	1500	17179.11	0.00	$46547^{\circ}_{5\frac{1}{2}} - 63726_{4\frac{1}{2}}$	4	0.98	(1.005)	w	0.84w
5814.76		2	17192.85	0.00	$57798^{\circ}_{2\frac{1}{2}} - 74991_{1\frac{1}{2}}$					
5813.58	3	40	17196.34	+0.01	$44940^{\circ}_{1\frac{1}{2}} - 62136_{0\frac{1}{2}}$	5	1.26	0.08	0.59	1.85
5811.90	1	40	17201.31	+0.06	$51248^{\circ}_{2\frac{1}{2}} - 68450_{3\frac{1}{2}}$					
5811.13	1	20	17203.59	+0.03	$56088^{\circ}_{4\frac{1}{2}} - 73291_{5\frac{1}{2}}$					
5808.66	3	120	17210.90	0.00	$47680^{\circ}_{6\frac{1}{2}} - 64891_{7\frac{1}{2}}$					
5807.86		30	17213.27	−0.02	$53644^{\circ}_{3\frac{1}{2}} - 70858_{4\frac{1}{2}}$					
5807.51	1	7	17214.31	−0.03	$59624^{\circ}_{3\frac{1}{2}} - 76839_{2\frac{1}{2}}$					
5801.50		8	17232.14	+0.02 −0.04	$47228^{\circ}_{0\frac{1}{2}} - 64461_{1\frac{1}{2}}$ $60649^{\circ}_{4\frac{1}{2}} - 77882_{3\frac{1}{2}}$					
5801.13	1	15	17233.24	0.00	$58672^{\circ}_{0\frac{1}{2}} - 75905_{0\frac{1}{2}}$					
5801.04	1	10	17233.51	+0.02	$44940^{\circ}_{1\frac{1}{2}} - 62174_{1\frac{1}{2}}$					
5799.57	1	40	17237.88	−0.01	$53716^{\circ}_{2\frac{1}{2}} - 70954_{2\frac{1}{2}}$					
5792.28	1	10	17259.57	−0.02 −0.03	$47663^{\circ}_{4\frac{1}{2}} - 64923_{4\frac{1}{2}}$ $57798^{\circ}_{2\frac{1}{2}} - 75058_{2\frac{1}{2}}$					
5789.17	2	50	17268.84	0.00	$47329^{\circ}_{2\frac{1}{2}} - 64598_{3\frac{1}{2}}$					

TABLE 6. Yb II—*Observed and classified lines*—Continued

1	2	3	4	5	6	7	8	9	10	11
Wave-length air	Intensity		Wave number	o–c	Classification	Zeeman type	1st g	2nd g	Zeeman components	
	Meggers lamp	Thomson lamp							Strong p	Strong n
Å			K	K						
5788.74	1	15	17270.13	0.00	$56480^{\circ}_{4\frac{1}{2}} - 73750_{4\frac{1}{2}}$					
5786.59	20	150	17276.54	−0.06	$59046^{\circ}_{4\frac{1}{2}} - 76323_{3\frac{1}{2}}$	5	1.08	(1.02)	w	1.30
5777.95	3	100	17302.38	+0.03	$50832^{\circ}_{1\frac{1}{2}} - 68135_{2\frac{1}{2}}$	5	(0.956)	1.08	w	1.27
5777.29	1	10	17304.35	+0.01	$48272^{\circ}_{2\frac{1}{2}} - 65577_{3\frac{1}{2}}$					
5775.61	1	50	17309.39	+0.01	$53644^{\circ}_{3\frac{1}{2}} - 70954_{2\frac{1}{2}}$					
5772.76		3	17317.93	+0.01	$50832^{\circ}_{1\frac{1}{2}} - 68150_{1\frac{1}{2}}$					
5771.66	500	2000	17321.23	−0.03	$31979^{\circ}_{3\frac{1}{2}} - 49301_{4\frac{1}{2}}$	4	1.32	1.19	(0.066)	0.72
5769.44		6	17327.90	−0.02	$64365^{\circ}_{4\frac{1}{2}} - 81692_{3\frac{1}{2}}$					
5767.95	3	30	17332.38	+0.05	$31568^{\circ}_{2\frac{1}{2}} - 48900_{3\frac{1}{2}}$					
5767.20	20	800	17334.63	+0.03	$47758^{\circ}_{3\frac{1}{2}} - 65093_{3\frac{1}{2}}$	6	1.073	0.968	0.37	1.020
5764.65	1	40	17342.30	+0.02	$49008^{\circ}_{3\frac{1}{2}} - 66351_{2\frac{1}{2}}$					
5760.18	30	20	17355.76	0.00	$24332_{2\frac{1}{2}} - 41688^{\circ}_{1\frac{1}{2}}$					
5757.84	2	15	17362.81	+0.06	$72779_{3\frac{1}{2}} - 90142^{\circ}_{3\frac{1}{2}}$					
5754.80	2	70	17371.98	+0.03	$48503^{\circ}_{5\frac{1}{2}} - 65875_{6\frac{1}{2}}$					
5753.57	1	25	17375.69	+0.04 −0.06	$52067^{\circ}_{0\frac{1}{2}} - 69443_{1\frac{1}{2}}$ $76170_{2\frac{1}{2}} - 93546^{\circ}_{2\frac{1}{2}}$					
5750.62		8	17384.61	+0.06	$44438^{\circ}_{3\frac{1}{2}} - 61822_{3\frac{1}{2}}$					
5749.91[a]	1000	400	17386.75	−0.04	$49008^{\circ}_{3\frac{1}{2}} - 66395_{2\frac{1}{2}}$					
5746.703		3	17396.46	0.00	$46547^{\circ}_{5\frac{1}{2}} - 63944_{5\frac{1}{2}}$					
5746.36	1	15	17397.50	+0.04	$53716^{\circ}_{2\frac{1}{2}} - 71113_{1\frac{1}{2}}$					
5741.75		2	17411.46	+0.06	$41678^{\circ}_{2\frac{1}{2}} - 59090_{3\frac{1}{2}}$					
5738.82		5	17420.35	+0.02	$60649^{\circ}_{4\frac{1}{2}} - 78070_{4\frac{1}{2}}$					
5737.09		20	17425.61	+0.02 +0.05	$73291_{5\frac{1}{2}} - 90717^{\circ}_{4\frac{1}{2}}$ $75550_{2\frac{1}{2}} - 92976^{\circ}_{3\frac{1}{2}}$					
5735.773	10	600	17429.61	−0.01 −0.07	$47663^{\circ}_{4\frac{1}{2}} - 65093_{3\frac{1}{2}}$ $(72779_{3\frac{1}{2}} - 90209^{\circ}_{4\frac{1}{2}})$	7	0.98	(0.973)	0	1.00
5735.50		5	17430.44	0.00	$56840^{\circ}_{1\frac{1}{2}} - 74270_{2\frac{1}{2}}$					
5734.26		3	17434.21	+0.02	$73283_{4\frac{1}{2}} - 90717^{\circ}_{4\frac{1}{2}}$					
5731.69		3	17442.02	−0.01	$62163^{\circ}_{2\frac{1}{2}} - 79605_{1\frac{1}{2}}$					
5730.001	20	1500	17447.16	+0.03 −0.02	$48503^{\circ}_{5\frac{1}{2}} - 65950_{4\frac{1}{2}}$ $(74568_{4\frac{1}{2}} - 92015^{\circ}_{4\frac{1}{2}})$	5	1.10	(1.08)	w	1.22
5727.21		5	17455.67	+0.05	$47005^{\circ}_{1\frac{1}{2}} - 64461_{1\frac{1}{2}}$					
5726.49		2	17457.86	+0.06	$79628_{3\frac{1}{2}} - 97086^{\circ}_{4\frac{1}{2}}$					
5724.21		3	17464.81	+0.02	$62163^{\circ}_{2\frac{1}{2}} - 79628_{3\frac{1}{2}}$					
5722.743		8	17469.29	+0.07	$59046^{\circ}_{4\frac{1}{2}} - 76516_{4\frac{1}{2}}$					
5717.25	10	300	17486.08	+0.04	$56480^{\circ}_{4\frac{1}{2}} - 73966_{3\frac{1}{2}}$	7	0.75	(0.763)	0	0.72
5716.70		2	17487.76	+0.02	$64169^{\circ}_{3\frac{1}{2}} - 81657_{2\frac{1}{2}}$					
5713.73	20	500	17496.85	+0.03	$45737^{\circ}_{1\frac{1}{2}} - 63234_{2\frac{1}{2}}$	4	(1.33)	1.21	w	1.03
5713.270	4	15	17498.26	+0.04	$35019^{\circ}_{4\frac{1}{2}} - 52517_{5\frac{1}{2}}$					
5712.844		15	17499.56	+0.03	$49916^{\circ}_{4\frac{1}{2}} - 67416_{4\frac{1}{2}}$					

TABLE 6. Yb II—*Observed and classified lines*—Continued

1	2	3	4	5	6	7	8	9	10	11
Wave-length air	Intensity		Wave number	o–c	Classification	Zeeman type	1st g	2nd g	Zeeman components	
	Meggers lamp	Thomson lamp							Strong p	Strong n
Å			K	K						
5710.733		25	17506.03	+0.05	$53716^{\circ}_{2\frac{1}{2}} - 71222_{3\frac{1}{2}}$					
5710.403	1	15	17507.04	+0.09	$59777^{\circ}_{1\frac{1}{2}} - 77284_{1\frac{1}{2}}$					
5709.715		2	17509.15	+0.03	$58661^{\circ}_{2\frac{1}{2}} - 76170_{2\frac{1}{2}}$					
5706.773	10	100	17518.18	+0.04	$31979^{\circ}_{3\frac{1}{2}} - 49498_{2\frac{1}{2}}$					
5704.98	2	70	17523.68	+0.02	$57534^{\circ}_{3\frac{1}{2}} - 75058_{2\frac{1}{2}}$	5	0.81	(0.76)	w	0.92
5704.14		3	17526.26	+0.02	$45335^{\circ}_{4\frac{1}{2}} - 62861_{5\frac{1}{2}}$					
5699.02		15	17542.01	−0.01	$48024^{\circ}_{1\frac{1}{2}} - 65566_{0\frac{1}{2}}$					
5697.65		2	17546.23	0.00	$45012^{\circ}_{2\frac{1}{2}} - 62559_{2\frac{1}{2}}$					
5696.717		5	17549.10	+0.03	$49008^{\circ}_{3\frac{1}{2}} - 66558_{3\frac{1}{2}}$					
5695.22		2	17553.71	+0.08	$53716^{\circ}_{2\frac{1}{2}} - 71270_{2\frac{1}{2}}$					
5694.906		15	17554.68	+0.06	$60910^{\circ}_{1\frac{1}{2}} - 78464_{1\frac{1}{2}}$					
5694.13		1	17557.07	+0.02	$46169^{\circ}_{4\frac{1}{2}} - 63726_{4\frac{1}{2}}$					
5693.694	10	400	17558.42	+0.05	$46902^{\circ}_{0\frac{1}{2}} - 64461_{1\frac{1}{2}}$	7	1.25	(1.176)	0	1.14
5689.67	3	70	17570.84	+0.05	$41688^{\circ}_{1\frac{1}{2}} - 59259_{2\frac{1}{2}}$					
5687.14	1*d*	20*d*	17578.65	−0.02	$43007^{\circ}_{0\frac{1}{2}} - 60586_{1\frac{1}{2}}$					
5686.53	80	800	17580.54	+0.03	$41678^{\circ}_{2\frac{1}{2}} - 59259_{2\frac{1}{2}}$	6	1.12	1.06	0.17	1.09
5685.832	1	9	17582.70	+0.06	$62046^{\circ}_{3\frac{1}{2}} - 79628_{3\frac{1}{2}}$					
5683.56	10	300	17589.73	+0.10 −0.07	$46354^{\circ}_{4\frac{1}{2}} - 63944_{5\frac{1}{2}}$ $(76839_{2\frac{1}{2}} - 94428^{\circ}_{1\frac{1}{2}})$					
5679.270	1	15	17603.01	+0.10	$59046^{\circ}_{4\frac{1}{2}} - 76649_{5\frac{1}{2}}$?					
5679.180	2	8	17603.29	+0.04	$46354^{\circ}_{4\frac{1}{2}} - 63957_{3\frac{1}{2}}$					
5675.180	2	50	17615.70	+0.01	$48272^{\circ}_{2\frac{1}{2}} - 65888_{1\frac{1}{2}}$					
5674.31	10	150	17618.40	−0.01	$44940^{\circ}_{1\frac{1}{2}} - 62559_{2\frac{1}{2}}$	7	(1.244)	1.22	0	1.18
5672.37		2	17624.42	+0.01	$65739^{\circ}_{2\frac{1}{2}} - 83363_{3\frac{1}{2}}$					
5672.16		8	17625.08	−0.04	$53644^{\circ}_{3\frac{1}{2}} - 71270_{2\frac{1}{2}}$					
5665.34		1	17646.29	+0.02	$66571_{5\frac{1}{2}} - 84217^{\circ}_{4\frac{1}{2}}$					
5660.152		4	17662.47	−0.04	$56088^{\circ}_{4\frac{1}{2}} - 73750_{4\frac{1}{2}}$					
5654.27	2	150	17680.84	+0.01	$50468^{\circ}_{5\frac{1}{2}} - 68148_{5\frac{1}{2}}$	7	(1.213)	1.19	0	1.20
5653.24	3	200	17684.06	+0.05 −0.05	$61442^{\circ}_{5\frac{1}{2}} - 79126_{4\frac{1}{2}}$ $78070_{4\frac{1}{2}} - 95754^{\circ}_{5\frac{1}{2}}$	7			0	1.14
5651.985	1000	4000	17687.99	+0.01	$30224^{\circ}_{4\frac{1}{2}} - 47912_{3\frac{1}{2}}$	4	0.93	1.29	0.18	−0.36
5637.812	80	600	17732.46	+0.06	$34784^{\circ}_{5\frac{1}{2}} - 52517_{5\frac{1}{2}}$	6	1.11	1.26	0.84	1.18
5637.33	1	6	17733.97	0.00	$45429^{\circ}_{3\frac{1}{2}} - 63163_{4\frac{1}{2}}$					
5634.45		1	17743.04	+0.02	$58162^{\circ}_{1\frac{1}{2}} - 75905_{0\frac{1}{2}}$					
5631.496	2	90	17752.34	+0.02 −0.09	$53716^{\circ}_{2\frac{1}{2}} - 71468_{2\frac{1}{2}}$ $57798^{\circ}_{2\frac{1}{2}} - 75550_{2\frac{1}{2}}$					
5627.89	4	200	17763.72	+0.02	$47329^{\circ}_{2\frac{1}{2}} - 65093_{3\frac{1}{2}}$	7	(0.990)	0.99	0	0.99
5624.494		10	17774.44	+0.04	$46169^{\circ}_{4\frac{1}{2}} - 63944_{5\frac{1}{2}}$					
5620.88	1	70	17785.87	+0.03	$49419^{\circ}_{0\frac{1}{2}} - 67204_{1\frac{1}{2}}$					
5620.19	50	700	17788.05	+0.03	$46169^{\circ}_{4\frac{1}{2}} - 63957_{3\frac{1}{2}}$	4	1.09	(1.148)	w	0.88

TABLE 6. Yb II—*Observed and classified lines*—Continued

1	2	3	4	5	6	7	8	9	10	11
Wave-length air	Intensity		Wave number	o–c	Classification	Zeeman type	1st g	2nd g	Zeeman components	
	Meggers lamp	Thomson lamp							Strong p	Strong n
Å			K	K						
5618.55		1	17793.25							
5609.89		1	17820.71	+0.04	$55462^{\circ}_{3\frac{1}{2}} - 73283_{4\frac{1}{2}}$					
5608.914	1	50	17823.82	+0.01	$53644^{\circ}_{3\frac{1}{2}} - 71468_{2\frac{1}{2}}$					
5608.64		2	17824.69	+0.03	$59624^{\circ}_{3\frac{1}{2}} - 77449_{3\frac{1}{2}}$					
5607.91		1	17827.01							
5607.345	10	150	17828.80	+0.04	$45335^{\circ}_{4\frac{1}{2}} - 63163_{4\frac{1}{2}}$					
5607.124		4	17829.51	0.00	$59777^{\circ}_{1\frac{1}{2}} - 77606_{2\frac{1}{2}}$					
5606.64		1	17831.04	+0.02	$51248^{\circ}_{2\frac{1}{2}} - 69079_{2\frac{1}{2}}$					
5604.145		9	17838.98	+0.03	$58484^{\circ}_{4\frac{1}{2}} - 76323_{3\frac{1}{2}}$					
5602.35	2	20	17844.70	+0.02	$58672^{\circ}_{0\frac{1}{2}} - 76517_{1\frac{1}{2}}$					
5602.264	3	40	17844.97	+0.03	$59439^{\circ}_{2\frac{1}{2}} - 77284_{1\frac{1}{2}}$					
5588.452	500	4000	17889.08	+0.05	$35831^{\circ}_{5\frac{1}{2}} - 53720_{4\frac{1}{2}}$					
5585.248		20	17899.34	−0.01	$64191^{\circ}_{1\frac{1}{2}} - 82091_{0\frac{1}{2}}$					
5583.57		1	17904.72	0.00	$60910^{\circ}_{1\frac{1}{2}} - 78814_{2\frac{1}{2}}$					
5582.236		2	17909.00	−0.01	$70793_{5\frac{1}{2}} - 88702^{\circ}_{5\frac{1}{2}}$					
5581.778		8	17910.47	+0.03	$45737^{\circ}_{1\frac{1}{2}} - 63467_{1\frac{1}{2}}$					
5581.05	2	40	17912.80							
5580.79	20	700	17913.64	+0.05	$47663^{\circ}_{4\frac{1}{2}} - 65577_{3\frac{1}{2}}$					
5578.483		4	17921.04	−0.02	$64970^{\circ}_{3\frac{1}{2}} - 82891_{2\frac{1}{2}}$					
5575.705	10	100	17929.97	+0.01	$31568^{\circ}_{2\frac{1}{2}} - 49498_{2\frac{1}{2}}$					
5573.64		1	17936.62	+0.06	$52921^{\circ}_{3\frac{1}{2}} - 70858_{4\frac{1}{2}}$					
5572.528	30	300	17940.20	+0.03	$41678^{\circ}_{2\frac{1}{2}} - 59618_{3\frac{1}{2}}$					
5566.04		3	17961.11	+0.02	$45273^{\circ}_{3\frac{1}{2}} - 63234_{2\frac{1}{2}}$					
				−0.06	$52067^{\circ}_{0\frac{1}{2}} - 70029_{0\frac{1}{2}}$					
5564.352		3	17966.56	+0.05	$52987^{\circ}_{1\frac{1}{2}} - 70954_{2\frac{1}{2}}$					
5559.58		1	17981.98	+0.06	$59624^{\circ}_{3\frac{1}{2}} - 77606_{2\frac{1}{2}}$					
5554.30		4	17999.07	+0.01	$45012^{\circ}_{2\frac{1}{2}} - 63011_{1\frac{1}{2}}$					
5551.69		2	18007.53	+0.03	$58162^{\circ}_{1\frac{1}{2}} - 76170_{2\frac{1}{2}}$					
5550.37		7	18011.81	+0.03	$56977^{\circ}_{0\frac{1}{2}} - 74989_{0\frac{1}{2}}$					
5549.79		20	18013.70	+0.03	$68135_{2\frac{1}{2}} - 86148^{c}_{2\frac{1}{2}}$					
				+0.05	$56977^{\circ}_{0\frac{1}{2}} - 74991_{1\frac{1}{2}}$					
5549.32		1	18015.22	+0.04	$58661^{\circ}_{2\frac{1}{2}} - 76676_{2\frac{1}{2}}$					
5548.918		50	18016.53	+0.04	$57534^{\circ}_{3\frac{1}{2}} - 75550_{2\frac{1}{2}}$					
5547.16	50	500	18022.24	+0.04	$41688^{\circ}_{1\frac{1}{2}} - 59710_{1\frac{1}{2}}$	7			0	0.75
				+0.06	$49916^{\circ}_{4\frac{1}{2}} - 67938_{3\frac{1}{2}}$					
5544.17		1*h*	18031.96	+0.04	$41678^{\circ}_{2\frac{1}{2}} - 59710_{1\frac{1}{2}}$					
5543.96		8	18032.64	−0.01	$52921^{\circ}_{3\frac{1}{2}} - 70954_{2\frac{1}{2}}$					
5540.03		10	18045.43	+0.03	$43075^{\circ}_{1\frac{1}{2}} - 61120_{0\frac{1}{2}}$					
5533.21		7	18067.67	−0.09	$48503^{\circ}_{5\frac{1}{2}} - 66571_{5\frac{1}{2}}$					
5533.14		10	18067.90	−0.04	$56500^{\circ}_{3\frac{1}{2}} - 74568_{4\frac{1}{2}}$					
5532.111		3	18071.26	+0.02	$44940^{\circ}_{1\frac{1}{2}} - 63011_{1\frac{1}{2}}$					

TABLE 6. Yb II—*Observed and classified lines*—Continued

1	2	3	4	5	6	7	8	9	10	11
Wave-length air	Intensity		Wave number	o–c	Classification	Zeeman type	1st g	2nd g	Zeeman components	
	Meggers lamp	Thomson lamp							Strong p	Strong n
Å			K	K						
5530.73	1	1	18075.78	+0.04	$68150_{1\frac{1}{2}} - 86226^{\circ}_{1\frac{1}{2}}$					
5529.92	4	150	18078.42	−0.02	$48272^{\circ}_{2\frac{1}{2}} - 66351_{2\frac{1}{2}}$	7	1.12	(1.125)	0	1.12
5529.08	5	250	18081.17	−0.01	$50468^{\circ}_{5\frac{1}{2}} - 68549_{4\frac{1}{2}}$	5	1.21	(1.157)	w	1.44
5521.61		3	18105.63	+0.02	$57534^{\circ}_{3\frac{1}{2}} - 75640_{3\frac{1}{2}}$					
5520.22	1	50	18110.19	−0.04	$59777^{\circ}_{1\frac{1}{2}} - 77887_{0\frac{1}{2}}$	4	1.63	2.21	0.29	1.34
5519.83		2	18111.47							
5516.334		10	18122.95	0.00	$48272^{\circ}_{2\frac{1}{2}} - 66395_{2\frac{1}{2}}$					
5515.38		3	18126.08	0.00	$52987^{\circ}_{1\frac{1}{2}} - 71113_{1\frac{1}{2}}$					
5511.764	1	30	18137.97	+0.03	$58661^{\circ}_{2\frac{1}{2}} - 76799_{1\frac{1}{2}}$	7	(0.86)	0.83	0	0.90
5511.401	2	70	18139.17	0.00	$54640^{\circ}_{4\frac{1}{2}} - 72779_{3\frac{1}{2}}$				0	1.20
5509.198		20	18146.42	+0.08	$51248^{\circ}_{2\frac{1}{2}} - 69395_{3\frac{1}{2}}$					
5509.046		3	18146.92	+0.03 +0.05	$71468_{2\frac{1}{2}} - 89615^{\circ}_{2\frac{1}{2}}$ $76676_{2\frac{1}{2}} - 94823^{\circ}_{1\frac{1}{2}}$					
5508.266		20	18149.49	+0.04 +0.06	$56840^{\circ}_{1\frac{1}{2}} - 74989_{0\frac{1}{2}}$ $(53120^{\circ}_{2\frac{1}{2}} - 71270_{2\frac{1}{2}})$	5	0.83	0.27	0.28?	1.11
5507.70		1	18151.36	+0.04	$56840^{\circ}_{1\frac{1}{2}} - 74991_{1\frac{1}{2}}$					
5502.802	1	10	18167.51	+0.01	$59439^{\circ}_{2\frac{1}{2}} - 77606_{2\frac{1}{2}}$					
5501.37	2	20	18172.24	+0.02	$40917^{\circ}_{4\frac{1}{2}} - 59090_{3\frac{1}{2}}$					
5499.65		2	18177.93	+0.06	$58661^{\circ}_{2\frac{1}{2}} - 76839_{2\frac{1}{2}}$					
5498.390		3	18182.09	0.00	$58051^{\circ}_{5\frac{1}{2}} - 76233_{6\frac{1}{2}}$					
5494.58		1	18194.70	+0.04	$51248^{\circ}_{2\frac{1}{2}} - 69443_{1\frac{1}{2}}$					
5494.364	1	10	18195.41	+0.04	$47680^{\circ}_{6\frac{1}{2}} - 65875_{6\frac{1}{2}}$					
5490.847		3	18207.07	+0.06	$64191^{\circ}_{1\frac{1}{2}} - 82398_{1\frac{1}{2}}$					
5488.883		8	18213.58	+0.01	$56056^{\circ}_{2\frac{1}{2}} - 74270_{2\frac{1}{2}}$					
5487.512	1	9	18218.13	+0.06	$56840^{\circ}_{1\frac{1}{2}} - 75058_{2\frac{1}{2}}$					
5486.535	7	150	18221.38	+0.06	$45012^{\circ}_{2\frac{1}{2}} - 63234_{2\frac{1}{2}}$	6	1.286	1.214	0.18	1.25
5483.212		3	18232.42	+0.04	$49916^{\circ}_{4\frac{1}{2}} - 68148_{5\frac{1}{2}}$					
5479.806	1	50	18243.75	+0.02	$46354^{\circ}_{4\frac{1}{2}} - 64598_{3\frac{1}{2}}$					
5479.122		2*d*	18246.03							
5478.50	100	1500	18248.10	+0.01	$40035^{\circ}_{3\frac{1}{2}} - 58283_{2\frac{1}{2}}$	4	(0.72)	0.77	w	0.60
5477.206		9	18252.41	+0.02	$50468^{\circ}_{5\frac{1}{2}} - 68720_{6\frac{1}{2}}$					
5475.706		10	18257.41	+0.03	$59624^{\circ}_{3\frac{1}{2}} - 77882_{3\frac{1}{2}}$					
5475.132		4	18259.33							
5471.17	30	400	18272.55	+0.05	$45429^{\circ}_{3\frac{1}{2}} - 63702_{2\frac{1}{2}}$	5	1.15	1.08	(0.036)	1.33
5468.260		3	18282.27	+0.02	$52987^{\circ}_{1\frac{1}{2}} - 71270_{2\frac{1}{2}}$					
5467.495	1	9	18284.83							
5466.714	1	25	18287.44	+0.01	$47663^{\circ}_{4\frac{1}{2}} - 65950_{4\frac{1}{2}}$					
5464.894	6	200	18293.53	+0.03 −0.03	$44940^{\circ}_{1\frac{1}{2}} - 63234_{2\frac{1}{2}}$ $(47912_{3\frac{1}{2}} - 66205^{\circ}_{2\frac{1}{2}})$	7	1.21	(1.208)	0	1.21

TABLE 6. Yb II—*Observed and classified lines*—Continued

1	2	3	4	5	6	7	8	9	10	11
Wave-length air	Intensity		Wave number	o–c	Classification	Zeeman type	1st g	2nd g	Zeeman components	
	Meggers lamp	Thomson lamp							Strong p	Strong n
Å			K	K						
5463.850		3	18297.03	+0.02	$45429°_{3\frac{1}{2}} - 63726_{4\frac{1}{2}}$					
5463.12		10	18299.47	−0.06 +0.07	$42915°_{5\frac{1}{2}} - 61214_{4\frac{1}{2}}$ $43075°_{1\frac{1}{2}} - 61374_{2\frac{1}{2}}$					
5458.088	2	60	18316.34	−0.01	$59753°_{5\frac{1}{2}} - 78070_{4\frac{1}{2}}$					
5457.427	4	150	18318.56	+0.03	$45737°_{1\frac{1}{2}} - 64055_{2\frac{1}{2}}$					
5455.046	5	250	18326.56	+0.05	$48024°_{1\frac{1}{2}} - 66351_{2\frac{1}{2}}$	4	1.365	1.119	0.123	0.75
5449.84		1	18344.06							
5449.270	500	2500	18345.98	+0.02	$35059°_{3\frac{1}{2}} - 53404_{2\frac{1}{2}}$	5	(1.124)	1.04	*w*	1.33
5448.565		4	18348.36	−0.03	$52921°_{3\frac{1}{2}} - 71270_{2\frac{1}{2}}$					
5445.492	1	40	18358.71	+0.03	$51248°_{2\frac{1}{2}} - 69607_{2\frac{1}{2}}$					
5441.615	2	5	18371.79	+0.05	$57798°_{2\frac{1}{2}} - 76170_{2\frac{1}{2}}$					
5440.548	10	200	18375.39	0.00	$46547°_{5\frac{1}{2}} - 64923_{4\frac{1}{2}}$					
5435.27		6	18393.24	+0.10 +0.01	$64970°_{3\frac{1}{2}} - 83363_{3\frac{1}{2}}$ $71222_{3\frac{1}{2}} - 89615°_{2\frac{1}{2}}$					
5432.71	60	1500	18401.91	+0.06	$47680°_{6\frac{1}{2}} - 66082_{5\frac{1}{2}}$	4	1.12	(1.141)	0	0.985
5431.167	2	80	18407.13	+0.03	$49008°_{3\frac{1}{2}} - 67416_{4\frac{1}{2}}$					
5429.838		8	18411.64	0.00	$62046°_{3\frac{1}{2}} - 80457_{3\frac{1}{2}}$					
5426.867	30	900	18421.72	+0.03	$49727°_{6\frac{1}{2}} - 68148_{5\frac{1}{2}}$	7	(1.20)	1.20	0	1.175
5424.627	30	300	18429.32	+0.02	$45273°_{3\frac{1}{2}} - 63702_{2\frac{1}{2}}$	5	1.20	1.08	(0.06)	1.51
5422.715		1	18435.82	−0.01	$55221°_{1\frac{1}{2}} - 73657_{1\frac{1}{2}}$					
5420.608		7	18442.99	+0.03	$59439°_{2\frac{1}{2}} - 77882_{3\frac{1}{2}}$					
5417.421		9	18453.84	+0.03	$45273°_{3\frac{1}{2}} - 63726_{4\frac{1}{2}}$					
5414.258	6	200	18464.62	+0.02	$58051°_{5\frac{1}{2}} - 76516_{4\frac{1}{2}}$	7	0.98	(1.01)	0	0.87
5411.038	1	40	18475.61	+0.01	$50468°_{5\frac{1}{2}} - 68943_{4\frac{1}{2}}$					
5410.635		15	18476.98	+0.01	$60649°_{4\frac{1}{2}} - 79126_{4\frac{1}{2}}$					
5409.473	2	60	18480.95	+0.01	$52987°_{1\frac{1}{2}} - 71468_{2\frac{1}{2}}$	4	(1.13)	1.02	*w*	0.86
5408.092		4	18485.67	+0.02	$53716°_{2\frac{1}{2}} - 72202_{3\frac{1}{2}}$					
5402.706		3	18504.10	−0.03	$55462°_{3\frac{1}{2}} - 73966_{3\frac{1}{2}}$					
5399.71	50	500	18514.37	+0.03	$44497°_{2\frac{1}{2}} - 63011_{1\frac{1}{2}}$	7	(0.734)	0.78	0	0.67
5397.23		1	18522.87							
5395.73	20	300	18528.02	+0.04	$45429°_{3\frac{1}{2}} - 63957_{3\frac{1}{2}}$	7	(1.150)	1.17	0	1.16
5394.084		3	18533.68	+0.07	$49916°_{4\frac{1}{2}} - 68450_{3\frac{1}{2}}$					
5393.37	5	150	18536.13	+0.03	$49419°_{0\frac{1}{2}} - 67955_{0\frac{1}{2}}$	6	1.40	0.90	0.25	1.15
5390.18		6	18547.10	+0.02	$52921°_{3\frac{1}{2}} - 71468_{2\frac{1}{2}}$					
5389.84	200	800	18548.27	+0.02	$34389°_{2\frac{1}{2}} - 52938_{1\frac{1}{2}}$	5	(1.007)	0.90	*w*	1.17
5386.72	1	50	18559.01	−0.01	$47329°_{2\frac{1}{2}} - 65888_{1\frac{1}{2}}$					
5386.07		10	18561.25	−0.01	$47005°_{1\frac{1}{2}} - 65566_{0\frac{1}{2}}$					
5384.48	5	50	18566.73	0.00	$70136_{6\frac{1}{2}} - 88702°_{5\frac{1}{2}}$	5	(1.07)	1.03	*w*	1.32
5383.95	3	60	18568.56	0.00	$46354°_{4\frac{1}{2}} - 64923_{4\frac{1}{2}}$					
5376.97	5	250	18592.66	−0.01	$47758°_{3\frac{1}{2}} - 66351_{2\frac{1}{2}}$	7	1.11	(1.125)	0	1.07

TABLE 6. Yb II—*Observed and classified lines*—Continued

1	2	3	4	5	6	7	8	9	10	11
Wavelength air	Intensity		Wave number	o–c	Classification	Zeeman type	1st g	2nd g	Zeeman components	
	Meggers lamp	Thomson lamp							Strong p	Strong n
Å			K	K						
5371.53		4	18611.49	0.00	$58672^{\circ}_{0\frac{1}{2}} - 77284_{1\frac{1}{2}}$					
5370.47		9	18615.17							
5368.28	50	400	18622.76	−0.01	$45335^{\circ}_{4\frac{1}{2}} - 63957_{3\frac{1}{2}}$	4	0.875	0.969	(0.047)	0.546
5367.78	10	100	18624.50	+0.02	$37077^{\circ}_{2\frac{1}{2}} - 55702_{1\frac{1}{2}}$					
5367.35	4	60	18625.99	−0.01	$45429^{\circ}_{3\frac{1}{2}} - 64055_{2\frac{1}{2}}$	7	1.11	(1.108)	0	1.17
5365.41	1	50	18632.72	−0.01	$49916^{\circ}_{4\frac{1}{2}} - 68549_{4\frac{1}{2}}$					
5364.78		15	18634.91	−0.03	$45012^{\circ}_{2\frac{1}{2}} - 63647_{1\frac{1}{2}}$					
5364.12		15	18637.20	+0.02	$47758^{\circ}_{3\frac{1}{2}} - 66395_{2\frac{1}{2}}$					
5362.43	1	20	18643.08	−0.01	$53120^{\circ}_{2\frac{1}{2}} - 71763_{1\frac{1}{2}}$					
5360.85		1	18648.57	−0.05	$74270_{2\frac{1}{2}} - 92919^{\circ}_{3\frac{1}{2}}$					
5360.10	1	30	18651.18	+0.05	$54640^{\circ}_{4\frac{1}{2}} - 73291_{5\frac{1}{2}}$					
5359.91	6	200	18651.84	+0.02	$46547^{\circ}_{5\frac{1}{2}} - 65199_{4\frac{1}{2}}$					
5358.64	400	2000	18656.26	0.00	$35059^{\circ}_{3\frac{1}{2}} - 53715_{3\frac{1}{2}}$	6	1.11	1.17	0.20	1.14
5357.71		3	18659.50	0.00	$47228^{\circ}_{0\frac{1}{2}} - 65888_{1\frac{1}{2}}$					
5357.08	20	200	18661.70	−0.01	$35059^{\circ}_{3\frac{1}{2}} - 53720_{4\frac{1}{2}}$					
5356.54	1	2	18663.58	+0.06	$75640_{3\frac{1}{2}} - 94303^{\circ}_{3\frac{1}{2}}$					
5356.41		10	18664.03	+0.02	$46902^{\circ}_{0\frac{1}{2}} - 65566_{0\frac{1}{2}}$					
5352.95	1000	6000	18676.09	+0.01	$30224^{\circ}_{4\frac{1}{2}} - 48900_{3\frac{1}{2}}$	4	0.934	1.048	0.057	0.535
5350.474	2	40	18684.74	−0.04	$45273^{\circ}_{3\frac{1}{2}} - 63957_{3\frac{1}{2}}$					
5349.626		5	18687.70	+0.01	$59777^{\circ}_{1\frac{1}{2}} - 78464_{1\frac{1}{2}}$					
5349.10	1	6	18689.54	+0.01	$45012^{\circ}_{2\frac{1}{2}} - 63702_{2\frac{1}{2}}$					
5347.22	1000	3000	18696.11	−0.02	$35019^{\circ}_{4\frac{1}{2}} - 53715_{3\frac{1}{2}}$	4	1.16	1.19	(0.014)	1.06
5345.83	200	900	18700.97	−0.02	$40917^{\circ}_{4\frac{1}{2}} - 59618_{3\frac{1}{2}}$					
5345.66	400	1500	18701.56	−0.02	$35019^{\circ}_{4\frac{1}{2}} - 53720_{4\frac{1}{2}}$					
5342.99		7	18710.91	+0.01	$56840^{\circ}_{1\frac{1}{2}} - 75550_{2\frac{1}{2}}$					
5339.69		1	18722.47	+0.06	$64169^{\circ}_{3\frac{1}{2}} - 82891_{2\frac{1}{2}}$					
5339.312		15	18723.80	+0.01	$45737^{\circ}_{1\frac{1}{2}} - 64461_{1\frac{1}{2}}$					
				−0.01	$73291_{5\frac{1}{2}} - 92015^{\circ}_{4\frac{1}{2}}$					
5338.75	10	100	18725.77	+0.01	$44438^{\circ}_{3\frac{1}{2}} - 63163_{4\frac{1}{2}}$	7	1.10	1.13	0	1.22
5337.11		7	18731.52	+0.08	$49419^{\circ}_{0\frac{1}{2}} - 68150_{1\frac{1}{2}}$					
5335.15	2000	7000	18738.40	+0.03	$30562^{\circ}_{5\frac{1}{2}} - 49301_{4\frac{1}{2}}$	4	1.10	1.16	(0.03)	0.83
5334.02	100	200	18742.37	−0.03	$24332_{2\frac{1}{2}} - 43075^{\circ}_{1\frac{1}{2}}$					
5331.536		20	18751.10							
5330.92		1	18753.27	−0.06	$46169^{\circ}_{4\frac{1}{2}} - 64923_{4\frac{1}{2}}$					
5328.526	3	50	18761.70	−0.01	$44940^{\circ}_{4\frac{1}{2}} - 63702_{2\frac{1}{2}}$					
5324.778		7	18774.90	+0.01	$50832^{\circ}_{1\frac{1}{2}} - 69607_{2\frac{1}{2}}$					
5324.486		9	18775.93	+0.02	$52987^{\circ}_{1\frac{1}{2}} - 71763_{1\frac{1}{2}}$					
5322.541		8	18782.79	−0.01	$45273^{\circ}_{3\frac{1}{2}} - 64055_{2\frac{1}{2}}$					
5321.14	10	250	18787.74	−0.02	$40035^{\circ}_{3\frac{1}{2}} - 58823_{2\frac{1}{2}}$					

TABLE 6. Yb II—*Observed and classified lines*—Continued

1	2	3	4	5	6	7	8	9	10	11
Wave-length air	Intensity		Wave number	o–c	Classification	Zeeman type	1st g	2nd g	Zeeman components	
	Meggers lamp	Thomson lamp							Strong p	Strong n
Å			K	K						
5320.774		15	18789.03	−0.01	$57534^{\circ}_{3\frac{1}{2}} - 76323_{3\frac{1}{2}}$					
5318.79		1	18796.04	−0.04	$44438^{\circ}_{3\frac{1}{2}} - 63234_{2\frac{1}{2}}$					
5315.462		6	18807.81	+0.01	$55462^{\circ}_{3\frac{1}{2}} - 74270_{2\frac{1}{2}}$					
5309.31	30	200	18829.60	+0.01	$34575^{\circ}_{1\frac{1}{2}} - 53404_{2\frac{1}{2}}$	4	1.43	1.03	0.20	0.43
5307.74		6	18835.17	+0.02	$59046^{\circ}_{4\frac{1}{2}} - 77882_{3\frac{1}{2}}$					
5306.506		40	18839.55	+0.01	$49916^{\circ}_{4\frac{1}{2}} - 68756_{3\frac{1}{2}}$					
5300.935	100	2000	18859.35	+0.03	$37516^{\circ}_{3\frac{1}{2}} - 56375_{2\frac{1}{2}}$	4	1.10	1.20	(0.05)	0.85
5295.755		5	18877.80	0.00 −0.06	$57798^{\circ}_{2\frac{1}{2}} - 76676_{2\frac{1}{2}}$ $75550_{2\frac{1}{2}} - 94428^{c}_{1\frac{1}{2}}$					
5293.726		3	18885.03	+0.01	$56088^{\circ}_{4\frac{1}{2}} - 74973_{3\frac{1}{2}}$					
5291.99		10	18891.23	+0.05	$47680^{\circ}_{6\frac{1}{2}} - 66571_{5\frac{1}{2}}$					
5291.077		5	18894.49	+0.01	$47663^{\circ}_{4\frac{1}{2}} - 66558_{3\frac{1}{2}}$					
5290.08	2	20	18898.05	+0.04	$41688^{\circ}_{1\frac{1}{2}} - 60586_{1\frac{1}{2}}$					
5289.45		2	18900.30							
5289.178	1	5	18901.27							
5287.285	5	100	18908.04	−0.02	$47663^{\circ}_{4\frac{1}{2}} - 66571_{5\frac{1}{2}}$					
5286.12	2	100	18912.20	−0.01	$48503^{\circ}_{5\frac{1}{2}} - 67416_{4\frac{1}{2}}$					
5283.825		3	18920.42	+0.04	$71222_{3\frac{1}{2}} - 90142^{c}_{3\frac{1}{2}}$					
5283.00		1	18923.37	+0.01	$46169^{\circ}_{4\frac{1}{2}} - 65093_{3\frac{1}{2}}$					
5281.210		20	18929.79	+0.04	$49008^{\circ}_{3\frac{1}{2}} - 67938_{3\frac{1}{2}}$					
5280.522	1	50	18932.25	+0.05	$48272^{\circ}_{2\frac{1}{2}} - 67204_{1\frac{1}{2}}$					
5279.53	1000	5000	18935.81	+0.05	$34784^{\circ}_{5\frac{1}{2}} - 53720_{4\frac{1}{2}}$	4	1.10	1.23	(0.066)	1.51
5265.63		8	18985.80	+0.05	$46902^{\circ}_{0\frac{1}{2}} - 65888_{1\frac{1}{2}}$					
5263.570	6	200	18993.23	−0.02	$49727^{\circ}_{6\frac{1}{2}} - 68720_{6\frac{1}{2}}$	6	1.20	1.16	0.26	1.18
5262.012	1	30	18998.85	−0.03	$64365^{\circ}_{4\frac{1}{2}} - 83363_{3\frac{1}{2}}$					
5261.52		1	19000.63	+0.07	$57798^{\circ}_{2\frac{1}{2}} - 76799_{1\frac{1}{2}}$					
5259.65		1	19007.38							
5257.490	800	3000	19015.19	−0.01	$34389^{\circ}_{2\frac{1}{2}} - 53404_{2\frac{1}{2}}$	6	1.01	1.03	0.06	1.02
5256.85		20	19017.51							
5255.680	4	150	19021.74	−0.03	$47329^{\circ}_{2\frac{1}{2}} - 66351_{2\frac{1}{2}}$					
5254.60		3	19025.65	−0.03	$59439^{\circ}_{2\frac{1}{2}} - 78464_{1\frac{1}{2}}$					
5254.20	1	20	19027.10	−0.05	$49916^{\circ}_{4\frac{1}{2}} - 68943_{4\frac{1}{2}}$					
5250.51	1	8	19040.47	−0.02	$57798^{\circ}_{2\frac{1}{2}} - 76839_{2\frac{1}{2}}$					
5249.80	5	150	19043.04	+0.01	$45012^{\circ}_{2\frac{1}{2}} - 64055_{2\frac{1}{2}}$					
5248.99		6	19045.98	+0.01	$52067^{\circ}_{0\frac{1}{2}} - 71113_{1\frac{1}{2}}$					
5248.17		1	19048.96	−0.06	$55221^{\circ}_{1\frac{1}{2}} - 74270_{2\frac{1}{2}}$					
5246.39	4	40	19055.42	−0.02	$43956^{\circ}_{2\frac{1}{2}} - 63011_{1\frac{1}{2}}$					
5244.61	100	300	19061.89	+0.04	$43075^{\circ}_{1\frac{1}{2}} - 62136_{0\frac{1}{2}}$	5	0.96	0.08	0.44	1.40
5243.56		1	19065.71	−0.02	$56840^{\circ}_{1\frac{1}{2}} - 75905_{0\frac{1}{2}}$					
5243.41		4	19066.25	−0.03	$47329^{\circ}_{2\frac{1}{2}} - 66395_{2\frac{1}{2}}$					

TABLE 6. Yb II—*Observed and classified lines*—Continued

1	2	3	4	5	6	7	8	9	10	11
Wave-length air	Intensity		Wave number	o–c	Classification	Zeeman type	1st g	2nd g	Zeeman components	
	Meggers lamp	Thomson lamp							Strong p	Strong t
Å			K	K						
5243.15		2	19067.20	−0.03	$57103^{\circ}_{3\frac{1}{2}} - 76170_{2\frac{1}{2}}$					
5240.51	300	1000	19076.80	−0.03	$30224^{\circ}_{4\frac{1}{2}} - 49301_{4\frac{1}{2}}$	6	0.94	1.20	1.15	1.07?
5239.25		2	19081.39	−0.06	$53120^{\circ}_{2\frac{1}{2}} - 72202_{3\frac{1}{2}}$					
5236.66	3	150	19090.83	−0.01	$54192^{\circ}_{5\frac{1}{2}} - 73283_{4\frac{1}{2}}$					
5234.28		2	19099.51	+0.07	$54192^{\circ}_{5\frac{1}{2}} - 73291_{5\frac{1}{2}}$					
5232.537	6	40	19105.87	+0.06 −0.03	$30392^{\circ}_{1\frac{1}{2}} - 49498_{2\frac{1}{2}}$ $55462^{\circ}_{3\frac{1}{2}} - 74568_{4\frac{1}{2}}$					
5229.963	1	60	19115.27	+0.06	$44940^{\circ}_{1\frac{1}{2}} - 64055_{2\frac{1}{2}}$					
5227.01	1	70	19126.07	0.00	$49008^{\circ}_{3\frac{1}{2}} - 68135_{2\frac{1}{2}}$					
5226.18	20	150	19129.11	−0.04	$43007^{\circ}_{0\frac{1}{2}} - 62136_{0\frac{1}{2}}$					
5222.68		3	19141.93	+0.07	$57534^{\circ}_{3\frac{1}{2}} - 76676_{2\frac{1}{2}}$					
5220.82		5	19148.75	+0.02	$62163^{\circ}_{2\frac{1}{2}} - 81312_{2\frac{1}{2}}$					
5220.41		10	19150.25	+0.03	$44497^{\circ}_{2\frac{1}{2}} - 63647_{1\frac{1}{2}}$					
5217.936	3	70	19159.33	+0.04	$56480^{\circ}_{4\frac{1}{2}} - 75640_{3\frac{1}{2}}$	7	0.77	(0.81)	0	0.63*h*
5215.44	4	100	19168.50	+0.04	$45429^{\circ}_{3\frac{1}{2}} - 64598_{3\frac{1}{2}}$					
5212.232		25	19180.30	+0.03	$48024^{\circ}_{1\frac{1}{2}} - 67204_{1\frac{1}{2}}$					
5209.54		1	19190.21	+0.01	$59624^{\circ}_{3\frac{1}{2}} - 78814_{2\frac{1}{2}}$					
5205.574	4	30	19204.83	+0.02	$44497^{\circ}_{2\frac{1}{2}} - 63702_{2\frac{1}{2}}$					
5204.57		1	19208.53							
5202.87		1	19214.81	+0.04	$58672^{\circ}_{0\frac{1}{2}} - 77887_{0\frac{1}{2}}$					
5201.32		1	19220.54	+0.07	$57103^{\circ}_{3\frac{1}{2}} - 76323_{3\frac{1}{2}}$					
5201.21		2	19220.94	+0.03	$58661^{\circ}_{2\frac{1}{2}} - 77882_{3\frac{1}{2}}$					
5200.75		4	19222.64	+0.08	$46354^{\circ}_{4\frac{1}{2}} - 65577_{3\frac{1}{2}}$					
5200.54	50	500	19223.42	0.00	$40035^{\circ}_{3\frac{1}{2}} - 59259_{2\frac{1}{2}}$	4	(0.720)	1.110	0.195	?
5199.14		1	19228.60	+0.04	$47329^{\circ}_{2\frac{1}{2}} - 66558_{3\frac{1}{2}}$					
5189.89		7	19262.87	+0.01	$58484^{\circ}_{4\frac{1}{2}} - 77747_{4\frac{1}{2}}$					
5189.50		8	19264.31	+0.02	$44438^{\circ}_{3\frac{1}{2}} - 63702_{2\frac{1}{2}}$					
5188.89		9	19266.58	0.00	$62046^{\circ}_{3\frac{1}{2}} - 81312_{2\frac{1}{2}}$					
5187.33		3	19272.37							
5185.15		1	19280.48	+0.07	$52921^{\circ}_{3\frac{1}{2}} - 72202_{3\frac{1}{2}}$					
5184.66		1	19282.30							
5184.15	150	1000	19284.19	+0.04	$33653^{\circ}_{0\frac{1}{2}} - 52938_{1\frac{1}{2}}$	4	1.34	0.90	0.22	0.68
5180.355	15	150	19298.32	0.00	$37077^{\circ}_{2\frac{1}{2}} - 56375_{2\frac{1}{2}}$	6	1.116	1.224	0.27	1.17
5173.11	2	200	19325.35	+0.09	$45273^{\circ}_{3\frac{1}{2}} - 64598_{3\frac{1}{2}}$					
5173.064	10	100	19325.52	+0.02	$34389^{\circ}_{2\frac{1}{2}} - 53715_{3\frac{1}{2}}$					
5172.40		1	19328.00	−0.05	$46547^{\circ}_{5\frac{1}{2}} - 65875_{6\frac{1}{2}}$					
5167.660		3	19345.73	−0.02	$47005^{\circ}_{1\frac{1}{2}} - 66351_{2\frac{1}{2}}$					
5160.99		1	19370.73	+0.01 +0.04	$63028^{\circ}_{1\frac{1}{2}} - 82398_{1\frac{1}{2}}$ $75058^{\circ}_{2\frac{1}{2}} - 94428^{\circ}_{1\frac{1}{2}}$					
5159.655		3	19375.74	−0.04	$59439^{\circ}_{2\frac{1}{2}} - 78814_{2\frac{1}{2}}$					

TABLE 6. Yb II—*Observed and classified lines*—Continued

1	2	3	4	5	6	7	8	9	10	11
Wave-length air	Intensity		Wave number	o–c	Classification	Zeeman type	1st g	2nd g	Zeeman components	
	Meggers lamp	Thomson lamp							Strong p	Strong n
Å			K	K						
5157.962	3	100	19382.10	−0.01	$48556^{\circ}_{3\frac{1}{2}} - 67938_{3\frac{1}{2}}$					
5152.34	7	200	19403.25	+0.02	$46547^{\circ}_{5\frac{1}{2}} - 65950_{4\frac{1}{2}}$					
5151.25		4	19407.36	+0.03	$46169^{\circ}_{4\frac{1}{2}} - 65577_{3\frac{1}{2}}$					
5149.04		1	19415.69	−0.02	$70793_{5\frac{1}{2}} - 90209^{\circ}_{4\frac{1}{2}}$					
5147.02	50	700	19423.31	+0.01	$38342^{\circ}_{4\frac{1}{2}} - 57765_{4\frac{1}{2}}$	6	(1.093)	1.13	w	1.11
5142.28	3	100	19441.21	+0.03	$49008^{\circ}_{3\frac{1}{2}} - 68450_{3\frac{1}{2}}$					
5141.61		3	19443.74	−0.09	$58162^{\circ}_{1\frac{1}{2}} - 77606_{2\frac{1}{2}}$					
5138.01		1	19457.37	−0.03	$47005^{\circ}_{1\frac{1}{2}} - 66462_{0\frac{1}{2}}$					
5137.43	2	4	19459.56							
5137.23		1	19460.32	+0.03	$44497^{\circ}_{2\frac{1}{2}} - 63957_{3\frac{1}{2}}$					
5136.49		1	19463.12							
5135.98	200	1500	19465.06	0.00	$33052^{\circ}_{4\frac{1}{2}} - 52517_{5\frac{1}{2}}$	7	(1.264)	1.25	0	1.29
5133.42		1	19474.76	−0.01	$63417^{\circ}_{2\frac{1}{2}} - 82891_{2\frac{1}{2}}$					
5132.40	1	60	19478.64	−0.06	$49916^{\circ}_{4\frac{1}{2}} - 69395_{3\frac{1}{2}}$					
5131.01	1	10	19483.91	−0.02	$43075^{\circ}_{1\frac{1}{2}} - 62559_{2\frac{1}{2}}$					
5130.711		2	19485.05	−0.07	$70793_{5\frac{1}{2}} - 90279^{c}_{5\frac{1}{2}}$					
5130.56		1	19485.62	+0.11	$57798^{\circ}_{2\frac{1}{2}} - 77284_{1\frac{1}{2}}$					
5129.56		60	19489.42	−0.02	$50468^{\circ}_{5\frac{1}{2}} - 69957_{4\frac{1}{2}}$					
5128.55	3	100	19493.26	−0.03 +0.05	$45429^{\circ}_{3\frac{1}{2}} - 64923_{4\frac{1}{2}}$ $62163^{\circ}_{2\frac{1}{2}} - 81657_{2\frac{1}{2}}$					
5121.58	30	300	19519.79	+0.02	$44438^{\circ}_{3\frac{1}{2}} - 63957_{3\frac{1}{2}}$	6	1.11	1.15	0.13	1.13
5117.72	1	25	19534.51	−0.02	$46547^{\circ}_{5\frac{1}{2}} - 66082_{5\frac{1}{2}}$					
5116.200		10	19540.31	+0.01	$49008^{\circ}_{3\frac{1}{2}} - 68549_{4\frac{1}{2}}$					
5111.47	1	60	19558.39	+0.08 0.00	$44497^{\circ}_{2\frac{1}{2}} - 64055_{2\frac{1}{2}}$ $54192^{\circ}_{5\frac{1}{2}} - 73750_{4\frac{1}{2}}$					
5107.58		1	19573.29	0.00	$57103^{\circ}_{3\frac{1}{2}} - 76676_{2\frac{1}{2}}$					
5106.12		1	19578.89							
5105.028	10	150	19583.07	−0.01 −0.08	$40035^{\circ}_{3\frac{1}{2}} - 59618_{3\frac{1}{2}}$ $56056^{\circ}_{2\frac{1}{2}} - 75640_{3\frac{1}{2}}$					
5104.42	20	400	19585.41	−0.08	$45012^{\circ}_{2\frac{1}{2}} - 64598_{3\frac{1}{2}}$	?	(1.28)	1.23	w	1.12h
5101.810		3	19595.43	0.00	$55462^{\circ}_{3\frac{1}{2}} - 75058_{2\frac{1}{2}}$					
5101.57	3	80	19596.35	−0.05	$46354^{\circ}_{4\frac{1}{2}} - 65950_{4\frac{1}{2}}$					
5099.11		3	19605.80							
5097.75		2	19611.03	−0.03	$62046^{\circ}_{3\frac{1}{2}} - 81657_{2\frac{1}{2}}$					
5095.99		3	19617.80	+0.01	$44438^{\circ}_{3\frac{1}{2}} - 64055_{2\frac{1}{2}}$					
5090.628		15	19638.47	+0.01	$53644^{\circ}_{3\frac{1}{2}} - 73283_{4\frac{1}{2}}$					
5088.92	1	30	19645.06	0.00	$48503^{\circ}_{5\frac{1}{2}} - 68148_{5\frac{1}{2}}$					
5087.61	10	150	19650.12	+0.03	$45273^{\circ}_{3\frac{1}{2}} - 64923_{4\frac{1}{2}}$	4	1.17	(1.10)	w	0.86
5085.70	2	80	19657.50	+0.01	$47758^{\circ}_{3\frac{1}{2}} - 67416_{4\frac{1}{2}}$					
5085.22		1	19659.35	−0.06	$53120^{\circ}_{2\frac{1}{2}} - 72779_{3\frac{1}{2}}$					

TABLE 6. Yb II—*Observed and classified lines*—Continued

1	2	3	4	5	6	7	8	9	10	11
Wave-length air	Intensity		Wave number	o–c	Classification	Zeeman type	1st g	2nd g	Zeeman components	
	Meggers lamp	Thomson lamp							Strong p	Strong n
Å			K	K						
5083.52		2	19665.93	+0.02	$48272_{2\frac{1}{2}}^{\circ} - 67938_{3\frac{1}{2}}$					
5082.934		7	19668.19	0.00	$50468_{5\frac{1}{2}}^{\circ} - 70136_{6\frac{1}{2}}$					
5076.957		6	19691.35	+0.03	$43956_{2\frac{1}{2}}^{\circ} - 63647_{1\frac{1}{2}}$					
5075.813		8	19695.79	+0.03 −0.01	$41678_{2\frac{1}{2}}^{\circ} - 61374_{2\frac{1}{2}}$ $52067_{0\frac{1}{2}}^{\circ} - 71763_{1\frac{1}{2}}$					
5074.609		80	19700.46							
5073.35		1	19705.35	−0.06	$51248_{2\frac{1}{2}}^{\circ} - 70954_{2\frac{1}{2}}$					
5067.600		10	19727.71	+0.01	$46354_{4\frac{1}{2}}^{\circ} - 66082_{5\frac{1}{2}}$					
5067.297	200	800	19728.89	−0.04	$34575_{1\frac{1}{2}}^{\circ} - 54304_{0\frac{1}{2}}$	4	1.435	2.005	0.285	1.150
5065.74		1	19734.95	−0.04	$52880_{4\frac{1}{2}}^{\circ} - 72615_{5\frac{1}{2}}$					
5065.488		4	19735.93	−0.05	$57103_{3\frac{1}{2}}^{\circ} - 76839_{2\frac{1}{2}}$					
5062.938	30	300	19745.87	−0.04	$43956_{2\frac{1}{2}}^{\circ} - 63702_{2\frac{1}{2}}$	6	(0.99)	1.01	d	1.00
5062.634		15	19747.06	−0.05	$49008_{3\frac{1}{2}}^{\circ} - 68756_{3\frac{1}{2}}$					
5061.24		1	19752.50	−0.01	$47663_{4\frac{1}{2}}^{\circ} - 67416_{4\frac{1}{2}}$					
5058.71		8	19762.38	−0.07	$61442_{5\frac{1}{2}}^{\circ} - 81205_{4\frac{1}{2}}$					
5057.275		2	19767.98	−0.05	$55221_{1\frac{1}{2}}^{\circ} - 74989_{0\frac{1}{2}}$					
5051.096		2	19792.17	−0.06	$58672_{0\frac{1}{2}}^{\circ} - 78464_{1\frac{1}{2}}$					
5049.832	5	250	19797.12	−0.02	$48923_{7\frac{1}{2}}^{\circ} - 68720_{6\frac{1}{2}}$	5	1.19	(1.157)	w	1.42
5047.08		15d	19807.91	−0.16 +0.06	$57798_{2\frac{1}{2}}^{\circ} - 77606_{2\frac{1}{2}}$ $60649_{4\frac{1}{2}}^{\circ} - 80457_{3\frac{1}{2}}$					
5043.28		1	19822.84	−0.01	$56500_{3\frac{1}{2}}^{\circ} - 76323_{3\frac{1}{2}}$					
5042.982	3	20	19824.01			7			0	1.20
5041.756		4	19828.83	−0.05	$59777_{1\frac{1}{2}}^{\circ} - 79605_{1\frac{1}{2}}$					
5039.86		2	19836.29	+0.02	$56840_{1\frac{1}{2}}^{\circ} - 76676_{2\frac{1}{2}}$					
5038.240		15	19842.67	−0.05	$56480_{4\frac{1}{2}}^{\circ} - 76323_{3\frac{1}{2}}$					
5033.289	1	20	19862.19	−0.04	$48272_{2\frac{1}{2}}^{\circ} - 68135_{2\frac{1}{2}}$					
5032.586	1	25	19864.96	−0.02	$51248_{2\frac{1}{2}}^{\circ} - 71113_{1\frac{1}{2}}$					
5029.342		3	19877.77	−0.03	$48272_{2\frac{1}{2}}^{\circ} - 68150_{1\frac{1}{2}}$					
5025.356	1	6	19893.54	0.00	$48556_{3\frac{1}{2}}^{\circ} - 68450_{3\frac{1}{2}}$					
5023.925	1	9	19899.21	−0.03	$52880_{4\frac{1}{2}}^{\circ} - 72779_{3\frac{1}{2}}$					
5021.13	50	400	19910.28	0.00	$33494_{3\frac{1}{2}}^{\circ} - 53404_{2\frac{1}{2}}$	7	(0.99)	1.02	0	0.90
5017.80		3	19923.50	−0.08	$70793_{5\frac{1}{2}} - 90717_{4\frac{1}{2}}^{\circ}$					
5014.98		2	19934.70	−0.02	$49008_{3\frac{1}{2}}^{\circ} - 68943_{4\frac{1}{2}}$					
5014.472	20	250	19936.72	−0.04	$43075_{1\frac{1}{2}}^{\circ} - 63011_{1\frac{1}{2}}$	6	0.97	0.79	0.26	0.70
5013.76		1	19939.55							
5010.04		1	19954.35	+0.11	$73291_{5\frac{1}{2}} - 93246_{6\frac{1}{2}}^{\circ}$					
5009.525	500	2000	19956.41	−0.01	$32981_{1\frac{1}{2}}^{\circ} - 52938_{1\frac{1}{2}}$	7	0.88	0.88	0	0.88
5009.025		2	19958.40	−0.05	$59624_{3\frac{1}{2}}^{\circ} - 79583_{2\frac{1}{2}}$					
5008.876	1	15	19958.99	−0.04 −0.05	$56840_{1\frac{1}{2}}^{\circ} - 76799_{1\frac{1}{2}}$ $73283_{4\frac{1}{2}} - 93242_{5\frac{1}{2}}^{\circ}$					

TABLE 6. Yb II—*Observed and classified lines*—Continued

1	2	3	4	5	6	7	8	9	10	11
Wave-length air	Intensity		Wave number	o–c	Classification	Zeeman type	1st g	2nd g	Zeeman components	
	Meggers lamp	Thomson lamp							Strong p	Strong n
Å			K	K						
5007.75		1	19963.48	−0.09	$44497^{\circ}_{2\frac{1}{2}} - 64461_{1\frac{1}{2}}$					
5005.25		1	19973.45	−0.05	$51248^{\circ}_{2\frac{1}{2}} - 71222_{3\frac{1}{2}}$					
5004.63		1	19975.93	−0.08	$47228^{\circ}_{0\frac{1}{2}} - 67204_{1\frac{1}{2}}$					
5002.98	5	70	19982.51	−0.02	$68720_{6\frac{1}{2}} - 88702^{\circ}_{5\frac{1}{2}}$	5	(1.157)	1.12	w	1.38
5000.452		2	19992.62	−0.04	$48556^{\circ}_{3\frac{1}{2}} - 68549_{4\frac{1}{2}}$					
4998.87		3	19998.94	−0.02	$56840^{\circ}_{1\frac{1}{2}} - 76839_{2\frac{1}{2}}$					
4998.266	3	15	20001.36	−0.03	$43956^{\circ}_{2\frac{1}{2}} - 63957_{3\frac{1}{2}}$					
4996.604		4	20008.01	−0.04	$69607_{2\frac{1}{2}} - 89615^{\circ}_{2\frac{1}{2}}$					
4994.74		1	20015.48	+0.01	$56500^{\circ}_{3\frac{1}{2}} - 76516_{4\frac{1}{2}}$					
4993.32		1	20021.17	−0.03	$47912_{3\frac{1}{2}} - 67933^{\circ}_{2\frac{1}{2}}$					
				+0.02	$51248^{\circ}_{2\frac{1}{2}} - 71270_{2\frac{1}{2}}$					
4992.654		6	20023.84	−0.02	$46547^{\circ}_{5\frac{1}{2}} - 66571_{5\frac{1}{2}}$					
4992.520		7	20024.38	−0.01	$49419^{\circ}_{0\frac{1}{2}} - 69443_{1\frac{1}{2}}$					
4989.794		4	20035.32	−0.02	$56480^{\circ}_{4\frac{1}{2}} - 76516_{4\frac{1}{2}}$					
4988.383	1	15	20040.99	0.00	$49916^{\circ}_{4\frac{1}{2}} - 69957_{4\frac{1}{2}}$					
4988.022		1	20042.44							
4987.292	1	15	20045.37	−0.04	$48503^{\circ}_{5\frac{1}{2}} - 68549_{4\frac{1}{2}}$					
4986.88[a]	6	3	20047.02	+0.03	$22960_{1\frac{1}{2}} - 43007^{\circ}_{0\frac{1}{2}}$					
4978.62	1	9	20080.28	−0.07	$45012^{\circ}_{2\frac{1}{2}} - 65093_{3\frac{1}{2}}$					
4976.65		2	20088.23	−0.03	$55462^{\circ}_{3\frac{1}{2}} - 75550_{2\frac{1}{2}}$					
4973.90		15	20099.34	−0.07	$43956^{\circ}_{2\frac{1}{2}} - 64055_{2\frac{1}{2}}$					
4972.26	1	20	20105.97	−0.04	$53644^{\circ}_{3\frac{1}{2}} - 73750_{4\frac{1}{2}}$					
4971.20		8	20110.26	−0.04	$48024^{\circ}_{1\frac{1}{2}} - 68135_{2\frac{1}{2}}$					
4970.203	3	4	20114.29	0.00	$22960_{1\frac{1}{2}} - 43075^{\circ}_{1\frac{1}{2}}$					
4967.35		2	20125.84	−0.03	$48024^{\circ}_{1\frac{1}{2}} - 68150_{1\frac{1}{2}}$					
4965.43	3	15	20133.62							
4963.18		2	20142.75	−0.09	$70136_{6\frac{1}{2}} - 90279^{\circ}_{5\frac{1}{2}}$					
4961.124		3	20151.10	−0.07	$45737^{\circ}_{1\frac{1}{2}} - 65888_{1\frac{1}{2}}$					
4958.895		2	20160.16	−0.09	$44438^{\circ}_{3\frac{1}{2}} - 64598_{3\frac{1}{2}}$					
4957.262		7	20166.80	−0.07	$59439^{\circ}_{2\frac{1}{2}} - 79605_{1\frac{1}{2}}$					
4955.98		1	20172.01	−0.06	$69443_{1\frac{1}{2}} - 89615^{\circ}_{2\frac{1}{2}}$					
4954.68	3	50	20177.31	−0.03	$48272^{\circ}_{2\frac{1}{2}} - 68450_{3\frac{1}{2}}$	7	0.98	0.98	0	0.98
				−0.07	$55462^{\circ}_{3\frac{1}{2}} - 75640_{3\frac{1}{2}}$					
4953.622		3	20181.62							
4952.740		2	20185.21	−0.04	$69957_{4\frac{1}{2}} - 90142^{\circ}_{3\frac{1}{2}}$					
4949.24		2	20199.48	−0.03	$47005^{\circ}_{1\frac{1}{2}} - 67204_{1\frac{1}{2}}$					
				+0.01	$48556^{\circ}_{3\frac{1}{2}} - 68756_{3\frac{1}{2}}$					
4946.524		1	20210.58	−0.02	$69395_{3\frac{1}{2}} - 89605^{\circ}_{4\frac{1}{2}}$					
4946.19		1	20211.94	0.00	$73291_{5\frac{1}{2}} - 93503^{\circ}_{4\frac{1}{2}}$					
4945.944		3	20212.95	0.00	$57534^{\circ}_{3\frac{1}{2}} - 77747_{4\frac{1}{2}}$					
4944.956	5	150	20216.98	−0.05	$46354^{\circ}_{4\frac{1}{2}} - 66571_{5\frac{1}{2}}$					

TABLE 6. Yb II—*Observed and classified lines*—Continued

1	2	3	4	5	6	7	8	9	10	11
Wave-length air	Intensity		Wave number	o–c	Classification	Zeeman type	1st g	2nd g	Zeeman components	
	Meggers lamp	Thomson lamp							Strong p	Strong n
Å			K	K						
4944.080	200	600	20220.57	−0.01 +0.03	$33494^{\circ}_{3\frac{1}{2}} - 53715_{3\frac{1}{2}}$ $(73283_{4\frac{1}{2}} - 93503^{\circ}_{4\frac{1}{2}})$	6	0.98	1.17	0.68	1.07
4942.742	20	200	20226.04	+0.01	$33494^{\circ}_{3\frac{1}{2}} - 53720_{4\frac{1}{2}}$					
4940.53		2	20235.10	0.00 +0.04	$56088^{\circ}_{4\frac{1}{2}} - 76323_{3\frac{1}{2}}$ $62163^{\circ}_{2\frac{1}{2}} - 82398_{1\frac{1}{2}}$					
4938.828		4	20242.07	−0.01	$45335^{\circ}_{4\frac{1}{2}} - 65577_{3\frac{1}{2}}$					
4937.222	100	2000	20248.65	−0.08 −0.01	$37516^{\circ}_{3\frac{1}{2}} - 57765_{4\frac{1}{2}}$ $42915^{\circ}_{5\frac{1}{2}} - 63163_{4\frac{1}{2}}$	7	1.12	1.11	0	1.09
4930.78		1	20275.11	−0.05	$47663^{\circ}_{4\frac{1}{2}} - 67938_{3\frac{1}{2}}$					
4929.31	1	20	20281.15	−0.04	$50832^{\circ}_{1\frac{1}{2}} - 71113_{1\frac{1}{2}}$	7	0.96	0.96	0	0.96
4928.184		4	20285.79							
4927.154		1	20290.03	+0.02	$69607_{2\frac{1}{2}} - 89897^{\circ}_{1\frac{1}{2}}$					
4924.187		2	20302.25	−0.01	$46902^{\circ}_{0\frac{1}{2}} - 67204_{1\frac{1}{2}}$					
4923.747		1	20304.07	−0.02	$45273^{\circ}_{3\frac{1}{2}} - 65577_{3\frac{1}{2}}$					
4918.45		10	20325.93	+0.02	$50468^{\circ}_{5\frac{1}{2}} - 70793_{5\frac{1}{2}}$					
4917.044	20	60	20331.75	−0.01	$39378^{\circ}_{0\frac{1}{2}} - 59710_{1\frac{1}{2}}$	4	1.84	0.80	0.52	0.28
4915.42		1	20338.46	+0.10	$56500^{\circ}_{3\frac{1}{2}} - 76839_{2\frac{1}{2}}$					
4909.81		3	20361.70	−0.03 +0.01	$52921^{\circ}_{3\frac{1}{2}} - 73283_{4\frac{1}{2}}$ $73636_{0\frac{1}{2}} - 93998^{\circ}_{1\frac{1}{2}}$					
4906.27		9	20376.39	−0.07	$47758^{\circ}_{3\frac{1}{2}} - 68135_{2\frac{1}{2}}$					
4905.48		2	20379.67	−0.09	$70858_{4\frac{1}{2}} - 91237^{\circ}_{3\frac{1}{2}}$					
4903.89	1	25	20386.28	+0.01	$49008^{\circ}_{3\frac{1}{2}} - 69395_{3\frac{1}{2}}$					
4903.71	3	50	20387.03	−0.05	$48556^{\circ}_{3\frac{1}{2}} - 68943_{4\frac{1}{2}}$	7	0.94	(0.89)	0	0.72
4900.16		4	20401.80	0.00	$46169^{\circ}_{4\frac{1}{2}} - 66571_{5\frac{1}{2}}$					
4899.980		2	20402.55	−0.05 +0.04	$52880^{\circ}_{4\frac{1}{2}} - 73283_{4\frac{1}{2}}$ $60910^{\circ}_{1\frac{1}{2}} - 81312_{2\frac{1}{2}}$					
4898.42		15	20409.05	0.00	$49727^{\circ}_{6\frac{1}{2}} - 70136_{6\frac{1}{2}}$					
4897.90	2	40	20411.21	+0.01	$52880^{\circ}_{4\frac{1}{2}} - 73291_{5\frac{1}{2}}$					
4894.983	50	400	20423.38	+0.01	$32981^{\circ}_{1\frac{1}{2}} - 53404_{2\frac{1}{2}}$	5	0.88	1.03	(0.08)	1.26
4891.654		3	20437.28	−0.08	$50832^{\circ}_{1\frac{1}{2}} - 71270_{2\frac{1}{2}}$					
4891.056	1	8	20439.77	−0.06	$48503^{\circ}_{5\frac{1}{2}} - 68943_{4\frac{1}{2}}$					
4890.07		1	20443.90	−0.08	$56840^{\circ}_{1\frac{1}{2}} - 77284_{1\frac{1}{2}}$					
4888.99		3	20448.41	−0.08	$41688^{\circ}_{1\frac{1}{2}} - 62136_{0\frac{1}{2}}$					
4887.662		2	20453.97	−0.06	$69443_{1\frac{1}{2}} - 89897^{\circ}_{1\frac{1}{2}}$					
4884.205		4	20468.44	−0.04	$47680^{\circ}_{6\frac{1}{2}} - 68148_{5\frac{1}{2}}$					
4880.674		8	20483.25	−0.02	$48272^{\circ}_{2\frac{1}{2}} - 68756_{3\frac{1}{2}}$					
4880.190		10	20485.28	−0.08	$47663^{\circ}_{4\frac{1}{2}} - 68148_{5\frac{1}{2}}$					
4875.852		2	20503.51	−0.05	$57103^{\circ}_{3\frac{1}{2}} - 77606_{2\frac{1}{2}}$					
4873.180		2	20514.75	−0.06	$51248^{\circ}_{2\frac{1}{2}} - 71763_{1\frac{1}{2}}$					
4871.670	2	40	20521.11	−0.02	$45429^{\circ}_{3\frac{1}{2}} - 65950_{4\frac{1}{2}}$	7	(1.150)	1.11	0	0.98

TABLE 6. Yb II—*Observed and classified lines*—Continued

1	2	3	4	5	6	7	8	9	10	11
Wave-length air	Intensity		Wave number	o–c	Classification	Zeeman type	1st g	2nd g	Zeeman components	
	Meggers lamp	Thomson lamp							Strong p	Strong n
Å			K	K						
4871.150	10	90	20523.30	−0.01	$48556^{\circ}_{3\frac{1}{2}} - 69079_{2\frac{1}{2}}$	7	0.91	(0.89)	0	0.95
4863.87		3	20554.02	−0.07	$68148_{5\frac{1}{2}} - 88702^{\circ}_{5\frac{1}{2}}$					
				−0.08	$53716^{\circ}_{2\frac{1}{2}} - 74270_{2\frac{1}{2}}$					
4863.56		1	20555.33	−0.08	$60649^{\circ}_{4\frac{1}{2}} - 81205_{4\frac{1}{2}}$					
4860.84		2	20566.83	−0.08	$32371^{\circ}_{2\frac{1}{2}} - 52938_{1\frac{1}{2}}$					
4859.49		2	20572.54	−0.10	$43075^{\circ}_{1\frac{1}{2}} - 63647_{1\frac{1}{2}}$					
4853.347		7	20598.58	−0.03	$49008^{\circ}_{3\frac{1}{2}} - 69607_{2\frac{1}{2}}$					
4851.150	300	600	20607.91	−0.01	$24332_{2\frac{1}{2}} - 44940^{\circ}_{1\frac{1}{2}}$	4?	(1.20)	1.22	0	1.18
4850.848	1	10	20609.19	−0.05	$47329^{\circ}_{2\frac{1}{2}} - 67938_{3\frac{1}{2}}$					
4849.265		2	20615.92	0.00	$45335^{\circ}_{4\frac{1}{2}} - 65950_{4\frac{1}{2}}$					
4848.455	50	300	20619.37	+0.02	$38342^{\circ}_{4\frac{1}{2}} - 58961_{5\frac{1}{2}}$					
				−0.03	$56056^{\circ}_{2\frac{1}{2}} - 76676_{2\frac{1}{2}}$					
4846.873	1	15	20626.10	−0.01	$44940^{\circ}_{1\frac{1}{2}} - 65566_{0\frac{1}{2}}$					
4846.612	4	20	20627.21	−0.02	$43075^{\circ}_{1\frac{1}{2}} - 63702_{2\frac{1}{2}}$					
4841.47		2	20649.11	+0.04	$52987^{\circ}_{1\frac{1}{2}} - 73636_{0\frac{1}{2}}$					
4841.153	50	150	20650.47	+0.03	$33653^{\circ}_{0\frac{1}{2}} - 54304_{0\frac{1}{2}}$	6	1.33	2.01	0.34	1.67
4839.279	1	15	20658.46	+0.03	$45737^{\circ}_{1\frac{1}{2}} - 66395_{2\frac{1}{2}}$					
4839.014	1	7	20659.59	0.00	$65566_{0\frac{1}{2}} - 86226^{\circ}_{1\frac{1}{2}}$					
4838.220	10	20	20662.99	+0.02	$33052^{\circ}_{4\frac{1}{2}} - 53715_{3\frac{1}{2}}$					
4837.045	500	1000	20668.00							
4836.96	500	1000	20668.37	−0.05	$33052^{\circ}_{4\frac{1}{2}} - 53720_{4\frac{1}{2}}$	6	1.26	1.28	(0.08)	1.27
4834.926	1	10	20677.06							
4834.72	10	100	20677.94	+0.01	$45273^{\circ}_{3\frac{1}{2}} - 65950_{4\frac{1}{2}}$	4	1.16	(1.08)	w	0.79
4834.23	2	3	20680.04	−0.06	$24332_{2\frac{1}{2}} - 45012^{\circ}_{2\frac{1}{2}}$					
4833.55		1	20682.95	−0.07	$72779_{3\frac{1}{2}} - 93463^{\circ}_{3\frac{1}{2}}$					
4833.24		1	20684.28	−0.03	$55221^{\circ}_{1\frac{1}{2}} - 75905_{0\frac{1}{2}}$					
4831.533	2	20	20691.58	+0.01	$47758^{\circ}_{3\frac{1}{2}} - 68450_{3\frac{1}{2}}$					
4827.81		2	20707.54	−0.03	$55462^{\circ}_{3\frac{1}{2}} - 76170_{2\frac{1}{2}}$					
4826.78		2	20711.96							
4823.615		2	20725.55	−0.02	$45737^{\circ}_{1\frac{1}{2}} - 66462_{0\frac{1}{2}}$					
				−0.06	$73283_{4\frac{1}{2}} - 94008^{\circ}_{3\frac{1}{2}}$					
4822.47		1	20730.47							
4822.010		3	20732.45	−0.02	$78070_{4\frac{1}{2}} - 98802^{\circ}_{5\frac{1}{2}}$					
4820.74		1	20737.91							
4820.242	400	1000	20740.05	−0.01	$28757^{\circ}_{1\frac{1}{2}} - 49498_{2\frac{1}{2}}$	4	1.432	1.145	0.143	0.72
4818.371	100	600	20748.10	−0.01	$38342^{\circ}_{4\frac{1}{2}} - 59090_{3\frac{1}{2}}$	4	(1.093)	1.12	0	1.01
4815.612		6	20759.99	−0.06	$69957_{4\frac{1}{2}} - 90717^{\circ}_{4\frac{1}{2}}$					
4815.28		1	20761.42	−0.09	$44438^{\circ}_{3\frac{1}{2}} - 65199_{4\frac{1}{2}}$					
4813.92	2	7	20767.29	−0.03	$37516^{\circ}_{3\frac{1}{2}} - 58283_{2\frac{1}{2}}$					
4809.451	2	30	20786.58	−0.01	$47663^{\circ}_{4\frac{1}{2}} - 68450_{3\frac{1}{2}}$					

TABLE 6. Yb II—*Observed and classified lines*—Continued

1	2	3	4	5	6	7	8	9	10	11
Wave-length air	Intensity		Wave number	o–c	Classification	Zeeman type	1st g	2nd g	Zeeman components	
	Meggers lamp	Thomson lamp							Strong p	Strong n
Å			K	K						
4808.502	2	50	20790.69	0.00	$47758^{\circ}_{3\frac{1}{2}} - 68549_{4\frac{1}{2}}$					
4803.653		10	20811.67	−0.03	$42915^{\circ}_{3\frac{1}{2}} - 63726_{4\frac{1}{2}}$					
4801.473		2	20821.12	−0.01	$47329^{\circ}_{2\frac{1}{2}} - 68150_{1\frac{1}{2}}$					
4799.96		1	20827.69	−0.05	$66558_{3\frac{1}{2}} - 87385^{\circ}_{3\frac{1}{2}}$					
4798.72		3	20833.07	+0.02	$59624^{\circ}_{3\frac{1}{2}} - 80457_{3\frac{1}{2}}$					
4792.63		3	20859.54	−0.01	$68756_{3\frac{1}{2}} - 89615^{\circ}_{2\frac{1}{2}}$					
4792.336		2	20860.82	+0.01	$55462^{\circ}_{3\frac{1}{2}} - 76323_{3\frac{1}{2}}$					
4790.61	1	15	20868.33	+0.02	$46547^{\circ}_{3\frac{1}{2}} - 67416_{4\frac{1}{2}}$					
4788.924		5	20875.68	+0.01	$45012^{\circ}_{2\frac{1}{2}} - 65888_{1\frac{1}{2}}$					
4786.61	2000	8000	20885.77	+0.01 +0.06	$31631^{\circ}_{6\frac{1}{2}} - 52517_{5\frac{1}{2}}$ $(47663^{\circ}_{4\frac{1}{2}} - 68549_{4\frac{1}{2}})$	4	1.24	1.28	(0.02)	1.02
4781.17		2*d*	20909.54	−0.05	$56977^{\circ}_{0\frac{1}{2}} - 77887_{0\frac{1}{2}}$					
4778.414		1	20921.60	−0.01	$47228^{\circ}_{0\frac{1}{2}} - 68150_{1\frac{1}{2}}$					
4778.35		1	20921.88	−0.10	$58661^{\circ}_{2\frac{1}{2}} - 79583_{2\frac{1}{2}}$					
4777.946		4	20923.65	−0.04	$53644^{\circ}_{3\frac{1}{2}} - 74568_{4\frac{1}{2}}$					
4777.56		1	20925.34	0.00	$59753^{\circ}_{5\frac{1}{2}} - 80679_{5\frac{1}{2}}$					
4774.145	4	8	20940.30	−0.03	$24332_{2\frac{1}{2}} - 45273^{\circ}_{3\frac{1}{2}}$					
4773.839		8	20941.65	−0.03	$49916^{\circ}_{4\frac{1}{2}} - 70858_{4\frac{1}{2}}$					
4773.13		3	20944.76	−0.06	$58661^{\circ}_{2\frac{1}{2}} - 79605_{1\frac{1}{2}}$					
4772.43		2	20947.83	−0.02	$44940^{\circ}_{1\frac{1}{2}} - 65888_{1\frac{1}{2}}$					
4772.23		6	20948.71	−0.08 +0.03	$55221^{\circ}_{1\frac{1}{2}} - 76170_{2\frac{1}{2}}$ $56500^{\circ}_{3\frac{1}{2}} - 77449_{3\frac{1}{2}}$					
4772.000		2	20949.72	−0.05	$47005^{\circ}_{1\frac{1}{2}} - 67955_{0\frac{1}{2}}$					
4768.32		6	20965.88	−0.02	$45429^{\circ}_{3\frac{1}{2}} - 66395_{2\frac{1}{2}}$					
4768.036		3	20967.13	−0.04	$57103^{\circ}_{3\frac{1}{2}} - 78070_{4\frac{1}{2}}$					
4761.139	2	40	20997.51	+0.01	$47758^{\circ}_{3\frac{1}{2}} - 68756_{3\frac{1}{2}}$					
4757.14		1	21015.16	−0.08	$40035^{\circ}_{3\frac{1}{2}} - 61051_{3\frac{1}{2}}$					
4756.36		1	21018.60	−0.03	$59439^{\circ}_{2\frac{1}{2}} - 80457_{3\frac{1}{2}}$					
4752.91	100	400	21033.86	0.00	$32371^{\circ}_{2\frac{1}{2}} - 53404_{2\frac{1}{2}}$	6	1.16	1.02	0.30	1.09
4749.948	2	30	21046.98	+0.01	$59632^{\circ}_{6\frac{1}{2}} - 80679_{5\frac{1}{2}}$					
4749.55		1	21048.74	−0.10	$52067^{\circ}_{0\frac{1}{2}} - 73116_{1\frac{1}{2}}$					
4749.06	1	5	21050.91	−0.06	$48556^{\circ}_{3\frac{1}{2}} - 69607_{2\frac{1}{2}}$					
4748.71		2	21052.46	−0.06	$46902^{\circ}_{0\frac{1}{2}} - 67955_{0\frac{1}{2}}$					
4748.08		2*d*	21055.26	+0.08 0.00	$48024^{\circ}_{1\frac{1}{2}} - 69079_{2\frac{1}{2}}$ $77747_{4\frac{1}{2}} - 98802^{\circ}_{5\frac{1}{2}}$					
4746.68	10	150	21061.47	−0.01	$46354^{\circ}_{4\frac{1}{2}} - 67416_{4\frac{1}{2}}$	6	1.30	(1.26)	*d*	1.28
4745.483	1	20	21066.78	+0.01	$49727^{\circ}_{6\frac{1}{2}} - 70793_{5\frac{1}{2}}$					
4743.57		3	21075.27	−0.05	$58051^{\circ}_{5\frac{1}{2}} - 79126_{4\frac{1}{2}}$					
4739.70	1	10	21092.48	−0.04	$47663^{\circ}_{4\frac{1}{2}} - 68756_{3\frac{1}{2}}$					
4738.656	5	7	21097.13	0.00	$24332_{2\frac{1}{2}} - 45429^{\circ}_{3\frac{1}{2}}$					
4736.69		2	21105.89	−0.05	$56500^{\circ}_{3\frac{1}{2}} - 77606_{2\frac{1}{2}}$					

TABLE 6. Yb II—*Observed and classified lines*—Continued

1	2	3	4	5	6	7	8	9	10	11
Wavelength air	Intensity		Wave number	o–c	Classification	Zeeman type	1st g	2nd g	Zeeman components	
	Meggers lamp	Thomson lamp							Strong p	Strong n
Å			K	K						
4732.935	1	25	21122.63	−0.07	$45273^{\circ}_{3\frac{1}{2}} - 66395_{2\frac{1}{2}}$					
4732.025	30	200	21126.69	−0.01	$34575^{\circ}_{1\frac{1}{2}} - 55702_{1\frac{1}{2}}$	6	1.43	1.69	0.40	1.56
4731.70		2	21128.14	−0.04	$45429^{\circ}_{3\frac{1}{2}} - 66558_{3\frac{1}{2}}$					
4729.25		3	21139.09	+0.01	$44438^{\circ}_{3\frac{1}{2}} - 65577_{3\frac{1}{2}}$					
4728.109		8	21144.19	+0.02	$58484^{\circ}_{4\frac{1}{2}} - 79628_{3\frac{1}{2}}$					
4727.901		7	21145.12	+0.01	$47005^{\circ}_{1\frac{1}{2}} - 68150_{1\frac{1}{2}}$					
4726.54		1	21151.21							
4726.08	1000	3000	21153.27	−0.02	$26759^{\circ}_{2} - 47912_{3\frac{1}{2}}$	4	1.57	1.28	0.15	0.54
4725.14		2	21157.48	−0.10	$70858_{4\frac{1}{2}} - 92015^{\circ}_{4\frac{1}{2}}$					
4723.404		4	21165.25	−0.08	$70136_{6\frac{1}{2}} - 91301^{\circ}_{6\frac{1}{2}}$					
4720.390		2	21178.77	−0.07	$40035^{\circ}_{3\frac{1}{2}} - 61214_{4\frac{1}{2}}$					
4715.672		3	21199.95	−0.01	$62163^{\circ}_{2\frac{1}{2}} - 83363_{3\frac{1}{2}}$					
4712.78	40	200	21212.96	+0.02	$48923^{\circ}_{2\frac{1}{2}} - 70136_{6\frac{1}{2}}$	5	(1.20)	1.16	w	1.47
4705.40		4	21246.23	−0.02	$46169^{\circ}_{4\frac{1}{2}} - 67416_{4\frac{1}{2}}$					
4705.04		7	21247.86	0.00	$46902^{\circ}_{0\frac{1}{2}} - 68150_{1\frac{1}{2}}$					
4704.23		1	21251.52	−0.01 +0.04	$69607_{2\frac{1}{2}} - 90859^{\circ}_{2\frac{1}{2}}$ $72615_{5\frac{1}{2}} - 93867^{\circ}_{4\frac{1}{2}}$					
4703.012		4	21257.02	−0.01	$53716^{\circ}_{2\frac{1}{2}} - 74973_{3\frac{1}{2}}$					
4699.045		6	21274.97	−0.01	$53716^{\circ}_{2\frac{1}{2}} - 74991_{1\frac{1}{2}}$					
4698.62	10	40	21276.89	+0.01	$38342^{\circ}_{4\frac{1}{2}} - 59618_{3\frac{1}{2}}$					
4697.688		2	21281.11							
4697.34		3	21282.69	−0.03	$52987^{\circ}_{1\frac{1}{2}} - 74270_{2\frac{1}{2}}$					
4696.842	1	15	21284.95	−0.03	$45273^{\circ}_{3\frac{1}{2}} - 66558_{3\frac{1}{2}}$					
4692.41		2	21305.05	−0.04	$67416_{4\frac{1}{2}} - 88721^{\circ}_{3\frac{1}{2}}$					
4691.982		4	21306.99	0.00	$37516^{\circ}_{3\frac{1}{2}} - 58823_{2\frac{1}{2}}$					
4690.810	20	90	21312.32	+0.01	$34389^{\circ}_{2\frac{1}{2}} - 55702_{1\frac{1}{2}}$					
4689.807	1	7	21316.87	−0.04	$35059^{\circ}_{3\frac{1}{2}} - 56375_{2\frac{1}{2}}$					
4688.515	40	100	21322.75	+0.04	$32981^{\circ}_{1\frac{1}{2}} - 54304_{0\frac{1}{2}}$	4	0.84	1.88	0.52	0.32
4688.38	5	20	21323.36	−0.04	$41688^{\circ}_{1\frac{1}{2}} - 63011_{1\frac{1}{2}}$					
4658.876		6	21334.76	−0.01	$48272^{\circ}_{2\frac{1}{2}} - 69607_{2\frac{1}{2}}$					
4685.071		3	21338.42	0.00	$45012^{\circ}_{2\frac{1}{2}} - 66351_{2\frac{1}{2}}$					
4683.810	200	1000	21344.17	+0.01	$32371^{\circ}_{2\frac{1}{2}} - 53715_{3\frac{1}{2}}$	7	(1.17)	1.19	0	1.22
4681.088		3	21356.58	0.00	$62861_{3\frac{1}{2}} - 84217^{\circ}_{4\frac{1}{2}}$					
4678.171	2	6	21369.89	−0.04	$31568^{\circ}_{2\frac{1}{2}} - 52938_{1\frac{1}{2}}$					
4675.66	2	4	21381.37	−0.03	$56500^{\circ}_{3\frac{1}{2}} - 77882_{3\frac{1}{2}}$					
4674.644		1	21386.02	+0.03	$43075^{\circ}_{1\frac{1}{2}} - 64461_{1\frac{1}{2}}$					
4674.493	1	3	21386.71	+0.01	$68756_{3\frac{1}{2}} - 90142^{\circ}_{3\frac{1}{2}}$					
4671.386		3	21400.93	+0.01	$48556^{\circ}_{3\frac{1}{2}} - 69957_{4\frac{1}{2}}$					
4670.586	50	200	21404.60	0.00	$24332_{2\frac{1}{2}} - 45737^{\circ}_{1\frac{1}{2}}$	4	(1.20)	1.30	w	1.06
4669.280		4	21410.58	−0.02	$44940^{\circ}_{1\frac{1}{2}} - 66351_{2\frac{1}{2}}$					
4667.05	1	1	21420.81	−0.03	$74270_{2\frac{1}{2}} - 95691^{\circ}_{3\frac{1}{2}}$					

TABLE 6. Yb II—*Observed and classified lines*—Continued

1	2	3	4	5	6	7	8	9	10	11
Wave-length air	Intensity		Wave number	o–c	Classification	Zeeman type	1st g	2nd g	Zeeman components	
	Meggers lamp	Thomson lamp							Strong p	Strong n
Å			K	K						
4666.145	2	1	21424.97	−0.09	$31979^{\circ}_{3\frac{1}{2}} - 53404_{2\frac{1}{2}}$					
4660.906		4	21449.05	+0.01	$56621^{\circ}_{5\frac{1}{2}} - 78070_{4\frac{1}{2}}$					
4659.910		5	21453.64	−0.03 +0.01	$48503^{\circ}_{5\frac{1}{2}} - 69957_{4\frac{1}{2}}$ $68756_{3\frac{1}{2}} - 90209^{\circ}_{4\frac{1}{2}}$					
4659.60		1	21455.06	−0.05	$44940^{\circ}_{1\frac{1}{2}} - 66395_{2\frac{1}{2}}$					
4658.746		3	21459.00							
4658.443	2	2	21460.39							
4657.43		1	21465.06	+0.04	$68150_{1\frac{1}{2}} - 89615^{\circ}_{2\frac{1}{2}}$					
4654.070	1	5	21480.56	−0.03	$68135_{2\frac{1}{2}} - 89615^{\circ}_{2\frac{1}{2}}$					
4652.667		5	21487.03	−0.02	$56977^{\circ}_{0\frac{1}{2}} - 78464_{1\frac{1}{2}}$					
4652.279		2	21488.82	−0.02	$60910^{\circ}_{1\frac{1}{2}} - 82398_{1\frac{1}{2}}$					
4649.756		2	21500.48							
4647.076		2	21512.88	−0.04	$44438^{\circ}_{3\frac{1}{2}} - 65950_{4\frac{1}{2}}$					
4645.05		10	21522.27	+0.02	$44940^{\circ}_{1\frac{1}{2}} - 66462_{0\frac{1}{2}}$					
4643.14		5	21531.12	−0.01	$51248^{\circ}_{2\frac{1}{2}} - 72779_{3\frac{1}{2}}$					
4640.11		15	21545.18	−0.03	$45012^{\circ}_{2\frac{1}{2}} - 66558_{3\frac{1}{2}}$					
4639.04		1	21550.15							
4637.226		3	21558.58	−0.06	$68720_{6\frac{1}{2}} - 90279^{\circ}_{5\frac{1}{2}}$					
4635.01		1	21568.89	−0.07	$52067^{\circ}_{0\frac{1}{2}} - 73636_{0\frac{1}{2}}$					
4634.014	20	200	21573.52	−0.02	$37516^{\circ}_{3\frac{1}{2}} - 59090_{3\frac{1}{2}}$	7			0	1.05?
4630.614		3	21589.36	−0.06 −0.06	$52067^{\circ}_{0\frac{1}{2}} - 73657_{1\frac{1}{2}}$ $56480^{\circ}_{4\frac{1}{2}} - 78070_{4\frac{1}{2}}$					
4629.75		2	21593.39							
4624.93		2	21615.89							
4623.91		1	21620.66	−0.04	$43956^{\circ}_{2\frac{1}{2}} - 65577_{3\frac{1}{2}}$					
4623.060		3	21624.64	−0.08	$56840^{\circ}_{1\frac{1}{2}} - 78464_{1\frac{1}{2}}$					
4621.83		2	21630.39	−0.01	$69607_{2\frac{1}{2}} - 91237^{\circ}_{3\frac{1}{2}}$					
4620.51		2	21636.57	−0.09	$47758^{\circ}_{3\frac{1}{2}} - 69395_{3\frac{1}{2}}$					
4615.740		2	21658.93	−0.08	$56088^{\circ}_{4\frac{1}{2}} - 77747_{4\frac{1}{2}}$					
4614.020	1	3	21667.01	−0.01	$77747_{4\frac{1}{2}} - 99414^{\circ}_{4\frac{1}{2}}$					
4611.90		1	21676.97	+0.06	$67938_{3\frac{1}{2}} - 89615^{\circ}_{2\frac{1}{2}}$					
4610.70		1	21682.61	−0.06	$54640^{\circ}_{4\frac{1}{2}} - 76323_{3\frac{1}{2}}$					
4609.600		1	21687.78	−0.05	$52880^{\circ}_{4\frac{1}{2}} - 74568_{4\frac{1}{2}}$					
4608.131		15	21694.69	−0.02	$49419^{\circ}_{0\frac{1}{2}} - 71113_{1\frac{1}{2}}$					
4600.300		2	21731.62	−0.06	$47663^{\circ}_{4\frac{1}{2}} - 69395_{3\frac{1}{2}}$					
4598.85		2	21738.48							
4598.361	300	800	21740.79	−0.02	$31979^{\circ}_{3\frac{1}{2}} - 53720_{4\frac{1}{2}}$ [d]	5	(1.33)	1.29	w	1.16
4597.980	5	30	21742.59	−0.06	$37516^{\circ}_{3\frac{1}{2}} - 59259_{2\frac{1}{2}}$					
4597.279	2	30	21745.90	−0.09	$37077^{\circ}_{2\frac{1}{2}} - 58823_{2\frac{1}{2}}$					
4597.087		1	21746.81							

TABLE 6. Yb II—*Observed and classified lines*—Continued

1	2	3	4	5	6	7	8	9	10	11
Wave-length air	Intensity		Wave number	o–c	Classification	Zeeman type	1st g	2nd g	Zeeman components	
	Meggers lamp	Thomson lamp							Strong p	Strong n
Å			K	K						
4596.342		7	21750.34	−0.10	$47329^{\circ}_{2\frac{1}{2}} - 69079_{2\frac{1}{2}}$					
4595.556		1	21754.06	−0.08	$71222_{3\frac{1}{2}} - 92976^{\circ}_{3\frac{1}{2}}$					
4593.214		4	21765.15	−0.08	$64461_{1\frac{1}{2}} - 86226^{\circ}_{1\frac{1}{2}}$					
4592-443		10	21768.80	−0.10	$46169^{\circ}_{1\frac{1}{2}} - 67938_{3\frac{1}{2}}$					
4588.677		1	21786.67	−0.09	$40035^{\circ}_{3\frac{1}{2}} - 61822_{3\frac{1}{2}}$					
4587.075		15	21794.28	−0.05	$46354^{\circ}_{4\frac{1}{2}} - 68148_{5\frac{1}{2}}$					
4585.767		10	21800.49	−0.05	$34575^{\circ}_{1\frac{1}{2}} - 56375_{2\frac{1}{2}}$					
4579.536		6	21830.16	−0.04	$57798^{\circ}_{2\frac{1}{2}} - 79628_{3\frac{1}{2}}$					
4578.620		3	21834.52	−0.04	$53716^{\circ}_{2\frac{1}{2}} - 75550_{2\frac{1}{2}}$					
4578.142		7	21836.80	−0.08	$31568^{\circ}_{2\frac{1}{2}} - 53404_{2\frac{1}{2}}$					
4574.800		2	21852.75	−0.08	$53120^{\circ}_{2\frac{1}{2}} - 74973_{3\frac{1}{2}}$					
4572.740		1	21862.60							
4572.027		1	21866.01							
4571.660		3	21867.76	−0.09	$51248^{\circ}_{2\frac{1}{2}} - 73116_{1\frac{1}{2}}$					
4571.064		1	21870.62							
4570.081		1	21875.32	+0.03	$54640^{\circ}_{1\frac{1}{2}} - 76516_{1\frac{1}{2}}$					
4563.680		3	21906.00	−0.05	$53644^{\circ}_{3\frac{1}{2}} - 75550_{2\frac{1}{2}}$					
4562.440		5	21911.95							
4560.022		3	21923.57	−0.11 0.00	$53716^{\circ}_{2\frac{1}{2}} - 75640_{3\frac{1}{2}}$ $67789^{\circ}_{1\frac{1}{2}} - 89713_{2\frac{1}{2}}$?					
4557.936	20	150	21933.61	−0.03	$35831^{\circ}_{3\frac{1}{2}} - 57765_{4\frac{1}{2}}$					
4555.50		2	21945.34	0.00	$49008^{\circ}_{3\frac{1}{2}} - 70954_{2\frac{1}{2}}$					
4554.032	1	3	21952.41							
4553.576	500	1500	21954.61	+0.05	$30562^{\circ}_{3\frac{1}{2}} - 52517_{3\frac{1}{2}}$	6	1.12	1.26	0.80	1.19
4552.619		8	21959.22	−0.06	$41688^{\circ}_{1\frac{1}{2}} - 63647_{1\frac{1}{2}}$					
4552.175		2	21961.36							
4551.792		2*d*	21963.21							
4550.601		6	21968.96	−0.04	$41678^{\circ}_{2\frac{1}{2}} - 63647_{1\frac{1}{2}}$					
4548.359	40	80	21979.79	−0.02	$22960_{1\frac{1}{2}} - 44940^{\circ}_{1\frac{1}{2}}$					
4547.960		3	21981.72	−0.08 +0.06	$56088^{\circ}_{4\frac{1}{2}} - 78070_{4\frac{1}{2}}$ $60910^{\circ}_{1\frac{1}{2}} - 82891_{2\frac{1}{2}}$					
4547.032	1	20	21986.20	+0.05 −0.01	$34389^{\circ}_{2\frac{1}{2}} - 56375_{2\frac{1}{2}}$ $45429^{\circ}_{3\frac{1}{2}} - 67416_{4\frac{1}{2}}$					
4545.383		1	21994.18							
4545.216		2	21994.99	−0.01	$69607_{2\frac{1}{2}} - 91602^{\circ}_{2\frac{1}{2}}$					
4543.879	2	40	22001.46	−0.05	$46547^{\circ}_{3\frac{1}{2}} - 68549_{4\frac{1}{2}}$					
4543.452		4	22003.53	−0.07	$52987^{\circ}_{1\frac{1}{2}} - 74991_{1\frac{1}{2}}$					
4543.302		3	22004.25	−0.09	$48024^{\circ}_{1\frac{1}{2}} - 70029_{0\frac{1}{2}}$					
4542.588	1*h*	5	22007.71	−0.03	$68135_{2\frac{1}{2}} - 90142^{\circ}_{3\frac{1}{2}}$					
4542.371		1	22008.76							

TABLE 6. Yb II—*Observed and classified lines*—Continued

1	2	3	4	5	6	7	8	9	10	11
Wavelength air	Intensity		Wave number	o–c	Classification	Zeeman type	1st g	2nd g	Zeeman components	
	Meggers lamp	Thomson lamp							Strong p	Strong n
Å			K	K						
4541.598		2	22012.51	−0.03	$37077^{\circ}_{2\frac{1}{2}} - 59090_{3\frac{1}{2}}$					
4541.325	20	100	22013.83	−0.04	$41688^{\circ}_{1\frac{1}{2}} - 63702_{2\frac{1}{2}}$	5	0.78	1.04	0.13	1.43
4539.323	5	20	22023.54	−0.05	$41678^{\circ}_{2\frac{1}{2}} - 63702_{2\frac{1}{2}}$					
4538.027		3	22029.83							
4537.494		2	22032.42	−0.05	$59624^{\circ}_{3\frac{1}{2}} - 81657_{2\frac{1}{2}}$					
4536.805		3	22035.77							
4535.718		2	22041.05	−0.04	$54192^{\circ}_{5\frac{1}{2}} - 76233_{6\frac{1}{2}}$					
4534.250		1	22048.18	−0.03	$33653^{\circ}_{0\frac{1}{2}} - 55702_{1\frac{1}{2}}$					
4530.657		3	22065.67	−0.09	$47329^{\circ}_{2\frac{1}{2}} - 69395_{3\frac{1}{2}}$					
4528.882		5	22074.31	−0.11	$47005^{\circ}_{1\frac{1}{2}} - 69079_{2\frac{1}{2}}$					
4527.526		2	22080.93	−0.07	$45335^{\circ}_{4\frac{1}{2}} - 67416_{4\frac{1}{2}}$					
4525.535		1	22090.64							
4525.108		3	22092.72	+0.06	$52880^{\circ}_{4\frac{1}{2}} - 74973_{3\frac{1}{2}}$					
4524.810		2	22094.18	−0.08	$57534^{\circ}_{3\frac{1}{2}} - 79628_{3\frac{1}{2}}$					
4524.549	1	4	22095.45	−0.11	$46354^{\circ}_{4\frac{1}{2}} - 68450_{3\frac{1}{2}}$					
4523.161		2	22102.23	−0.08	$37516^{\circ}_{3\frac{1}{2}} - 59618_{3\frac{1}{2}}$					
4520.746		8	22114.04	−0.04	$47329^{\circ}_{2\frac{1}{2}} - 69443_{1\frac{1}{2}}$					
4517.218		2	22131.31	−0.08	$66571_{5\frac{1}{2}} - 88702^{\circ}_{5\frac{1}{2}}$					
4517.051		1	22132.13							
4516.094	1	2	22136.82							
4515.636		2	22139.07							
4515.161	200	800	22141.40	+0.01	$26759^{\circ}_{2\frac{1}{2}} - 48900_{3\frac{1}{2}}$	4	1.57	1.05	0.26	−0.25
4514.846		10	22142.94	−0.07	$45273^{\circ}_{3\frac{1}{2}} - 67416_{4\frac{1}{2}}$					
4513.990	6	20	22147.14	−0.04	$31568^{\circ}_{2\frac{1}{2}} - 53715_{3\frac{1}{2}}$					
4512.909		1	22152.44							
4511.725		3	22158.26	−0.12	$59046^{\circ}_{4\frac{1}{2}} - 81205_{4\frac{1}{2}}$					
4510.744		3	22163.08	−0.04	$66558_{3\frac{1}{2}} - 88721^{\circ}_{3\frac{1}{2}}$					
4509.700		3	22168.21	−0.10	$68549_{4\frac{1}{2}} - 90717^{\circ}_{4\frac{1}{2}}$					
4508.788	1	9	22172.69	−0.03	$46547^{\circ}_{5\frac{1}{2}} - 68720_{6\frac{1}{2}}$					
4506.95		2*d*	22181.73	+0.08	$37077^{\circ}_{2\frac{1}{2}} - 59259_{2\frac{1}{2}}$					
4506.045	1	4	22186.19	−0.01	$65199_{4\frac{1}{2}} - 87385^{\circ}_{3\frac{1}{2}}$					
4505.900		5	22186.90							
4505.345		3	22189.63							
4504.850		2	22192.07	−0.11	$45012^{\circ}_{2\frac{1}{2}} - 67204_{1\frac{1}{2}}$					
4504.331	1	9	22194.63	−0.05 −0.01	$46354^{\circ}_{4\frac{1}{2}} - 68549_{4\frac{1}{2}}$ $58484^{\circ}_{4\frac{1}{2}} - 80679_{5\frac{1}{2}}$					
4503.463		5	22198.91	−0.04	$47758^{\circ}_{3\frac{1}{2}} - 69957_{4\frac{1}{2}}$					
4500.542		3	22213.31	−0.12	$49008^{\circ}_{3\frac{1}{2}} - 71222_{3\frac{1}{2}}$					
4500.304		1	22214.49	−0.07	$47228^{\circ}_{0\frac{1}{2}} - 69443_{1\frac{1}{2}}$					
4499.621		3	22217.86	−0.08	$45737^{\circ}_{1\frac{1}{2}} - 67955_{0\frac{1}{2}}$					
4499.462		1	22218.65							

TABLE 6. Yb II—*Observed and classified lines*—Continued

1	2	3	4	5	6	7	8	9	10	11
Wave-length air	Intensity		Wave number	o–c	Classification	Zeeman type	1st g	2nd g	Zeeman components	
	Meggers lamp	Thomson lamp							Strong p	Strong n
Å			K	K						
4495.520		1	22238.13							
4493.965	50	150	22245.82	−0.06	$40917^{\circ}_{4\frac{1}{2}} - 63163_{4\frac{1}{2}}$	6	0.964	1.116	0.685	1.04
4493.244		1	22249.39							
4491.422		1	22258.42							
4490.240		1	22264.28	−0.08	$44940^{\circ}_{1\frac{1}{2}} - 67204_{1\frac{1}{2}}$					
4487.266	50	200	22279.03	−0.04	$41678^{\circ}_{2\frac{1}{2}} - 63957_{3\frac{1}{2}}$	7	(1.193)	1.17	0	1.12
4487.03		2*h*	22280.21	−0.12	$46169^{\circ}_{4\frac{1}{2}} - 68450_{3\frac{1}{2}}$					
4486.794		1	22281.38							
4486.225		1	22284.20							
4485.986		1	22285.39							
4485.326		6	22288.67							
4485.040		2	22290.09	−0.05	$48503^{\circ}_{5\frac{1}{2}} - 70793_{5\frac{1}{2}}$					
4484.466	20	60	22292.94	−0.08	$30224^{\circ}_{4\frac{1}{2}} - 52517_{5\frac{1}{2}}$					
4484.280	1	5	22293.87	−0.10	$47663^{\circ}_{4\frac{1}{2}} - 69957_{4\frac{1}{2}}$					
4475.666		2	22336.78	−0.07	$70858_{4\frac{1}{2}} - 93195^{\circ}_{3\frac{1}{2}}$					
4474.115		3	22344.52	−0.02	$49419^{\circ}_{0\frac{1}{2}} - 71763_{1\frac{1}{2}}$					
4473.884		1	22345.67	−0.08	$69957_{4\frac{1}{2}} - 92303^{\circ}_{3\frac{1}{2}}$					
4472.146		8	22354.36	0.00	$48503^{\circ}_{5\frac{1}{2}} - 70858_{4\frac{1}{2}}$					
4470.958		1	22360.30							
4469.566		3	22367.26	−0.11	$41688^{\circ}_{1\frac{1}{2}} - 64055_{2\frac{1}{2}}$					
4467.642		1	22376.89							
4467.128	1	10	22379.47	+0.02	$46169^{\circ}_{4\frac{1}{2}} - 68549_{4\frac{1}{2}}$					
4466.002		7	22385.11	−0.01	$55221^{\circ}_{1\frac{1}{2}} - 77606_{2\frac{1}{2}}$					
4465.663		2	22386.81							
4463.965		2	22395.32	+0.05	$61822_{3\frac{1}{2}} - 84217^{\circ}_{4\frac{1}{2}}$					
4463.855	1	8	22395.88	−0.05	$46547^{\circ}_{5\frac{1}{2}} - 68943_{4\frac{1}{2}}$					
4463.493	1	9	22397.69	−0.02 −0.01	$45737^{\circ}_{1\frac{1}{2}} - 68135_{2\frac{1}{2}}$ $48556^{\circ}_{3\frac{1}{2}} - 70954_{2\frac{1}{2}}$					
4460.923	1	5	22410.60	−0.02	$67204_{1\frac{1}{2}} - 89615^{\circ}_{2\frac{1}{2}}$					
4460.405		1	22413.20	−0.08	$45737^{\circ}_{1\frac{1}{2}} - 68150_{1\frac{1}{2}}$					
4459.181		1	22419.35	−0.01	$55462^{\circ}_{3\frac{1}{2}} - 77882_{3\frac{1}{2}}$					
4457.428		2	22428.17							
4457.311		1	22428.76							
4456.994		4	22430.35	−0.01	$53120^{\circ}_{2\frac{1}{2}} - 75550_{2\frac{1}{2}}$					
4452.663		3	22452.17	−0.06	$70793_{5\frac{1}{2}} - 93246^{\circ}_{6\frac{1}{2}}$					
4452.153		1	22454.74							
4451.930		20	22455.86	+0.02	$47680^{\circ}_{6\frac{1}{2}} - 70136_{6\frac{1}{2}}$					
4451.11		2*d*	22460.00							
4450.60		1	22462.58	−0.05	$64923_{4\frac{1}{2}} - 87385^{\circ}_{3\frac{1}{2}}$					
4444.860		3	22491.58	−0.05	$43075^{\circ}_{1\frac{1}{2}} - 65566_{0\frac{1}{2}}$					
4442.075		3	22505.68	0.00	$56621^{\circ}_{5\frac{1}{2}} - 79126_{4\frac{1}{2}}$					

TABLE 6. Yb II—*Observed and classified lines*—Continued

1	2	3	4	5	6	7	8	9	10	11
Wave-length air	Intensity		Wave number	o–c	Classification	Zeeman type	1st g	2nd g	Zeeman components	
	Meggers lamp	Thomson lamp							Strong p	Strong n
Å			K	K						
4441.484		2	22508.68	−0.06	$70954_{2\frac{1}{2}} - 93463^{\circ}_{3\frac{1}{2}}$					
4438.142		7	22525.63	−0.06	$57103^{\circ}_{3\frac{1}{2}} - 79628_{3\frac{1}{2}}$					
4435.150		5	22540.82	+0.01	$46902^{\circ}_{0\frac{1}{2}} - 69443_{1\frac{1}{2}}$					
4434.178	40	100	22545.76	−0.02	$30392^{\circ}_{1\frac{1}{2}} - 52938_{1\frac{1}{2}}$					
4431.595		1	22558.91	−0.02	$43007^{\circ}_{0\frac{1}{2}} - 65566_{0\frac{1}{2}}$					
4428.153		3*h*	22576.44							
4423.129		1	22602.08	0.00	$47005^{\circ}_{1\frac{1}{2}} - 69607_{2\frac{1}{2}}$					
4422.150		3	22607.09	−0.02	$53716^{\circ}_{2\frac{1}{2}} - 76323_{3\frac{1}{2}}$					
4419.495		1	22620.67	−0.05	$66082_{5\frac{1}{2}} - 88702^{\circ}_{5\frac{1}{2}}$					
4418.132		3	22627.65	−0.02	$58051^{\circ}_{5\frac{1}{2}} - 80679_{5\frac{1}{2}}$					
4417.814		1	22629.27	−0.05	$52921^{\circ}_{3\frac{1}{2}} - 75550_{2\frac{1}{2}}$					
4417.080		3	22633.03	−0.03	$37077^{\circ}_{2\frac{1}{2}} - 59710_{1\frac{1}{2}}$					
4414.548		1	22646.02	−0.04 −0.01	$56480^{\circ}_{4\frac{1}{2}} - 79126_{4\frac{1}{2}}$ $59046^{\circ}_{4\frac{1}{2}} - 81692_{3\frac{1}{2}}$					
4410.740		2*h*	22665.57	−0.09	$45273^{\circ}_{3\frac{1}{2}} - 67938_{3\frac{1}{2}}$					
4409.685		2*h*	22670.99							
4409.346	200	300	22672.73	−0.04	$24332_{2\frac{1}{2}} - 47005^{\circ}_{1\frac{1}{2}}$	5	1.20	1.02	0.09	1.47
4408.220		1	22678.52	−0.08	$53644^{\circ}_{3\frac{1}{2}} - 76323_{3\frac{1}{2}}$					
4407.650	1	4	22681.46	−0.04	$48272^{\circ}_{2\frac{1}{2}} - 70954_{2\frac{1}{2}}$					
4405.496		1	22692.55	−0.03	$67204_{1\frac{1}{2}} - 89897^{\circ}_{1\frac{1}{2}}$					
4404.208		1	22699.18	−0.06	$49916^{\circ}_{4\frac{1}{2}} - 72615_{5\frac{1}{2}}$					
4403.037		1	22705.22	+0.04	$45429^{\circ}_{3\frac{1}{2}} - 68135_{2\frac{1}{2}}$					
4402.824		5	22706.32	0.00	$35059^{\circ}_{3\frac{1}{2}} - 57765_{4\frac{1}{2}}$					
4402.300	40	200	22709.02	−0.02	$38342^{\circ}_{4\frac{1}{2}} - 61051_{3\frac{1}{2}}$	4	(1.093)	1.18	*w*	0.80
4401.824		1	22711.48							
4401.445	1	6	22713.43	−0.01	$48556^{\circ}_{3\frac{1}{2}} - 71270_{2\frac{1}{2}}$					
4400.583		1	22717.88	−0.07	$51248^{\circ}_{2\frac{1}{2}} - 73966_{3\frac{1}{2}}$					
4399.391		1	22724.04	−0.03	$68135_{2\frac{1}{2}} - 90859^{\circ}_{2\frac{1}{2}}$					
4396.499	10	40	22738 .98	−0.04 +0.03	$26759^{\circ}_{2\frac{1}{2}} - 49498_{2\frac{1}{2}}$ $71270_{2\frac{1}{2}} - 94008^{\circ}_{3\frac{1}{2}}$					
4392.825	50	100	22758.00	−0.05 +0.05	$39378^{\circ}_{0\frac{1}{2}} - 62136_{0\frac{1}{2}}$ $(56056^{\circ}_{2\frac{1}{2}} - 78814_{2\frac{1}{2}})$	6	1.84	0.08	0.88	0.96
4390.49		1	22770.10	−0.07	$65950_{4\frac{1}{2}} - 88721^{\circ}_{3\frac{1}{2}}$					
4390.43		1	22770.42							
4389.764	50	200	22773.87	0.00	$46169^{\circ}_{4\frac{1}{2}} - 68943_{4\frac{1}{2}}$					
4388.528		8	22780.28	−0.08	$68756_{3\frac{1}{2}} - 91536^{\circ}_{3\frac{1}{2}}$					
4387.46		1	22785.83							
4387.144	1	10	22787.47	+0.01	$64598_{3\frac{1}{2}} - 87385^{\circ}_{3\frac{1}{2}}$					
4385.97	2	20	22793.57	−0.07	$67416_{4\frac{1}{2}} - 90209^{\circ}_{4\frac{1}{2}}$					
4385.66	3	10	22795.18	−0.03	$39378^{\circ}_{0\frac{1}{2}} - 62174_{1\frac{1}{2}}$					

TABLE 6. Yb II—*Observed and classified lines*—Continued

1	2	3	4	5	6	7	8	9	10	11
Wave-length air	Intensity		Wave number	o–c	Classification	Zeeman type	1st g	2nd g	Zeeman components	
	Meggers lamp	Thomson lamp							Strong p	Strong n
Å			K	K						
4384.72		2	22800.07	−0.01	$47228^{\circ}_{0\frac{1}{2}} - 70029_{0\frac{1}{2}}$					
4383.93		10	22804.18	0.00	$50832^{\circ}_{1\frac{1}{2}} - 73636_{0\frac{1}{2}}$					
4383.11		1	22808.44	−0.06	$54640^{\circ}_{4\frac{1}{2}} - 77449_{3\frac{1}{2}}$					
4383.02		2	22808.91	−0.01	$40917^{\circ}_{4\frac{1}{2}} - 63726_{4\frac{1}{2}}$					
4382.16		1	22813.39	+0.02	$43075^{\circ}_{1\frac{1}{2}} - 65888_{1\frac{1}{2}}$					
4382.08		2	22813.80	−0.05	$45335^{\circ}_{3\frac{1}{2}} - 68148_{3\frac{1}{2}}$					
4381.80		20	22815.26	−0.04	$50468^{\circ}_{5\frac{1}{2}} - 73283_{4\frac{1}{2}}$					
4379.50	20	300	22827.24	+0.04	$65875_{6\frac{1}{2}} - 88702^{\circ}_{5\frac{1}{2}}$					
4377.80		1	22836.11							
4376.851	1	40	22841.06	−0.01	$48272^{\circ}_{2\frac{1}{2}} - 71113_{1\frac{1}{2}}$					
4376.649		2	22842.11							
4374.861		3	22851.45	−0.04	$58661^{\circ}_{2\frac{1}{2}} - 81512_{1\frac{1}{2}}$					
4372.854		1	22861.94	−0.04	$45273^{\circ}_{3\frac{1}{2}} - 68135_{2\frac{1}{2}}$					
4372.65		2	22863.00	−0.05	$67416_{4\frac{1}{2}} - 90279^{\circ}_{5\frac{1}{2}}$					
4372.560	2	30	22863.47	−0.02	$49916^{\circ}_{1\frac{1}{2}} - 72779_{3\frac{1}{2}}$					
4371.083		3	22871.20	−0.02	$53644^{\circ}_{3\frac{1}{2}} - 76516_{4\frac{1}{2}}$					
4371.05		1	22871.37							
4370.810	200	2000	22872.63	−0.01	$38342^{\circ}_{4\frac{1}{2}} - 61214_{4\frac{1}{2}}$	6	1.10	1.07	0.15	1.08
4368.89		1	22882.68							
4368.520		1	22884.62	−0.06	$71113_{1\frac{1}{2}} - 93998^{\circ}_{1\frac{1}{2}}$					
4365.948		2	22898.10							
4364.056		5	22908.02	−0.02	$69395_{3\frac{1}{2}} - 92303^{\circ}_{3\frac{1}{2}}$					
4363.54		1	22910.73	+0.02	$53322^{\circ}_{7\frac{1}{2}} - 76233_{6\frac{1}{2}}$					
4363.280	6	90	22912.10	−0.03	$48556^{\circ}_{3\frac{1}{2}} - 71468_{2\frac{1}{2}}$					
4362.333		4	22917.07	−0.07	$66796^{\circ}_{3\frac{1}{2}} - 89713_{2\frac{1}{2}}$					
4362.156	1	6	22918.00	−0.01	$52987^{\circ}_{1\frac{1}{2}} - 75905_{0\frac{1}{2}}$					
4361.868		2	22919.52	−0.03	$41678^{\circ}_{2\frac{1}{2}} - 64598_{3\frac{1}{2}}$					
4361.468	1	10	22921.62	0.00	$52067^{\circ}_{0\frac{1}{2}} - 74989_{0\frac{1}{2}}$	7	0.50	0.50	0	0.500
4360.663		4	22925.85	−0.04	$45012^{\circ}_{2\frac{1}{2}} - 67938_{3\frac{1}{2}}$					
4360.140	1	2	22928.60							
4359.958		20	22929.56	−0.01	$48024^{\circ}_{1\frac{1}{2}} - 70954_{2\frac{1}{2}}$					
4359.165[a]	3	2	22933.73							
4356.160		3	22949.55	−0.04	$48272^{\circ}_{2\frac{1}{2}} - 71222_{3\frac{1}{2}}$					
4355.58		1	22952.60							
4354.191	3	10	22959.93	0.00 +0.03	$53716^{\circ}_{2\frac{1}{2}} - 76676_{2\frac{1}{2}}$ $59439^{\circ}_{2\frac{1}{2}} - 82398_{1\frac{1}{2}}$					
4350.801		15	22977.81							
4349.952		2	22982.30							
4348.087	3	15	22992.16	−0.04	$63234_{2\frac{1}{2}} - 86226^{\circ}_{1\frac{1}{2}}$					
4347.358		3	22996.01	+0.01	$58661^{\circ}_{2\frac{1}{2}} - 81657_{2\frac{1}{2}}$					

TABLE 6. Yb II—*Observed and classified lines*—Continued

1	2	3	4	5	6	7	8	9	10	11
Wave-length air	Intensity		Wave number	o–c	Classification	Zeeman type	1st g	2nd g	Zeeman components	
	Meggers lamp	Thomson lamp							Strong p	Strong n
Å			K	K						
4347.223	10	20	22996.73	−0.02	$24332_{2\frac{1}{2}} - 47329^{\circ}_{2\frac{1}{2}}$					
4347.13		1	22997.22	−0.02	$48272^{\circ}_{2\frac{1}{2}} - 71270_{2\frac{1}{2}}$					
4346.00		1	23003.20	+0.01	$61214_{4\frac{1}{2}} - 84217^{\circ}_{4\frac{1}{2}}$					
4344.894	1	20	23009.05	+0.01	$70858_{4\frac{1}{2}} - 93867^{\circ}_{4\frac{1}{2}}$					
4344.204	60	300	23012.71	−0.02	$30392^{\circ}_{1\frac{1}{2}} - 53404_{2\frac{1}{2}}$	4	1.320	1.034	0.143	0.605
4343.845		5	23014.61	−0.01	$44940^{\circ}_{1\frac{1}{2}} - 67955_{0\frac{1}{2}}$					
4342.753		3	23020.40	+0.11	$45429^{\circ}_{3\frac{1}{2}} - 68450_{3\frac{1}{2}}$					
4342.151	6	80	23023.59	+0.01	$47005^{\circ}_{1\frac{1}{2}} - 70029_{0\frac{1}{2}}$	5	0.98	0.68	0.15	1.15
4341.646		10	23026.27	0.00	$40917^{\circ}_{4\frac{1}{2}} - 63944_{5\frac{1}{2}}$					
4340.673	2	7	23031.43	+0.01	$53644^{\circ}_{3\frac{1}{2}} - 76676_{2\frac{1}{2}}$					
4340.269		1	23033.57	0.00	$71270_{2\frac{1}{2}} - 94303^{\circ}_{3\frac{1}{2}}$					
4340.147	1	15	23034.22	0.00	$66571_{5\frac{1}{2}} - 89605^{\circ}_{4\frac{1}{2}}$					
4339.082	150	1000	23039.87	−0.02	$40917^{\circ}_{4\frac{1}{2}} - 63957_{3\frac{1}{2}}$	4	0.977	1.147	0.085	0.383
4337.235		2	23049.68	+0.01	$53120^{\circ}_{2\frac{1}{2}} - 76170_{2\frac{1}{2}}$					
4336.30		1	23054.65	−0.04	$70954_{2\frac{1}{2}} - 94008^{\circ}_{3\frac{1}{2}}$					
4334.914	3	4	23062.02							
4332.809		4	23073.23	−0.03	$70793_{5\frac{1}{2}} - 93867^{\circ}_{4\frac{1}{2}}$					
4331.942		2	23077.85							
4331.762		3	23078.81	0.00	$69957_{4\frac{1}{2}} - 93036^{\circ}_{5\frac{1}{2}}$					
4331.318		1	23081.17	−0.05	$71222_{3\frac{1}{2}} - 94303^{\circ}_{3\frac{1}{2}}$					
4331.032		5	23082.69	0.00	$53716^{\circ}_{2\frac{1}{2}} - 76799_{1\frac{1}{2}}$					
4329.818		15	23089.17	+0.03	$48024^{\circ}_{1\frac{1}{2}} - 71113_{1\frac{1}{2}}$					
4329.654		1	23090.04	−0.07	$73291_{5\frac{1}{2}} - 96382^{\circ}_{5\frac{1}{2}}$					
4327.853		9	23099.65	+0.01	$47758^{\circ}_{3\frac{1}{2}} - 70858_{4\frac{1}{2}}$					
4327.238		2	23102.93	−0.01	$68135_{2\frac{1}{2}} - 91237^{\circ}_{3\frac{1}{2}}$					
4326.637	1	15	23106.14	−0.01	$70136_{6\frac{1}{2}} - 93242^{\circ}_{5\frac{1}{2}}$					
4326.556		9	23106.57	−0.01	$54640^{\circ}_{4\frac{1}{2}} - 77747_{4\frac{1}{2}}$					
4325.240	6	90	23113.60	+0.04	$47680^{\circ}_{6\frac{1}{2}} - 70793_{5\frac{1}{2}}$					
4325.033		2	23114.71	−0.02	$59777^{\circ}_{1\frac{1}{2}} - 82891_{2\frac{1}{2}}$					
4324.962		1	23115.09	+0.01	$45335^{\circ}_{4\frac{1}{2}} - 68450_{3\frac{1}{2}}$					
4324.500		7	23117.56	0.00	$57561^{\circ}_{6\frac{1}{2}} - 80679_{5\frac{1}{2}}$					
4324.160		1	23119.38	−0.03	$45429^{\circ}_{3\frac{1}{2}} - 68549_{4\frac{1}{2}}$					
4323.630		8	23122.21	0.00	$45012^{\circ}_{2\frac{1}{2}} - 68135_{2\frac{1}{2}}$					
4323.554	1	5	23122.62	0.00	$53716^{\circ}_{2\frac{1}{2}} - 76839_{2\frac{1}{2}}$					
4322.851		1	23126.38	+0.05	$46902^{\circ}_{0\frac{1}{2}} - 70029_{0\frac{1}{2}}$					
4322.56	2	30	23127.93	−0.04	$40035^{\circ}_{3\frac{1}{2}} - 63163_{4\frac{1}{2}}$					
4322.53	1	20	23128.10	+0.03	$56500^{\circ}_{3\frac{1}{2}} - 79628_{3\frac{1}{2}}$					
4322.230	200	2000	23129.70	+0.01	$35831^{\circ}_{5\frac{1}{2}} - 58961_{5\frac{1}{2}}$	6	1.22	0.98	1.30	1.11
4320.723		2	23137.77	−0.01	$45012^{\circ}_{2\frac{1}{2}} - 68150_{1\frac{1}{2}}$					
4319.556	1	9	23144.02	+0.01	$65577_{3\frac{1}{2}} - 88721^{\circ}_{3\frac{1}{2}}$					

TABLE 6. Yb II—*Observed and classified lines*—Continued

1	2	3	4	5	6	7	8	9	10	11
Wave-length air	Intensity		Wave number	o–c	Classification	Zeeman type	1st g	2nd g	Zeeman components	
	Meggers lamp	Thomson lamp							Strong p	Strong n
Å			K	K						
4318.978		1	23147.12	−0.01	$73750_{4\frac{1}{2}} - 96898^{\circ}_{5\frac{1}{2}}$					
4318.820		1	23147.96	+0.02	$56480^{\circ}_{4\frac{1}{2}} - 79628_{3\frac{1}{2}}$					
4318.750		2	23148.34							
4318.459	2	10	23149.90	0.00	$58162^{\circ}_{1\frac{1}{2}} - 81312_{2\frac{1}{2}}$					
4318.010		3	23152.31							
4317.751	1	15	23153.69	−0.07	$58051^{\circ}_{5\frac{1}{2}} - 81205_{4\frac{1}{2}}$					
4316.954	2000	8000	23157.97	+0.05	$30562^{\circ}_{5\frac{1}{2}} - 53720_{4\frac{1}{2}}$	4	1.126	1.276	0.075	0.451
4315.302		3	23166.83	+0.04	$61051_{3\frac{1}{2}} - 84217^{\circ}_{4\frac{1}{2}}$					
4315.15		1	23167.65							
4310.230	1	10	23194.09	−0.02	$53644^{\circ}_{3\frac{1}{2}} - 76839_{2\frac{1}{2}}$					
4310.124		20	23194.66	0.00	$47663^{\circ}_{4\frac{1}{2}} - 70858_{4\frac{1}{2}}$					
4309.886		15	23195.95	+0.02	$48272^{\circ}_{2\frac{1}{2}} - 71468_{2\frac{1}{2}}$					
4309.308		4	23199.06	−0.03	$73283_{4\frac{1}{2}} - 96482^{\circ}_{4\frac{1}{2}}$					
4308.586		7	23202.94	+0.03	$53120^{\circ}_{2\frac{1}{2}} - 76323_{3\frac{1}{2}}$					
4307.583		4	23208.35	−0.03	$58484^{\circ}_{4\frac{1}{2}} - 81692_{3\frac{1}{2}}$					
4307.29		3	23209.93	−0.03	$44940^{\circ}_{1\frac{1}{2}} - 68150_{1\frac{1}{2}}$					
4306.494	2	80	23214.22	+0.02	$45335^{\circ}_{4\frac{1}{2}} - 68549_{4\frac{1}{2}}$					
4304.512		2	23224.90	−0.01	$35059^{\circ}_{3\frac{1}{2}} - 58283_{2\frac{1}{2}}$					
4304.422		2	23225.39	−0.03	$46169^{\circ}_{4\frac{1}{2}} - 69395_{3\frac{1}{2}}$					
4303.675		2	23229.42	+0.01	$61214_{4\frac{1}{2}} - 84444^{\circ}_{3\frac{1}{2}}$					
4301.496	5	15	23241.19	−0.03	$54640^{\circ}_{4\frac{1}{2}} - 77882_{3\frac{1}{2}}$					
4300.736		4	23245.30	−0.01	$48024^{\circ}_{1\frac{1}{2}} - 71270_{2\frac{1}{2}}$					
4298.075		1	23259.69	−0.03	$68756_{3\frac{1}{2}} - 92015^{\circ}_{4\frac{1}{2}}$					
4296.696		3	23267.15	+0.01	$59624^{\circ}_{3\frac{1}{2}} - 82891_{2\frac{1}{2}}$					
4296.338		3	23269.09							
4293.421		8	23284.90	0.00	$69957_{4\frac{1}{2}} - 93242^{\circ}_{5\frac{1}{2}}$					
4290.357		7	23301.53	+0.02	$67416_{4\frac{1}{2}} - 90717^{\circ}_{4\frac{1}{2}}$					
4289.91		1	23303.96							
4288.800		9	23309.99							
4286.839		7	23320.65	+0.02	$43075^{\circ}_{1\frac{1}{2}} - 66395_{2\frac{1}{2}}$					
4285.878		9	23325.88							
4285.816		1	23326.22	0.00	$45429^{\circ}_{3\frac{1}{2}} - 68756_{3\frac{1}{2}}$					
4285.258	1	9	23329.25							
4285.127	2	15	23329.97	+0.05	$64055_{2\frac{1}{2}} - 87385^{\circ}_{3\frac{1}{2}}$					
4284.942	7	80	23330.97	0.00	$32371^{\circ}_{2\frac{1}{2}} - 55702_{1\frac{1}{2}}$					
4283.453		1	23339.08							
4282.808		10	23342.60	+0.01	$45737^{\circ}_{1\frac{1}{2}} - 69079_{2\frac{1}{2}}$					
4281.972	20	50	23347.16							
4281.584		5	23349.27	−0.04	$70954_{2\frac{1}{2}} - 94303^{\circ}_{3\frac{1}{2}}$					
4280.636		2	23354.44	−0.04	$71468_{2\frac{1}{2}} - 94823^{\circ}_{1\frac{1}{2}}$					

TABLE 6. Yb II—*Observed and classified lines*—Continued

1	2	3	4	5	6	7	8	9	10	11
Wavelength air	Intensity		Wave number	o–c	Classification	Zeeman type	1st g	2nd g	Zeeman components	
	Meggers lamp	Thomson lamp							Strong p	Strong n
Å			K	K						
4280.594		1	23354.67	−0.02	$57103^{\circ}_{3\frac{1}{2}} - 80457_{3\frac{1}{2}}$					
4277.092		2	23373.79							
4276.78		1	23375.50	+0.05	$49916^{\circ}_{4\frac{1}{2}} - 73291_{5\frac{1}{2}}$					
4273.340	20	150	23394.32	0.00	$32981^{\circ}_{1\frac{1}{2}} - 56375_{2\frac{1}{2}}$	5	(0.87)	1.23	0.18	?
4271.963		2	23401.86	−0.01	$52921^{\circ}_{3\frac{1}{2}} - 76323_{3\frac{1}{2}}$					
4270.515	4	60	23409.79	+0.02	$46547^{\circ}_{5\frac{1}{2}} - 69957_{4\frac{1}{2}}$					
4268.882		1	23418.75	−0.04	$58672^{\circ}_{0\frac{1}{2}} - 82091_{0\frac{1}{2}}$					
4267.590	50	100	23425.84	−0.01	$24332_{2\frac{1}{2}} - 47758^{\circ}_{3\frac{1}{2}}$					
4266.952	10	100	23429.34	−0.03	$54640^{\circ}_{4\frac{1}{2}} - 78070_{4\frac{1}{2}}$					
4265.976		2	23434.70	+0.01	$66462_{0\frac{1}{2}} - 89897^{\circ}_{1\frac{1}{2}}$					
4265.498		1	23437.32	0.00	$45012^{\circ}_{2\frac{1}{2}} - 68450_{3\frac{1}{2}}$					
4264.802	1	30	23441.15	−0.02	$44497^{\circ}_{2\frac{1}{2}} - 67938_{3\frac{1}{2}}$					
4264.520		1	23442.70	−0.04	$52880^{\circ}_{4\frac{1}{2}} - 76323_{3\frac{1}{2}}$					
4264.282		5	23444.01	+0.01	$48024^{\circ}_{1\frac{1}{2}} - 71468_{2\frac{1}{2}}$					
4264.029		6	23445.40	0.00	$70858_{4\frac{1}{2}} - 94303^{\circ}_{3\frac{1}{2}}$					
4262.826	2	5	23452.02	+0.05	$68150_{1\frac{1}{2}} - 91602^{\circ}_{2\frac{1}{2}}$					
4262.691		6	23452.76	+0.04	$59439^{\circ}_{2\frac{1}{2}} - 82891_{2\frac{1}{2}}$					
4262.273		1	23455.06	−0.01	$43007^{\circ}_{0\frac{1}{2}} - 66462_{0\frac{1}{2}}$					
4260.678		7	23463.84	+0.02	$47758^{\circ}_{3\frac{1}{2}} - 71222_{3\frac{1}{2}}$					
4259.17		1	23472.15							
4258.194	2	20	23477.53	+0.01	$70858_{4\frac{1}{2}} - 94335^{\circ}_{5\frac{1}{2}}$					
4257.640	200	2000	23480.58	+0.02	$38342^{\circ}_{4\frac{1}{2}} - 61822_{3\frac{1}{2}}$	4	1.10	1.34	0.12	0.26
4257.198		6	23483.02	0.00	$45273^{\circ}_{3\frac{1}{2}} - 68756_{3\frac{1}{2}}$					
4255.765	500	2000	23490.93	0.00 +0.03	$30224^{\circ}_{4\frac{1}{2}} - 53715_{3\frac{1}{2}}$ $(48272^{\circ}_{2\frac{1}{2}} - 71763_{1\frac{1}{2}})$	4	(0.94)	1.19	0.125	?
4254.775	200	800	23496.39	+0.01	$30224^{\circ}_{4\frac{1}{2}} - 53720_{4\frac{1}{2}}$	6	0.95	1.27	1.50	1.11
4254.000		9	23500.67	+0.02	$44438^{\circ}_{3\frac{1}{2}} - 67938_{3\frac{1}{2}}$					
4253.790		1	23501.83	0.00 +0.01	$66395_{2\frac{1}{2}} - 89897^{\circ}_{1\frac{1}{2}}$ $70858_{4\frac{1}{2}} - 94360^{\circ}_{4\frac{1}{2}}$					
4252.806		3	23507.27	−0.03	$66205^{\circ}_{2\frac{1}{2}} - 89713_{2\frac{1}{2}}$					
4252.515	300	3000	23508.88	+0.01	$37077^{\circ}_{2\frac{1}{2}} - 60586_{1\frac{1}{2}}$	4	1.113	1.326	0.107	0.794
4252.040		15	23511.50	+0.03	$47758^{\circ}_{3\frac{1}{2}} - 71270_{2\frac{1}{2}}$					
4250.21		5	23521.63	+0.05	$65199_{4\frac{1}{2}} - 88721^{\circ}_{3\frac{1}{2}}$					
4249.861		2	23523.56	+0.01	$66082_{5\frac{1}{2}} - 89605^{\circ}_{4\frac{1}{2}}$					
4249.81		2	23523.84	−0.06	$69395_{3\frac{1}{2}} - 92919^{\circ}_{3\frac{1}{2}}$					
4249.748		4	23524.18	+0.01	$66189^{\circ}_{1\frac{1}{2}} - 89713_{2\frac{1}{2}}$					
4248.12		2	23533.20							
4247.885	40	300	23534.50	+0.03	$37516^{\circ}_{3\frac{1}{2}} - 61051_{3\frac{1}{2}}$	6	1.11	1.17	0.22	1.14
4247.04		2	23539.18							
4246.835		10	23540.32	0.00	$56088^{\circ}_{4\frac{1}{2}} - 79628_{3\frac{1}{2}}$					
4246.586	4	20	23541.70	−0.04	$70793_{5\frac{1}{2}} - 94335^{\circ}_{5\frac{1}{2}}$					

TABLE 6. Yb II—*Observed and classified lines*—Continued

1	2	3	4	5	6	7	8	9	10	11
Wave-length air	Intensity		Wave number	o–c	Classification	Zeeman type	1st g	2nd g	Zeeman components	
	Meggers lamp	Thomson lamp							Strong p	Strong n
Å			K	K						
4245.740	3	15	23546.39	$\begin{cases}+0.05\\-0.01\end{cases}$	$66351_{2\frac{1}{2}} - 89897^{\circ}_{1\frac{1}{2}}$ $69957_{4\frac{1}{2}} - 93503^{\circ}_{4\frac{1}{2}}$					
4245.597		2	23547.18	−0.02	$68756_{3\frac{1}{2}} - 92303^{\circ}_{3\frac{1}{2}}$					
4244.73		1	23551.99							
4244.51		8	23553.21	+0.04	$71270_{2\frac{1}{2}} - 94823^{\circ}_{1\frac{1}{2}}$					
4244.21	6	80	23554.88	−0.01	$54192^{\circ}_{5\frac{1}{2}} - 77747_{4\frac{1}{2}}$	5?	1.11	(1.07)	w	1.18
4244.054	6	15	23555.75	+0.02	$53120^{\circ}_{2\frac{1}{2}} - 76676_{2\frac{1}{2}}$					
4243.494		9	23558.85	+0.01	$47663^{\circ}_{4\frac{1}{2}} - 71222_{3\frac{1}{2}}$					
4242.425	4	60	23564.79	+0.03	$49727^{\circ}_{6\frac{1}{2}} - 73291_{5\frac{1}{2}}$					
4242.299		4	23565.49							
4241.67	2	6	23568.98							
4241.24		2	23571.37							
4241.159	1	15	23571.82	+0.02	$56056^{\circ}_{2\frac{1}{2}} - 79628_{3\frac{1}{2}}$					
4241.116		5	23572.06							
4239.455		1	23581.30	0.00	$69395_{3\frac{1}{2}} - 92976^{\circ}_{3\frac{1}{2}}$					
4238.84		1	23584.72	−0.02	$66558_{3\frac{1}{2}} - 90142^{\circ}_{3\frac{1}{2}}$					
4238.345		1	23587.47	−0.02	$69607_{2\frac{1}{2}} - 93195^{\circ}_{3\frac{1}{2}}$					
4238.157	2	30	23588.52	0.00	$46547^{\circ}_{5\frac{1}{2}} - 70136_{6\frac{1}{2}}$					
4237.284		3	23593.38	−0.02	$55221^{\circ}_{1\frac{1}{2}} - 78814_{2\frac{1}{2}}$					
4235.565	1	20	23602.95	+0.01	$46354^{\circ}_{4\frac{1}{2}} - 69957_{4\frac{1}{2}}$					
4235.012	1	20	23606.04	−0.04	$73291_{5\frac{1}{2}} - 96898^{\circ}_{5\frac{1}{2}}$					
4234.545	50	800	23608.64	+0.02	$45335^{\circ}_{4\frac{1}{2}} - 68943_{4\frac{1}{2}}$	6	1.014	0.870	0.667	0.942
4232.427		1	23620.45	−0.03	$49419^{\circ}_{0\frac{1}{2}} - 73039_{0\frac{1}{2}}$					
4231.648		6	23624.80	−0.03	$47329^{\circ}_{2\frac{1}{2}} - 70954_{2\frac{1}{2}}$					
4230.184	200	400	23632.98	+0.02	$39378^{\circ}_{0\frac{1}{2}} - 63011_{1\frac{1}{2}}$	4	1.865	0.775	0.545	0.230
4229.681		3	23635.79							
4229.271	3	30	23638.08	−0.01	$66571_{5\frac{1}{2}} - 90209^{\circ}_{4\frac{1}{2}}$					
4227.952	50	700	23645.45	−0.01	$48556^{\circ}_{3\frac{1}{2}} - 72202_{3\frac{1}{2}}$	6	0.91	0.85	0.22	0.880
4226.85		2	23651.62	−0.05	$66558_{3\frac{1}{2}} - 90209^{\circ}_{4\frac{1}{2}}$					
4226.595		4	23653.05	−0.01	$44497^{\circ}_{2\frac{1}{2}} - 68150_{1\frac{1}{2}}$					
4226.273	1	20	23654.85	0.00	$65950_{4\frac{1}{2}} - 89605^{\circ}_{4\frac{1}{2}}$					
4225.998		8	23656.39	−0.06	$42915^{\circ}_{5\frac{1}{2}} - 66571_{5\frac{1}{2}}$					
4225.548	10	30	23658.91	0.00	$63726_{4\frac{1}{2}} - 87385^{\circ}_{3\frac{1}{2}}$					
4224.196	20	150	23666.48	−0.02	$40035^{\circ}_{3\frac{1}{2}} - 63702_{2\frac{1}{2}}$	4	(0.720)	1.08	0.18	
4224.064		1	23667.22	−0.07	$62559_{2\frac{1}{2}} - 86226^{\circ}_{1\frac{1}{2}}$					
4223.466		2	23670.57	−0.06	$45273^{\circ}_{3\frac{1}{2}} - 68943_{4\frac{1}{2}}$					
4222.486		10	23676.06							
4222.057		4	23678.47	−0.02	$53120^{\circ}_{2\frac{1}{2}} - 76799_{1\frac{1}{2}}$					
4220.260		1	23688.55	0.00	$52987^{\circ}_{1\frac{1}{2}} - 76676_{2\frac{1}{2}}$					
42[illegible].646		10	23692.00	−0.01	$24332_{2\frac{1}{2}} - 48024^{\circ}_{1\frac{1}{2}}$					
421[illegible].565	1000	5000	23698.07	0.00	$37516^{\circ}_{3\frac{1}{2}} - 61214_{4\frac{1}{2}}$	4	1.115	1.05	(0.035)	0.80

TABLE 6. Yb II—*Observed and classified lines*—Continued

1	2	3	4	5	6	7	8	9	10	11
Wave-length air	Intensity		Wave number	o–c	Classification	Zeeman type	1st g	2nd g	Zeeman components	
	Meggers lamp	Thomson lamp							Strong p	Strong n
Å			K	K						
4217.79		2	23702.42	−0.03	$72779_{3\frac{1}{2}} - 96482^{\circ}_{4\frac{1}{2}}$					
4217.69		2	23702.98							
4217.110		4	23706.24	+0.01	$45737^{\circ}_{1\frac{1}{2}} - 69443_{1\frac{1}{2}}$					
4216.885	6	60	23707.51	+0.01	$66571_{5\frac{1}{2}} - 90279^{\circ}_{5\frac{1}{2}}$					
4216.704	60	300	23708.53	−0.01	$34575^{\circ}_{1\frac{1}{2}} - 58283_{2\frac{1}{2}}$	4	1.432	0.766	0.331	−0.233
4216.569		2	23709.29	−0.05	$71113_{1\frac{1}{2}} - 94823^{\circ}_{1\frac{1}{2}}$					
4216.417		8	23710.14	−0.02	$47758^{\circ}_{3\frac{1}{2}} - 71468_{2\frac{1}{2}}$					
4215.519	6	20	23715.19							
4214.942	2	15	23718.44	+0.02	$53120^{\circ}_{2\frac{1}{2}} - 76839_{2\frac{1}{2}}$					
4213.856		2	23724.55	0.00	$51248^{\circ}_{2\frac{1}{2}} - 74973_{3\frac{1}{2}}$					
4213.407		3	23727.08	−0.05	$65888_{1\frac{1}{2}} - 89615^{\circ}_{2\frac{1}{2}}$					
4212.361		6	23732.97	+0.03	$53716^{\circ}_{2\frac{1}{2}} - 77449_{3\frac{1}{2}}$					
4211.957		1	23735.25							
4211.502		2	23737.81	−0.04	$58661^{\circ}_{2\frac{1}{2}} - 82398_{1\frac{1}{2}}$					
4211.298		4	23738.96	−0.01	$48024^{\circ}_{1\frac{1}{2}} - 71763_{1\frac{1}{2}}$					
4210.664	4	40	23742.54	+0.04	$51248^{\circ}_{2\frac{1}{2}} - 74991_{1\frac{1}{2}}$	7	(1.034)	1.05	0	1.01
4209.870		5	23747.01	−0.01	$66395_{2\frac{1}{2}} - 90142^{\circ}_{3\frac{1}{2}}$					
4208.625		4	23754.04	+0.03	$68549_{4\frac{1}{2}} - 92303^{\circ}_{3\frac{1}{2}}$					
4208.519		1	23754.64	−0.05	$52921^{\circ}_{3\frac{1}{2}} - 76676_{2\frac{1}{2}}$					
4207.65		1	23759.54							
4205.608		4	23771.08	+0.02	$49008^{\circ}_{3\frac{1}{2}} - 72779_{3\frac{1}{2}}$					
4204.058		5	23779.84	−0.02	$64923_{4\frac{1}{2}} - 88702^{\circ}_{5\frac{1}{2}}$					
4203.254		2	23784.39	−0.01	$47329^{\circ}_{2\frac{1}{2}} - 71113_{1\frac{1}{2}}$					
4204.666		2	23787.72	+0.01	$46169^{\circ}_{4\frac{1}{2}} - 69957_{4\frac{1}{2}}$					
4202.44	15	30*hl*	23789.00							
4201.991		1	23791.54	+0.01	$66351_{2\frac{1}{2}} - 90142^{\circ}_{3\frac{1}{2}}$					
4201.460	2	20	23794.55	−0.01	$73291_{5\frac{1}{2}} - 97086^{\circ}_{4\frac{1}{2}}$					
4200.841		5	23798.05	+0.04	$64923_{4\frac{1}{2}} - 88721^{\circ}_{3\frac{1}{2}}$					
4199.939		4	23803.16	0.00	$73283_{4\frac{1}{2}} - 97086^{\circ}_{4\frac{1}{2}}$					
4199.713		10	23804.44	+0.01	$53644^{\circ}_{3\frac{1}{2}} - 77449_{3\frac{1}{2}}$					
4198.863		1	23809.26	+0.01	$51248^{\circ}_{2\frac{1}{2}} - 75058_{2\frac{1}{2}}$					
4196.632	1	9	23821.92	+0.01	$67416_{4\frac{1}{2}} - 91237^{\circ}_{3\frac{1}{2}}$					
4193.807	2	10	23837.97	+0.07	$52067^{\circ}_{0\frac{1}{2}} - 75905_{0\frac{1}{2}}$	6	(0.54)	1.30	0.38	
4193.533		4	23839.52							
4192.725		3	23844.12							
4191.473		2	23851.24	0.00	$52987^{\circ}_{1\frac{1}{2}} - 76839_{2\frac{1}{2}}$					
4190.297	200	2000	23857.93	+0.03	$37516^{\circ}_{3\frac{1}{2}} - 61374_{2\frac{1}{2}}$	4	1.13	1.30	0.085	0.73
4188.723		7	23866.90	+0.02	$68148_{1\frac{1}{2}} - 92015^{\circ}_{4\frac{1}{2}}$					
4188.371		2	23868.90	−0.01	$70954_{2\frac{1}{2}} - 94823^{\circ}_{1\frac{1}{2}}$					
4188.130	1	20	23870.28	+0.03	$45737^{\circ}_{1\frac{1}{2}} - 69607_{2\frac{1}{2}}$					

TABLE 6. Yb II—*Observed and classified lines*—Continued

1	2	3	4	5	6	7	8	9	10	11
Wavelength air	Intensity		Wave number	o–c	Classification	Zeeman type	1st g	2nd g	Zeeman components	
	Meggers lamp	Thomson lamp							Strong p	Strong n
Å			K	K						
4186.83	15	300	23877.69	+0.01	$54192^{\circ}_{5\frac{1}{2}} - 78070_{4\frac{1}{2}}$	7	(1.11)	1.11	0	1.11
4186.027		2	23882.27							
4185.565	2	30	23884.91	+0.03	$47228^{\circ}_{0\frac{1}{2}} - 71113_{1\frac{1}{2}}$	5	0.74	1.00	0.13	1.13
4184.635	1	20	23890.21	+0.01	$53716^{\circ}_{2\frac{1}{2}} - 77606_{2\frac{1}{2}}$	7	(1.183)	1.12	0	1.15
4184.164		3	23892.90	−0.02	$47329^{\circ}_{2\frac{1}{2}} - 71222_{3\frac{1}{2}}$					
4183.905		1	23894.38	−0.03	$57798^{\circ}_{2\frac{1}{2}} - 81692_{3\frac{1}{2}}$					
4182.553		2	23902.11							
4180.809	10000	20000	23912.08	+0.01	$30392^{\circ}_{1\frac{1}{2}} - 54304_{0\frac{1}{2}}$	4	1.33	2.01	0.34	0.99
4179.084	10	80	23921.95	−0.03	$40035^{\circ}_{3\frac{1}{2}} - 63957_{3\frac{1}{2}}$					
4178.585	4	6	23924.80	0.00	$59439^{\circ}_{2\frac{1}{2}} - 83363_{3\frac{1}{2}}$					
4178.225		8	23926.86	−0.04	$68720_{6\frac{1}{2}} - 92647^{\circ}_{5\frac{1}{2}}$					
4177.81	4	80	23929.24	−0.02	$48272^{\circ}_{2\frac{1}{2}} - 72202_{3\frac{1}{2}}$	4	1.14	0.86	0.144	0.149
4177.40	2	50	23931.59							
4176.204		3	23938.44	−0.02	$69607_{2\frac{1}{2}} - 93546^{\circ}_{2\frac{1}{2}}$					
4175.928	10	90	23940.03	−0.05	$24332_{2\frac{1}{2}} - 48272^{\circ}_{2\frac{1}{2}}$					
4175.835		30	23940.56	−0.01	$47329^{\circ}_{2\frac{1}{2}} - 71270_{2\frac{1}{2}}$					
4175.602	2	30	23941.89	−0.02	$22960_{1\frac{1}{2}} - 46902^{\circ}_{0\frac{1}{2}}$	4	0.80	1.32	0.26	0.54
4175.545	1	20	23942.22	−0.02	$35019^{\circ}_{4\frac{1}{2}} - 58961_{5\frac{1}{2}}$					
4174.399		6	23948.79	−0.02	$47005^{\circ}_{1\frac{1}{2}} - 70954_{2\frac{1}{2}}$					
4172.15		20	23961.70	+0.01	$53644^{\circ}_{3\frac{1}{2}} - 77606_{2\frac{1}{2}}$	7	(1.18)	1.16	0	1.23
4170.106	200	2000	23973.45	−0.02	$37077^{\circ}_{2\frac{1}{2}} - 61051_{3\frac{1}{2}}$	5	1.09	1.15	(0.03)	1.30
4169.499	2	8	23976.94	0.00	$56480^{\circ}_{4\frac{1}{2}} - 80457_{3\frac{1}{2}}$					
4165.692		2	23998.85							
4165.143		6	24002.01							
4164.660	5	50	24004.80	−0.01	$32371^{\circ}_{2\frac{1}{2}} - 56375_{2\frac{1}{2}}$					
4164.587		15	24005.22	+0.02	$40917^{\circ}_{4\frac{1}{2}} - 64923_{4\frac{1}{2}}$					
4162.023		5	24020.01	+0.01	$40035^{\circ}_{3\frac{1}{2}} - 64055_{2\frac{1}{2}}$					
4161.572		1	24022.61							
4160.299		2	24029.96							
4160.090	3	40	24031.17	+0.04	$35059^{\circ}_{3\frac{1}{2}} - 59090_{3\frac{1}{2}}$					
4157.755	100	200	24044.66	0.00	$22960_{1\frac{1}{2}} - 47005^{\circ}_{1\frac{1}{2}}$					
4156.575	1	4	24051.49	+0.02	$69957_{4\frac{1}{2}} - 94008^{\circ}_{3\frac{1}{2}}$					
4156.444		1	24052.25	+0.04	$62174_{1\frac{1}{2}} - 86226^{\circ}_{1\frac{1}{2}}$					
4153.88		6	24067.09	0.00	$45012^{\circ}_{2\frac{1}{2}} - 69079_{2\frac{1}{2}}$					
4153.758		4	24067.80	−0.01	$69395_{3\frac{1}{2}} - 93463^{\circ}_{3\frac{1}{2}}$					
4153.197		7	24071.05	+0.05	$35019^{\circ}_{4\frac{1}{2}} - 59090_{3\frac{1}{2}}$					
4152.79		3	24073.41							
4148.440		8	24098.65							
4147.774	1	30	24102.52	+0.01 +0.04	$53644^{\circ}_{3\frac{1}{2}} - 77747_{4\frac{1}{2}}$ $69443_{1\frac{1}{2}} - 93546^{\circ}_{2\frac{1}{2}}$					
4146.984		2	24107.11							

TABLE 6. Yb II—*Observed and classified lines*—Continued

1	2	3	4	5	6	7	8	9	10	11
Wave-length air	Intensity		Wave number	o–c	Classification	Zeeman type	1st g	2nd g	Zeeman components	
	Meggers lamp	Thomson lamp							Strong p	Strong n
Å			K	K						
4146.764	1	30	24108.39	+0.01	$47005^{\circ}_{1\frac{1}{2}} - 71113_{1\frac{1}{2}}$					
4146.160		3	24111.90	−0.02	$48503^{\circ}_{3\frac{1}{2}} - 72615_{3\frac{1}{2}}$					
4144.700	1	20	24120.40	−0.03 +0.03	$55462^{\circ}_{3\frac{1}{2}} - 79583_{2\frac{1}{2}}$ $67416_{4\frac{1}{2}} - 91536^{\circ}_{3\frac{1}{2}}$					
4144.273	1	15	24122.88	+0.04	$64598_{3\frac{1}{2}} - 88721^{\circ}_{3\frac{1}{2}}$					
4143.070		4	24129.89	+0.01	$43075^{\circ}_{1\frac{1}{2}} - 67204_{1\frac{1}{2}}$					
4142.364	1	30	24134.00	+0.01	$31568^{\circ}_{2\frac{1}{2}} - 55702_{1\frac{1}{2}}$					
4141.457	2	60	24139.28	+0.01 +0.02	$44940^{\circ}_{1\frac{1}{2}} - 69079_{2\frac{1}{2}}$ $47329^{\circ}_{2\frac{1}{2}} - 71468_{2\frac{1}{2}}$					
4139.332	10	30	24151.68	+0.05	$63234_{2\frac{1}{2}} - 87385^{\circ}_{3\frac{1}{2}}$					
4138.445		4	24156.85	+0.01	$50832^{\circ}_{1\frac{1}{2}} - 74989_{0\frac{1}{2}}$					
4138.166		3	24158.48	+0.01	$57534^{\circ}_{3\frac{1}{2}} - 81692_{3\frac{1}{2}}$					
4138.13		1	24158.69	−0.02	$50832^{\circ}_{1\frac{1}{2}} - 74991_{1\frac{1}{2}}$					
4138.11		1	24158.81							
4137.985		2	24159.54	0.00	$66558_{3\frac{1}{2}} - 90717^{\circ}_{4\frac{1}{2}}$					
4137.378		4	24163.08	+0.02	$68756_{3\frac{1}{2}} - 92919^{\circ}_{3\frac{1}{2}}$					
4136.930		7	24165.70	+0.04	$53716^{\circ}_{2\frac{1}{2}} - 77882_{3\frac{1}{2}}$					
4136.872		1	24166.04	+0.01	$55462^{\circ}_{3\frac{1}{2}} - 79628_{3\frac{1}{2}}$					
4135.088	500	5000	24176.46	+0.04	$34784^{\circ}_{5\frac{1}{2}} - 58961_{5\frac{1}{2}}$	6	1.126	0.987	0.765	1.062
4134.476	20	80	24180.04	+0.01	$28757^{\circ}_{1\frac{1}{2}} - 52938_{1\frac{1}{2}}$	6	1.46	0.89	0.845	1.180
4132.465		4	24191.81	+0.02	$65950_{4\frac{1}{2}} - 90142^{\circ}_{3\frac{1}{2}}$					
4132.063		2	24194.16	0.00	$43956^{\circ}_{2\frac{1}{2}} - 68150_{1\frac{1}{2}}$					
4131.600	2	20	24196.87	+0.04	$66082_{5\frac{1}{2}} - 90279^{\circ}_{5\frac{1}{2}}$					
4131.325		3	24198.48	+0.07	$56480^{\circ}_{4\frac{1}{2}} - 80679_{5\frac{1}{2}}$					
4131.15		4	24199.51	+0.05	$70136_{6\frac{1}{2}} - 94335^{\circ}_{5\frac{1}{2}}$					
4131.024	6	40	24200.25	+0.01	$35059^{\circ}_{3\frac{1}{2}} - 59259_{2\frac{1}{2}}$					
4130.878	1	4	24201.10							
4129.413		1	24209.69	−0.04 +0.06	$41678^{\circ}_{2\frac{1}{2}} - 65888_{1\frac{1}{2}}$ $57103^{\circ}_{3\frac{1}{2}} - 81312_{2\frac{1}{2}}$					
4129.329		2	24210.18							
4129.157	2	30	24211.19	+0.06	$46902^{\circ}_{0\frac{1}{2}} - 71113_{1\frac{1}{2}}$	4	1.30	0.98	0.16	0.82
4128.046		3	24217.70	0.00	$49419^{\circ}_{0\frac{1}{2}} - 73636_{0\frac{1}{2}}$					
4127.202		4	24222.66	+0.04	$71468_{2\frac{1}{2}} - 95691^{\circ}_{3\frac{1}{2}}$					
4126.992	20	30	24223.89	+0.01	$24332_{2\frac{1}{2}} - 48556^{\circ}_{3\frac{1}{2}}$					
4126.726	1	15	24225.45	−0.01	$50832^{\circ}_{1\frac{1}{2}} - 75058_{2\frac{1}{2}}$					
4126.030		2	24229.54							
4124.736	2	30	24237.14	−0.01	$53644^{\circ}_{3\frac{1}{2}} - 77882_{3\frac{1}{2}}$					
4124.564		1	24238.15	−0.01	$49419^{\circ}_{0\frac{1}{2}} - 73657_{1\frac{1}{2}}$					
4123.180	1	20	24246.28	+0.04	$46547^{\circ}_{3\frac{1}{2}} - 70793_{3\frac{1}{2}}$					
4122.853	50	500	24248.21	0.00	$34575^{\circ}_{1\frac{1}{2}} - 58823_{2\frac{1}{2}}$	4	1.34	1.18	0.08	0.94
4121.345		3	24257.08	+0.05	$69607_{2\frac{1}{2}} - 93864^{\circ}_{2\frac{1}{2}}$					

TABLE 6. Yb II—*Observed and classified lines*—Continued

1	2	3	4	5	6	7	8	9	10	11
Wavelength air	Intensity		Wave number	o–c	Classification	Zeeman type	1st g	2nd g	Zeeman components	
	Meggers lamp	Thomson lamp							Strong p	Strong n
Å			K	K						
4120.071	1	40	24264.58	+0.03	$47005^{\circ}_{1\frac{1}{2}} - 71270_{2\frac{1}{2}}$					
4119.812		2	24266.11							
4119.464	200	1500	24268.16	0.00	$22960_{1\frac{1}{2}} - 47228^{\circ}_{0\frac{1}{2}}$	5	0.76?	0.56?	0.10w?	0.86
4119.25	20	30	24269.42							
4119.046	3	60	24270.62	−0.02	$33494^{\circ}_{3\frac{1}{2}} - 57765_{4\frac{1}{2}}$					
4118.395		3	24274.46	+0.04	$49008^{\circ}_{3\frac{1}{2}} - 73283_{4\frac{1}{2}}$					
4117.177	1	30	24281.64	+0.01	$40917^{\circ}_{4\frac{1}{2}} - 65199_{4\frac{1}{2}}$					
4116.654		4	24284.72							
4115.454		9	24291.80	+0.05	$45737^{\circ}_{1\frac{1}{2}} - 70029_{0\frac{1}{2}}$					
4114.591	2	30	24296.90	0.00	$37077^{\circ}_{2\frac{1}{2}} - 61374_{2\frac{1}{2}}$					
4113.879	1	20	24301.10	+0.03	$66558_{3\frac{1}{2}} - 90859^{\circ}_{2\frac{1}{2}}$					
4113.707		5	24302.12	+0.04	$51248^{\circ}_{2\frac{1}{2}} - 75550_{2\frac{1}{2}}$					
4113.046	40	400	24306.02	+0.03	$37516^{\circ}_{3\frac{1}{2}} - 61822_{3\frac{1}{2}}$	6	1.13	1.33	0.71	1.23
4111.381		6	24315.87	+0.01	$68720_{6\frac{1}{2}} - 93036^{\circ}_{5\frac{1}{2}}$					
4110.448		2	24321.39							
4110.168		10	24323.04	0.00	$67955_{0\frac{1}{2}} - 92278^{\circ}_{1\frac{1}{2}}$					
4109.654		400	24326.08	−0.01	$61822_{3\frac{1}{2}} - 86148^{\circ}_{2\frac{1}{2}}$	4	1.33	1.57	0.12	0.73
4109.306	2	40	24328.14	+0.01 −0.05	$65950_{4\frac{1}{2}} - 90279^{\circ}_{5\frac{1}{2}}$ $71222_{3\frac{1}{2}} - 95550^{\circ}_{4\frac{1}{2}}$					
4108.845	5	15	24330.87	+0.04	$65566_{0\frac{1}{2}} - 89897^{\circ}_{1\frac{1}{2}}$					
4106.284		3	24346.05	−0.04	$69957_{4\frac{1}{2}} - 94303^{\circ}_{3\frac{1}{2}}$					
4106.070		5	24347.32							
4103.416	1	10	24363.06							
4103.113		2	24364.86	−0.06	$68549_{4\frac{1}{2}} - 92914^{\circ}_{4\frac{1}{2}}$					
4102.478	20	20	24368.64	0.00	$22960_{1\frac{1}{2}} - 47329^{\circ}_{2\frac{1}{2}}$					
4102.264		5	24369.91	+0.04	$68549_{4\frac{1}{2}} - 92919^{\circ}_{3\frac{1}{2}}$					
4100.877		1	24378.15	−0.06	$69957_{4\frac{1}{2}} - 94335^{\circ}_{5\frac{1}{2}}$					
4100.160		8	24382.41	0.00	$45012^{\circ}_{2\frac{1}{2}} - 69395_{3\frac{1}{2}}$					
4099.820		2	24384.43	−0.06	$55221^{\circ}_{1\frac{1}{2}} - 79605_{1\frac{1}{2}}$					
4099.482		3	24386.44							
4098.848		2	24390.22							
4098.096		2	24394.69							
4097.885	100	600	24395.95	−0.06	$31979^{\circ}_{3\frac{1}{2}} - 56375_{2\frac{1}{2}}$	5	1.34	1.24	0.05	1.59
4096.968		1	24401.41	−0.01	$69607_{2\frac{1}{2}} - 94008^{\circ}_{3\frac{1}{2}}$					
4096.785		3	24402.50	−0.01	$69957_{4\frac{1}{2}} - 94360^{\circ}_{4\frac{1}{2}}$					
4096.644	2	20	24403.34	+0.03	$65875_{6\frac{1}{2}} - 90279^{\circ}_{5\frac{1}{2}}$					
4096.156	1	15	24406.24	−0.02	$65199_{4\frac{1}{2}} - 89605^{\circ}_{4\frac{1}{2}}$					
4094.351		2	24417.00							
4093.634	2	20	24421.28	−0.03	$71270_{2\frac{1}{2}} - 95691^{\circ}_{3\frac{1}{2}}$					

TABLE 6. Yb II—*Observed and classified lines*—Continued

1	2	3	4	5	6	7	8	9	10	11
Wave-length air	Intensity		Wave number	o–c	Classification	Zeeman type	1st g	2nd g	Zeeman components	
	Meggers lamp	Thomson lamp							Strong p	Strong n
Å			K	K						
4092.959		10	24425.31	+0.01	$53644^{\circ}_{3\frac{1}{2}} - 78070_{4\frac{1}{2}}$					
4092.052	1	4	24430.72	−0.01	$45012^{\circ}_{2\frac{1}{2}} - 69443_{1\frac{1}{2}}$					
4091.53	6	100	24433.84	+0.02	$34389^{\circ}_{2\frac{1}{2}} - 58823_{2\frac{1}{2}}$					
4091.466	2	40	24434.22	−0.01	$47329^{\circ}_{2\frac{1}{2}} - 71763_{1\frac{1}{2}}$	4	1.01	1.12	0.053	0.850
4090.594		3	24439.43	+0.02	$46354^{\circ}_{4\frac{1}{2}} - 70793_{5\frac{1}{2}}$					
4088.633		2	24451.15							
4088.528		1	24451.78							
4086.61	7	100	24463.25	+0.01	$47005^{\circ}_{1\frac{1}{2}} - 71468_{2\frac{1}{2}}$	7	(0.990)	1.01	0	1.03
4085.66	1	8	24468.94	−0.05 −0.02	$68450_{3\frac{1}{2}} - 92919^{\circ}_{3\frac{1}{2}}$ $71222_{3\frac{1}{2}} - 95691^{\circ}_{3\frac{1}{2}}$					
4085.05		3	24472.60	−0.01	$56840^{\circ}_{1\frac{1}{2}} - 81312_{2\frac{1}{2}}$					
4084.845		3	24473.82							
4084.515		1	24475.80							
4083.870		1	24479.67							
4082.814		4	24486.00	0.00 −0.01	$53120^{\circ}_{2\frac{1}{2}} - 77606_{2\frac{1}{2}}$ $54640^{\circ}_{4\frac{1}{2}} - 79126_{4\frac{1}{2}}$					
4082.64		1	24487.04	−0.03	$68549_{4\frac{1}{2}} - 93036^{\circ}_{5\frac{1}{2}}$					
4082.529		1	24487.71							
4081.05		1	24496.58							
4079.991	2	40	24502.94	+0.03	$44940^{\circ}_{1\frac{1}{2}} - 69443_{1\frac{1}{2}}$	6	1.24	1.14	0.14	1.19
4079.88		6	24503.61	−0.02	$46354^{\circ}_{4\frac{1}{2}} - 70858_{4\frac{1}{2}}$					
4079.542		3	24505.64	+0.02	$44438^{\circ}_{3\frac{1}{2}} - 68943_{4\frac{1}{2}}$					
4079.164	2	20	24507.91	+0.05	$66351_{2\frac{1}{2}} - 90859^{\circ}_{2\frac{1}{2}}$					
4078.36	7	70	24512.74	+0.08	$65093_{3\frac{1}{2}} - 89605^{\circ}_{4\frac{1}{2}}$	4	(0.973)	0.94	w	0.830
4077.713	10	20	24516.63							
4077.276	200	2000	24519.26	+0.01 −0.10	$38342^{\circ}_{4\frac{1}{2}} - 62861_{5\frac{1}{2}}$ $(68943_{4\frac{1}{2}} - 93463^{\circ}_{3\frac{1}{2}})$	5	1.06	1.10	(0.022)	1.30
4076.82		1	24522.00	+0.05	$68720_{6\frac{1}{2}} - 93242^{\circ}_{5\frac{1}{2}}$					
4076.198		3	24525.74	−0.01	$68720_{6\frac{1}{2}} - 93246^{\circ}_{6\frac{1}{2}}$					
4076.09		3	24526.39	0.00	$68450_{3\frac{1}{2}} - 92976^{\circ}_{3\frac{1}{2}}$					
4075.873		3	24527.70	+0.03 0.00	$45429^{\circ}_{3\frac{1}{2}} - 69957_{4\frac{1}{2}}$ $52921^{\circ}_{3\frac{1}{2}} - 77449_{3\frac{1}{2}}$					
4074.705	8	60	24534.73	+0.02	$47228^{\circ}_{0\frac{1}{2}} - 71763_{1\frac{1}{2}}$	5	0.698	1.098	0.200	1.298
4074.074		1	24538.53	+0.02	$47663^{\circ}_{4\frac{1}{2}} - 72202_{3\frac{1}{2}}$					
4071.442		1	24554.39							
4071.334		3	24555.04	+0.004	$69443_{1\frac{1}{2}} - 93998^{\circ}_{1\frac{1}{2}}$					
4070.527	8	50	24559.91	+0.01	$35059^{\circ}_{3\frac{1}{2}} - 59618_{3\frac{1}{2}}$					
4069.013		4	24569.05							
4068.50		2	24572.14							
4068.229		2	24573.78							
4067.031		2	24581.02							

TABLE 6. Yb II—*Observed and classified lines*—Continued

1	2	3	4	5	6	7	8	9	10	11
Wavelength air	Intensity		Wave number	o–c	Classification	Zeeman type	1st g	2nd g	Zeeman components	
	Meggers lamp	Thomson lamp							Strong p	Strong n
Å			K	K						
4066.809		15	24582.36	−0.01	$44497^{\circ}_{2\frac{1}{2}} - 69079_{2\frac{1}{2}}$					
4066.520		2	24584.11	−0.01	$56621^{\circ}_{5\frac{1}{2}} - 81205_{4\frac{1}{2}}$					
4064.757		15	24594.77	+0.02	$45012^{\circ}_{2\frac{1}{2}} - 69607_{2\frac{1}{2}}$					
4063.927	1	30	24599.79	+0.02 +0.06	$35019^{\circ}_{4\frac{1}{2}} - 59618_{3\frac{1}{2}}$ $67416_{4\frac{1}{2}} - 92015^{\circ}_{4\frac{1}{2}}$					
4062.35		1	24609.34							
4062.100		2	24610.86							
4061.614		7	24613.80	+0.04	$69395_{3\frac{1}{2}} - 94008^{\circ}_{3\frac{1}{2}}$					
4060.180		1	24622.50	+0.04	$45335^{\circ}_{4\frac{1}{2}} - 69957_{4\frac{1}{2}}$					
4060.04		1	24623.34							
4059.893		2	24624.24	+0.06	$46169^{\circ}_{4\frac{1}{2}} - 70793_{5\frac{1}{2}}$					
4058.238		1	24634.28							
4058.065	1	6	24635.33	+0.04	$66082_{5\frac{1}{2}} - 90717^{\circ}_{4\frac{1}{2}}$					
4056.142	500	2000	24647.01	+0.03	$28757^{\circ}_{1\frac{1}{2}} - 53404_{2\frac{1}{2}}$	4	1.44	1.03	0.21	0.42
4055.468		3	24651.10							
4054.588		1	24656.45							
4053.547		2	24662.79	+0.03	$41688^{\circ}_{1\frac{1}{2}} - 66351_{2\frac{1}{2}}$					
4053.235		1*h*	24664.68							
4053.11		10	24665.44							
4052.860		20	24666.97	+0.04	$44940^{\circ}_{1\frac{1}{2}} - 69607_{2\frac{1}{2}}$					
4051.339	20	60	24676.23	−0.01	$24332_{2\frac{1}{2}} - 49008^{\circ}_{3\frac{1}{2}}$	4	1.19	1.04	0.074	0.67
4050.083	20	150	24683.88	+0.01	$34575^{\circ}_{1\frac{1}{2}} - 59259_{2\frac{1}{2}}$	4	1.446	1.110	0.168	0.606
4049.982		5	24684.49	+0.02	$45273^{\circ}_{3\frac{1}{2}} - 69957_{4\frac{1}{2}}$					
4049.335		7	24688.44	+0.04	$46169^{\circ}_{4\frac{1}{2}} - 70858_{4\frac{1}{2}}$					
4048.683		5	24692.41	+0.04	$70858_{4\frac{1}{2}} - 95550^{\circ}_{4\frac{1}{2}}$					
4048.554		2	24693.20	+0.04	$68549_{4\frac{1}{2}} - 93242^{\circ}_{5\frac{1}{2}}$					
4048.21		1	24695.30							
4048.090		2	24696.03	−0.01	$69607_{2\frac{1}{2}} - 94303^{\circ}_{3\frac{1}{2}}$					
4047.38	20	200	24700.36	−0.01	$34389^{\circ}_{2\frac{1}{2}} - 59090_{3\frac{1}{2}}$	5	1.000	1.122	0.061	1.427
4046.998		2	24702.70	−0.05	$58661^{\circ}_{2\frac{1}{2}} - 83363_{3\frac{1}{2}}$					
4046.56		1	24705.37							
4046.52		1	24705.61							
4046.297		4	24706.97	0.00	$68756_{3\frac{1}{2}} - 93463^{\circ}_{3\frac{1}{2}}$					
4045.605		1	24711.20							
4045.302	6	80	24713.05	+0.02	$33052^{\circ}_{4\frac{1}{2}} - 57765_{4\frac{1}{2}}$					
4044.657		2	24716.99	0.00	$41678^{\circ}_{2\frac{1}{2}} - 66395_{2\frac{1}{2}}$					
4043.426		4	24724.52	+0.02	$56480^{\circ}_{4\frac{1}{2}} - 81205_{4\frac{1}{2}}$					
4043.05	20	300	24726.82	+0.04	$48556^{\circ}_{3\frac{1}{2}} - 73283_{4\frac{1}{2}}$	5	1.00	1.07	(0.037)	1.33
4042.532	3	40	24729.99	0.00	$66571_{5\frac{1}{2}} - 91301^{\circ}_{6\frac{1}{2}}$					
4042.328		4	24731.23	+0.03	$52067^{\circ}_{6\frac{1}{2}} - 76799_{1\frac{1}{2}}$					

277-259 O - 68 - 6

TABLE 6. Yb II—*Observed and classified lines*—Continued

1	2	3	4	5	6	7	8	9	10	11
Wave-length air	Intensity		Wave number	o–c	Classification	Zeeman type	1st g	2nd g	Zeeman components	
	Meggers lamp	Thomson lamp							Strong p	Strong n
Å			K	K						
4040.563	1	30	24742.04	+0.07	$49008^{\circ}_{3\frac{1}{2}} - 73750_{4\frac{1}{2}}$	4	1.023	0.987	(0.018)	0.861
4040.498		8	24742.43	0.00	$64970^{\circ}_{3\frac{1}{2}} - 89713_{2\frac{1}{2}}$					
4040.29		1	24743.71							
4040.08	60	1000	24744.99	0.00 +0.07	$37077^{\circ}_{2\frac{1}{2}} - 61882_{3\frac{1}{2}}$ $(68450_{3\frac{1}{2}} - 93195^{\circ}_{3\frac{1}{2}})$	5	1.120	1.334	0.107	1.87
4039.613		4	24747.85	0.00	$68756_{3\frac{1}{2}} - 93503^{\circ}_{4\frac{1}{2}}$					
4039.140		3	24750.75							
4038.187		6	24756.59	0.00	$70793_{5\frac{1}{2}} - 95550^{\circ}_{4\frac{1}{2}}$					
4037.916		9	24758.25	+0.04	$47005^{\circ}_{1\frac{1}{2}} - 71763_{1\frac{1}{2}}$					
4037.822	20	50	24758.83	+0.04	$63944_{5\frac{1}{2}} - 88702^{\circ}_{5\frac{1}{2}}$	7	(1.115)	1.095	0	1.105
4036.772[a]	20	15	24765.27							
4036.550	1	15	24766.63	+0.04	$65950_{4\frac{1}{2}} - 90717^{\circ}_{4\frac{1}{2}}$					
4035.315	9	90	24774.21	+0.03	$61374_{2\frac{1}{2}} - 86148^{\circ}_{2\frac{1}{2}}$	6	1.304	1.578	0.685	1.441
4034.438		6	24779.60	+0.07	$48503^{\circ}_{5\frac{1}{2}} - 73283_{4\frac{1}{2}}$					
4033.695		4	24784.16	+0.06	$68135_{2\frac{1}{2}} - 92919^{\circ}_{3\frac{1}{2}}$					
4032.869	10	100	24789.24	+0.01	$33494^{\circ}_{3\frac{1}{2}} - 58283_{2\frac{1}{2}}$	5	1.000	0.784	0.109	1.540
4032.756		2	24789.93	−0.03	$68756_{3\frac{1}{2}} - 93546^{\circ}_{2\frac{1}{2}}$					
4032.441		2	24791.87							
4030.712		1	24802.50							
4029.844	2	60	24807.85	+0.02	$31568^{\circ}_{2\frac{1}{2}} - 56375_{2\frac{1}{2}}$					
4027.580		10	24821.79	+0.02	$38342^{\circ}_{4\frac{1}{2}} - 63163_{4\frac{1}{2}}$					
4027.19		1	24824.19							
4026.922		2	24825.85	+0.07	$52921^{\circ}_{3\frac{1}{2}} - 77747_{4\frac{1}{2}}$					
4025.740		2	24833.14	0.00	$70858_{4\frac{1}{2}} - 95691^{\circ}_{3\frac{1}{2}}$					
4024.375		4	24841.56	+0.06	$68135_{2\frac{1}{2}} - 92976^{\circ}_{3\frac{1}{2}}$					
4023.987	6	30	24843.95	+0.01	$48272^{\circ}_{2\frac{1}{2}} - 73116_{1\frac{1}{2}}$	5	1.141	0.861	0.140	1.561
4022.712	3	40	24851.83	+0.01	$61374_{2\frac{1}{2}} - 86226^{\circ}_{1\frac{1}{2}}$					
4021.956		1	24856.50							
4020.310		2	24866.68	+0.03	$52880^{\circ}_{4\frac{1}{2}} - 77747_{4\frac{1}{2}}$					
4019.852	1	10	24869.51	+0.03	$34389^{\circ}_{2\frac{1}{2}} - 59259_{2\frac{1}{2}}$					
4019.35	6	150	24872.61	+0.02	$47329^{\circ}_{2\frac{1}{2}} - 72202_{3\frac{1}{2}}$	4	0.989	0.859	0.065	0.534
4018.264		2	24879.34	+0.07 0.00	$41678^{\circ}_{2\frac{1}{2}} - 66558_{3\frac{1}{2}}$ $58484^{\circ}_{4\frac{1}{2}} - 83363_{3\frac{1}{2}}$					
4018.134		2	24880.14	0.00	$43075^{\circ}_{1\frac{1}{2}} - 67955_{0\frac{1}{2}}$					
4017.94		1	24881.34							
4017.060		3	24886.79	+0.06	$66351_{2\frac{1}{2}} - 91237^{\circ}_{3\frac{1}{2}}$					
4016.976		9	24887.31	+0.02	$40035^{\circ}_{3\frac{1}{2}} - 64923_{4\frac{1}{2}}$					
4015.296		4	24897.73	+0.04	$44497^{\circ}_{2\frac{1}{2}} - 69395_{3\frac{1}{2}}$					
4015.004		1	24899.54	0.00	$52987^{\circ}_{1\frac{1}{2}} - 77887_{0\frac{1}{2}}$					
4013.579	1	15	24908.38	0.00	$69395_{3\frac{1}{2}} - 94303^{\circ}_{3\frac{1}{2}}$					

TABLE 6. Yb II—*Observed and classified lines*—Continued

1	2	3	4	5	6	7	8	9	10	11
Wave-length air	Intensity		Wave number	o–c	Classification	Zeeman type	1st g	2nd g	Zeeman components	
	Meggers lamp	Thomson lamp							Strong p	Strong n
Å			K	K						
4013.464		3	24909.09							
4012.704		1	24913.81	+0.03	$68549_{4\frac{1}{2}} - 93463^{\circ}_{3\frac{1}{2}}$					
4012.204		1	24916.91							
4010.84		2	24925.39							
4009.237		20	24935.35	+0.01	$47680^{\circ}_{6\frac{1}{2}} - 72615_{5\frac{1}{2}}$					
4008.94	4	1	24937.20							
4008.775		3	24938.23							
4007.518		20	24946.05	+0.04	$44497^{\circ}_{2\frac{1}{2}} - 69443_{1\frac{1}{2}}$					
4006.962		2	24949.51							
4006.672		1	24951.32							
4006.53		2	24952.20	−0.02	$47663^{\circ}_{4\frac{1}{2}} - 72615_{5\frac{1}{2}}$					
4005.619		1	24957.87	−0.01	$49008^{\circ}_{3\frac{1}{2}} - 73966_{3\frac{1}{2}}$					
4005.218		1	24960.37	+0.03	$70793_{5\frac{1}{2}} - 95754^{\circ}_{5\frac{1}{2}}$					
				−0.05	$52921^{\circ}_{3\frac{1}{2}} - 77882_{3\frac{1}{2}}$					
4003.574		1	24970.62	+0.01	$65888_{1\frac{1}{2}} - 90859^{\circ}_{2\frac{1}{2}}$					
4003.224		2	24972.81							
4002.798		2	24975.46							
4002.68		1	24976.20	+0.06	$63726_{4\frac{1}{2}} - 88702^{\circ}_{5\frac{1}{2}}$					
4002.326		10	24978.41	+0.01	$66558_{3\frac{1}{2}} - 91536^{\circ}_{3\frac{1}{2}}$					
4002.002		1	24980.43	+0.01	$67938_{3\frac{1}{2}} - 92919^{\circ}_{3\frac{1}{2}}$					
4000.808	5	150	24987.89	0.00	$54640^{\circ}_{4\frac{1}{2}} - 79628_{3\frac{1}{2}}$	7	1.12	(1.11)	0	1.15
3999.777	2	40	24994.33	+0.04	$63726_{4\frac{1}{2}} - 88721^{\circ}_{3\frac{1}{2}}$					
3998.430		7	25002.75							
3998.38		1	25003.06							
3997.244		4	25010.17	+0.04	$65199_{4\frac{1}{2}} - 90209^{\circ}_{4\frac{1}{2}}$					
3995.859		1	25018.83	+0.03	$63702_{2\frac{1}{2}} - 88721^{\circ}_{3\frac{1}{2}}$					
3995.432	1	20	25021.51	+0.06	$47758^{\circ}_{3\frac{1}{2}} - 72779_{3\frac{1}{2}}$	7	(1.08)	1.12	0	1.10
3994.563		2	25026.95							
3994.300		1	25028.60							
3992.826		1	25037.84	+0.02	$67938_{3\frac{1}{2}} - 92976^{\circ}_{3\frac{1}{2}}$					
3992.09		8	25042.45	+0.02	$37516^{\circ}_{3\frac{1}{2}} - 62559_{2\frac{1}{2}}$					
3991.09		1	25048.73							
3990.603		2	25051.78	+0.02	$73750_{4\frac{1}{2}} - 98802^{\circ}_{5\frac{1}{2}}$					
3990.473		2	25052.60	+0.02	$46169^{\circ}_{4\frac{1}{2}} - 71222_{3\frac{1}{2}}$					
3990.280		1	25053.81	+0.03	$68450_{3\frac{1}{2}} - 93503^{\circ}_{4\frac{1}{2}}$					
3989.717		6	25057.35	+0.03	$40035^{\circ}_{3\frac{1}{2}} - 65093_{3\frac{1}{2}}$					
3988.666		70	25063.95	+0.05	$22960_{1\frac{1}{2}} - 48024^{\circ}_{1\frac{1}{2}}$					
3986.962		5	25074.66	+0.03	$51248^{\circ}_{2\frac{1}{2}} - 76323_{3\frac{1}{2}}$					
3986.830		5	25075.49	+0.01	$43075^{\circ}_{1\frac{1}{2}} - 68150_{1\frac{1}{2}}$					
3986.179		10	25079.59	+0.05	$65199_{4\frac{1}{2}} - 90279^{\circ}_{5\frac{1}{2}}$					
3985.125		1	25086.22							

TABLE 6. Yb II—*Observed and classified lines*—Continued

1	2	3	4	5	6	7	8	9	10	11
Wave-length air	Intensity		Wave number	o–c	Classification	Zeeman type	1st g	2nd g	Zeeman components	
	Meggers lamp	Thomson lamp							Strong p	Strong n
Å			K	K						
3984.765		3	25088.49	+0.06	$44940^{\circ}_{1\frac{1}{2}} - 70029_{0\frac{1}{2}}$					
3983.748		1	25094.89							
3983.314	2	60	25097.63	+0.02	$61051_{3\frac{1}{2}} - 86148^{\circ}_{2\frac{1}{2}}$	4	1.17	1.55	0.187	0.240
3983.179		1	25098.48	0.00	$53716^{\circ}_{2\frac{1}{2}} - 78814_{2\frac{1}{2}}$					
3982.009	2	20	25105.85	+0.03	$61120_{0\frac{1}{2}} - 86226^{\circ}_{1\frac{1}{2}}$	4	1.699	1.365	0.167	1.198
3981.574		1	25108.59	+0.06	$68756_{3\frac{1}{2}} - 93864^{\circ}_{2\frac{1}{2}}$					
3981.160		5	25111.20	+0.02	$68756_{3\frac{1}{2}} - 93867^{\circ}_{4\frac{1}{2}}$					
3980.78		1	25113.60	−0.01	$56977^{\circ}_{0\frac{1}{2}} - 82091_{0\frac{1}{2}}$					
3980.318		10	25116.52	+0.05 −0.01	$47663^{\circ}_{4\frac{1}{2}} - 72779_{3\frac{1}{2}}$ $65093_{3\frac{1}{2}} - 90209^{\circ}_{4\frac{1}{2}}$					
3978.543	2	10	25127.72	0.00	$59090_{3\frac{1}{2}} - 84217^{\circ}_{4\frac{1}{2}}$					
3977.342	2	20	25135.31	+0.03	$34575^{\circ}_{1\frac{1}{2}} - 59710_{1\frac{1}{2}}$					
3977.113		1	25136.76							
3976.527		1	25140.46	+0.03	$65577_{3\frac{1}{2}} - 90717^{\circ}_{4\frac{1}{2}}$					
3976.148		7	25142.86	+0.08	$43007^{\circ}_{0\frac{1}{2}} - 68150_{1\frac{1}{2}}$					
3974.91		1	25150.69							
3974.30		2	25154.55	+0.04	$64461_{1\frac{1}{2}} - 89615^{\circ}_{2\frac{1}{2}}$					
3972.91		1	25163.35							
3972.848		3	25163.74	+0.02	$40035^{\circ}_{3\frac{1}{2}} - 65199_{4\frac{1}{2}}$					
3972.517		4	25165.84							
3972.267		3	25167.42							
3972.08		1	25168.61							
3971.739		2	25170.77							
3971.014		2*h*	25175.36							
3969.519		1	25184.84	+0.01	$59259_{2\frac{1}{2}} - 84444^{\circ}_{3\frac{1}{2}}$					
3969.461		1	25185.21	+0.02	$66351_{2\frac{1}{2}} - 91536^{\circ}_{3\frac{1}{2}}$					
3969.082		3	25187.62							
3968.79		20	25189.47	+0.03	$52880^{\circ}_{4\frac{1}{2}} - 78070_{4\frac{1}{2}}$					
3968.68		1	25190.17							
3968.024	10	100	25194.33	0.00	$48556^{\circ}_{3\frac{1}{2}} - 73750_{4\frac{1}{2}}$	5	1.00	1.06	(0.03)	1.27
3966.062		2	25206.80	−0.02	$66395_{2\frac{1}{2}} - 91602^{\circ}_{2\frac{1}{2}}$					
3964.584		1	25216.19	+0.04	$52067^{\circ}_{0\frac{1}{2}} - 77284_{1\frac{1}{2}}$					
3964.459	1	20	25216.99	+0.01	$45737^{\circ}_{1\frac{1}{2}} - 70954_{2\frac{1}{2}}$	4	1.360	1.016	0.172	0.500
3963.301		2	25224.36							
3962.457		4	25229.73	−0.05	$73291_{5\frac{1}{2}} - 98521^{\circ}_{4\frac{1}{2}}$					
3961.832		4	25233.71	−0.04	$42915^{\circ}_{5\frac{1}{2}} - 68148_{5\frac{1}{2}}$					
3961.288		1	25237.17							
3961.104		2	25238.35	−0.03	$73283_{4\frac{1}{2}} - 98521^{\circ}_{4\frac{1}{2}}$					
3960.866		2	25239.86							
3960.34		1	25243.21							
3960.27		1	25243.66							

TABLE 6. Yb II—*Observed and classified lines*—Continued

1	2	3	4	5	6	7	8	9	10	11
Wave-length air	Intensity		Wave number	o–c	Classification	Zeeman type	1st g	2nd g	Zeeman components	
	Meggers lamp	Thomson lamp							Strong p	Strong n
Å			K	K						
3959.730		1	25247.10	+0.02	$48503^{\circ}_{5\frac{1}{2}} - 73750_{4\frac{1}{2}}$					
3959.060	1	9	25251.38	+0.10 +0.05	$56840^{\circ}_{1\frac{1}{2}} - 82091_{0\frac{1}{2}}$ $66351_{2\frac{1}{2}} - 91602^{\circ}_{2\frac{1}{2}}$					
3958.818		2	25252.92	0.00	$68756_{3\frac{1}{2}} - 94008^{\circ}_{3\frac{1}{2}}$					
3958.376		3	25255.74	0.00	$56056^{\circ}_{2\frac{1}{2}} - 81312_{2\frac{1}{2}}$					
3954.266		4	25281.99	+0.03	$65577_{3\frac{1}{2}} - 90859^{\circ}_{2\frac{1}{2}}$					
3953.546		1	25286.59	+0.03	$64923_{4\frac{1}{2}} - 90209^{\circ}_{4\frac{1}{2}}$					
3951.08		10	25302.37	+0.05	$32981^{\circ}_{1\frac{1}{2}} - 58283_{2\frac{1}{2}}$					
3949.91	10	100	25309.87	+0.03	$30392^{\circ}_{1\frac{1}{2}} - 55702_{1\frac{1}{2}}$	6	1.339	1.701	0.545	1.520
3949.58	100	200	25311.98	+0.01	$22960_{1\frac{1}{2}} - 48272^{\circ}_{2\frac{1}{2}}$	5	0.774	1.132	0.179	1.669
3948.64		4	25318.01	+0.02	$68549_{4\frac{1}{2}} - 93867^{\circ}_{4\frac{1}{2}}$					
3948.18	20	100	25320.96	+0.07	$34389^{\circ}_{2\frac{1}{2}} - 59710_{1\frac{1}{2}}$	5	1.047	0.857	0.095	1.332
3946.94	20	150	25328.91	+0.01	$33494^{\circ}_{3\frac{1}{2}} - 58823_{2\frac{1}{2}}$	4	0.989	1.261	0.137	0.309
3945.577		2	25337.66	+0.06	$50832^{\circ}_{1\frac{1}{2}} - 76170_{2\frac{1}{2}}$					
3944.55		1	25344.26	+0.08	$53120^{\circ}_{2\frac{1}{2}} - 78464_{1\frac{1}{2}}$					
3944.509		1	25344.52							
3943.692		2	25349.77							
3942.72		6	25356.02	+0.05	$64923_{4\frac{1}{2}} - 90279^{\circ}_{5\frac{1}{2}}$					
3939.517	1	20	25376.64	+0.09	$45737^{\circ}_{1\frac{1}{2}} - 71113_{1\frac{1}{2}}$					
3938.53	40	400	25383.00	+0.02	$35831^{\circ}_{5\frac{1}{2}} - 61214_{4\frac{1}{2}}$					
3938.25	40	500	25384.80	−0.01	$38342^{\circ}_{4\frac{1}{2}} - 63726_{4\frac{1}{2}}$	6	1.095	1.005	0.41	1.05
3937.984		1	25386.52							
3936.596		2	25395.47	+0.04	$68150_{1\frac{1}{2}} - 93546^{\circ}_{2\frac{1}{2}}$					
3936.385		5	25396.83							
3935.086		3	25405.21							
3934.30	4	100	25410.29	+0.05	$48556^{\circ}_{3\frac{1}{2}} - 73966_{3\frac{1}{2}}$					
3933.87		2	25413.07							
3933.25		2*h*	25417.07	−0.04	$68450_{3\frac{1}{2}} - 93867^{\circ}_{4\frac{1}{2}}$					
3931.90	10	100	25425.80	0.00	$65875_{6\frac{1}{2}} - 91301^{\circ}_{6\frac{1}{2}}$	6	1.21	1.23	0.164	1.22
3931.634		2	25427.52	+0.07	$51248^{\circ}_{2\frac{1}{2}} - 76676_{2\frac{1}{2}}$					
3931.44		1	25428.77							
3930.900		1	25432.27							
3930.004		2	25438.06							
3929.885		1	25438.83	+0.04	$43956^{\circ}_{2\frac{1}{2}} - 69395_{3\frac{1}{2}}$					
3929.053		6	25444.22	+0.04	$66571_{5\frac{1}{2}} - 92015^{\circ}_{4\frac{1}{2}}$					
3928.068		10	25450.60	+0.05	$47329^{\circ}_{2\frac{1}{2}} - 72779_{3\frac{1}{2}}$					
3927.60		1	25453.63							
3926.962		1	25457.77	+0.01	$66558_{3\frac{1}{2}} - 92015^{\circ}_{4\frac{1}{2}}$					
3926.651		2	25459.79	+0.06	$68549_{4\frac{1}{2}} - 94008^{\circ}_{3\frac{1}{2}}$					
3924.656		2	25472.73							
3923.230		4	25481.99	+0.05	$53644^{\circ}_{3\frac{1}{2}} - 79126_{4\frac{1}{2}}$					

TABLE 6. Yb II—*Observed and classified lines*—Continued

1	2	3	4	5	6	7	8	9	10	11
Wave-length air	Intensity		Wave number	o–c	Classification	Zeeman type	1st g	2nd g	Zeeman components	
	Meggers lamp	Thomson lamp							Strong p	Strong n
Å			K	K						
3922.443	1	15	25487.10	−0.01	$43956^{\circ}_{2\frac{1}{2}} - 69443_{1\frac{1}{2}}$					
3921.201		2	25495.17							
3920.745		4	25498.14	+0.02	$67416_{4\frac{1}{2}} - 92914^{\circ}_{4\frac{1}{2}}$					
3920.602		2*h*	25499.07							
3919.980	1	15	25503.11	+0.04	$67416_{4\frac{1}{2}} - 92919^{\circ}_{3\frac{1}{2}}$					
3918.804		9	25510.77	+0.06	$73291_{5\frac{1}{2}} - 98802^{\circ}_{5\frac{1}{2}}$					
3917.685		3	25518.05	+0.05	$65199_{4\frac{1}{2}} - 90717^{\circ}_{4\frac{1}{2}}$					
3917.473		5	25519.43	−0.03	$44438^{\circ}_{3\frac{1}{2}} - 69957_{4\frac{1}{2}}$					
3916.892		2	25523.22	+0.07	$45335^{\circ}_{4\frac{1}{2}} - 70858_{4\frac{1}{2}}$					
3916.783	2	15	25523.93	+0.05	$70858_{4\frac{1}{2}} - 96382^{\circ}_{5\frac{1}{2}}$					
3916.702		1	25524.46	+0.01	$45429^{\circ}_{3\frac{1}{2}} - 70954_{2\frac{1}{2}}$					
3916.425		10	25526.26	+0.02	$41678^{\circ}_{2\frac{1}{2}} - 67204_{1\frac{1}{2}}$					
3916.316		1	25526.97							
3916.268		1	25527.28							
3915.427		10	25532.77	+0.05	$45737^{\circ}_{1\frac{1}{2}} - 71270_{2\frac{1}{2}}$					
3914.690		3	25537.57	+0.03	$73291_{5\frac{1}{2}} - 98829^{\circ}_{6\frac{1}{2}}$					
3913.923		7	25542.58	0.00	$59090_{3\frac{1}{2}} - 84632^{\circ}_{2\frac{1}{2}}$					
3913.729		7	25543.84	+0.06	$64169^{\circ}_{3\frac{1}{2}} - 89713_{2\frac{1}{2}}$					
3913.347	30	200	25546.34	+0.02	$28757^{\circ}_{1\frac{1}{2}} - 54304_{0\frac{1}{2}}$	4	1.441	2.001	0.280	1.161
3910.911		6	25562.25	+0.04	$60586_{1\frac{1}{2}} - 86148^{\circ}_{2\frac{1}{2}}$					
3910.429		2	25565.40	+0.03	$57798^{\circ}_{2\frac{1}{2}} - 83363_{3\frac{1}{2}}$					
3910.364		4	25565.83							
3909.98		1	25568.34							
3909.186		1	25573.53							
3908.020		5	25581.16							
3907.355	2	40	25585.51	+0.06	$65950_{4\frac{1}{2}} - 91536^{\circ}_{3\frac{1}{2}}$	4	(1.09)	1.13	*w*	0.955
3906.960	4	30	25588.10	0.00	$70793_{5\frac{1}{2}} - 96382^{\circ}_{5\frac{1}{2}}$	6	1.21	1.23	0.07	1.22
3906.64		3	25590.20	+0.06	$51248^{\circ}_{2\frac{1}{2}} - 76839_{2\frac{1}{2}}$					
3906.196	4	30	25593.10	+0.04	$69957_{4\frac{1}{2}} - 95550^{\circ}_{4\frac{1}{2}}$					
3905.832	20	200	25595.49	+0.04	$33494^{\circ}_{3\frac{1}{2}} - 59090_{3\frac{1}{2}}$	6	0.926	1.060	0.474	0.992
3904.812	100	1500	25602.18	+0.02	$38342^{\circ}_{4\frac{1}{2}} - 63944_{5\frac{1}{2}}$	5	(1.093)	1.13	*w*	1.30
3904.537		2	25603.98	+0.02	$68756_{3\frac{1}{2}} - 94360^{\circ}_{4\frac{1}{2}}$					
3904.447		1	25604.57	+0.04	$56088^{\circ}_{4\frac{1}{2}} - 81692_{3\frac{1}{2}}$					
3903.74		1*h*	25609.21							
3903.397		4	25611.46	−0.09 +0.07	$47680^{\circ}_{6\frac{1}{2}} - 73291_{5\frac{1}{2}}$ $64598_{3\frac{1}{2}} - 90209^{\circ}_{4\frac{1}{2}}$					
3903.288		3	25612.17	+0.04	$48024^{\circ}_{1\frac{1}{2}} - 73636_{0\frac{1}{2}}$					
3902.814		5	25615.28	+0.02	$68720_{6\frac{1}{2}} - 94335^{\circ}_{5\frac{1}{2}}$					
3902.43		3*h*	25617.80							
3902.109		5	25619.91	+0.08	$47663^{\circ}_{4\frac{1}{2}} - 73283_{4\frac{1}{2}}$					

TABLE 6. Yb II—*Observed and classified lines*—Continued

1	2	3	4	5	6	7	8	9	10	11
Wave-length air	Intensity		Wave number	o–c	Classification	Zeeman type	1st g	2nd g	Zeeman components	
	Meggers lamp	Thomson lamp							Strong p	Strong n
Å			K	K						
3902.042	1	20	25620.35	$\begin{cases}-0.14\\+0.08\end{cases}$	$58823_{2\frac{1}{2}} - 84444^{\circ}_{3\frac{1}{2}}$ $67416_{4\frac{1}{2}} - 93036^{\circ}_{5\frac{1}{2}}$					
3901.44		1	25624.30	$\begin{cases}-0.10\\+0.04\end{cases}$	$65093_{3\frac{1}{2}} - 90717^{\circ}_{4\frac{1}{2}}$ $70858_{4\frac{1}{2}} - 96482^{\circ}_{4\frac{1}{2}}$					
3899.245		3	25638.73							
3899.07	4	80	25639.88	+0.03	$60586_{1\frac{1}{2}} - 86226^{\circ}_{1\frac{1}{2}}$	7	(1.323)	1.36	0	1.34
3898.450		1	25643.96							
3897.946		8	25647.27	+0.07	$37516^{\circ}_{3\frac{1}{2}} - 63163_{4\frac{1}{2}}$					
3897.34		2*d*	25651.26	+0.13	$43956^{\circ}_{2\frac{1}{2}} - 69607_{2\frac{1}{2}}$					
3897.060		1	25653.10							
3896.966		4	25653.72	+0.05	$40917^{\circ}_{4\frac{1}{2}} - 66571_{5\frac{1}{2}}$					
3895.884		2	25660.84	+0.01	$65577_{3\frac{1}{2}} - 91237^{\circ}_{3\frac{1}{2}}$					
3895.758	1	30	25661.67	+0.05	$63944_{5\frac{1}{2}} - 89605^{\circ}_{4\frac{1}{2}}$					
3893.740		2	25674.97							
3892.285		1	25684.57	+0.01	$50832^{\circ}_{1\frac{1}{2}} - 76517_{1\frac{1}{2}}$					
3891.696		1	25688.46	−0.02	$70793_{5\frac{1}{2}} - 96482^{\circ}_{4\frac{1}{2}}$					
3890.850	2	50	25694.04	0.00	$48272^{\circ}_{2\frac{1}{2}} - 73966_{3\frac{1}{2}}$	4	1.117	0.745	0.186	−0.185
3889.664		2	25701.88							
3887.826		10	25714.03	$\begin{cases}-0.05\\+0.03\end{cases}$	$65888_{1\frac{1}{2}} - 91602^{\circ}_{2\frac{1}{2}}$ $68150_{1\frac{1}{2}} - 93864^{\circ}_{2\frac{1}{2}}$					
3887.50		1	25716.19							
3887.290	20	300	25717.57	+0.05	$37516^{\circ}_{3\frac{1}{2}} - 63234_{2\frac{1}{2}}$	4	1.13	1.20	(0.036)	0.95
3886.63		1	25721.94							
3886.378		4	25723.61	+0.05	$49916^{\circ}_{4\frac{1}{2}} - 75640_{3\frac{1}{2}}$					
3885.647		1	25728.45							
3885.470		1	25729.62	+0.05	$68135_{2\frac{1}{2}} - 93864^{\circ}_{2\frac{1}{2}}$					
3885.195		4	25731.44	+0.03	$45737^{\circ}_{1\frac{1}{2}} - 71468_{2\frac{1}{2}}$					
3884.833		1	25733.84	+0.01	$69957_{4\frac{1}{2}} - 95691^{\circ}_{3\frac{1}{2}}$					
3883.638		1	25741.76	+0.02	$72779_{3\frac{1}{2}} - 98521^{\circ}_{4\frac{1}{2}}$					
3883.105		1	25745.29	+0.05	$66558_{3\frac{1}{2}} - 92303^{\circ}_{3\frac{1}{2}}$					
3881.738		3	25754.36	+0.01	$68549_{4\frac{1}{2}} - 94303^{\circ}_{3\frac{1}{2}}$					
3880.684		1	25761.35							
3880.332		2	25763.69							
3880.197	5	70	25764.58	+0.02	$33494^{\circ}_{3\frac{1}{2}} - 59259_{2\frac{1}{2}}$	4	(0.991)	1.10	*w*	0.73
3880.044		1	25765.60	+0.05	$50468^{\circ}_{5\frac{1}{2}} - 76233_{6\frac{1}{2}}$					
3879.140		7	25771.61							
3878.023		4	25779.03	+0.03	$67416_{4\frac{1}{2}} - 93195^{\circ}_{3\frac{1}{2}}$					
3877.06	4	60	25785.43	+0.01	$31979^{\circ}_{3\frac{1}{2}} - 57765_{4\frac{1}{2}}$					
3876.902		1	25786.48	+0.01	$68549_{4\frac{1}{2}} - 94335^{\circ}_{5\frac{1}{2}}$					
3876.776	1	20	25787.32	+0.05	$47329^{\circ}_{2\frac{1}{2}} - 73116_{1\frac{1}{2}}$	5	0.995	0.863	0.067	1.193

TABLE 6. Yb II—*Observed and classified lines*—Continued

1	2	3	4	5	6	7	8	9	10	11
Wave-length air	Intensity		Wave number	o–c	Classification	Zeeman type	1st g	2nd g	Zeeman components	
	Meggers lamp	Thomson lamp							Strong p	Strong n
Å			K	K						
3876.33		2h	25790.29							
3874.610		3h	25801.74							
3874.066		10	25805.36	+0.05	$42915^{\circ}_{5\frac{1}{2}} - 68720_{6\frac{1}{2}}$					
3873.497		4	25809.15	+0.02	$58823_{2\frac{1}{2}} - 84632^{\circ}_{2\frac{1}{2}}$					
3872.555		5	25815.43	+0.02	$66462_{0\frac{1}{2}} - 92278^{\circ}_{1\frac{1}{2}}$					
3872.338		8	25816.87	−0.02	$54640^{\circ}_{4\frac{1}{2}} - 80457_{3\frac{1}{2}}$					
3871.946		1	25819.49	+0.06	$52067^{\circ}_{0\frac{1}{2}} - 77887_{0\frac{1}{2}}$					
3870.447		2	25829.49	+0.06	$57534^{\circ}_{3\frac{1}{2}} - 83363_{3\frac{1}{2}}$					
3870.197		2h	25831.16							
3868.838		4	25840.23	+0.04	$45429^{\circ}_{3\frac{1}{2}} - 71270_{2\frac{1}{2}}$					
3868.602	1	9	25841.81	+0.08	$64055_{2\frac{1}{2}} - 89897^{\circ}_{1\frac{1}{2}}$					
3868.570	1	20	25842.02	+0.03	$32981^{\circ}_{1\frac{1}{2}} - 58823_{2\frac{1}{2}}$					
3867.75		1	25847.50	+0.02	$46354^{\circ}_{4\frac{1}{2}} - 72202_{3\frac{1}{2}}$					
3867.675		3	25848.00	+0.05	$68150_{1\frac{1}{2}} - 93998^{\circ}_{1\frac{1}{2}}$					
3867.48		5h	25849.30							
3867.378		1	25849.98	+0.01	$55462^{\circ}_{3\frac{1}{2}} - 81312_{2\frac{1}{2}}$					
3866.862		1	25853.43	−0.04	$68450_{3\frac{1}{2}} - 94303^{\circ}_{3\frac{1}{2}}$					
3865.351		1	25863.54	+0.02	$68135_{2\frac{1}{2}} - 93998^{\circ}_{1\frac{1}{2}}$					
3865.255		3	25864.18	+0.03	$71222_{3\frac{1}{2}} - 97086^{\circ}_{4\frac{1}{2}}$					
3863.784		2	25874.03	+0.07	$68135_{2\frac{1}{2}} - 94008^{\circ}_{3\frac{1}{2}}$					
3863.455	200	800	25876.23	+0.04	$27061^{\circ}_{5\frac{1}{2}} - 52938_{1\frac{1}{2}}$	5	0.68	0.88	0.10	0.98
3863.046	10	100	25878.97	0.00	$63726_{4\frac{1}{2}} - 89605^{\circ}_{4\frac{1}{2}}$					
3862.511	1	20	25882.56	+0.01	$66395_{2\frac{1}{2}} - 92278^{\circ}_{1\frac{1}{2}}$ [d]	5	(1.235)	1.49	w	0.86
3861.792		3	25887.37	+0.04	$45335^{\circ}_{4\frac{1}{2}} - 71222_{3\frac{1}{2}}$					
3861.730		2	25887.79	+0.04	$47228^{\circ}_{0\frac{1}{2}} - 73116_{1\frac{1}{2}}$					
3861.566		1	25888.89							
3861.467		1	25889.55	−0.02	$53716^{\circ}_{2\frac{1}{2}} - 79605_{1\frac{1}{2}}$					
3860.917		1	25893.24	0.00	$52921^{\circ}_{3\frac{1}{2}} - 78814_{2\frac{1}{2}}$					
3859.887		2	25900.15							
3859.35		2h	25903.75							
3858.555	10	100	25909.09	+0.01	$33052^{\circ}_{4\frac{1}{2}} - 58961_{5\frac{1}{2}}$	4	1.265	0.975	0.145	−0.290
3858.434		1	25909.90	+0.01	$68450_{3\frac{1}{2}} - 94360^{\circ}_{4\frac{1}{2}}$					
3858.07		9	25912.35	+0.02	$53716^{\circ}_{2\frac{1}{2}} - 79628_{3\frac{1}{2}}$					
3857.860		2	25913.76							
3857.586	10	20	25915.60							
3856.514		3	25922.80							
3854.91	4	30	25933.59	+0.08	$66082_{5\frac{1}{2}} - 92015^{\circ}_{4\frac{1}{2}}$					
3854.806	20	100	25934.29	+0.03	$37077^{\circ}_{2\frac{1}{2}} - 63011_{1\frac{1}{2}}$	5	1.117	0.787	0.165	1.612
3853.731		3	25941.52	+0.04	$45012^{\circ}_{2\frac{1}{2}} - 70954_{2\frac{1}{2}}$					
3853.238	1	2	25944.84							

TABLE 6. Yb II—*Observed and classified lines*—Continued

1	2	3	4	5	6	7	8	9	10	11
Wave-length air	Intensity		Wave number	o–c	Classification	Zeeman type	1st g	2nd g	Zeeman components	
	Meggers lamp	Thomson lamp							Strong p	Strong n
Å			K	K						
3852.562		10	25949.39	+0.05	$45273^{\circ}_{3\frac{1}{2}} - 71222_{3\frac{1}{2}}$					
3852.160	4	40	25952.10	+0.07	$66351_{2\frac{1}{2}} - 92303^{\circ}_{3\frac{1}{2}}$					
3851.80		2	25954.53	+0.11	$73291_{5\frac{1}{2}} - 99246^{\circ}_{5\frac{1}{2}}$?					
3851.242		1	25958.29							
3851.090		2	25959.31	+0.02	$65577_{3\frac{1}{2}} - 91536^{\circ}_{3\frac{1}{2}}$					
3850.366		4	25964.19							
3850.32		2	25964.50	+0.02	$49008^{\circ}_{3\frac{1}{2}} - 74973_{3\frac{1}{2}}$					
3847.473	30	200	25983.72	+0.04 −0.10	$30392^{\circ}_{1\frac{1}{2}} - 56375_{2\frac{1}{2}}$ $(53644^{\circ}_{3\frac{1}{2}} - 79628_{3\frac{1}{2}})$	4	1.32	1.24	(0.04)	1.12
3846.237		4	25992.07	+0.01	$35059^{\circ}_{3\frac{1}{2}} - 61051_{3\frac{1}{2}}$					
3846.186	1	15	25992.41	+0.05	$47758^{\circ}_{3\frac{1}{2}} - 73750_{4\frac{1}{2}}$					
3845.402		4	25997.71	0.00	$48272^{\circ}_{2\frac{1}{2}} - 74270_{2\frac{1}{2}}$					
3844.988	2	6	26000.51							
3844.349	1	15	26004.83	+0.04	$43075^{\circ}_{1\frac{1}{2}} - 69079_{2\frac{1}{2}}$					
3843.811		6	26008.47							
3843.420	5	80	26011.12	+0.03	$34575^{\circ}_{1\frac{1}{2}} - 60586_{1\frac{1}{2}}$	6	1.446	1.334	0.168	1.390
3843.032	1	20	26013.74	+0.08	$44940^{\circ}_{1\frac{1}{2}} - 70954_{2\frac{1}{2}}$					
3842.653		1	26016.31							
3841.950	1	9	26021.07							
3841.296	1	10	26025.50	+0.07	$65577_{3\frac{1}{2}} - 91602^{\circ}_{2\frac{1}{2}}$					
3840.70		1	26029.54							
3840.341	3	70	26031.97	+0.04	$35019^{\circ}_{4\frac{1}{2}} - 61051_{3\frac{1}{2}}$	7	(1.158)	1.17	0	1.10
3840.297	2	40	26032.27	+0.02	$46169^{\circ}_{4\frac{1}{2}} - 72202_{3\frac{1}{2}}$					
3840.013		2	26034.19	+0.04	$47005^{\circ}_{1\frac{1}{2}} - 73039_{0\frac{1}{2}}$					
3839.469	30	300	26037.88	+0.04	$33052^{\circ}_{4\frac{1}{2}} - 59090_{3\frac{1}{2}}$	5	1.259	1.111	0.072	1.777
3839.382	1	20	26038.47	+0.11 +0.07	$54640^{\circ}_{4\frac{1}{2}} - 80679_{5\frac{1}{2}}$ $65199_{4\frac{1}{2}} - 91237^{\circ}_{3\frac{1}{2}}$					
3838.900	10	100	26041.74	+0.02	$35831^{\circ}_{5\frac{1}{2}} - 61873_{6\frac{1}{2}}$	4				
3838.67		2	26043.30	+0.01	$67955_{0\frac{1}{2}} - 93998^{\circ}_{1\frac{1}{2}}$					
3838.123		3	26047.01	+0.03	$67416_{4\frac{1}{2}} - 93463^{\circ}_{3\frac{1}{2}}$					
3837.411		4	26051.85	+0.09	$56840^{\circ}_{1\frac{1}{2}} - 82891_{2\frac{1}{2}}$					
3836.677		2	26056.83	+0.04	$33653^{\circ}_{0\frac{1}{2}} - 59710_{1\frac{1}{2}}$					
3836.541		1	26057.75							
3835.952		2	26061.75							
3835.872		1	26062.30							
3835.495		3	26064.86	+0.10 +0.05	$48503^{\circ}_{5\frac{1}{2}} - 74568_{4\frac{1}{2}}$ $65950_{4\frac{1}{2}} - 92015^{\circ}_{4\frac{1}{2}}$					
3833.884		9	26075.81	+0.05	$66571_{5\frac{1}{2}} - 92647^{\circ}_{5\frac{1}{2}}$					
3832.701		4	26083.86	+0.08	$69607_{2\frac{1}{2}} - 95691^{\circ}_{3\frac{1}{2}}$					
3832.664		1	26084.11							
3832.180		3	26087.41	+0.03	$47663^{\circ}_{4\frac{1}{2}} - 73750_{4\frac{1}{2}}$					

TABLE 6. Yb II—*Observed and classified lines*—Continued

1	2	3	4	5	6	7	8	9	10	11
Wavelength air	Intensity		Wave number	o–c	Classification	Zeeman type	1st g	2nd g	Zeeman components	
	Meggers lamp	Thomson lamp							Strong p	Strong n
Å			K	K						
3832.108		3	26087.90	+0.04	$67416_{4\frac{1}{2}} - 93503^{\circ}_{4\frac{1}{2}}$					
3831.610	3	20	26091.29	+0.10	$55221^{\circ}_{1\frac{1}{2}} - 81312_{2\frac{1}{2}}$	7	(1.11)	1.11	0	1.12
3831.288		1	26093.48							
3831.13		1	26094.56							
3830.178		2	26101.04	−0.01	$45012^{\circ}_{2\frac{1}{2}} - 71113_{1\frac{1}{2}}$					
3829.767		2	26103.84							
3829.736		1	26104.05	−0.02	$70793_{5\frac{1}{2}} - 96898^{\circ}_{5\frac{1}{2}}$					
3827.494		4	26119.34	+0.08	$64598_{3\frac{1}{2}} - 90717^{\circ}_{4\frac{1}{2}}$					
3827.030		2	26122.51	+0.04	$73291_{5\frac{1}{2}} - 99414^{\circ}_{4\frac{1}{2}}$					
3826.768		8	26124.30	+0.08	$33494^{\circ}_{3\frac{1}{2}} - 59618_{3\frac{1}{2}}$					
3826.51		1	26126.06							
3822.216		1	26155.41	+0.06	$69395_{3\frac{1}{2}} - 95550^{\circ}_{4\frac{1}{2}}$					
3822.17		1	26155.73	+0.07	$35059^{\circ}_{3\frac{1}{2}} - 61214_{4\frac{1}{2}}$					
3821.526		1	26160.13	−0.03	$58283_{2\frac{1}{2}} - 84444^{\circ}_{3\frac{1}{2}}$					
3821.224		1	26162.20	+0.10	$62559_{2\frac{1}{2}} - 88721^{\circ}_{3\frac{1}{2}}$					
3820.825		8	26164.93							
3820.288		5	26168.61	+0.03	$68135_{2\frac{1}{2}} - 94303^{\circ}_{3\frac{1}{2}}$					
3819.916	1	15	26171.16	+0.08	$61214_{4\frac{1}{2}} - 87385^{\circ}_{3\frac{1}{2}}$					
3818.365		1	26181.79	+0.04	$50468^{\circ}_{5\frac{1}{2}} - 76649_{5\frac{1}{2}}$					
3817.777	3	20	26185.82	+0.09	$37516^{\circ}_{3\frac{1}{2}} - 63702_{2\frac{1}{2}}$	5	(1.12)	1.05	w	1.30
3817.624		7	26186.87	+0.05	$68148_{5\frac{1}{2}} - 94335^{\circ}_{5\frac{1}{2}}$					
				−0.05	$72615_{5\frac{1}{2}} - 98802^{\circ}_{5\frac{1}{2}}$					
3816.345	15	150	26195.65	+0.12	$35019^{\circ}_{4\frac{1}{2}} - 61214_{4\frac{1}{2}}$	6				
				−0.03	$(45273^{\circ}_{3\frac{1}{2}} - 71468_{2\frac{1}{2}})$					
3816.189	30	300	26196.72	+0.02	$34389^{\circ}_{2\frac{1}{2}} - 60586_{1\frac{1}{2}}$	4	1.007	1.327	0.160	1.166
3815.640		1	26200.49	+0.03	$51248^{\circ}_{2\frac{1}{2}} - 77449_{3\frac{1}{2}}$					
3814.310		10	26209.62	+0.05	$45012^{\circ}_{2\frac{1}{2}} - 71222_{3\frac{1}{2}}$					
3814.215	15	200	26210.28	+0.04	$37516^{\circ}_{3\frac{1}{2}} - 63726_{4\frac{1}{2}}$	4	1.12	1.00	0.06	0.57
3814.084		4	26211.18	+0.06	$68148_{5\frac{1}{2}} - 94360^{\circ}_{4\frac{1}{2}}$					
3813.665		3	26214.06	+0.06	$46902^{\circ}_{0\frac{1}{2}} - 73116_{1\frac{1}{2}}$					
3811.584		2	26228.37	+0.04	$70858_{4\frac{1}{2}} - 97086^{\circ}_{4\frac{1}{2}}$					
3809.04	5	30	26245.88	+0.10	$48024^{\circ}_{1\frac{1}{2}} - 74270_{2\frac{1}{2}}$					
				+0.06	$70136_{6\frac{1}{2}} - 96382^{\circ}_{5\frac{1}{2}}$					
3808.544		1	26249.30	−0.02	$70793_{5\frac{1}{2}} - 97043^{\circ}_{6\frac{1}{2}}$					
3808.460	1	2	26249.88	+0.06	$63647_{1\frac{1}{2}} - 89897^{\circ}_{1\frac{1}{2}}$					
3808.35		2	26250.64							
3808.315		2	26250.88							
3807.574	50	500	26255.99							
3807.545	100	1000	26256.19	−0.07	$38342^{\circ}_{4\frac{1}{2}} - 64598_{3\frac{1}{2}}$	4	1.08	1.23	0.076	0.55
3806.996		3	26259.98	+0.03	$41678^{\circ}_{2\frac{1}{2}} - 67938_{3\frac{1}{2}}$					

TABLE 6. Yb II—*Observed and classified lines*—Continued

1	2	3	4	5	6	7	8	9	10	11
Wave-length air	Intensity		Wave number	o–c	Classification	Zeeman type	1st g	2nd g	Zeeman components	
	Meggers lamp	Thomson lamp							Strong p	Strong n
Å			K	K						
3806.869		1	26260.85	−0.01 +0.06	$57103^{\circ}_{3\frac{1}{2}} - 83363_{3\frac{1}{2}}$ $64598_{3\frac{1}{2}} - 90859^{\circ}_{2\frac{1}{2}}$					
3806.818		2	26261.20	+0.01	$46354^{\circ}_{4\frac{1}{2}} - 72615_{5\frac{1}{2}}$					
3806.188	2	20	26265.55	+0.06	$63944_{5\frac{1}{2}} - 90209^{\circ}_{4\frac{1}{2}}$					
3806.011		1	26266.77	−0.01	$41688^{\circ}_{1\frac{1}{2}} - 67955_{0\frac{1}{2}}$					
3804.99		1	26273.82							
3804.431	4	40	26277.68	+0.03	$32981^{\circ}_{1\frac{1}{2}} - 59259_{2\frac{1}{2}}$	5	0.891	1.125	0.117	1.476
3804.35		2	26278.24	+0.01	$68150_{1\frac{1}{2}} - 94428^{\circ}_{1\frac{1}{2}}$					
3803.680		1	26282.87							
3802.47		1	26291.23	+0.07	$55221^{\circ}_{1\frac{1}{2}} - 81512_{1\frac{1}{2}}$					
3802.28		1	26292.54	−0.01	$70793_{5\frac{1}{2}} - 97086^{\circ}_{4\frac{1}{2}}$					
3801.752	1	20	26296.20	+0.06 +0.08	$63417^{\circ}_{2\frac{1}{2}} - 89713_{2\frac{1}{2}}$ $69395_{3\frac{1}{2}} - 95691^{\circ}_{3\frac{1}{2}}$					
3801.026		3*h*	26301.22							
3800.622	20	80	26304.01	0.00	$31979^{\circ}_{3\frac{1}{2}} - 58283_{2\frac{1}{2}}$	5	1.36	0.80	0.28	2.76
3799.054		1	26314.87	+0.04	$64923_{4\frac{1}{2}} - 91237^{\circ}_{3\frac{1}{2}}$					
3798.960	4	20	26315.52	+0.03	$35059^{\circ}_{3\frac{1}{2}} - 61374_{2\frac{1}{2}}$					
3798.854		1	26316.26							
3797.915		2	26322.76							
3797.219		2	26327.59							
3797.181		3	26327.85	0.00	$47329^{\circ}_{2\frac{1}{2}} - 73657_{1\frac{1}{2}}$					
3796.950		10	26329.45	+0.05	$44940^{\circ}_{1\frac{1}{2}} - 71270_{2\frac{1}{2}}$	4	1.265	0.911	0.177	0.380
3796.157	7	80	26334.95	+0.05	$63944_{5\frac{1}{2}} - 90279^{\circ}_{5\frac{1}{2}}$	6	1.107	1.125	0.098	1.116
3795.916		4	26336.62							
3795.878		3	26336.89	+0.03	$65199_{4\frac{1}{2}} - 91536^{\circ}_{3\frac{1}{2}}$					
3795.061		4	26342.56	−0.01	$66571_{5\frac{1}{2}} - 92914^{\circ}_{4\frac{1}{2}}$					
3794.906		3	26343.63							
3793.934		4	26350.38							
3793.104		3	26356.15	0.00	$66558_{3\frac{1}{2}} - 92914^{\circ}_{4\frac{1}{2}}$					
3792.87		4	26357.78	+0.06	$51248^{\circ}_{2\frac{1}{2}} - 77606_{2\frac{1}{2}}$					
3792.557		1	26359.95	+0.05	$40035^{\circ}_{3\frac{1}{2}} - 66395_{2\frac{1}{2}}$					
3792.39		2	26361.11	+0.01	$66558_{3\frac{1}{2}} - 92919^{\circ}_{3\frac{1}{2}}$					
3791.336		2	26368.44	+0.01	$43075^{\circ}_{1\frac{1}{2}} - 69443_{1\frac{1}{2}}$					
3789.457		6	26381.51	+0.03	$63234_{2\frac{1}{2}} - 89615^{\circ}_{2\frac{1}{2}}$					
3789.37		1	26382.12							
3788.267		4	26389.80	−0.01	$65888_{1\frac{1}{2}} - 92278^{\circ}_{1\frac{1}{2}}$					
3787.418	1	5	26395.72							
3787.080	1	10	26398.07	+0.08	$64461_{1\frac{1}{2}} - 90859^{\circ}_{2\frac{1}{2}}$					
3786.465		1	26402.36							
3785.960		1	26405.88							
3785.666	1	20	26407.93	+0.06	$47228^{\circ}_{0\frac{1}{2}} - 73636_{0\frac{1}{2}}$	7	0.70	0.70	0	0.70

TABLE 6. Yb II—*Observed and classified lines*—Continued

1	2	3	4	5	6	7	8	9	10	11
Wave-length air	Intensity		Wave number	o–c	Classification	Zeeman type	1st g	2nd g	Zeeman components	
	Meggers lamp	Thomson lamp							Strong p	Strong n
Å			K	K						
3785.330	6	80	26410.28	+0.01	$64891_{7\frac{1}{2}} - 91301^{\circ}_{6\frac{1}{2}}$	4	(1.19)	1.21	?	1.05
3784.512		1	26415.98	+0.07	$63726_{4\frac{1}{2}} - 90142^{\circ}_{3\frac{1}{2}}$					
3784.384	7	100	26416.88	+0.04	$48556^{\circ}_{3\frac{1}{2}} - 74973_{3\frac{1}{2}}$	6	0.935	1.069	0.465	1.002
3784.144	1	10	26418.55	+0.05	$66558_{3\frac{1}{2}} - 92976^{\circ}_{3\frac{1}{2}}$					
3783.914		1	26420.16	+0.01	$44438^{\circ}_{3\frac{1}{2}} - 70858_{4\frac{1}{2}}$					
3782.736		4	26428.39	+0.06	$47228^{\circ}_{0\frac{1}{2}} - 73657_{1\frac{1}{2}}$					
3782.540	70	700	26429.76	+0.05	$34784^{\circ}_{5\frac{1}{2}} - 61214_{4\frac{1}{2}}$	5	1.15	1.09	(0.030)	1.42
3781.684		8	26435.74	+0.01 +0.07	$43007^{\circ}_{0\frac{1}{2}} - 69443_{1\frac{1}{2}}$ $55221^{\circ}_{1\frac{1}{2}} - 81657_{2\frac{1}{2}}$					
3781.268		1	26438.65	0.00	$65577_{3\frac{1}{2}} - 92015^{\circ}_{4\frac{1}{2}}$					
3781.046		3	26440.20							
3780.605		1	26443.28	+0.0	$65093_{3\frac{1}{2}} - 91536^{\circ}_{3\frac{1}{2}}$					
3780.217	2	20	26446.00	+0.0	$46169^{\circ}_{4\frac{1}{2}} - 72615_{5\frac{1}{2}}$					
3779.838		1	26448.65							
3779.472		2	26451.21	+0.02	$67416_{4\frac{1}{2}} - 93867^{\circ}_{4\frac{1}{2}}$					
3779.286	20	150	26452.51	+0.03 −0.02	$32371^{\circ}_{2\frac{1}{2}} - 58823_{2\frac{1}{2}}$ $(57765_{4\frac{1}{2}} - 84217^{\circ}_{4\frac{1}{2}})$	6	1.177	1.275	0.244	1.226
3779.184	1	15	26453.22							
3778.800		2	26455.91	0.00	$45012^{\circ}_{2\frac{1}{2}} - 71468_{2\frac{1}{2}}$					
3778.452		3	26458.35	+0.02	$22960_{1\frac{1}{2}} - 49419^{\circ}_{0\frac{1}{2}}$					
3777.906	1	20	26462.17	+0.05	$41688^{\circ}_{1\frac{1}{2}} - 68150_{1\frac{1}{2}}$					
3777.534	2	30	26464.78	+0.06	$66571_{5\frac{1}{2}} - 93036^{\circ}_{5\frac{1}{2}}$	6	(1.189)	1.23	*d*?	1.21
3776.520	3	40	26471.88	+0.04	$41678^{\circ}_{2\frac{1}{2}} - 68150_{1\frac{1}{2}}$	5	1.197	0.931	0.132	1.595
3776.362		1	26472.99							
3775.906		2	26476.19							
3774.956		2	26482.85	+0.01	$63726_{4\frac{1}{2}} - 90209^{\circ}_{4\frac{1}{2}}$					
3773.625		1	26492.19							
3773.428	200	600	26493.58	+0.02	$21418^{\circ}_{3\frac{1}{2}} - 47912_{3\frac{1}{2}}$	6	1.156	1.300	0.496	1.228
3772.517	20	100	26499.97	+0.01	$24332_{2\frac{1}{2}} - 50832^{\circ}_{1\frac{1}{2}}$	5	1.213	0.963	0.126	1.588
3772.294	3	40	26501.54	0.00	$48556^{\circ}_{3\frac{1}{2}} - 75058_{2\frac{1}{2}}$	5	0.932	0.758	0.087	1.367
3771.596		2	26506.44	+0.03	$49727^{\circ}_{6\frac{1}{2}} - 76233_{6\frac{1}{2}}$					
3771.350		3	26508.17	+0.04	$53120^{\circ}_{2\frac{1}{2}} - 79628_{3\frac{1}{2}}$					
3771.155	1	10	26509.54	−0.03	$39378^{\circ}_{0\frac{1}{2}} - 65888_{1\frac{1}{2}}$					
3770.814		1	26511.94	0.00	$47758^{\circ}_{3\frac{1}{2}} - 74270_{2\frac{1}{2}}$					
3770.28		1	26515.70	+0.04	$59710_{1\frac{1}{2}} - 86226^{\circ}_{1\frac{1}{2}}$					
3770.195	2	40	26516.29	+0.05	$44438^{\circ}_{3\frac{1}{2}} - 70954_{2\frac{1}{2}}$					
3769.35		1	26522.24	+0.06	$40035^{\circ}_{3\frac{1}{2}} - 66558_{3\frac{1}{2}}$					
3769.189		1	26523.37	−0.01	$66395_{2\frac{1}{2}} - 92919^{\circ}_{3\frac{1}{2}}$					
3768.966		2	26524.94	−0.01	$69957_{4\frac{1}{2}} - 96482^{\circ}_{4\frac{1}{2}}$					
3767.891		10	26532.51	+0.06	$43075^{\circ}_{1\frac{1}{2}} - 69607_{2\frac{1}{2}}$					

TABLE 6. Yb II—*Observed and classified lines*—Continued

1	2	3	4	5	6	7	8	9	10	11
Wave-length air	Intensity		Wave number	o–c	Classification	Zeeman type	1st g	2nd g	Zeeman components	
	Meggers lamp	Thomson lamp							Strong p	Strong n
Å			K	K						
3767.175		1	26537.55							
3766.925	2	20	26539.31	+0.08	$37516^{\circ}_{3\frac{1}{2}} - 64055_{2\frac{1}{2}}$	5	(1.12)	1.11	0	1.15
3766.736		8*h*	26540.64							
3766.527		4	26542.12	+0.11	$49008^{\circ}_{3\frac{1}{2}} - 75550_{2\frac{1}{2}}$					
3766.101	20	200	26545.12	0.00	$34575^{\circ}_{1\frac{1}{2}} - 61120_{0\frac{1}{2}}$	4	1.438	1.666	0.112	1.327
3765.080	1	8	26552.32	+0.07	$63726_{4\frac{1}{2}} - 90279^{\circ}_{5\frac{1}{2}}$					
3764.56		3*h*	26555.98							
3764.03		1	26559.72							
3763.35		1	26564.52	+0.07	$54640^{\circ}_{4\frac{1}{2}} - 81205_{4\frac{1}{2}}$					
3763.27		1	26565.09	0.00	$66082_{5\frac{1}{2}} - 92647^{\circ}_{5\frac{1}{2}}$					
3763.045	1	6	26566.67	+0.06	$33052^{\circ}_{4\frac{1}{2}} - 59618_{3\frac{1}{2}}$					
3762.98		1	26567.13							
3762.550	40	400	26570.17	+0.03	$37077^{\circ}_{2\frac{1}{2}} - 63647_{1\frac{1}{2}}$	4	(1.113)	1.14	*w*	1.07
3762.12		1	26573.21							
3761.31		1	26578.93							
3760.999	10	200	26581.13	+0.04	$38342^{\circ}_{4\frac{1}{2}} - 64923_{4\frac{1}{2}}$	6	1.103	1.089	0.06	1.096
3760.23		2*d*	26586.56							
3757.355		1	26606.91	+0.01	$68943_{4\frac{1}{2}} - 95550^{\circ}_{4\frac{1}{2}}$					
3756.888		2	26610.21	0.00	$46169^{\circ}_{4\frac{1}{2}} - 72779_{3\frac{1}{2}}$					
3756.445		6	26613.35	+0.06	$64923_{4\frac{1}{2}} - 91536^{\circ}_{3\frac{1}{2}}$					
3755.762		2	26618.19	0.00	$52987^{\circ}_{1\frac{1}{2}} - 79605_{1\frac{1}{2}}$					
3755.32		1	26621.32							
3754.83		2	26624.80	+0.07	$37077^{\circ}_{2\frac{1}{2}} - 63702_{2\frac{1}{2}}$					
3754.74		1	26625.44							
3754.606	2	6	26626.39							
3753.897	8	100	26631.41	+0.04	$47005^{\circ}_{1\frac{1}{2}} - 73636_{0\frac{1}{2}}$	5	0.990	0.690	0.15	1.15
3753.65		1	26633.17	−0.01	$51248^{\circ}_{2\frac{1}{2}} - 77882_{3\frac{1}{2}}$					
3753.49		2	26634.30							
3753.053	4	60	26637.40	+0.03	$47329^{\circ}_{2\frac{1}{2}} - 73966_{3\frac{1}{2}}$					
3752.730		4	26639.70	+0.04	$64598_{3\frac{1}{2}} - 91237^{\circ}_{3\frac{1}{2}}$					
3752.56		1	26640.90							
3751.847	10	40	26645.97	+0.03	$26759^{\circ}_{2\frac{1}{2}} - 53404_{2\frac{1}{2}}$	6	1.58	1.04	1.36	1.31
3751.206	1	2	26650.52							
3751.030		1	26651.77	−0.06	$47005^{\circ}_{1\frac{1}{2}} - 73657_{1\frac{1}{2}}$					
3750.045		8	26658.77							
3749.688	40	400	26661.31	+0.01	$34389^{\circ}_{2\frac{1}{2}} - 61051_{3\frac{1}{2}}$	5	1.015	1.196	0.452	1.650
3749.388	1	6	26663.44	0.00	$63234_{2\frac{1}{2}} - 89897^{\circ}_{1\frac{1}{2}}$					
3748.345	3	10	26670.86	+0.05	$66571_{5\frac{1}{2}} - 93242^{\circ}_{5\frac{1}{2}}$					
3748.204		2	26671.86							
3748.102		1	26672.59	−0.02	$68150_{1\frac{1}{2}} - 94823^{\circ}_{1\frac{1}{2}}$					

TABLE 6. Yb II—*Observed and classified lines*—Continued

1	2	3	4	5	6	7	8	9	10	11
Wave-length air	Intensity		Wave number	o–c	Classification	Zeeman type	1st g	2nd g	Zeeman components	
	Meggers lamp	Thomson lamp							Strong p	Strong n
Å			K	K						
3747.817	2	20	26674.62	+0.01	$66571_{5\frac{1}{2}} - 93246^{\circ}_{6\frac{1}{2}}$					
3747.229		10	26678.80	+0.05	$57765_{4\frac{1}{2}} - 84444^{\circ}_{3\frac{1}{2}}$					
3746.67		1	26682.78							
3744.762		1	26696.38	−0.01	$65950_{4\frac{1}{2}} - 92647^{\circ}_{5\frac{1}{2}}$					
3744.166		4	26700.63	−0.01	$48272^{\circ}_{2\frac{1}{2}} - 74973_{3\frac{1}{2}}$					
3743.97		1	26702.02							
3743.390		3	26706.16							
3743.26		6	26707.09	0.00	$52921^{\circ}_{3\frac{1}{2}} - 79628_{3\frac{1}{2}}$					
3743.138		15*h*	26707.96							
3742.627		1	26711.61	+0.06	$65566_{0\frac{1}{2}} - 92278^{\circ}_{1\frac{1}{2}}$					
3742.358		1	26713.53							
3742.036	4	20	26715.82	−0.01	$31568^{\circ}_{2\frac{1}{2}} - 58283_{2\frac{1}{2}}$					
3741.642	3	15	26718.64	+0.05	$48272^{\circ}_{2\frac{1}{2}} - 74991_{1\frac{1}{2}}$					
3741.59	8	80	26719.01	−0.02	$32371^{\circ}_{2\frac{1}{2}} - 59090_{3\frac{1}{2}}$	4	1.18	1.13	(0.024)	1.01
3740.772		10	26724.85	0.00	$44497^{\circ}_{2\frac{1}{2}} - 71222_{3\frac{1}{2}}$					
3740.59		2	26726.15	+0.02	$65577_{3\frac{1}{2}} - 92303^{\circ}_{3\frac{1}{2}}$					
3739.59		1	26733.30	0.00	$49916^{\circ}_{4\frac{1}{2}} - 76649_{5\frac{1}{2}}$					
3739.56		1	26733.51	−0.11	$73291_{5\frac{1}{2}} - 100025^{\circ}_{5\frac{1}{2}}$					
3738.009		10	26744.61	+0.08	$62861_{5\frac{1}{2}} - 89605^{\circ}_{4\frac{1}{2}}$					
3737.537	1	40	26747.98	+0.02	$52880^{\circ}_{4\frac{1}{2}} - 79628_{3\frac{1}{2}}$					
3737.123		6	26750.95	+0.07	$45012^{\circ}_{2\frac{1}{2}} - 71763_{1\frac{1}{2}}$					
3736.901	7	10	26752.54			4	2.00[e]	1.34[e]	0.33	1.01
3735.606		9	26761.81	+0.02	$70136_{6\frac{1}{2}} - 96898^{\circ}_{5\frac{1}{2}}$					
3735.352		10	26763.63	+0.05	$35059^{\circ}_{3\frac{1}{2}} - 61822_{3\frac{1}{2}}$					
3734.96		1	26766.44							
3734.150		8	26772.24	+0.03	$45429^{\circ}_{3\frac{1}{2}} - 72202_{3\frac{1}{2}}$					
3734.12		2	26772.46	−0.04	$44497^{\circ}_{2\frac{1}{2}} - 71270_{2\frac{1}{2}}$					
3733.989		10	26773.40	+0.04	$63944_{5\frac{1}{2}} - 90717^{\circ}_{4\frac{1}{2}}$					
3733.762		5	26775.03							
3733.19		1	26779.13							
3732.458		5	26784.38	+0.05	$44438^{\circ}_{3\frac{1}{2}} - 71222_{3\frac{1}{2}}$					
3732.33	1	10	26785.30	−0.04	$48272^{\circ}_{2\frac{1}{2}} - 75058_{2\frac{1}{2}}$					
3731.166		7	26793.65	+0.10	$67204_{1\frac{1}{2}} - 93998^{\circ}_{1\frac{1}{2}}$					
3731.044		8	26794.53	+0.02	$68756_{3\frac{1}{2}} - 95550^{\circ}_{4\frac{1}{2}}$					
3730.409	20	200	26799.09	−0.03	$34575^{\circ}_{1\frac{1}{2}} - 61374_{2\frac{1}{2}}$	4	1.44	1.30	0.70	1.10
3729.81	10	100	26803.39	−0.06	$35019^{\circ}_{4\frac{1}{2}} - 61822_{3\frac{1}{2}}$	4	(1.16)	1.32	0.08	
3728.24		2	26814.68							
3727.073		1	26823.08	+0.02	$44940^{\circ}_{1\frac{1}{2}} - 71763_{1\frac{1}{2}}$					
3726.169	1	5	26829.59	+0.02	$61873_{6\frac{1}{2}} - 88702^{\circ}_{5\frac{1}{2}}$					

TABLE 6. Yb II—*Observed and classified lines*—Continued

1	2	3	4	5	6	7	8	9	10	11
Wave-length air	Intensity		Wave number	o–c	Classification	Zeeman type	1st g	2nd g	Zeeman components	
	Meggers lamp	Thomson lamp							Strong p	Strong n
Å			K	K						
3725.84	5	70	26831.95	$\begin{cases}-0.03\\+0.05\end{cases}$	$44438^{\circ}_{3\frac{1}{2}} - 71270_{2\frac{1}{2}}$ $66082_{5\frac{1}{2}} - 92914^{\circ}_{4\frac{1}{2}}$					
3724.91		3	26838.65							
3724.213	150	800	26843.68	0.00	$31979^{\circ}_{3\frac{1}{2}} - 58823_{2\frac{1}{2}}$	5	1.32	1.25	(0.034)	1.49
3723.06		2	26851.99							
3722.626		7	26855.12							
3722.296	40	600	26857.50	−0.02	$38342^{\circ}_{4\frac{1}{2}} - 65199_{4\frac{1}{2}}$	7	1.09	1.09	0	1.09
3720.98	6	100	26867.00	0.00	$45335^{\circ}_{4\frac{1}{2}} - 72202_{3\frac{1}{2}}$	5	1.03	0.88	0.075	1.555
3720.846		3	26867.97	+0.02	$67955_{0\frac{1}{2}} - 94823^{\circ}_{1\frac{1}{2}}$					
3720.584		2	26869.86	0.00	$55221^{\circ}_{1\frac{1}{2}} - 82091_{0\frac{1}{2}}$					
3720.192		3	26872.69							
3719.924		3	26874.63							
3719.148		2	26880.23	+0.02	$37077^{\circ}_{2\frac{1}{2}} - 63957_{3\frac{1}{2}}$					
3718.887		1	26882.12							
3718.749		2	26883.12	+0.01	$56480^{\circ}_{4\frac{1}{2}} - 83363_{3\frac{1}{2}}$					
3718.482	1	10	26885.05							
3718.139		4	26887.53	−0.02	$67416_{4\frac{1}{2}} - 94303^{\circ}_{3\frac{1}{2}}$					
3718.052	3	15	26888.16	+0.02	$32371^{\circ}_{2\frac{1}{2}} - 59259_{2\frac{1}{2}}$					
3717.885		2	26889.36	−0.07	$59259_{2\frac{1}{2}} - 86148^{\circ}_{2\frac{1}{2}}$					
3717.412		3	26892.78							
3717.15		1	26894.68							
3716.596		2	26898.69							
3716.139	10	40	26902.00							
3715.725		4	26904.99	$\begin{cases}-0.07\\-0.02\end{cases}$	$47663^{\circ}_{4\frac{1}{2}} - 74568_{4\frac{1}{2}}$ $66558_{3\frac{1}{2}} - 93463^{\circ}_{3\frac{1}{2}}$					
3715.440		10	26907.06	+0.02	$70136_{6\frac{1}{2}} - 97043^{\circ}_{6\frac{1}{2}}$					
3714.186	50	150	26916.14	−0.03	$24332_{2\frac{1}{2}} - 51248^{\circ}_{2\frac{1}{2}}$	6	1.207	1.037	0.440	1.122
3713.93		1	26918.00							
3713.70		2	26919.67	0.00	$67416_{4\frac{1}{2}} - 94335^{\circ}_{5\frac{1}{2}}$					
3713.298		2	26922.58	$\begin{cases}-0.03\\-0.04\end{cases}$	$49727^{\circ}_{6\frac{1}{2}} - 76649_{5\frac{1}{2}}$ $65093_{3\frac{1}{2}} - 92015^{\circ}_{4\frac{1}{2}}$					
3712.438	1	10	26928.82	+0.02	$46354^{\circ}_{4\frac{1}{2}} - 73283_{4\frac{1}{2}}$					
3712.416		4	26928.98	−0.03	$45273^{\circ}_{3\frac{1}{2}} - 72202_{3\frac{1}{2}}$					
3712.06		1	26931.56							
3711.245		6	26937.47	+0.07	$46354^{\circ}_{4\frac{1}{2}} - 73291_{5\frac{1}{2}}$					
3710.825		3	26940.52	−0.02	$69957_{4\frac{1}{2}} - 96898^{\circ}_{5\frac{1}{2}}$					
3710.340	100	1000	26944.04	$\begin{cases}-0.05\\+0.07\end{cases}$	$28757^{\circ}_{1\frac{1}{2}} - 55702_{1\frac{1}{2}}$ $(67416_{4\frac{1}{2}} - 94360^{\circ}_{4\frac{1}{2}})$	6	1.443	1.692	0.37	1.57
3710.090		2	26945.86	−0.03	$66558_{3\frac{1}{2}} - 93503^{\circ}_{4\frac{1}{2}}$					
3708.97		10	26953.99	$\begin{cases}+0.04\\-0.06\end{cases}$	$43075^{\circ}_{1\frac{1}{2}} - 70029_{0\frac{1}{2}}$ $66082_{5\frac{1}{2}} - 93036^{\circ}_{5\frac{1}{2}}$					

TABLE 6. Yb II—*Observed and classified lines*—Continued

1	2	3	4	5	6	7	8	9	10	11
Wavelength air	Intensity		Wave number	o–c	Classification	Zeeman type	1st g	2nd g	Zeeman components	
	Meggers lamp	Thomson lamp							Strong p	Strong n
Å			K	K						
3708.663	150	600	26956.23	−0.01	$26759^{\circ}_{2\frac{1}{2}} - 53715_{3\frac{1}{2}}$	4	1.57	1.18	0.195	0.221
3708.218		3	26959.46							
3707.707		2	26963.18	−0.02	$65950_{4\frac{1}{2}} - 92914^{\circ}_{4\frac{1}{2}}$					
3707.486	1	7	26964.78	−0.01	$48024^{\circ}_{1\frac{1}{2}} - 74989_{0\frac{1}{2}}$	5	1.374	0.510	0.434	1.806
3707.234		1	26966.62	−0.04	$48024^{\circ}_{1\frac{1}{2}} - 74991_{1\frac{1}{2}}$					
3707.020		4	26968.17	+0.02	$65950_{4\frac{1}{2}} - 92919^{\circ}_{3\frac{1}{2}}$					
3706.833		4	26969.53							
3706.32		1	26973.27							
3705.64	2	30	26978.22	−0.01	$37077^{\circ}_{2\frac{1}{2}} - 64055_{2\frac{1}{2}}$	7	1.12	1.12	0	1.12
3704.750		20	26984.70	−0.03	$34389^{\circ}_{2\frac{1}{2}} - 61374_{2\frac{1}{2}}$					
3704.300		1	26987.97	−0.03	$66558_{3\frac{1}{2}} - 93546^{\circ}_{2\frac{1}{2}}$					
3703.92		7	26990.74	+0.03	$63726_{4\frac{1}{2}} - 90717^{\circ}_{4\frac{1}{2}}$					
3703.423	10	200	26994.37	0.00	$48556^{\circ}_{3\frac{1}{2}} - 75550_{2\frac{1}{2}}$	7	0.94	0.94	0	0.94
3702.94		6	26997.89	+0.03	$43956^{\circ}_{2\frac{1}{2}} - 70954_{2\frac{1}{2}}$					
3702.42	1	5	27001.68							
3702.07		8	27004.23	−0.03	$64598_{3\frac{1}{2}} - 91602^{\circ}_{2\frac{1}{2}}$					
3699.800	5	100	27020.80	+0.03	$40917^{\circ}_{4\frac{1}{2}} - 67938_{3\frac{1}{2}}$	7	(0.967)	0.958	0	0.997
3698.596	40	400	27029.59	0.00	$35831^{\circ}_{5\frac{1}{2}} - 62861_{5\frac{1}{2}}$	6	1.21	1.13	0.42	1.117
3698.446	2	40	27030.69	+0.02	$44438^{\circ}_{3\frac{1}{2}} - 71468_{2\frac{1}{2}}$					
3698.070		2	27033.44	+0.03	$48024^{\circ}_{1\frac{1}{2}} - 75058_{2\frac{1}{2}}$					
3698.012		6	27033.86	0.00	$68720_{6\frac{1}{2}} - 95754^{\circ}_{5\frac{1}{2}}$					
3697.688		2	27036.23							
3694.190	1000000.4	80000	27061.83	+0.01	$0_{0\frac{1}{2}} - 27061^{\circ}_{0\frac{1}{2}}$	6	1.996	0.666	0.666	1.330
3692.072		4	27077.35	+0.04	$41678^{\circ}_{2\frac{1}{2}} - 68756_{3\frac{1}{2}}$					
3691.67	2	6	27080.30							
3691.472	10	200	27081.76	+0.07	$37516^{\circ}_{3\frac{1}{2}} - 64598_{3\frac{1}{2}}$	6	1.113	1.221	0.364	1.167
3691.34		1	27082.72							
3691.230	1	10	27083.53	+0.04	$48556^{\circ}_{3\frac{1}{2}} - 75640_{3\frac{1}{2}}$					
3690.560	30	300	27088.45	0.00	$34784^{\circ}_{5\frac{1}{2}} - 61873_{6\frac{1}{2}}$	7	(1.119)	1.114	0	1.086
3689.99		8	27092.63	−0.02	$64923_{4\frac{1}{2}} - 92015^{\circ}_{4\frac{1}{2}}$					
3688.937		4	27100.37	−0.07	$68450_{3\frac{1}{2}} - 95550^{\circ}_{4\frac{1}{2}}$					
3688.490		1	27103.65	−0.05	$65199_{4\frac{1}{2}} - 92303^{\circ}_{3\frac{1}{2}}$					
3687.598	20	150	27110.21	−0.02	$31979^{\circ}_{3\frac{1}{2}} - 59090_{3\frac{1}{2}}$	6	1.337	1.131	0.735	1.234
3687.142	7	80	27113.56	−0.01	$46169^{\circ}_{4\frac{1}{2}} - 73283_{4\frac{1}{2}}$	6	1.10	1.04	0.29	1.07
3685.973		15	27122.16	−0.01	$46169^{\circ}_{4\frac{1}{2}} - 73291_{5\frac{1}{2}}$					
3684.068		1	27136.18							
3683.352	2	30	27141.46	0.00	$64461_{1\frac{1}{2}} - 91602^{\circ}_{2\frac{1}{2}}$	7	(1.176)	1.172	0	1.166
3683.277	1	15	27142.01	−0.08	$68549_{4\frac{1}{2}} - 95691^{\circ}_{3\frac{1}{2}}$					
3682.777		2	27145.69							
3682.20		1	27149.95							

TABLE 6. Yb II—*Observed and classified lines*—Continued

1	2	3	4	5	6	7	8	9	10	11
Wavelength air	Intensity		Wave number	o–c	Classification	Zeeman type	1st g	2nd g	Zeeman components	
	Meggers lamp	Thomson lamp							Strong p	Strong n
Å			K	K						
3681.29		1	27156.66	−0.09	$63702_{2\frac{1}{2}} - 90859^{\circ}_{2\frac{1}{2}}$					
3681.195		15	27157.36	−0.07	$43956^{\circ}_{2\frac{1}{2}} - 71113_{1\frac{1}{2}}$					
3680.770		7	27160.50	−0.03	$65875_{6\frac{1}{2}} - 93036^{\circ}_{5\frac{1}{2}}$					
3680.667		4	27161.26	−0.06	$49008^{\circ}_{3\frac{1}{2}} - 76170_{2\frac{1}{2}}$					
3679.521		2	27169.71							
3678.26		1	27179.03							
3678.15		1	27179.84							
3677.906		6	27181.65							
3677.853	1	15	27182.04	−0.08	$64055_{2\frac{1}{2}} - 91237^{\circ}_{3\frac{1}{2}}$					
3676.89		1	27189.16	−0.08	$45012^{\circ}_{2\frac{1}{2}} - 72202_{3\frac{1}{2}}$					
3676.14		2	27194.70	−0.09	$66351_{2\frac{1}{2}} - 93546^{\circ}_{2\frac{1}{2}}$					
3675.085	300	2000	27202.51	−0.02	$30562^{\circ}_{5\frac{1}{2}} - 57765_{4\frac{1}{2}}$	7	(1.112)	1.105	0	1.144
3674.065	2	20	27210.06	−0.04	$65093_{3\frac{1}{2}} - 92303^{\circ}_{3\frac{1}{2}}$					
3673.900		8	27211.28	−0.06	$63647_{1\frac{1}{2}} - 90859^{\circ}_{2\frac{1}{2}}$					
3673.423		8	27214.82	−0.05	$47758^{\circ}_{3\frac{1}{2}} - 74973_{3\frac{1}{2}}$					
3673.286		1	27215.83	−0.07	$51248^{\circ}_{2\frac{1}{2}} - 78464_{1\frac{1}{2}}$					
3670.69	50	600	27235.08	−0.01	$38342^{\circ}_{4\frac{1}{2}} - 65577_{3\frac{1}{2}}$	5	1.09	1.04	(0.024)	1.26
3669.69	2000*r*	6000	27242.50	+0.02	$27061^{\circ}_{0\frac{1}{2}} - 54304_{0\frac{1}{2}}$	6	0.668	2.007	0.667	1.340
3668.992	3	50	27247.68	−0.12	$32371^{\circ}_{2\frac{1}{2}} - 59618_{3\frac{1}{2}}$?					
3668.16		1	27253.86							
3667.951		8	27255.42	−0.08	$31568^{\circ}_{2\frac{1}{2}} - 58823_{2\frac{1}{2}}$					
3666.67	1	30	27264.94	−0.08	$47005^{\circ}_{1\frac{1}{2}} - 74270_{2\frac{1}{2}}$					
3666.522		5	27266.04	+0.09	$43956^{\circ}_{2\frac{1}{2}} - 71222_{3\frac{1}{2}}$					
3666.09		10	27269.25							
3664.895	3	40	27278.14	−0.03	$48272^{\circ}_{2\frac{1}{2}} - 75550_{2\frac{1}{2}}$					
3664.744	40	200	27279.27	−0.07 −0.08	$31979^{\circ}_{3\frac{1}{2}} - 59259_{2\frac{1}{2}}$ $(50468^{\circ}_{5\frac{1}{2}} - 77747_{4\frac{1}{2}})$	5	1.34	1.12	0.11	1.91
3664.560	8	90	27280.64	−0.07	$45335^{\circ}_{4\frac{1}{2}} - 72615_{5\frac{1}{2}}$	7	0.99	(0.99)	0	0.94
3663.11		6	27291.43	−0.01	$65950_{4\frac{1}{2}} - 93242^{\circ}_{5\frac{1}{2}}$					
3662.545	1	20	27295.64	0.00	$66571_{5\frac{1}{2}} - 93867^{\circ}_{4\frac{1}{2}}$					
3662.297		2	27297.49							
3662.061		7	27299.25	−0.12	$71222_{3\frac{1}{2}} - 98521^{\circ}_{4\frac{1}{2}}$?					
3662.033		5	27299.46	−0.11	$47758^{\circ}_{3\frac{1}{2}} - 75058_{2\frac{1}{2}}$?					
3661.656		2	27302.27	−0.05	$45737^{\circ}_{1\frac{1}{2}} - 73039_{0\frac{1}{2}}$					
3661.135		2	27306.16							
3661.08		6	27306.57	0.00	$66558_{3\frac{1}{2}} - 93864^{\circ}_{2\frac{1}{2}}$					
3660.99		1	27307.24							
3660.73	1	8	27309.18	−0.04	$66558_{3\frac{1}{2}} - 93867^{\circ}_{4\frac{1}{2}}$					
3660.64		1	27309.85	−0.04	$47663^{\circ}_{4\frac{1}{2}} - 74973_{3\frac{1}{2}}$					
3660.58	1	15	27310.30	0.00	$48923^{\circ}_{7\frac{1}{2}} - 76233_{6\frac{1}{2}}$					

277-259 O - 68 - 7

TABLE 6. Yb II—*Observed and classified lines*—Continued

1	2	3	4	5	6	7	8	9	10	11
Wavelength air	Intensity		Wave number	o–c	Classification	Zeeman type	1st g	2nd g	Zeeman components	
	Meggers lamp	Thomson lamp							Strong p	Strong n
Å			K	K						
3660.42		1	27311.49							
3660.137	1	10	27313.60	0.00	$43956^{\circ}_{2\frac{1}{2}} - 71270_{2\frac{1}{2}}$					
3658.605	5	70	27325.04	−0.05	$58823_{2\frac{1}{2}} - 86148^{\circ}_{2\frac{1}{2}}$					
3657.665		3	27332.06	−0.05	$35831^{\circ}_{5\frac{1}{2}} - 63163_{4\frac{1}{2}}$					
3657.131		1	27336.05							
3657.007		2	27336.98	−0.06	$65577_{3\frac{1}{2}} - 92914^{\circ}_{4\frac{1}{2}}$					
3656.81		1	27338.45	−0.08	$62559_{2\frac{1}{2}} - 89897^{\circ}_{1\frac{1}{2}}$					
3656.672		2	27339.48	−0.07	$32371^{\circ}_{2\frac{1}{2}} - 59710_{1\frac{1}{2}}$					
3655.48	1	20	27348.40	0.00	$62861_{5\frac{1}{2}} - 90209^{\circ}_{4\frac{1}{2}}$					
3654.417	1	5	27356.35							
3654.28	1	20	27357.38	−0.01	$63944_{5\frac{1}{2}} - 91301^{\circ}_{6\frac{1}{2}}$					
3653.041	2	20	27366.66	+0.04	$65875_{6\frac{1}{2}} - 93242^{\circ}_{5\frac{1}{2}}$					
3652.953	3	40	27367.32	+0.03	$48272^{\circ}_{2\frac{1}{2}} - 75640_{3\frac{1}{2}}$					
3652.538	1	15	27370.42	0.00	$65875_{6\frac{1}{2}} - 93246^{\circ}_{6\frac{1}{2}}$					
3651.24	1	10	27380.15	−0.06 +0.02	$40035^{\circ}_{3\frac{1}{2}} - 67416_{4\frac{1}{2}}$ $64923_{4\frac{1}{2}} - 92303^{\circ}_{3\frac{1}{2}}$					
3651.15		1	27380.83							
3650.80	4	50	27383.45	−0.04	$37077^{\circ}_{2\frac{1}{2}} - 64461_{1\frac{1}{2}}$	4	(1.113)	1.174	w	1.02
3649.739	10	150	27391.41	−0.02	$41688^{\circ}_{1\frac{1}{2}} - 69079_{2\frac{1}{2}}$	5	0.784	0.911	0.065	1.101
3649.084		6	27396.33	−0.02	$46354^{\circ}_{4\frac{1}{2}} - 73750_{4\frac{1}{2}}$					
3648.827		2	27398.26							
3648.676		1	27399.39	0.00	$65577_{3\frac{1}{2}} - 92976^{\circ}_{3\frac{1}{2}}$					
3648.440	10	100	27401.17	+0.02	$41678^{\circ}_{2\frac{1}{2}} - 69079_{2\frac{1}{2}}$	6	(1.193)	0.90	0.72	?
3648.38	4	50	27401.62	−0.05	$68148_{5\frac{1}{2}} - 95550^{\circ}_{4\frac{1}{2}}$					
3648.29		1	27402.29							
3648.242		2	27402.65	−0.08	$58823_{2\frac{1}{2}} - 86226^{\circ}_{1\frac{1}{2}}$					
3647.730	2	40	27406.50	−0.02	$37516^{\circ}_{3\frac{1}{2}} - 64923_{4\frac{1}{2}}$	7	(1.119)	1.11	0	1.076
3646.277	1	10	27417.42	−0.06	$64598_{3\frac{1}{2}} - 92015^{\circ}_{4\frac{1}{2}}$					
3646.24		7	27417.70	−0.11	$62861_{5\frac{1}{2}} - 90279^{\circ}_{5\frac{1}{2}}$?					
3645.72		7	27421.61	−0.03	$66082_{5\frac{1}{2}} - 93503^{\circ}_{4\frac{1}{2}}$					
3644.236	40	400	27432.78	−0.04	$34389^{\circ}_{2\frac{1}{2}} - 61822_{3\frac{1}{2}}$	5	1.013	1.329	0.160	2.13
3643.28	1	10	27439.97							
3642.63		3	27444.87	−0.09	$45335^{\circ}_{4\frac{1}{2}} - 72779_{3\frac{1}{2}}$					
3642.37		7*h*	27446.83							
3642.24		4	27447.81	+0.01	$65199_{4\frac{1}{2}} - 92647^{\circ}_{5\frac{1}{2}}$					
3640.79		1	27458.74							
3639.97		1	27464.93							
3639.746	1	15	27466.62	−0.01	$33653^{\circ}_{0\frac{1}{2}} - 61120_{0\frac{1}{2}}$					
3639.030		2	27472.02							
3637.757	2000*R*	3000	27481.63	−0.03	$21418^{\circ}_{3\frac{1}{2}} - 48900_{3\frac{1}{2}}$	6	1.156	1.064	0.33	1.11

TABLE 6. Yb II—*Observed and classified lines*—Continued

1	2	3	4	5	6	7	8	9	10	11
Wave-length air	Intensity		Wave number	o–c	Classification	Zeeman type	1st g	2nd g	Zeeman components	
	Meggers lamp	Thomson lamp							Strong p	Strong n
Å			K	K						
3636.899		2	27488.12							
3636.23		2	27493.17							
3635.330		1	27499.98	−0.04	$35059^{\circ}_{3\frac{1}{2}} - 62559_{2\frac{1}{2}}$					
3634.86		2	27503.54							
3634.74		1	27504.44							
3634.525 [a]	30	20	27506.07							
3634.40		10	27507.02	+0.05	$45273^{\circ}_{3\frac{1}{2}} - 72779_{3\frac{1}{2}}$					
3634.27		2	27508.00							
3633.858		10	27511.12	+0.01	$63726_{4\frac{1}{2}} - 91237^{\circ}_{3\frac{1}{2}}$					
3633.70	1	20	27512.32	+0.03	$43956^{\circ}_{2\frac{1}{2}} - 71468_{2\frac{1}{2}}$	7	1.01	1.01	0	1.01
3632.595	20	150	27520.68	−0.01	$37077^{\circ}_{2\frac{1}{2}} - 64598_{3\frac{1}{2}}$	5	1.091	1.234	0.070	1.591
3632.415	20	100	27522.05	0.00	$31568^{\circ}_{2\frac{1}{2}} - 59090_{3\frac{1}{2}}$	5	0.875	1.145	0.129	1.820
3631.86		8	27526.25	+0.01	$48024^{\circ}_{1\frac{1}{2}} - 75550_{2\frac{1}{2}}$					
3631.073	7	80	27532.22	+0.02	$40917^{\circ}_{4\frac{1}{2}} - 68450_{3\frac{1}{2}}$	4	0.96	1.04	(0.04)	0.68
3630.621		4	27535.65	+0.03 −0.01	$63702_{2\frac{1}{2}} - 91237^{\circ}_{3\frac{1}{2}}$ $66462_{0\frac{1}{2}} - 93998^{\circ}_{1\frac{1}{2}}$					
3630.337		2	27537.80							
3630.301		4	27538.07	−0.01	$52067^{\circ}_{0\frac{1}{2}} - 79605_{1\frac{1}{2}}$					
3629.919	30	300	27540.97	−0.02	$30224^{\circ}_{4\frac{1}{2}} - 57765_{4\frac{1}{2}}$	6	0.933	1.112	0.803	1.022
3628.340		6	27552.96	+0.02	$65950_{4\frac{1}{2}} - 93503^{\circ}_{4\frac{1}{2}}$					
3627.89	2	30	27556.38	0.00 +0.06	$33494^{\circ}_{3\frac{1}{2}} - 61051_{3\frac{1}{2}}$ $68135_{2\frac{1}{2}} - 95691^{\circ}_{3\frac{1}{2}}$					
3627.205	2	30	27561.58	+0.01	$34575^{\circ}_{1\frac{1}{2}} - 62136_{0\frac{1}{2}}$	5	1.45	0.07	0.69	2.14
3627.078		1	27562.54							
3626.80	1	6	27564.66							
3625.230	2	60	27576.59	+0.04	$37516^{\circ}_{3\frac{1}{2}} - 65093_{3\frac{1}{2}}$					
3624.634	15	200	27581.13	+0.01	$46169^{\circ}_{4\frac{1}{2}} - 73750_{4\frac{1}{2}}$	6	1.00	1.07	0.33	1.03
3623.627	1	10	27588.79							
3622.320	20	80	27598.75	+0.02	$34575^{\circ}_{1\frac{1}{2}} - 62174_{1\frac{1}{2}}$	6	1.44	0.80	0.96	1.13
3621.873		7	27602.15	+0.01	$50468^{\circ}_{3\frac{1}{2}} - 78070_{4\frac{1}{2}}$					
3621.80		2	27602.71	−0.09	$66395_{2\frac{1}{2}} - 93998^{\circ}_{1\frac{1}{2}}$					
3621.513	1	15	27604.90	+0.03	$32981^{\circ}_{1\frac{1}{2}} - 60586_{1\frac{1}{2}}$					
3621.18		1	27607.44							
3620.988	30	400	27608.90	−0.03	$38342^{\circ}_{4\frac{1}{2}} - 65950_{4\frac{1}{2}}$	7	(1.093)	1.103	0	1.098
3620.362		4	27613.67	−0.01	$48556^{\circ}_{3\frac{1}{2}} - 76170_{2\frac{1}{2}}$					
3619.803	700*r*	3000	27617.94	+0.01 +0.02	$28757^{\circ}_{1\frac{1}{2}} - 56375_{2\frac{1}{2}}$ $(65577_{3\frac{1}{2}} - 93195^{\circ}_{3\frac{1}{2}})$	4	1.433	1.222	0.105	0.91
3618.887		1	27624.93	−0.03	$63234_{2\frac{1}{2}} - 90859^{\circ}_{3\frac{1}{2}}$					
3618.040	50	200	27631.39	+0.07	$40917^{\circ}_{4\frac{1}{2}} - 68549_{4\frac{1}{2}}$	6	0.975	1.151	0.81	1.063
3617.045	1	10	27639.00	0.00	$31979^{\circ}_{3\frac{1}{2}} - 59618_{3\frac{1}{2}}$					
3616.395		10	27643.96	−0.01	$47329^{\circ}_{2\frac{1}{2}} - 74973_{3\frac{1}{2}}$					

TABLE 6. Yb II—*Observed and classified lines*—Continued

1	2	3	4	5	6	7	8	9	10	11
Wave-length air	Intensity		Wave number	o–c	Classification	Zeeman type	1st g	2nd g	Zeeman components	
	Meggers lamp	Thomson lamp							Strong p	Strong n
Å			K	K						
3616.031		3	27646.75							
3615.957		2	27647.31	0.00	$66351_{2\frac{1}{2}} - 93998^{\circ}_{1\frac{1}{2}}$					
3614.63		1	27657.46	−0.08	$65888_{1\frac{1}{2}} - 93546^{\circ}_{2\frac{1}{2}}$					
3614.593		6	27657.74	−0.01	$66351_{2\frac{1}{2}} - 94008^{\circ}_{3\frac{1}{2}}$					
3614.048	5	100	27661.92	0.00	$47329^{\circ}_{2\frac{1}{2}} - 74991_{1\frac{1}{2}}$	4	(0.990)	1.04	w	0.91
3613.38		3	27667.03	−0.07	$62046^{\circ}_{3\frac{1}{2}} - 89713_{2\frac{1}{2}}$					
3613.340		3	27667.33	−0.05	$49008^{\circ}_{3\frac{1}{2}} - 76676_{2\frac{1}{2}}$					
3613.295		2	27667.68	−0.08	$53644^{\circ}_{3\frac{1}{2}} - 81312_{2\frac{1}{2}}$					
3612.950		4	27670.32	−0.02	$55221^{\circ}_{1\frac{1}{2}} - 82891_{2\frac{1}{2}}$					
3611.300	60	800	27682.96	+0.01	$37516^{\circ}_{3\frac{1}{2}} - 65199_{4\frac{1}{2}}$	4	1.14	1.10	(0.02)	0.96
3610.233	100	700	27691.15	−0.01	$31568^{\circ}_{2\frac{1}{2}} - 59259_{2\frac{1}{2}}$	6	0.862	1.105	0.613	0.99
3609.24		l	27698.76							
3608.936		3	27701.10							
3608.488	10	150	27704.54	+0.02	$44497^{\circ}_{2\frac{1}{2}} - 72202_{3\frac{1}{2}}$	5	0.711	0.835	0.06	1.145
3607.186		2	27714.54	−0.07	$65199_{4\frac{1}{2}} - 92914^{\circ}_{4\frac{1}{2}}$					
3606.478	300	2000	27719.98	0.00	$33494^{\circ}_{3\frac{1}{2}} - 61214_{4\frac{1}{2}}$	5	0.98	1.04	(0.03)	1.24
3605.347	2	20	27728.67	0.00	$47329^{\circ}_{2\frac{1}{2}} - 75058_{2\frac{1}{2}}$	6	1.00	0.78	0.60	0.88
3605.208		1	27729.74	−0.04	$48503^{\circ}_{5\frac{1}{2}} - 76233_{6\frac{1}{2}}$					
3603.848	20	300	27740.20	−0.03	$38342^{\circ}_{4\frac{1}{2}} - 66082_{5\frac{1}{2}}$	5	1.10	1.14	(0.019)	1.31
3602.237		1	27752.61	−0.03	$67938_{3\frac{1}{2}} - 95691^{\circ}_{3\frac{1}{2}}$					
3601.917	2	20	27755.08	+0.01	$41688^{\circ}_{1\frac{1}{2}} - 69443_{1\frac{1}{2}}$	6	0.77	1.15	0.58	0.96
3601.209	2	15	27760.53	0.00 −0.08	$47228^{\circ}_{0\frac{1}{2}} - 74989_{0\frac{1}{2}}$ $62136_{0\frac{1}{2}} - 89897^{\circ}_{1\frac{1}{2}}$					
3600.966	10	100	27762.41	+0.01	$47228^{\circ}_{0\frac{1}{2}} - 74991_{1\frac{1}{2}}$					
3600.763	20	300	27763.97	−0.03	$44438^{\circ}_{3\frac{1}{2}} - 72202_{3\frac{1}{2}}$					
3600.663	2	30	27764.74	−0.05	$41678^{\circ}_{2\frac{1}{2}} - 69443_{1\frac{1}{2}}$					
3600.383	10	150	27766.90	−0.02 +0.06	$48556^{\circ}_{3\frac{1}{2}} - 76323_{3\frac{1}{2}}$ $(59618_{3\frac{1}{2}} - 87385^{\circ}_{3\frac{1}{2}})$	6	0.957	1.003	0.16	0.98
3598.87		2h	27778.57							
3598.043	2	20	27784.96	−0.01	$66082_{5\frac{1}{2}} - 93867^{\circ}_{4\frac{1}{2}}$					
3597.60		1	27788.38	−0.04	$66571_{5\frac{1}{2}} - 94360^{\circ}_{4\frac{1}{2}}$					
3597.078		10	27792.41	+0.01	$47758^{\circ}_{3\frac{1}{2}} - 75550_{2\frac{1}{2}}$					
3596.488	1	30	27796.97	−0.06	$46169^{\circ}_{4\frac{1}{2}} - 73966_{3\frac{1}{2}}$					
3596.300		4	27798.42	−0.01	$52880^{\circ}_{4\frac{1}{2}} - 80679_{5\frac{1}{2}}$					
3595.844		5	27801.95	−0.05	$66558_{3\frac{1}{2}} - 94360^{\circ}_{4\frac{1}{2}}$					
3595.649		2	27803.46							
3595.162		9	27807.22	−0.04	$43956^{\circ}_{2\frac{1}{2}} - 71763_{1\frac{1}{2}}$					
3594.864	1	10	27809.53	−0.04	$63726_{4\frac{1}{2}} - 91536^{\circ}_{3\frac{1}{2}}$					
3593.882		1	27817.13	−0.06	$64461_{1\frac{1}{2}} - 92278^{\circ}_{1\frac{1}{2}}$					
3593.728		2	27818.32							

TABLE 6. Yb II—*Observed and classified lines*—Continued

1	2	3	4	5	6	7	8	9	10	11
Wave-length air	Intensity		Wave number	o–c	Classification	Zeeman type	1st g	2nd g	Zeeman components	
	Meggers lamp	Thomson lamp							Strong p	Strong n
Å			K	K						
3593.060		1	27823.49							
3592.734	1	20	27826.02	−0.06 +0.06 −0.04	$39378^{\circ}_{0\frac{1}{2}} - 67204_{1\frac{1}{2}}$ $65093_{3\frac{1}{2}} - 92919^{\circ}_{3\frac{1}{2}}$ $70793_{5\frac{1}{2}} - 98620^{\circ}_{6\frac{1}{2}}$					
3592.217	1	10	27830.02	−0.05	$49008^{\circ}_{3\frac{1}{2}} - 76839_{2\frac{1}{2}}$					
3591.24		1	27837.59							
3591.18		2	27838.06	−0.07	$40917^{\circ}_{4\frac{1}{2}} - 68756_{3\frac{1}{2}}$					
3591.141		4	27838.36							
3590.657	5	50	27842.11	−0.03	$35019^{\circ}_{4\frac{1}{2}} - 62861_{5\frac{1}{2}}$	7	(1.158)	1.144	0	1.079
3589.997		1	27847.23	+0.01	$63011_{1\frac{1}{2}} - 90859^{\circ}_{2\frac{1}{2}}$					
3589.186		7	27853.52	−0.01	$45429^{\circ}_{3\frac{1}{2}} - 73283_{4\frac{1}{2}}$					
3588.832	1	20	27856.27	0.00	$62861_{5\frac{1}{2}} - 90717^{\circ}_{4\frac{1}{2}}$					
3588.456		2	27859.19							
3587.736		7	27864.78	+0.02	$58283_{2\frac{1}{2}} - 86148^{\circ}_{2\frac{1}{2}}$					
3587.569		1	27866.08							
3586.824	30	90	27871.86	+0.01	$22960_{1\frac{1}{2}} - 50832^{\circ}_{1\frac{1}{2}}$	6	0.795	0.948	0.224	0.876
3586.536		6	27874.10							
3585.878		8	27879.22	+0.04	$43075^{\circ}_{1\frac{1}{2}} - 70954_{2\frac{1}{2}}$					
3585.794	1	20	27879.87	+0.06	$33494^{\circ}_{3\frac{1}{2}} - 61374_{2\frac{1}{2}}$					
3585.466	2000*R*	4000	27882.42	+0.01	$21418^{\circ}_{3\frac{1}{2}} - 49301_{4\frac{1}{2}}$	5	1.14	1.19	(0.023)	1.35
3583.96		4*h*	27894.14							
3583.827	7	70	27895.17	+0.02	$35831^{\circ}_{5\frac{1}{2}} - 63726_{4\frac{1}{2}}$					
3583.532		5	27897.47	−0.01	$48272^{\circ}_{2\frac{1}{2}} - 76170_{2\frac{1}{2}}$					
3583.26		7	27899.58	+0.04	$45737^{\circ}_{1\frac{1}{2}} - 73636_{0\frac{1}{2}}$					
3583.180		1	27900.21	−0.01	$63702_{2\frac{1}{2}} - 91602^{\circ}_{2\frac{1}{2}}$					
3582.841	3	40	27902.85	−0.01	$40035^{\circ}_{3\frac{1}{2}} - 67938_{3\frac{1}{2}}$					
3582.20		3	27907.84	−0.02	$66395_{2\frac{1}{2}} - 94303^{\circ}_{3\frac{1}{2}}$					
3580.755		10	27919.10	+0.01	$41688^{\circ}_{1\frac{1}{2}} - 69607_{2\frac{1}{2}}$					
3580.640	1	15	27920.00	0.00	$45737^{\circ}_{1\frac{1}{2}} - 73657_{1\frac{1}{2}}$					
3580.474		1	27921.29							
3579.511	3	40	27928.80	−0.01	$41678^{\circ}_{2\frac{1}{2}} - 69607_{2\frac{1}{2}}$	7	1.23	1.23	0	1.226
3578.95		1	27933.18	−0.03	$68549_{4\frac{1}{2}} - 96482^{\circ}_{4\frac{1}{2}}$					
3577.985		1	27940.72	−0.03	$53716^{\circ}_{2\frac{1}{2}} - 81657_{2\frac{1}{2}}$					
3577.690	1	10	27943.02	−0.03	$42915^{\circ}_{5\frac{1}{2}} - 70858_{4\frac{1}{2}}$					
3577.504		3	27944.47	−0.01	$70858_{4\frac{1}{2}} - 98802^{\circ}_{5\frac{1}{2}}$					
3577.008	30	300	27948.35	+0.03	$45335^{\circ}_{4\frac{1}{2}} - 73283_{4\frac{1}{2}}$	7	0.98	1.04	0	1.009
3576.288		8	27953.97							
3576.188		1	27954.75	−0.06	$63647_{1\frac{1}{2}} - 91602^{\circ}_{2\frac{1}{2}}$					
3575.905	1	20	27956.97	+0.05	$45335^{\circ}_{4\frac{1}{2}} - 73291_{5\frac{1}{2}}$					
3575.704		5	27958.54							
3575.573	3	60	27959.56	+0.02	$48556^{\circ}_{3\frac{1}{2}} - 76516_{4\frac{1}{2}}$	5	(0.941)	1.01	*w*	1.23

TABLE 6. Yb II—*Observed and classified lines*—Continued

1	2	3	4	5	6	7	8	9	10	11
Wave-length air	Intensity		Wave number	o–c	Classification	Zeeman type	1st g	2nd g	Zeeman components	
	Meggers lamp	Thomson lamp							Strong p	Strong n
Å			K	K						
3574.58		30h	27967.33							
3573.750	1	10	27973.82			7			0	1.013
3573.67		1	27974.45							
3573.458[a]	3	3	27976.11							
3573.41		4	27976.49	−0.05 −0.05	$47663^{\circ}_{4\frac{1}{2}} - 75640_{3\frac{1}{2}}$ $53716^{\circ}_{2\frac{1}{2}} - 81692_{3\frac{1}{2}}$					
3572.498	200	800	27983.63	−0.02	$34575^{\circ}_{1\frac{1}{2}} - 62559_{2\frac{1}{2}}$	4			0	1.33?
3572.212	2	15	27985.87	−0.03	$47005^{\circ}_{1\frac{1}{2}} - 74991_{1\frac{1}{2}}$					
3570.987	1	8	27995.47	−0.02	$65199_{4\frac{1}{2}} - 93195^{\circ}_{3\frac{1}{2}}$					
3570.566	200	1000	27998.77	0.00	$33052^{\circ}_{4\frac{1}{2}} - 61051_{3\frac{1}{2}}$	5	1.27	1.20	(0.034)	1.51
3569.925	2	20	28003.80	−0.03	$63234_{2\frac{1}{2}} - 91237^{\circ}_{3\frac{1}{2}}$					
3569.308		2	28008.64	−0.06	$70793_{5\frac{1}{2}} - 98802^{\circ}_{5\frac{1}{2}}$					
3569.094	1	10	28010.32	−0.01	$45273^{\circ}_{3\frac{1}{2}} - 73283_{4\frac{1}{2}}$					
3568.430	5	50	28015.53	−0.02	$37077^{\circ}_{2\frac{1}{2}} - 65093_{3\frac{1}{2}}$	4	(1.113)	1.01	w	0.74
3567.130	50	500	28025.74	0.00	$40917^{\circ}_{4\frac{1}{2}} - 68943_{4\frac{1}{2}}$	6	0.97	0.87	0.47	0.92
3566.519		2	28030.54							
3565.891		4	28035.48	−0.05	$70793_{5\frac{1}{2}} - 98829^{\circ}_{6\frac{1}{2}}$					
3565.823		1	28036.01							
3565.477		6	28038.73	−0.02	$43075^{\circ}_{1\frac{1}{2}} - 71113_{1\frac{1}{2}}$					
3565.404		3	28039.31							
3564.955		1	28042.84	−0.01	$65199_{4\frac{1}{2}} - 93242^{\circ}_{5\frac{1}{2}}$					
3563.941	200	800	28050.82	0.00	$31568^{\circ}_{2\frac{1}{2}} - 59618_{3\frac{1}{2}}$	5	0.862	1.010	0.077	1.40
3563.712	2	20	28052.62	−0.03	$47005^{\circ}_{1\frac{1}{2}} - 75058_{2\frac{1}{2}}$					
3562.706	7	80	28060.54	+0.02	$37516^{\circ}_{3\frac{1}{2}} - 65577_{3\frac{1}{2}}$	6	1.132	1.058	0.26	1.095
3561.738	1	10	28068.16	0.00	$56375_{2\frac{1}{2}} - 84444^{\circ}_{3\frac{1}{2}}$					
3561.444	2	6	28070.48							
3561.309		2	28071.55	−0.03	$63944_{5\frac{1}{2}} - 92015^{\circ}_{4\frac{1}{2}}$					
3560.704	500r	2000	28076.32	0.00	$34784^{\circ}_{5\frac{1}{2}} - 62861_{5\frac{1}{2}}$	6	1.112	1.142	(0.165)	1.127
3560.327	2000R	3000	28079.29	0.00	$21418^{\circ}_{3\frac{1}{2}} - 49498_{2\frac{1}{2}}$	7	1.134	1.134	0	1.134
3559.139		4	28088.66	+0.01	$46902^{\circ}_{0\frac{1}{2}} - 74991_{1\frac{1}{2}}$					
3557.825		2	28099.03	+0.03	$44940^{\circ}_{1\frac{1}{2}} - 73039_{0\frac{1}{2}}$					
3557.466		1	28101.87	−0.02	$65093_{3\frac{1}{2}} - 93195^{\circ}_{3\frac{1}{2}}$					
3557.100	2	20	28104.76	−0.03	$35059^{\circ}_{3\frac{1}{2}} - 63163_{4\frac{1}{2}}$	7	(1.124)	1.14	0	1.18
3556.940		4	28106.03	−0.02	$43007^{\circ}_{0\frac{1}{2}} - 71113_{1\frac{1}{2}}$					
3556.435		3	28110.02	−0.04	$65888_{1\frac{1}{2}} - 93998^{\circ}_{1\frac{1}{2}}$					
3556.124		1	28112.47	−0.03	$35831^{\circ}_{5\frac{1}{2}} - 63944_{5\frac{1}{2}}$					
3556.042		1	28113.12	−0.07	$64923_{4\frac{1}{2}} - 93036^{\circ}_{5\frac{1}{2}}$					
3555.204	5	30	28119.75	+0.01	$48556^{\circ}_{3\frac{1}{2}} - 76676_{2\frac{1}{2}}$	4	0.95	1.13	0.091	0.495
3555.055		3	28120.93							
3554.347		5	28126.53	+0.03	$59259_{2\frac{1}{2}} - 87385^{\circ}_{3\frac{1}{2}}$					

TABLE 6. Yb II—*Observed and classified lines*—Continued

1	2	3	4	5	6	7	8	9	10	11
Wave-length air	Intensity		Wave number	o–c	Classification	Zeeman type	1st g	2nd g	Zeeman components	
	Meggers lamp	Thomson lamp							Strong p	Strong n
Å			K	K						
3553.82		1	28130.70							
3553.340		7	28134.50	−0.02	$67416_{4\frac{1}{2}} - 95550^{\circ}_{4\frac{1}{2}}$					
3553.192		3	28135.67							
3553.153		3	28135.98							
3552.324	100	1000	28142.55	−0.02	$31568^{\circ}_{2\frac{1}{2}} - 59710_{1\frac{1}{2}}$	5	0.854	0.810	(0.022)	0.92
3549.822	200	2000	28162.38	+0.01	$33052^{\circ}_{4\frac{1}{2}} - 61214_{4\frac{1}{2}}$	6	1.264	1.050	0.980	1.167
3548.470		2	28173.11							
3548.096		7	28176.08	−0.02	$44940^{\circ}_{1\frac{1}{2}} - 73116_{1\frac{1}{2}}$					
3546.085		1	28192.06	−0.01 0.00	$53120^{\circ}_{2\frac{1}{2}} - 81312_{2\frac{1}{2}}$ $71222_{3\frac{1}{2}} - 99414^{\circ}_{4\frac{1}{2}}$					
3545.725	1	40*h*	28194.92	0.00	$43075^{\circ}_{1\frac{1}{2}} - 71270_{2\frac{1}{2}}$					
3543.890		1	28209.52							
3543.324	1	10	28214.03	0.00	$46354^{\circ}_{4\frac{1}{2}} - 74568_{4\frac{1}{2}}$					
3543.159	30	200	28215.34	−0.02	$32371^{\circ}_{2\frac{1}{2}} - 60586_{1\frac{1}{2}}$	4	1.202	1.370	0.084	0.960
3542.385	7	100	28221.50		$47329^{\circ}_{2\frac{1}{2}} - 75550_{2\frac{1}{2}}$	6	0.990	0.902	0.22	0.946
3542.272	1	6	28222.40	−0.05	$64055_{2\frac{1}{2}} - 92278^{\circ}_{1\frac{1}{2}}$					
3541.375	7	80	28229.55	−0.01	$38342^{\circ}_{4\frac{1}{2}} - 66571_{5\frac{1}{2}}$	5	(1.093)	1.18	*w*	1.58
3540.926		3	28233.13	−0.05	$68148_{5\frac{1}{2}} - 96382^{\circ}_{5\frac{1}{2}}$					
3540.61		1	28235.65							
3540.21		2	28238.84							
3540.09		1	28239.80							
3540.02		1	28240.36							
3539.932		3	28241.06	−0.04	$61374_{2\frac{1}{2}} - 89615^{\circ}_{2\frac{1}{2}}$					
3539.362	20	200	28245.61	−0.01	$43956^{\circ}_{2\frac{1}{2}} - 72202_{3\frac{1}{2}}$	4	0.990	0.865	0.067	0.530
3538.369		2	28253.53	+0.08	$66082_{5\frac{1}{2}} - 94335^{\circ}_{5\frac{1}{2}}$					
3537.964		1	28256.77	−0.03	$56375_{2\frac{1}{2}} - 84632^{\circ}_{2\frac{1}{2}}$					
3537.127		6	28263.45	−0.02	$65199_{4\frac{1}{2}} - 93463^{\circ}_{3\frac{1}{2}}$					
3536.068	1	8	28271.92	0.00	$64923_{4\frac{1}{2}} - 93195^{\circ}_{3\frac{1}{2}}$					
3534.752	4	20	28282.44	−0.04 +0.01	$44497^{\circ}_{2\frac{1}{2}} - 72779_{3\frac{1}{2}}$ $48556^{\circ}_{3\frac{1}{2}} - 76839_{2\frac{1}{2}}$					
3534.13		2	28287.42	−0.04	$65577_{3\frac{1}{2}} - 93864^{\circ}_{2\frac{1}{2}}$					
3534.05	50	100	28288.06	0.00	$22960_{1\frac{1}{2}} - 51248^{\circ}_{2\frac{1}{2}}$	5	0.815	1.041	0.113	1.380
3533.80		3	28290.06	−0.05	$65577_{3\frac{1}{2}} - 93867^{\circ}_{4\frac{1}{2}}$					
3533.107	20	60	28295.61	0.00	$59090_{3\frac{1}{2}} - 87385^{\circ}_{3\frac{1}{2}}$	6	1.12	1.14	*d*	1.13
3531.24	5	100	28310.57	−0.05	$47329^{\circ}_{2\frac{1}{2}} - 75640_{3\frac{1}{2}}$	4	0.995	0.813	0.091	0.358
3530.58		1	28315.86	−0.01	$64598_{3\frac{1}{2}} - 92914^{\circ}_{4\frac{1}{2}}$					
3530.16		3	28319.23	−0.05	$64923_{4\frac{1}{2}} - 93242^{\circ}_{5\frac{1}{2}}$					
3530.05		1	28320.12	−0.04	$61822_{3\frac{1}{2}} - 90142^{\circ}_{3\frac{1}{2}}$					
3529.715	2	20	28322.80	−0.04	$68720_{6\frac{1}{2}} - 97043^{\circ}_{6\frac{1}{2}}$					
3529.458		2	28324.87	−0.02	$52987^{\circ}_{1\frac{1}{2}} - 81312_{2\frac{1}{2}}$					
3529.085	8	100	28327.86	−0.04	$33494^{\circ}_{3\frac{1}{2}} - 61822_{3\frac{1}{2}}$	6	1.001	1.340	1.185	1.171

TABLE 6. Yb II—*Observed and classified lines*—Continued

1	2	3	4	5	6	7	8	9	10	11
Wave-length air	Intensity		Wave number	o–c	Classification	Zeeman type	1st g	2nd g	Zeeman components	
	Meggers lamp	Thomson lamp							Strong p	Strong n
Å			K	K						
3528.771		2	28330.38	−0.09	$68756_{3\frac{1}{2}} - 97086^{\circ}_{4\frac{1}{2}}$					
3527.501	1	15	28340.58	−0.01	$41688^{\circ}_{1\frac{1}{2}} - 70029_{0\frac{1}{2}}$	7	(0.784)	0.736	0	0.808
3527.332	2	20	28341.94	−0.02	$44438^{\circ}_{3\frac{1}{2}} - 72779_{3\frac{1}{2}}$	7	1.10	1.10	0	1.105
3526.477		1	28348.81	+0.01	$68549_{4\frac{1}{2}} - 96898^{\circ}_{5\frac{1}{2}}$					
3525.722	5	50	28354.88	−0.01	$64891_{7\frac{1}{2}} - 93246^{\circ}_{6\frac{1}{2}}$	7?	(1.19)	1.21	w	1.08
3525.456		3	28357.02	−0.07	$51248^{\circ}_{2\frac{1}{2}} - 79605_{1\frac{1}{2}}$					
3525.171		2	28359.31							
3525.05		1	28360.28	−0.04	$66462_{0\frac{1}{2}} - 94823^{\circ}_{1\frac{1}{2}}$					
3524.82		1	28362.13							
3524.044		1	28368.38	−0.05	$63234_{2\frac{1}{2}} - 91602^{\circ}_{2\frac{1}{2}}$					
3523.734		3*h*	28370.88							
3523.148[a]	3	2	28375.59							
3522.826		3	28378.19	−0.03	$64598_{3\frac{1}{2}} - 92976^{\circ}_{3\frac{1}{2}}$					
3522.747	1	10	28378.82	−0.02	$34784^{\circ}_{5\frac{1}{2}} - 63163_{4\frac{1}{2}}$					
3522.021		1	28384.67	−0.08	$65950_{4\frac{1}{2}} - 94335^{\circ}_{5\frac{1}{2}}$					
3521.727		3	28387.04	−0.05	$61822_{3\frac{1}{2}} - 90209^{\circ}_{4\frac{1}{2}}$					
3521.664		2	28387.55							
3521.585	1	7	28388.19	0.00	$70858_{4\frac{1}{2}} - 99246^{\circ}_{5\frac{1}{2}}$					
3521.224		7	29391.10	+0.07	$52921^{\circ}_{3\frac{1}{2}} - 81312_{2\frac{1}{2}}$					
				−0.04	$61214_{4\frac{1}{2}} - 89605^{\circ}_{4\frac{1}{2}}$					
3521.007	5	20	28392.85	−0.05	$32981^{\circ}_{1\frac{1}{2}} - 61374_{2\frac{1}{2}}$					
3520.917		10	28393.57	−0.04	$43075^{\circ}_{1\frac{1}{2}} - 71468_{2\frac{1}{2}}$					
3520.293	600*r*	3000	28398.61	+0.03	$30562^{\circ}_{5\frac{1}{2}} - 58961_{5\frac{1}{2}}$	6	1.111	0.972	0.770	1.043
3519.690		2	28403.47	−0.07	$48272^{\circ}_{2\frac{1}{2}} - 76676_{2\frac{1}{2}}$					
3519.417	5	50	28405.67	−0.01	$61873_{6\frac{1}{2}} - 90279^{\circ}_{5\frac{1}{2}}$	7	(1.11)	1.11	0	1.096
3519.10		1	28408.23							
3518.89		1	28409.93							
3518.795		3	28410.70	−0.05	$65093_{3\frac{1}{2}} - 93503^{\circ}_{4\frac{1}{2}}$					
3518.674		1	28411.67	−0.04	$47758^{\circ}_{3\frac{1}{2}} - 76170_{2\frac{1}{2}}$					
3518.353	1	10	28414.26	−0.03	$40035^{\circ}_{3\frac{1}{2}} - 68450_{3\frac{1}{2}}$					
3518.156	20	300	28415.86	−0.01	$45335^{\circ}_{4\frac{1}{2}} - 73750_{4\frac{1}{2}}$	7	1.00	1.00	0	1.00
3516.60		1	28428.43							
3516.180		2	28431.82	+0.02	$65566_{0\frac{1}{2}} - 93998^{\circ}_{1\frac{1}{2}}$					
				−0.03	$65577_{3\frac{1}{2}} - 94008^{\circ}_{3\frac{1}{2}}$					
3515.865	30	300	28434.37	+0.01	$37516^{\circ}_{3\frac{1}{2}} - 65950_{4\frac{1}{2}}$	4	(1.119)	1.09	w	0.99
3515.610	10	50	28436.43	−0.05	$34575^{\circ}_{1\frac{1}{2}} - 63011_{1\frac{1}{2}}$	6	1.450	0.780	0.90	1.120
3515.138	1	15	28440.25	−0.05	$62861_{5\frac{1}{2}} - 91301^{\circ}_{6\frac{1}{2}}$					
3513.640		4	28452.38	−0.03	$70793_{5\frac{1}{2}} - 99246^{\circ}_{5\frac{1}{2}}$					
3513.412		2	28454.22							
3512.708	2	20	28459.93	0.00	$65875_{6\frac{1}{2}} - 94335^{\circ}_{5\frac{1}{2}}$					

TABLE 6. Yb II—*Observed and classified lines*—Continued

1	2	3	4	5	6	7	8	9	10	11
Wave-length air	Intensity		Wave number	o–c	Classification	Zeeman type	1st g	2nd g	Zeeman components	
	Meggers lamp	Thomson lamp							Strong p	Strong n
Å			K	K						
3512.441		6	28462.09							
3511.283		8	28471.48							
3510.942		3	28474.24							
3510.500	1	15	28477.83	−0.05	$45273^{\circ}_{3\frac{1}{2}} - 73750_{4\frac{1}{2}}$					
3509.86	1	10	28483.02	−0.06	$33653^{\circ}_{0\frac{1}{2}} - 62136_{0\frac{1}{2}}$					
3509.776		3	28483.70	−0.08	$70136_{6\frac{1}{2}} - 98620^{\circ}_{6\frac{1}{2}}$					
3508.95		1	28490.40							
3507.830	200	2000	28499.50	−0.02	$37077^{\circ}_{2\frac{1}{2}} - 65577_{3\frac{1}{2}}$	4	1.12	1.06	(0.028)	0.92
3506.125	8	200	28513.36	−0.05	$40035^{\circ}_{3\frac{1}{2}} - 68549_{4\frac{1}{2}}$	5	0.714	1.160	0.223	2.72
3505.282	50	150	28520.22	−0.02	$33653^{\circ}_{0\frac{1}{2}} - 62174_{1\frac{1}{2}}$	4	1.30	0.80	0.26	0.54
3504.936	3	15	28523.03	−0.03	$61374_{2\frac{1}{2}} - 89897^{\circ}_{1\frac{1}{2}}$					
3504.542	1	15	28526.24	−0.06	$48272^{\circ}_{2\frac{1}{2}} - 76799_{1\frac{1}{2}}$					
3503.690	4	40	28533.18	−0.01	$45737^{\circ}_{1\frac{1}{2}} - 74270_{2\frac{1}{2}}$	4	1.315	0.911	0.202	0.305
3503.277		2	28536.54	−0.01	$53120^{\circ}_{2\frac{1}{2}} - 81657_{2\frac{1}{2}}$					
3503.190		3	28537.25	−0.03	$68549_{4\frac{1}{2}} - 97086^{\circ}_{4\frac{1}{2}}$					
3503.011		1	28538.71							
3502.572		4*h*	28542.28							
3502.180	10	100	28545.48	0.00	$47005^{\circ}_{1\frac{1}{2}} - 75550_{2\frac{1}{2}}$	4	1.00	0.92	(0.04)	0.80
3500.863		5	28556.22	−0.02	$70858_{4\frac{1}{2}} - 99414^{\circ}_{4\frac{1}{2}}$					
3500.131	10	30	28562.19	+0.03	$58823_{2\frac{1}{2}} - 87385^{\circ}_{3\frac{1}{2}}$					
3499.886		3	28564.19	−0.05	$69957_{4\frac{1}{2}} - 98521^{\circ}_{4\frac{1}{2}}$					
3499.85		1	28564.48	−0.05	$61051_{3\frac{1}{2}} - 89615^{\circ}_{2\frac{1}{2}}$					
3499.791		2	28564.96	+0.01	$47758^{\circ}_{3\frac{1}{2}} - 76323_{3\frac{1}{2}}$					
3499.636	1	9	28566.23	0.00	$48272^{\circ}_{2\frac{1}{2}} - 76839_{2\frac{1}{2}}$					
3499.419	5	10	28568.00							
3498.392	2	40	28576.38	+0.04 −0.03	$39378^{\circ}_{0\frac{1}{2}} - 67955_{0\frac{1}{2}}$ $63726_{4\frac{1}{2}} - 92303^{\circ}_{3\frac{1}{2}}$					
3497.86		2	28580.73	−0.05	$64923_{4\frac{1}{2}} - 93503^{\circ}_{4\frac{1}{2}}$					
3496.858	5	20	28588.92	−0.01	$24332_{2\frac{1}{2}} - 52921^{\circ}_{3\frac{1}{2}}$					
3495.90		50	28596.76	+0.01	$64598_{3\frac{1}{2}} - 93195^{\circ}_{3\frac{1}{2}}$					
3495.780		3	28597.74	+0.09	$49008^{\circ}_{3\frac{1}{2}} - 77606_{2\frac{1}{2}}$					
3493.154	1	15	28619.23	+0.03	$44497^{\circ}_{2\frac{1}{2}} - 73116_{1\frac{1}{2}}$					
3492.807	5	30	28622.08	−0.01	$34389^{\circ}_{2\frac{1}{2}} - 63011_{1\frac{1}{2}}$					
3491.624	6	100	28631.77	−0.01	$45335^{\circ}_{4\frac{1}{2}} - 73966_{3\frac{1}{2}}$					
3491.063		3	28636.38	−0.02	$68450_{3\frac{1}{2}} - 97086^{\circ}_{4\frac{1}{2}}$					
3490.880		2*h*	28637.88							
3490.58		1	28640.34	+0.09	$27061^{\circ}_{0\frac{1}{2}} - 55702_{1\frac{1}{2}}$					
3490.213	1	20	28643.35	+0.03	$35059^{\circ}_{3\frac{1}{2}} - 63702_{2\frac{1}{2}}$					
3488.786	200	700	28655.06	−0.01	$24332_{2\frac{1}{2}} - 52987^{\circ}_{1\frac{1}{2}}$	5	1.18	1.12	(0.03)	1.27
3488.43		10*h*	28657.99							

TABLE 6. Yb II—*Observed and classified lines*—Continued

1	2	3	4	5	6	7	8	9	10	11
Wave-length air	Intensity		Wave number	o–c	Classification	Zeeman type	1st g	2nd g	Zeeman components	
	Meggers lamp	Thomson lamp							Strong p	Strong n
Å			K	K						
3488.34	6	50	28658.73	−0.01 −0.05	$34575^{\circ}_{1\frac{1}{2}} - 63234_{2\frac{1}{2}}$ $50468^{\circ}_{5\frac{1}{2}} - 79126_{4\frac{1}{2}}$					
3487.402		3	28666.44	+0.02	$70136_{6\frac{1}{2}} - 98802^{\circ}_{5\frac{1}{2}}$					
3487.233	6	100	28667.83	0.00	$35059^{\circ}_{3\frac{1}{2}} - 63726_{4\frac{1}{2}}$					
3487.041		2	28669.40	+0.03	$52987^{\circ}_{1\frac{1}{2}} - 81657_{2\frac{1}{2}}$					
3486.137	1	8	28676.84	+0.03	$47228^{\circ}_{0\frac{1}{2}} - 75905_{0\frac{1}{2}}$					
3485.757	200	1500	28679.96	0.00	$32371^{\circ}_{2\frac{1}{2}} - 61051_{3\frac{1}{2}}$	7	(1.170)	1.18	0	1.21
3484.656		1	28689.03							
3484.38		2	28691.30							
3484.143	1	15	28693.25	0.00	$70136_{6\frac{1}{2}} - 98829^{\circ}_{6\frac{1}{2}}$					
3484.09		2	28693.69	−0.10	$45273^{\circ}_{3\frac{1}{2}} - 73966_{3\frac{1}{2}}$					
3484.06		2	28693.93							
3483.782	1	10	28696.22	0.00	$44940^{\circ}_{1\frac{1}{2}} - 73636_{0\frac{1}{2}}$					
3482.942	1	10	28703.14	−0.02	$63944_{5\frac{1}{2}} - 92647^{\circ}_{5\frac{1}{2}}$					
3482.564	5	30*h*	28706.26							
3482.390		1	28707.69	−0.01	$35019^{\circ}_{4\frac{1}{2}} - 63726_{4\frac{1}{2}}$					
3481.706		2	28713.33							
3481.302	1	20	28716.66	−0.02	$44940^{\circ}_{1\frac{1}{2}} - 73657_{1\frac{1}{2}}$					
3479.912		2	28728.14							
3478.835	3000*r*	10000	28737.03	−0.01	$30224^{\circ}_{4\frac{1}{2}} - 58961_{5\frac{1}{2}}$	5	0.93	0.97	(0.022)	1.17
3477.022	20	30	28752.01							
3476.303	10000*A*	8000	28757.96	−0.02	$0_{0\frac{1}{2}} - 28757^{\circ}_{1\frac{1}{2}}$	4	1.999	1.437	0.281	1.160
3474.82	60	400	28770.23	−0.06	$33052^{\circ}_{4\frac{1}{2}} - 61822_{3\frac{1}{2}}$	4	1.28	1.33	(0.026)	1.10
3474.512		3	28772.78							
3473.996		5	28777.06	0.00	$61120_{0\frac{1}{2}} - 89897^{\circ}_{1\frac{1}{2}}$					
3473.75		3	28779.09							
3473.01		2	28785.23							
3472.58		1	28788.79							
3472.324	5	20	28790.91							
3471.891		2	28794.50							
3471.46		1	28798.08							
3470.79	8	80	28803.64	+0.01	$46169^{\circ}_{4\frac{1}{2}} - 74973_{3\frac{1}{2}}$	5	(1.10)	1.09	*w*	1.13
3469.925	5	70	28810.82	−0.05	$37077^{\circ}_{2\frac{1}{2}} - 65888_{1\frac{1}{2}}$	4	1.117	1.209	0.046	0.979
3469.253	3	5	28816.40							
3468.395	1	20	28823.53	−0.05	$43956^{\circ}_{2\frac{1}{2}} - 72779_{3\frac{1}{2}}$					
3468.00		3*h*	28826.81							
3467.066	10	200	28834.57	−0.05	$37516^{\circ}_{3\frac{1}{2}} - 66351_{2\frac{1}{2}}$	7	(1.119)	1.115	0	1.128
3466.346		10	28840.56	−0.10	$45429^{\circ}_{3\frac{1}{2}} - 74270_{2\frac{1}{2}}$					
3465.898	3	40	28844.29	−0.06	$34389^{\circ}_{2\frac{1}{2}} - 63234_{2\frac{1}{2}}$	6	1.00	1.19	0.48	1.090
3465.792		3	28845.17	0.00	$69957_{4\frac{1}{2}} - 98802^{\circ}_{5\frac{1}{2}}$					

TABLE 6. Yb II—*Observed and classified lines*—Continued

1	2	3	4	5	6	7	8	9	10	11
Wave-length air	Intensity		Wave number	o–c	Classification	Zeeman type	1st g	2nd g	Zeeman components	
	Meggers lamp	Thomson lamp							Strong p	Strong n
Å			K	K						
3464.905		1	28852.56	−0.03	$47663^{\circ}_{4\frac{1}{2}} - 76516_{4\frac{1}{2}}$					
3463.325	2	30	28865.72	−0.08	$30224^{\circ}_{4\frac{1}{2}} - 59090_{3\frac{1}{2}}$					
3463.179	2	20	28866.94	−0.07	$30392^{\circ}_{1\frac{1}{2}} - 59259_{2\frac{1}{2}}$					
3462.79		1*h*	28870.18							
3462.338[a]	20	15	28873.95							
3461.719	30	300	28879.11	−0.02	$37516^{\circ}_{3\frac{1}{2}} - 66395_{2\frac{1}{2}}$	4	1.11	1.23	(0.06)	0.82
3461.327		5	28882.38							
3460.137		4	28892.31							
3460.092		10	28892.69	−0.06	$48556^{\circ}_{3\frac{1}{2}} - 77449_{3\frac{1}{2}}$					
3459.902		2	28894.28							
3459.828		4	28894.89	−0.07	$61822_{3\frac{1}{2}} - 90717^{\circ}_{4\frac{1}{2}}$					
3459.183	10	40	28900.28	−0.03	$47005^{\circ}_{1\frac{1}{2}} - 75905_{0\frac{1}{2}}$	4	0.988	1.278	0.145	0.843
3458.792		2	28903.55							
3458.286	200	1500	28907.78	−0.05	$40035^{\circ}_{3\frac{1}{2}} - 68943_{4\frac{1}{2}}$	5	0.73	0.88	0.077	1.47
3457.333		2	28915.75	−0.07	$65093_{3\frac{1}{2}} - 94088^{\circ}_{3\frac{1}{2}}$					
3457.10		2	28917.69	−0.08	$47758^{\circ}_{3\frac{1}{2}} - 76676_{2\frac{1}{2}}$					
3457.04		1	28918.20							
3456.953		1	28918.92							
3456.774		6	28920.42	−0.09	$63726_{4\frac{1}{2}} - 92647^{\circ}_{5\frac{1}{2}}$					
3456.231	5	20	28924.97	−0.08	$35019^{\circ}_{4\frac{1}{2}} - 63944_{5\frac{1}{2}}$					
3455.863		5	28928.05	−0.03	$61214_{4\frac{1}{2}} - 90142^{\circ}_{3\frac{1}{2}}$					
3454.92		3	28935.94							
3454.215	50	300	28941.85	−0.03	$34784^{\circ}_{5\frac{1}{2}} - 63726_{4\frac{1}{2}}$					
3454.080	2000*r*	10000	28942.98	−0.07	$26759^{\circ}_{2\frac{1}{2}} - 55702_{1\frac{1}{2}}$	4	1.560	1.687	0.065	1.370?
3453.524		5	28947.64	−0.08	$64598_{3\frac{1}{2}} - 93546^{\circ}_{2\frac{1}{2}}$					
3453.207		2	28950.29							
3452.264		7	28958.20							
3451.33	1	20	28966.04	+0.01	$67416_{4\frac{1}{2}} - 96382^{\circ}_{5\frac{1}{2}}$					
3451.305		3	28966.25							
3450.929		2	28969.40	0.00	$47680^{\circ}_{6\frac{1}{2}} - 76649_{5\frac{1}{2}}$					
3450.269		5	28974.95							
3449.362		1	28982.56							
3449.15		7*h*	28984.35							
3448.906		1	28986.40	+0.12	$47663^{\circ}_{4\frac{1}{2}} - 76649_{5\frac{1}{2}}$?					
3447.993	4	40	28994.07	+0.02	$47329^{\circ}_{2\frac{1}{2}} - 76323_{3\frac{1}{2}}$	7	(0.990)	0.982	0	0.971
3447.668	1	20	28996.80	−0.02	$35059^{\circ}_{3\frac{1}{2}} - 64055_{2\frac{1}{2}}$	7	(1.124)	1.120	0	1.134
3446.887	100	600	29003.37	−0.02	$32371^{\circ}_{2\frac{1}{2}} - 61374_{2\frac{1}{2}}$	6	1.178	1.306	0.32	1.242
3445.950	7	100	29011.26	+0.01	$48272^{\circ}_{2\frac{1}{2}} - 77284_{1\frac{1}{2}}$	5	1.16	0.93	0.116	1.51
3445.107		3	29018.36	−0.02	$31568^{\circ}_{2\frac{1}{2}} - 60586_{1\frac{1}{2}}$					
3444.544		2	29023.10							
3443.895		2*h*	29028.57							

TABLE 6. Yb II—*Observed and classified lines*—Continued

1	2	3	4	5	6	7	8	9	10	11
Wave-length air	Intensity		Wave number	o–c	Classification	Zeeman type	1st g	2nd g	Zeeman components	
	Meggers lamp	Thomson lamp							Strong p	Strong n
Å			K	K						
3443.587[a]	30	20	29031.17			?			0	1.18
3443.391		6*h*	29032.82							
3442.586	10	5	29039.61	+0.03	$40917^{\circ}_{4\frac{1}{2}} - 69957_{4\frac{1}{2}}$					
3442.368	3	40	29041.45	+0.04	$37516^{\circ}_{3\frac{1}{2}} - 66558_{3\frac{1}{2}}$	6	1.13	1.11	*d*	1.12
3442.058	1	10	29044.06	0.00 −0.10	$40035^{\circ}_{3\frac{1}{2}} - 69079_{2\frac{1}{2}}$ $63234_{2\frac{1}{2}} - 92278^{\circ}_{1\frac{1}{2}}$?					
3441.354		7	29050.00	−0.01	$48556^{\circ}_{3\frac{1}{2}} - 77606_{2\frac{1}{2}}$					
3441.30		1	29050.46							
3440.894		8*h*	29053.89							
3440.016		5	29061.30	+0.04	$49008^{\circ}_{3\frac{1}{2}} - 78070_{4\frac{1}{2}}$					
3439.648	1	20	29064.41	+0.07 −0.01	$33494^{\circ}_{3\frac{1}{2}} - 62559_{2\frac{1}{2}}$ $61214_{4\frac{1}{2}} - 90279^{\circ}_{5\frac{1}{2}}$					
3438.848	400	2000	29071.17	+0.01	$31979^{\circ}_{3\frac{1}{2}} - 61051_{3\frac{1}{2}}$	6	1.337	1.187	0.525	1.262
3438.709	200	1500	29072.35	−0.01	$34575^{\circ}_{1\frac{1}{2}} - 63647_{1\frac{1}{2}}$	6	1.439	1.149	0.435	1.004
3438.516		10	29073.98	−0.03	$38342^{\circ}_{4\frac{1}{2}} - 67416_{4\frac{1}{2}}$					
3437.754		3	29080.42	−0.04	$47758^{\circ}_{3\frac{1}{2}} - 76839_{2\frac{1}{2}}$					
3437.222		2	29084.92	0.00	$64461_{1\frac{1}{2}} - 93546^{\circ}_{2\frac{1}{2}}$					
3437.114		2	29085.84	−0.01	$64923_{4\frac{1}{2}} - 94008^{\circ}_{3\frac{1}{2}}$					
3436.452	100	700	29091.44	+0.01	$35831^{\circ}_{5\frac{1}{2}} - 64923_{4\frac{1}{2}}$					
3435.74		4*h*	29097.47							
3435.516		2	29099.37							
3435.429		3	29100.10							
3434.610	200	600	29107.04	−0.03	$22960_{1\frac{1}{2}} - 52067^{\circ}_{0\frac{1}{2}}$	5	0.810	0.560	0.125	0.936
3434.244	1	10	29110.15	+0.02	$70136_{6\frac{1}{2}} - 99246^{\circ}_{5\frac{1}{2}}$					
3433.650		1	29115.18							
3433.160		10	29119.34							
3432.732	1	3	29122.97							
3432.261	1	30	29126.96	+0.01	$34575^{\circ}_{1\frac{1}{2}} - 63702_{2\frac{1}{2}}$					
3431.780		4*h*	29131.05							
3431.63		1	29132.32							
3431.512		2	29133.32	0.00	$66558_{3\frac{1}{2}} - 95691^{\circ}_{3\frac{1}{2}}$					
3431.377	5	9	29134.47							
3430.872		3	29138.76	0.00	$45429^{\circ}_{3\frac{1}{2}} - 74568_{4\frac{1}{2}}$					
3430.65		1	29140.64							
3430.632		2	29140.79							
3429.96		1	29146.50							
3429.80		1	29147.86	+0.03	$67938_{3\frac{1}{2}} - 97086^{\circ}_{4\frac{1}{2}}$					
3428.463	200	2000	29159.23	0.00	$34784^{\circ}_{5\frac{1}{2}} - 63944_{5\frac{1}{2}}$	6	1.12	1.10	0.09	1.11
3427.808	1	20	29164.80	+0.01	$47005^{\circ}_{1\frac{1}{2}} - 76170_{2\frac{1}{2}}$					
3427.508		3	29167.35	−0.04	$70858_{4\frac{1}{2}} - 100025^{\circ}_{5\frac{1}{2}}$					
3426.558		2	29175.44	+0.02	$53716^{\circ}_{2\frac{1}{2}} - 82891_{2\frac{1}{2}}$					
3426.43		1	29176.53	−0.02	$48272^{\circ}_{2\frac{1}{2}} - 77449_{3\frac{1}{2}}$					

TABLE 6. Yb II—*Observed and classified lines*—Continued

1	2	3	4	5	6	7	8	9	10	11
Wave-length air	Intensity		Wave number	o–c	Classification	Zeeman type	1st g	2nd g	Zeeman components	
	Meggers lamp	Thomson lamp							Strong p	Strong n
Å			K	K						
3425.71		1	29182.66	−0.06	$66571_{5\frac{1}{2}} - 95754^{\circ}_{5\frac{1}{2}}$					
3424.750		5	29190.84	+0.01	$48556^{\circ}_{3\frac{1}{2}} - 77747_{4\frac{1}{2}}$					
3424.554	3	15	29192.51	0.00	$32981^{\circ}_{1\frac{1}{2}} - 62174_{1\frac{1}{2}}$					
3424.182		1	29195.68							
3422.454		6	29210.42	−0.02 +0.09	$65093_{3\frac{1}{2}} - 94303^{\circ}_{3\frac{1}{2}}$ $49916^{\circ}_{4\frac{1}{2}} - 79126_{4\frac{1}{2}}$					
3421.409		1	29219.34							
3419.742	2	20	29233.59	+0.04	$45335^{\circ}_{4\frac{1}{2}} - 74568_{4\frac{1}{2}}$	7	1.01	(1.04)	0	1.023
3419.606	20	100	29234.75	−0.01	$31979^{\circ}_{3\frac{1}{2}} - 61214_{4\frac{1}{2}}$	4	1.33	1.07	0.13	0.16
3418.571		1	29243.60	+0.02	$48503^{\circ}_{5\frac{1}{2}} - 77747_{4\frac{1}{2}}$					
3417.565	3	30	29252.21	+0.01	$45737^{\circ}_{1\frac{1}{2}} - 74989_{0\frac{1}{2}}$	5	1.36	0.54	0.41	1.77
3417.345	1	10	29254.09	+0.02	$45737^{\circ}_{1\frac{1}{2}} - 74991_{1\frac{1}{2}}$					
3416.894	40	200	29257.95	−0.02	$34389^{\circ}_{2\frac{1}{2}} - 63647_{1\frac{1}{2}}$	4	1.00	1.14	0.070	0.79
3416.314		1	29262.92							
3415.974	10	100	29265.83	+0.01	$41688^{\circ}_{1\frac{1}{2}} - 70954_{2\frac{1}{2}}$	5	0.800	1.028	0.114	1.370
3415.853		2	29266.87	+0.01	$65093_{3\frac{1}{2}} - 94360^{\circ}_{1\frac{1}{2}}$					
3415.610		6	29268.95	+0.01	$64598_{3\frac{1}{2}} - 93867^{\circ}_{4\frac{1}{2}}$					
3415.062	10	80	29273.65	+0.03	$37077^{\circ}_{2\frac{1}{2}} - 66351_{2\frac{1}{2}}$	7	1.125	1.125	0	1.125
3414.838	20	200	29275.57	+0.03	$41678^{\circ}_{2\frac{1}{2}} - 70954_{2\frac{1}{2}}$	6	1.191	1.008	0.454	1.099
3413.357	5	15	29288.27	+0.02	$47228^{\circ}_{0\frac{1}{2}} - 76517_{1\frac{1}{2}}$	5	0.77	0.87	0.05	0.92
3412.507		5	29295.57	+0.01 −0.03	$45273^{\circ}_{3\frac{1}{2}} - 74568_{4\frac{1}{2}}$ $66395_{2\frac{1}{2}} - 95691^{\circ}_{3\frac{1}{2}}$					
3412.453[a]	80	40	29296.03			7			0	1.13
3411.750		6	29302.07	+0.06	$63944_{5\frac{1}{2}} - 93246^{\circ}_{6\frac{1}{2}}$					
3411.240[a]	10	8	29306.45							
3410.880		4	29309.54	+0.07	$63726_{4\frac{1}{2}} - 93036^{\circ}_{5\frac{1}{2}}$					
3410.689	1	6	29311.18	+0.09	$60586_{1\frac{1}{2}} - 89897^{\circ}_{1\frac{1}{2}}$					
3410.566	50	60	29312.24	+0.04	$24332_{2\frac{1}{2}} - 53644^{\circ}_{3\frac{1}{2}}$	7	(1.202)	1.198	0	1.188
3410.487	1	10	29312.92	+0.05	$44438^{\circ}_{3\frac{1}{2}} - 73750_{4\frac{1}{2}}$					
3409.875	6	70	29318.18	+0.05	$37077^{\circ}_{2\frac{1}{2}} - 66395_{2\frac{1}{2}}$					
3409.568	1	10	29320.82	0.00	$45737^{\circ}_{1\frac{1}{2}} - 75058_{2\frac{1}{2}}$					
3409.022		3	29325.51	+0.04	$48556^{\circ}_{3\frac{1}{2}} - 77882_{3\frac{1}{2}}$					
3408.516	10	100	29329.87	0.00	$44940^{\circ}_{1\frac{1}{2}} - 74270_{2\frac{1}{2}}$	4	1.234	0.920	0.157	0.449
3408.20		3	29332.59							
3408.058		7	29333.81	0.00	$48272^{\circ}_{2\frac{1}{2}} - 77606_{2\frac{1}{2}}$					
3406.536	1	6	29346.91	+0.04	$47329^{\circ}_{2\frac{1}{2}} - 76676_{2\frac{1}{2}}$					
3405.79		1	29353.34							
3405.249	5	30	29358.00	+0.01	$33653^{\circ}_{0\frac{1}{2}} - 63011_{1\frac{1}{2}}$					
3405.093		2	29359.35	−0.03	$40035^{\circ}_{3\frac{1}{2}} - 69395_{3\frac{1}{2}}$					
3405.03		1	29359.89							
3404.103	150	800	29367.89	+0.03	$35831^{\circ}_{5\frac{1}{2}} - 65199_{4\frac{1}{2}}$	5	1.23	1.10	(0.065)	1.815

TABLE 6. Yb II—*Observed and classified lines*—Continued

1	2	3	4	5	6	7	8	9	10	11
Wave-length air	Intensity		Wave number	o–c	Classification	Zeeman type	1st g	2nd g	Zeeman components	
	Meggers lamp	Thomson lamp							Strong p	Strong n
Å			K	K						
3402.640		5	29380.51	+0.04	$64923_{4\frac{1}{2}} - 94303^{\circ}_{3\frac{1}{2}}$					
3402.273	200	300	29383.68	−0.01	$24332_{2\frac{1}{2}} - 53716^{\circ}_{2\frac{1}{2}}$	6	1.206	1.180	0.067	1.193
3401.010	200	1000	29394.59	0.00 +0.02	$31979^{\circ}_{3\frac{1}{2}} - 61374_{2\frac{1}{2}}$ $(30224^{\circ}_{4\frac{1}{2}} - 59618_{3\frac{1}{2}})$	5	1.33	(1.30)	w	1.39
3400.603		4d	29398.11							
3400.445		3	29399.48							
3399.548		3	29407.24	+0.05	$64055_{2\frac{1}{2}} - 93463^{\circ}_{3\frac{1}{2}}$					
3398.649	2	10	29415.01							
3397.446	2	20	29425.43	+0.04	$41688^{\circ}_{1\frac{1}{2}} - 71113_{1\frac{1}{2}}$					
3397.125	2	20	29428.21	+0.04	$61873_{6\frac{1}{2}} - 91301^{\circ}_{6\frac{1}{2}}$					
3396.328	40	400	29435.12	+0.01	$41678^{\circ}_{2\frac{1}{2}} - 71113_{1\frac{1}{2}}$	5	1.21	1.00	0.105	1.530
3395.14		5h	29445.41							
3394.437	60	300	29451.51	+0.03	$32371^{\circ}_{2\frac{1}{2}} - 61822_{3\frac{1}{2}}$	5	1.170	1.325	0.077	1.716
3394.152		1	29453.99							
3393.815		1	29456.91	−0.02	$69957_{4\frac{1}{2}} - 99414^{\circ}_{4\frac{1}{2}}$					
3393.636		2	29458.46							
3393.252		1	29461.80	−0.08	$59259_{2\frac{1}{2}} - 88721^{\circ}_{3\frac{1}{2}}$					
3392.390	7	100	29469.28	−0.02	$44497^{\circ}_{2\frac{1}{2}} - 73966_{3\frac{1}{2}}$	5	(0.734)	0.76	w	0.81
3392.356	2	20	29469.58	−0.05	$47329^{\circ}_{2\frac{1}{2}} - 76799_{1\frac{1}{2}}$					
3392.276		4	29470.27	−0.01	$46169^{\circ}_{4\frac{1}{2}} - 75640_{3\frac{1}{2}}$					
3391.104	100r	900	29480.46	+0.01 +0.05	$34575^{\circ}_{1\frac{1}{2}} - 64055_{2\frac{1}{2}}$ $(37077^{\circ}_{2\frac{1}{2}} - 66558_{3\frac{1}{2}})$	4	1.42	1.11	0.15	0.64
3390.817	3	40	29482.95	−0.03	$31568^{\circ}_{2\frac{1}{2}} - 61051_{3\frac{1}{2}}$					
3390.63		1	29484.58	0.00	$61374_{2\frac{1}{2}} - 90859^{\circ}_{2\frac{1}{2}}$					
3390.421	1h	30h	29486.40							
3390.246	1h	40h	29487.92							
3389.985		2	29490.19	+0.01	$64055_{2\frac{1}{2}} - 93546^{\circ}_{2\frac{1}{2}}$					
3389.439		4	29494.94							
3388.523		7	29502.91	+0.03	$61214_{4\frac{1}{2}} - 90717^{\circ}_{4\frac{1}{2}}$					
3387.760		3	29509.56	0.00	$47329^{\circ}_{2\frac{1}{2}} - 76839_{2\frac{1}{2}}$					
3387.293	2	20	29513.63	+0.01	$48556^{\circ}_{3\frac{1}{2}} - 78070_{4\frac{1}{2}}$					
3387.120		2	29515.13							
3387.073		3	29515.54	−0.02	$63726_{4\frac{1}{2}} - 93242^{\circ}_{5\frac{1}{2}}$					
3386.560		1	29520.01							
3385.883	20	40	29525.92	−0.01	$28757^{\circ}_{1\frac{1}{2}} - 58283_{2\frac{1}{2}}$					
3385.559	10	100	29528.74	−0.04	$44438^{\circ}_{3\frac{1}{2}} - 73966_{3\frac{1}{2}}$	6	1.098	0.762	1.18	0.930
3384.560		1	29537.46	+0.02	$64461_{1\frac{1}{2}} - 93998^{\circ}_{1\frac{1}{2}}$					
3384.352		4	29539.27	−0.01	$35059^{\circ}_{3\frac{1}{2}} - 64598_{3\frac{1}{2}}$					
3383.862	3	20	29543.55	−0.04 −0.08	$45429^{\circ}_{3\frac{1}{2}} - 74973_{3\frac{1}{2}}$ $(41678^{\circ}_{2\frac{1}{2}} - 71222_{3\frac{1}{2}})$	6	1.16	1.08	0.28	1.12
3381.255		1	29566.33	−0.04	$48503^{\circ}_{5\frac{1}{2}} - 78070_{4\frac{1}{2}}$					

TABLE 6. Yb II—*Observed and classified lines*—Continued

1	2	3	4	5	6	7	8	9	10	11
Wave-length air	Intensity		Wave number	o–c	Classification	Zeeman type	1st g	2nd g	Zeeman components	
	Meggers lamp	Thomson lamp							Strong p	Strong n
Å			K	K						
3381.060	2	15	29568.03	−0.01	$34389^{\circ}_{2\frac{1}{2}} - 63957_{3\frac{1}{2}}$					
3380.820	1	20	29570.13	+0.02	$47228^{\circ}_{0\frac{1}{2}} - 76799_{1\frac{1}{2}}$	5?	0.72	0.84	0.06	0.90
3380.644		1	29571.67	−0.05	$40035^{\circ}_{3\frac{1}{2}} - 69607_{2\frac{1}{2}}$					
3380.340		1	29574.33							
3379.986	40	100	29577.43	0.00	$32981^{\circ}_{1\frac{1}{2}} - 62559_{2\frac{1}{2}}$	5	0.88	1.21	0.165	1.70
3379.788	100	700	29579.16	+0.01	$35019^{\circ}_{4\frac{1}{2}} - 64598_{3\frac{1}{2}}$	4	1.15	1.22	(0.034)	0.91
3379.517	6	70	29581.53	−0.03	$41688^{\circ}_{1\frac{1}{2}} - 71270_{2\frac{1}{2}}$	5	0.78	0.90	(0.06)	1.08
3379.386[a]	2	2	29582.68							
3378.404	10	100	29591.28	0.00	$41678^{\circ}_{2\frac{1}{2}} - 71270_{2\frac{1}{2}}$	6	1.19	0.91	(0.70)	1.05
3377.792	3	40	29596.64	−0.02	$38342^{\circ}_{4\frac{1}{2}} - 67938_{3\frac{1}{2}}$					
3377.456		3	29599.58	−0.02	$65950_{4\frac{1}{2}} - 95550^{\circ}_{4\frac{1}{2}}$					
3376.780		2	29605.51							
3376.623	3	30	29606.89							
3375.483	2000r	5000	29616.88	−0.01	$26759^{\circ}_{2\frac{1}{2}} - 56375_{2\frac{1}{2}}$	6	1.580	1.238	0.860	1.410
3375.079	30	70	29620.43	+0.01	$57765_{4\frac{1}{2}} - 87385^{\circ}_{3\frac{1}{2}}$					
3374.184		1	29628.29	0.00	$45429^{\circ}_{3\frac{1}{2}} - 75058_{2\frac{1}{2}}$					
3374.07		1	29629.29							
3373.873	2	20	29631.02	+0.03	$59090_{3\frac{1}{2}} - 88721^{\circ}_{3\frac{1}{2}}$					
3373.736		1	29632.22							
3373.033	1	10	29638.40	+0.02	$45335^{\circ}_{4\frac{1}{2}} - 74973_{3\frac{1}{2}}$					
3372.00		1	29647.47	−0.03	$53716^{\circ}_{2\frac{1}{2}} - 83363_{3\frac{1}{2}}$					
3369.886	10	80	29666.07	+0.01	$34389^{\circ}_{2\frac{1}{2}} - 64055_{2\frac{1}{2}}$	6	1.006	1.110	0.262	1.058
3369.544	70	200	29669.08	−0.03	$33494^{\circ}_{3\frac{1}{2}} - 63163_{4\frac{1}{2}}$	5	0.98	1.13	0.075	1.65
3369.344	20	60	29670.84	−0.01	$47005^{\circ}_{1\frac{1}{2}} - 76676_{2\frac{1}{2}}$	5	0.990	1.102	(0.056)	1.270
3367.738		6	29684.99	0.00	$63234_{2\frac{1}{2}} - 92919^{\circ}_{3\frac{1}{2}}$					
3367.077		4	29690.82	+0.04	$47758^{\circ}_{3\frac{1}{2}} - 77449_{3\frac{1}{2}}$					
3366.964		3	29691.82							
3365.969	80	800	29700.59	−0.02	$42915^{\circ}_{5\frac{1}{2}} - 72615_{5\frac{1}{2}}$	6	1.126	1.000	0.70	1.063
3365.658		2	29703.34							
3365.444		1	29705.23	−0.07	$64598_{3\frac{1}{2}} - 94303^{\circ}_{3\frac{1}{2}}$					
3365.059		4	29708.63							
3364.471		4	29713.82	0.00	$61822_{3\frac{1}{2}} - 91536^{\circ}_{3\frac{1}{2}}$					
3364.125		2	29716.87							
3363.886		1	29718.98	−0.01	$53644^{\circ}_{3\frac{1}{2}} - 83363_{3\frac{1}{2}}$					
3363.645	10	20	29721.11							
3362.705	4	6	29729.42							
3362.438	10	70	29731.78							
3361.573	15	100	29739.43	0.00	$33494^{\circ}_{3\frac{1}{2}} - 63234_{2\frac{1}{2}}$	4	0.983	1.196	0.106	0.451
3361.467	1	8	29740.37	0.00	$65950_{4\frac{1}{2}} - 95691^{\circ}_{3\frac{1}{2}}$					
3361.329	3	30	29741.59	−0.01	$58961_{5\frac{1}{2}} - 88702^{\circ}_{5\frac{1}{2}}$					
3359.49		1	29757.87							

TABLE 6. Yb II—*Observed and classified lines*—Continued

1	2	3	4	5	6	7	8	9	10	11
Wave-length air	Intensity		Wave number	o–c	Classification	Zeeman type	1st g	2nd g	Zeeman components	
	Meggers lamp	Thomson lamp							Strong p	Strong n
Å			K	K						
3359.193		3h	29760.50							
3358.612		2	29765.65	−0.04	$68756_{3\frac{1}{2}} - 98521^{\circ}_{4\frac{1}{2}}$					
3357.802	5	40	29772.83	+0.07	$56375_{2\frac{1}{2}} - 86148^{\circ}_{2\frac{1}{2}}$					
3356.966	20	200	29780.25	0.00	$41688^{\circ}_{1\frac{1}{2}} - 71468_{2\frac{1}{2}}$	5	0.790	1.027	0.118	1.381
3356.683		1	29782.76							
3356.305	6	40	29786.11	+0.04	$62861_{5\frac{1}{2}} - 92647^{\circ}_{5\frac{1}{2}}$					
3355.870	20	200	29789.97	0.00	$41678^{\circ}_{2\frac{1}{2}} - 71468_{2\frac{1}{2}}$	6	1.189	1.007	0.463	1.098
3354.020		3	29806.40	−0.01	$31568^{\circ}_{2\frac{1}{2}} - 61374_{2\frac{1}{2}}$					
3353.966	2	30	29806.88	+0.02	$38342^{\circ}_{4\frac{1}{2}} - 68148_{5\frac{1}{2}}$					
3353.733	20	150	29808.95	−0.03	$33052^{\circ}_{4\frac{1}{2}} - 62861_{5\frac{1}{2}}$	4	1.260	1.138	0.061	0.589
3353.563	1	6	29810.46	−0.02	$66571_{5\frac{1}{2}} - 96382^{\circ}_{5\frac{1}{2}}$					
3353.200	3	40	29813.69	+0.04	$45737^{\circ}_{1\frac{1}{2}} - 75550_{2\frac{1}{2}}$	4	1.334	0.908	0.213	0.269
3352.491	10	30	29820.00							
3351.265[a]	20	20	29830.90							
3351.087	6	60	29832.49	+0.04	$44438^{\circ}_{3\frac{1}{2}} - 74270_{2\frac{1}{2}}$	5	1.103	0.921	0.091	1.558
3350.967	5	40	29833.56	+0.02	$47005^{\circ}_{1\frac{1}{2}} - 76839_{2\frac{1}{2}}$	5	0.996	1.116	0.06	1.296
3349.942	20	150	29842.69	+0.01	$31979^{\circ}_{3\frac{1}{2}} - 61822_{3\frac{1}{2}}$	7	1.333	1.333	0	1.333
3349.074	10	60	29850.42	+0.02	$56375_{2\frac{1}{2}} - 86226^{\circ}_{1\frac{1}{2}}$	4	(1.226)	1.314	w	1.094
3347.537	150	1000	29864.12	+0.01	$35059^{\circ}_{3\frac{1}{2}} - 64923_{4\frac{1}{2}}$	7	(1.124)	1.117	0	1.092
3346.504[a]	30	30	29873.34							
3346.192		7	29876.13	+0.08	$40917^{\circ}_{4\frac{1}{2}} - 70793_{5\frac{1}{2}}$					
3345.921		7	29878.55	+0.02	$65875_{6\frac{1}{2}} - 95754^{\circ}_{5\frac{1}{2}}$					
3345.187		9	29885.10							
3344.715		3	29889.32	−0.01	$70136_{6\frac{1}{2}} - 100025^{\circ}_{5\frac{1}{2}}$					
3343.78		1	29897.68							
3343.705		2	29898.35	+0.08	$63647_{1\frac{1}{2}} - 93546^{\circ}_{2\frac{1}{2}}$					
3343.566		2	29899.59	+0.01	$68720_{6\frac{1}{2}} - 98620^{\circ}_{6\frac{1}{2}}$					
3343.071	80	400	29904.02	+0.04 −0.02	$35019^{\circ}_{4\frac{1}{2}} - 64923_{4\frac{1}{2}}$ $(52987^{\circ}_{1\frac{1}{2}} - 82891_{2\frac{1}{2}})$	6	1.16	1.11	0.21	1.14
3342.93	20h	100h	29905.28							
3342.310		1	29910.83	−0.03	$66571_{5\frac{1}{2}} - 96482^{\circ}_{4\frac{1}{2}}$					
3341.097	3	40	29921.69	+0.02	$40035^{\circ}_{3\frac{1}{2}} - 69957_{4\frac{1}{2}}$	5	0.66	1.08	0.208	2.54
3340.791		1	29924.43	−0.01	$66558_{3\frac{1}{2}} - 96482^{\circ}_{4\frac{1}{2}}$					
3339.476		3	29936.21							
3339.305		3	29937.74							
3339.274		1	29938.02							
3339.022		1	29940.28	+0.01	$40917^{\circ}_{4\frac{1}{2}} - 70858_{4\frac{1}{2}}$					
3338.749	1	8	29942.73	+0.03	$64055_{2\frac{1}{2}} - 93998^{\circ}_{1\frac{1}{2}}$					
3337.581		1	29953.21	+0.07	$64055_{2\frac{1}{2}} - 94008^{\circ}_{3\frac{1}{2}}$					
3337.420	5	20	29954.65	+0.07	$47329^{\circ}_{2\frac{1}{2}} - 77284_{1\frac{1}{2}}$	5	1.00	(0.90)	w	1.14

TABLE 6. Yb II—*Observed and classified lines*—Continued

1	2	3	4	5	6	7	8	9	10	11
Wave-length air	Intensity		Wave number	o–c	Classification	Zeeman type	1st g	2nd g	Zeeman components	
	Meggers lamp	Thomson lamp							Strong p	Strong n
Å			K	K						
3337.171	30	100	29956.89			7			0	1.019
3337.005		5*h*	29958.38							
3336.88		1	29959.50							
3336.718		4	29960.95	+0.03	$63234_{2\frac{1}{2}} - 93195^{\circ}_{3\frac{1}{2}}$					
3335.826	1	10	29968.96	+0.02	$46354^{\circ}_{1\frac{1}{2}} - 76323_{3\frac{1}{2}}$					
3335.435		2	29972.48	−0.02	$68549_{4\frac{1}{2}} - 98521^{\circ}_{4\frac{1}{2}}$					
3335.327		3	29973.45	+0.01	$65577_{3\frac{1}{2}} - 95550^{\circ}_{4\frac{1}{2}}$					
3334.321	1	3	29982.49							
3333.800		4	29987.18							
3333.057	200	1000	29993.86	−0.01	$33653^{\circ}_{0\frac{1}{2}} - 63647_{1\frac{1}{2}}$	4	1.329	1.157	0.086	1.071
3332.774		7	29996.41							
3331.220	5	50	30010.40	0.00	$43956^{\circ}_{2\frac{1}{2}} - 73966_{3\frac{1}{2}}$	4	0.991	0.765	0.113	0.200
3330.238		1	30019.25	+0.03	$69395_{3\frac{1}{2}} - 99414^{\circ}_{4\frac{1}{2}}$					
3329.50	3	5	30025.90							
3329.382	50	100	30026.97	+0.01	$22960_{1\frac{1}{2}} - 52987^{\circ}_{1\frac{1}{2}}$	6	0.806	1.134	0.500	0.970
3329.087		4	30029.63							
3329.017	3	10	30030.26	0.00	$32981^{\circ}_{1\frac{1}{2}} - 63011_{1\frac{1}{2}}$					
3328.584		8	30034.17	+0.03	$35059^{\circ}_{3\frac{1}{2}} - 65093_{3\frac{1}{2}}$					
3328.39		1	30035.92							
3327.756	8	80	30041.64	+0.02	$43075^{\circ}_{1\frac{1}{2}} - 73116_{1\frac{1}{2}}$	6	0.960	0.870	0.135	0.915
3327.485	1	15	30044.08	−0.01	$35831^{\circ}_{5\frac{1}{2}} - 65875_{6\frac{1}{2}}$					
3327.195[a]	3	3	30046.70							
3326.949	2	20	30048.93	+0.05	$44940^{\circ}_{1\frac{1}{2}} - 74989_{0\frac{1}{2}}$	5	1.252	0.512	0.370	1.622
3326.745		4	30050.77	+0.02	$44940^{\circ}_{1\frac{1}{2}} - 74991_{1\frac{1}{2}}$					
3326.266	40	200	30055.09	+0.03	$47228^{\circ}_{0\frac{1}{2}} - 77284_{1\frac{1}{2}}$	5	0.711	0.894	0.091	0.985
3325.104	9	50	30065.60	0.00	$28757^{\circ}_{1\frac{1}{2}} - 58823_{2\frac{1}{2}}$	4	1.440	1.256	0.092	0.980
3324.80		2	30068.35							
3324.470	10	70	30071.33	+0.01	$34389^{\circ}_{2\frac{1}{2}} - 64461_{1\frac{1}{2}}$	4	1.001	1.171	0.085	0.746
3324.172	40	300	30074.03	+0.02	$35019^{\circ}_{1\frac{1}{2}} - 65093_{3\frac{1}{2}}$	5	1.16	0.99	0.083	1.74
3324.043	2	12	30075.19	−0.03	$41688^{\circ}_{1\frac{1}{2}} - 71763_{1\frac{1}{2}}$					
3323.46		3*h*	30080.47							
3322.963	20	250	30084.97	+0.03	$41678^{\circ}_{2\frac{1}{2}} - 71763_{1\frac{1}{2}}$	5	(1.193)	1.10	*w*	1.33?
3322.87	1	2	30085.81							
3322.58		1	30088.44	−0.07	$59624^{\circ}_{3\frac{1}{2}} - 89713_{2\frac{1}{2}}$					
3320.802		1	30104.55							
3320.642		2	30106.00							
3320.314	10	200	30108.97	+0.05 −0.08	$43007^{\circ}_{0\frac{1}{2}} - 73116_{1\frac{1}{2}}$ $(68720_{6\frac{1}{2}} - 98829^{\circ}_{6\frac{1}{2}})$	5	0.158	0.862	0.352	1.213
3320.032	5	30	30111.53	+0.03	$33052^{\circ}_{4\frac{1}{2}} - 63163_{4\frac{1}{2}}$					
3319.737		2	30114.20	−0.01	$65577_{3\frac{1}{2}} - 95691^{\circ}_{3\frac{1}{2}}$					

TABLE 6. Yb II—*Observed and classified lines*—Continued

1	2	3	4	5	6	7	8	9	10	11
Wavelength air	Intensity		Wave number	o–c	Classification	Zeeman type	1st g	2nd g	Zeeman components	
	Meggers lamp	Thomson lamp							Strong p	Strong n
Å			K	K						
3319.180	80	500	30119.26	−0.01	$35831^{\circ}_{5\frac{1}{2}} - 65950_{4\frac{1}{2}}$	5	1.21	1.08	(0.063)	1.78
3318.973	50	100	30121.13	+0.01	$45429^{\circ}_{3\frac{1}{2}} - 75550_{2\frac{1}{2}}$	5	1.15	0.92	0.115	1.73
3318.590		1	30124.61							
3318.283	3	40	30127.40	+0.02	$37077^{\circ}_{2\frac{1}{2}} - 67204_{1\frac{1}{2}}$	5	(1.113)	1.06	0	1.18
3317.939	2	30	30130.52	−0.03	$44438^{\circ}_{3\frac{1}{2}} - 74568_{4\frac{1}{2}}$					
3317.094		3	30138.20	+0.04	$34784^{\circ}_{5\frac{1}{2}} - 64923_{4\frac{1}{2}}$					
3316.834	10	200	30140.56	+0.02	$35059^{\circ}_{3\frac{1}{2}} - 65199_{4\frac{1}{2}}$	4	(1.124)	1.09	w	0.98
3315.390	20	200	30153.69	−0.02	$46169^{\circ}_{4\frac{1}{2}} - 76323_{3\frac{1}{2}}$	5	1.12	1.03	(0.043)	1.42
3315.101	1h	15h	30156.31							
3314.720	10	20	30159.78	0.00	$22960_{1\frac{1}{2}} - 53120^{\circ}_{2\frac{1}{2}}$					
3314.52		10	30161.60	+0.04	$46354^{\circ}_{4\frac{1}{2}} - 76516_{4\frac{1}{2}}$					
3313.763	5	40	30168.49	+0.01	$45737^{\circ}_{1\frac{1}{2}} - 75905_{0\frac{1}{2}}$	7	(1.333)	1.30	0	1.35
3313.039		3	30175.08	+0.05	$62861_{5\frac{1}{2}} - 93036^{\circ}_{5\frac{1}{2}}$					
3312.450	1	20	30180.45	+0.04	$35019^{\circ}_{4\frac{1}{2}} - 65199_{4\frac{1}{2}}$					
3311.742	2	10	30186.90	+0.08	$49419^{\circ}_{0\frac{1}{2}} - 79605_{1\frac{1}{2}}$					
				0.00	$59710_{1\frac{1}{2}} - 89897^{\circ}_{1\frac{1}{2}}$					
				+0.02	$61051_{3\frac{1}{2}} - 91237^{\circ}_{3\frac{1}{2}}$					
3311.630	3	8	30187.92	0.00	$32371^{\circ}_{2\frac{1}{2}} - 62559_{2\frac{1}{2}}$					
3311.180		2	30192.02	+0.03	$48272^{\circ}_{2\frac{1}{2}} - 78464_{1\frac{1}{2}}$					
3311.050	4	30	30193.21	+0.03	$61822_{3\frac{1}{2}} - 92015^{\circ}_{4\frac{1}{2}}$					
3310.937	10	80	30194.24	+0.01	$30392^{\circ}_{1\frac{1}{2}} - 60586_{1\frac{1}{2}}$	7	1.320	1.320	0	1.320
3310.815		1	30195.35							
3310.20		1	30200.96							
3309.512	10	70	30207.24	+0.03	$38342^{\circ}_{4\frac{1}{2}} - 68549_{4\frac{1}{2}}$					
3309.470	2	20	30207.62	−0.02	$33494^{\circ}_{3\frac{1}{2}} - 63702_{2\frac{1}{2}}$					
3309.372	70	300	30208.52	0.00	$34389^{\circ}_{2\frac{1}{2}} - 64598_{3\frac{1}{2}}$	5	1.01	1.25	0.119	1.850
3309.185	5	50	30210.22	−0.02	$45429^{\circ}_{3\frac{1}{2}} - 75640_{3\frac{1}{2}}$					
3308.461		2	30216.84	0.00	$63647_{1\frac{1}{2}} - 93864^{\circ}_{2\frac{1}{2}}$					
3308.210		1	30219.13							
3306.783	100	400	30232.17	+0.02	$33494^{\circ}_{3\frac{1}{2}} - 63726_{4\frac{1}{2}}$	7	1.005	1.005	0	1.005
3305.733	500r	2000	30241.77	−0.04	$31631^{\circ}_{6\frac{1}{2}} - 61873_{6\frac{1}{2}}$	6	1.23	1.11	0.76	1.16
3305.252[a]	20	20	30246.17							
3304.770	70	400	30250.58	+0.01	$35831^{\circ}_{5\frac{1}{2}} - 66082_{5\frac{1}{2}}$	6	1.217	1.145	0.40	1.181
3304.558	80	400	30252.52	0.00	$32981^{\circ}_{1\frac{1}{2}} - 63234_{2\frac{1}{2}}$	5	0.865	1.216	0.176	1.742
3304.346		6	30254.46	−0.04	$31568^{\circ}_{2\frac{1}{2}} - 61822_{3\frac{1}{2}}$					
3303.926		1	30258.31	+0.02	$48556^{\circ}_{3\frac{1}{2}} - 78814_{2\frac{1}{2}}$					
3303.864		2	30258.88							
3303.449		1	30262.68							
3303.203		2	30264.93							
3302.202		1	30274.11	+0.02	$59439^{\circ}_{2\frac{1}{2}} - 89713_{2\frac{1}{2}}$					
3301.780	1	10	30277.98	+0.06	$45273^{\circ}_{3\frac{1}{2}} - 75550_{2\frac{1}{2}}$					

TABLE 6. Yb II—*Observed and classified lines*—Continued

1	2	3	4	5	6	7	8	9	10	11
Wave-length air	Intensity		Wave number	o–c	Classification	Zeeman type	1st g	2nd g	Zeeman components	
	Meggers lamp	Thomson lamp							Strong p	Strong n
Å			K	K						
3301.711	10	20	30278.61	+0.05	$47005^{\circ}_{1\frac{1}{2}} - 77284_{1\frac{1}{2}}$	6	1.00	0.88	0.18	0.94
3301.328		1	30282.12	−0.01	$63726_{4\frac{1}{2}} - 94008^{\circ}_{3\frac{1}{2}}$					
3299.447		1	30299.38							
3299.400	1	6	30299.82	+0.01	$66082_{5\frac{1}{2}} - 96382^{\circ}_{5\frac{1}{2}}$					
3298.896		8	30304.45	0.00	$40917^{\circ}_{4\frac{1}{2}} - 71222_{3\frac{1}{2}}$					
3298.826	1	10	30305.09	+0.06	$45335^{\circ}_{4\frac{1}{2}} - 75640_{3\frac{1}{2}}$					
3298.102		2	30311.74	+0.09	$47758^{\circ}_{3\frac{1}{2}} - 78070_{4\frac{1}{2}}$					
3297.851	10	100	30314.05	−0.02	$43956^{\circ}_{2\frac{1}{2}} - 74270_{2\frac{1}{2}}$	6	1.00	0.93	0.165	0.970
3296.501		4	30326.46	+0.01	$66571_{5\frac{1}{2}} - 96898^{\circ}_{5\frac{1}{2}}$					
3295.825		4	30332.68							
3294.58		2	30344.14							
3294.341	7	100	30346.35	+0.02	$46169^{\circ}_{4\frac{1}{2}} - 76516_{4\frac{1}{2}}$	6	1.10	1.02	0.34	1.06
3293.836		2	30351.00	−0.01	$65199_{4\frac{1}{2}} - 95550^{\circ}_{4\frac{1}{2}}$					
3293.66		3	30352.62							
3293.25		1	30356.40	+0.05	$59259_{2\frac{1}{2}} - 89615^{\circ}_{2\frac{1}{2}}$					
3292.92		1	30359.44							
3292.089	5	20	30367.10	+0.06	$45273^{\circ}_{3\frac{1}{2}} - 75640_{3\frac{1}{2}}$					
3291.967		10	30368.23	+0.01	$42915^{\circ}_{5\frac{1}{2}} - 73283_{4\frac{1}{2}}$					
3291.028		4	30376.89	+0.07	$42915^{\circ}_{5\frac{1}{2}} - 73291_{5\frac{1}{2}}$					
3290.554		8	30381.27	−0.04	$46902^{\circ}_{0\frac{1}{2}} - 77284_{1\frac{1}{2}}$					
3290.14		4	30385.09							
3289.370	60000*A*	40000	30392.20	−0.03	$0_{0\frac{1}{2}} - 30392^{\circ}_{1\frac{1}{2}}$	4	2.000	1.334	0.333	1.001
3287.81		1	30406.62	−0.05	$47663^{\circ}_{4\frac{1}{2}} - 78070_{4\frac{1}{2}}$					
3286.960	10	70	30414.49	−0.10	$34784^{\circ}_{5\frac{1}{2}} - 65199_{4\frac{1}{2}}$	5	(1.119)	1.09	*w*	1.25
3285.78		1	30425.41							
3285.35		1	30429.39							
3285.168		2	30431.08	−0.03	$65950_{4\frac{1}{2}} - 96382^{\circ}_{5\frac{1}{2}}$					
3283.494	4	40	30446.59	−0.01	$55702_{1\frac{1}{2}} - 86148^{\circ}_{2\frac{1}{2}}$	4	1.690	1.568	0.061	1.385
3282.03		5	30460.17							
3281.715	1	7	30463.09	−0.03	$33494^{\circ}_{3\frac{1}{2}} - 63957_{3\frac{1}{2}}$					
3280.850		4	30471.13	−0.01	$68148_{5\frac{1}{2}} - 98620^{\circ}_{6\frac{1}{2}}$					
3280.335	1	10	30475.91	+0.01	$44497^{\circ}_{2\frac{1}{2}} - 74973_{3\frac{1}{2}}$					
3279.89		4	30480.04	+0.02 +0.04	$46169^{\circ}_{4\frac{1}{2}} - 76649_{5\frac{1}{2}}$ $50832^{\circ}_{1\frac{1}{2}} - 81312_{2\frac{1}{2}}$					
3279.32		4	30485.34	0.00	$61051_{3\frac{1}{2}} - 91536^{\circ}_{3\frac{1}{2}}$					
3278.99		1	30488.41							
3278.400	2	20	30493.90	+0.05	$44497^{\circ}_{2\frac{1}{2}} - 74991_{1\frac{1}{2}}$	4	0.74	1.06	0.16	0.26
3278.057	7	70	30497.09	−0.05	$53720_{4\frac{1}{2}} - 84217^{\circ}_{4\frac{1}{2}}$	6	1.25	1.19	0.25	1.21
3277.73		4	30500.13							
3277.607	4	15	30501.27	+0.01	$28757^{\circ}_{1\frac{1}{2}} - 59259_{2\frac{1}{2}}$					

TABLE 6. Yb II—*Observed and classified lines*—Continued

1	2	3	4	5	6	7	8	9	10	11
Wave-length air	Intensity		Wave number	o–c	Classification	Zeeman type	1st g	2nd g	Zeeman components	
	Meggers lamp	Thomson lamp							Strong p	Strong n
Å			K	K						
3277.575		1	30501.57							
3277.07		1	30506.27	−0.02	$65875_{6\frac{1}{2}} - 96382^{\circ}_{5\frac{1}{2}}$					
3275.801	50	200	30518.09	−0.02	$35059^{\circ}_{3\frac{1}{2}} - 65577_{3\frac{1}{2}}$	6	1.12	1.06	0.22	1.09
3275.19		7	30523.78	−0.06	$59618_{3\frac{1}{2}} - 90142^{\circ}_{3\frac{1}{2}}$					
3275.14		1	30524.25	+0.01	$55702_{1\frac{1}{2}} - 86226^{\circ}_{1\frac{1}{2}}$					
3275.01	1	8	30525.46	0.00	$59090_{3\frac{1}{2}} - 89615^{\circ}_{2\frac{1}{2}}$					
3274.96		2	30525.93	0.00	$68720_{6\frac{1}{2}} - 99246^{\circ}_{5\frac{1}{2}}$					
3273.940	7	70	30535.44	+0.06	$44438^{\circ}_{3\frac{1}{2}} - 74973_{3\frac{1}{2}}$					
3273.65		1	30538.14	−0.01	$45012^{\circ}_{2\frac{1}{2}} - 75550_{2\frac{1}{2}}$					
3272.98		2	30544.39							
3271.528	20	150	30557.95	−0.03	$35019^{\circ}_{4\frac{1}{2}} - 65577_{3\frac{1}{2}}$					
3271.247	2	20	30560.57	−0.03	$44497^{\circ}_{2\frac{1}{2}} - 75058_{2\frac{1}{2}}$					
3271.190	10	40	30561.11	−0.03	$33494^{\circ}_{3\frac{1}{2}} - 64055_{2\frac{1}{2}}$					
3271.125	3	30	30561.71	−0.03	$43075^{\circ}_{1\frac{1}{2}} - 73636_{0\frac{1}{2}}$					
3270.57		2	30566.90							
3269.265	50	200	30579.10	−0.02	$31979^{\circ}_{3\frac{1}{2}} - 62559_{2\frac{1}{2}}$					
3268.94		2	30582.14	−0.06	$43075^{\circ}_{1\frac{1}{2}} - 73657_{1\frac{1}{2}}$					
3268.84		1	30583.08	+0.03	$67938_{3\frac{1}{2}} - 98521^{\circ}_{4\frac{1}{2}}$					
3266.915		6	30601.10	−0.02	$47005^{\circ}_{1\frac{1}{2}} - 77606_{2\frac{1}{2}}$					
3266.39		4*d*	30606.01	−0.01	$31568^{\circ}_{2\frac{1}{2}} - 62174_{1\frac{1}{2}}$					
3266.163		4	30608.14							
3265.930	3	30	30610.32	−0.01	$44940^{\circ}_{1\frac{1}{2}} - 75550_{2\frac{1}{2}}$					
3265.068	7	60	30618.41	0.00	$37516^{\circ}_{3\frac{1}{2}} - 68135_{2\frac{1}{2}}$					
3264.889	8	80	30620.08	0.00	$44438^{\circ}_{3\frac{1}{2}} - 75058_{2\frac{1}{2}}$					
3264.114		4	30627.35	+0.08	$45012^{\circ}_{2\frac{1}{2}} - 75640_{3\frac{1}{2}}$					
				−0.09	$64923_{4\frac{1}{2}} - 95550^{\circ}_{4\frac{1}{2}}$					
3263.938	1	10	30629.01	−0.03	$43007^{\circ}_{0\frac{1}{2}} - 73636_{0\frac{1}{2}}$					
3263.79		1	30630.40	−0.06	$63234_{2\frac{1}{2}} - 93864^{\circ}_{2\frac{1}{2}}$					
3262.296	6	60	30644.42	−0.01	$58961_{5\frac{1}{2}} - 89605^{\circ}_{4\frac{1}{2}}$					
3261.759	5	50	30649.47	−0.03	$43007^{\circ}_{0\frac{1}{2}} - 73657_{1\frac{1}{2}}$					
3261.686	20	200	30650.15	0.00	$39378^{\circ}_{0\frac{1}{2}} - 70029_{0\frac{1}{2}}$	6	1.85	0.67	0.59	1.26
3261.508	500	1500	30651.83	−0.04	$30562^{\circ}_{5\frac{1}{2}} - 61214_{4\frac{1}{2}}$	5	1.10	1.04	(0.03)	1.37
3261.02		1	30656.41							
3260.82		5	30658.29	−0.05	$47228^{\circ}_{0\frac{1}{2}} - 77887_{0\frac{1}{2}}$					
3259.99	1	8	30666.10	−0.04	$32981^{\circ}_{1\frac{1}{2}} - 63647_{1\frac{1}{2}}$					
3259.100	100	500	30674.47	−0.07	$33052^{\circ}_{4\frac{1}{2}} - 63726_{4\frac{1}{2}}$	6	1.272	1.008	0.132	1.140
3258.663	1	10	30678.59							
3258.453		8	30680.56	−0.05	$68148_{5\frac{1}{2}} - 98829^{\circ}_{6\frac{1}{2}}$					
3256.86		1	30695.57							
3256.030	5	50	30703.39	+0.01	$34389^{\circ}_{2\frac{1}{2}} - 65093_{3\frac{1}{2}}$					
				−0.04	$63163_{4\frac{1}{2}} - 93867^{\circ}_{4\frac{1}{2}}$					
3255.24		1	30710.84							

TABLE 6. Yb II—*Observed and classified lines*—Continued

1	2	3	4	5	6	7	8	9	10	11
Wave-length air	Intensity		Wave number	o–c	Classification	Zeeman type	1st g	2nd g	Zeeman components	
	Meggers lamp	Thomson lamp							Strong p	Strong n
Å			K	K						
3254.62		2	30716.69							
3254.197	100	300	30720.69	−0.04	$32981^{\circ}_{1\frac{1}{2}} - 63702_{2\frac{1}{2}}$					
3253.911	10	100	30723.39	+0.03	$53720_{4\frac{1}{2}} - 84444^{\circ}_{3\frac{1}{2}}$					
3253.340	20	120	30728.78	−0.03	$53715_{3\frac{1}{2}} - 84444^{\circ}_{3\frac{1}{2}}$					
3252.106	1	10	30740.44	+0.01	$45429^{\circ}_{3\frac{1}{2}} - 76170_{2\frac{1}{2}}$					
3250.505	1	5	30755.58	0.00	$22960_{1\frac{1}{2}} - 53716^{\circ}_{2\frac{1}{2}}$					
3249.80		1	30762.25							
3249.57		1	30764.43	+0.02	$63234_{2\frac{1}{2}} - 93998^{\circ}_{1\frac{1}{2}}$					
3249.17		4	30768.22	+0.01	$64923_{4\frac{1}{2}} - 95691^{\circ}_{3\frac{1}{2}}$					
3248.446	2	10	30775.07							
3247.932	1	5	30779.94	+0.02	$45737^{\circ}_{1\frac{1}{2}} - 76517_{1\frac{1}{2}}$					
3246.85		1	30790.20	+0.04	$48024^{\circ}_{1\frac{1}{2}} - 78814_{2\frac{1}{2}}$					
3246.657	1	7	30792.03	+0.02	$58823_{2\frac{1}{2}} - 89615^{\circ}_{2\frac{1}{2}}$					
3246.28		1	30795.61							
3246.060		10	30797.69							
3245.70		5	30801.11	+0.01	$61214_{4\frac{1}{2}} - 92015^{\circ}_{4\frac{1}{2}}$					
3245.05		6	30807.28	+0.06	$33653^{\circ}_{0\frac{1}{2}} - 64461_{1\frac{1}{2}}$					
3243.46		5	30822.38	+0.02	$40035^{\circ}_{3\frac{1}{2}} - 70858_{4\frac{1}{2}}$					
3243.00	4	30	30826.75	+0.02	$30224^{\circ}_{4\frac{1}{2}} - 61051_{3\frac{1}{2}}$					
3242.12	1	10	30835.12							
3242.048	4	50	30835.80	+0.03	$42915^{\circ}_{3\frac{1}{2}} - 73750_{4\frac{1}{2}}$					
3239.39	1	8	30861.10	+0.01	$37077^{\circ}_{2\frac{1}{2}} - 67938_{3\frac{1}{2}}$					
3239.195	50	200	30862.96	−0.05	$32371^{\circ}_{2\frac{1}{2}} - 63234_{2\frac{1}{2}}$	6	1.18	1.22	0.09	1.20
3237.215		5	30881.84	0.00	$47005^{\circ}_{1\frac{1}{2}} - 77887_{0\frac{1}{2}}$					
3236.488	20	60	30888.77	0.00	$24332_{2\frac{1}{2}} - 55221^{\circ}_{1\frac{1}{2}}$					
3236.160	40	300	30891.91	−0.04 +0.02	$35059^{\circ}_{3\frac{1}{2}} - 65950_{4\frac{1}{2}}$ $(33052^{\circ}_{4\frac{1}{2}} - 63944_{5\frac{1}{2}})$	4	(1.124)	1.10	w	1.03
3235.975	3	30	30893.67	0.00	$45429^{\circ}_{3\frac{1}{2}} - 76323_{3\frac{1}{2}}$					
3235.858		6	30894.79							
3235.61		8	30897.16	−0.07	$45273^{\circ}_{3\frac{1}{2}} - 76170_{2\frac{1}{2}}$					
3234.740	2	10	30905.47	−0.04	$33052^{\circ}_{4\frac{1}{2}} - 63957_{3\frac{1}{2}}$					
3233.487	3	40	30917.44	−0.01	$53715_{3\frac{1}{2}} - 84632^{\circ}_{2\frac{1}{2}}$					
3233.38		1	30918.46	+0.01	$40035^{\circ}_{3\frac{1}{2}} - 70954_{2\frac{1}{2}}$					
3232.29		4	30928.89							
3231.986	50	300	30931.80	−0.02	$35019^{\circ}_{4\frac{1}{2}} - 65950_{4\frac{1}{2}}$	6	1.15	1.07	0.36	1.11
3231.90	1	10	30932.62							
3231.81		10	30933.48	−0.04	$37516^{\circ}_{3\frac{1}{2}} - 68450_{3\frac{1}{2}}$					
3231.376	10	50	30937.64	−0.01	$57765_{4\frac{1}{2}} - 88702^{\circ}_{3\frac{1}{2}}$					
3231.228		2	30939.06	+0.04	$45737^{\circ}_{1\frac{1}{2}} - 76676_{2\frac{1}{2}}$					
3229.814	50	150	30952.60	−0.07	$28757^{\circ}_{1\frac{1}{2}} - 59710_{1\frac{1}{2}}$	6	1.44	0.80	0.96	1.12
3229.475	2	20	30955.85	+0.05	$57765_{4\frac{1}{2}} - 88721^{\circ}_{3\frac{1}{2}}$					

TABLE 6. Yb II—*Observed and classified lines*—Continued

1	2	3	4	5	6	7	8	9	10	11
Wave-length air	Intensity		Wave number	o–c	Classification	Zeeman type	1st g	2nd g	Zeeman components	
	Meggers lamp	Thomson lamp							Strong p	Strong n
Å			K	K						
3228.503	5	40	30965.17	+0.01	$44940^{\circ}_{1\frac{1}{2}} - 75905_{0\frac{1}{2}}$					
3226.725	20	80	30982.23	−0.03	$30392^{\circ}_{1\frac{1}{2}} - 61374_{2\frac{1}{2}}$	4	(1.333)	1.31	0	1.27
3225.885	100	400	30990.30	−0.03	$30224^{\circ}_{4\frac{1}{2}} - 61214_{4\frac{1}{2}}$	6	0.94	1.05	0.50	1.00
3225.78	20	200	30991.31	−0.04	$34575^{\circ}_{1\frac{1}{2}} - 65566_{0\frac{1}{2}}$	7	1.43	1.43	0	1.43
3224.890		4	30999.86							
3224.752		3	31001.19							
3224.43		4	31004.28	+0.02	$66082_{5\frac{1}{2}} - 97086^{\circ}_{4\frac{1}{2}}$					
3224.25		1	31006.01	+0.06	$62861_{5\frac{1}{2}} - 93867^{\circ}_{4\frac{1}{2}}$					
3223.854	4	20	31009.82	−0.01	$56375_{2\frac{1}{2}} - 87385^{\circ}_{3\frac{1}{2}}$					
3223.105	4	40	31017.03	+0.03	$43956^{\circ}_{2\frac{1}{2}} - 74973_{3\frac{1}{2}}$					
3222.55		1	31022.37	+0.11	$65875_{6\frac{1}{2}} - 96898^{\circ}_{5\frac{1}{2}}$					
3222.11		5	31026.60	+0.06	$48556^{\circ}_{3\frac{1}{2}} - 79583_{2\frac{1}{2}}$					
3221.486	10	70	31032.61	−0.03	$37516^{\circ}_{3\frac{1}{2}} - 68549_{4\frac{1}{2}}$	5	(1.12)	1.15	u	1.24
3221.246	15	150	31034.93	−0.02	$43956^{\circ}_{2\frac{1}{2}} - 74991_{1\frac{1}{2}}$	4	(0.99)	1.04	w	0.92
3220.96		2	31037.68							
3220.814		8	31039.09	−0.02	$53404_{2\frac{1}{2}} - 84444^{\circ}_{3\frac{1}{2}}$					
3219.633		8	31050.47	0.00	$45273^{\circ}_{3\frac{1}{2}} - 76323_{3\frac{1}{2}}$					
3219.408	2	9	31052.64	+0.03	$59090_{3\frac{1}{2}} - 90142^{\circ}_{3\frac{1}{2}}$					
3219.325	1	10	31053.44	+0.01	$44497^{\circ}_{2\frac{1}{2}} - 75550_{2\frac{1}{2}}$					
3218.913	2	15	31057.42	+0.01	$37077^{\circ}_{2\frac{1}{2}} - 68135_{2\frac{1}{2}}$					
3218.323	100	600	31063.11	−0.01	$35019^{\circ}_{4\frac{1}{2}} - 66082_{5\frac{1}{2}}$	7	1.11	1.11	0	1.11
3217.96		1	31066.62							
3217.66		3	31069.51	+0.04	$63234_{2\frac{1}{2}} - 94303^{\circ}_{3\frac{1}{2}}$					
3217.45		1	31071.54							
3217.29	1	7	31073.09	+0.11	$37077^{\circ}_{2\frac{1}{2}} - 68150_{1\frac{1}{2}}$?					
3217.176	200	1000	31074.19	−0.04	$32981^{\circ}_{1\frac{1}{2}} - 64055_{2\frac{1}{2}}$	5	0.862	1.110	0.124	1.482
3215.927	10	100	31086.25	−0.04	$45429^{\circ}_{3\frac{1}{2}} - 76516_{4\frac{1}{2}}$					
3215.68		2	31088.64	+0.06	$61214_{4\frac{1}{2}} - 92303^{\circ}_{3\frac{1}{2}}$					
3215.456	10	60	31090.81	−0.01	$34784^{\circ}_{5\frac{1}{2}} - 65875_{6\frac{1}{2}}$					
3215.38		2	31091.54	−0.03	$61822_{3\frac{1}{2}} - 92914^{\circ}_{4\frac{1}{2}}$					
3214.330	2	20	31101.70	0.00 −0.01	$43956^{\circ}_{2\frac{1}{2}} - 75058_{2\frac{1}{2}}$ $45737^{\circ}_{1\frac{1}{2}} - 76839_{2\frac{1}{2}}$					
3214.14		1	31103.54	−0.06	$33494^{\circ}_{3\frac{1}{2}} - 64598_{3\frac{1}{2}}$					
3213.172		6	31112.91	0.00	$44438^{\circ}_{3\frac{1}{2}} - 75550_{2\frac{1}{2}}$					
3212.485		5	31119.56	+0.02	$59090_{3\frac{1}{2}} - 90209^{\circ}_{4\frac{1}{2}}$					
3210.84		7	31135.50	−0.06	$65950_{4\frac{1}{2}} - 97086^{\circ}_{4\frac{1}{2}}$					
3210.112	20	200	31142.56	+0.01	$44497^{\circ}_{2\frac{1}{2}} - 75640_{3\frac{1}{2}}$	5	0.74	0.80	(0.03)	0.96
3208.01		3	31162.97	+0.07	$61873_{6\frac{1}{2}} - 93036^{\circ}_{5\frac{1}{2}}$					
3207.702	4	30	31165.96	−0.04	$34784^{\circ}_{5\frac{1}{2}} - 65950_{4\frac{1}{2}}$	5	(1.119)	1.10	w	1.19
3207.538	2	10	31167.55	+0.04	$65875_{6\frac{1}{2}} - 97043^{\circ}_{6\frac{1}{2}}$					
3207.40		1	31168.90							

TABLE 6. Yb II—*Observed and classified lines*—Continued

1	2	3	4	5	6	7	8	9	10	11
Wave-length air	Intensity		Wave number	o–c	Classification	Zeeman type	1st g	2nd g	Zeeman components	
	Meggers lamp	Thomson lamp							Strong p	Strong n
Å			K	K						
3206.148	20	200	31181.07	−0.01	$45335^{\circ}_{4\frac{1}{2}} - 76516_{4\frac{1}{2}}$	7	1.01	1.01	0	1.01
3205.863	20	50	31183.84	−0.05	$31979^{\circ}_{3\frac{1}{2}} - 63163_{4\frac{1}{2}}$					
3205.58		1	31186.59	+0.05	$40035^{\circ}_{3\frac{1}{2}} - 71222_{3\frac{1}{2}}$					
3204.681	20	200	31195.34	−0.05	$43075^{\circ}_{1\frac{1}{2}} - 74270_{2\frac{1}{2}}$	4	(0.96)	0.93	0	0.89
3203.989	1	10	31202.08	+0.05	$44438^{\circ}_{3\frac{1}{2}} - 75640_{3\frac{1}{2}}$					
3202.76		2	31214.05							
3201.35	5	30	31227.80	+0.05	$53404_{2\frac{1}{2}} - 84632^{\circ}_{2\frac{1}{2}}$					
3201.160	800r	2000	31229.65	−0.03 +0.01	$31631^{\circ}_{6\frac{1}{2}} - 62861_{5\frac{1}{2}}$ $(44940^{\circ}_{1\frac{1}{2}} - 76170_{2\frac{1}{2}})$	5	1.23	1.15	(0.04)	1.69
3200.69		1	31234.24	+0.05	$40035^{\circ}_{3\frac{1}{2}} - 71270_{2\frac{1}{2}}$					
3199.785	5	50	31243.07	−0.02	$45273^{\circ}_{3\frac{1}{2}} - 76516_{4\frac{1}{2}}$					
3199.24		1	31248.39	+0.09	$58961_{5\frac{1}{2}} - 90209^{\circ}_{4\frac{1}{2}}$					
3198.647	400	1000	31254.19	−0.02	$31979^{\circ}_{3\frac{1}{2}} - 63234_{2\frac{1}{2}}$	5	1.320	1.196	0.062	1.630
3196.354	10	50	31276.61	−0.02	$32371^{\circ}_{2\frac{1}{2}} - 63647_{1\frac{1}{2}}$	7	(1.170)	1.16	0	1.18
3196.052	2	20	31279.56	+0.02	$46169^{\circ}_{4\frac{1}{2}} - 77449_{3\frac{1}{2}}$					
3195.585	20	200	31284.13	+0.01	$40917^{\circ}_{4\frac{1}{2}} - 72202_{3\frac{1}{2}}$	5	0.96	0.86	(0.05)	1.31
3194.765	10	100	31292.16	−0.05	$35059^{\circ}_{3\frac{1}{2}} - 66351_{2\frac{1}{2}}$	7	1.11	1.11	0	1.11
3194.242	8	70	31297.28	−0.02	$34784^{\circ}_{5\frac{1}{2}} - 66082_{5\frac{1}{2}}$	6	1.12	1.14	0.09	1.13
3192.885	1000r	3000	31310.59	−0.02	$30562^{\circ}_{5\frac{1}{2}} - 61873_{6\frac{1}{2}}$	7	1.08	1.08	0	1.08
3192.62	4	30	31313.18	+0.09	$34575^{\circ}_{1\frac{1}{2}} - 65888_{1\frac{1}{2}}$					
3192.45	1	8	31314.85	+0.08	$45335^{\circ}_{4\frac{1}{2}} - 76649_{5\frac{1}{2}}$					
3192.15		5	31317.79	+0.08	$58961_{5\frac{1}{2}} - 90279^{\circ}_{5\frac{1}{2}}$					
3190.780	8	30	31331.24	+0.02	$32371^{\circ}_{2\frac{1}{2}} - 63702_{2\frac{1}{2}}$					
3190.58		5	31333.20	+0.02	$48272^{\circ}_{2\frac{1}{2}} - 79605_{1\frac{1}{2}}$					
3188.26		1	31356.00	+0.06	$48272^{\circ}_{2\frac{1}{2}} - 79628_{3\frac{1}{2}}$					
3187.51		2	31363.38							
3187.01		3	31368.30	+0.01	$47758^{\circ}_{3\frac{1}{2}} - 79126_{4\frac{1}{2}}$					
3186.580	10	100	31372.53	+0.01 +0.08	$37077^{\circ}_{2\frac{1}{2}} - 68450_{3\frac{1}{2}}$ $(61822_{3\frac{1}{2}} - 93195^{\circ}_{3\frac{1}{2}})$	4	(1.113)	1.09	w	1.04
3185.64		1	31381.79							
3185.03		1	31387.80							
3184.71		1	31390.96							
3183.498	1	5	31402.91							
3183.46	1	5	31403.28	−0.01	$45273^{\circ}_{3\frac{1}{2}} - 76676_{2\frac{1}{2}}$					
3182.86		4	31409.20	+0.02	$45429^{\circ}_{3\frac{1}{2}} - 76839_{2\frac{1}{2}}$					
3182.52	1	8	31412.56							
3182.165	2	10	31416.06							
3181.64		1	31421.24							
3181.27	1	4	31424.90							
3181.03	1	9	31427.27							
3180.919	200	800	31428.37	−0.06	$33494^{\circ}_{3\frac{1}{2}} - 64923_{4\frac{1}{2}}$	5	(0.99)	1.10	w	1.47
3180.48		1	31432.70	+0.02	$61214_{4\frac{1}{2}} - 92647^{\circ}_{5\frac{1}{2}}$					

TABLE 6. Yb II—*Observed and classified lines*—Continued

1	2	3	4	5	6	7	8	9	10	11
Wave-length air	Intensity		Wave number	o–c	Classification	Zeeman type	1st g	2nd g	Zeeman components	
	Meggers lamp	Thomson lamp							Strong p	Strong n
Å			K	K						
3179.94	1	10	31438.04	+0.06	$41678^{\circ}_{2\frac{1}{2}} - 73116_{1\frac{1}{2}}$					
3179.344	30	70	31443.93							
3178.85		1	31448.82	+0.04	$49008^{\circ}_{3\frac{1}{2}} - 80457_{3\frac{1}{2}}$					
3177.815		1	31459.06							
3177.78		2	31459.41	+0.11	$47005^{\circ}_{1\frac{1}{2}} - 78464_{1\frac{1}{2}}$?					
3176.26		3	31474.46	+0.03	$62861_{5\frac{1}{2}} - 94335^{\circ}_{5\frac{1}{2}}$					
3176.06		1	31476.45	+0.11	$68549_{4\frac{1}{2}} - 100025^{\circ}_{5\frac{1}{2}}$?					
3175.759	25	150	31479.43	−0.06	$32981^{\circ}_{1\frac{1}{2}} - 64461_{1\frac{1}{2}}$	6	0.873	1.177	0.455	1.025
3174.22		2	31494.69							
3173.797	20	150	31498.89	−0.11	$35059^{\circ}_{3\frac{1}{2}} - 66558_{3\frac{1}{2}}$?	7	(1.124)	1.10	0	1.11
3171.176	100	300	31524.92	+0.03	$26759^{\circ}_{2\frac{1}{2}} - 58283_{2\frac{1}{2}}$	6	1.58	0.78	2.00	1.18
3169.056	200	1200	31546.01	+0.02	$33052^{\circ}_{4\frac{1}{2}} - 64598_{3\frac{1}{2}}$	5	(1.264)	1.244	w	1.334
3168.985	3	10	31546.72	−0.01	$45737^{\circ}_{1\frac{1}{2}} - 77284_{1\frac{1}{2}}$					
3168.405	8	60	31552.49	+0.04	$35019^{\circ}_{3\frac{1}{2}} - 66571_{3\frac{1}{2}}$	5	(1.158)	1.18	w	1.27
3167.72		1	31559.31	−0.02	$64923_{4\frac{1}{2}} - 96482^{\circ}_{4\frac{1}{2}}$					
3167.044	1	8	31566.05	+0.07	$45273^{\circ}_{3\frac{1}{2}} - 76839_{2\frac{1}{2}}$					
3166.727	2	20	31569.21							
3165.981	1	5	31576.65	+0.05	$44940^{\circ}_{1\frac{1}{2}} - 76517_{1\frac{1}{2}}$					
3165.875		7	31577.70	+0.08	$46169^{\circ}_{4\frac{1}{2}} - 77747_{4\frac{1}{2}}$					
3165.206	60	500	31584.38	+0.03	$35831^{\circ}_{3\frac{1}{2}} - 67416_{4\frac{1}{2}}$	4	(1.214)	1.25	w	1.065
3164.973	6	15	31586.70	0.00	$32371^{\circ}_{2\frac{1}{2}} - 63957_{3\frac{1}{2}}$					
3163.796	100	600	31598.45	−0.01	$33494^{\circ}_{3\frac{1}{2}} - 65093_{3\frac{1}{2}}$	7	0.987	0.987	0	0.987
3161.80		2	31618.40							
3160.894	1	8	31627.46	+0.05	$59090_{3\frac{1}{2}} - 90717^{\circ}_{3\frac{1}{2}}$					
3160.12		1	31635.21							
3160.01		3	31636.31							
3159.79		2	31638.51							
3159.59		1	31640.52	+0.09	$61822_{3\frac{1}{2}} - 93463^{\circ}_{3\frac{1}{2}}$					
3159.49		2	31641.52							
3159.34		1	31643.02	+0.08	$51248^{\circ}_{2\frac{1}{2}} - 82891_{2\frac{1}{2}}$					
3159.04		2	31646.03							
3158.869	5	10	31647.74							
3158.43	1	7	31652.14							
3158.300	40	300	31653.44	−0.01	$42915^{\circ}_{3\frac{1}{2}} - 74568_{4\frac{1}{2}}$	5	1.12	1.04	(0.04)	1.48
3157.043		7	31666.04	+0.01	$31568^{\circ}_{2\frac{1}{2}} - 63234_{2\frac{1}{2}}$					
3156.365		4	31672.84	+0.10	$44497^{\circ}_{2\frac{1}{2}} - 76170_{2\frac{1}{2}}$					
3155.798	30	40	31678.54	+0.09	$37077^{\circ}_{2\frac{1}{2}} - 68756_{3\frac{1}{2}}$					
3155.52		2	31681.33	+0.02	$61822_{3\frac{1}{2}} - 93503^{\circ}_{4\frac{1}{2}}$					
3155.284	5	50	31683.69	+0.04	$43956^{\circ}_{2\frac{1}{2}} - 75640_{3\frac{1}{2}}$					
3155.183	40	200	31684.71	−0.01	$32371^{\circ}_{2\frac{1}{2}} - 64055_{2\frac{1}{2}}$	6	1.160	1.110	0.125	1.135

TABLE 6. Yb II—*Observed and classified lines*—Continued

1	2	3	4	5	6	7	8	9	10	11
Wave-length air	Intensity		Wave number	o–c	Classification	Zeeman type	1st g	2nd g	Zeeman components	
	Meggers lamp	Thomson lamp							Strong p	Strong n
Å			K	K						
3154.194	5	40	31694.64	−0.06	$52938_{1\frac{1}{2}} - 84632^{\circ}_{2\frac{1}{2}}$					
3153.880	100	700	31697.80	−0.03	$40917^{\circ}_{4\frac{1}{2}} - 72615_{5\frac{1}{2}}$	7	(0.967)	0.978	0	1.028
3153.616	20	100	31700.45	−0.05	$52517_{5\frac{1}{2}} - 84217^{\circ}_{4\frac{1}{2}}$					
3153.180	40	300	31704.84	−0.02	$33494^{\circ}_{3\frac{1}{2}} - 65199_{4\frac{1}{2}}$	5	0.99	1.08	(0.044)	1.38
3152.44	4	40	31712.28	+0.02	$46169^{\circ}_{4\frac{1}{2}} - 77882_{3\frac{1}{2}}$					
3151.90		1	31717.71							
3151.436	15	100	31722.38	−0.04	$31979^{\circ}_{3\frac{1}{2}} - 63702_{2\frac{1}{2}}$					
3151.255	3	8	31724.20	−0.02	$24332_{2\frac{1}{2}} - 56056^{\circ}_{2\frac{1}{2}}$					
3150.46	3	30	31732.21	−0.01	$44438^{\circ}_{3\frac{1}{2}} - 76170_{2\frac{1}{2}}$					
3150.19		6	31734.93	−0.02	$39378^{\circ}_{0\frac{1}{2}} - 71113_{1\frac{1}{2}}$					
3150.12		2	31735.63	−0.07	$44940^{\circ}_{1\frac{1}{2}} - 76676_{2\frac{1}{2}}$					
3148.998	30	200	31746.94	+0.01	$31979^{\circ}_{3\frac{1}{2}} - 63726_{4\frac{1}{2}}$					
3148.43		2	31752.67							
3148.08		1	31756.20	+0.03	$58961_{5\frac{1}{2}} - 90717^{\circ}_{4\frac{1}{2}}$					
3146.134	8	60	31775.84	0.00	$34575^{\circ}_{1\frac{1}{2}} - 66351_{2\frac{1}{2}}$					
3145.540	150	500	31781.84	−0.03	$30392^{\circ}_{1\frac{1}{2}} - 62174_{1\frac{1}{2}}$					
3145.063	80	600	31786.66	+0.03	$34784^{\circ}_{5\frac{1}{2}} - 66571_{5\frac{1}{2}}$	6	1.120	1.188	0.36	1.154
3142.813	1	7	31809.41	+0.01	$47005^{\circ}_{1\frac{1}{2}} - 78814_{2\frac{1}{2}}$					
3142.74		2	31810.15	+0.03	$63944_{5\frac{1}{2}} - 95754^{\circ}_{5\frac{1}{2}}$					
3141.733	60	400	31820.35	0.00	$34575^{\circ}_{1\frac{1}{2}} - 66395_{2\frac{1}{2}}$	4	1.420	1.234	0.093	0.954
3141.17		3	31826.05	+0.07	$44497^{\circ}_{2\frac{1}{2}} - 76323_{3\frac{1}{2}}$					
3140.936	1000r	2000	31828.42	−0.06	$28757^{\circ}_{1\frac{1}{2}} - 60586_{1\frac{1}{2}}$	6	1.440	1.320	0.180	1.380
3140.28		2	31835.07							
3139.75	1	6	31840.44	−0.04	$57765_{4\frac{1}{2}} - 89605^{\circ}_{4\frac{1}{2}}$					
3139.27		2	31845.31							
3138.276		5	31855.40							
3138.07		2	31857.49							
3137.622		10	31862.04	−0.04	$40917^{\circ}_{4\frac{1}{2}} - 72779_{3\frac{1}{2}}$					
3137.51		1	31863.18	+0.09	$61051_{3\frac{1}{2}} - 92914^{\circ}_{4\frac{1}{2}}$					
3136.760	80	400	31870.79	−0.03	$33052^{\circ}_{4\frac{1}{2}} - 64923_{4\frac{1}{2}}$	6	1.265	1.105	0.72	1.185
3136.67	1	10	31871.71							
3136.18		2	31876.69	0.00	$68148_{5\frac{1}{2}} - 100025^{\circ}_{5\frac{1}{2}}$					
3135.989		4	31878.63	+0.02	$37516^{\circ}_{3\frac{1}{2}} - 69395_{3\frac{1}{2}}$					
3135.93		1	31879.23							
3135.43		1	31884.31							
3135.316	1	10	31885.47	+0.01	$44438^{\circ}_{3\frac{1}{2}} - 76323_{3\frac{1}{2}}$					
3135.12	4	30	31887.47	−0.02	$34575^{\circ}_{1\frac{1}{2}} - 66462_{0\frac{1}{2}}$					
3133.96		1	31899.27							
3133.845		3	31900.44	+0.03	$46169^{\circ}_{4\frac{1}{2}} - 78070_{4\frac{1}{2}}$					
3133.778		3	31901.12	−0.02	$48556^{\circ}_{3\frac{1}{2}} - 80457_{3\frac{1}{2}}$					

TABLE 6. Yb II—*Observed and classified lines*—Continued

1	2	3	4	5	6	7	8	9	10	11
Wavelength air	Intensity		Wave number	o–c	Classification	Zeeman type	1st g	2nd g	Zeeman components	
	Meggers lamp	Thomson lamp							Strong p	Strong n
Å			K	K						
3132.628	15	150	31912.83	−0.03	$33653^{\circ}_{0\frac{1}{2}} - 65566_{0\frac{1}{2}}$	6	1.32	1.42	(0.05)	1.37
3132.478	2	15	31914.36	−0.04	$43075^{\circ}_{1\frac{1}{2}} - 74989_{0\frac{1}{2}}$					
3132.294	1	8	31916.23	−0.04	$43075^{\circ}_{1\frac{1}{2}} - 74991_{1\frac{1}{2}}$					
3131.397		1	31925.38	−0.06	$61051_{3\frac{1}{2}} - 92976^{\circ}_{3\frac{1}{2}}$					
3131.38		3	31925.55							
3129.145	8	80	31948.35	−0.03	$41688^{\circ}_{1\frac{1}{2}} - 73636_{0\frac{1}{2}}$	5	0.78	0.70	(0.04)	0.82
3128.60		1	31953.92							
3127.866	20	120	31961.41	−0.04	$34389^{\circ}_{2\frac{1}{2}} - 66351_{2\frac{1}{2}}$	6	(1.01)	1.12	0.27	?
3127.64		2	31963.72	−0.01	$66558_{3\frac{1}{2}} - 98521^{\circ}_{4\frac{1}{2}}$					
3127.49		2	31965.26	+0.07	$47663^{\circ}_{4\frac{1}{2}} - 79628_{3\frac{1}{2}}$					
3127.31		2*h*	31967.10							
3127.138	4	40	31968.86	+0.02	$41688^{\circ}_{1\frac{1}{2}} - 73657_{1\frac{1}{2}}$					
3126.25	1	5	31977.94	+0.04	$31979^{\circ}_{3\frac{1}{2}} - 63957_{3\frac{1}{2}}$					
3126.192	4	20	31978.53	−0.03	$41678^{\circ}_{2\frac{1}{2}} - 73657_{1\frac{1}{2}}$					
3125.885	1	10	31981.67	−0.03	$43007^{\circ}_{0\frac{1}{2}} - 74989_{0\frac{1}{2}}$					
3125.700	5	20	31983.56	−0.01 −0.08	$43007^{\circ}_{0\frac{1}{2}} - 74991_{1\frac{1}{2}}$ $59618_{3\frac{1}{2}} - 91602^{\circ}_{2\frac{1}{2}}$					
3125.443	50	100	31986.19	−0.02	$21418^{\circ}_{3\frac{1}{2}} - 53404_{2\frac{1}{2}}$					
3124.25		2	31998.41	+0.02	$67416_{4\frac{1}{2}} - 99414^{\circ}_{4\frac{1}{2}}$					
3123.870		6	32002.30	+0.01	$37077^{\circ}_{2\frac{1}{2}} - 69079_{2\frac{1}{2}}$					
3123.510	8	60	32005.99	+0.03	$34389^{\circ}_{2\frac{1}{2}} - 66395_{2\frac{1}{2}}$					
3122.74		1	32013.88							
3122.48		3	32016.54							
3122.185	2	20	32019.57	+0.07	$45429^{\circ}_{3\frac{1}{2}} - 77449_{3\frac{1}{2}}$					
3121.38		2	32027.83	+0.10	$61214_{4\frac{1}{2}} - 93242^{\circ}_{3\frac{1}{2}}$					
3119.73		1	32044.76	+0.12	$61822_{3\frac{1}{2}} - 93867^{\circ}_{4\frac{1}{2}}$?					
3119.37		2	32048.46	+0.02	$66571_{5\frac{1}{2}} - 98620^{\circ}_{6\frac{1}{2}}$					
3119.10		1	32051.24							
3117.806	1000*r*	3000	32064.54	−0.02	$26759^{\circ}_{2\frac{1}{2}} - 58823_{2\frac{1}{2}}$	6	1.568	1.260	0.770	1.414
3116.702	60	300	32075.90	−0.02	$31979^{\circ}_{3\frac{1}{2}} - 64055_{2\frac{1}{2}}$	5	1.333	1.111	0.110	1.888
3116.487	10	70	32078.11	+0.03	$44438^{\circ}_{3\frac{1}{2}} - 76516_{4\frac{1}{2}}$					
3116.342	10	40	32079.60	−0.05	$31568^{\circ}_{2\frac{1}{2}} - 63647_{1\frac{1}{2}}$					
3116.070	15	70	32082.40	−0.03	$33494^{\circ}_{3\frac{1}{2}} - 65577_{3\frac{1}{2}}$	6	1.00	1.05	0.18	1.02
3115.340	100	400	32089.92	−0.06	$32371^{\circ}_{2\frac{1}{2}} - 64461_{1\frac{1}{2}}$	7	1.162	1.162	0	1.162
3115.25	1	8	32090.85	−0.10	$37516^{\circ}_{3\frac{1}{2}} - 69607_{2\frac{1}{2}}$					
3114.905	3	20	32094.40							
3114.69		1	32096.62							
3114.505		4	32098.52							
3112.980	1	10	32114.25	−0.04	$45335^{\circ}_{4\frac{1}{2}} - 77449_{3\frac{1}{2}}$					
3112.91		4	32114.97	−0.05	$51248^{\circ}_{2\frac{1}{2}} - 83363_{3\frac{1}{2}}$					
3111.047	1	6	32134.20	−0.04	$31568^{\circ}_{2\frac{1}{2}} - 63702_{2\frac{1}{2}}$					

TABLE 6. Yb II—*Observed and classified lines*—Continued

1	2	3	4	5	6	7	8	9	10	11
Wave-length air	Intensity		Wave number	o–c	Classification	Zeeman type	1st g	2nd g	Zeeman components	
	Meggers lamp	Thomson lamp							Strong p	Strong n
Å			K	K						
3109.786	5	40	32147.23	−0.02	$33052^{\circ}_{4\frac{1}{2}} - 65199_{4\frac{1}{2}}$					
3109.52		2	32149.98	−0.03	$45737^{\circ}_{1\frac{1}{2}} - 77887_{0\frac{1}{2}}$					
3109.10	1	5	32154.32							
3107.902	1000r	3000	32166.72	−0.07	$30392^{\circ}_{1\frac{1}{2}} - 62559_{2\frac{1}{2}}$	4	(1.333)	1.25	w	1.14
3107.760	100	500	32168.18	−0.06	$34389^{\circ}_{2\frac{1}{2}} - 66558_{3\frac{1}{2}}$	5	(1.007)	1.08	w	1.26
3106.97		2	32176.36	+0.06	$45273^{\circ}_{3\frac{1}{2}} - 77449_{3\frac{1}{2}}$					
3106.94	1	6	32176.67	−0.09	$45429^{\circ}_{3\frac{1}{2}} - 77606_{2\frac{1}{2}}$					
3106.740	2	10	32178.75	−0.05 +0.03	$44497^{\circ}_{2\frac{1}{2}} - 76676_{2\frac{1}{2}}$ $57534^{\circ}_{3\frac{1}{2}} - 89713_{2\frac{1}{2}}$					
3106.133		3	32185.03	+0.09	$48272^{\circ}_{2\frac{1}{2}} - 80457_{3\frac{1}{2}}$					
3106.007		4	32186.34	−0.04	$61822_{3\frac{1}{2}} - 94008^{\circ}_{3\frac{1}{2}}$					
3105.37		1	32192.94							
3103.81		4	32209.12							
3103.36		1	32213.79	−0.05	$43956^{\circ}_{2\frac{1}{2}} - 76170_{2\frac{1}{2}}$					
3102.71		2	32220.54							
3102.074	30	150	32227.15	−0.03	$32371^{\circ}_{2\frac{1}{2}} - 64598_{3\frac{1}{2}}$	5	(1.170)	1.23	w	1.37
3101.688		5	32231.16	+0.08	$66571_{5\frac{1}{2}} - 98802^{\circ}_{5\frac{1}{2}}$					
3101.361	50	250	32234.55	−0.05	$33653^{\circ}_{0\frac{1}{2}} - 65888_{1\frac{1}{2}}$	4	1.32	1.22	(0.05)	1.17
3101.004	15	100	32238.26	−0.02	$44438^{\circ}_{3\frac{1}{2}} - 76676_{2\frac{1}{2}}$					
3100.25		4	32246.11							
3100.03		2	32248.39	+0.04	$61214_{4\frac{1}{2}} - 93463^{\circ}_{3\frac{1}{2}}$					
3099.114	1	10	32257.93	+0.02	$66571_{5\frac{1}{2}} - 98829^{\circ}_{6\frac{1}{2}}$					
3098.850	4	10	32260.67	+0.01	$22960_{1\frac{1}{2}} - 55221^{\circ}_{1\frac{1}{2}}$					
3098.384		3	32265.52							
3097.331	1	8	32276.49	−0.02	$47329^{\circ}_{2\frac{1}{2}} - 79605_{1\frac{1}{2}}$					
3096.278		4	32287.47							
3096.10		1	32289.33	+0.10	$61214_{4\frac{1}{2}} - 93503^{\circ}_{4\frac{1}{2}}$					
3095.415	30	60	32296.47	−0.04	$21418^{\circ}_{3\frac{1}{2}} - 53715_{3\frac{1}{2}}$					
3095.221	10	60	32298.50	+0.02	$30562^{\circ}_{5\frac{1}{2}} - 62861_{5\frac{1}{2}}$	6	(1.112)	1.15	w	1.13
3094.894	100	200	32301.91	−0.05	$21418^{\circ}_{3\frac{1}{2}} - 53720_{4\frac{1}{2}}$					
3093.870	200r	1000	32312.60	+0.01	$31631^{\circ}_{6\frac{1}{2}} - 63944_{5\frac{1}{2}}$	5	1.24	1.13	(0.056)	1.86
3093.423	3	30	32317.27	+0.07	$35831^{\circ}_{5\frac{1}{2}} - 68148_{5\frac{1}{2}}$	6	(1.214)	1.23	w	1.22
3093.40	1	10	32317.51	−0.10 −0.07	$37077^{\circ}_{2\frac{1}{2}} - 69395_{3\frac{1}{2}}$ $45429^{\circ}_{3\frac{1}{2}} - 77747_{4\frac{1}{2}}$					
3092.10	1	8	32331.10	−0.01	$26759^{\circ}_{2\frac{1}{2}} - 59090_{3\frac{1}{2}}$					
3091.10	1	6	32341.55	+0.06	$44497^{\circ}_{2\frac{1}{2}} - 76839_{2\frac{1}{2}}$					
3090.924	6	15	32343.40	−0.01	$44940^{\circ}_{1\frac{1}{2}} - 77284_{1\frac{1}{2}}$					
3090.747	1	10	32345.25	+0.04	$56375_{2\frac{1}{2}} - 88721^{\circ}_{3\frac{1}{2}}$					
3089.61	3	20	32357.15	+0.12	$35059^{\circ}_{3\frac{1}{2}} - 67416_{4\frac{1}{2}}$					
3089.102	150r	500	32362.47	−0.04	$28757^{\circ}_{1\frac{1}{2}} - 61120_{0\frac{1}{2}}$	4	1.437	1.658	0.110	1.325

TABLE 6. Yb II—*Observed and classified lines*—Continued

1	2	3	4	5	6	7	8	9	10	11
Wave-length air	Intensity		Wave number	o–c	Classification	Zeeman type	1st g	2nd g	Zeeman components	
	Meggers lamp	Thomson lamp							Strong p	Strong n
Å			K	K						
3088.823	3	30	32365.39	−0.05	$40917_{4\frac{1}{2}}^{\circ} - 73283_{4\frac{1}{2}}$					
3088.78	1	9	32365.84	−0.09	$37077_{2\frac{1}{2}}^{\circ} - 69443_{1\frac{1}{2}}$					
3088.66		3	32367.10	+0.02	$43956_{2\frac{1}{2}}^{\circ} - 76323_{3\frac{1}{2}}$					
3087.998	1	15	32374.04	0.00	$40917_{4\frac{1}{2}}^{\circ} - 73291_{5\frac{1}{2}}$					
3087.720		6	32376.96	−0.03	$47228_{0\frac{1}{2}}^{\circ} - 79605_{1\frac{1}{2}}$					
3087.46		2	32379.68							
3086.971	10	100	32384.81	+0.03	$39378_{0\frac{1}{2}}^{\circ} - 71763_{1\frac{1}{2}}$	4	1.84	1.10	0.37	0.72
3086.508	8	40	32389.67	−0.05	$31568_{2\frac{1}{2}}^{\circ} - 63957_{3\frac{1}{2}}$					
3085.817	10	70	32396.92	+0.02	$35019_{4\frac{1}{2}}^{\circ} - 67416_{4\frac{1}{2}}$	6	1.16	1.26	0.44	1.21
3085.434	9	60	32400.94	−0.03	$44438_{3\frac{1}{2}}^{\circ} - 76839_{2\frac{1}{2}}$					
3084.347	7	70	32412.36	−0.01	$45335_{4\frac{1}{2}}^{\circ} - 77747_{4\frac{1}{2}}$	6	1.00	1.07	0.30	1.04?
3083.809		3	32418.02							
3083.44		1	32421.89							
3082.34		1	32433.46	+0.05	$53715_{3\frac{1}{2}} - 86148_{2\frac{1}{2}}^{\circ}$					
3082.264		6	32434.26							
3082.05		1	32436.52	−0.01	$45012_{2\frac{1}{2}}^{\circ} - 77449_{3\frac{1}{2}}$					
3081.625		8	32440.99	+0.09	$37516_{3\frac{1}{2}}^{\circ} - 69957_{4\frac{1}{2}}$					
3081.18		1	32445.67							
3080.552	3	30	32452.29	+0.07	$45429_{3\frac{1}{2}}^{\circ} - 77882_{3\frac{1}{2}}$	6	1.15	1.13	(0.07)	1.14
3080.49		3	32452.94	+0.11	$61051_{3\frac{1}{2}} - 93503_{4\frac{1}{2}}^{\circ}$?					
3080.17	3	20	32456.31	+0.04	$33494_{3\frac{1}{2}}^{\circ} - 65950_{4\frac{1}{2}}$					
3079.593		7	32462.39	+0.09	$61873_{6\frac{1}{2}} - 94335_{5\frac{1}{2}}^{\circ}$					
3078.450	1	10	32474.45	+0.07	$45273_{3\frac{1}{2}}^{\circ} - 77747_{4\frac{1}{2}}$					
3078.31	1	10	32475.92	+0.07	$43075_{1\frac{1}{2}}^{\circ} - 75550_{2\frac{1}{2}}$					
3077.82		2	32481.09	+0.09	$61822_{3\frac{1}{2}} - 94303_{3\frac{1}{2}}^{\circ}$					
3077.34		7	32486.16							
3077.18		8	32487.85	+0.11	$31568_{2\frac{1}{2}}^{\circ} - 64055_{2\frac{1}{2}}$?					
3077.14		6	32488.27	+0.04	$64598_{3\frac{1}{2}} - 97086_{4\frac{1}{2}}^{\circ}$					
3076.50		1	32495.03	+0.09	$61051_{3\frac{1}{2}} - 93546_{2\frac{1}{2}}^{\circ}$					
3076.013	30	150	32500.17	−0.05	$26759_{2\frac{1}{2}}^{\circ} - 59259_{2\frac{1}{2}}$	6	1.572	1.104	1.170	1.338
3075.10		2	32509.82							
3074.92		2	32511.73							
3074.84		3	32512.57							
3074.50	1	10	32516.17	+0.01	$38342_{4\frac{1}{2}}^{\circ} - 70858_{4\frac{1}{2}}$					
3073.89		3	32522.62							
3073.680	20	100	32524.84	+0.02	$33052_{4\frac{1}{2}}^{\circ} - 65577_{3\frac{1}{2}}$					
3073.19		3	32530.03	+0.08	$37077_{2\frac{1}{2}}^{\circ} - 69607_{2\frac{1}{2}}$					
3072.486	6	60	32537.48	+0.06	$61822_{3\frac{1}{2}} - 94360_{4\frac{1}{2}}^{\circ}$					
3072.41		4	32538.29	+0.03	$63944_{5\frac{1}{2}} - 96482_{4\frac{1}{2}}^{\circ}$					
3071.583	5	50	32547.05	+0.04	$45335_{4\frac{1}{2}}^{\circ} - 77882_{3\frac{1}{2}}$					
3071.26		1	32550.47							

TABLE 6. Yb II—*Observed and classified lines*—Continued

1	2	3	4	5	6	7	8	9	10	11
Wave-length air	Intensity		Wave number	o–c	Classification	Zeeman type	1st g	2nd g	Zeeman components	
	Meggers lamp	Thomson lamp							Strong p	Strong n
Å			K	K						
3070.28	2	7	32560.86	+0.06	$43956^{\circ}_{2\frac{1}{2}} - 76517_{1\frac{1}{2}}$					
3069.34		2	32570.83	+0.05	$65950_{4\frac{1}{2}} - 98521^{\circ}_{4\frac{1}{2}}$					
3068.69	1	10	32577.73	+0.08	$47005^{\circ}_{1\frac{1}{2}} - 79583_{2\frac{1}{2}}$					
3068.284	7	60	32582.04	+0.01	$41688^{\circ}_{1\frac{1}{2}} - 74270_{2\frac{1}{2}}$					
3067.986	2	10	32585.20	+0.07	$32981^{\circ}_{1\frac{1}{2}} - 65566_{0\frac{1}{2}}$					
3067.365	10	70	32591.80	+0.05	$41678^{\circ}_{2\frac{1}{2}} - 74270_{2\frac{1}{2}}$	6	(1.19)	0.93	0.65	?
3066.54		2	32600.57	+0.08	$47005^{\circ}_{1\frac{1}{2}} - 79605_{1\frac{1}{2}}$					
3066.487	2	6	32601.13	+0.13	$30562^{\circ}_{5\frac{1}{2}} - 63163_{4\frac{1}{2}}$?					
3065.74		7	32609.07	+0.05	$45273^{\circ}_{3\frac{1}{2}} - 77882_{3\frac{1}{2}}$					
3065.52		2	32611.41							
3065.48		1	32611.84							
3065.040	300	1000	32616.52	+0.01	$28757^{\circ}_{1\frac{1}{2}} - 61374_{2\frac{1}{2}}$	4	1.45	1.30	0.075	1.08
3064.868	30	150	32618.35	−0.03	$31979^{\circ}_{3\frac{1}{2}} - 64598_{3\frac{1}{2}}$					
3064.75		2	32619.61	−0.01	$30392^{\circ}_{1\frac{1}{2}} - 63011_{1\frac{1}{2}}$					
3063.80		4	32629.72	+0.12	$34575^{\circ}_{1\frac{1}{2}} - 67204_{1\frac{1}{2}}$?					
3063.671	20	100	32631.10	+0.02	$34784^{\circ}_{5\frac{1}{2}} - 67416_{4\frac{1}{2}}$					
3063.350	2	10	32634.51	+0.04	$61374_{2\frac{1}{2}} - 94008^{\circ}_{3\frac{1}{2}}$					
3063.125	40	200	32636.91	−0.03	$30224^{\circ}_{4\frac{1}{2}} - 62861_{5\frac{1}{2}}$	5	0.935	1.137	0.101	2.047
3062.524		4	32643.32							
3062.06		1	32648.26	+0.06	$49008^{\circ}_{3\frac{1}{2}} - 81657_{2\frac{1}{2}}$					
3061.646		6	32652.68	+0.12	$61214_{4\frac{1}{2}} - 93867^{\circ}_{4\frac{1}{2}}$?					
3060.394		7	32666.03	+0.06	$44940^{\circ}_{1\frac{1}{2}} - 77606_{2\frac{1}{2}}$					
3059.568		7	32674.85	+0.06	$66571_{5\frac{1}{2}} - 99246^{\circ}_{5\frac{1}{2}}$					
3059.362		4	32677.05							
3058.71		2	32684.02	+0.03	$49008^{\circ}_{3\frac{1}{2}} - 81692_{3\frac{1}{2}}$					
3058.66		5	32684.55							
3058.288		4	32688.53							
3058.20		1	32689.47							
3057.29		1	32699.20	+0.03	$47758^{\circ}_{3\frac{1}{2}} - 80457_{3\frac{1}{2}}$					
3056.01		2	32712.89	+0.07	$58823_{2\frac{1}{2}} - 91536^{\circ}_{3\frac{1}{2}}$					
3055.60		1	32717.28							
3055.46		2	32718.78							
3055.350	5	15	32719.96	+0.06	$43956^{\circ}_{2\frac{1}{2}} - 76676_{2\frac{1}{2}}$					
3055.157	10	60	32722.03	−0.01	$32371^{\circ}_{2\frac{1}{2}} - 65093_{3\frac{1}{2}}$	4	1.168	0.978	0.095	0.503
3054.649	1	10	32727.47	0.00	$45737^{\circ}_{1\frac{1}{2}} - 78464_{1\frac{1}{2}}$					
3053.928	2	20	32735.20	+0.04	$45335^{\circ}_{4\frac{1}{2}} - 78070_{4\frac{1}{2}}$					
3053.452		8	32740.30							
3053.084	1	10	32744.24	+0.07 −0.01	$40035^{\circ}_{3\frac{1}{2}} - 72779_{3\frac{1}{2}}$ $65875_{6\frac{1}{2}} - 98620^{\circ}_{6\frac{1}{2}}$					
3052.20		2	32753.73							

TABLE 6. Yb II—*Observed and classified lines*—Continued

1	2	3	4	5	6	7	8	9	10	11
Wave-length air	Intensity		Wave number	o–c	Classification	Zeeman type	1st g	2nd g	Zeeman components	
	Meggers lamp	Thomson lamp							Strong p	Strong n
Å			K	K						
3052.021	1	7	32755.65	+0.04	$63726_{4\frac{1}{2}} - 96482^{\circ}_{4\frac{1}{2}}$					
3051.98		2	32756.09	+0.01	$48556^{\circ}_{3\frac{1}{2}} - 81312_{2\frac{1}{2}}$					
3051.11		2	32765.43							
3050.64		1	32770.48							
3050.50		6	32771.98							
3049.84		2	32779.07	+0.11	$58823_{2\frac{1}{2}} - 91602^{\circ}_{2\frac{1}{2}}$					
3049.14		7	32786.60	+0.09	$44497^{\circ}_{2\frac{1}{2}} - 77284_{1\frac{1}{2}}$					
3048.82		2	32790.04							
3048.41		6	32794.45	+0.15	$61214_{4\frac{1}{2}} - 94008^{\circ}_{3\frac{1}{2}}$?					
3048.15		2	32797.24	+0.07	$45273^{\circ}_{3\frac{1}{2}} - 78070_{4\frac{1}{2}}$					
3047.052	20	100	32809.06	+0.06	$33653^{\circ}_{0\frac{1}{2}} - 66462_{0\frac{1}{2}}$	6	1.315	1.107	0.104	1.211
3046.482	30	200	32815.20	−0.01	$34389^{\circ}_{2\frac{1}{2}} - 67204_{1\frac{1}{2}}$	4	(1.007)	1.03	w	0.97
3046.27		3	32817.48							
3045.91		2	32821.36	+0.01	$53404_{2\frac{1}{2}} - 86226^{\circ}_{1\frac{1}{2}}$					
3045.84		1	32822.12							
3045.46		4	32826.21							
3045.044	1	7	32830.70	+0.02	$43075^{\circ}_{1\frac{1}{2}} - 75905_{0\frac{1}{2}}$					
3044.83	10	60	32833.00	+0.01	$40917^{\circ}_{4\frac{1}{2}} - 73750_{4\frac{1}{2}}$	6	0.97	0.99	0.07?	0.98?
3044.004	20	100	32841.91	+0.03	$30392^{\circ}_{1\frac{1}{2}} - 63234_{2\frac{1}{2}}$	4	1.335	1.205	(0.065)	1.01
3043.93		4	32842.71	+0.05	$43956^{\circ}_{2\frac{1}{2}} - 76799_{1\frac{1}{2}}$					
3043.07		1	32851.99							
3042.78		3	32855.12							
3042.650	50	300	32856.53	0.00	$33494^{\circ}_{3\frac{1}{2}} - 66351_{2\frac{1}{2}}$	4	0.990	1.122	(0.066)	0.66
3042.34		2	32859.87	−0.01	$26759^{\circ}_{2\frac{1}{2}} - 59618_{3\frac{1}{2}}$					
3040.83		2	32876.19							
3040.504	5	30	32879.72	+0.04	$35059^{\circ}_{3\frac{1}{2}} - 67938_{3\frac{1}{2}}$					
3040.444	2	15	32880.37	+0.03	$38342^{\circ}_{4\frac{1}{2}} - 71222_{3\frac{1}{2}}$					
3040.235	5	15	32882.63	+0.04	$43956^{\circ}_{2\frac{1}{2}} - 76839_{2\frac{1}{2}}$					
3039.665	40	300	32888.79	+0.03	$35831^{\circ}_{5\frac{1}{2}} - 68720_{6\frac{1}{2}}$	4	1.211	1.159	(0.026)	0.871
3039.276		6	32893.00	0.00	$31568^{\circ}_{2\frac{1}{2}} - 64461_{1\frac{1}{2}}$					
				−0.03	$62861_{5\frac{1}{2}} - 95754^{\circ}_{5\frac{1}{2}}$					
3038.81		2	32898.04	+0.06	$43007^{\circ}_{0\frac{1}{2}} - 75905_{0\frac{1}{2}}$					
3038.75	2	10	32898.69	+0.03	$33052^{\circ}_{4\frac{1}{2}} - 65950_{4\frac{1}{2}}$					
3038.531	5	30	32901.07	+0.03	$33494^{\circ}_{3\frac{1}{2}} - 66395_{2\frac{1}{2}}$					
3037.992	15	90	32906.90	+0.03	$32981^{\circ}_{1\frac{1}{2}} - 65888_{1\frac{1}{2}}$	6	0.865	1.204	0.508	1.035
3036.820	10	60	32919.60	+0.05	$35019^{\circ}_{4\frac{1}{2}} - 67938_{3\frac{1}{2}}$					
3036.13		1	32927.08							
3035.945	1	7	32929.09	0.00	$61374_{2\frac{1}{2}} - 94303^{\circ}_{3\frac{1}{2}}$					
3034.99	1	5	32939.45	−0.01	$30224^{\circ}_{4\frac{1}{2}} - 63163_{4\frac{1}{2}}$					
3034.642	40	200	32943.23	+0.02	$31979^{\circ}_{3\frac{1}{2}} - 64923_{4\frac{1}{2}}$	4	1.336	1.113	0.111	0.330

TABLE 6. Yb II—*Observed and classified lines*—Continued

1	2	3	4	5	6	7	8	9	10	11
Wavelength air	Intensity		Wave number	o–c	Classification	Zeeman type	1st g	2nd g	Zeeman components	
	Meggers lamp	Thomson lamp							Strong p	Strong n
Å			K	K						
3034.52		2	32944.55	−0.07	$65577_{3\frac{1}{2}} - 98521^{\circ}_{4\frac{1}{2}}$					
3034.32		1	32946.72	+0.03	$44940^{\circ}_{1\frac{1}{2}} - 77887_{0\frac{1}{2}}$					
3033.860	30	100	32951.72	+0.09 −0.09	$26759^{\circ}_{2\frac{1}{2}} - 59710_{1\frac{1}{2}}$ $44497^{\circ}_{2\frac{1}{2}} - 77449_{3\frac{1}{2}}$					
3033.664	2	10	32953.85	0.00	$63944_{5\frac{1}{2}} - 96898^{\circ}_{5\frac{1}{2}}$					
3033.40		2	32956.72							
3033.28		1	32958.02	+0.12	$61051_{3\frac{1}{2}} - 94008^{\circ}_{3\frac{1}{2}}$					
3033.14		1	32959.54	0.00	$60586_{1\frac{1}{2}} - 93546^{\circ}_{2\frac{1}{2}}$					
3031.110	5000*A*	3000	32981.61	+0.02	$0_{0\frac{1}{2}} - 32981^{\circ}_{1\frac{1}{2}}$	4	1.996	0.864	0.566	0.298
3028.38	2	20	33011.34	+0.05	$44438^{\circ}_{3\frac{1}{2}} - 77449_{3\frac{1}{2}}$					
3026.669	100	700	33030.00	+0.04	$33052^{\circ}_{4\frac{1}{2}} - 66082_{5\frac{1}{2}}$	4	1.266	1.140	(0.063)	0.570
3025.76		2	33039.93	+0.05	$48272^{\circ}_{2\frac{1}{2}} - 81312_{2\frac{1}{2}}$					
3025.38		6	33044.08	+0.08	$59259_{2\frac{1}{2}} - 92303^{\circ}_{3\frac{1}{2}}$					
3024.935	2	15	33048.94	+0.04	$40917^{\circ}_{4\frac{1}{2}} - 73966_{3\frac{1}{2}}$					
3023.614	5	30	33063.38	+0.06	$33494^{\circ}_{3\frac{1}{2}} - 66558_{3\frac{1}{2}}$	6	0.99	1.09	0.35	1.04
3022.58		1	33074.69							
3022.454	10	60	33076.07	+0.07	$35059^{\circ}_{3\frac{1}{2}} - 68135_{2\frac{1}{2}}$	7	1.11	(1.087)	*w*	1.17
3021.27		1	33089.03	+0.11	$61214_{4\frac{1}{2}} - 94303^{\circ}_{3\frac{1}{2}}$					
3020.99		4	33092.09							
3020.703	20	100	33095.24	+0.08	$43075^{\circ}_{1\frac{1}{2}} - 76170_{2\frac{1}{2}}$	5				
3020.345	2	10	33099.16	+0.06	$63944_{5\frac{1}{2}} - 97043^{\circ}_{6\frac{1}{2}}$					
3020.211		5	33100.63	+0.07	$48556^{\circ}_{3\frac{1}{2}} - 81657_{2\frac{1}{2}}$					
3019.440	2	15	33109.08	+0.01	$44497^{\circ}_{2\frac{1}{2}} - 77606_{2\frac{1}{2}}$					
3019.17		2	33112.04	+0.07	$35831^{\circ}_{5\frac{1}{2}} - 68943_{4\frac{1}{2}}$					
3019.058	8	40	33113.27	+0.03	$31979^{\circ}_{3\frac{1}{2}} - 65093_{3\frac{1}{2}}$					
3017.560	100	800	33129.71	−0.04	$35019^{\circ}_{4\frac{1}{2}} - 68148_{5\frac{1}{2}}$	5	(1.158)	1.20	*w*	1.40
3016.95		6	33136.41	+0.06	$48556^{\circ}_{3\frac{1}{2}} - 81692_{3\frac{1}{2}}$					
3016.40		1	33142.45							
3014.97		2	33158.17							
3014.526	10	60	33163.05			7			0	1.12
3014.427	40	200	33164.14	+0.10 +0.02	$30562^{\circ}_{5\frac{1}{2}} - 63726_{4\frac{1}{2}}$ $(66082_{5\frac{1}{2}} - 99246^{\circ}_{5\frac{1}{2}})$	5	1.11	1.01	(0.05)	1.56
3014.02		8	33168.62	+0.07	$44438^{\circ}_{3\frac{1}{2}} - 77606_{2\frac{1}{2}}$					
3013.08		2	33178.96							
3012.80		3	33182.05							
3012.28		1	33187.77							
3011.842		4	33192.60							
3011.00		1	33201.88	+0.12	$24332_{2\frac{1}{2}} - 57534^{\circ}_{3\frac{1}{2}}$					
3010.625	50	300	33206.02	+0.01	$32371^{\circ}_{2\frac{1}{2}} - 65577_{3\frac{1}{2}}$	4	1.17	1.05	0.06	0.75
3009.392	100	500	33219.62	−0.02	$31979^{\circ}_{3\frac{1}{2}} - 65199_{4\frac{1}{2}}$	4	1.328	1.076	0.126	0.195

TABLE 6. Yb II—*Observed and classified lines*—Continued

1	2	3	4	5	6	7	8	9	10	11
Wave-length air	Intensity		Wave number	o–c	Classification	Zeeman type	1st g	2nd g	Zeeman components	
	Meggers lamp	Thomson lamp							Strong p	Strong n
Å			K	K						
3007.923	5	30	33235.85							
3007.56		3	33239.86	+0.01	$48272^{\circ}_{2\frac{1}{2}} - 81512_{1\frac{1}{2}}$					
3006.863	10	70	33247.56	+0.03	$40035^{\circ}_{3\frac{1}{2}} - 73283_{4\frac{1}{2}}$	5	0.720	1.020	0.150	2.070
3006.30		3	33253.79							
3006.14	5	40	33255.56	+0.06	$30392^{\circ}_{1\frac{1}{2}} - 63647_{1\frac{1}{2}}$					
3005.766	800*r*	3000	33259.70	−0.01	$31631^{\circ}_{6\frac{1}{2}} - 64891_{7\frac{1}{2}}$	4	(1.230)	1.20	*w*	1.02
3004.642	1	15	33272.14							
3004.46	3	10*h*	33274.15	−0.01	$46354^{\circ}_{4\frac{1}{2}} - 79628_{3\frac{1}{2}}$					
3004.097	1	5	33278.17	+0.06	$60586_{1\frac{1}{2}} - 93864^{\circ}_{2\frac{1}{2}}$					
3003.60		2	33283.68							
3002.608	30	200	33294.68	0.00	$41678^{\circ}_{2\frac{1}{2}} - 74973_{3\frac{1}{2}}$					
3002.47		2	33296.21							
3002.035	5	30	33301.03	−0.01	$41688^{\circ}_{1\frac{1}{2}} - 74989_{0\frac{1}{2}}$	5	0.80	0.52	0.14	0.94
3001.864	2	10	33302.93	+0.02	$41688^{\circ}_{1\frac{1}{2}} - 74991_{1\frac{1}{2}}$					
3001.283	4	40	33309.37	0.00	$44438^{\circ}_{3\frac{1}{2}} - 77747_{4\frac{1}{2}}$	4	(1.10)	1.10	*w*	1.09
3000.987	2	15	33312.66	+0.03	$41678^{\circ}_{2\frac{1}{2}} - 74991_{1\frac{1}{2}}$					
3000.465	100	300	33318.45	−0.02	$42915^{\circ}_{5\frac{1}{2}} - 76233_{6\frac{1}{2}}$	4	(1.115)	1.10	*w*	1.05
3000.13		2	33322.17	−0.02	$65199_{4\frac{1}{2}} - 98521^{\circ}_{3\frac{1}{2}}$					
2999.642	5	10	33327.59	−0.02	$43956^{\circ}_{2\frac{1}{2}} - 77284_{1\frac{1}{2}}$					
2998.377	4	30	33341.66	+0.07	$37516^{\circ}_{3\frac{1}{2}} - 70858_{4\frac{1}{2}}$					
2996.75		2	33359.76	+0.08	$63726_{4\frac{1}{2}} - 97086^{\circ}_{4\frac{1}{2}}$					
2996.373		5	33363.95	+0.02	$34784^{\circ}_{5\frac{1}{2}} - 68148_{5\frac{1}{2}}$					
2995.862	20	100	33369.64	+0.02 −0.02	$32981^{\circ}_{1\frac{1}{2}} - 66351_{2\frac{1}{2}}$ $(41688^{\circ}_{1\frac{1}{2}} - 75058_{2\frac{1}{2}})$	5	0.880	1.128	0.124	1.500
2995.03	6	30	33378.91	−0.05	$28757^{\circ}_{1\frac{1}{2}} - 62136_{0\frac{1}{2}}$					
2994.94	2	20	33379.92	+0.06	$34575^{\circ}_{1\frac{1}{2}} - 67955_{0\frac{1}{2}}$					
2994.805	150	600	33381.42	+0.03	$30562^{\circ}_{5\frac{1}{2}} - 63944_{5\frac{1}{2}}$	6	1.101	1.119	0.10	1.110
2994.53	2	20	33384.49	−0.04	$44497^{\circ}_{2\frac{1}{2}} - 77882_{3\frac{1}{2}}$					
2994.48	1	10	33385.04	0.00	$45429^{\circ}_{3\frac{1}{2}} - 78814_{2\frac{1}{2}}$					
2993.939	10	70	33391.08	−0.03	$35059^{\circ}_{3\frac{1}{2}} - 68450_{3\frac{1}{2}}$	6	1.12	1.08	0.14	1.10
2992.28		5	33409.59							
2991.872	40	200	33414.14	+0.01	$32981^{\circ}_{1\frac{1}{2}} - 66395_{2\frac{1}{2}}$	5	0.867	1.248	0.189	1.813
2991.70	5	9	33416.07	−0.05	$28757^{\circ}_{1\frac{1}{2}} - 62174_{1\frac{1}{2}}$					
2991.33		1	33420.20	+0.05	$48272^{\circ}_{2\frac{1}{2}} - 81692_{3\frac{1}{2}}$					
2991.240	1	6	33421.20							
2990.366	30	200	33430.97	−0.01	$35019^{\circ}_{4\frac{1}{2}} - 68450_{3\frac{1}{2}}$	5	(1.158)	1.09	*w*	1.38
2989.768	2	15	33437.66	−0.02	$37516^{\circ}_{3\frac{1}{2}} - 70954_{2\frac{1}{2}}$					
2989.376	6	10	33442.04	−0.08	$43075^{\circ}_{1\frac{1}{2}} - 76517_{1\frac{1}{2}}$					
2989.20	2	20	33444.01	0.00	$44438^{\circ}_{3\frac{1}{2}} - 77882_{3\frac{1}{2}}$	6	1.09	1.12	0.12	1.106
2988.95		5*h*	33446.81	+0.08	$47758^{\circ}_{3\frac{1}{2}} - 81205_{4\frac{1}{2}}$					
2988.56		1	33451.17							

TABLE 6. Yb II—*Observed and classified lines*—Continued

1	2	3	4	5	6	7	8	9	10	11
Wavelength air	Intensity		Wave number	o–c	Classification	Zeeman type	1st g	2nd g	Zeeman components	
	Meggers lamp	Thomson lamp							Strong p	Strong n
Å			K	K						
2988.30		2	33454.08	+0.09	$66571_{5\frac{1}{2}} - 100025^{\circ}_{5\frac{1}{2}}$					
2987.862	1	10	33458.99	+0.06	$46169^{\circ}_{4\frac{1}{2}} - 79628_{3\frac{1}{2}}$					
2987.25	1	6	33465.84	+0.02	$24332_{2\frac{1}{2}} - 57798^{\circ}_{2\frac{1}{2}}$					
2986.64		2	33472.68	+0.06	$57765_{4\frac{1}{2}} - 91237^{\circ}_{3\frac{1}{2}}$					
2986.47		1	33474.58							
2985.876	10	70	33481.24	−0.03	$32981^{\circ}_{1\frac{1}{2}} - 66462_{0\frac{1}{2}}$	4	0.864	1.100	0.118	0.746
2985.078	50	300	33490.19	−0.04	$35059^{\circ}_{3\frac{1}{2}} - 68549_{4\frac{1}{2}}$	5	(1.124)	1.15	w	1.24
2984.84	7	60	33492.86	−0.05	$43956^{\circ}_{2\frac{1}{2}} - 77449_{3\frac{1}{2}}$					
2984.44		1	33497.35							
2983.990	200r	1000	33502.40	−0.10	$30224^{\circ}_{4\frac{1}{2}} - 63726_{4\frac{1}{2}}$	6	0.94	1.00	0.26	0.97
2983.702	15	100	33505.64	−0.07	$33052^{\circ}_{4\frac{1}{2}} - 66558_{3\frac{1}{2}}$					
2983.369	4	8	33509.37	−0.05	$43007^{\circ}_{0\frac{1}{2}} - 76517_{1\frac{1}{2}}$					
2982.659	10	70	33517.35	−0.01	$32371^{\circ}_{2\frac{1}{2}} - 65888_{1\frac{1}{2}}$	4	(1.170)	1.20	w	1.13
2982.494	20	150	33519.21	−0.08	$33052^{\circ}_{4\frac{1}{2}} - 66571_{5\frac{1}{2}}$	4	(1.264)	1.20	w	0.90
2982.055	2	8	33524.14	−0.01	$44940^{\circ}_{1\frac{1}{2}} - 78464_{1\frac{1}{2}}$					
2982.01		5	33524.65	+0.01	$27061^{\circ}_{0\frac{1}{2}} - 60586_{1\frac{1}{2}}$					
2981.519	3	20	33530.17	+0.07	$35019^{\circ}_{4\frac{1}{2}} - 68549_{4\frac{1}{2}}$					
2980.482		5	33541.83	−0.01 +0.08	$45273^{\circ}_{3\frac{1}{2}} - 78814_{2\frac{1}{2}}$ $47663^{\circ}_{4\frac{1}{2}} - 81205_{4\frac{1}{2}}$					
2979.859	10	60	33548.84	−0.08	$34389^{\circ}_{2\frac{1}{2}} - 67938_{3\frac{1}{2}}$	4	(1.007)	0.98	w	0.90
2979.658	3	20	33551.11	0.00	$33653^{\circ}_{0\frac{1}{2}} - 67204_{1\frac{1}{2}}$	4	1.32	1.04	0.14	0.90
2979.44		1	33553.56							
2978.906	6	40	33559.58	−0.05	$34575^{\circ}_{1\frac{1}{2}} - 68135_{2\frac{1}{2}}$	4	1.435	1.085	0.175	0.560
2977.76		1	33572.49							
2977.695		4	33573.22							
2977.525	10	60	33575.14	−0.06	$34575^{\circ}_{1\frac{1}{2}} - 68150_{1\frac{1}{2}}$	6	1.435	0.925	0.776	1.180
2977.270	1	9	33578.02							
2976.53		1	33586.36							
2975.567	3	20	33597.23	+0.02	$31979^{\circ}_{3\frac{1}{2}} - 65577_{3\frac{1}{2}}$					
2975.238		6	33600.95	−0.03	$42915^{\circ}_{5\frac{1}{2}} - 76516_{4\frac{1}{2}}$					
2973.36		1	33622.17							
2972.94		6	33626.92							
2972.47	3	30	33632.24	+0.08	$44438^{\circ}_{3\frac{1}{2}} - 78070_{4\frac{1}{2}}$	7	(1.10)	1.11	0	1.13
2970.84	20	200	33650.69	+0.02	$40917^{\circ}_{4\frac{1}{2}} - 74568_{4\frac{1}{2}}$	6	0.97	1.03	0.27	1.00
2970.564	4000A	3000	33653.82	−0.04	$0_{0\frac{1}{2}} - 33653^{\circ}_{0\frac{1}{2}}$	6	2.001	1.324	0.338	1.663
2969.70	1	7	33663.61	+0.02	$30392^{\circ}_{1\frac{1}{2}} - 64055_{2\frac{1}{2}}$					
2967.72		4	33686.06	+0.09	$58961_{5\frac{1}{2}} - 92647^{\circ}_{5\frac{1}{2}}$					
2966.763	20	100	33696.93	−0.11 −0.08	$35059^{\circ}_{3\frac{1}{2}} - 68756_{3\frac{1}{2}}$ $45429^{\circ}_{3\frac{1}{2}} - 79126_{4\frac{1}{2}}$	7			0	1.144
2965.168	8	60	33715.06	−0.02	$40035^{\circ}_{3\frac{1}{2}} - 73750_{4\frac{1}{2}}$	5				
2964.82		4	33719.01							

277-259 O - 68 - 9

TABLE 6. Yb II—*Observed and classified lines*—Continued

1	2	3	4	5	6	7	8	9	10	11
Wave-length air	Intensity		Wave number	o–c	Classification	Zeeman type	1st g	2nd g	Zeeman components	
	Meggers lamp	Thomson lamp							Strong p	Strong n
Å			K	K						
2964.755	100r	500	33719.75	−0.10	$30224^{\circ}_{4\frac{1}{2}} - 63944_{5\frac{1}{2}}$	5	0.944	1.110	0.083	1.852
2964.39	15	100	33723.90	−0.08	$43075^{\circ}_{1\frac{1}{2}} - 76799_{1\frac{1}{2}}$	6	0.97	0.85	0.17	0.91
2963.96		4	33728.80	+0.08	$64891_{7\frac{1}{2}} - 98620^{\circ}_{6\frac{1}{2}}$					
2963.46	40	300	33734.49			6			0.16	1.08
2963.255	10	70	33736.82	−0.09	$35019^{\circ}_{4\frac{1}{2}} - 68756_{3\frac{1}{2}}$					
2963.17	8	50	33737.79	−0.03	$39378^{\circ}_{0\frac{1}{2}} - 73116_{1\frac{1}{2}}$					
2962.522	40	250	33745.17	−0.07	$34389^{\circ}_{2\frac{1}{2}} - 68135_{2\frac{1}{2}}$	6	1.00	1.08	0.19	1.04
2961.801	4	30	33753.38	−0.04	$37516^{\circ}_{3\frac{1}{2}} - 71270_{2\frac{1}{2}}$					
2961.150	1	6	33760.80	−0.01	$34389^{\circ}_{2\frac{1}{2}} - 68150_{1\frac{1}{2}}$					
2960.850	10	60	33764.22	−0.06	$34784^{\circ}_{5\frac{1}{2}} - 68549_{4\frac{1}{2}}$	4	1.13	(1.157)	w	1.01
2958.425		3	33791.90	+0.10	$45335^{\circ}_{4\frac{1}{2}} - 79126_{4\frac{1}{2}}$					
2957.632	40	150	33800.96	−0.08	$28757^{\circ}_{1\frac{1}{2}} - 62559_{2\frac{1}{2}}$					
2957.05		3	33807.61							
2955.61		2	33824.08	+0.06	$59090_{3\frac{1}{2}} - 92914^{\circ}_{4\frac{1}{2}}$					
2955.318	40	200	33827.42	−0.02	$26759^{\circ}_{2\frac{1}{2}} - 60586_{1\frac{1}{2}}$	5	1.576	1.334	0.121	1.940
2955.09	1	4	33830.03	−0.03	$24332_{2\frac{1}{2}} - 58162^{\circ}_{1\frac{1}{2}}$					
2954.45		1	33837.36	+0.05	$65577_{3\frac{1}{2}} - 99414^{\circ}_{4\frac{1}{2}}$					
2953.016	5	40	33853.79	−0.02	$45273^{\circ}_{3\frac{1}{2}} - 79126_{4\frac{1}{2}}$	4	(1.18)	1.15	w	1.03
2952.475		4	33859.99	−0.02	$38342^{\circ}_{3\frac{1}{2}} - 72202_{3\frac{1}{2}}$					
2952.253	1	10	33862.54	+0.05	$41688^{\circ}_{1\frac{1}{2}} - 75550_{2\frac{1}{2}}$					
2951.716	1	8	33868.70	+0.04	$45737^{\circ}_{1\frac{1}{2}} - 79605_{1\frac{1}{2}}$					
				−0.04	$61822_{3\frac{1}{2}} - 95691^{\circ}_{3\frac{1}{2}}$					
2951.406	5	40	33872.26	+0.05	$41678^{\circ}_{2\frac{1}{2}} - 75550_{2\frac{1}{2}}$					
2951.022	8	50	33876.67	−0.01	$37077^{\circ}_{2\frac{1}{2}} - 70954_{2\frac{1}{2}}$					
2950.80	2	8	33879.21	−0.03	$22960_{1\frac{1}{2}} - 56840^{\circ}_{1\frac{1}{2}}$					
2950.64		1	33881.05							
2950.52	2	20	33882.43							
2950.326	20	150	33884.66	+0.01	$35059^{a}_{3\frac{1}{2}} - 68943_{4\frac{1}{2}}$	4	1.143	0.889	0.127	0
2949.840		5	33890.24							
2948.65		2	33903.92							
2947.76		3	33914.15							
2947.131	4	30	33921.39	+0.04	$33494^{\circ}_{3\frac{1}{2}} - 67416_{4\frac{1}{2}}$					
2946.95		5	33923.47	+0.02	$64598_{3\frac{1}{2}} - 98521^{\circ}_{4\frac{1}{2}}$					
2946.852	2	20	33924.60	+0.08	$35019^{\circ}_{4\frac{1}{2}} - 68943_{4\frac{1}{2}}$					
2946.765	10	70	33925.60	−0.03	$43956^{\circ}_{2\frac{1}{2}} - 77882_{3\frac{1}{2}}$	5	(0.99)	1.15	w	1.55
2946.305	30	200	33930.90	−0.09	$40035^{\circ}_{3\frac{1}{2}} - 73966_{3\frac{1}{2}}$	6	0.71	0.76	0.17	0.733
2945.907	100r	600	33935.48	−0.01	$34784^{\circ}_{5\frac{1}{2}} - 68720_{6\frac{1}{2}}$	5	(1.119)	1.14	w	1.28
2945.22		3	33943.40	+0.08	$66082_{5\frac{1}{2}} - 100025^{\circ}_{5\frac{1}{2}}$					
2944.465	5	30	33952.10	−0.01	$37516^{\circ}_{3\frac{1}{2}} - 71468_{2\frac{1}{2}}$					
2944.19		2	33955.27							

TABLE 6. Yb II—*Observed and classified lines*—Continued

1	2	3	4	5	6	7	8	9	10	11
Wavelength air	Intensity		Wave number	o–c	Classification	Zeeman type	1st g	2nd g	Zeeman components	
	Meggers lamp	Thomson lamp							Strong p	Strong n
Å			K	K						
2943.20		2	33966.69							
2943.15		1	33967.27	+0.02	$44497^{\circ}_{2\frac{1}{2}} - 78464_{1\frac{1}{2}}$					
2942.823	10	50	33971.04	−0.01	$31979^{\circ}_{3\frac{1}{2}} - 65950_{4\frac{1}{2}}$	4	1.33	1.08	0.12	0.20
2942.60		2	33973.62							
2942.038	15	80	33980.11	0.00	$32371^{\circ}_{2\frac{1}{2}} - 66351_{2\frac{1}{2}}$	6	1.169	1.125	0.11	1.145
2941.77	1	4	33983.20	−0.01	$47329^{\circ}_{2\frac{1}{2}} - 81312_{2\frac{1}{2}}$					
2941.11		1	33990.83							
2940.517	25	150	33997.68			5			w	1.44
2940.25		2	34000.77							
2939.534	20	100	34009.05	+0.02	$31568^{\circ}_{2\frac{1}{2}} - 65577_{3\frac{1}{2}}$	5	0.863	1.049	0.093	1.514
2938.85	1	4	34016.97	+0.06	$22960_{1\frac{1}{2}} - 56977^{\circ}_{0\frac{1}{2}}$					
2938.51	3	20	34020.90	+0.02	$35059^{\circ}_{3\frac{1}{2}} - 69079_{2\frac{1}{2}}$					
2938.188	7	50	34024.63	+0.01	$32371^{\circ}_{2\frac{1}{2}} - 66395_{2\frac{1}{2}}$	6	1.165	1.235	0.176	1.200
2937.186	15	100	34036.24	−0.01	$37077^{\circ}_{2\frac{1}{2}} - 71113_{1\frac{1}{2}}$	5	1.097	0.965	0.066	1.300
2935.52		4	34055.56	+0.06	$40917^{\circ}_{4\frac{1}{2}} - 74973_{3\frac{1}{2}}$					
2935.245	1	7	34058.74	+0.07	$27061^{\circ}_{0\frac{1}{2}} - 61120_{0\frac{1}{2}}$					
2935.108	30	200	34060.33	−0.02	$34389^{\circ}_{2\frac{1}{2}} - 68450_{3\frac{1}{2}}$	5	(1.007)	1.07	w	1.23
2932.90		1	34085.98							
2932.21		1	34094.00							
2932.08		2	34095.51	−0.01	$58823_{2\frac{1}{2}} - 92919^{\circ}_{3\frac{1}{2}}$					
2931.27		1	34104.93	+0.03	$59090_{3\frac{1}{2}} - 93195^{\circ}_{3\frac{1}{2}}$					
2929.70		5	34123.20							
2929.48		3	34125.77	−0.04	$35831^{\circ}_{5\frac{1}{2}} - 69957_{4\frac{1}{2}}$					
2929.44		1	34126.23	+0.02	$48272^{\circ}_{2\frac{1}{2}} - 82398_{1\frac{1}{2}}$					
2927.850	10	70	34144.76	−0.01	$37077^{\circ}_{2\frac{1}{2}} - 71222_{3\frac{1}{2}}$	5	(1.113)	1.14	w	1.206
2927.42		1	34149.78	−0.02	$65875_{6\frac{1}{2}} - 100025^{\circ}_{5\frac{1}{2}}$					
2927.116	1	10	34153.33	+0.04	$45429^{\circ}_{3\frac{1}{2}} - 79583_{2\frac{1}{2}}$					
2926.65	2	15	34158.76	+0.06	$34784^{\circ}_{5\frac{1}{2}} - 68943_{4\frac{1}{2}}$					
2926.28		1	34163.08							
2924.65	2	9	34182.12	+0.11	$62861_{5\frac{1}{2}} - 97043^{\circ}_{6\frac{1}{2}}$					
2924.560		4	34183.17	−0.01	$47329^{\circ}_{2\frac{1}{2}} - 81512_{1\frac{1}{2}}$					
2924.235	20	100	34186.97	+0.07	$32371^{\circ}_{2\frac{1}{2}} - 66558_{3\frac{1}{2}}$	4	(1.17)	1.11	w	0.96
2922.35	2	7	34209.02	+0.09	$43075^{\circ}_{1\frac{1}{2}} - 77284_{1\frac{1}{2}}$					
2921.85		1	34214.88	0.00	$65199_{4\frac{1}{2}} - 99414^{\circ}_{4\frac{1}{2}}$					
2921.64		2	34217.34	+0.02	$41688^{\circ}_{1\frac{1}{2}} - 75905_{0\frac{1}{2}}$					
2921.119	40	200	34223.44	+0.06	$32981^{\circ}_{1\frac{1}{2}} - 67204_{1\frac{1}{2}}$	6	0.861	1.033	0.258	0.946
2920.16	1	10	34234.68	+0.02	$40035^{\circ}_{3\frac{1}{2}} - 74270_{2\frac{1}{2}}$					
2919.346	400r	1000	34244.22	+0.04	$31631^{\circ}_{6\frac{1}{2}} - 65875_{6\frac{1}{2}}$	6	1.227	1.201	0.165	1.214
2918.89		2	34249.57							
2918.53		1	34253.80	−0.07	$28757^{\circ}_{1\frac{1}{2}} - 63011_{1\frac{1}{2}}$					

TABLE 6. Yb II—*Observed and classified lines*—Continued

1	2	3	4	5	6	7	8	9	10	11
Wave-length air	Intensity		Wave number	o–c	Classification	Zeeman type	1st g	2nd g	Zeeman components	
	Meggers lamp	Thomson lamp							Strong p	Strong n
Å			K	K						
2916.83	2	10	34273.76	+0.04	$38342^{\circ}_{4\frac{1}{2}} - 72615_{5\frac{1}{2}}$					
2916.61	7	30	34276.35	+0.12	$43007^{\circ}_{0\frac{1}{2}} - 77284_{1\frac{1}{2}}$					
2916.431	10	70	34278.45	+0.05	$39378^{\circ}_{0\frac{1}{2}} - 73657_{1\frac{1}{2}}$	4	1.86	1.05	0.40	0.64
2915.99		4	34283.63	−0.03	$47228^{\circ}_{0\frac{1}{2}} - 81512_{1\frac{1}{2}}$					
2915.275	100r	300	34292.04	0.00	$26759^{\circ}_{2\frac{1}{2}} - 61051_{3\frac{1}{2}}$	4	1.56	1.18	0.19	0.22
2915.14		4	34293.63	−0.05	$45335^{\circ}_{4\frac{1}{2}} - 79628_{3\frac{1}{2}}$					
2914.84	1	8	34297.16							
2914.48	7	40	34301.39	+0.02	$33653^{\circ}_{0\frac{1}{2}} - 67955_{0\frac{1}{2}}$	6	1.310	0.900	0.205	1.105
2914.210	100r	600	34304.57	+0.01	$35831^{\circ}_{3\frac{1}{2}} - 70136_{6\frac{1}{2}}$	4	1.22	1.15	(0.034)	0.78
2913.75		3	34309.99	−0.10	$45273^{\circ}_{3\frac{1}{2}} - 79583_{2\frac{1}{2}}$					
2913.12	1	10	34317.41	+0.06	$44497^{\circ}_{2\frac{1}{2}} - 78814_{2\frac{1}{2}}$					
2912.865	10	50	34320.41	+0.03	$31568^{\circ}_{2\frac{1}{2}} - 65888_{1\frac{1}{2}}$	4	0.86	1.20	0.17	0.36
2912.51		5	34324.59	−0.04	$46354^{\circ}_{4\frac{1}{2}} - 80679_{5\frac{1}{2}}$					
2912.25		2	34327.66	−0.03	$47329^{\circ}_{2\frac{1}{2}} - 81657_{2\frac{1}{2}}$					
2911.61		3	34335.20	−0.03	$48556^{\circ}_{3\frac{1}{2}} - 82891_{2\frac{1}{2}}$					
2911.523	40	200	34336.23	+0.03	$35059^{\circ}_{3\frac{1}{2}} - 69395_{3\frac{1}{2}}$	6	1.12	0.94	0.63	1.05
2910.43		2	34349.12							
2909.88		4	34355.62	−0.07	$45273^{\circ}_{3\frac{1}{2}} - 79628_{3\frac{1}{2}}$					
2909.48	30	150	34360.34	+0.02	$30562^{\circ}_{5\frac{1}{2}} - 64923_{4\frac{1}{2}}$	5	(1.112)	1.10	0	1.153
2909.19	20	100	34363.76	+0.02	$33052^{\circ}_{4\frac{1}{2}} - 67416_{4\frac{1}{2}}$	7	1.26	1.26	0	1.266
2908.55	1	9	34371.33	+0.02	$31979^{\circ}_{3\frac{1}{2}} - 66351_{2\frac{1}{2}}$					
2908.33	10	50	34373.93	−0.02	$30224^{\circ}_{4\frac{1}{2}} - 64598_{3\frac{1}{2}}$	4	0.93	1.23	0.150	−0.12
2908.15		4	34376.05	−0.02	$35019^{\circ}_{4\frac{1}{2}} - 69395_{3\frac{1}{2}}$					
2908.09	5	40	34376.76	−0.07	$44438^{\circ}_{3\frac{1}{2}} - 78814_{2\frac{1}{2}}$					
2906.88	7	60	34391.07	−0.04	$37077^{\circ}_{2\frac{1}{2}} - 71468_{2\frac{1}{2}}$	6	1.110	1.018	0.23	1.064
2905.61		3	34406.10							
2904.97		3	34413.68	−0.08	$59090_{3\frac{1}{2}} - 93503^{\circ}_{4\frac{1}{2}}$					
2904.79	1	7	34415.81	−0.01	$31979^{\circ}_{3\frac{1}{2}} - 66395_{2\frac{1}{2}}$					
2904.20		1	34422.81							
2902.924	8	80	34437.94	−0.03	$38342^{\circ}_{4\frac{1}{2}} - 72779_{3\frac{1}{2}}$	5	(1.093)	1.064	w	1.065
2902.41	6	40	34444.03	+0.03	$33494^{\circ}_{3\frac{1}{2}} - 67938_{3\frac{1}{2}}$	6	0.99	0.97	0.06	0.98
2901.86		1	34450.56	−0.10	$31631^{\circ}_{6\frac{1}{2}} - 66082_{5\frac{1}{2}}$					
2901.60		1	34453.65							
2900.39		2	34468.02							
2899.705	40	200	34476.16	+0.03	$28757^{\circ}_{1\frac{1}{2}} - 63234_{2\frac{1}{2}}$	4	1.44	1.21	0.115	0.86
2899.236	5	40	34481.74	−0.06	$41688^{\circ}_{1\frac{1}{2}} - 76170_{2\frac{1}{2}}$	5	0.77	1.12	0.175us	1.646us
2897.98		2	34496.68	−0.03	$33653^{\circ}_{0\frac{1}{2}} - 68150_{1\frac{1}{2}}$					
2897.32		4	34504.54	+0.03	$34575^{\circ}_{1\frac{1}{2}} - 69079_{2\frac{1}{2}}$					
2896.902	10	100	34509.52	+0.12	$46169^{\circ}_{4\frac{1}{2}} - 80679_{5\frac{1}{2}}$	4	1.06	1.00	(0.03?)	0.73
2895.06	2	15	34531.48	−0.01	$43075^{\circ}_{1\frac{1}{2}} - 77606_{2\frac{1}{2}}$					

TABLE 6. Yb II—*Observed and classified lines*—Continued

1	2	3	4	5	6	7	8	9	10	11
Wave-length air	Intensity		Wave number	o–c	Classification	Zeeman type	1st g	2nd g	Zeeman components	
	Meggers lamp	Thomson lamp							Strong p	Strong n
Å			K	K						
2894.95	3	30	34532.79	+0.03	$40035^{\circ}_{3\frac{1}{2}} - 74568_{4\frac{1}{2}}$	5				
2893.620	10	100	34548.66	+0.12	$35059^{\circ}_{3\frac{1}{2}} - 69607_{2\frac{1}{2}}$	4	1.12	1.21	(0.044)	0.90
2891.384	5000A	2000	34575.38	+0.01	$0_{0\frac{1}{2}} - 34575^{\circ}_{1\frac{1}{2}}$	4	1.999	1.430	0.285	1.145
2891.16	4	40	34578.06	−0.04	$31979^{\circ}_{3\frac{1}{2}} - 66558_{3\frac{1}{2}}$					
2890.28	1	8	34588.58							
2888.04	100r	300	34615.41	−0.06	$26759^{\circ}_{2\frac{1}{2}} - 61374_{2\frac{1}{2}}$	6	1.567	1.292	0.692	1.430
2887.74	2	7	34619.00	−0.03	$48272^{\circ}_{2\frac{1}{2}} - 82891_{2\frac{1}{2}}$					
2886.263	30	200	34636.72	−0.03	$30562_{5\frac{1}{2}} - 65199_{4\frac{1}{2}}$	5	1.10	1.06	(0.02)	1.28
2885.97	10	70	34640.24	−0.08 −0.02	$33494^{\circ}_{3\frac{1}{2}} - 68135_{2\frac{1}{2}}$ $(61051_{3\frac{1}{2}} - 95691^{\circ}_{3\frac{1}{2}})$	4	1.00	1.09	(0.044)	0.78
2885.594		7	34644.75	−0.01	$41678^{\circ}_{2\frac{1}{2}} - 76323_{3\frac{1}{2}}$					
2885.02	1	8	34651.64	−0.03	$47005^{\circ}_{1\frac{1}{2}} - 81657_{2\frac{1}{2}}$					
2884.51		2	34657.77							
2883.87	1	10	34665.46	+0.12	$44940^{\circ}_{1\frac{1}{2}} - 79605_{1\frac{1}{2}}$	6	1.236	1.152	0.125	1.194
2883.01		6	34675.80	−0.04	$63944_{5\frac{1}{2}} - 98620^{\circ}_{6\frac{1}{2}}$					
2882.155	7	50	34686.09	+0.01	$37077^{\circ}_{2\frac{1}{2}} - 71763_{1\frac{1}{2}}$	7	1.12	1.12	0	1.122
2882.01		1	34687.83							
2881.93	7	60	34688.79			5			w	1.24
2881.10		6	34698.79	+0.01	$30224^{\circ}_{4\frac{1}{2}} - 64923_{4\frac{1}{2}}$					
2879.83		1	34714.09							
2879.159	10	70	34722.18	+0.03	$40917^{\circ}_{4\frac{1}{2}} - 75640_{3\frac{1}{2}}$	5	0.976	0.820	0.078	1.522
2876.45		1	34754.88							
2874.83		1	34774.46	+0.02	$59090_{3\frac{1}{2}} - 93864^{\circ}_{2\frac{1}{2}}$					
2874.11		6	34783.17	+0.04	$31568^{\circ}_{2\frac{1}{2}} - 66351_{2\frac{1}{2}}$					
2873.14		3	34794.91	+0.01	$63726_{4\frac{1}{2}} - 98521^{\circ}_{4\frac{1}{2}}$					
2872.82		1	34798.79							
2872.11	2	10	34807.39	+0.08	$48556^{\circ}_{3\frac{1}{2}} - 83363_{3\frac{1}{2}}$					
2871.712	2	10	34812.22	+0.01	$43075^{\circ}_{1\frac{1}{2}} - 77887_{0\frac{1}{2}}$					
2870.57		3	34826.06	+0.03	$65199_{4\frac{1}{2}} - 100025^{\circ}_{5\frac{1}{2}}$					
2870.51		3	34826.79							
2870.061	20	100	34832.24	−0.03	$42915^{\circ}_{5\frac{1}{2}} - 77747_{4\frac{1}{2}}$	5	1.10	1.07	(0.017)	1.25
2869.61		1	34837.71	0.00	$22960_{1\frac{1}{2}} - 57798^{\circ}_{2\frac{1}{2}}$					
2869.546	1	15	34838.49	+0.01	$41678^{\circ}_{2\frac{1}{2}} - 76517_{1\frac{1}{2}}$					
2868.536		5	34850.76	+0.04	$46354^{\circ}_{4\frac{1}{2}} - 81205_{4\frac{1}{2}}$					
2867.90		7	34858.49	+0.01 +0.04	$63944_{5\frac{1}{2}} - 98802^{\circ}_{5\frac{1}{2}}$ $43956^{\circ}_{2\frac{1}{2}} - 78814_{2\frac{1}{2}}$					
2867.58	5	15	34862.38	+0.02	$47228^{\circ}_{0\frac{1}{2}} - 82091_{0\frac{1}{2}}$					
2867.20	1	7	34867.00	−0.10	$48024^{\circ}_{1\frac{1}{2}} - 82891_{2\frac{1}{2}}$					
2867.06	100r	500	34868.70	−0.11	$30224^{\circ}_{4\frac{1}{2}} - 65093_{3\frac{1}{2}}$	4	0.94	1.00	(0.03)	0.72
2866.179	4	30	34879.42	−0.09	$43007^{\circ}_{0\frac{1}{2}} - 77887_{0\frac{1}{2}}$	6	0.14	2.18	1.02	1.16

TABLE 6. Yb II—*Observed and classified lines*—Continued

1	2	3	4	5	6	7	8	9	10	11
Wave-length air	Intensity		Wave number	o–c	Classification	Zeeman type	1st g	2nd g	Zeeman components	
	Meggers lamp	Thomson lamp							Strong p	Strong n
Å			K	K						
2865.96	1	6	34882.08	+0.06	$57765_{4\frac{1}{2}} - 92647^{\circ}_{5\frac{1}{2}}$					
2865.74		1	34884.76							
2865.60	1	7	34886.46	+0.07	$33052^{\circ}_{4\frac{1}{2}} - 67938_{3\frac{1}{2}}$					
2865.328	5	30	34889.77	+0.02	$28757^{\circ}_{1\frac{1}{2}} - 63647_{1\frac{1}{2}}$	6	1.454	1.146	0.44	1.300
2864.725	4	40	34897.12			4			w	0.94
2864.62	1	10	34898.40	−0.09	$35059^{\circ}_{3\frac{1}{2}} - 69957_{4\frac{1}{2}}$					
2864.19		1	34903.64							
2863.13	5	30	34916.56	−0.13	$49301_{4\frac{1}{2}} - 84217^{\circ}_{4\frac{1}{2}}$					
2862.97	2	5	34918.51							
2862.85	1	8	34919.97							
2861.34	20	200	34938.40	+0.04	$35019^{\circ}_{4\frac{1}{2}} - 69957_{4\frac{1}{2}}$	6	1.15	1.11	0.18	1.12
2861.212	40	300	34939.96	−0.03	$31631^{\circ}_{6\frac{1}{2}} - 66571_{5\frac{1}{2}}$	5	1.22	1.18	(0.018)	1.41
2861.11	5	30	34941.21	−0.12	$38342^{\circ}_{4\frac{1}{2}} - 73283_{4\frac{1}{2}}$					
2860.71	3	15	34946.10	+0.07	$49498_{2\frac{1}{2}} - 84444^{\circ}_{3\frac{1}{2}}$					
2860.393	20	100	34949.97	+0.04	$38342^{\circ}_{4\frac{1}{2}} - 73291_{5\frac{1}{2}}$	7	(1.093)	1.09	0	1.07
2859.94	4	20	34955.50	+0.07	$33494^{\circ}_{3\frac{1}{2}} - 68450_{3\frac{1}{2}}$					
2859.805	1000*R*	1000	34957.15	−0.01	$21418^{\circ}_{3\frac{1}{2}} - 56375_{2\frac{1}{2}}$	4	(1.145)	1.24	?	0.91
2859.392	30	200	34962.20	−0.08	$35831^{\circ}_{5\frac{1}{2}} - 70793_{5\frac{1}{2}}$	6	1.21	1.19	w	1.20
2858.460	8	40	34973.60	−0.04	$32981^{\circ}_{1\frac{1}{2}} - 67955_{0\frac{1}{2}}$	4	0.87	0.89	(0.01)	0.880
2858.332	15	60	34975.17	−0.04	$30224^{\circ}_{4\frac{1}{2}} - 65199_{4\frac{1}{2}}$	6	0.971	1.118	(0.666)	1.044
2857.75		2	34982.29	+0.03	$53720_{4\frac{1}{2}} - 88702^{\circ}_{5\frac{1}{2}}$					
2857.29	4	20	34987.92	+0.06	$41688^{\circ}_{1\frac{1}{2}} - 76676_{2\frac{1}{2}}$	5	0.770	1.110	0.170	1.620
2857.13		3	34989.88	−0.04	$31568^{\circ}_{2\frac{1}{2}} - 66558_{3\frac{1}{2}}$					
2855.85	1	7	35005.56	+0.12	$34389^{\circ}_{2\frac{1}{2}} - 69395_{3\frac{1}{2}}$					
2854.490	10	50	35022.24	−0.05	$40035^{\circ}_{3\frac{1}{2}} - 75058_{2\frac{1}{2}}$	4	(0.72)	0.76	w	0.63
2854.144	10	60	35026.48	−0.02	$35831^{\circ}_{5\frac{1}{2}} - 70858_{4\frac{1}{2}}$	4	1.21	1.27?	(0.03)	0.94
2854.04	4	40	35027.76	−0.13	$45429^{\circ}_{3\frac{1}{2}} - 80457_{3\frac{1}{2}}$					
2853.68	3	30	35032.18	+0.01	$34575^{\circ}_{1\frac{1}{2}} - 69607_{2\frac{1}{2}}$	4	1.44	1.21	0.12	0.86
2853.409	5	60	35035.51	+0.02	$46169^{\circ}_{4\frac{1}{2}} - 81205_{4\frac{1}{2}}$	6	1.123	1.087	0.16	1.10
2852.63		1	35045.07							
2851.92		4	35053.80	+0.04	$34389^{\circ}_{2\frac{1}{2}} - 69443_{1\frac{1}{2}}$					
2851.86	10	70	35054.53	−0.02	$33494^{\circ}_{3\frac{1}{2}} - 68549_{4\frac{1}{2}}$	5	1.000	1.167	0.083	1.755
2851.126	500*R*	1000	35063.56	0.00	$26759^{\circ}_{2\frac{1}{2}} - 61822_{3\frac{1}{2}}$	4	1.560	1.310	0.125	0.686
2850.64		3	35069.54	0.00	$47329^{\circ}_{2\frac{1}{2}} - 82398_{1\frac{1}{2}}$					
2850.13		1	35075.81	−0.02	$63726_{4\frac{1}{2}} - 98802^{\circ}_{5\frac{1}{2}}$					
2849.90		3	35078.64							
2849.84		1	35079.38							
2849.336	6	40	35085.58	−0.02	$44497^{\circ}_{2\frac{1}{2}} - 79583_{2\frac{1}{2}}$	6	0.746	0.674	0.18	0.71
2848.88	1	7	35091.20	+0.09	$48272^{\circ}_{2\frac{1}{2}} - 83363_{3\frac{1}{2}}$					
2848.445	20	100	35096.56	−0.03	$33052^{\circ}_{4\frac{1}{2}} - 68148_{5\frac{1}{2}}$	4	1.29	1.24	(0.027)	1.00

TABLE 6. Yb II—*Observed and classified lines*—Continued

1	2	3	4	5	6	7	8	9	10	11
Wavelength air	Intensity		Wave number	o–c	Classification	Zeeman type	1st g	2nd g	Zeeman components	
	Meggers lamp	Thomson lamp							Strong p	Strong n
Å			K	K						
2847.97		3	35102.41	−0.05	$64923_{4\frac{1}{2}} - 100025^{\circ}_{5\frac{1}{2}}$					
2847.75		2	35105.12							
2847.64		2	35106.48	+0.09	$24332_{2\frac{1}{2}} - 59439^{\circ}_{2\frac{1}{2}}$					
2847.28		4	35110.92							
2847.175	400r	1000	35112.21	−0.07	$27061^{\circ}_{0\frac{1}{2}} - 62174_{1\frac{1}{2}}$	5	(0.667)	0.79	w	0.85
2847.03		1	35114.00							
2846.324		5	35122.71	+0.03	$45335^{\circ}_{4\frac{1}{2}} - 80457_{3\frac{1}{2}}$					
2846.183	1	5	35124.45	+0.01	$37077^{\circ}_{2\frac{1}{2}} - 72202_{3\frac{1}{2}}$					
2845.355		4	35134.67	0.00	$49498_{2\frac{1}{2}} - 84632^{\circ}_{2\frac{1}{2}}$					
2844.685	4	20	35142.95	+0.04	$49301_{4\frac{1}{2}} - 84444^{\circ}_{3\frac{1}{2}}$					
2844.067	4	10	35150.58	+0.03	$41688^{\circ}_{1\frac{1}{2}} - 76839_{2\frac{1}{2}}$					
2843.83	3	15	35153.51	+0.10	$32981^{\circ}_{1\frac{1}{2}} - 68135_{2\frac{1}{2}}$					
2843.702	1	7	35155.09	+0.03	$42915^{\circ}_{5\frac{1}{2}} - 78070_{4\frac{1}{2}}$					
2842.586	6	30	35168.90	−0.08	$32981^{\circ}_{1\frac{1}{2}} - 68150_{1\frac{1}{2}}$	6	0.88	0.92	0.05	0.90
2842.51	2	8	35169.84	−0.04	$61873_{6\frac{1}{2}} - 97043^{\circ}_{6\frac{1}{2}}$					
2842.291	1	7	35172.55	+0.01	$34784^{\circ}_{5\frac{1}{2}} - 69957_{4\frac{1}{2}}$					
2842.140	3	15	35174.42	−0.07	$30392^{\circ}_{1\frac{1}{2}} - 65566_{0\frac{1}{2}}$	7	(1.333)	1.38	0	1.31
2841.308	2	20	35184.71	+0.02	$45273^{\circ}_{3\frac{1}{2}} - 80457_{3\frac{1}{2}}$	6	(1.18)	0.97	0.709	?
2841.26		1	35185.31	−0.07	$58823_{2\frac{1}{2}} - 94008^{\circ}_{3\frac{1}{2}}$					
2841.02		2	35188.28							
2839.91		2	35202.03	+0.08	$22960_{1\frac{1}{2}} - 58162^{\circ}_{1\frac{1}{2}}$					
2839.85		1	35202.78							
2839.17		1	35211.21	+0.03	$57765_{4\frac{1}{2}} - 92976^{\circ}_{3\frac{1}{2}}$					
2838.64	3	15	35217.78	0.00	$34389^{\circ}_{2\frac{1}{2}} - 69607_{2\frac{1}{2}}$					
2837.92		2	35226.72	+0.09	$56375_{2\frac{1}{2}} - 91602^{\circ}_{2\frac{1}{2}}$					
2837.09		1	35237.02							
2835.95		1	35251.19							
2835.48		2	35257.03							
2835.13		1	35261.38	+0.02	$33494^{\circ}_{3\frac{1}{2}} - 68756_{3\frac{1}{2}}$					
2834.972	10	70	35263.35	−0.05	$37516^{\circ}_{3\frac{1}{2}} - 72779_{3\frac{1}{2}}$	6	1.13	1.11	0.07	1.12
2834.63		4	35267.60							
2833.68		1	35279.42							
2832.201	4	20	35297.85	+0.01	$28757^{\circ}_{1\frac{1}{2}} - 64055_{2\frac{1}{2}}$	4	1.44	1.11	0.16	0.62
2830.989	30	200	35312.96	−0.02	$30562^{\circ}_{5\frac{1}{2}} - 65875_{6\frac{1}{2}}$	5	1.13	1.20	(0.035)	1.60
2830.88	4	30	35314.32			7			0	0.99
2830.639	1	8	35317.32	−0.12	$48900_{3\frac{1}{2}} - 84217^{\circ}_{4\frac{1}{2}}$					
2828.49	1	10	35344.16	+0.01	$45335^{\circ}_{4\frac{1}{2}} - 80679_{5\frac{1}{2}}$					
2827.921	3	20	35351.26	−0.03	$34784^{\circ}_{5\frac{1}{2}} - 70136_{6\frac{1}{2}}$	7	(1.12)	1.14	w	1.23
2827.80	1	5	35352.78	0.00	$30224^{\circ}_{4\frac{1}{2}} - 65577_{3\frac{1}{2}}$					
2826.735		3	35366.10							

TABLE 6. Yb II—*Observed and classified lines*—Continued

1	2	3	4	5	6	7	8	9	10	11
Wave-length air	Intensity		Wave number	o–c	Classification	Zeeman type	1st g	2nd g	Zeeman components	
	Meggers lamp	Thomson lamp							Strong p	Strong n
Å			K	K						
2826.522		2	35368.76							
2824.974	20	100	35388.14	−0.02	$30562^{\circ}_{5\frac{1}{2}} - 65950_{4\frac{1}{2}}$	5	(1.112)	1.10	w	1.19
2824.86	1	4	35389.57	−0.10	$43075^{\circ}_{1\frac{1}{2}} - 78464_{1\frac{1}{2}}$					
2824.54	2	9	35393.58	+0.06	$47005^{\circ}_{1\frac{1}{2}} - 82398_{1\frac{1}{2}}$					
2824.20	2	10	35397.84	+0.02	$33052^{\circ}_{4\frac{1}{2}} - 68450_{3\frac{1}{2}}$					
2823.585	7	50	35405.55	−0.03	$40917^{\circ}_{4\frac{1}{2}} - 76323_{3\frac{1}{2}}$	7	0.97	0.97	0	0.97
2823.320		4	35408.87	−0.01	$38342^{\circ}_{4\frac{1}{2}} - 73750_{4\frac{1}{2}}$					
2821.52		3	35431.46	+0.08	$61051_{3\frac{1}{2}} - 96482^{\circ}_{4\frac{1}{2}}$					
2821.152	30r	200	35436.08	−0.05	$31979^{\circ}_{3\frac{1}{2}} - 67416_{4\frac{1}{2}}$	4	1.34	1.27	(0.037)	1.01
2820.12		3	35449.05	+0.08	$33494^{\circ}_{3\frac{1}{2}} - 68943_{4\frac{1}{2}}$					
2819.75		2	35453.70	+0.03	$34575^{\circ}_{1\frac{1}{2}} - 70029_{0\frac{1}{2}}$					
2819.49	2	10	35456.97	0.00	$43007^{\circ}_{0\frac{1}{2}} - 78464_{1\frac{1}{2}}$	?	0.09	1.15	0.53	1.68
2817.66		2	35480.00	0.00	$58823_{2\frac{1}{2}} - 94303^{\circ}_{3\frac{1}{2}}$					
2816.368	2	8	35496.27	+0.04 0.00	$30392^{\circ}_{1\frac{1}{2}} - 65888_{1\frac{1}{2}}$ $46902^{\circ}_{0\frac{1}{2}} - 82398_{1\frac{1}{2}}$					
2816.317	4	20	35496.91	−0.03	$33052^{\circ}_{4\frac{1}{2}} - 68549_{4\frac{1}{2}}$					
2815.20		1	35511.00							
2814.87	2	10	35515.16	+0.04	$40035^{\circ}_{3\frac{1}{2}} - 75550_{2\frac{1}{2}}$					
2814.528	20	100	35519.48	+0.02 −0.06	$30562^{\circ}_{5\frac{1}{2}} - 66082_{5\frac{1}{2}}$ $(63726_{4\frac{1}{2}} - 99246^{\circ}_{5\frac{1}{2}})$	6	1.12	1.14	0.09	1.13
2814.241	2	10	35523.10	−0.04	$46169^{\circ}_{4\frac{1}{2}} - 81692_{3\frac{1}{2}}$					
2813.00		1	35538.77							
2812.612	2	6	35543.67	+0.01	$48900_{3\frac{1}{2}} - 84444^{\circ}_{3\frac{1}{2}}$					
2811.133	3	8	35562.37	+0.01	$47329^{\circ}_{2\frac{1}{2}} - 82891_{2\frac{1}{2}}$					
2810.723	5	20	35567.56	−0.02	$32371^{\circ}_{2\frac{1}{2}} - 67938_{3\frac{1}{2}}$	4	1.164	0.966	0.099	0.471
2810.109	4	15	35575.33	−0.03	$45737^{\circ}_{1\frac{1}{2}} - 81312_{2\frac{1}{2}}$					
2809.326	2	9	35585.24	+0.04	$33494^{\circ}_{3\frac{1}{2}} - 69079_{2\frac{1}{2}}$					
2808.75		2	35592.54							
2808.305	4	20	35598.18	−0.02	$40917^{\circ}_{4\frac{1}{2}} - 76516_{4\frac{1}{2}}$	6	0.99	1.01	0.09	1.00
2807.83	2	10	35604.20	−0.04	$40035^{\circ}_{3\frac{1}{2}} - 75640_{3\frac{1}{2}}$					
2807.744	2	6	35605.29	0.00 −0.05	$41678^{\circ}_{2\frac{1}{2}} - 77284_{1\frac{1}{2}}$ $47758^{\circ}_{3\frac{1}{2}} - 83363_{3\frac{1}{2}}$					
2807.32	1	4	35610.67	+0.07	$39378^{\circ}_{0\frac{1}{2}} - 74989_{0\frac{1}{2}}$					
2807.180	2	8	35612.45	−0.02	$39378^{\circ}_{0\frac{1}{2}} - 74991_{1\frac{1}{2}}$					
2806.43		1	35621.96							
2806.057	1	4	35626.70	0.00	$43956^{\circ}_{2\frac{1}{2}} - 79583_{2\frac{1}{2}}$					
2804.807	1	3	35642.58							
2804.260	5	30	35649.53	−0.01	$43956^{\circ}_{2\frac{1}{2}} - 79605_{1\frac{1}{2}}$	4	1.00	1.17	0.083	0.74
2801.598	1	5	35683.40	+0.03	$61214_{4\frac{1}{2}} - 96898^{\circ}_{5\frac{1}{2}}$					
2801.272		1	35687.55	−0.04	$63726_{4\frac{1}{2}} - 99414^{\circ}_{4\frac{1}{2}}$					
2800.109	2	10	35702.37	−0.03	$37077^{\circ}_{2\frac{1}{2}} - 72779_{3\frac{1}{2}}$					

TABLE 6. Yb II—*Observed and classified lines*—Continued

1	2	3	4	5	6	7	8	9	10	11
Wave-length air	Intensity		Wave number	o–c	Classification	Zeeman type	1st g	2nd g	Zeeman components	
	Meggers lamp	Thomson lamp							Strong p	Strong n
Å			K	K						
2800.060	6	30	35703.00	−0.10	$28757°_{1\frac{1}{2}} - 64461_{1\frac{1}{2}}$					
2800.006	8	50	35703.69	−0.06	$33052°_{4\frac{1}{2}} - 68756_{3\frac{1}{2}}$					
2799.376	30	40	35711.72	−0.01	$22960_{1\frac{1}{2}} - 58672°_{0\frac{1}{2}}$	5	0.807	0.541	0.133	0.940
2798.211	20	100	35726.59	−0.03	$30224°_{4\frac{1}{2}} - 65950_{4\frac{1}{2}}$	6	0.931	1.091	0.720	1.10
2797.796	10	80	35731.89	0.00	$40917°_{4\frac{1}{2}} - 76649_{5\frac{1}{2}}$ [d]	5			0.43w	1.58
2797.28		2	35738.48	−0.09	$57765_{4\frac{1}{2}} - 93503°_{4\frac{1}{2}}$					
2796.764		2	35745.07							
2795.292	6	20	35763.89	−0.01	$32371°_{2\frac{1}{2}} - 68135_{2\frac{1}{2}}$	6	1.17	1.09	0.20	1.13
2795.074	8	40	35766.68	−0.08	$37516°_{3\frac{1}{2}} - 73283_{4\frac{1}{2}}$ [d]	4			(0.04)	0.63
2794.774	7	40	35770.52	−0.07	$41678°_{2\frac{1}{2}} - 77449_{3\frac{1}{2}}$	7	(1.193)	1.18	0	1.14
2794.441	10	70	35774.79	−0.04	$35019°_{4\frac{1}{2}} - 70793_{5\frac{1}{2}}$	5	1.15	1.20	(0.025)	1.43
2794.08	2	10	35779.41	−0.06	$32371°_{2\frac{1}{2}} - 68150_{1\frac{1}{2}}$					
2793.280	10	60	35789.65	−0.01	$33653°_{0\frac{1}{2}} - 69443_{1\frac{1}{2}}$	4	1.32	1.15	0.09	1.06
2792.54		3	35799.14	−0.04	$35059°_{3\frac{1}{2}} - 70858_{4\frac{1}{2}}$					
2789.431	3	15	35839.04	−0.01	$35019°_{4\frac{1}{2}} - 70858_{4\frac{1}{2}}$					
2787.965	7	30	35857.88	−0.04	$30224°_{4\frac{1}{2}} - 66082_{5\frac{1}{2}}$	5	(0.935)	1.15	0.107	?
2787.010	1	7	35870.17	−0.07	$45335°_{4\frac{1}{2}} - 81205_{4\frac{1}{2}}$					
2786.025	1	5	35882.85	+0.02	$45429°_{3\frac{1}{2}} - 81312_{2\frac{1}{2}}$					
2785.750	8	30	35886.39	+0.05	$47005°_{1\frac{1}{2}} - 82891_{2\frac{1}{2}}$	5	(0.99)	1.03	w	1.09
2785.066		2	35895.20	−0.07	$35059°_{3\frac{1}{2}} - 70954_{2\frac{1}{2}}$					
2784.656	30	150	35900.49	−0.03 +0.02	$33494°_{3\frac{1}{2}} - 69395_{3\frac{1}{2}}$ $(55702_{1\frac{1}{2}} - 91602°_{2\frac{1}{2}})$	6	0.99	0.95	0.15	0.97
2783.16		2	35919.78	−0.06	$45737°_{1\frac{1}{2}} - 81657_{2\frac{1}{2}}$					
2782.58		3	35927.27	−0.06	$56375_{2\frac{1}{2}} - 92303°_{3\frac{1}{2}}$					
2782.54	1	5	35927.79	−0.06	$41678°_{2\frac{1}{2}} - 77606_{2\frac{1}{2}}$					
2782.203	1	5	35932.14	−0.11	$45273°_{3\frac{1}{2}} - 81205_{4\frac{1}{2}}$					
2782.102	1	2	35933.44							
2781.493		2	35941.31	−0.08	$62861_{5\frac{1}{2}} - 98802°_{5\frac{1}{2}}$					
2780.820	1	3	35950.01	−0.02	$27061°_{0\frac{1}{2}} - 63011_{1\frac{1}{2}}$					
2780.125		3	35958.99	+0.01	$30392°_{1\frac{1}{2}} - 66351_{2\frac{1}{2}}$					
2780.032	2	15	35960.20	0.00	$44497°_{2\frac{1}{2}} - 80457_{3\frac{1}{2}}$					
2776.688	1	5	36003.50	+0.01	$30392°_{1\frac{1}{2}} - 66395_{2\frac{1}{2}}$					
2776.280	60r	200	36008.79	0.00	$30562°_{2\frac{1}{2}} - 66571_{3\frac{1}{2}}$	6	1.12	1.19	0.36	1.16
2775.440	2	10	36019.69	+0.01 +0.02	$44438°_{3\frac{1}{2}} - 80457_{3\frac{1}{2}}$ $(58283_{2\frac{1}{2}} - 94303°_{3\frac{1}{2}})$	6	(1.10)	0.99?	0.38	
2774.304	5	20	36034.44	0.00	$47329°_{2\frac{1}{2}} - 83363_{3\frac{1}{2}}$	7	(0.990)	0.97	0	0.911
2773.91		2	36039.56	−0.07	$45273°_{3\frac{1}{2}} - 81312_{2\frac{1}{2}}$					
2771.86		2	36066.21							
2771.324	20	100	36073.18	−0.05	$34784°_{5\frac{1}{2}} - 70858_{4\frac{1}{2}}$	4	1.12	1.28	0.080	0.40
2770.405		2	36085.15							

TABLE 6. Yb II—*Observed and classified lines*—Continued

1	2	3	4	5	6	7	8	9	10	11
Wavelength air	Intensity		Wave number	o–c	Classification	Zeeman type	1st g	2nd g	Zeeman components	
	Meggers lamp	Thomson lamp							Strong p	Strong n
Å			K	K						
2769.402		2	36098.22	−0.07	$32981^{\circ}_{1\frac{1}{2}} - 69079_{2\frac{1}{2}}$					
2768.281	2	20	36112.84	−0.02	$33494^{\circ}_{3\frac{1}{2}} - 69607_{2\frac{1}{2}}$					
2766.624	2	7	36134.46	+0.03	$40035^{\circ}_{3\frac{1}{2}} - 76170_{2\frac{1}{2}}$					
2766.167	1	3	36140.43							
2765.046	2	8	36155.08	−0.02	$31979^{\circ}_{3\frac{1}{2}} - 68135_{2\frac{1}{2}}$					
2764.414	10	50	36163.35	−0.01	$35059^{\circ}_{3\frac{1}{2}} - 71222_{3\frac{1}{2}}$	6	1.13	1.15	0.07	1.14
2762.716	1	3	36185.58	−0.04	$52517_{5\frac{1}{2}} - 88702^{\circ}_{5\frac{1}{2}}$					
2761.70		4	36198.89	+0.04	$41688^{\circ}_{1\frac{1}{2}} - 77887_{0\frac{1}{2}}$					
2761.373	10	70	36203.17	−0.06	$35019^{\circ}_{4\frac{1}{2}} - 71222_{3\frac{1}{2}}$	7	(1.158)	1.15	w	1.175
2760.780	10	70	36210.95	−0.06	$35059^{\circ}_{3\frac{1}{2}} - 71270_{2\frac{1}{2}}$	5	1.12	0.90	0.11	1.67
2759.532	3	20	36227.32	+0.01	$45429^{\circ}_{3\frac{1}{2}} - 81657_{2\frac{1}{2}}$					
2759.257		3	36230.93							
2759.003	7	40	36234.27	−0.04	$37516^{\circ}_{3\frac{1}{2}} - 73750_{4\frac{1}{2}}$	4	1.15	1.03	(0.063)	0.58
2758.263		1	36243.99							
2758.065		1	36246.59							
2757.542		3	36253.47							
2754.943	3	20	36287.67	0.00	$40035^{\circ}_{3\frac{1}{2}} - 76323_{3\frac{1}{2}}$	6	(0.72)	0.99	0.936	?
2754.105		2	36298.71	−0.03	$63726_{4\frac{1}{2}} - 100025^{\circ}_{5\frac{1}{2}}$					
2753.584	5	20	36305.57	+0.03	$47912_{3\frac{1}{2}} - 84217^{\circ}_{4\frac{1}{2}}$					
2751.452	20	80	36333.71	+0.04	$30224^{\circ}_{1\frac{1}{2}} - 66558_{3\frac{1}{2}}$	4	0.94	1.11	0.085	0.345
2750.477	600R	500	36346.58	+0.01	$21418^{\circ}_{3\frac{1}{2}} - 57765_{4\frac{1}{2}}$	4	(1.145)	1.12	0	1.05
2749.624	3	20	36357.86	−0.03	$45335^{\circ}_{3\frac{1}{2}} - 81692_{3\frac{1}{2}}$					
2748.664	50r	150	36370.56	−0.04	$31568^{\circ}_{2\frac{1}{2}} - 67938_{3\frac{1}{2}}$	5	0.85	0.96	(0.06)	1.24
2748.56	3	10	36371.93	−0.11	$44940^{\circ}_{1\frac{1}{2}} - 81312_{2\frac{1}{2}}$					
2748.036	5	30	36378.87	−0.03	$34575^{\circ}_{1\frac{1}{2}} - 70954_{2\frac{1}{2}}$	4	1.450	1.016	0.213	0.363
2747.641	3	10	36384.10	−0.01	$45273^{\circ}_{3\frac{1}{2}} - 81657_{2\frac{1}{2}}$					
2747.580	20	80	36384.90	−0.04	$32371^{\circ}_{2\frac{1}{2}} - 68756_{3\frac{1}{2}}$	5	1.165	1.330	0.082	1.743
2746.83		1	36394.84							
2745.712	5	30	36409.66	−0.04	$35059^{\circ}_{3\frac{1}{2}} - 71468_{2\frac{1}{2}}$	5	1.12	1.02	(0.05)	1.38
2745.115	2	8	36417.58						(0.14)	
2744.782	1	3	36421.99	−0.04	$53720_{4\frac{1}{2}} - 90142^{\circ}_{3\frac{1}{2}}$					
2744.372		1	36427.43	−0.05	$53715_{3\frac{1}{2}} - 90142^{\circ}_{3\frac{1}{2}}$					
2742.741		2	36449.10							
2742.651	1	5	36450.29	+0.07	$37516^{\circ}_{3\frac{1}{2}} - 73966_{3\frac{1}{2}}$					
2741.779	4	15	36461.88	−0.05	$32981^{\circ}_{1\frac{1}{2}} - 69443_{1\frac{1}{2}}$					
2741.714	8	40	36462.75	−0.06	$33494^{\circ}_{3\frac{1}{2}} - 69957_{4\frac{1}{2}}$	5	1.00	1.11	0.05	1.49
2741.150	2	8	36470.25	+0.04	$31979^{\circ}_{3\frac{1}{2}} - 68450_{3\frac{1}{2}}$					
2740.79	3	9	36475.04	−0.05	$26759^{\circ}_{2\frac{1}{2}} - 63234_{2\frac{1}{2}}$					
2740.551	3	6	36478.22	−0.06	$22960_{1\frac{1}{2}} - 59439^{\circ}_{2\frac{1}{2}}$					
2740.397	1	4	36480.27	−0.02	$40035^{\circ}_{3\frac{1}{2}} - 76516_{4\frac{1}{2}}$					

TABLE 6. Yb II—*Observed and classified lines*—Continued

1	2	3	4	5	6	7	8	9	10	11
Wave-length air	Intensity		Wave number	o–c	Classification	Zeeman type	1st g	2nd g	Zeeman components	
	Meggers lamp	Thomson lamp							Strong p	Strong n
Å			K	K						
2740.215	2	6	36482.69							
2739.475	1	2	36492.55	−0.04	$53404_{2\frac{1}{2}} - 89897^{\circ}_{1\frac{1}{2}}$					
2738.818	2	8	36501.30	0.00	$43956^{\circ}_{2\frac{1}{2}} - 80457_{3\frac{1}{2}}$	7	(0.99)	0.99	0	0.99
2738.31		1	36508.07	+0.05	$43075^{\circ}_{1\frac{1}{2}} - 79583_{2\frac{1}{2}}$					
2737.61	3	15	36517.41	+0.12	$31631^{\circ}_{0\frac{1}{2}} - 68148_{1\frac{1}{2}}$	5	(1.230)	1.22	0	1.28
2736.553	4	20	36531.51	+0.10	$40917^{\circ}_{1\frac{1}{2}} - 77449_{2\frac{1}{2}}$					
2736.050		2	36538.23	−0.03	$57765_{4\frac{1}{2}} - 94303^{\circ}_{3\frac{1}{2}}$					
2735.673	2	6	36543.26	+0.07	$56375_{2\frac{1}{2}} - 92919^{\circ}_{3\frac{1}{2}}$					
2734.928		2	36553.22	+0.07	$62861_{5\frac{1}{2}} - 99414^{\circ}_{4\frac{1}{2}}$					
2734.413		1	36560.10							
2734.087	5	30	36564.46	−0.05	$34389^{\circ}_{2\frac{1}{2}} - 70954_{2\frac{1}{2}}$	7	1.00	1.00	0	1.00
2733.724		4	36569.31	−0.02	$31979^{\circ}_{3\frac{1}{2}} - 68549_{4\frac{1}{2}}$					
2733.65		2	36570.30	−0.08	$57765_{4\frac{1}{2}} - 94335^{\circ}_{5\frac{1}{2}}$					
2733.112	5	10	36577.50	+0.05	$24332_{2\frac{1}{2}} - 60910^{\circ}_{1\frac{1}{2}}$	5	(1.202)	1.12	w	1.32
2732.942	1	4	36579.78	+0.08	$37077^{\circ}_{2\frac{1}{2}} - 73657_{1\frac{1}{2}}$					
2732.742	30r	150	36582.45	−0.04	$31568^{\circ}_{2\frac{1}{2}} - 68150_{1\frac{1}{2}}$	4	(0.862)	0.90	d	0.81
2732.50		1	36585.69							
2732.033		1	36591.95							
2731.83		1	36594.67	−0.01	$57765_{4\frac{1}{2}} - 94360^{\circ}_{4\frac{1}{2}}$					
2731.573		3	36598.11	−0.05	$43007^{\circ}_{0\frac{1}{2}} - 79605_{1\frac{1}{2}}$					
2731.517		3	36598.86							
2730.62		1	36610.88							
2729.50	2	8	36625.90	−0.05	$32981^{\circ}_{1\frac{1}{2}} - 69607_{2\frac{1}{2}}$	5	(0.866)	1.21	0.17	
2729.093	1	5	36631.36	−0.03	$38342^{\circ}_{1\frac{1}{2}} - 74973_{3\frac{1}{2}}$					
2728.47		1	36639.73							
2728.420	6	20	36640.40	−0.09	$40035^{\circ}_{3\frac{1}{2}} - 76676_{2\frac{1}{2}}$	4	0.726	1.112	0.193	0.240
2727.66		1	36650.61	−0.02	$49498_{2\frac{1}{2}} - 86148^{\circ}_{2\frac{1}{2}}$					
2727.22		1	36656.52							
2724.65	1	3	36691.09							
2724.41		2	36694.33							
2723.338		3	36708.77	−0.01	$32371^{\circ}_{2\frac{1}{2}} - 69079_{2\frac{1}{2}}$					
2722.759		2	36716.58	+0.06	$44940^{\circ}_{1\frac{1}{2}} - 81657_{2\frac{1}{2}}$					
2722.475	1	5	36720.41	+0.01	$47912_{3\frac{1}{2}} - 84632^{\circ}_{2\frac{1}{2}}$					
2722.205	8	40	36724.05	−0.03	$34389^{\circ}_{2\frac{1}{2}} - 71113_{1\frac{1}{2}}$	7	0.99	(0.967)	0	1.03
2721.895		3	36728.23	−0.04	$49498_{2\frac{1}{2}} - 86226^{\circ}_{1\frac{1}{2}}$					
2721.183		3	36737.84	+0.06	$53404_{2\frac{1}{2}} - 90142^{\circ}_{3\frac{1}{2}}$					
2720.522	1	5	36746.77							
2719.996		2	36753.87	−0.02	$37516^{\circ}_{3\frac{1}{2}} - 74270_{2\frac{1}{2}}$					
2719.005	3	15	36767.27	+0.03	$44438^{\circ}_{3\frac{1}{2}} - 81205_{4\frac{1}{2}}$	7	(1.10)	1.11	0	1.157
2718.349	40r	200	36776.14	0.00	$31979^{\circ}_{3\frac{1}{2}} - 68756_{3\frac{1}{2}}$	7	1.328	1.328	0	1.328

TABLE 6. Yb II—*Observed and classified lines*—Continued

1	2	3	4	5	6	7	8	9	10	11
Wave-length air	Intensity		Wave number	o–c	Classification	Zeeman type	1st g	2nd g	Zeeman components	
	Meggers lamp	Thomson lamp							Strong p	Strong n
Å			K	K						
2717.76		2	36784.11	+0.05	$35831^{\circ}_{5\frac{1}{2}} - 72615_{5\frac{1}{2}}$					
2717.661	3	10	36785.45							
2717.617	1	4	36786.04	+0.01	$41678^{\circ}_{2\frac{1}{2}} - 78464_{1\frac{1}{2}}$					
2717.106	4	20	36792.96	+0.03	$58961_{5\frac{1}{2}} - 95754^{\circ}_{5\frac{1}{2}}$	7	0.89	0.89	0	0.89
2716.354	3	5	36803.15	−0.03	$40035^{\circ}_{3\frac{1}{2}} - 76839_{2\frac{1}{2}}$					
2716.177		3	36805.55							
2715.94	3	15	36808.76	+0.02	$28757^{\circ}_{1\frac{1}{2}} - 65566_{0\frac{1}{2}}$	7	1.45	1.45	0	1.45
2715.640	1	4	36812.82	+0.08	$30392^{\circ}_{1\frac{1}{2}} - 67204_{1\frac{1}{2}}$					
2715.383	4	7	36816.31	+0.04	$22960_{1\frac{1}{2}} - 59777^{\circ}_{1\frac{1}{2}}$					
2715.17		1	36819.19	+0.07	$56375_{2\frac{1}{2}} - 93195^{\circ}_{3\frac{1}{2}}$					
2714.408	4	30	36829.53	+0.04	$40917^{\circ}_{4\frac{1}{2}} - 77747_{4\frac{1}{2}}$	6	0.965	1.073	0.49	1.02
2714.18		2	36832.62	+0.02	$34389^{\circ}_{2\frac{1}{2}} - 71222_{3\frac{1}{2}}$					
2713.718		2	36838.89							
2712.658	15	80	36853.29	+0.05	$30562^{\circ}_{5\frac{1}{2}} - 67416_{4\frac{1}{2}}$	4	(1.112)	1.23	?	0.52
2711.785	20	30	36865.15	−0.01	$21418^{\circ}_{3\frac{1}{2}} - 58283_{2\frac{1}{2}}$	5	1.141	0.770	0.190	2.071
2711.09		1	36874.60	−0.02	$44438^{\circ}_{3\frac{1}{2}} - 81312_{2\frac{1}{2}}$					
2710.674	6	30	36880.26	+0.01	$34389^{\circ}_{2\frac{1}{2}} - 71270_{2\frac{1}{2}}$	6	1.02	0.92	0.26	0.97
2710.544	20	80	36882.03	0.00	$31568^{\circ}_{2\frac{1}{2}} - 68450_{3\frac{1}{2}}$	5	0.87	1.09	0.111	1.651
2710.046	2	5	36888.81	+0.10	$26759^{\circ}_{2\frac{1}{2}} - 63647_{1\frac{1}{2}}$					
2709.715	4	20	36893.31	−0.02	$34575^{\circ}_{1\frac{1}{2}} - 71468_{2\frac{1}{2}}$	4	1.46	1.02	0.22	0.36
2708.842	5	30	36905.20	0.00	$33052^{\circ}_{4\frac{1}{2}} - 69957_{4\frac{1}{2}}$	6	1.27	1.13	0.65	1.20
2708.46		2	36910.41							
2705.108		3	36956.14	+0.05	$61873_{6\frac{1}{2}} - 98829^{\circ}_{6\frac{1}{2}}$					
2704.75		2	36961.03							
2704.53	3	15	36964.04	−0.09	$40917^{\circ}_{4\frac{1}{2}} - 77882_{3\frac{1}{2}}$					
2702.133	1	4	36996.83	0.00	$53720_{4\frac{1}{2}} - 90717^{\circ}_{4\frac{1}{2}}$					
2701.733	1	4	37002.30	+0.02	$53715_{3\frac{1}{2}} - 90717^{\circ}_{4\frac{1}{2}}$					
2701.130	3	5	37010.56							
2700.797	6	40	37015.13	+0.02	$44497^{\circ}_{2\frac{1}{2}} - 81512_{1\frac{1}{2}}$	5	0.74	0.48	0.130	1.14
2698.617	2	8	37045.03							
2698.447		1	37047.36	−0.09	$32981^{\circ}_{1\frac{1}{2}} - 70029_{0\frac{1}{2}}$					
2696.625	4	20	37072.39	−0.03	$32371^{\circ}_{2\frac{1}{2}} - 69443_{1\frac{1}{2}}$	7	(1.170)	1.16	0	1.19
2696.150		2	37078.92	−0.02	$34389^{\circ}_{2\frac{1}{2}} - 71468_{2\frac{1}{2}}$					
2695.556		2	37087.09	−0.01	$56375_{2\frac{1}{2}} - 93463^{\circ}_{3\frac{1}{2}}$					
2695.427	8	60	37088.87	+0.02	$31631^{\circ}_{6\frac{1}{2}} - 68720_{6\frac{1}{2}}$	6	(1.230)	1.16	0.44	?
2694.622	1	4	37099.95	−0.03	$31979^{\circ}_{3\frac{1}{2}} - 69079_{2\frac{1}{2}}$					
2692.703	2	10	37126.38	−0.03	$41688^{\circ}_{1\frac{1}{2}} - 78814_{2\frac{1}{2}}$					
2692.408	3	15	37130.45	−0.03	$28757^{\circ}_{1\frac{1}{2}} - 65888_{1\frac{1}{2}}$					
2691.996	5	30	37136.14	+0.01	$41678^{\circ}_{2\frac{1}{2}} - 78814_{2\frac{1}{2}}$	6	(1.193)	1.26	d	1.225
2691.49		3	37143.12	+0.09	$35059^{\circ}_{3\frac{1}{2}} - 72202_{3\frac{1}{2}}$					

TABLE 6. Yb II—*Observed and classified lines*—Continued

1	2	3	4	5	6	7	8	9	10	11
Wave-length air	Intensity		Wave number	o–c	Classification	Zeeman type	1st g	2nd g	Zeeman components	
	Meggers lamp	Thomson lamp							Strong p	Strong n
Å			K	K						
2691.44		2	37143.81	0.00	$53715_{3\frac{1}{2}} - 90859^{\circ}_{2\frac{1}{2}}$					
2690.669	2	2	37154.45	−0.06	$45737^{\circ}_{1\frac{1}{2}} - 82891_{2\frac{1}{2}}$					
2690.298	1	3	37159.57	−0.05	$44497^{\circ}_{2\frac{1}{2}} - 81657_{2\frac{1}{2}}$					
2688.22		1	37188.29	−0.01	$34575^{\circ}_{1\frac{1}{2}} - 71763_{1\frac{1}{2}}$					
2687.980	4	30	37191.62	−0.08	$30224^{\circ}_{4\frac{1}{2}} - 67416_{4\frac{1}{2}}$	6	(0.935)	1.261	1.467	?
2687.900	1	5	37192.72							
2687.08		1	37204.07							
2685.990	2	10	37219.17	+0.07	$44438^{\circ}_{3\frac{1}{2}} - 81657_{2\frac{1}{2}}$					
2685.30		2	37228.73							
2684.747	10	70	37236.40	−0.04	$32371^{\circ}_{2\frac{1}{2}} - 69607_{2\frac{1}{2}}$	6	1.172	1.208	0.09	1.190
2683.895		2	37248.22	−0.04	$48900_{3\frac{1}{2}} - 86148^{\circ}_{2\frac{1}{2}}$					
2683.416	4	30	37254.87	−0.02	$44438^{\circ}_{3\frac{1}{2}} - 81692_{3\frac{1}{2}}$	6	1.11	1.16	0.18	1.14
2681.180		2	37285.94							
2680.404	6	40	37296.73	−0.07	$26759^{\circ}_{2\frac{1}{2}} - 64055_{2\frac{1}{2}}$	6	1.576	1.100	1.164	1.338
2678.847	1	3	37318.41							
2676.131	3	6	37356.28	+0.04	$43956^{\circ}_{2\frac{1}{2}} - 81312_{2\frac{1}{2}}$					
2674.866	3	10	37373.94	+0.03	$34389^{\circ}_{2\frac{1}{2}} - 71763_{1\frac{1}{2}}$	4	(1.007)	1.06	d	0.924
2672.656	200R	200	37404.85	+0.02	$21418^{\circ}_{3\frac{1}{2}} - 58823_{2\frac{1}{2}}$	4	1.15	1.28	(0.064)	0.83
2672.035		2	37413.54	+0.04	$40035^{\circ}_{3\frac{1}{2}} - 77449_{3\frac{1}{2}}$					
2671.554		2	37420.27	+0.09	$39378^{\circ}_{0\frac{1}{2}} - 76799_{1\frac{1}{2}}$					
2670.605		1	37433.57							
2669.305		1	37451.80	+0.13	$35831^{\circ}_{5\frac{1}{2}} - 73283_{4\frac{1}{2}}$					
2669.131	1	3	37454.24	+0.13	$53404_{2\frac{1}{2}} - 90859^{\circ}_{2\frac{1}{2}}$					
2668.94		2	37456.92	+0.10	$37516^{\circ}_{3\frac{1}{2}} - 74973_{3\frac{1}{2}}$					
2668.752	8	40	37459.56	−0.03	$33494^{\circ}_{3\frac{1}{2}} - 70954_{2\frac{1}{2}}$	7	(0.991)	1.00	0	0.98
2668.707	4	20	37460.19	−0.08	$35831^{\circ}_{5\frac{1}{2}} - 73291_{5\frac{1}{2}}$					
2668.587	1	3	37461.88	−0.10	$45429^{\circ}_{3\frac{1}{2}} - 82891_{2\frac{1}{2}}$					
2667.965		2	37470.61	−0.06	$61051_{3\frac{1}{2}} - 98521^{\circ}_{4\frac{1}{2}}$					
2665.038	60	100	37511.76	−0.04	$31568^{\circ}_{2\frac{1}{2}} - 69079_{2\frac{1}{2}}$	6	0.859	0.893	0.085	0.876
2664.39		2	37520.88							
2663.900	2	5	37527.79							
2661.888		3	37556.15	−0.06	$43956^{\circ}_{2\frac{1}{2}} - 81512_{1\frac{1}{2}}$					
2660.861	1	4	37570.64	−0.12	$40035^{\circ}_{3\frac{1}{2}} - 77606_{2\frac{1}{2}}$					
2660.73		2	37572.49							
2659.635		2	37587.96	−0.04	$61214_{4\frac{1}{2}} - 98802^{\circ}_{5\frac{1}{2}}$					
2659.267	4	20	37593.16	−0.07	$28757^{\circ}_{1\frac{1}{2}} - 66351_{2\frac{1}{2}}$	4	1.443	1.129	0.157	0.658
2657.46		1	37618.72	−0.06	$45273^{\circ}_{3\frac{1}{2}} - 82891_{2\frac{1}{2}}$					
2657.20		2	37622.40							
2656.838	2	15	37627.53	−0.11	$31979^{\circ}_{3\frac{1}{2}} - 69607_{2\frac{1}{2}}$ [d]	7	(1.33)	1.45	0	1.03
2656.125	10	40	37637.63	−0.11	$28757^{\circ}_{1\frac{1}{2}} - 66395_{2\frac{1}{2}}$	4	1.44	1.24	0.10	0.94

TABLE 6. Yb II—*Observed and classified lines*—Continued

1	2	3	4	5	6	7	8	9	10	11
Wavelength air	Intensity		Wave number	o–c	Classification	Zeeman type	1st g	2nd g	Zeeman components	
	Meggers lamp	Thomson lamp							Strong p	Strong n
Å			K	K						
2653.75	1000R	1000	37671.31	−0.07	$21418^{\circ}_{3\frac{1}{2}} - 59090_{3\frac{1}{2}}$	7	(1.145)	1.13	0	1.136
2650.795	2	10	37713.30	−0.08	$24332_{2\frac{1}{2}} - 62046^{\circ}_{3\frac{1}{2}}$					
2650.728	9	30	37714.26	−0.09	$30224^{\circ}_{4\frac{1}{2}} - 67938_{3\frac{1}{2}}$	4	(0.935)	0.96		0.863
2649.787	10	40	37727.65	−0.03	$33494^{\circ}_{3\frac{1}{2}} - 71222_{3\frac{1}{2}}$	6	0.98	1.14	0.54	1.06
2649.165		3	37736.51	0.00	$43956^{\circ}_{2\frac{1}{2}} - 81692_{3\frac{1}{2}}$					
2648.803	6	30	37741.66	−0.01	$33052^{\circ}_{4\frac{1}{2}} - 70793_{5\frac{1}{2}}$	4	1.24	1.20	(0.017)	1.05
2647.455	8	40	37760.88	+0.02	$35019^{\circ}_{4\frac{1}{2}} - 72779_{3\frac{1}{2}}$	5	1.16	1.12	(0.02)	1.30
2647.233	2	10	37764.05	0.00	$42915^{\circ}_{5\frac{1}{2}} - 80679_{5\frac{1}{2}}$					
2646.442	6	30	37775.33	0.00	$33494^{\circ}_{3\frac{1}{2}} - 71270_{2\frac{1}{2}}$	5	0.98	0.90	(0.04)	1.18
2645.691		2	37786.06							
2644.306	20r	80	37805.85	−0.04	$33052^{\circ}_{4\frac{1}{2}} - 70858_{4\frac{1}{2}}$	6	1.265	1.279	(0.06)	1.272
2643.237		3	37821.13	−0.01	$53715_{3\frac{1}{2}} - 91536^{\circ}_{3\frac{1}{2}}$					
2642.815		5	37827.17	+0.05	$31568^{\circ}_{2\frac{1}{2}} - 69395_{3\frac{1}{2}}$					
2642.558	10	1000	37830.85	+0.06	$34784^{\circ}_{5\frac{1}{2}} - 72615_{5\frac{1}{2}}$	6	1.20	1.07	0.73	1.132
2641.97	2	10	37839.27	+0.01	$26759^{\circ}_{2\frac{1}{2}} - 64598_{3\frac{1}{2}}$					
2641.886	50	50	37840.47	−0.02	$21418^{\circ}_{3\frac{1}{2}} - 59259_{2\frac{1}{2}}$	5	(1.145)	1.12	w	1.20
2641.485		2	37846.22	0.00	$40035^{\circ}_{3\frac{1}{2}} - 77882_{3\frac{1}{2}}$					
2639.448	10	40	37875.42	−0.02	$31568^{\circ}_{2\frac{1}{2}} - 69443_{1\frac{1}{2}}$	4	0.86	1.14	0.14	0.42
2638.596	4	5	37887.65	−0.05	$49498_{2\frac{1}{2}} - 87385^{\circ}_{3\frac{1}{2}}$					
2637.637		2	37901.43	−0.04	$44497^{\circ}_{2\frac{1}{2}} - 82398_{1\frac{1}{2}}$					
2637.378	2	2	37905.15	+0.02	$39378^{\circ}_{0\frac{1}{2}} - 77284_{1\frac{1}{2}}$					
2636.519	1	6	37917.50	0.00	$41688^{\circ}_{1\frac{1}{2}} - 79605_{1\frac{1}{2}}$	6	(0.784)	1.16	0.58	
2636.399		3	37919.22	0.00	$35831^{\circ}_{5\frac{1}{2}} - 73750_{4\frac{1}{2}}$					
2636.275	2	8	37921.01	−0.05	$52938_{1\frac{1}{2}} - 90859^{\circ}_{2\frac{1}{2}}$					
2635.197	1	4	37936.52	−0.14	$58961_{5\frac{1}{2}} - 96898^{\circ}_{5\frac{1}{2}}$					
2634.306	30	40	37949.35	+0.01	$22960_{1\frac{1}{2}} - 60910^{\circ}_{1\frac{1}{2}}$	6	0.806	1.000	0.29	0.903
2634.183		3	37951.12	−0.07	$44940^{\circ}_{1\frac{1}{2}} - 82891_{2\frac{1}{2}}$					
2632.69	2	8	37972.64	−0.04	$32981^{\circ}_{1\frac{1}{2}} - 70954_{2\frac{1}{2}}$					
2631.73	3	15	37986.49	+0.05	$30562^{\circ}_{5\frac{1}{2}} - 68549_{4\frac{1}{2}}$	4	(1.112)	1.14	w	1.00
2628.80	2	7	38028.83	−0.02	$45335^{\circ}_{4\frac{1}{2}} - 83363_{3\frac{1}{2}}$					
2628.605	1	4	38031.65	−0.06	$61214_{4\frac{1}{2}} - 99246^{\circ}_{5\frac{1}{2}}$					
2628.424		2	38034.27	−0.08	$37516^{\circ}_{3\frac{1}{2}} - 75550_{2\frac{1}{2}}$					
				−0.10	$40035^{\circ}_{3\frac{1}{2}} - 78070_{4\frac{1}{2}}$					
2628.07	3	20	38039.39	−0.07	$31568^{\circ}_{2\frac{1}{2}} - 69607_{2\frac{1}{2}}$	6	(0.862)	1.22	0.88	
2624.949	3	5	38084.62	+0.04	$49301_{4\frac{1}{2}} - 87385^{\circ}_{3\frac{1}{2}}$					
2624.52		2	38090.84	−0.02	$45273^{\circ}_{3\frac{1}{2}} - 83363_{3\frac{1}{2}}$					
2623.22	2	9	38109.72	−0.09	$33653^{\circ}_{0\frac{1}{2}} - 71763_{1\frac{1}{2}}$	4	1.32	1.10	0.11	0.99
2621.67	4	20	38132.25	0.00	$32981^{\circ}_{1\frac{1}{2}} - 71113_{1\frac{1}{2}}$					
2619.93	3	15	38157.57	−0.08	$30562^{\circ}_{5\frac{1}{2}} - 68720_{6\frac{1}{2}}$	5	(1.112)	1.13	d	1.25
2619.074	4	20	38170.04	−0.03	$33052^{\circ}_{4\frac{1}{2}} - 71222_{3\frac{1}{2}}$					

TABLE 6. Yb II—*Observed and classified lines*—Continued

1	2	3	4	5	6	7	8	9	10	11
Wavelength air	Intensity		Wave number	o–c	Classification	Zeeman type	1st g	2nd g	Zeeman components	
	Meggers lamp	Thomson lamp							Strong p	Strong n
Å			K	K						
2618.948		2	38171.88							
2617.01	100r	100	38200.15	0.00 −0.04	$21418^{\circ}_{3\frac{1}{2}} - 59618_{3\frac{1}{2}}$ $(52517_{3\frac{1}{2}} - 90717^{\circ}_{4\frac{1}{2}})$	6	1.16	1.02	0.46	1.09
2615.35	1	5	38224.39	+0.04	$35059^{\circ}_{3\frac{1}{2}} - 73283_{4\frac{1}{2}}$					
2615.262	6	30	38225.68	−0.10	$30224^{\circ}_{4\frac{1}{2}} - 68450_{3\frac{1}{2}}$	4	(0.935)	1.06	(0.06)	
2614.55	1	3	38236.08							
2614.45	2	3	38237.55	−0.01	$43075^{\circ}_{1\frac{1}{2}} - 81312_{2\frac{1}{2}}$					
2612.63	2	10	38264.18	−0.04	$35019^{\circ}_{4\frac{1}{2}} - 73283_{4\frac{1}{2}}$					
2612.041	4	20	38272.81	−0.01	$35019^{\circ}_{4\frac{1}{2}} - 73291_{5\frac{1}{2}}$					
2611.645	2	2	38278.61							
2610.860	5	30	38290.12	−0.02	$42915^{\circ}_{5\frac{1}{2}} - 81205_{4\frac{1}{2}}$	7	(1.115)	1.11	0	1.14
2610.531	1	4	38294.95	−0.10	$53720_{4\frac{1}{2}} - 92015^{\circ}_{4\frac{1}{2}}$					
2608.498	1	4	38324.79	−0.11	$30224^{\circ}_{4\frac{1}{2}} - 68549_{4\frac{1}{2}}$					
2607.864	5	30	38334.11	−0.01	$26759^{\circ}_{2\frac{1}{2}} - 65093_{3\frac{1}{2}}$	4				
2605.43	2	3	38369.92							
2604.69		2	38380.82	−0.04	$30562^{\circ}_{5\frac{1}{2}} - 68943_{4\frac{1}{2}}$					
2604.053	5	30	38390.21	−0.02	$34389^{\circ}_{2\frac{1}{2}} - 72779_{3\frac{1}{2}}$	5	(1.007)	1.08	w	1.25
2602.40		2	38414.59							
2600.850	2	9	38437.48	−0.05	$43075^{\circ}_{1\frac{1}{2}} - 81512_{1\frac{1}{2}}$					
2600.508	1	2	38442.54	−0.03	$43956^{\circ}_{2\frac{1}{2}} - 82398_{1\frac{1}{2}}$					
2600.21	3	15	38446.94	−0.05	$28757^{\circ}_{1\frac{1}{2}} - 67204_{1\frac{1}{2}}$					
2599.75	1	2	38453.74	−0.03	$44438^{\circ}_{3\frac{1}{2}} - 82891_{2\frac{1}{2}}$					
2598.43	2	6	38473.28	−0.07	$37077^{\circ}_{2\frac{1}{2}} - 75550_{2\frac{1}{2}}$					
2598.11		2	38478.02							
2597.69	1	3	38484.24							
2597.619	2	2	38485.29	−0.04	$48900_{3\frac{1}{2}} - 87385^{\circ}_{3\frac{1}{2}}$					
2597.495	1	5	38487.13	+0.02	$32981^{\circ}_{1\frac{1}{2}} - 71468_{2\frac{1}{2}}$					
2596.735	3	30	38498.39	−0.01	$34784^{\circ}_{5\frac{1}{2}} - 73283_{4\frac{1}{2}}$					
2596.320	6	80	38504.54	−0.11	$31631^{\circ}_{6\frac{1}{2}} - 70136_{6\frac{1}{2}}$	6	(1.23)	1.15?	0.51	
2596.16	6	80	38506.92	−0.08	$34784^{\circ}_{5\frac{1}{2}} - 73291_{5\frac{1}{2}}$	6	1.12	1.09	0.17	1.10w
2594.493	3	20	38531.65	−0.06	$30224^{\circ}_{4\frac{1}{2}} - 68756_{3\frac{1}{2}}$					
2594.20	3	15	38536.01			6			0.22	
2591.026	3	10	38583.21	+0.04	$32371^{\circ}_{2\frac{1}{2}} - 70954_{2\frac{1}{2}}$	6	(1.17)	1.00	0.43	
2590.711	2	5	38587.90	−0.08	$53715_{3\frac{1}{2}} - 92303^{\circ}_{3\frac{1}{2}}$					
2586.30	3	10	38653.71	+0.05	$37516^{\circ}_{3\frac{1}{2}} - 76170_{2\frac{1}{2}}$	7	(1.12)	1.10	0	1.17
2583.748	1	4	38691.89	−0.01	$35059^{\circ}_{3\frac{1}{2}} - 73750_{4\frac{1}{2}}$					
2582.489		2	38710.75	−0.05	$40917^{\circ}_{4\frac{1}{2}} - 79628_{3\frac{1}{2}}$					
2582.068		3	38717.06	−0.06	$57765_{4\frac{1}{2}} - 96482^{\circ}_{4\frac{1}{2}}$					
2581.41	1	4	38726.93	−0.02	$34389^{\circ}_{2\frac{1}{2}} - 73116_{1\frac{1}{2}}$					
2581.092		3	38731.70	−0.07	$35019^{\circ}_{4\frac{1}{2}} - 73750_{4\frac{1}{2}}$					

TABLE 6. Yb II—*Observed and classified lines*—Continued

1	2	3	4	5	6	7	8	9	10	11
Wavelength air	Intensity		Wave number	o–c	Classification	Zeeman type	1st g	2nd g	Zeeman components	
	Meggers lamp	Thomson lamp							Strong p	Strong n
Å			K	K						
2577.74	3	10	38782.06	−0.02	$32981^{\circ}_{1\frac{1}{2}} - 71763_{1\frac{1}{2}}$					
2577.605	5	20	38784.09	−0.13	$52517_{3\frac{1}{2}} - 91301^{\circ}_{6\frac{1}{2}}$					
2576.09		2	38806.90	0.00	$37516^{\circ}_{3\frac{1}{2}} - 76323_{3\frac{1}{2}}$					
2574.78	2	10	38826.64	0.00	$27061^{\circ}_{0\frac{1}{2}} - 65888_{1\frac{1}{2}}$					
2573.147	6	30	38851.28	+0.02	$32371^{\circ}_{2\frac{1}{2}} - 71222_{3\frac{1}{2}}$	7	(1.17)	1.16	0	1.12
2572.15	1	4	38866.34	−0.03	$44497^{\circ}_{2\frac{1}{2}} - 83363_{3\frac{1}{2}}$					
2571.69	1	2	38873.29	−0.02	$53404_{2\frac{1}{2}} - 92278^{\circ}_{1\frac{1}{2}}$					
2571.36	7	50	38878.28	0.00	$31979^{\circ}_{3\frac{1}{2}} - 70858_{4\frac{1}{2}}$	4	(1.331)	1.30	w	1.18
2569.61	1	2	38904.76							
2568.60		2	38920.05							
2568.17	3	10	38926.57	−0.06	$53720_{4\frac{1}{2}} - 92647^{\circ}_{5\frac{1}{2}}$					
2565.573	10	40	38965.97	+0.02	$34784^{\circ}_{5\frac{1}{2}} - 73750_{4\frac{1}{2}}$					
2563.92	2	2	38991.09							
2559.972	2	5	39051.22	−0.07	$30392^{\circ}_{1\frac{1}{2}} - 69443_{1\frac{1}{2}}$					
2558.40	3	2	39075.21							
2557.804	4	5	39084.32	−0.02	$24332_{2\frac{1}{2}} - 63417^{\circ}_{2\frac{1}{2}}$					
2557.703	1	5	39085.86	−0.01	$39378^{\circ}_{0\frac{1}{2}} - 78464_{1\frac{1}{2}}$					
2557.259	4	20	39092.64	−0.02	$37077^{\circ}_{2\frac{1}{2}} - 76170_{2\frac{1}{2}}$	7	(1.113)	1.13	0	1.12
2556.30		3	39107.31	+0.01	$38342^{\circ}_{4\frac{1}{2}} - 77449_{3\frac{1}{2}}$					
2554.641		2	39132.70	−0.01	$57765_{4\frac{1}{2}} - 96898^{\circ}_{5\frac{1}{2}}$					
2552.88	2	2	39159.70	−0.02	$37516^{\circ}_{3\frac{1}{2}} - 76676_{2\frac{1}{2}}$					
2552.70	10	60	39162.46	+0.09	$31631^{\circ}_{6\frac{1}{2}} - 70793_{5\frac{1}{2}}$	7	(1.230)	1.224	0	1.264
2552.147	15	80	39170.94	+0.07	$30224^{\circ}_{4\frac{1}{2}} - 69395_{3\frac{1}{2}}$	7	(0.935)	0.942	0	0.912
2550.786		1	39191.84							
2550.68	3	10	39193.47	+0.03	$53720_{4\frac{1}{2}} - 92914^{\circ}_{4\frac{1}{2}}$					
2550.060	10	20	39203.00	−0.12	$22960_{1\frac{1}{2}} - 62163^{\circ}_{2\frac{1}{2}}$					
2550.023		3	39203.57							
2548.756	3	15	39223.05	−0.03	$49498_{2\frac{1}{2}} - 88721^{\circ}_{3\frac{1}{2}}$	7	(1.145)	1.156	0	1.182
2548.00		3	39234.69							
2547.498	2	8	39242.42	−0.04	$31979^{\circ}_{3\frac{1}{2}} - 71222_{3\frac{1}{2}}$					
2547.23	2	5	39246.55							
2547.20		2	39247.01							
2546.886	1	2	39251.85							
2546.28	2	5	39261.19	−0.05	$53715_{3\frac{1}{2}} - 92976^{\circ}_{3\frac{1}{2}}$					
2545.871	2	4	39267.50	−0.03	$34389^{\circ}_{2\frac{1}{2}} - 73657_{1\frac{1}{2}}$					
2545.545		3	39272.53							
2544.72		2	39285.26	−0.05	$33494^{\circ}_{3\frac{1}{2}} - 72779_{3\frac{1}{2}}$					
2542.76	3	10	39315.54	−0.05 +0.13	$53720_{4\frac{1}{2}} - 93036^{\circ}_{5\frac{1}{2}}$ $56375_{2\frac{1}{2}} - 95691^{\circ}_{3\frac{1}{2}}$					
2542.318	4	10	39322.37	−0.04	$37516^{\circ}_{3\frac{1}{2}} - 76839_{2\frac{1}{2}}$					
2541.82		1	39330.08							

TABLE 6. Yb II—*Observed and classified lines*—Continued

1	2	3	4	5	6	7	8	9	10	11
Wave-length air	Intensity		Wave number	o–c	Classification	Zeeman type	1st g	2nd g	Zeeman components	
	Meggers lamp	Thomson lamp							Strong p	Strong n
Å			K	K						
2541.16	2	6	39340.29	+0.03	$52938_{1\frac{1}{2}} - 92278^{\circ}_{1\frac{1}{2}}$					
2540.60		1	39348.96							
2539.64		4	39363.84							
2538.79	2	20	39377.02	0.00	$28757^{\circ}_{1\frac{1}{2}} - 68135_{2\frac{1}{2}}$					
2538.67	300*A*	200	39378.88	−0.01	$0_{0\frac{1}{2}} - 39378^{\circ}_{0\frac{1}{2}}$	6	2.00	1.86	0.07	1.93
2538.203	4	30	39386.12	−0.07	$31568^{\circ}_{2\frac{1}{2}} - 70954_{2\frac{1}{2}}$	6				
2537.65	10	70	39394.70	0.00	$30562^{\circ}_{5\frac{1}{2}} - 69957_{4\frac{1}{2}}$	7	(1.11)	1.11	0	1.135
2537.240	1	5	39401.07	+0.03	$27061^{\circ}_{0\frac{1}{2}} - 66462_{0\frac{1}{2}}$					
2537.08		1	39403.55							
2536.962	2	10	39405.39	+0.01	$38342^{\circ}_{4\frac{1}{2}} - 77747_{4\frac{1}{2}}$	6	(1.09)	1.07	0	1.08
2536.027	4	20	39419.91	−0.05	$49301_{4\frac{1}{2}} - 88721^{\circ}_{3\frac{1}{2}}$	5	(1.19)	1.18	*w*	1.23
2534.05		2	39450.67							
2532.55	2	6	39474.03							
2532.19	2	3	39479.64	−0.13	$53715_{3\frac{1}{2}} - 93195^{\circ}_{3\frac{1}{2}}$					
2531.00		1	39498.20	−0.21	$52517_{5\frac{1}{2}} - 92015^{\circ}_{4\frac{1}{2}}$?					
2529.98	1	3	39514.13	−0.01	$53404_{2\frac{1}{2}} - 92919^{\circ}_{3\frac{1}{2}}$					
2529.50	3	9	39521.62	−0.06	$53720_{4\frac{1}{2}} - 93242^{\circ}_{5\frac{1}{2}}$					
2528.836	1	1	39532.00							
2528.339	3	25	39539.77	−0.03	$40917^{\circ}_{4\frac{1}{2}} - 80457_{3\frac{1}{2}}$	7	(0.967)	0.98	0	0.938
2527.954		3	39545.79	+0.03	$31568^{\circ}_{2\frac{1}{2}} - 71113_{1\frac{1}{2}}$					
2727.864	4	30	39547.20	−0.09	$40035^{\circ}_{3\frac{1}{2}} - 79583_{2\frac{1}{2}}$	5	(0.72)	0.70	*w*	0.77
2527.49		2	39553.05							
2526.31	2	5	39571.52	−0.02	$53404_{2\frac{1}{2}} - 92976^{\circ}_{3\frac{1}{2}}$					
2526.189		3	39573.42	−0.03	$30562^{\circ}_{5\frac{1}{2}} - 70136_{6\frac{1}{2}}$					
2524.990	2	10	39592.21	+0.02	$26759^{\circ}_{2\frac{1}{2}} - 66351_{2\frac{1}{2}}$					
2524.573	4	8	39598.75	+0.03	$37077^{\circ}_{2\frac{1}{2}} - 76676_{2\frac{1}{2}}$					
2522.438	15	50	39632.26	−0.05	$21418^{\circ}_{3\frac{1}{2}} - 61051_{3\frac{1}{2}}$	6	1.14	1.18	0.14	1.16*w*
2521.04	3	15	39654.24	−0.04	$31568^{\circ}_{2\frac{1}{2}} - 71222_{3\frac{1}{2}}$					
2519.39		2	39680.21							
2518.59		2	39692.81							
2518.47		1	39694.70							
2518.01	3	10	39701.95	+0.02	$31568^{\circ}_{2\frac{1}{2}} - 71270_{2\frac{1}{2}}$	6	0.86	0.90	0.09	0.88
2516.82	50	300	39720.72			7			0	1.348
2516.35	6	30	39728.14	−0.03	$38342^{\circ}_{4\frac{1}{2}} - 78070_{4\frac{1}{2}}$	6	1.09	1.10	0.06	1.094
2516.031	3	15	39733.18	+0.02	$30224^{\circ}_{4\frac{1}{2}} - 69957_{4\frac{1}{2}}$					
2515.600	2	7	39739.99			7			0	0.91
2515.460	2	3	39742.20	−0.10	$53720_{4\frac{1}{2}} - 93463^{\circ}_{3\frac{1}{2}}$					
2515.165		2	39746.86							
2514.69		1	39754.37							
2514.248	7	20	39761.35	−0.06 +0.08	$37077^{\circ}_{2\frac{1}{2}} - 76839_{2\frac{1}{2}}$ $(40917^{\circ}_{4\frac{1}{2}} - 80679_{5\frac{1}{2}})$	7	1.116	1.116	0	1.116

277-259 O - 68 - 10

TABLE 6. Yb II—*Observed and classified lines*—Continued

1	2	3	4	5	6	7	8	9	10	11
Wave-length air	Intensity		Wave number	o–c	Classification	Zeeman type	1st g	2nd g	Zeeman components	
	Meggers lamp	Thomson lamp							Strong p	Strong n
Å			K	K						
2513.64		1	39770.97							
2512.87		2	39783.16	−0.02	$53720_{4\frac{1}{2}} - 93503^{\circ}_{4\frac{1}{2}}$					
2512.524	5	20	39788.64	−0.03 +0.01	$33494^{\circ}_{3\frac{1}{2}} - 73283_{4\frac{1}{2}}$ $(53715_{3\frac{1}{2}} - 93503^{\circ}_{4\frac{1}{2}})$	5	(0.99)	1.02	w	1.11
2512.061	50r	100	39795.97	+0.06	$21418^{\circ}_{3\frac{1}{2}} - 61214_{4\frac{1}{2}}$	4	1.12	1.05	(0.036)	0.80
2511.868	4	20	39799.03	+0.05	$26759^{\circ}_{2\frac{1}{2}} - 66558_{3\frac{1}{2}}$					
2510.50	2	7	39820.71	0.00	$48900_{3\frac{1}{2}} - 88721^{\circ}_{3\frac{1}{2}}$					
2510.29	1	2	39824.04	−0.13	$41688^{\circ}_{1\frac{1}{2}} - 81512_{1\frac{1}{2}}$					
2510.03	1	1	39828.17							
2509.86	2	5	39830.86	−0.07	$32371^{\circ}_{2\frac{1}{2}} - 72202_{3\frac{1}{2}}$					
2508.073	10	20	39859.24	−0.04	$24332_{2\frac{1}{2}} - 64191^{\circ}_{1\frac{1}{2}}$					
2505.477	6	30	39900.54	−0.08	$31568^{\circ}_{2\frac{1}{2}} - 71468_{2\frac{1}{2}}$	6	0.86	1.00	0.36?	0.93
2503.46		1	39932.68	−0.05	$37516^{\circ}_{3\frac{1}{2}} - 77449_{3\frac{1}{2}}$					
2502.02	30	70	39955.66	−0.08	$21418^{\circ}_{3\frac{1}{2}} - 61374_{2\frac{1}{2}}$	4	1.14	1.29	(0.07)	0.77
2501.21	1	3	39968.60	−0.08	$41688^{\circ}_{1\frac{1}{2}} - 81657_{2\frac{1}{2}}$					
2500.568	2	6	39978.86							
2498.73		2	40008.27							
2498.36	2	5	40014.19	0.00	$41678^{\circ}_{2\frac{1}{2}} - 81692_{3\frac{1}{2}}$				0	
2496.85		2	40038.39							
2495.63	5	20	40057.96	−0.06 −0.09	$32981^{\circ}_{1\frac{1}{2}} - 73039_{0\frac{1}{2}}$ $53404_{2\frac{1}{2}} - 93463^{\circ}_{3\frac{1}{2}}$					
2495.05	4	3	40067.27							
2493.64	3	10	40089.93	−0.06	$37516^{\circ}_{3\frac{1}{2}} - 77606_{2\frac{1}{2}}$				0	
2491.15	3	5	40130.00	+0.01	$52517_{5\frac{1}{2}} - 92647^{\circ}_{5\frac{1}{2}}$					
2488.92		3	40165.95							
2487.08	1	3	40195.66	+0.07	$31568^{\circ}_{2\frac{1}{2}} - 71763_{1\frac{1}{2}}$					
2484.89	5	20	40231.09	−0.08 +0.03	$30562^{\circ}_{5\frac{1}{2}} - 70793_{5\frac{1}{2}}$ $(33052^{\circ}_{4\frac{1}{2}} - 73283_{4\frac{1}{2}})$	6	(1.112)	1.20	0.49	
2481.42	1	3	40287.34	−0.02	$40917^{\circ}_{4\frac{1}{2}} - 81205_{4\frac{1}{2}}$					
2481.36		2	40288.32	+0.07	$53720_{4\frac{1}{2}} - 94008^{\circ}_{3\frac{1}{2}}$					
2481.03	1	2	40293.67	−0.03	$53715_{3\frac{1}{2}} - 94008^{\circ}_{3\frac{1}{2}}$					
2479.29		2	40321.95	+0.05	$28757^{\circ}_{1\frac{1}{2}} - 69079_{2\frac{1}{2}}$					
2479.15	1	5	40324.23	−0.06	$59090_{3\frac{1}{2}} - 99414^{\circ}_{4\frac{1}{2}}$					
2477.76		1	40346.85							
2476.62		2	40365.42	−0.03	$37516^{\circ}_{3\frac{1}{2}} - 77882_{3\frac{1}{2}}$					
2475.92		2	40376.83							
2474.52	2	1	40399.67	+0.16	$49498_{2\frac{1}{2}} - 89897^{\circ}_{1\frac{1}{2}}$					
2474.27	1	3	40403.75	−0.08	$21418^{\circ}_{3\frac{1}{2}} - 61822_{3\frac{1}{2}}$					
2473.95		1	40408.98	+0.09	$32371^{\circ}_{2\frac{1}{2}} - 72779_{3\frac{1}{2}}$					
2473.16		2	40421.89	0.00	$40035^{\circ}_{3\frac{1}{2}} - 80457_{3\frac{1}{2}}$					
2471.06	2	3	40456.24	+0.01	$22960_{1\frac{1}{2}} - 63417^{\circ}_{2\frac{1}{2}}$					

TABLE 6. Yb II—*Observed and classified lines*—Continued

1	2	3	4	5	6	7	8	9	10	11
Wave-length air	Intensity		Wave number	o–c	Classification	Zeeman type	1st g	2nd g	Zeeman components	
	Meggers lamp	Thomson lamp							Strong p	Strong n
Å			K	K						
2470.85		2	40459.67	+0.06	$53404_{2\frac{1}{2}} - 93864^{\circ}_{2\frac{1}{2}}$					
2469.89	1	2	40475.40							
2469.52		1	40481.46							
2467.24		2	40518.87	−0.08 −0.01	$52517_{5\frac{1}{2}} - 93036^{\circ}_{5\frac{1}{2}}$ $54304_{0\frac{1}{2}} - 94823^{\circ}_{1\frac{1}{2}}$					
2466.63	5	20	40528.89	−0.10	$37077^{\circ}_{2\frac{1}{2}} - 77606_{2\frac{1}{2}}$	6				
2465.13		2	40553.55	−0.05	$37516^{\circ}_{3\frac{1}{2}} - 78070_{4\frac{1}{2}}$					
2464.59	1	10	40562.43							
2463.79		1	40575.60							
2463.35	2	4	40582.85	−0.02	$53720_{4\frac{1}{2}} - 94303^{\circ}_{3\frac{1}{2}}$					
2463.04		1	40587.96							
2462.71		1	40593.40	−0.16	$53404_{2\frac{1}{2}} - 93998^{\circ}_{1\frac{1}{2}}$					
2461.98		2	40605.43							
2461.83		1	40607.90	−0.09	$52938_{1\frac{1}{2}} - 93546^{\circ}_{2\frac{1}{2}}$					
2461.40	3	10	40615.00	+0.01	$53720_{4\frac{1}{2}} - 94335^{\circ}_{5\frac{1}{2}}$					
2460.25	10	40	40633.98	+0.03	$31568^{\circ}_{2\frac{1}{2}} - 72202_{3\frac{1}{2}}$	7	(0.86)	0.86	0	0.86
2460.00	1	1	40638.11	+0.06	$24332_{2\frac{1}{2}} - 64970^{\circ}_{3\frac{1}{2}}$					
2459.93	1	4	40639.27	−0.02	$53720_{4\frac{1}{2}} - 94360^{\circ}_{4\frac{1}{2}}$					
2458.22		2	40667.54							
2457.73		2	40675.64	−0.06	$32981^{\circ}_{1\frac{1}{2}} - 73657_{1\frac{1}{2}}$					
2456.74		1	40692.03							
2456.35		1	40698.49	−0.12	$33052^{\circ}_{4\frac{1}{2}} - 73750_{4\frac{1}{2}}$					
2456.08		6	40702.97							
2455.97		3	40704.79							
2454.75	1	10	40725.02	−0.02	$52517_{5\frac{1}{2}} - 93242^{\circ}_{5\frac{1}{2}}$					
2454.52	3	20	40728.83	−0.01	$52517_{5\frac{1}{2}} - 93246^{\circ}_{6\frac{1}{2}}$					
2453.51		2	40745.60	−0.01	$32371^{\circ}_{2\frac{1}{2}} - 73116_{1\frac{1}{2}}$					
2451.94	2	3	40771.69							
2451.15		1	40784.83	+0.02	$38342^{\circ}_{4\frac{1}{2}} - 79126_{4\frac{1}{2}}$					
2450.26	3	5	40799.64							
2449.71	1	3	40808.80	−0.01	$47912_{3\frac{1}{2}} - 88721^{\circ}_{3\frac{1}{2}}$					
2449.45		2	40813.13							
2447.26	3	10	40849.65	+0.09	$28757^{\circ}_{1\frac{1}{2}} - 69607_{2\frac{1}{2}}$					
2446.41		1	40863.84							
2445.92	1	2	40872.03							
2444.64		2	40893.43	+0.02	$27061^{\circ}_{0\frac{1}{2}} - 67955_{0\frac{1}{2}}$					
2443.74		2	40908.49	−0.02	$49301_{4\frac{1}{2}} - 90209^{\circ}_{4\frac{1}{2}}$					
2442.64	1	3	40926.91							
2440.01		1	40971.02							
2439.72		2	40975.89							

TABLE 6. Yb II—*Observed and classified lines*—Continued

1	2	3	4	5	6	7	8	9	10	11
Wavelength air	Intensity		Wave number	o–c	Classification	Zeeman type	1st g	2nd g	Zeeman components	
	Meggers lamp	Thomson lamp							Strong p	Strong n
Å			K	K						
2439.59	3	5	40978.07	+0.15	$49301_{4\frac{1}{2}} - 90279^{\circ}_{5\frac{1}{2}}$					
2437.24	4	7	41017.58							
2436.87	1	2	41023.81	−0.03	$53404_{2\frac{1}{2}} - 94428^{\circ}_{1\frac{1}{2}}$					
2436.06		5	41037.45	+0.11	$57765_{4\frac{1}{2}} - 98802^{\circ}_{5\frac{1}{2}}$					
2434.02		2	41071.84							
2433.74		1	41076.56	+0.09	$30392^{\circ}_{1\frac{1}{2}} - 71468_{2\frac{1}{2}}$					
2433.62	1	3	41078.59							
2433.16	1	2	41086.35							
2433.05		1	41088.21							
2432.62	2	3	41095.47							
2432.01		2	41105.78							
2431.69		1	41111.19	−0.06	$35059^{\circ}_{3\frac{1}{2}} - 76170_{2\frac{1}{2}}$					
2429.01	1	10	41156.55	−0.05	$48556^{\circ}_{3\frac{1}{2}} - 89713_{2\frac{1}{2}}$					
2428.74		1	41161.12	−0.06	$34389^{\circ}_{2\frac{1}{2}} - 75550_{2\frac{1}{2}}$					
2428.30		1	41168.58							
2428.12		6	41171.63							
2427.66		1	41179.43							
2427.20		1	41187.23							
2426.19		1	41204.38							
2425.68		1	41213.04	−0.03	$41678^{\circ}_{2\frac{1}{2}} - 82891_{2\frac{1}{2}}$					
2424.61	4	6	41231.23	+0.06	$22960_{1\frac{1}{2}} - 64191^{\circ}_{1\frac{1}{2}}$					
2423.96		1	41242.28	−0.05	$48900_{3\frac{1}{2}} - 90142^{\circ}_{3\frac{1}{2}}$					
2422.84	10	20	41261.35	−0.02	$24332_{2\frac{1}{2}} - 65594^{\circ}_{2\frac{1}{2}}$					
2421.35	10	50	41286.74	+0.05	$38342^{\circ}_{4\frac{1}{2}} - 79628_{3\frac{1}{2}}$	4	(1.09)	1.12	w	1.00
2420.03	1	4	41309.25	−0.01	$48900_{3\frac{1}{2}} - 90209^{\circ}_{4\frac{1}{2}}$					
2419.41		1	41319.84							
2419.20		2	41323.42							
2418.38		2	41337.44	−0.06	$33653^{\circ}_{0\frac{1}{2}} - 74991_{1\frac{1}{2}}$					
2417.01		3	41360.86	−0.17	$49498_{2\frac{1}{2}} - 90859^{\circ}_{2\frac{1}{2}}$					
2415.39		2	41388.60							
2414.33	2	6	41406.77	−0.01	$24332_{2\frac{1}{2}} - 65739^{\circ}_{2\frac{1}{2}}$					
2413.77		2	41416.38	0.00	$49301_{4\frac{1}{2}} - 90717^{\circ}_{4\frac{1}{2}}$					
2413.66	1	5	41418.27	+0.05	$53404_{2\frac{1}{2}} - 94823^{\circ}_{1\frac{1}{2}}$					
2409.44		1	41490.80	+0.01	$52938_{1\frac{1}{2}} - 94428^{\circ}_{1\frac{1}{2}}$					
2409.06		5	41497.35							
2407.98		1	41515.96							
2407.76		1	41519.75							
2406.79		1	41536.48							
2406.09	1	10	41548.57	−0.06	$31568^{\circ}_{2\frac{1}{2}} - 73116_{1\frac{1}{2}}$					
2403.41		4	41594.89	+0.01	$34575^{\circ}_{1\frac{1}{2}} - 76170_{2\frac{1}{2}}$					

TABLE 6. Yb II—*Observed and classified lines*—Continued

1	2	3	4	5	6	7	8	9	10	11
Wave-length air	Intensity		Wave number	o–c	Classification	Zeeman type	1st g	2nd g	Zeeman components	
	Meggers lamp	Thomson lamp							Strong p	Strong n
Å			K	K						
2402.71		2	41607.01							
2399.93		1	41655.20							
2398.02	40	20	41688.38	−0.07	$0_{0\frac{1}{2}} - 41688^{\circ}_{1\frac{1}{2}}$					
2397.87		3	41690.98	−0.11	$26759^{\circ}_{2\frac{1}{2}} - 68450_{3\frac{1}{2}}$					
2397.73		3	41693.42	−0.07	$47912_{3\frac{1}{2}} - 89605^{\circ}_{4\frac{1}{2}}$					
2397.34		1	41700.20							
2390.74	20*R*	70	41815.31	−0.05	$21418^{\circ}_{3\frac{1}{2}} - 63234_{2\frac{1}{2}}$	4	(1.143)	1.20	*w*	1.01
2390.57	2	8	41818.29	−0.06	$52517_{5\frac{1}{2}} - 94335^{\circ}_{5\frac{1}{2}}$					
2389.18		3	41842.61	−0.04	$52517_{5\frac{1}{2}} - 94360^{\circ}_{4\frac{1}{2}}$					
2388.40	2	7	41856.28	−0.03	$24332_{2\frac{1}{2}} - 66189^{\circ}_{1\frac{1}{2}}$					
2386.75		2	41885.21	+0.04	$52938_{1\frac{1}{2}} - 94823^{\circ}_{1\frac{1}{2}}$					
2385.94		1	41899.43	+0.05	$32371^{\circ}_{2\frac{1}{2}} - 74270_{2\frac{1}{2}}$					
2385.01	1	5	41915.77	+0.05	$35831^{\circ}_{5\frac{1}{2}} - 77747_{4\frac{1}{2}}$					
2383.44		1	41943.37							
2382.98		2	41951.47							
2382.57	1	10	41958.69	+0.03	$48900_{3\frac{1}{2}} - 90859^{\circ}_{2\frac{1}{2}}$					
2380.39	2	15	41997.11	+0.09	$26759^{\circ}_{2\frac{1}{2}} - 68756_{3\frac{1}{2}}$					
2375.18		3	42089.23	+0.02	$31568^{\circ}_{2\frac{1}{2}} - 73657_{1\frac{1}{2}}$					
2374.74		1	42097.02							
2374.52	1	5	42100.92	−0.02	$34575^{\circ}_{1\frac{1}{2}} - 76676_{2\frac{1}{2}}$					
2374.32		3	42104.47	−0.03	$49498_{2\frac{1}{2}} - 91602^{\circ}_{2\frac{1}{2}}$					
2373.89	2	20	42112.10	−0.02	$37516^{\circ}_{3\frac{1}{2}} - 79628_{3\frac{1}{2}}$	7	(1.119)	1.10	0	1.11
2373.06		7	42126.82							
2371.64		1	42152.04							
2369.59		2	42188.51	0.00	$22960_{1\frac{1}{2}} - 65149^{\circ}_{0\frac{1}{2}}$					
2369.42		50	42191.53							
2366.97		2	42235.20	−0.04	$49301_{4\frac{1}{2}} - 91536^{\circ}_{3\frac{1}{2}}$					
2364.10		2	42286.47	−0.08 +0.11	$34389^{\circ}_{2\frac{1}{2}} - 76676_{2\frac{1}{2}}$ $53404_{2\frac{1}{2}} - 95691^{\circ}_{3\frac{1}{2}}$					
2363.49	1	9	42297.38	+0.02	$47912_{3\frac{1}{2}} - 90209^{\circ}_{4\frac{1}{2}}$					
2362.89	10	60	42308.12	+0.04	$21418^{\circ}_{3\frac{1}{2}} - 63726_{4\frac{1}{2}}$					
2362.30		1	42318.69							
2358.67		2	42383.81	+0.08	$47329^{\circ}_{2\frac{1}{2}} - 89713_{2\frac{1}{2}}$					
2357.84	1	7	42398.73	0.00	$31568^{\circ}_{2\frac{1}{2}} - 73966_{3\frac{1}{2}}$					
2355.03		1	42449.32	+0.08	$34389^{\circ}_{2\frac{1}{2}} - 76839_{2\frac{1}{2}}$					
2350.06		2	42539.08	+0.03	$21418^{\circ}_{3\frac{1}{2}} - 63957_{3\frac{1}{2}}$					
2349.39		7	42551.21	+0.09	$37077^{\circ}_{2\frac{1}{2}} - 79628_{3\frac{1}{2}}$					
2347.41		1	42587.10							
2344.66	4	20	42637.05	−0.02	$21418^{\circ}_{3\frac{1}{2}} - 64055_{2\frac{1}{2}}$					
2344.09	4	7	42647.41	+0.03	$30392^{\circ}_{1\frac{1}{2}} - 73039_{0\frac{1}{2}}$					

TABLE 6. Yb II—*Observed and classified lines*—Continued

1	2	3	4	5	6	7	8	9	10	11
Wavelength air	Intensity		Wave number	o–c	Classification	Zeeman type	1st g	2nd g	Zeeman components	
	Meggers lamp	Thomson lamp							Strong p	Strong n
Å			K	K						
2340.78		1	42707.72	+0.01	$47005^{\circ}_{1\frac{1}{2}} - 89713_{2\frac{1}{2}}$					
2340.40	1	6	42714.65	+0.05	$49301_{1\frac{1}{2}} - 92015^{\circ}_{1\frac{1}{2}}$					
2339.61		1	42729.07	−0.09	$30562^{\circ}_{5\frac{1}{2}} - 73291_{5\frac{1}{2}}$					
2336.83		1	42779.90							
2335.44	2	10	42805.36	+0.13 +0.16	$47912_{3\frac{1}{2}} - 90717^{\circ}_{4\frac{1}{2}}$ $49498_{2\frac{1}{2}} - 92303^{\circ}_{3\frac{1}{2}}$					
2335.11		1	42811.41							
2332.28		1	42863.35	0.00 +0.10	$33653^{\circ}_{0\frac{1}{2}} - 76517_{1\frac{1}{2}}$ $38342^{\circ}_{4\frac{1}{2}} - 81205_{4\frac{1}{2}}$					
2331.56		1	42876.59							
2330.39		1	42898.11							
2328.06		1	42941.04	−0.08	$37516^{\circ}_{3\frac{1}{2}} - 80457_{3\frac{1}{2}}$					
2327.74		3	42946.94	+0.18	$47912_{3\frac{1}{2}} - 90859^{\circ}_{2\frac{1}{2}}$					
2327.38		1	42953.59							
2326.92	1	10	42962.08							
2323.18		4	43031.23	+0.02	$34575^{\circ}_{1\frac{1}{2}} - 77606_{2\frac{1}{2}}$					
2323.02		1	43034.20							
2322.63		1	43041.42							
2321.38		1	43064.60							
2320.81	200*A*	150	43075.17	+0.08	$0_{0\frac{1}{2}} - 43075^{\circ}_{1\frac{1}{2}}$	4	2.01	0.95	0.53	0.41
2318.65		2	43115.30	−0.05	$48900_{3\frac{1}{2}} - 92015^{\circ}_{4\frac{1}{2}}$					
2315.20	3	10	43179.54	+0.01	$21418^{\circ}_{3\frac{1}{2}} - 64598_{3\frac{1}{2}}$					
2312.59	1	3	43228.27	+0.07	$22960_{1\frac{1}{2}} - 66189^{\circ}_{1\frac{1}{2}}$					
2311.18		1	43254.64							
2309.54	2	5	43285.35	+0.11	$34784^{\circ}_{5\frac{1}{2}} - 78070_{4\frac{1}{2}}$					
2307.39	1	6	43325.68	+0.05	$47912_{3\frac{1}{2}} - 91237^{\circ}_{3\frac{1}{2}}$					
2306.30		2	43346.16	−0.02	$49301_{4\frac{1}{2}} - 92647^{\circ}_{5\frac{1}{2}}$					
2303.28		2	43402.98	+0.15	$48900_{3\frac{1}{2}} - 92303^{\circ}_{3\frac{1}{2}}$					
2303.16		1	43405.25	−0.08	$31568^{\circ}_{2\frac{1}{2}} - 74973_{3\frac{1}{2}}$					
2298.67		2	43490.02	−0.01	$31568^{\circ}_{2\frac{1}{2}} - 75058_{2\frac{1}{2}}$					
2297.91		4	43504.40	+0.04	$21418^{\circ}_{3\frac{1}{2}} - 64923_{4\frac{1}{2}}$					
2296.63		2	43528.65							
2292.83		4	43600.78	−0.04	$24332_{2\frac{1}{2}} - 67933^{\circ}_{2\frac{1}{2}}$					
2292.19		3	43612.96	−0.03	$49301_{4\frac{1}{2}} - 92914^{\circ}_{4\frac{1}{2}}$					
2291.61		1	43623.99	−0.10	$47912_{3\frac{1}{2}} - 91536^{\circ}_{3\frac{1}{2}}$					
2288.96	2	10	43674.49	+0.10	$21418^{\circ}_{3\frac{1}{2}} - 65093_{3\frac{1}{2}}$					
2288.14		1	43690.15	−0.08	$47912_{3\frac{1}{2}} - 91602^{\circ}_{2\frac{1}{2}}$					
2285.79		4	43735.06	−0.08	$49301_{4\frac{1}{2}} - 93036^{\circ}_{5\frac{1}{2}}$					
2284.99		30	43750.37							
2283.40	3	9	43780.83	+0.04	$21418^{\circ}_{3\frac{1}{2}} - 65199_{4\frac{1}{2}}$					
2279.44		1	43856.88							

TABLE 6. Yb II—*Observed and classified lines*—Continued

1	2	3	4	5	6	7	8	9	10	11
Wave-length air	Intensity		Wave number	o–c	Classification	Zeeman type	1st g	2nd g	Zeeman components	
	Meggers lamp	Thomson lamp							Strong p	Strong n
Å			K	K						
2276.11		1	43921.04							
2275.07		3	43941.12	−0.11	$49301_{4\frac{1}{2}} - 93242^{\circ}_{5\frac{1}{2}}$					
2271.31		1	44013.85	+0.11	$48900_{3\frac{1}{2}} - 92914^{\circ}_{4\frac{1}{2}}$					
2269.57		1	44047.59							
2268.57		4	44067.01							
2268.31		3	44072.06	+0.08	$31568^{\circ}_{2\frac{1}{2}} - 75640_{3\frac{1}{2}}$					
2267.16		3	44094.41							
2263.89		1	44158.10							
2263.12		3	44173.12							
2255.48		3	44322.73							
2253.97		1	44352.42							
2253.27		2	44366.20							
2251.93		1	44392.60							
2243.18		1	44565.74							
2237.51		2	44678.67							
2224.89		1	44932.07							
2224.46	100	80	44940.75	+0.14	$0_{0\frac{1}{2}} - 44940^{\circ}_{1\frac{1}{2}}$	4	(2.00)	1.24	0.38	?
2222.25		1	44985.44							
2216.20		1	45108.23	0.00	$31568^{\circ}_{2\frac{1}{2}} - 76676_{2\frac{1}{2}}$					
2214.68		3	45139.19	−0.06	$21418^{\circ}_{3\frac{1}{2}} - 66558_{3\frac{1}{2}}$					
2213.06		1	45172.23							
2211.91		1	45195.71							
2203.11		2	45376.22							
2201.20		3	45415.59	−0.14	$30224^{\circ}_{4\frac{1}{2}} - 75640_{3\frac{1}{2}}$					
2189.45		6	45659.29							
2185.71	100	80	45737.41	+0.12	$0_{0\frac{1}{2}} - 45737^{\circ}_{1\frac{1}{2}}$	?	(2.00)	1.32	0.34	?
2178.70		4	45884.56							
2174.28	1	3	45977.83	+0.04	$27061^{\circ}_{0\frac{1}{2}} - 73039_{0\frac{1}{2}}$					
2169.79		2	46072.96							
2165.21		3	46170.40							
2161.60	10	40	46247.50							
2160.20		6	46277.47							
2159.89		1	46284.12	+0.04	$30392^{\circ}_{1\frac{1}{2}} - 76676_{2\frac{1}{2}}$					
2155.50		30	46378.37							
2155.20		3	46384.82							
2152.32		3	46446.88	+0.11	$30392^{\circ}_{1\frac{1}{2}} - 76839_{2\frac{1}{2}}$					
2148.94		2	46519.93	0.00	$21418^{\circ}_{3\frac{1}{2}} - 67938_{3\frac{1}{2}}$					
2142.21		2	46666.06							
2137.71		4	46764.28							
2135.27		3	46817.72							

TABLE 6. Yb II—*Observed and classified lines*—Continued

1	2	3	4	5	6	7	8	9	10	11
Wavelength air	Intensity		Wave number	o–c	Classification	Zeeman type	1st g	2nd g	Zeeman components	
	Meggers lamp	Thomson lamp							Strong p	Strong n
Å			K	K						
2131.40	6	5	46902.72	+0.01	$0_{0\frac{1}{2}} - 46902^{\circ}_{0\frac{1}{2}}$					
2126.74	100	80	47005.47	+0.01	$0_{0\frac{1}{2}} - 47005^{\circ}_{1\frac{1}{2}}$					
2125.57		4	47031.34	−0.02	$21418^{\circ}_{3\frac{1}{2}} - 68450_{3\frac{1}{2}}$					
2120.36		3	47146.89	−0.04	$31979^{\circ}_{3\frac{1}{2}} - 79126_{4\frac{1}{2}}$					
2117.62		6	47207.89	+0.10	$26759^{\circ}_{2\frac{1}{2}} - 73966_{3\frac{1}{2}}$					
2116.67	100	80	47229.07	+0.11	$0_{0\frac{1}{2}} - 47228^{\circ}_{0\frac{1}{2}}$					
2102.73	5	20	47542.14							
2022.03		2	49439.31	−0.12	$21418^{\circ}_{3\frac{1}{2}} - 70858_{4\frac{1}{2}}$					
2021.36		2	49455.70							
2018.08		2	49536.06							

[a] Line is a blend of Yb I and Yb II.
[b] Parentheses in column 6 denote masked lines.
[c] $J = 0\frac{1}{2}$ assumed in deriving g-values for λ 8093.030.
[d] Observed Zeeman Effect and classification are discordant.
[e] For λ 7362.920 $J = 1\frac{1}{2}$, 1st g: $0\frac{1}{2}$ 2nd g.
For λ 3736.901 $J = 0\frac{1}{2}$, 1st g: $1\frac{1}{2}$ 2nd g.

(Paper 71A6–470)

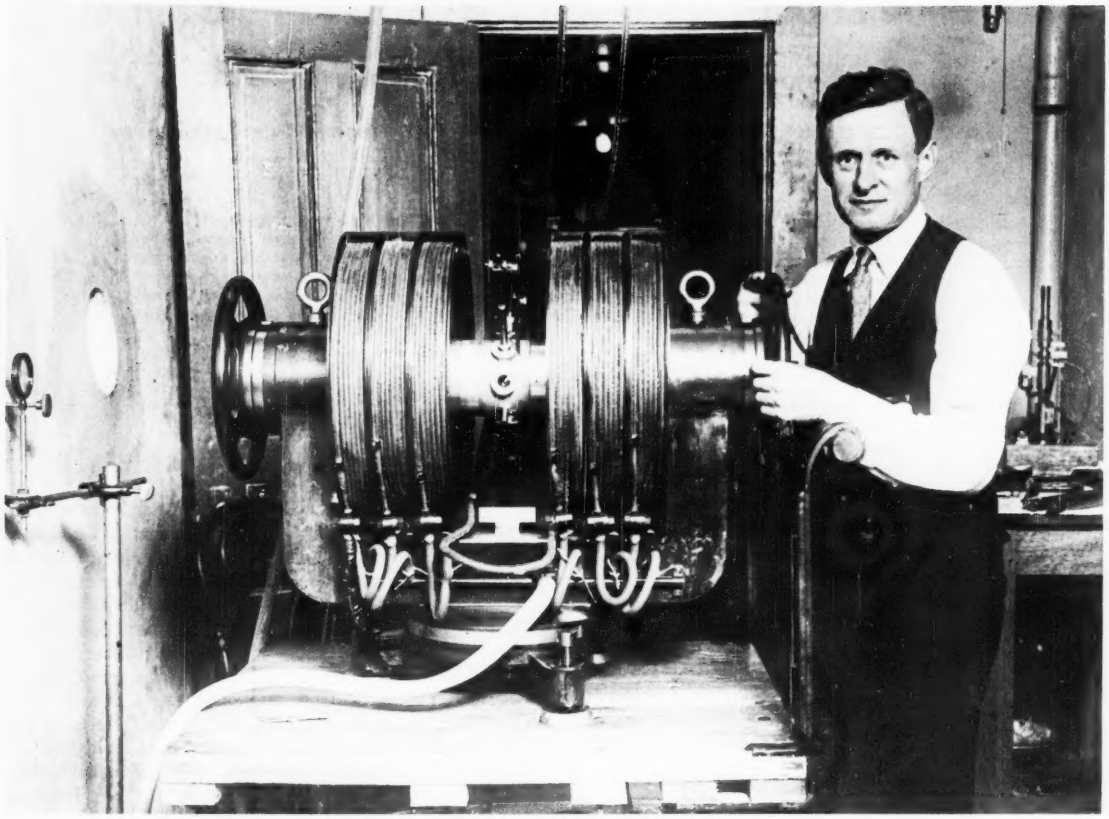

W. F. Meggers shown in 1925 with the electromagnet used by him in his pioneering application of the Zeeman effect to the interpretation of atomic spectra.

JOURNAL OF RESEARCH of the National Bureau of Standards—A. Physics and Chemistry
Vol. 71A, No. 6, November–December 1967

An Improved Description of Technetium Spectra (Tc I and Tc II), 2000 to 9000 Å

W. R. Bozman, W. F. Meggers, and C. H. Corliss

Institute for Basic Standards, National Bureau of Standards, Washington, D.C. 20234

(June 26, 1967)

A new description of technetium spectra has been made that is more complete and provides more accurate data on wavelengths than those reported heretofore. The observations were made in the region 2000 to 9000 Å with arc and spark sources. Larger samples of technetium and spectrographs of higher resolution were used and the number of lines reported (4500) is more than doubled. The intensities are estimated over a range from 1 to 20,000 and the relative strengths in arc and spark permit assignment of the origin of the lines to neutral atoms (3300 lines) or ions (1200 lines).

Key Words: Spectra of technetium; technetium, spectra of; wavelengths of technetium

1. Introduction

It is nearly a hundred years since Mendeléeff predicted the existence of the chemical analog of manganese, which we now call technetium. Because it was first produced artificially, the element was named from the Greek work τεχνικὸς, artificial [1].[1] Over the past 30 years increasingly larger amounts of the element have been artificially prepared. By 1949 Meggers and Scribner were able to obtain 6 mg of ^{99}Tc from the Atomic Energy Commission. With this sample they made a description of arc and spark spectra of technetium [2] which they hoped would "serve for spectrochemical identification and for structural analyses of these spectra."

Although the list of lines published by Meggers and Scribner did not entirely fulfill their hopes, it provided material for a preliminary analysis of the structures of Tc I and Tc II by Meggers [3] and for the remarkable discovery by Merrill [4] of naturally occurring technetium in R Andromedae and other S stars.

In order to make a substantial extension to the preliminary analyses of Meggers [3] it has been necessary to reobserve the spectrum with larger samples of technetium and higher spectrographic resolution. The new observations, which are reported in the present paper, have doubled the number of known lines and significantly improved the accuracy of the wavelengths.

Using this new list of lines, and also observations of the Zeeman effect, Bozman [5, 6] has reported the classification of 900 lines of Tc I as transitions among 40 even and 70 odd levels. Most of these levels have been compiled and published by C. E. Moore [7]. Further analysis and details of the work already reported will be published shortly.

Moore and Catalán extended the analysis of Tc II from this list and provided new terms and g-values for her compilation, *Atomic Energy Levels* [8]. The analysis of Tc II is far from complete. Further observations below 2000 Å are needed.

[1] Figures in brackets indicate the literature references at the end of this paper.

2. Observations

2.1. Samples and Sources

These new observations were made possible by the generous loan of 20 mg of ^{99}Tc as ammonium pertechnetate (NH_4TcO_4) from the Atomic Energy Commission, obtained with the help of G. W. Parker of the Oak Ridge National Laboratory.

Preliminary experiments in the manipulation and excitation of the sample were conducted with $(NH_4)_6Mo_7O_{24}$ because of the rarity and radioactivity of the technetium. As a result of studies of various electrical parameters and electrode configurations the following conditions were adopted for the exposures.

For the arc exposures 400 μg of Tc was evaporated from solution in a shallow cup on the end of a ¼-in diam copper or silver rod which served as the lower anode. The upper cathode of the same material was tipped with a 90° cone. A 2-min exposure was made from the center portion of a 5 A arc in air drawn across a 3-mm gap between the electrodes.

For the spark exposures 200 μg of Tc was evaporated from solution on the flat ends of a pair of truncated wedges forming the tips of ¼-in diam copper or silver rods. A 30-sec exposure was made with light from the portion of a 5-mm gap next to one electrode surface. The spark was produced by the discharge from a capacitor of 0.006 μF charged by a 30,000 V transformer. Several successive exposures from freshly loaded pairs of electrodes were necessary to obtain spark spectra of adequate strength on the plates.

All regions of the spectrum were photographed with both silver and copper electrodes to permit observation of Tc lines masked by lines of the electrode material. A typical spectrogram consisted of successive juxtaposed spectra as follows: standard iron arc, Cu or Ag blank arc, arc of Tc on Cu or Ag, spark of Tc on Cu or Ag, Cu or Ag blank spark, standard iron arc.

The arcs and sparks were always operated in a brass housing with quartz windows to prevent contamination of the surroundings with the radioactive ^{99}Tc. A current of air was drawn through the housing with a vacuum pump and the exhaust was filtered through glass wool where the used Tc was collected.

2.2. Spectrographs and Standards

The region from 2000 to 6900 Å was photographed with a 1200 line/mm concave grating ruled by R. W. Wood and mounted in parallel light. This mounting produces stigmatic images of the slit to allow use of juxtaposed spectra. The average resolution with the slit width used was about 1/50,000, i.e., the equivalent slit width was about 0.06 Å at 3000 Å. This region was photographed on Eastman 103–O–UV and 103a–F(3) plates. One set of exposures was made on the Hilger E–1 Littrow quartz prism spectrograph in the region 2000 to 2300 Å.

The region from 6600 to 9000 Å was observed with a 600 line/mm grating mounted in parallel light and with an equivalent slit width of about 0.2 or 0.3 Å. No spark exposures were made in this region.

A few exposures were made beyond 9000 Å and below 2000 Å by using electrodeless lamps but the lamps did not run well.

Every region of the spectrum was photographed from two to four times and each plate was measured twice, each time by a different observer. Each wavelength represents about five measurements, on the average.

Since this work was all done in 1952 and 1953 before the advent of standard wavelengths from thorium, the iron arc was used to provide the standard lines.

3. Results

The results of this investigation are presented in table 1, where wavelengths and relative intensities of 4500 spectral lines characteristic of technetium atoms and ions are given. In the region from 2000 to 2300 Å the wavelengths represent the average of eight measurements for most of the lines. From 2300 to 4200 Å, six observations were made and from 4200 to 9000 Å the averages were made from four observations. All regions were observed in both arc and spark and on both copper and silver electrodes except for wavelengths longer than 6900 Å where no spark observations were made.

In the earlier experiments reported in [2], all the spectra were excited from copper electrodes; in the present work the use of silver electrodes as well as higher resolving power has revealed lines previously obscured by copper lines. In particular, the Tc II line at 2529.34 was not previously resolved from the Cu II line at 2529.30 and its absence from the earlier line list prevented the discovery of the $4d^6\,a^5$D term of Tc II by Meggers [3].

The probable error in the wavelengths depends, of course, on the region of the spectrum and on the number of measurements. The agreement observed among the measurements was sufficient to warrant the retention of three decimal places at wavelengths shorter than 6900 Å; at longer wavelengths only two decimal places are given.

The relative intensities of the lines have been estimated on a scale extending from 1 to 20,000. The relative intensities of the very strong lines are undoubtedly distorted by severe self-absorption and the true relative intensities among these lines are better represented by the numbers reported in reference [2], where a smaller amount of Tc was used in each exposure. No attempt has been made to represent a true scale of relative power radiated in different regions of the spectrum. It is probable that the intensities in the short wavelength regions, expecially those below 2300 Å are much underestimated relative to the visible and near ultraviolet, whereas intensities in the infrared portion are probably slightly overestimated.

The lines which are stronger in the arc originate in the neutral atom and those of equal or greater intensity in the spark originate in the singly charged ion or, perhaps in a few cases in the shortest wavelength region, in the doubly charged ion.

The intensity numbers are in some cases accompanied by literal symbols indicating characteristic features of the lines as follows:

c—complex
d—double
e—enhanced at the electrode
h—hazy
H—very hazy
l—shaded to longer waves
s—shaded to shorter waves
w—wide
W—very wide
tr—intensity < 1.

The complex characteristic exhibited by some Tc lines is due to hyperfine structure arising from interaction of valence electrons with the atomic nucleus. This structure has been studied in detail at higher resolution by Kessler and Trees [9].

TABLE 1. *Spectrum of technetium*

Wavelength	Intensity		Wavelength	Intensity		Wavelength	Intensity		Wavelength	Intensity	
	Arc	Spark		Arc	Spark		Arc	Spark		Arc	Spark
2054.468		4	2140.738		6	2258.410		1	2376.040		8
2057.704	2		2140.943	1		2260.870		1	2377.770	1	
2058.880	2		2141.830		3h	2261.247	3	15	2382.098	6	
2060.266		2	2144.900	2		2263.533		2	2382.386		2
2060.961	2e	6	2145.322	5		2266.220	10	30	2382.992	3	
2062.929		2e	2147.193	2	2	2267.424	2	2	2384.650	1	15
2064.022	4	1	2148.305	4	4	2268.100		1	2385.338		2
2064.211		1	2149.764		2	2270.722		1	2386.030		1
2064.853	tr		2151.250		5	2271.094	5	50	2387.188	3	
2065.154		1	2153.390	2		2271.218	5	40	2392.012	8	
2067.630		3	2154.668	2		2271.662	3		2393.422		1
2068.323	1		2155.278		12	2272.441	5	10	2394.498		2
2071.289	1		2156.272	30	1	2272.976	2		2394.777		1
2072.072		4	2156.608		1	2274.825	2		2394.974	6	
2073.563	2		2156.908		2	2274.624	2		2395.291		1
2076.700		1	2157.780	1		2278.403	1	3	2396.628		2
2077.210		1	2157.800		10	2280.304	2		2396.984		1
2079.071		6	2158.702	1		2280.884	4		2397.400		2
2079.504		10	2159.292	2	3	2282.121	10		2398.652	2	
2079.808		1	2159.843	5e	50h	2282.361		1	2398.682		60
2081.466		2	2160.606		1	2282.713	10		2399.368	4	
2084.088	5	2	2160.771	2	10	2285.451	50	15	2400.896		4
2084.683	1		2163.546	3	4	2287.470	2	1	2404.101	2	50
2086.853	1		2164.988		8	2287.931		1	2405.128	8	
2087.628	3		2165.902	5	10	2291.637	1	3	2406.651		3
2089.268	3	10	2168.554		1	2292.104	1	2	2407.099		3
2089.657		3	2170.123	1	10	2298.080	100	30	2407.875	5	
2090.682	4	20	2170.546	1		2299.095		1	2408.158		6
2090.987		2	2173.446	3	5	2299.947	1	2	2408.815	7	
2091.730		1	2177.980		4	2300.405		2h	2410.193		2
2092.830	1		2178.935		8	2300.950	3	4	2412.610	6	
2093.310	1		2180.454		6	2302.556		1	2414.471		3
2094.551		1	2182.032		30	2310.706		2h	2416.217	30	
2096.307	2	10	2183.001		15	2313.897		1	2417.524		3
2096.519	3		2184.244		2	2318.731		3	2418.031	7	
2098.119	5		2185.394	30		2324.596	2		2418.647	5	
2098.756	2		2187.476	1	1	2328.389		2	2418.737		1
2099.330	1		2188.218	5	20	2334.046		1	2419.818	2	
2099.680		1	2189.055	30		2336.041		2	2420.775		1
2101.520	4		2191.623	2	15	2337.526		2	2421.296	2h	2h
2101.580		1	2193.347	40	1	2338.278		3w	2423.228	50	3
2101.811	1		2193.999	4	20	2341.028		2	2424.538	20	1
2103.808	6		2196.669		4	2341.610		6	2425.250		1
2104.054		1	2197.501		15	2341.970		1	2425.904		1
2104.340		1	2198.344		2	2344.719	1	10	2427.084	2	
2105.248		2	2198.517		1	2344.845		6	2427.848	3	
2106.234	15	30	2199.825		8	2345.088	2		2431.360		1
2107.617		1	2204.151	4		2345.162		7	2432.337	2	
2107.848		6	2206.006	2		2346.592		5	2432.596		2h
2108.680		1	2207.310		1	2349.167		5	2433.728	8	
2109.056	1	4h	2214.224		2h	2349.594		1	2434.364		2
2110.302	5		2215.245		20	2350.096		1	2434.859		1
2111.252	5		2216.031		4	2350.320		1	2435.628		1
2114.259	3		2216.244		8	2353.166		2	2435.829	20	
2114.484	5		2221.000		2	2353.742		3	2436.824		5
2116.436	20	30	2221.133	3		2354.096		3	2436.994	10	
2118.218	2	2	2221.349		3	2354.448		1	2439.081	5	
2119.114	4		2221.918		4	2355.979		1	2441.284		1
2119.406	15		2226.626		6	2356.839	4		2441.494	1	2
2123.830	3	8	2227.876		6	2360.456		1	2445.560	1	4
2124.074	1		2233.860		8	2360.770		8	2446.049	3	
2125.302	4h	30h	2234.642	1	10w	2361.827	5		2446.864	4	
2126.542		1h	2236.270		6	2365.533		1	2447.440		1
2130.284		2	2237.176		3	2365.856		2	2447.860	3	
2131.912	3		2237.466		1	2366.539		6	2447.900		2
2132.061		5	2237.919		3	2367.660		1	2448.603		2
2133.182		4	2248.533	6		2368.010		1	2448.950	3	
2133.658		2	2252.319	1	1	2368.349		2	2449.119		10w
2135.169		30h	2254.524		3hw	2369.026		2	2450.093		4
2138.133		6h	2256.790		5	2372.104		1	2450.614		6

TABLE 1. *Spectrum of technetium* – Continued

Wavelength	Intensity		Wavelength	Intensity		Wavelength	Intensity		Wavelength	Intensity	
	Arc	Spark		Arc	Spark		Arc	Spark		Arc	Spark
2451.602	5		2493.432	20	8	2529.340	80	400	2565.669		3
2451.759		2h	2493.696		2	2529.550	2		2566.024		25
2452.415		8	2494.129	8		2530.340	3	150	2566.322		10
2453.691	15		2495.025		2	2530.922	2h		2567.011	50	
2453.946		1	2496.767	100	500	2531.372		30	2567.034		250
2454.446		1	2497.232	1	70	2532.027		25	2567.510		2
2455.056	2		2497.317	2		2532.965		40c	2567.733		20cw
2455.936		1	2499.139		2	2533.247		1	2568.376	1	
2456.144		1	2499.582		15	2533.467	10	1	2568.405		3
2456.386	2		2500.654	2		2534.576	1	30	2568.664		4
2456.480	10		2500.837		1	2535.893		1	2569.623		2c
2456.715		1	2500.990	15	1	2536.626		1	2569.874		40
2457.276		1	2501.361		5	2536.966		2	2571.164		8
2458.994	10		2501.882		2	2537.274		2	2571.590		30wl
2460.764		2	2502.363	7	1	2537.405		3	2572.644		1
2461.523	9		2503.284		15c	2537.513		4	2572.923		10
2461.655		2	2503.550	6		2538.039	1	5	2573.166		6
2461.876	3		2503.969		40	2538.507		1	2573.387		5
2463.500		2	2505.031		15c	2538.688		10	2573.482		5
2463.694	80w	2w	2506.782	7		2538.804	2		2573.883		9
2464.340	3		2507.131	5c	300	2539.025	3	1	2574.442	5	30c
2464.470	1	10	2508.000		15c	2539.790		2	2575.061	30	30
2464.804		1	2508.410		4	2540.468		6h	2575.234	1	40
2465.086	20	1	2508.783		5hw	2540.600		10	2575.581	15	
2465.740	10	1	2508.853	10		2540.767		1	2576.281	80	90
2466.100		2	2509.449		3	2541.367		10	2576.756		1
2466.382		1	2510.021		1	2543.227	500	5000c	2577.000		2
2466.873	30	1	2510.167	30	4	2544.144	2		2577.861	40	40
2467.058		2	2510.878		3h	2544.405		15c	2578.301	10	200
2467.520		5w	2511.270		10	2544.807	60	400	2578.791	300h l	100hl
2468.114	3		2512.134	2		2545.565	15	1	2580.871	1	5
2468.715		2	2512.265		8	2545.754		5	2581.004	1	12
2471.286		4	2512.565	1c	2hw	2546.043	1		2582.277		30h
2472.132		10	2512.957	2h	2h	2546.306		1h	2583.091		5
2473.915	8		2513.602	4		2546.993		10	2584.966		1
2474.106	1	4	2514.890	1		2547.919	50		2585.091		6
2474.570	2		2515.925		15	2547.930		150	2585.454		2
2475.107	20		2516.107		1	2548.526		3hw	2585.545		2
2475.158		2h	2516.267		20	2549.353		2	2585.946		8
2475.852		1h	2516.897		50hw	2549.763		2	2586.258		4
2476.283		1	2517.146	1c	100w	2549.860	2		2586.678	10	
2477.800	1	2	2519.170		50hw	2550.043		30	2586.726		10
2478.843		10	2519.435		10	2550.832		2	2586.953		20h
2480.699	50		2519.604	2		2552.055		1	2587.437	5h	
2481.010		1	2519.825	1	4	2553.202		2h	2587.760		15
2481.160		1	2520.030	1	8	2554.346		3	2587.926	4	
2482.381		2	2520.204		3h	2554.759		10	2588.920		40
2482.600		2	2520.678		10hw	2556.090		30	2589.861	200	3
2483.224	50	1	2521.058		2	2556.587		4	2590.007		1
2484.080	4		2521.640		4	2556.867		2	2590.189	20w s	
2484.572	8	8	2521.679	2		2557.391		15hc	2590.713		4
2485.598		5	2521.857	5	6	2558.206	2	80	2591.147		15
2486.496	20		2522.299		4	2558.606	50	300	2591.386		2
2486.884	2		2522.451		4	2559.004		7	2591.790	3	
2487.086		6h	2522.538		20	2559.237	3		2591.879		3h
2487.234		15	2523.409		50	2559.434		3	2592.416		2
2487.735		2	2523.527	2		2559.902	2		2592.816	100	5
2488.049	1h	10hw	2523.876	1	20	2560.209		1	2593.053	5	80
2488.111	5c		2525.028	4		2560.614	10	2	2593.247	10	
2489.058		50c	2525.259		6	2560.673		1	2593.594	10h	30h
2489.456	2	15	2525.460		1	2561.141		6	2593.921	4	
2489.800	2	15	2525.767		2	2561.996		10	2594.067		2
2490.115		50c	2526.039		1	2562.818	10		2594.519		4
2490.319		1	2526.548	3		2563.183		1	2595.740	12	
2490.729		4	2526.769		50c	2563.349	2		2596.768	3	30
2490.854	10		2527.082		2	2564.647		7	2596.944		1
2491.062		20	2527.247		2	2564.825		2	2597.194	20	150
2491.279	15		2527.624		40	2565.173		4	2598.621		10h
2492.124		4	2528.088		6	2565.463		1	2600.403	1	80
2492.721	25	3	2528.716		3	2565.560	4		2600.925		10

TABLE 1. *Spectrum of technetium* – Continued

Wavelength	Intensity		Wavelength	Intensity		Wavelength	Intensity		Wavelength	Intensity	
	Arc	Spark		Arc	Spark		Arc	Spark		Arc	Spark
2601.491	10		2639.865		3h	2673.024	6		2714.656		4
2601.807		2w	2640.038	8		2673.412	15	200	2715.205	30	
2602.093	10	100	2640.159	1	60w	2673.854		2	2715.460		20
2602.535		20	2640.482		5	2674.079		3	2715.818	5	30
2603.727		20h	2641.255	30	1	2674.614		6	2716.542		40
2604.866	8	30	2642.101		4	2674.825	10		2716.671	6	35
2605.391	3	70	2642.372	100		2675.223	3c	200c	2718.186		4
2605.753	4		2642.531		4	2675.634		20	2718.996		10
2605.840		7h	2643.006	20	200	2676.364		3h	2719.321	6	100
2606.796		1	2644.496	40	500c	2677.027		2h	2719.794		10
2607.236		20	2644.864	1	1	2678.057		7h	2720.891		2
2608.134		20	2645.380		5	2678.571	2	30c	2721.552		2
2608.570	3		2645.585		15	2679.012		5	2722.296		1
2608.855	500	15	2645.662	20		2679.417		3	2722.503		1
2609.064		4	2646.245	15	100	2680.659		8	2723.010		3
2609.323	6		2646.751	20c		2680.929		7	2723.400		80
2609.993	1000c	2000c	2647.011	1000c	3000c	2681.190	80	500	2723.550	30	
2610.645		3	2647.359		10	2682.316		15	2723.750		20
2610.889		10	2647.980		3	2682.699	15cw	200cw	2724.193	2w	200w
2612.171	4		2648.306	20	200	2683.054		5h	2725.418		5h
2612.421		1	2649.162		40h	2683.139	60		2725.656	4c	400c
2612.979	3h		2649.207	300c		2683.740		6	2726.171		10
2613.219	3h		2650.217		3	2683.886	80	1	2726.691	1000	40
2613.283		40	2650.394	10		2684.191	5		2727.078	3	30
2613.742	8		2650.603	1	20h	2684.234		6	2727.634		20
2613.941		2	2651.801		2	2684.507		60c	2727.802	3	1
2614.233	1500	30	2652.083		5h	2684.959		2	2728.306		2
2614.637		12	2652.351	100	600	2685.396	3c	100c	2728.471	30c	1
2615.127		10	2652.898		20	2686.023		8	2729.743		5h
2615.873	1000	20	2653.400		2	2686.900		1	2730.225		6
2616.068		80	2653.526		2	2687.326		30	2730.377		1
2617.565		20	2653.566	30		2688.033		3	2730.529	500	10
2618.279	30		2653.746		10	2688.059	20		2732.251		2h
2618.670		2	2654.306	100	3	2688.255		100c	2732.872	300	10
2618.790		5	2654.902	8		2690.451		9	2733.039		1,
2619.063	10		2657.327	15		2690.673	12		2733.248		2'
2619.302		60	2657.572	1	1	2691.294		20	2733.782		7
2619.691	3		2657.975		1	2691.361		7	2733.969		3
2619.944		70	2658.180		2	2691.812	8	200	2734.097	4	
2620.285		6	2658.578		3	2693.112	80	2	2735.135		30
2620.501		1	2659.931	5h		2693.744		40	2735.912		10
2620.803		20	2660.884	120	30 l	2694.533		3	2736.200		15
2620.932	10		2661.156		3	2694.768		20	2736.231	150	
2622.823		6	2661.642	1	100	2694.780	10		2736.503	2	40
2623.123	6		2662.032		2h	2695.259		2	2736.830	60c	300c
2623.381		1	2662.296	100	2	2696.537	1	100	2737.122		30h
2623.780		1	2662.642	1	80	2696.636	50		2737.680		60
2624.376		15	2663.162	3		2696.755	15	1	2737.973	100	1
2625.487	10	200	2663.897	12		2697.383		20	2738.148		1
2625.983		50	2663.947		4	2697.598		5	2738.826	20c	500c
2626.422		7	2664.66	8		2699.433		3	2739.302		2
2626.654		2	2664.69		20	2699.788		30	2739.819	3	
2626.914		1	2665.100		15	2700.664		20	2740.060	3	100 hl
2627.786		2	2665.404		1	2701.494		1	2741.142		12
2627.967		100	2665.733	20	70	2701.640		15	2741.406		1
2629.509		2	2666.463		2	2702.271	70		2742.526		3
2630.052	8		2666.636	3		2702.447		20	2742.745		4
2630.288		4	2667.175		9	2702.959	40	800	2742.904		2
2631.617	20		2667.780		3	2703.239		10	2743.821	8	80
2631.806		4w	2668.308		2	2706.936		8	2744.309		2
2634.444		10	2668.958		30c	2707.327		10	2745.724		1
2634.909	200	1000	2669.654	1		2707.896	100	700	2746.517		5
2635.618	4		2669.872		15 s	2708.785	1000	10	2747.375	1	15
2635.769		6	2670.110	2	20	2710.536		30c	2749.226		50 cw
2636.334		15	2670.341		2h	2710.745		50c	2749.831		2
2636.357	80		2670.818		3	2711.481		5	2751.489	1	250c
2636.500		3	2671.014		25	2712.591	8	100	2752.295		10
2638.802		9	2671.380		1	2713.551		20w	2753.051		15
2639.070		15	2671.878		1	2714.568		9	2753.291		1
2639.320		4	2672.333		2h	2714.600	2		2755.761	100	8

TABLE 1. *Spectrum of technetium* – Continued

Wavelength	Intensity		Wavelength	Intensity		Wavelength	Intensity		Wavelength	Intensity	
	Arc	Spark		Arc	Spark		Arc	Spark		Arc	Spark
2757.008		1	2795.286		2	2838.547	5c	50c	2883.508		5
2757.282		6	2795.650	80		2838.876		8	2883.670	5	
2757.577		6	2795.778	200	500	2839.140		1	2884.748		10
2758.714		5	2796.709	4	80	2839.854		30	2885.548		20c
2759.211		1	2797.730	3	10	2840.375	50	400	2886.079		20
2759.790		2	2798.079	2	300	2841.656		1	2887.429	1	2
2760.132		15h	2798.208	8		2842.303		4	2887.734	1000	8
2760.380	7		2800.450		4	2843.352		20	2888.458	100	25
2761.281		8	2800.770		10	2843.766	8		2889.200	30	300c
2762.134	100	3	2802.455		2	2845.044	60	3	2889.487	3	
2762.337	200	8	2802.810	1000	8	2845.472	7	4	2890.438		20
2763.231		50	2803.018	150	3	2845.786	2	3	2890.793	6	300c
2763.871		5	2803.389		4	2846.392	10	200	2891.176		5
2763.957	8		2803.921	8		2846.617		3	2891.324		15
2764.501		5	2804.855	6		2846.742	10	30	2892.347		60
2765.507		3	2805.179		10	2847.327	6		2892.759	4	150
2765.713	1	20c	2805.983		2	2847.700		5w	2893.160	200	2
2765.947	60	1	2806.626		15	2847.874	1		2893.448	150	2
2766.886	500	10	2807.100		2	2847.909		2	2893.900		10
2767.363		10h	2807.433		3	2848.157		4w	2894.322	200	2
2769.051	15	4	2807.915		15d	2849.196	60	3	2894.831		15
2769.590		15	2808.356	500	10	2850.154		2	2895.473		15
2769.714	5		2809.646	50c	150c	2850.931		10	2896.340	1000	10
2769.879		5	2810.046	8		2850.956	150	10	2897.776	6	
2771.216	2h	100c	2810.225	15		2851.222		3	2899.363		2
2771.797		10	2810.240		20	2851.358	1	3	2900.692		80
2772.052	1	6	2811.152		1h	2851.732		4	2902.134	7	10
2773.303		30	2811.614	500	1000	2851.985		20w	2902.539		4
2773.786	2	200	2812.447	3		2852.294		15	2902.910		4
2774.278		4	2812.999		4	2853.319		2	2903.813	40	3
2774.809		1h	2813.499		5d	2853.554		1	2904.956	10	
2775.076		10	2813.784		60c	2853.643		2	2905.420		1
2775.328	6		2814.184	8	100	2855.637	10	1	2906.251		8
2775.601	3	70	2814.626		6	2857.128	500h	7	2906.618		100
2776.041		10	2814.847		6	2858.482	10h		2906.882		9c
2776.559		4	2814.860	30		2859.110	2000c	200c	2907.625		10c
2777.313	20	500	2814.959	2		2859.852		2	2907.856		4
2777.645		2	2815.965		8	2860.770	6c	600c	2907.982	15	
2778.117		9	2816.515		10h	2860.988	15		2909.036	7	
2778.269		1	2816.999	3	40	2861.361		3h	2909.074		30h
2778.908	150	9	2817.286		7	2861.684		30	2909.508		1
2779.773	1	30	2817.612	1	15	2862.772		4	2909.852	5	
2781.222	25		2818.630		15	2863.335	10		2910.202	10w	150w
2782.052	1000	15	2819.050		4	2863.528		4	2910.689		6
2782.235		3	2819.460	40	1	2864.486	500	8	2911.702		6
2782.955		1	2820.198		20	2864.892		6	2911.996	2	10
2784.372		10h	2820.645		6 l	2866.069	8c	300c	2913.147	1000	7
2784.726		5	2821.352	100	500	2867.213	8		2913.792	8	
2785.134		8	2821.590	5	100w	2867.430	8		2914.242		3
2785.288		20	2822.910		8h	2867.673		3	2915.394		6
2785.586	500	10	2824.380		3h	2868.087	100	3	2915.850		3
2786.941		1	2825.042	6c	80c	2868.788	4	1	2919.650		3
2787.234	15	2	2825.342	6c	100c	2869.283	20		2920.850	7	
2787.609		2	2825.967	10		2869.303		30	2921.054	15w	100w
2787.937		30	2826.166	2c	100c	2869.497	10	1	2921.496		50
2788.797		7h	2828.042	200	10	2870.295		4	2921.912	500	2
2788.888	40		2829.090		4	2870.422		15	2922.736	3	70
2789.246	500		2829.375	5		2871.438		3h	2923.155	5	
2789.273		100w	2829.607		10s	2871.986		4	2923.342	20c	200c
2790.293		2	2830.202		1	2872.234		30cw	2924.254		70
2790.443		9	2830.823	4		2873.660	20		2924.870		3
2790.628		1	2830.869		3	2874.101		10	2925.065		7
2790.920		2h	2831.180	60	600	2877.196		3	2927.098	3	
2791.739		3	2833.599		200	2877.606		1	2927.318		10
2792.070		7c	2834.326		3	2878.703	1	30	2927.783		1
2792.973		4	2834.762		2	2879.133		50	2927.960		1
2793.672		4	2836.117	12	150	2880.406	5	200c	2928.198	1000	2
2794.228	3	60	2836.900		3	2881.269		20hw	2928.434	1	40
2794.526	100	1	2837.382		10hw	2882.362		60	2929.515		20
2795.072		6	2838.231		1	2882.891		4	2930.035		18

TABLE 1. *Spectrum of technetium* – Continued

Wavelength	Intensity		Wavelength	Intensity		Wavelength	Intensity		Wavelength	Intensity	
	Arc	Spark		Arc	Spark		Arc	Spark		Arc	Spark
2930.485	20	1	2978.254		2	3026.445		4	3074.270	20	1
2931.134		20	2979.338	100	3	3026.887	300w	200w	3076.238	80	2
2931.552		6	2979.752	10		3029.220		3	3076.528	10	
2932.062	4		2979.780		7	3030.276	6		3076.855	12	
2932.118		4	2980.832		2h	3030.718	2		3077.591	3	
2932.923	3		2982.217		3h	3031.220		3w	3077.701		100
2932.975		1	2982.552	8	400	3031.486		1	3078.630		3h
2933.888	80		2983.712		20h	3032.089		10	3079.907		10
2933.924		50	2984.137	20	1	3033.158	50	2	3081.075	15	1
2936.921	3	50	2984.362	30		3033.621		4	3082.098		2h
2937.801	6		2984.388		60	3034.568	80		3082.886	3w	3h
2938.868	10		2985.046	15		3034.642		3	3083.289		15c
2938.993	1	70	2985.364	150	7	3034.963		2	3083.354	20	
2939.501		1	2985.601	8		3035.512		1	3084.499		4h
2939.990	15	1	2985.932	8		3036.014		7	3085.752		1
2940.487		2	2986.453	15		3036.878	40	2	3085.906	12	
2940.928		3	2987.235		3	3037.449	3		3089.120		3
2941.835		8	2988.172	20c		3037.902	20	800	3089.340	150	2
2942.082	30	1	2988.468	5		3038.226	100	2	3090.222	30	1
2942.912	4c	100c	2988.614		10	3040.228		3	3092.517		2h
2945.518		20	2990.132	8w	5h lw	3040.605	15	1	3092.749		30c
2946.220		2	2990.748		2h lw	3040.874	12	1	3093.617		10
2946.581		8	2992.873	30h		3042.213		2	3093.988		1
2947.107	15	1	2993.232	18h		3042.359		3	3095.014	20w	
2948.070		3	2993.460	8		3042.643	40	2	3095.740	30	
2948.473	8	100c	2993.762		15	3043.049	12	1	3095.834		7
2948.633	15	400c	2993.910	1	1	3043.774	8		3096.672	5	
2949.255	20		2994.097	15	8	3043.938	8		3096.710		2
2949.456		10h	2996.882		4	3044.686		15w	3097.269		20
2949.580	25	1	2997.076	20		3044.978	10		3097.582	5	
2950.248		15	2997.186		8	3045.292		10c	3098.556		40
2950.375	3	50	2997.635	1		3046.502		20c	3098.657	20	
2950.803	2	30	2997.906	20		3047.113	4		3099.098	1000	10
2951.033		10	2997.953		2	3047.529		15h	3099.517	200	2
2952.068		20	2998.235	6		3049.047		6h	3100.462		4
2952.544		40	2998.356		8h	3050.818	6		3100.638		3
2953.162		4	2999.690		2	3051.332	4		3100.880	1	30
2953.838	8h		3000.418		1	3051.550	100h		3101.582	5	
2954.046	10h		3001.055	1	150	3051.600		5	3101.782		2
2954.149	10h		3001.590		2	3052.128	20w		3102.822	2	
2955.928	200	3	3002.269	10		3052.474	40		3103.443	10	
2956.229		3	3002.669	15	5	3052.507		10w	3104.293	30	1
2957.823	6	1	3003.022		10	3053.106	10	7	3105.107		70
2958.357	3		3003.698	30	1	3055.464		5	3105.387		10
2958.424		7	3004.379		15	3056.670	5		3106.937	30	2
2958.547	2		3004.601		5	3057.014	20	4	3108.254	60	2
2958.832		5	3005.488		9w	3057.327	30	2	3108.576		1
2961.636	1	30	3007.007	1	100c	3057.515		10	3109.122		20c
2962.086	7	40	3008.782		2	3058.509		20	3109.151	40	
2962.569		4	3009.746		6	3059.308		1	3110.563		30
2964.287	20		3010.831	100	2	3059.550	6		3110.759	15	
2964.487	10	800	3011.868		1h	3060.103	4		3110.938	3	
2965.488		3	3012.388		1h	3060.672	30	1	3111.392	10w	
2966.196		50	3015.161	2	30	3060.904		4	3115.296		4
2966.550		15	3016.298	12		3061.283	3		3115.977	60	2
2967.084	1		3017.232	300	7	3061.780		10	3116.382		3
2967.242		10h l	3018.341	4		3062.112	80	2	3116.698	2	
2967.956		2h	3019.179	3	15	3062.361	200	2	3116.914	10	
2968.233		1	3020.452	3	3	3064.667	300	3	3118.644	5	
2968.769	8		3021.555	150	2	3066.393		4	3119.171	80	6
2969.770	3		3022.035	20		3066.602	100c		3119.662	40	1
2970.186		2	3022.203		20h	3068.337	120c		3119.888	1	40
2970.740		40h l	3022.578		10h	3069.956	3	200	3120.937		2h
2970.760		20h	3022.665	100		3070.241	30		3121.306	10h	
2970.900	20		3022.998		1	3072.702	8		3121.970		50
2973.179	18		3023.680	200	3	3072.898		15	3122.642	700	3
2973.650	200	5	3024.208		1	3073.046	10		3123.556	10	
2976.179		25	3025.263	80	3	3073.326	12		3126.184		5
2976.379	5		3025.523	3		3073.726		2	3126.390	8w	
2976.561	15c	400c	3025.932		1	3073.969		2	3126.807	5	

277-259 O - 68 - 11

TABLE 1. *Spectrum of technetium* – Continued

Wavelength	Intensity		Wavelength	Intensity		Wavelength	Intensity		Wavelength	Intensity	
	Arc	Spark		Arc	Spark		Arc	Spark		Arc	Spark
3127.464	2		3178.366		5	3226.044	15		3290.974		5
3127.855	10		3178.630	3		3227.412	4		3291.233		5
3128.878		8h	3179.168	1		3227.589	1		3291.960	20	1
3129.049	20		3180.305	200	3	3228.040		2h	3292.364		2h
3131.003	6		3181.158	2		3230.022	60		3292.930		7h
3131.233	1500	20	3181.648	1		3230.336	1		3293.649		5
3131.553	5		3182.367	2000	60	3230.640	1		3296.270		20
3132.555	10		3182.783	8	3	3230.938	1	200	3296.504	10	
3133.128		30c	3183.108	2000	60	3231.114	15		3297.074	3	
3133.336		15c	3183.577	1		3231.936	5		3297.360		50h
3136.593		100	3184.472	1		3234.984		4	3298.297		10
3137.054		1	3187.327	3		3236.439	5		3298.842	30	600
3138.322	20		3188.077	1		3237.017	1000	3000	3300.572	1	
3138.968	5		3189.707		4h	3237.922	1		3300.770	100	4
3139.936	25		3190.355	2	100	3238.487		4	3301.168		2
3140.656		20c	3191.620	10		3239.518	12	4	3301.572	3	
3140.994	5h	40h	3192.051	20		3239.789	5		3301.960		120h
3143.561	4		3192.310		3	3240.682		6	3301.990	20	
3143.640		15	3192.574	2		3241.837	100	5	3302.864	1	
3144.166		20	3192.905	2		3242.251	4h	1h	3303.510	6	
3144.291	20		3193.078	1		3244.193	500	15	3305.607		30c
3144.568		15	3195.202	800c	1000c	3245.509		3	3305.669	2	
3145.591		20	3195.485	20		3245.708		3	3305.891	80	10
3145.937	6		3195.658	3		3246.191		8	3306.817		3h
3145.996		5	3195.766		6	3247.273		2	3309.412		8
3146.212	12		3196.591	3w		3249.340		6	3309.607		2h
3146.471		1	3196.945		2	3249.600	10		3310.646	200	15
3147.160	15	1	3197.530	40w		3250.389	10	2	3311.051	20	2
3148.414		2	3197.711	10		3250.638	10		3312.135		2
3149.897	2		3197.766		3h	3252.048	300	10	3312.240	2	
3150.265	40c	5c	3198.069	3		3254.700	10		3312.524		100
3150.650	8		3198.497	15	3	3254.960		40	3313.652	150	5
3152.779	3		3199.149		3	3256.102	40	2	3314.051		5
3153.172		20	3200.062	1		3256.326	2	500	3315.755	4	
3153.353	20		3200.980	8		3257.679		1	3315.806		50c
3155.079	2		3202.831	300c	6c	3259.261	3	1	3317.626		6h
3155.476	5		3203.108		2	3259.910	10	5	3318.772		4
3156.794		50h	3205.345	1		3261.370	20	3	3319.252		5
3157.339	5		3205.474	4		3261.937	40	6	3320.134		7h
3157.636		5	3205.847		1	3262.099		20	3322.288	40	1
3158.046		30	3207.866	4		3262.896	6	2h	3322.966	5h	1
3158.688	6		3208.270	6		3263.308		3h	3323.888		7
3159.378		6	3208.390		3	3263.870	2		3324.200		3
3159.789	2		3208.430	4		3264.664	1h	20h	3325.140	8	
3160.463	2		3208.770		6	3266.305		20h	3325.552	200	6
3160.579	3		3208.904	5		3266.911	20	400	3326.605	1	
3161.674	300	8	3209.838	1		3269.427		15c	3327.102	150cw	1c
3162.542		1	3210.245	1		3269.660	4	60	3327.665	1	
3163.140	12		3212.021	1000	2000	3269.800		50	3328.252	5	
3165.003	6		3213.286	8		3270.060	20	10h	3330.766	100	2
3165.167		40w	3214.738	3		3270.608	5	1	3331.319		5
3166.993	3		3214.901	7		3271.164	5	1	3331.700		1
3168.271	1		3215.764	3		3271.754		1	3331.740		10
3168.918	3		3216.518	6		3272.111	10	2	3332.227		3
3169.258		5w	3217.130		4	3272.534		10h l	3332.468	50	2
3170.380		50	3217.463	25		3276.29	5	10h l	3334.500	2	7h
3170.484	1		3217.956	2		3281.392	6		3336.089	5c	
3170.833	3		3218.254		15h	3281.848	4		3336.715	4	
3171.064	4		3218.559	10		3282.390	8	200	3337.486	10	2hl
3171.199	3		3219.052	3		3283.918	1		3337.977	5	
3171.598		20hw	3219.174	1		3284.768	5		3338.252		20
3171.912	8		3219.726		25	3285.816		20h	3338.873		18
3172.013	6		3220.315	3		3286.297		10	3339.202		10
3173.295	3000	100	3220.737	40	2	3286.688	2		3339.332	6	
3174.738		30c	3221.320	2		3287.143	100		3340.697		1
3175.554		6	3221.573	1		3287.194		50	3341.198		2
3176.025		3	3223.585		20	3287.900		2h	3342.141	3	
3177.714	6		3223.762	3		3288.293		3h	3343.113	4	
3177.909		10	3223.880	6		3290.250		3	3343.770	10	
3178.186	10		3225.500	2		3290.624		8	3344.295	2	

TABLE 1. *Spectrum of technetium* – Continued

Wavelength	Intensity		Wavelength	Intensity		Wavelength	Intensity		Wavelength	Intensity	
	Arc	Spark		Arc	Spark		Arc	Spark		Arc	Spark
3345.016	15w		3402.105	200	4	3447.451	3		3504.052	2	
3345.597	3	200	3403.330	3		3449.652		2h	3504.163	3	
3348.460		20h	3403.481	10		3449.897	15		3505.359	40	30
3348.930	4		3403.579	10		3450.647		2h	3505.558	3	
3349.356		3	3403.931	200c	2	3451.050	200	8	3506.114	50	1
3349.880	6	1	3404.559		1	3451.507	3		3506.431	8	
3350.218		2	3405.328	80	5	3453.020	30	1	3506.931	10	
3350.563	60	3	3405.826	20	1	3453.751		1	3507.187	100c	1
3350.830	50c	1h	3406.669	4		3454.073	30	1	3508.271	100	1
3351.985	1		3406.964	10		3454.623	8		3509.519	4	
3352.844	1		3407.281	80		3456.127		20	3509.869	2	
3353.156	2		3408.331	50		3456.476		15	3510.193		1
3354.093	20		3409.506	1		3456.637	5		3510.594	10	
3354.954	5	2hw	3411.646	1	80h	3456.849	200	5	3510.912	100	4
3356.884	8		3411.804	40		3457.243	400	20	3511.328	20	
3358.038	12		3413.843	1		3457.603	40	3	3511.919	20	1
3358.421	2		3414.600	10		3458.023	20	10	3512.546	5	
3358.468		2h	3415.448	15	1	3459.102		4	3512.768	6	
3359.232	15	2	3415.867	15	1	3460.916	1		3514.302	10	
3362.156	1		3417.738	10		3461.406	1		3514.700	2	
3362.322	3		3418.053	20	1	3461.714	10	1	3515.174	12	1
3362.603		10	3418.101		3wd	3462.413		6w	3515.973		2h
3363.038	4	100	3418.203	40cw	1	3463.507		2	3517.206	40	1
3363.549	2		3418.556		4	3464.214	3w		3517.442	10	
3363.678		5	3418.581	15		3465.212	5		3518.126	8	
3363.700	2		3419.100	100	6	3466.278	5000cw	500cw	3519.092		2
3366.753	400	15	3419.451	15		3467.213		10	3519.414		10
3367.198	3		3420.583	2		3467.959		25c	3520.054	30c	
3368.420	5		3421.450		5h	3468.087	3		3520.276	20	
3371.402	5		3421.987		2h	3470.188	10		3520.514	30c	
3371.646	10		3422.675	2		3470.299	5		3520.832	1	
3371.902	15		3422.972	3	4	3470.514	150	5	3521.305	20	1
3372.543	8		3424.321	1	40	3470.726	10		3521.641	5	1
3373.429	30	1	3425.382	20		3472.165	30	6	3522.082	60	1
3373.572	25	1	3426.414	3		3472.896	15		3522.275	30	
3373.906	3		3426.653		10	3473.726	20		3522.516	15	
3374.626	8		3427.853	60		3475.178	80	2	3524.523	20	1
3375.368	4		3428.958	1h		3475.592	1000	10	3525.271	1	
3375.560		4h	3431.150	2w		3476.980	1		3525.828	800	15
3376.014		1	3431.750	40	2	3477.838	1		3526.178	300	5
3377.781	10		3431.920		2	3478.432	10		3526.730	6w	
3378.067		10h	3432.263		2h	3478.926		2h	3526.869		2h
3379.606	10		3433.155	6c		3479.315	8		3527.626	50	2
3379.925	4h		3434.182		2h	3479.452	10		3527.976	30	
3380.343	3		3434.701	200	4	3480.787	8		3528.285	1	
3380.410	15	2	3435.213	20		3481.400		20c	3528.996		3h
3380.574	5		3435.679	40	1	3482.288	2h		3529.829	100	2
3382.096	4		3436.110	3		3482.676	1	10	3530.813	10	
3382.676		15	3436.300	4		3484.620	60	1	3531.002	3	
3385.004	10		3436.440		1	3486.226	1000c	30c	3531.318	15	
3385.490		1h	3436.644	3		3490.139		10hw	3531.733	3	
3386.387	20		3437.439	150	1	3490.299	100	2	3534.878	150	3
3386.674	40	1	3438.248		10	3493.394	400	5	3535.399		10
3388.166		20	3438.525		1	3493.884	1		3535.506	500	12
3388.459	8		3438.729	80	1	3494.168	20	1	3536.086	1	
3389.492	12		3439.217	3		3494.623	500	4	3537.194	10	
3390.808	1	15	3439.819	12		3494.866		7h	3538.119	300	
3391.364	1	10	3440.451	6		3495.827	20		3538.374		2
3392.227	50		3440.724	3		3496.950	1		3538.678	800	3
3392.604	3		3441.086		15	3499.141	40	1	3539.148	20	
3394.179	300	10	3441.217	3w		3499.895	3		3539.759	12	
3394.808		2	3441.818	3h		3500.161	6		3540.174	1	
3396.903	60	1	3442.233		5h	3500.704	1000	20	3541.772	2000c	20c
3397.830	40		3442.337	10		3501.241	200	2	3542.616	8c	
3398.120	1		3442.803	4		3501.507	20	10h	3543.212		3h
3398.327	300	6	3442.916		3	3502.467	80	2	3544.096	4	
3398.545		2	3443.472	200c	2	3502.704	800c	20c	3544.382	20	1
3398.738	10		3444.012		8h	3503.336	30	20hw	3544.500	2	
3400.118	3		3444.428	3		3503.586	30		3546.934	20	
3401.681	25	1	3445.021	1		3503.786	40		3548.113	2h	

TABLE 1. *Spectrum of technetium* – Continued

Wavelength	Intensity		Wavelength	Intensity		Wavelength	Intensity		Wavelength	Intensity	
	Arc	Spark		Arc	Spark		Arc	Spark		Arc	Spark
3548.825	2h		3595.661	1000cw	10cw	3643.950	8		3702.366	8	
3549.725	6000c	60c	3596.181	4		3644.134	50	2	3702.498		2h
3550.645	4000c	40c	3597.401	12		3644.427	3		3703.176	60	2
3551.206	30		3598.261		1	3645.630	2		3703.830	800	20
3551.998	3		3598.830	30		3645.796		2	3704.797	300	5
3552.828	4		3599.152		2h	3646.851	2		3705.481	100	2
3553.539	60	1	3599.750	50	1	3648.040	1000c	50c	3705.712	80	1
3554.580	30		3602.191	20	1	3648.860	10		3706.705	200	4
3554.919	2		3602.639	1		3650.344	60	2	3707.627	200	5
3556.056	40	2h	3604.794	1	3h	3651.467	600	20	3708.261	200	3
3556.178		1	3605.717	7		3654.054	10	1	3709.226	2	
3558.209	2		3605.938	15		3656.458	1		3709.527	15	
3558.260		1h	3606.265		2h	3658.152	10		3709.831	80	1
3558.662	15		3607.321	1000c	30c	3658.588	1000c	60c	3710.126	90	2
3559.111	3	1h	3607.625	200	5	3659.882	3		3710.428	4	
3559.390	1h	1h	3608.271	2000c	80c	3661.452	400c	30c	3711.048	2	
3559.754	300	5	3609.045	60		3662.032	6		3711.388	80	1
3560.319	800	15	3609.527	1		3662.838	30	1	3712.256	1000	10
3560.876	50		3609.843	6		3663.091	8		3712.819	300	3
3561.192	50	1	3609.906	5	9h	3664.455	6		3713.838	25	
3562.303	4		3610.354	1		3664.575		7h	3714.516	100	1
3563.000	5		3610.550	10c		3664.916	200	2	3715.944	500	5
3563.994		2	3611.109	2	10c	3667.349	10		3716.706	4	
3564.359	5		3611.156	50		3667.510	30	1	3716.809	20	2
3564.566	1		3611.788	4		3667.794	10		3717.024	15	1
3565.008		3	3612.108	60		3667.991	10		3717.287	1	8
3565.217	100	1	3612.346	3		3668.940	20	1	3718.861	10000	300
3565.490	80	1	3612.833	4	3h	3669.152	40	2	3720.407		2h
3566.883	3		3613.163		1	3669.918	40	1h	3720.688		2h
3568.853	800	5	3613.232	3	1	3671.710		2	3721.056	3	
3569.852	30s		3614.282	15		3672.087	8		3721.160		4h
3570.654	100	1	3615.814	50	1	3672.553	3		3722.885		5hw
3572.631	1	10	3616.346		10h	3673.014	1		3723.132	40	
3573.083	50		3616.528	30		3673.285		4h	3723.674	1500	15
3573.306	10h	4h	3617.692	20		3675.003	3		3724.176	10	
3573.654	1		3618.582	8h		3675.429	30		3724.395	2000	20
3574.410	25		3618.943	200	3	3675.584		5	3725.082	20	
3574.610	80	1	3619.664	20		3675.855	10w		3726.152	100	2
3575.420	100	1	3619.795	10	15	3675.899		4hw	3726.351	5000	40
3575.463		2h	3622.453	1		3678.089	80	2	3727.364	200	
3575.964	20		3623.508	5		3678.388	70	2	3728.291	2	
3576.324	50		3625.555	150	3	3679.146	1000	30	3728.886	30	
3576.495		4h	3626.294	10		3679.603	1		3729.177	400c	5c
3577.228	6		3627.364	1000c	10c	3680.318	300	6	3729.618	2	
3577.796	1		3627.858	100	2	3680.518		8h	3730.358	10	
3577.986	15		3628.476	2		3680.575	50		3730.836	60	1
3578.764	12		3628.901	30	1	3681.683	40		3731.412	8	
3578.969	60		3630.388	200	2	3682.592	100	2	3731.735	500	3
3580.059	1000	10c	3631.227	2		3683.073	2		3735.501	30	
3581.258	600	3	3633.244	150	2	3684.744	5000	100	3735.753	4	
3581.744	10		3634.258	1h	8	3686.027		1h	3737.420	300	2
3582.075	800	4	3634.764		3h	3687.772	20	1	3737.662	10h	
3582.628	2000	10	3634.800	10		3691.324	1		3737.693		20h
3583.464	12		3635.146	3000c	50c	3691.608	50	1h	3738.501	20	
3584.005	1		3636.070	10000c	500c	3691.674		5c	3739.342	1	
3585.684	30	1	3637.447	8		3692.759	300	4	3740.388	1	
3586.566	3		3638.012	1		3693.400	8		3740.494	1	
3587.386	1		3638.220	1000	15	3694.327	30d	1	3740.988	2	
3587.942	4000	40	3638.848	200	4	3695.404		1	3742.789	150	3
3589.471	15		3639.069	1		3695.734	1		3743.508	1	
3589.890	3h	2h	3639.379	900	15	3695.999	30w	1h	3743.610	2	
3590.471	1		3640.095		10w	3696.297	150	3	3744.026	150	2
3591.222	50	1	3640.226	400	10	3696.747		2h	3744.801		6h
3591.483	80	4	3641.093	6	1	3697.415	100	1	3745.012	400	5
3591.942	8cw		3641.183	15	1	3697.736	30	1	3745.808	4hl	
3592.920		1h	3641.534	30	1	3698.694		3hw	3746.148	1000	10
3593.471	200	3	3642.576		2	3698.959	3		3746.640	100	2
3593.580	10		3642.985	30	1	3701.478	5	1	3746.845	5000	150
3594.573	300	4	3643.157	3		3701.966	1		3748.406	1	
3594.908	50cw		3643.376	10		3702.077		3h	3749.634	10	

TABLE 1. *Spectrum of technetium* – Continued

Wavelength	Intensity		Wavelength	Intensity		Wavelength	Intensity		Wavelength	Intensity	
	Arc	Spark		Arc	Spark		Arc	Spark		Arc	Spark
3749.928	60	4	3791.524	3		3847.351	100	1	3908.596	20	
3750.061	40		3791.734	300	7	3847.596	500	3	3909.038	8	
3750.566	6		3792.102	20		3847.870	10h	1	3909.782	20	
3751.056	6		3792.674	6		3848.310	5h		3909.958	10	
3752.024	30	1	3792.774	1		3849.519	1		3911.157	5	
3752.134	1000	10	3793.087	3		3850.553	5		3911.921	3	
3752.944	20		3793.207	1		3851.222	300	3	3914.538	3	
3754.048	60	3	3793.721	2		3852.328	80	1	3914.723	1	
3754.368	4000	40	3793.986	3c		3853.323	2		3915.174	2	
3754.885	4		3794.800	60	1	3854.074	8		3915.889	10	
3755.048	3		3795.502		4h	3854.326	50		3916.536	60	1
3755.221	80	3	3796.522	12		3854.768	10		3916.941	5	
3755.652	10c		3797.435	200	5	3855.555	20		3917.443	10c	
3756.230	12		3797.767	1000	10	3855.914	1		3917.743		4h
3756.334		2h	3798.055	40	1	3856.543	20		3919.148	50	
3757.722	3		3798.981	20c		3856.734	500c	5h	3919.375	300	3
3758.535	1000	10	3799.692	80	2	3857.388	20		3920.550	30cw	
3758.948	5		3801.645		5hw	3858.063		4	3922.134	100	1
3759.170		7	3802.025	2h		3860.129	8		3923.663	300c	3c
3759.305	5		3803.976	40	1	3861.259	25c		3924.131	20	
3759.553	20	1	3804.534	2		3863.068	200	3	3924.469	2	
3761.481	8		3806.144	15		3863.830	100	1	3925.143	10	
3761.807	2000	20	3806.424	5		3864.106	400	4	3925.953	20	
3762.880	6		3807.381	10		3865.112	3		3927.356	5	
3763.974	40	1	3808.633	10d		3866.012	30		3927.573	200	2
3764.566	2		3809.798	1	6	3866.190		20cw	3928.323	10	
3765.576	1		3810.355	2		3866.608	5		3928.770	30	
3765.962	2		3810.568	30		3868.240	1000	8	3928.913	20	
3767.858	2d		3811.253	80	2	3870.292	10		3929.113	10	
3768.365	30		3812.390	10		3871.055	12		3929.378	40	
3768.774	5000	100	3813.040	15cw	1c	3871.223	12		3929.821	5	
3769.352	6		3813.846	10		3874.609	12		3931.319	3	
3769.680	3		3814.339	6	2h	3875.658	200	2	3931.907	8	
3769.783		1	3814.667	200	3	3876.366	80	1	3932.218	2	
3770.320		1h	3815.509	80	1	3877.139	30		3933.438	150	2
3770.498	15		3816.888	300	4	3878.295	4		3933.705	200	
3771.031	3000	50	3817.967	150	3	3879.160	500c	10c	3934.832	30	
3771.467	4		3818.119	100	2	3880.715	600c	20c	3936.175	1	
3772.088	60	2	3819.103	1	10c	3882.497	10		3936.648	70	
3772.388	40	2	3820.761	50	2	3885.638	3		3939.726	25	
3772.782	20	1	3821.083	4		3886.896	2		3940.054	70	
3773.413	50	4	3822.672	80		3888.177	1h		3940.478		2h
3773.930	1		3823.066	1		3888.440	80	1	3942.866	30	
3774.783	15		3824.102	1		3888.665	7		3943.868	120	1
3774.970	10		3824.467	300	4	3888.814	2		3946.571	4000c	20c
3775.355	50c	1	3825.531	5		3889.130	150	2	3947.087	2000	10
3775.560	15		3826.013	20		3890.033	1		3948.151	1	
3776.288	1		3826.352	1		3890.320	20		3948.513	2	
3776.999	6h		3827.193	2		3892.122	300cw	100cw	3948.844	4	
3777.274	500	10	3827.593	60	1	3892.332	100	1	3949.224	9	
3778.194	10		3828.537	500	4	3893.220	200	2	3950.391	80	
3779.032		2hw	3828.750	3		3893.837	4		3951.016	7	
3779.373	2000	40	3829.220	150		3894.201	15		3951.831	180	
3779.693	40	1	3829.274		10h	3894.482	15		3952.193	6	
3780.680	3000cw	100cw	3830.352	200	3	3894.688	2		3953.651	100	1
3782.299	15		3831.883	20		3895.390	2		3953.765	30	
3784.057	500	6	3832.448	200	1	3898.531	2		3955.734	200	3
3784.802	1		3832.817	600	5	3899.120	100	1	3956.410	3	
3785.222	20	1	3833.425		3h	3899.827	600	5	3958.114	10	
3785.560	6		3837.559	1500	15	3901.473	5		3958.793	15	
3786.064	200	3	3839.577	1		3902.832	10		3959.090	80c	1c
3786.494	10		3840.137	60		3903.740	60		3959.520	150	2
3786.566		3h	3841.307	800	8	3903.934	80	1	3959.943		15w
3787.537		3h	3842.342	80		3904.195	3		3960.770	20w	
3787.772	1		3843.349	2		3905.322	8		3961.520		1
3788.154	2		3843.968	100	2	3905.517	30		3963.361	2	
3788.370	1		3844.061	20		3905.774	100	1	3963.714	2	
3789.232	2		3844.347	60	1	3906.400	20		3964.266	30	
3789.955	2h		3845.974	800	8	3907.681	1		3964.467	20	
3791.282	500	8	3846.941	8		3907.958	30		3965.619	3	

TABLE I. *Spectrum of technetium* – Continued

Wavelength	Intensity		Wavelength	Intensity		Wavelength	Intensity		Wavelength	Intensity	
	Arc	Spark		Arc	Spark		Arc	Spark		Arc	Spark
3967.500	100c		4036.267	1		4110.221	1000	5	4201.850	20	1
3967.912	2		4036.787	3		4111.199	6		4206.568	50	5
3969.207	10		4037.195		2	4111.386	150	1	4211.430	20	1
3970.239		6h	4038.253	8		4113.341	30		4212.420	1	3
3971.232	8		4039.246	1000	8	4114.340	6		4214.220	5	
3971.503	80	1	4041.016	5h		4115.077	10000	300	4215.510	10	1
3971.914	40		4041.559	100		4117.021	4		4218.609	300	20
3972.264	20		4041.781	200		4118.740	6		4220.346	50h	1
3974.554	30h		4042.657	10		4119.274	600	5	4221.619	10	
3975.020	150cw	30c	4043.401	8		4120.163	2h		4229.948	6	
3976.526	3		4046.697	80		4121.576	100		4230.207	10	1
3978.706	8		4048.086	20		4122.206	4		4230.832	150	5
3979.095	20		4049.108	10000c	150c	4124.217	8000	200	4231.195	5	
3979.637	300	2	4050.888	60	1	4127.899	1		4232.096	40	1
3980.354	500	3	4051.569	2		4128.268	1000	20	4235.709	1h	
3981.279	6		4051.949	500	4	4128.557	80	1	4238.191	5000c	100c
3981.688	8		4053.177	200	3	4129.862	6		4238.991	5	
3982.171	100	1	4054.415	30		4130.453	150	2	4239.567	20	1
3984.967	10000c	100c	4056.082	200c	4c	4130.877	30		4241.996	8	
3985.903	10		4057.283	60	2h	4131.212	2		4242.979	40	1
3987.780	400	3	4058.232	30	1	4132.530	40		4246.613	1	
3988.961	10		4058.666	2		4133.276	20		4247.038	4	
3989.216	20		4060.853	40	1	4133.679	2		4248.953	30	1
3989.449	8		4061.516	20		4134.490	3		4252.756	2h	
3989.888	15		4062.095	8		4134.813	300	3	4253.527	4	1h
3990.392	2		4064.868	3		4137.234	15		4253.776	4h	
3991.320	20		4069.023	100	1	4137.660	4		4256.134	10	
3992.094	50		4070.834	40	1	4139.116	300	3	4257.338	30	1
3992.965	3h		4071.059	100	1	4139.849	800	8	4258.587	20	1
3994.038	300	1	4071.454	5		4141.267	400	4	4262.270	10000	400
3994.509	2000	10	4073.802	1		4142.917	20		4262.687	1000	20
3995.741	3		4074.034	6		4144.950	6000	30	4264.027	6w	
3996.974	200	1	4074.857	20		4145.080	3000	15	4264.303	8	
3997.257	3		4076.463	2		4146.202	80	1	4266.158	80	1
3998.755	40		4077.074	15		4146.882	20		4266.532	2h	
4001.332	20		4078.159	1		4147.615	200	2	4266.983	2	
4001.843	20		4079.004	5h		4150.200	15		4267.978	8	
4003.867	4		4079.786	30		4151.241	10		4268.503	30	1
4003.976	4		4079.914	3		4153.672	150	1	4269.531		8w
4004.182	15		4080.042		2	4155.867	2		4269.660	4	
4004.689	300	2	4081.966	3		4158.547	10		4270.767	6h	
4005.886	15		4082.800	10		4159.319	20		4270.880		8h
4006.161	30		4083.537	400	3	4159.820	3h		4274.971	800	1000
4006.631	30c		4084.500	6h		4160.346	1		4275.504	18	2
4007.136	500		4084.650	10		4160.998	1		4275.906	20	2
4007.603	10		4085.085	20		4161.547	100	1	4277.514	5h	1h
4007.874	40		4086.325	18		4162.970	1		4278.895	800	100
4008.152	20		4087.299	50	1	4163.271	10	1	4279.263	18	2
4008.837	50		4088.707	10000	100	4163.702	20		4285.559	1	
4009.179	15		4089.285	60		4165.609	10000	100	4286.353	4	1
4010.897	1		4091.555	100 1d	1	4167.424	500	6	4286.843	1	
4011.043	10		4092.373	12		4169.680	1000	10	4287.854	2h	
4011.358	12		4093.694	200	2	4170.274	4000	40	4288.404	2h	
4011.996	1000	5	4094.163	80	1	4172.532	5000	60	4289.115	5	1
4014.293	20		4095.668	15000	500	4174.462	70		4289.563	20	2
4015.474	30		4098.004	2h		4176.276	1000	50	4290.783		3h
4015.760	20		4098.784	100	1	4182.629	5		4294.351	80	12
4016.683	400	2	4100.114	150cw		4185.815	3		4297.058	10000	1000
4017.223	600	4	4100.902	20		4186.506	800	30	4299.523	1h	
4020.755	2000	10	4101.312	100	1	4188.910	10		4301.301	2h	
4023.576	4w		4101.989	30		4189.609	50		4302.319	1	
4024.865		1	4103.368	10		4190.306	2		4302.452		2h
4025.475	60		4103.501	10		4190.477	4		4303.372		1h
4029.108	80	1	4103.987	3		4191.415	10		4303.717	1	
4030.034	3		4105.089	80		4193.557	1		4304.848	4	1
4031.626	20000cw	300cw	4106.246	60		4194.224	3		4305.516	15	2
4033.677	1		4106.723	80	1	4196.063	1		4305.819	80	8
4034.014	80		4107.644	20		4198.312		5w	4308.615	15	2
4034.673	20		4108.979	50c		4199.466	30	1	4309.370	2	
4035.658	5w		4109.646	40		4200.228	3w		4309.858	1	

TABLE 1. *Spectrum of technetium* – Continued

Wavelength	Intensity		Wavelength	Intensity		Wavelength	Intensity		Wavelength	Intensity	
	Arc	Spark		Arc	Spark		Arc	Spark		Arc	Spark
4310.222	60	6	4395.571	2		4472.512	2h		4547.088	1	
4311.376	3		4397.254	1		4473.662	15c	2	4548.614	1	
4312.504	10	1	4398.003	1		4474.506	8	1	4549.156	1h	
4314.021	9	1	4398.689		1	4475.003	7	1	4549.439	80	8
4314.679	1		4399.337	4		4477.233		3	4550.270	4h	
4318.061	6	1	4401.518	10		4478.078	2		4551.728	2	
4318.983	5	1	4402.054	1h		4478.673	4	1	4552.204	400	40
4319.887	2		4402.819		2h	4480.251	100	10	4552.456	150	15
4320.505	3		4403.905	6	1	4481.533	1000	100	4552.854	800	80
4321.068	1		4404.176	2		4484.351	10	1	4554.042	1	3
4322.015		2h	4404.403	1		4486.050	6c	1	4557.046	1000	100
4323.016	2		4405.081	7	1	4487.061	3000	300	4558.711	40	4
4323.356	80	7	4405.485	2		4488.624	3		4560.205	15	2
4323.958	12	2	4405.922	3		4490.128	1		4560.421	20c	2
4324.867	12	2	4406.427	1		4491.473	1h	2h	4562.522	8	1
4326.393	3	1	4407.346	7	1	4492.173	2		4562.913	30	3
4328.778	60	6	4409.034	3	1	4492.735	10	1	4563.741	25	2
4330.231	2		4409.815	2		4493.388	8h	7h	4564.539	2000	300
4331.866	1		4412.004	100	7	4495.027	400	50	4565.436	4	1
4332.452	150	10	4412.685	2	1	4495.213	20		4566.421	7	1
4334.768	3	1	4413.322	1		4497.337	2w		4567.216	1h	
4335.187	4	1	4415.452	20c	1	4497.713	5		4568.135	3	
4336.855	400cw	40cw	4415.718	5	1	4498.529	60	8	4568.769	1	
4338.248	2h		4417.269	1		4499.295	7h	1h	4569.751	1	
4339.914	3h		4418.412	7	1	4500.170	1h		4570.599	15	
4341.109	2		4420.302	80	6	4501.743	60	6	4570.861	60	10
4342.242	20	2	4421.430	2h		4503.399	100	10	4571.453	2	
4342.570	4	1	4421.878	3h		4504.058	1h		4572.062	5	1
4343.584	1		4423.089	2h		4505.081	1		4573.977	8	1
4343.918	4	1	4423.781	3hw		4505.473	2		4576.521	2	
4344.579	70	7	4425.139	1h		4505.881	3		4577.129	20	3
4345.442	10		4427.294	10	1	4506.068	1		4578.447	1000	100
4350.013	5h		4428.702	2	1	4506.640	2		4579.084	60	5
4350.415	1	1	4429.592	1000	200	4507.177	4		4579.559	3	
4352.487	2h		4431.716	15	2	4507.775	3		4580.291	3w	
4354.823	2		4432.571	12	2	4508.719	8	1	4580.613	7	1
4355.398	15w	2	4433.783	1h		4511.312	3h		4582.377	25	3
4356.093	3	1	4434.486	1		4512.691	8		4582.726	4	1
4358.491	400	40	4434.845		20c	4514.019	2h		4583.246	1	
4359.257	200	30	4436.731	2		4515.978	1000	100	4583.686	2	
4361.959	20	2	4437.056	1h		4516.601		2h	4584.710	3h	1h
4363.014	80	8	4438.999	5		4521.263	20	2	4584.851	50	4
4363.838		1	4441.418	2h		4522.075	4	1	4585.884	150	15
4364.017	1		4445.316	6	1	4522.841	10000	1000	4586.309	4	1
4364.889	1		4446.502	8	2	4525.760	2		4587.037	6	1
4365.425	1		4447.015	12c		4526.321	10	2	4587.628	4	1
4365.999	4		4450.790	5c	1	4526.507	8	1	4588.232	30	3
4368.340	2		4451.433	1		4531.157	30	4	4588.536	2	2
4368.616	1		4452.078	6		4531.219	5	1	4588.857		3
4368.940	30	4	4452.273	60	6	4531.391	8	1	4589.297	2h	
4369.255	25	3	4452.581	1		4531.703	20	3	4590.690	1h	
4370.094	70	7	4454.142	3		4534.236	1		4591.689	3w	
4370.717	60	7	4454.811	1		4534.299	1		4591.988	1	
4371.661	1		4456.621	20	3	4534.760	3h	1h	4592.306	1	
4372.086	10	1	4458.057	3		4536.110	1		4593.346	1000	100
4373.181	15	2	4459.395	10	2	4536.365	2		4594.059	100	10
4373.952	70	7	4463.038	20	2	4536.680	2		4597.273		2h
4378.519		2h	4463.535	1		4537.052	2		4597.393	2h	
4380.132	2		4463.852	60	6	4537.347	100	10	4598.217	10	1
4381.583	4	1	4464.277	15	1	4537.844	5	1	4600.164	1	
4383.075	60	6	4464.864	6		4538.556	3	1	4601.231	3	
4384.317	1		4465.090	20	2	4539.530	2000	500	4601.586	2	
4384.574	1		4465.613	80	8	4540.200	3		4602.408	30	3
4385.626	1		4466.575	3	1	4541.247	5		4602.721	100	10
4385.881	1		4467.384	3	1	4542.090	400	40	4603.162	15	2
4387.501	15	1	4468.309	1h		4543.900	5	1	4607.170	3	
4388.605	3	1	4469.173	10	1	4544.609	3		4608.005	80	8
4391.923	3	1	4470.061	4	1	4545.546	50	5	4608.314	20	2
4392.265	1		4470.369	1		4546.672	2		4608.833	8	1
4393.787	7		4471.986	3		4546.896	2		4609.159	300c	30c

TABLE 1. *Spectrum of technetium* – Continued

Wavelength	Intensity		Wavelength	Intensity		Wavelength	Intensity		Wavelength	Intensity	
	Arc	Spark		Arc	Spark		Arc	Spark		Arc	Spark
4610.531	20	2	4686.406	150	15	4762.362	200	20	4848.716	3	
4611.171	40		4687.627	20	1	4763.931	1		4849.608	40	2
4611.386	2		4687.978	100	15	4764.796	5		4850.368	4	
4611.811	3		4688.365	3h		4764.987	3		4850.740	1h	
4613.089	1		4689.359	400	40	4765.381	8	1	4853.588	20000	2000
4616.857	1000	100	4689.810	150	5	4766.305	7	1	4855.343	1	
4617.447	20	2	4692.384	60	2	4770.363	1		4857.211	100	10
4618.192		2	4694.282	300	30	4771.543	4000	400	4858.446	2	
4619.725	1		4695.788	15	3	4773.237	5	1	4859.216	40c	2c
4620.048	3		4697.047	3		4773.890	200	20	4860.424	1	
4621.129	30		4697.513	25h	2h	4776.355	120	12	4861.232	20	2
4621.458	40		4700.186	1		4777.557	1		4862.193	100c	8c
4622.691	200c	20c	4701.169	2		4778.820	5	1	4862.931	40	4
4622.950	30c	1c	4701.814	5	1	4779.501	8c	1c	4863.323	20	2
4624.122	3	1	4702.586	1		4779.898	50	5	4864.125	6	1
4624.961	300	30	4702.880	50	5	4780.607	80	3	4866.733	10000	1000
4625.628	5	1	4704.802	15	2	4781.012	1h		4869.240	3c	
4625.753	5	1	4705.542	5	1	4783.925	200	20	4870.772	200	20
4626.557	20		4706.918	1000	100	4784.137	20	2	4873.799	10c	
4626.803	2		4707.575	20	2	4784.720	100	10	4874.325	1	
4628.063	60	4	4709.786	1		4785.597	500	50	4874.768	30	1
4629.253	1		4710.758	2		4787.589	40	2	4875.142	1	
4630.572	1000		4711.448	2		4787.758	100	8	4876.444	1	
4630.978	4		4712.120	8c		4789.492	150	15	4876.768	12c	1
4631.378	80	3	4713.610	3		4790.482	200c	20c	4877.016	30	3
4631.815	10	1	4714.222	200	20	4791.623	250	20	4877.344	15	2
4632.740	30	3	4714.605	40	4	4792.120	5	1	4878.094	12	1
4633.152	200	20	4716.787	80	8	4796.176	3		4882.586	8	1
4635.433	1		4717.766	2000	200	4796.480	10	1	4885.044	30	3
4635.752	150	15	4719.018	500c	50c	4797.895	6h		4885.889	12	1
4637.500	3000	300	4719.281	4000c	400c	4799.079	4		4886.190	4	
4640.015	2		4720.726	6		4799.978	300	30	4888.695	100	10
4641.296	6	1	4723.828	3	1	4800.700	80c	5c	4889.444	50	5
4641.669	1		4724.842	1		4803.291	30		4890.884	150c	10c
4643.280	500	20	4725.202	1		4803.623	2		4891.918	8000	800
4645.490	150c	5c	4726.798	10	1	4804.777	1h		4892.490	150	15
4646.620	80	8	4728.082	50	5	4805.688	100	10	4893.153	1h	
4647.573	120	10	4729.302	15	2	4806.992	8	1	4893.651	10c	1c
4648.332	2000	200	4731.023	2cw		4807.349	8	1	4894.780	5cw	20cw
4650.556	8	1	4731.918	10	1	4807.988	1h		4895.977	2	
4652.005	2		4732.044	10	1	4809.094	1		4896.832	1	
4653.609	100	1	4732.469	25	1	4809.416	100	10	4897.251	8	1
4654.658	120	10	4733.869	20c	2c	4810.633	2		4899.704	1	
4655.363	1		4735.058	8	1	4811.842	60	6	4900.046	30	3
4656.440	12	1	4736.515	200cd	20cd	4812.630	3		4900.955	10	1
4657.006	60sd	6	4737.434	1		4813.324	50	5	4901.708	20	2
4658.934	2		4738.652	2		4814.073	60	6	4902.085	1	
4659.798	30	3	4739.551	100c	10c	4816.062	30c	1	4903.747	2	
4660.212	2000c	200	4740.608	10000	1000	4816.794	500	80	4906.410	50	5
4660.590	30c	3	4741.284	50	5	4819.024	1h		4906.791	10	1
4663.237	2h		4741.532	6	1	4820.739	10000	1000	4908.509	1000	100
4664.337	100	10	4742.940	8	1	4825.236	1		4909.053	5	1
4666.311	3		4744.250	1h		4825.748	20	2	4909.566	2000	200
4667.326	1		4746.009	100csd	10csd	4828.203	1		4912.422	5c	
4668.354	40		4747.833	1		4828.698	2		4913.020	500	50
4668.879	100	10	4749.614	500	20	4831.347	300	30	4914.166	10	1
4669.305	2000	200	4750.552	3		4834.367	1000	100	4914.699	150c	15c
4671.749	10	1	4750.759	8	1	4835.394	1000	100	4915.372	1	
4672.170	400	40	4751.548	15	2	4838.034	1		4915.810	30	3
4672.545	3		4752.717	1000	60	4839.017	1		4918.917	3	
4672.824	40	4	4755.362	1h		4840.974	20	2	4919.229	5	
4673.077	45	4	4756.111	100	10	4841.364	100	10	4920.668	200cl	20c
4674.245	30	1	4756.498	1		4842.022	10h	1h	4921.646	20	2
4678.073	3		4757.502	40c	2	4842.488	1		4922.482	2w	
4678.903	200	20	4757.840	2		4843.559	6	1	4923.601	300	3
4682.129	1h	1h	4758.094	80	6	4843.850	1h	1	4925.412	2	
4682.732	20c	1	4759.280	40	3	4844.326	2		4927.031	5	1
4683.599	150	15	4759.806	50	3	4845.642	2		4928.676	3	
4684.716	2		4760.160	2		4845.980	1		4929.749	25	2
4685.423	1		4761.968	40	3	4846.444	1		4930.360	20	2

TABLE 1. *Spectrum of technetium* – Continued

Wavelength	Intensity		Wavelength	Intensity		Wavelength	Intensity		Wavelength	Intensity	
	Arc	Spark		Arc	Spark		Arc	Spark		Arc	Spark
4930.904	15		5046.622	3h		5167.774	8	1	5286.886	10cw	1
4932.271	10 l	30wd	5046.903	2h		5168.470	2		5287.228	10c	1
4933.430	10		5051.303	40	4	5169.324	2		5288.330	1	
4933.798	25c	2	5055.274	300	30	5172.292	4hd		5291.060	2h	
4934.586	25c	2	5058.331	60	6	5173.910	2		5291.905	3h	
4936.132	40	3	5060.686	500	50	5174.812	2000	200	5292.263	30c	3c
4938.821	30	4	5062.136	2		5177.018	2		5299.669	20	1
4939.112	2		5067.632	1		5177.387	3		5304.310	4h	
4940.576	1		5069.549	50	5	5177.746	10c		5305.307	100	6
4941.567	1		5070.378	4		5178.104	10		5306.210	1h	
4944.246	30c	3c	5074.051	3		5181.930	2hs		5307.558	5	
4945.219	1		5074.690	1	1	5183.999	50	2	5307.875	1	
4947.078	50c	5c	5075.184	10	1	5184.994	10	1	5311.163	10	1
4948.064	400	40	5079.561	2		5186.791	2w		5313.696	1h	
4948.839	20	2	5080.268	1h		5189.687	40	4	5314.964	400	40
4949.111	2		5081.860	3		5193.144	20h	2h	5317.056	2h	
4949.264	5		5083.969	30	3	5202.152	10cw		5317.509	30c	3c
4950.743	2		5085.611	2		5205.268	2h		5318.186	15c	1c
4951.056		10hw	5086.922	40	4	5206.561	100		5320.198	600	60
4953.351	1h		5088.200	1		5206.862	10		5325.132	5	
4954.508	2h		5090.743	80	8	5207.358	4		5325.848	4	
4954.713	10	1	5093.182	10	1	5208.623	25		5328.406	10	1
4954.985	20	2	5095.575	2		5211.262	6		5329.620	4	
4956.337	40	4	5096.280	5000	500	5211.477	6		5332.201	2	
4959.942	4		5100.033	6	1	5214.087	20	4	5334.790	200	20
4961.532	1		5100.327	3	1	5220.239	15	3	5335.080	6	1
4962.654	10	1	5100.653	4	1	5221.447	10	1	5336.594	1	
4963.023	2		5102.525	30	3	5223.517	2		5337.066	5	1
4964.735	2h	2h	5103.240	200c	20c	5225.360	10	1	5339.754	1h	
4966.255	10	1	5103.531	10	1	5225.554	200	20	5345.690	8	
4967.200	60cw	6	5104.321	500	50	5228.648	40cw	4cw	5345.890	15c	1c
4968.854	5c		5107.080	3c	1h	5228.756	10		5350.498	4	
4976.340	5000	500	5107.581	8	1	5230.342	12	1	5350.873	15	
4978.569	20	2	5109.079	4	1	5231.268	15	1	5353.480	500cw	50cw
4979.028	8	1	5109.809	200	20	5232.164	5	1	5355.110	6	1
4980.214	3		5111.113	1		5232.929	1h		5356.634	200	20
4980.448	50	4	5111.377	1		5233.326	1		5358.646	300	30
4988.083	2		5112.019	3		5236.130	7	1	5359.222	40	4
4988.710	1		5113.370	5		5236.452	5	1	5360.142	200	20
4989.332	3h		5113.686	30	3	5237.180	2		5360.690	15	1
4990.428	2h		5116.141	2h		5237.521	2		5362.420	4wd	
4991.346	1h		5116.564	2		5238.247	1		5364.050	20	2
4993.978	80c		5118.483	2		5240.304	2h		5366.082	10	1
4994.997	400	40	5118.940	8		5240.953	20c	2c	5367.090	2	
4999.120	30	2	5120.605	100	10	5242.641	2		5367.166	4hw	10hw
5000.831	50c	3	5122.180	20	2	5243.094	2		5370.824	7	1
5002.674	200	20	5122.739	6	1	5245.600	4w		5372.086	1h	
5003.405	2		5123.400	5wd		5246.653	4w		5372.719	1h	
5005.737	100	5	5125.158	6c	1c	5247.006	20	2	5375.201	500h	50h
5010.766	30	2	5126.626		3h	5249.428	20c	2	5376.298	10h	1h
5014.517	200cw	20cw	5129.152	1h		5251.421	40c	3c	5377.414	20	2
5017.324	1h		5130.260	1h		5252.768	3w		5378.457	2	1
5019.628	1h		5134.320	40h	3	5253.052	5		5378.970	1h	
5022.250	2h		5135.789	6	1	5253.421	6		5380.416	1	
5022.669	1h		5136.156	40	4	5254.762	20c	2c	5381.585	1h	
5024.722	20	2	5138.886	3		5260.217	200cw	20c	5382.704	20c	1c
5026.238	500	50	5139.262	500	50	5261.444	200c	20c	5383.509	30c	2c
5026.793	300	30	5140.450	1		5262.925	1		5385.832	10h	
5027.894	150	15	5141.227	1		5266.227	6	1	5386.872	10	1
5031.663	4		5146.542	30w	3w	5266.402	8	1	5387.630	6h	
5032.107	10	1	5147.030	20w	1w	5267.214	4	1h	5389.320	20cw	1h
5032.446	80	8	5147.997	4		5267.350	3		5390.214	1	
5033.613	5	1	5150.630	500	50	5273.229	20h	1h	5390.697	1	
5035.760	3		5152.053	1		5273.930	15	2	5393.629	5h	
5036.002	4		5157.991	10	1	5274.824	50	5	5394.569	3h	
5036.833	5	1	5158.858	30c	3c	5275.512	1000	100	5395.149	1	
5039.572	10	1	5160.130	1		5279.330	30c	2c	5395.802	4h	
5041.905	1h		5161.810	2000	200	5281.101	20c	1c	5396.690	2	
5043.699	2		5162.410	5h		5285.067	800	80	5397.539	5	
5045.580	2h		5167.038	1		5285.838	8	1	5400.480	20	

TABLE 1. *Spectrum of technetium* – Continued

Wavelength	Intensity		Wavelength	Intensity		Wavelength	Intensity		Wavelength	Intensity	
	Arc	Spark		Arc	Spark		Arc	Spark		Arc	Spark
5407.910	50c	3c	5524.107	150	15	5645.694	2		5773.656	20	2
5411.928	20	1	5526.878	6		5650.259	1		5775.069	10cw	1c
5412.915	20h	1	5528.233	100	10	5651.335		7	5777.360	1	
5413.624	2h		5532.793	1		5652.123	1		5777.976	6	1
5417.121	3		5535.098	10		5652.909	1		5792.474	10cw	
5418.934	2h		5536.394	20	1	5654.338	6		5794.646	100	10
5421.787	5		5538.875	10cw	1c	5656.005	100	8	5795.956	5cw	
5422.382	2		5539.304	1		5657.490	3		5799.850	80c	8c
5423.048	150c	15c	5540.596	10	1	5658.106	8	1	5802.433	10	1
5425.956	6	1	5541.939	200	20	5661.557	20	2	5805.214	20	2
5430.712	2		5543.627	80	8	5662.104	10	1	5805.525	10	1
5431.246	15h	1	5545.860	5h		5664.232	4		5806.126	2h	
5432.437	5		5548.227	2		5664.900	40cw	2cw	5806.672	3h	
5433.894	1		5550.528	100	10	5666.338	7		5807.107	1w	
5435.139	1		5554.516	1h		5667.058	15		5809.536	1	
5436.993	2		5555.551	1h		5667.615	15		5814.241	100cw	10c
5438.774	2h		5556.110	2		5672.153	60	6	5814.639	2	
5439.507	20c	1c	5560.712	3h		5675.178	5hs		5815.038	1h	
5441.440	2		5563.006	10cw		5678.478	50	2	5817.348	2h	
5442.071	4cw		5564.840	3h		5679.174	5		5819.176	15h1	
5444.258	50	5	5565.140	1		5680.973	15		5820.292	1	
5447.402	200	20	5566.102	4hd		5682.298	1h		5820.785	2	
5447.800	20c		5567.748	2h		5685.567	8c		5821.310	10	1
5448.384	20		5568.700	5		5687.301	200	20	5823.196	8	1
5449.335	2cw		5570.032	3		5688.730	20	2	5826.552	30 1d	1h
5449.720	2		5570.880	10cw	2	5689.046	200	20	5827.189	10	1
5450.471	10		5572.858	20	1	5692.212	15h	1	5831.477	200	20
5451.900	500c	50c	5575.438	10h		5694.330	15c	2c	5831.858	2	
5454.124	3		5576.283	20	1	5696.056	20h	2	5832.836	2	
5455.112	20wd		5576.800	25	1	5696.626	18cw	2c	5833.314	2h	
5455.952	100		5577.649	15w		5702.894	5h		5834.358	2h	
5456.494	1		5578.255	4h		5704.900	2c		5835.865	6	1
5458.159	30cw		5580.231	8cw		5705.403	1h		5836.329	150c	15c
5459.118	2c		5580.828	1		5711.460	4hw		5838.366	10	1
5460.747	10		5581.931	2c		5718.775	1h		5846.973	1	
5461.092	9c		5584.031	20	2	5719.542	10	1	5847.754	1	
5462.422	4h		5589.019	3000cw	300cw	5720.205	1h		5850.364	6	1
5467.471	10		5591.400	1h		5721.090	10h	1h	5851.707	1h	
5468.768	3		5594.491	1h		5723.255	2h		5853.376	25h	2h
5471.072	1		5596.614	2h		5725.314	700	70	5855.439	7cw	
5471.962	300		5602.229	200	20	5732.791	3		5855.898	1	
5473.258	2		5603.543	5h	1h	5734.691	2h		5856.656	5	
5474.435	2		5604.069	2h		5735.636	3		5863.865	30h	
5475.624	2		5604.762	1h		5737.543	5w		5865.146	5h	
5477.540	20cws		5605.534	2		5739.108	2h		5865.393	15c	1c
5480.035	3c		5606.376	10h		5739.479	1h		5865.826	10cw	1
5480.635	4h		5611.482	20	2	5741.301	5		5867.484	10c	1
5482.840	50	5	5613.021	3h		5741.943	10hw	1h	5871.273	20	1
5483.012	70	7	5613.863	2h		5745.020	3h		5873.635	7	1
5485.026	50c	1c	5615.272	8	1	5748.307	3		5874.804	20	1
5485.373	60	3	5616.347	5h		5749.542	10c		5879.288	18h	
5486.028	2		5616.795	10		5750.098	2h		5882.067	25	2
5490.391	30c	2	5617.651	7	1	5751.050	1h		5885.365	10cw	
5490.903	5		5620.450	2000c	200	5751.614	1h		5890.704	1	
5496.054	10	1	5622.748	2h		5752.219	2		5891.658	1h	
5500.096	20	2	5625.232	6		5754.775	20h		5893.590	15	1
5501.168	1		5626.180	1		5755.199	3h		5894.662	1h	
5502.110	5		5627.469	2		5758.298	1h		5896.406	6	
5502.971	30h	1h	5628.956	1		5760.389	2		5897.420	3	
5504.608	2h		5629.568	5		5761.734	1		5901.728	2	
5505.274	30h	2h	5629.937	300	30	5762.449	5		5903.415	3	
5506.890	80cw	5c	5633.820	1		5764.119	1h		5903.570	2	
5507.476	3h		5636.253	30	3	5765.698	5h		5905.477	8h	
5510.866	10	1	5636.840	40h	2h	5767.232	4hc		5905.904	10	1
5511.478	2		5637.792	8h	1	5767.546	6		5908.577	15cw	1c
5511.811	1		5640.782	40c	2c	5768.002	2		5914.939	1	
5512.876	4h		5642.132	1500	150	5769.704	3		5915.751	3h	
5513.630	10h		5643.940	6		5770.249	4		5917.250	1	
5514.216	20h		5644.357	12	1	5771.468	500c	50c	5917.963	2h	
5518.051	30	3	5644.944	800	80	5772.500	1h		5918.780	1	

TABLE 1. *Spectrum of technetium* – Continued

Wavelength	Intensity		Wavelength	Intensity		Wavelength	Intensity		Wavelength	Intensity	
	Arc	Spark		Arc	Spark		Arc	Spark		Arc	Spark
5919.462	5	1	6063.930	20c	2	6267.598	2		6511.774	1	
5923.357	150	10	6065.090	200	20	6274.014	1		6515.160	20	
5924.468	1000cw	100cw	6066.182	5h		6275.425	4		6515.660	2h	
5925.384	20c	1c	6069.785	30	3	6277.250	2cw		6516.192	2	
5925.714	10	1	6076.041	2		6278.234	2c		6519.740	1	
5926.286	200	20	6077.819	1		6287.962	4cw		6526.817	200	20
5926.687	3h		6080.327	1		6288.358	1h		6528.038	5c	
5928.111	2		6083.456	1		6290.397	5		6532.494	2	
5930.310	20		6085.229	800	80	6292.239	1h		6533.606	2	
5930.544	2		6089.828	2h		6295.943	1		6534.063	6	
5931.929	600c	60c	6091.146	1		6296.423	2		6534.659	10	
5937.136	5h		6093.741	20c	2c	6296.765	6h		6535.947	3h	
5938.394	20	2	6097.790	1		6299.959	1h		6536.633	5	
5942.259	20cw	1	6098.891	3h		6303.104	2hw		6537.425	2c	
5946.514	10cw		6099.387	300	30	6304.048	6		6563.197	4	
5951.484	40c	3c	6102.961	500cw	50c	6305.028	30	3	6564.004	50w	
5951.924	8c		6106.898	1h		6306.260	8		6568.820	2h	
5955.318	2		6107.205	2h		6310.420	40c	3c	6576.820	50wld	
5958.646	1h		6111.120	20	1	6312.179	100	10	6579.243	150	
5961.256	2		6112.030	20h	1h	6318.408	1w		6581.747	8	
5969.013	6	1	6112.630	1		6319.033	1		6586.147	3	
5974.845	8	1	6115.490	4h		6320.700	5		6590.039	15	
5977.678	1		6120.684	1000	100	6321.099	1		6595.124	4	
5979.170	2h		6122.196	1		6326.116	1		6595.244	6	
5979.893	4		6124.339	5		6328.690	2h		6598.037	10	
5980.512	20c	1c	6127.167	8	1	6330.962	2		6602.099	5	
5980.694	10		6127.791	1		6332.742	2		6609.746	3hs	
5986.820	6		6130.805	1000	100	6347.458	1		6614.304	3	
5988.406	1h		6132.230	150c	10c	6352.866	2		6618.080	2	
5993.208	10cws		6145.959	3		6354.632	50cw	2c	6625.573	500cws	10cws
5995.204	1		6148.136	1h		6354.860	100	10	6627.896	50c	1c
5996.700	15c	1c	6148.320	1h		6356.732	100	10	6629.071	1	
5997.130	5		6150.522	2		6369.313	4		6646.143	1	
5999.701	3c		6151.460	7h		6380.889	5c		6647.489	4	
6002.900	2h		6154.274	5	1	6382.724	3		6648.383	30	1
6003.496	1		6156.540	1h		6386.778	5h		6649.388	3	
6004.566	3h		6159.510	1h		6388.426	30cw	1	6650.177	2	
6005.099	1h	1h	6162.172	3	2	6389.871	80	6	6656.906	2	
6005.099	1h	1h	6163.603	8	1	6392.408	30c	2c	6661.433	5	
6006.099	2h		6167.399	1		6392.716	3		6662.015	20	
6010.191	20c	2c	6174.723	1h		6408.830	100	8	6664.722	2	
6011.790	4		6182.668	20	2	6412.941	3h		6673.263		1h
6012.104	15cw	1cw	6183.771	10	1	6416.316		2h	6673.656	300c	5c
6013.183	10h		6184.698	100	2	6419.206	2		6684.967	3	
6018.624	8c		6185.908	5		6419.353	2		6687.099	100	1
6020.726	10	1	6187.702	3		6428.104	3		6691.680	3	
6023.500	50	5	6192.665	800	80	6432.774	5		6694.386	4	
6024.046	2h		6193.908	1		6439.080	3	5	6696.684	2	
6024.423	10	1	6195.384	40	2	6442.684	1h		6699.464	2	
6026.085	2		6197.312	1		6445.100	30cw	1cw	6701.142	5	
6028.542	6	1	6198.853	4h		6449.026	4		6707.478	8	
6030.297	5	1	6202.095	1		6449.552	1		6710.202	10	
6032.355	60	6	6202.630	5		6452.922	2		6712.512	4	
6035.193	2h		6202.902	3		6453.357	1		6718.327	1h	
6036.500	1		6204.446	4		6453.925	3		6721.629	3	
6037.506	1		6205.040	2h		6455.896	1000	30	6731.187	50	
6038.504	4h		6213.347	3h		6460.338	5h		6733.847	7	
6039.271	6h		6214.032	30	2	6461.928	600c	20c	6738.066	1	
6041.982	2		6218.473	2		6462.548	1		6742.901	5	
6043.390	1h l		6220.783	4h		6467.134	1		6745.042	6	
6047.358	1		6231.258	1h		6467.570	2h		6747.530	7h	
6047.992	60	6	6232.076	2h		6469.605	20h		6748.838	5	
6051.632	1		6236.621	3c		6470.270	100	6	6749.077	50	
6052.397	1h		6236.865	8	1	6472.663	3h		6753.399	10	
6052.685	1h		6238.625	2		6478.692	4		6754.509	15	
6053.042	1		6239.698	20	1	6479.620	1h		6758.326	20	
6055.056	2hs		6244.178	600cw	50c	6491.676	200cw	5	6761.469	30	1
6056.454	1		6248.971	15	1	6493.570	2c		6764.101	2	
6057.249	20	2	6255.807	5	1	6496.606	10		6764.574	5	
6063.473	30	3	6266.102	2w		6499.312	3		6764.758	8	

TABLE 1. *Spectrum of technetium* – Continued

Wavelength	Intensity		Wavelength	Intensity		Wavelength	Intensity		Wavelength	Intensity	
	Arc	Spark		Arc	Spark		Arc	Spark		Arc	Spark
6767.183	2		6998.653	15		7350.29	1		7782.99	15	
6770.387	1h		7002.37	150		7360.06	10		7793.04	800cw	
6772.562	1h		7004.78	6		7362.46	5w		7795.70	2	
6773.899	4		7006.29	20c		7366.33	40cw		7798.28	60	
6776.580	8		7011.44	2		7395.06	50		7807.20	10	
6781.305	1h		7012.56	3h		7396.80	100		7811.10	2	
6786.003	80	2	7014.10	10c		7402.61	100cw	l	7812.65	4	
6786.452	1		7016.57	100		7405.36	200		7816.74	60	
6786.965	10		7020.02	20		7421.12	8		7817.72	800	
6787.951	2		7022.91	5		7424.01	20		7826.31	10	
6788.665	3		7023.63	6		7427.15	60		7826.91	10	
6795.564	2		7029.72	8		7429.12	1		7848.36	2c	
6798.629	70	2	7032.89	10		7431.65	2		7854.40	10	
6800.793	2		7045.97	3		7434.12	150		7856.38	100	
6805.049	5		7048.47	30		7452.49	600		7858.25	10	
6805.942	15		7054.80	10		7461.59	60		7861.44	200	
6813.340	5		7061.63	7		7470.14	50		7863.22	10	
6813.590	5		7065.59	10		7471.77	20		7871.25	400	ld
6815.382	1		7071.44	30		7494.28	6		7874.76	60cw	
6818.126	10		7076.77	15		7512.28	3		7876.19	2	
6823.962	1		7077.56	2		7516.40	3w		7879.37	8c	
6825.480	3		7083.59	15		7534.95	80		7881.63	5	
6826.146	5		7084.87	1		7540.26	800		7885.98	40cw	
6826.686	5		7086.18	500cwd		7543.39	80		7894.75	2	
6830.007	8		7093.12	60		7545.51	30		7898.56	3	
6833.736	3		7097.24	3		7547.26	5		7905.72	20c	
6837.906	4hw		7109.81	8		7548.44	50		7911.29	4c	
6854.469	3h		7115.78	8		7550.99	10w		7912.19	4c	
6855.365	5		7117.17	4		7554.48	5		7920.37	10h	
6856.902	60	1	7117.39	5		7555.35	2		7949.71	15c	
6860.726	30	1	7123.97	4		7574.02	200		7958.09	5	
6862.371	15		7124.78	30		7577.61	2		7960.65	1	
6866.473	15		7134.82	1		7579.26	500		7963.92	20	
6866.677	25		7140.18	3		7583.93	5		7965.45	70	
6867.526	2		7141.28	200		7584.33	3		7968.30	50	
6871.646	2		7144.67	15		7586.44	5		7981.80	50cw	
6872.303	1		7156.87	20		7587.56	5		7999.73	500	
6873.070	2		7157.62	200c		7588.61	7		8001.88	10	
6874.626	10		7169.73	2w		7593.15	7		8014.78	1	
6876.690	50		7173.04	3		7600.96	3		8017.22	8	
6894.386	20		7177.91	3hw		7605.80	10wd		8021.57	2	
6899.136	3		7179.04	10		7618.42	30		8029.46	8c	
6901.620	2		7191.59	3		7619.79	3		8036.95	2	
6905.117	10		7194.65	2		7624.53	90		8042.47	30	
6907.514	30		7207.02	8		7631.14	1		8045.33	25	
6923.552	1		72[illegible].36	4w		7631.82	4		8057.76	4	
6924.055	15		72[illegible].54	2		7634.53	7		8065.72	3	
6928.934	3h		7226.46	1		7635.08	4		8067.21	2	
6930.264	6		7228.63	4		7649.80	2		8068.79	40c	
6931.795	30		7229.02	4		7652.00	1		8073.66	10c	
6933.236	30		7243.35	3w		7655.82	1		8112.77	1	
6939.892	4		7248.12	4		7657.04	2		8113.54	1	
6941.465	4		7251.68	15		7658.37	30c		8116.91	5	
6944.988	2		7253.09	5		7661.98	1		8119.86	40	
6945.597	15		7256.08	70		7667.64	2		8126.55	200	
6949.320	7h		7264.84	3		7672.72	2		8127.78	15	
6951.282	3		7283.16	15		7676.95	4		8132.65	5h	
6952.625	3		7296.24	5wd		7679.20	2		8134.10	3h	
6958.593	4		7304.60	6		7681.79	15		8142.63	30	
6960.046	2		7305.00	5		7684.45	100		8153.48	8	
6968.151	30		7316.44	15d		7697.37	500		8160.53	10c	
6969.394	4		7320.30	5w		7698.19	80cw		8160.94	15	
6971.534	1		7322.38	100		7701.92	1		8170.55	200	
6974.191	2		7327.32	4h		7719.59	2h		8175.13	1	
6975.067	7		7329.14	80		7722.19	3		8176.18	5	
6980.153	10		7331.89	5		7733.63	5c		8200.05	3	
6985.402	30		7338.20	50		7737.36	50c		8205.27	150	
6988.946	1		7340.13	4		7746.60	10		8206.49	100	
6990.300	40		7341.85	2		7777.22	40		8208.41	2	
6998.037	8		7345.81	4		7779.59	6c		8211.31	150	

TABLE 1. *Spectrum of technetium*—Continued

Wavelength	Intensity		Wavelength	Intensity		Wavelength	Intensity		Wavelength	Intensity	
	Arc	Spark		Arc	Spark		Arc	Spark		Arc	Spark
8225.07	50		8309.16	200		8497.12	5h		8735.34	3	
8231.21	2		8315.50	60		8507.15	1		8737.93	100cw	
8237.08	500cw		8319.07	20cw		8514.70	30		8751.77	20	
8248.96	40		8322.49	5		8519.73	1		8756.86	15	
8250.43	3		8323.35	1		8522.53	20		8757.41	4w	
8254.50	30		8330.37	1		8531.06	100		8766.68	6	
8264.13	10		8346.57	40		8537.65	30		8787.24	3	
8265.64	3		8383.67	40		8543.61	100		8790.90	2	
8269.84	1h		8399.36	1		8595.93	10		8808.81	2h	
8270.83	2h		8404.00	7		8604.09	3		8812.42	5c	
8271.93	2hd		8415.55	50cw		8639.39	4		8820.91	10c	
8276.20	1h		8422.43	5		8645.03	3		8829.82	200cw	
8278.00	1		8445.82	20		8652.76	50		8897.64	2c	
8283.27	1		8462.80	10c		8664.12	6		8901.47	30c	
8285.09	1		8477.91	2		8673.62	8		8909.93	2	
8285.68	2		8481.34	50c		8707.21	100cw		8917.73	8	
8306.22	2		8484.00	40		8719.95	30				
8308.15	200		8492.13	1		8722.68	25				

4. References

[1] C. Perrier and E. Segré, Nature **159,** 24 (1947).
[2] W. F. Meggers and B. F. Scribner, J. Res. NBS **45,** 476 (1950) RP2161.
[3] W. F. Meggers, J. Res. NBS **47,** 7 (1951) RP2221.
[4] P. W. Merrill, Astrophys. J. **116,** 21 (1952).
[5] W. R. Bozman, J. Opt. Soc. Am. **44,** 824(A) (1954).
[6] W. R. Bozman, J. Opt. Soc. Am. **46,** 383(A) (1956).
[7] C. E. Moore, Atomic Energy Levels, Vol **III,** NBS Circ. 467 (Washington, 1958) p. 17.
[8] ibid. p. 19.
[9] K. G. Kessler and R. E. Trees, Phys. Rev. **92,** 303 (1953).

(Paper 71A6–471)

JOURNAL OF RESEARCH of the National Bureau of Standards—A. Physics and Chemistry
Vol. 71A, No. 6, November–December 1967

Lifetimes of Energy Levels in Neutral Iron

C. H. Corliss and J. L. Tech

Institute for Basic Standards, National Bureau of Standards, Washington, D.C. 20234

(August 15, 1967)

Mean radiative lifetimes for 408 energy levels of neutral iron are calculated from the known transition probabilities of 3288 lines of Fe I.

Key Words: Atomic spectra, energy levels, iron, iron—lifetimes in, lifetimes in Fe I, radiative lifetimes, spectroscopy.

1. Introduction

Let us first briefly review the concept of mean radiative lifetime. Even in the absence of de-excitation caused by such external factors as collisional processes or an ambient radiation field, an atom in an excited state E_i will eventually suffer a spontaneous transition to a state of lower energy E_j and will emit a photon of energy in accordance with Bohr's energy relation, $h\nu = E_i - E_j$. The probability per unit time, A_{ij}, associated with this type of spontaneous decay is a physical constant for the particular transition and was first described by Einstein [1917]. For a system of N_i atoms in an excited state of energy E_i, we can write the decay rate as

$$\frac{dN_i}{dt} = -\Sigma_j A_{ij} N_i$$

the summation being extended over all states E_j of energy lower than E_i. By setting $1/\tau_i = \Sigma_j A_{ij}$ and integrating, we obtain

$$N_i = N_i^0 e^{-t/\tau_i}$$

where N_i^0 is the number of atoms in the excited state at time $t = 0$. After a time interval equal to τ_i, therefore, the number of atoms remaining in the excited level will have been reduced by a factor $1/e$. This time interval is defined as the mean radiative lifetime of the given energy state and can be measured by a variety of well-established experimental methods, as described in the well-known work by Mitchell and Zemansky [1934].

As a result of the connection between transition probabilities (A-values) and oscillator strengths (f-values), namely

$$A_{ij} = \frac{6.670}{\lambda^2} \frac{g_j}{g_i} f_{ji}$$

where g is the statistical weight, $2J+1$, of the level, it is possible to calculate the lifetime of an energy level

$$\tau_i = 1/\Sigma_j A_{ij}$$

provided only that the f-values for all possible downward transitions are known. The practicability of this indirect method is seriously limited, however, because for levels other than those yielding simple resonance lines the method requires not only a rather complete knowledge of the energy-level structure of the given atom, but also f-values in quantities not usually available. In the case of iron, however, these requirements no longer are insurmountable.

2. Discussion of the Data

For a variety of reasons, the spectrum of iron has traditionally been the object of considerable attention. The term analysis is sufficiently advanced that it was possible for Corliss and Bozman [1962] to derive f-values for a large number of iron lines by a simple reduction of accurate arc emission intensities. Corliss and Warner [1964, 1966] later extended this work by adding new and fainter lines. For many of the lines, the evaluation of 19 other sets of measurements in

the literature made it possible for them to arrive at a "best" value for *gf*.

In these previous compilations the calculation of *gf*-values included the application of an empirically determined normalization to put the relative *gf*-values on an absolute scale, the normalization being given as a function of upper energy level for the transition. This function, which was essentially a correction to level populations for departures from a Boltzmann distribution in the arc, reduces the value of *gf* calculated from line intensities measured in the free-burning arc below that which would have been calculated with a simple Boltzmann factor. The correction affected all lines that arise from upper energy levels lying above 46,000 cm^{-1}, the magnitude of the correction becoming progressively larger as the value of the upper level increased.

Recent investigations by Huber and Tobey [1967], who measured oscillator strengths for Fe I by use of a shock tube, do not support these excitation corrections in the case of Fe I. A similar conclusion may be drawn from the work of Cowley and Warner [1967], who have decided on the basis of a theoretical model for the arc that a single normalization function is not applicable to all spectra but that the function depends on both the ionization potential and the ionization stage of the atom under study. For iron, their work indicates that no correction at all should be applied. In view of these concordant results, we have recalculated *gf*-values for all lines to which the excitation correction had previously been applied. The recalculated *gf*-values, together with other supporting material for the present calculation of lifetimes, are being published separately in a monograph by Corliss and Tech [1967]. That monograph covers the spectral range from 2084 to 9900 angstroms. As demonstrated there, the best available evidence indicates that the data presented in this new compilation do not now suffer from any serious systematic error.

Using these revised data we have calculated a number of intensity-related quantities, including *A*-values, for over 3000 spectral lines, and from these have been able to derive mean radiative lifetimes for over 400 energy levels of neutral iron. In a work of this kind, it is essential that the spectral range considered be sufficiently extensive to contain most of the lines in which the energy of the system is radiated and that no systematic error affects the data over that spectral range. We feel that the homogeneity and the extensive wavelength coverage of the present material on iron meets these requirements.

It has thus become possible for the first time to present for a complex atom a fairly comprehensive picture of individual lifetimes for a large number of its energy states. Apart from their own intrinsic interest, these lifetimes can additionally serve as the basis for a computation of the radiation damping constant for any line given in the aforementioned monograph. These constants, required in any calculation of line absorption coefficients for pure radiation damping, are given simply by the sum of the reciprocal lifetimes of the upper and lower energy levels involved in the transition. Thus, for a line produced by the transition $E_i \rightarrow E_j$, the damping constant will be given by

$$\Gamma_{ij}=\frac{1}{\tau_i}+\frac{1}{\tau_j}=\Gamma_i+\Gamma_j.$$

Of course, in most actual sources, for example those at high temperatures or high particle densities, other factors affecting the lifetimes come into play in fixing the damping constants and must be included in any such calculation of absorption coefficients or line profiles. However, the above expression for the contribution owing to pure radiation damping is exact and determines the natural width of the line.

3. Results

The calculated lifetimes for energy levels in iron are given in table 1, which is arranged in six columns as follows:

col. 1—electron configuration (with parent term)
col. 2—term designation
col. 3—*J*-value for the individual levels of the term
col. 4—level value rounded to the nearest cm^{-1}
col. 5—lifetime in nanoseconds given in most cases to three significant figures, although not more than two figures are meaningful.
col. 6—the number of downward transitions contributing to the lifetime determination.

TABLE 1. *Radiative lifetimes for energy levels in neutral iron*

Configuration	Term	J	Level cm^{-1}	Lifetime ns	Number of transitions
$3d^6\,4s(a\,^6D)4p$	$z\,^7D°$	5	19351	182000.	2
		4	19562	73700.	2
		3	19757	75600.	4
		2	19913	89200.	2
		1	20020	137000.	2
$3d^6\,4s(a\,^6D)4p$	$z\,^7F°$	6	22650	788000.	1
		5	22846	12000.	2
		4	22997	8370.	3
		3	23111	10500.	2
		2	23193	9540.	5
		1	23245	15700.	4
$3d^6\,4s(a\,^6D)4p$	$z\,^7P°$	4	23711	17200.	3
		3	24181	26900.	4
		2	24507	85100.	3
$3d^6\,4s(a\,^6D)4p$	$z\,^5D°$	4	25900	59.8	6
		3	26140	60.6	6
		2	26340	59.1	6
		1	26479	54.4	5
		0	26550	54.4	2
$3d^6\,4s(a\,^6D)4p$	$z\,^5F°$	5	26875	47.4	4
		4	27167	50.8	6
		3	27395	45.8	6
		2	27560	43.2	6
		1	27666	39.2	5
$3d^6\,4s(a\,^6D)4p$	$z\,^5P°$	3	29056	23.4	7
		2	29469	23.7	9
		1	29733	19.7	6
$3d^6\,4s(a\,^4D)4p$	$z\,^3F°$	4	31307	238.	7
		3	31805	249.	10
		2	32134	370.	7
$3d^6\,4s(a\,^4D)4p$	$z\,^3D°$	3	31323	119.	9
		2	31686	101.	7
		1	31937	98.5	6
$3d^7\,(a\,^4F)4p$	$y\,^5D°$	4	33096	4.38	7
		3	33507	3.33	10
		2	33802	4.13	13
		1	34017	3.04	12
		0	34122	2.58	4
$3d^7\,(a\,^4F)4p$	$y\,^5F°$	5	33695	4.69	5
		4	34040	4.13	10
		3	34329	3.58	9
		2	34547	3.58	8
		1	34692	3.29	6
$3d^6\,4s(a\,^4D)4p$	$z\,^3P°$	2	33947	14.4	14
		1	34363	5.97	12
		0	34556	31.7	4
$3d^7\,(a\,^4F)4p$	$z\,^5G°$	6	34844	6.28	1
		5	34782	5.80	7
		4	35257	5.31	12
		3	35612	4.68	11
		2	35856	4.29	7
$3d^7\,(a\,^4F)4p$	$z\,^3G°$	5	35379	5.35	7
		4	35768	4.80	12
		3	36079	4.92	13
$3d^7\,(a\,^4F)4p$	$y\,^3F°$	4	36686	3.85	12
		3	37163	3.82	13
		2	37521	3.48	11
$3d^6\,4s(a\,^4D)4p$	$y\,^5P°$	3	36767	4.09	10
		2	37158	3.58	9
		1	37410	3.15	8
$3d^7\,(b\,^2F)4s$	$d\,^3F$	2	36941	<4320.	2
$3d^7\,(a\,^4F)4p$	$y\,^3D°$	3	38175	2.92	16
		2	38678	2.43	14
		1	38996	2.09	16
$3d^6\,4s(a\,^4D)4p$	$x\,^5D°$	4	39626	1.64	7
		3	39970	1.35	13
		2	40231	1.23	13
		1	40405	1.00	9
		0	40491	1.03	3
$3d^5\,4s^2\,(a\,^6S)4p$	$y\,^7P°$	2	40052	119.	6
		3	40207	21.8	7
		4	40422	33.1	4
$3d^6\,4s(a\,^4D)4p$	$x\,^5F°$	5	40257	2.65	3
		4	40594	1.81	7
		3	40842	1.49	9
		2	41018	1.28	9
		1	41131	.86	5
$3d^6\,4s(b\,^4P)4p$	$z\,^5S°$	2	40895	8.04	9
$3d^6\,4s(b\,^4P)4p$	$x\,^5P°$	3	42533	7.87	11
		2	42860	4.44	11
		1	43079	10.8	7
$3d^6\,4s(a\,^4H)4p$	$y\,^5G°$	6	42784	5.63	1
		5	42912	5.96	4
		4	43023	7.05	5
		3	43138	4.90	4
		2	43210	4.36	3
$3d^6\,4s(a\,^6D)5s$	$e\,^7D$	5	42816	3.15	7
		4	43163	2.83	10
		3	43435	2.61	10
		2	43634	2.40	8
		1	43764	2.12	6
$3d^6\,4s(a\,^4H)4p$	$z\,^5H°$	6	43321	10.9	1
		5	42992	11.5	5
		4	43109	11.4	5
		3	43326	47.9	5
$3d^6\,4s(b\,^4P)4p$	$w\,^5D°$	4	43500	2.02	8
		3	43923	1.66	10
		2	44184	1.65	14
		1	44411	1.51	13
		0	44459	1.63	3
$3d^6\,4s(b\,^4F)4p$	$w\,^5F°$	5	44244	7.21	4
		4	44023	12.5	8
		3	44166	8.98	9
		2	44285	7.54	8
		1	44378	7.37	4
$3d^6\,4s(b\,^4F)4p$	$v\,^5D°$	4	44415	5.54	6
		3	44551	4.87	6
		2	44664	4.72	10
		1	44761	3.14	5
		0	44827	1.93	2
$3d^7\,(a\,^4P)4p$	$y\,^5S°$	2	44512	1.09	9

277-259 O - 68 - 12

TABLE 1. *Radiative lifetimes for energy levels in neutral iron*—Continued

Configuration	Term	J	Level cm^{-1}	Lifetime ns	Number of transitions
$3d^6\,4s(a\,^6D)5s$	$e\,^5D$	4	44677	4.50	13
		3	45061	4.44	15
		2	45334	3.80	14
		1	45509	3.63	8
		0	45595	3.29	3
$3d^6\,4s(b\,^4P)4p$	$x\,^3D°$	3	45221	2.91	12
		2	45282	2.69	15
		1	45552	2.37	13
$3d^6\,4s(a\,^4H)4p$	$y\,^3G°$	5	45295	8.05	9
		4	45428	8.20	14
		3	45563	18.6	12
$3d^6\,4s(b\,^4F)4p$	$x\,^5G°$	6	45608	9.01	1
		5	45726	5.92	5
		4	45833	3.89	7
		3	45914	4.44	7
		2	45965	3.70	4
$3d^6\,4s(a\,^4H)4p$	$z\,^3I°$	7	45978	22.5	1
		6	46027	28.7	3
		5	46136	34.0	3
$3d^5\,4s^2(a\,^6S)4p$	$w\,^5P°$	3	46137	.28	4
		2	46314	.30	6
		1	46410	.25	8
$3d^6\,4s(b\,^4P)4p$	$z\,^3S°$	1	46601	.51	11
$3d^7\,(a\,^4P)4p$	$y\,^3P°$	0	46673	2.84	5
		1	46902	1.15	13
		2	46727	1.48	10
$3d^7\,(a\,^4P\,)4p$	$u\,^5D°$	4	46721	1.58	15
		3	46745	.37	17
		2	46889	.56	14
		1	47177	.96	12
		0	47172	.63	4
$3d^7\,(a\,^2G)4p$	$x\,^3F°$	4	46889	1.64	14
		3	47093	1.80	17
		2	47197	2.40	14
$3d^6\,4s(a\,^4H)4p$	$z\,^3H°$	6	46982	5.19	7
		5	47008	4.07	14
		4	47107	2.87	16
$3d^7\,(a\,^4F)5s$	$e\,^5F$	5	47006	4.24	9
		4	47378	3.99	17
		3	47756	3.58	19
		2	48037	3.47	16
		1	48221	2.86	12
$3d^7\,(a\,^4P)4p$	$w\,^3D°$	3	47017	1.27	15
		2	47136	1.13	16
		1	47272	1.61	11
$3d^6\,4s(a\,^4G)4p$	$w\,^5G°$	6	47363	5.90	5
		5	47420	3.29	7
		4	47590	5.36	10
		3	47693	< 6.28	8
		2	47831	4.12	7
	1°	2	47420	3.43	13
$3d^7\,(a\,^2G)4p$:	$z\,^1G°$	4	47453	10.5	13
$3d^7\,(a\,^4P)4p$	$y\,^3S°$	1	47556	1.62	13
$3d^6\,4s(a\,^4G)4p$	$v\,^5F°$	5	47606	4.25	6
		4	47930	2.09	13
		3	48123	2.22	11
		2	48239	1.50	17
		1	48351	1.50	7
$3d^6\,4s(b\,^4F)4p$	$x\,^3G°$	3	47834	6.64	12
		4	47812	6.70	15
		5	47835	5.69	10
$3d^7\,(a\,^4F)5s$	$e\,^3F$	4	47961	4.74	19
		3	48532	3.99	20
		2	48928	3.73	9
$3d^7\,(a\,^4P)4p$	$v\,^5P°$	3	47967	.23	6
		2	48163	.68	13
		1	48290	.86	9
	$w\,^3G°$	5	48231	18.8	9
		4	48362	15.7	8
		3	48476	6.14	9
$3d^6\,4s(b\,^4P)4p$	$x\,^3P°$	2	48305	1.33	19
		1	48516	1.46	14
		0	48460	1.41	7
$3d^7\,(a\,^2G)4p$	$z\,^1H°$	5	48383	3.07	12
$3d^7\,(a\,^2H)4p$:	$y\,^1G°$	4	48703	2.55	13
	2°	2	49053	7.21	2
$3d^6\,4s(b\,^4F)4p$	$w\,^3F°$	4	49109	1.49	11
		3	49243	1.45	14
		2	49433	1.26	11
$3d^6\,4s(b\,^4F)4p$	$v\,^3D°$	3	49135	1.72	11
		2	49243	1.57	12
		1	49298	1.55	13
	3°	3	49227	30.9	1
$3d^7\,(a\,^2G)4p$	$y\,^3H°$	6	49434	1.51	7
		5	49604	1.07	9
		4	49727	.80	12
$3d^7\,(a\,^2G)4p$	$v\,^3G°$	5	49461	1.05	12
		4	49628	1.00	16
		3	49851	.86	11
	$z\,^1D°$	2	49477	9.44	10
$3d^6\,4s(a\,^6D)5p$	$x\,^7P°$	3	49805	7.73	1
$3d^7\,(a\,^2D)4p$:	$w\,^3P°$	0	49951	1.09	6
		1	50043	1.29	13
		2	50187	1.50	11
$3d^6\,4s(a\,^6D)4d$	$e\,^7F$	6	50342	0.63	3
		5	50833	.60	9
		4	51192	.55	11
		3	51149	.63	12
		2	51331	.83	10
		1	51208	.50	6
$3d^6\,4s(a\,^6D)4d$	$f\,^7D$	5	50378	.72	4
		4	50808	.54	13
		3	50862	.59	7
		2	50999	.74	13
		1	51048	.65	12

TABLE 1. *Radiative lifetimes for energy levels in neutral iron*—Continued

Configuration	Term	J	Level cm^{-1}	Lifetime ns	Number of transitions
$3d^6\,4s(a\,^6D)4d$	$f\,^5D$	4	50423	.80	14
		3	50534	.75	17
		2	50699	1.17	15
		1	50880	1.25	10
		0	50981	1.00	6
$3d^6\,4s(a\,^6D)4d$	$e\,^7P$	4	50475	.86	8
		3	50611	1.17	13
		2	50861	1.93	9
$3d^6\,4s(a\,^6D)4d$	$e\,^5G$	6	50523	1.96	6
		5	50704	1.30	10
		4	50980	1.81	10
		3	51219	.92	11
		2	51370	1.14	12
$3d^7\,(a\,^2G)4p$:	$z\,^1F°$	3	50587	2.54	11
	$x\,^1G°$	4	50614	3.90	7
$3d^6\,4s(a\,^6D)4d$	$e\,^7G$	7	50652	.74	1
		6	50968	.91	4
		5	51229	.89	9
		4	51335	.79	13
		3	51461	.57	8
		2	51540	.58	6
		1	51567	.61	4
$3d^6\,4s(a\,^6D)5p$	$u\,^5F°$	5	51017	7.44	2
		4	51381	6.09	3
		3	51619	12.3	3
		2	51828	2.14	4
$3d^6\,4s(a\,^4G)4p$:	$x\,^3H°$	6	51023	6.97	7
		5	51069	6.31	12
$3d^6\,4s(a\,^6D)5p$	$t\,^5D°$	4	51077	< 6.28	2
		3	51361	2.73	8
		2	51630	2.75	6
		1	51837	8.01	1
		0	51942	5.08	1
$3d^6\,4s(a\,^6D)4d$	$f\,^5F$	5	51103	1.28	9
		4	51462	1.12	11
		3	51604	2.09	13
		2	51705	2.12	12
		1	51755	3.45	8
$3d^6\,4s(a\,^6D)4d$	$e\,^5S$	2	51149	1.05	8
$3d^6\,4s(a\,^4G)4p$:	$v\,^3F°$	2	51201	2.47	11
		3	51365	3.48	9
		4	51305	2.05	13
$3d^6\,4s(a\,^4D)5s$	$e\,^3D$	3	51294	2.56	19
		2	51740	2.05	19
		1	52040	2.64	10
$3d^6\,4s(a\,^4D)5s$	$g\,^5D$	4	51351	1.50	19
		3	51771	1.57	23
		2	52050	1.91	23
		1	52214	1.52	19
		0	52257	1.48	6
$3d^7\,(a\,^2H)4p$	$u\,^3G°$	5	51374	1.11	11
		4	51668	.80	18
		3	51826	1.10	10
	4°	4	51409	2.79	11
	5°	3	51436	10.3	3
$3d^6\,4s(a\,^6D)4d$	$e\,^7S$	3	51570	.50	11
	6°	5	51630	3.47	8
$3d^6\,4s(a\,^6D)5p$	$u\,^5P°$	3	51692	71.1	1
$3d^7\,(a\,^2P)4p$	$y\,^1D°$	2	51708	1.34	11
	7°	2	51756	6.96	3
	$x\,^1D°$	2	51762	5.07	6
$3d^6\,4s(a\,^6D)4d$	$e\,^5P$	3	51837	2.44	13
		2	52067	2.65	15
		1	52020	2.71	8
$3d^7\,(a\,^2P)4p$	$u\,^3D°$	3	51969	.81	12
		2	52297	.47	11
		1	52512	.38	14
$3d^7\,(a\,^2D)4p$:	$t\,^3D°$	1	52181	1.97	8
		2	52683	1.17	11
		3	52213	1.09	10
$3d^7\,(a\,^2H)4p$	$w\,^3H°$	6	52431	.96	5
		5	52613	.84	6
		4	52769	1.06	7
$3d^7\,(a\,^2H)4p$	$y\,^3I°$	7	52655	1.46	2
		6	52514	1.24	7
		5	52899	1.22	6
$3d^7\,(a\,^2P)4p$	$x\,^3S°$	1	52858	.46	11
$3d^7\,(a\,^2P)4p$:	$v\,^3P°$	2	52916	.61	9
		1	53808	.47	12
	$s\,^3D°$	3	52954	3.94	4
		2	53275	7.87	2
$3d^7\,(a\,^4F)4d$	$g\,^5F$	5	53061	2.95	6
		4	53394	3.72	11
		3	53831	4.21	11
		2	54258	7.36	6
		1	54386	1.84	10
$3d^7\,(a\,^2H)4p$	$z\,^1I°$	6	53094	1.06	4
$3d^7\,(a\,^4F)4d$	$h\,^5D$	4	53155	4.39	6
		3	53546	2.66	11
		2	53967	2.73	8
		1	54132	< 5.26	6
$3d^7\,(a\,^4F)4d$	$f\,^5P$	3	53161	< 4.78	4
		2	53569	2.09	12
		1	53925	2.62	11
$3d^7\,(a\,^4F)4d$	$f\,^5G$	6	53169	4.15	5
		5	53282	1.82	6
		4	53769	2.97	12
		3	54161	2.02	12
		2	54376	3.48	5
$3d^7\,(a\,^2P)4p$	$z\,^1P°$	1	53230	.57	11
$3d^7\,(a\,^4F)4d$	$e\,^5H$	7	53275	4.35	1
		6	53353	3.79	2

TABLE 1. *Radiative lifetimes for energy levels in neutral iron*—Continued

Configuration	Term	J	Level cm^{-1}	Lifetime ns	Number of transitions
		5	53874	3.21	3
		4	54237	3.60	3
		3	54491	3.72	1
	9°	4	53329	3.35	5
$3d^6\,4s(b\,^4D)4p$	$t\,^5P°$	3	53389	9.82	1
		2	54112	1.13	3
		1	54271	1.98	6
	$y\,^1F°$	3	53661	1.94	9
$3d^7\,(a\,^2H)4p$	$y\,^1H°$	5	53722	1.69	2
$3d^7\,(a\,^4F)4d$	$e\,^3G$	5	53739	2.28	12
		4	54067	2.79	9
		3	54379	3.71	3
$3d^7\,(a\,^4F)4d$	$f\,^3D$	3	53748	2.66	12
		2	54067	2.21	14
		1	54449	.99	14
	$x\,^1F°$	3	53763	1.57	10
$3d^6\,4s(a\,^6D)6s$	$g\,^7D$	5	53801	3.90	4
		4	54125	2.23	6
		3	54414		
		2	54612	< 3.98	4
		1	54748	3.30	3
$3d^7\,(a\,^4F)4d$	$e\,^3H$	6	53841	3.51	2
		5	54267	19.6	1
		4	54555	2.90	4
$3d^6\,4s(b\,^4D)4d$:	10°($^5D°$?)	3	53892	1.18	9
$3d^6\,4s(a\,^4G)4p$:	$t\,^3G°$	5	53983	.67	8
		4	54237	.78	11
		3	54600	.67	13
	11°	3	54005	9.69	7
$3d^6\,4s(b\,^4D)4d$:	12°($^3F°$?)	5	54014	1.77	5
	13°	4	54301	2.05	9
$3d^7\,(a\,^4F)4d$	$f\,^3F$	4	54683	3.62	9
		3	55125	2.57	9
		2	55379	2.15	6
	$w\,^1G°$	4	54811	2.94	4
$3d^7\,(a\,^4F)4d$	$e\,^3P$	2	54880	3.85	5
		1	55376	2.47	5
		0	55727	1.08	2
	$v\,^3H°$	4	55446	.88	6
		5	55430	.74	9
		6	55490	.66	5
	$x\,^1H°$	5	55526	1.96	5
$3d^7\,(a\,^2D)4p$:	$w\,^1D°$	2	55754	.17	8
	$w\,^1F°$	3	55791	.74	8
	$s\,^3G°$	5	55907	.74	7
		4	55906	.65	9
		3	56098	1.33	3
$3d^6\,4s(b\,^2H)4p$:	$u\,^3H°$	6	56334	.89	4
		5	56383	.45	7
		4	56423	.46	9
$3d^6\,4s(a\,^6D)5d$	1	5	56428	.91	4
$3d^6\,4s(a\,^6D)5d$	2	4	56452	1.29	5
$3d^7\,(a\,^2D)4p$:	$u\,^3F°$	4	56593	.52	6
		3	56783	.53	6
		2	56859	.44	7
$3d^6\,4s(a\,^6D)5d$	3	4	56843	1.02	5
	$v\,^1G°$	4	56951	.42	5
$3d^6\,4s(b\,^2H)4p$	$x\,^3I°$	7	57028	.65	2
		6	57070	.70	3
		5	57104	.73	3
	$t\,^3F°$	4	57550	.51	5
		3	57641	1.26	8
		2	57709	.44	5
$3d^6\,4s(a\,^4D)4d$	$i\,^5D$	4	57698	.59	7
		3	57814	.56	8
		2	57974	.49	9
$3d^6\,4s(a\,^6D)7s$	$h\,^7D$	5	57897	2.75	2
$3d^6\,4s(a\,^4D)4d$	$g\,^5G$	6	58002	.50	3
		5	58272	1.80	4
		4	58520	2.17	5
		3	58710	< 8.82	2
		2	58825	2.10	3
$3d^6\,4s(a\,^4D)4d$	4	2	58213	.71	7
	$r\,^3G°$	5	59927	.37	1
		4	60172	.13	3
		3	60365	.09	2
	$t\,^3H°$	6	60366	.17	4
		5	60549	.16	4
		4	60758	.18	5
	$q\,^3G°$	3	60807	.32	4
		3	53358	3.88	7
		4	53610	7.73	3
		3	53734	8.45	6
		2	53749	2.88	6
		3	53785	6.62	3
		4	53882	7.13	4
		3	54289	4.58	7
		3	54357	2.30	7
		3	57565	2.48	4
		3	60564	.93	5
		2	62081	1.14	3
Fe II ($a\,^6D_{4\frac{1}{2}}$)	*Limit*		63700		

In pure *LS* coupling the lowest three terms in table 1 would be metastable. This metastability is clearly exhibited in our results for the lifetimes of these levels. Though finite because of slight departures from *LS* coupling, the lifetimes obtained for these levels are nevertheless several orders of magnitude longer than those obtained for the nonmetastable levels. Another point of interest is the marked tendency throughout the table towards equality in the lifetimes of the individual levels of a single term, as expected.

Although the 3300 lines entering into these determinations represent more than three quarters of the classified lines observed in the laboratory, and the strongest ones at that, there are a few cases where the values stated for the lifetimes must be considered as an upper limit. For example, the $d\,^3F_2$ level at 36941 cm^{-1}, which is the lowest even level in our list, must make its strongest downward combinations in the infrared, beyond the range of our list of lines. For a few other levels, lines of significant intensity lacked reliable values of log *gf*. Where known, such values are marked with the "less than" (<) symbol.

Of the 408 lifetimes reported in table 1, three have been measured elsewhere by more direct methods. Karstensen and Richter [1965] measured lifetimes for $z\,^3F_4^\circ$ and $z\,^3D_1^\circ$ by a delayed coincidence method in a hollow cathode and Otten and Wagner [1967] measured the lifetime for $z\,^5F_5^\circ$ by a double resonance experiment in an atomic beam. The lifetimes in nanoseconds are compared below.

Level	This Paper	Elsewhere
$z\,^5F_5^\circ$	47	54
$z\,^3F_4^\circ$	238	220
$z\,^3D_1^\circ$	98	100

A detailed discussion of the accuracy of the absolute scale of the oscillator strengths from which our lifetimes are derived is given in section 5 of Corliss and Warner [1966]. From that discussion we conclude that our general scale of lifetimes may be small by about 30 ± 10 percent. In the comparison of values for the three levels shown in the preceding paragraph our scale is small by about 3 percent, which is well within the uncertainty of the individual values. This latter uncertainty cannot be precisely evaluated, but may be about 50 percent.

The work reported in this paper is based on the work originally conceived by the late W. F. Meggers and brought to fruition in his monumental "Tables of Spectral-Line Intensities," which was published in 1961 as NBS Monograph 32.

The present authors were privileged to be associated for many years with Dr. Meggers. His encouragement and good counsel were always a source of inspiration to us.

4. References

Corliss, C. H. and Bozman, W. R. (1962), Experimental transition probabilities for spectral lines of seventy elements, NBS Mono. **53** (July 20, 1962).

Corliss, C. H. and Tech, J. L. (1967), Oscillator strengths and transition probabilities for 3328 Lines of Fe I. NBS Mono. 108.

Corliss, C. H. and Warner, B. (1964), Ap. J. Suppl. **8,** 395, No. 83.

Corliss, C. H. and Warner, B. (1966), J. Res. NBS **70A** (Phys. and Chem.), No. 4, 325.

Einstein, A. (1917), Phys. Zeits. **18,** 121.

Huber, M. and Tobey, F. L. (1967), Shock Tube Spectroscopy Laboratory, Scientific Report No. 16, Harvard College Observatory. Also Astrophys. J. (in press).

Karstensen, F. and Richter J. (1965), New Method of Measuring Transition Probabilities, AF EOAR Grant 63–110.

Mitchell, A. G. C. and Zemansky, M. W., Resonance Radiation and Excited Atoms, p. 145 (Cambridge University Press, 1934).

Otten, E. W. and Wagner, R. (1967), Physica **33,** 283.

Warner, B. and Cowley, C. R. (1967), J. Quant. Spectrosc. Radiative Transfer **7,** 751.

(Paper 71A6–472)

JOURNAL OF RESEARCH of the National Bureau of Standards—A. Physics and Chemistry
Vol. 71A, No. 6, November–December 1967

Transition Probabilities in Argon I

C. H. Corliss and J. B. Shumaker, Jr.

Institute for Basic Standards, National Bureau of Standards, Washington, D.C. 20234

(April 27, 1967)

In order to derive transition probabilities from intensity measurements of Ar I lines made by Dieke and Crosswhite, new transition probabilities for 26 lines from high levels in Ar I have been measured in a high current constricted arc. With these data, relative level populations of Ar I in Dieke and Crosswhite's micrewave discharge are determined and transition probabilities for 240 lines of Ar I in the wavelength range 4100 to 9800 Å are derived. The new values are compared with other published values.

Key Words: Argon, atomic spectra, transition probabilities.

1. Introduction

In 1954 G. H. Dieke and H. M. Crosswhite published a report [1][1] on the first spectrum of argon that included original intensity measurements made at The Johns Hopkins University spectroscopic laboratory. In the report, line intensities are tabulated for several types of discharges at argon pressures of 3 torr[2] and below. In addition a photoelectric tracing of the argon spectrum produced by a microwave discharge in argon at 6.5 torr pressure is reproduced. The traces and the tabulated values are corrected for changes of response of the apparatus with wavelength by comparison with a calibrated tungsten lamp.

By using absolute transition probabilities for a number of lines whose upper energy levels are well distributed throughout the energy level structure of Ar I, we have been able to determine the relative populations of the energy levels excited in the argon microwave discharge and derive transition probabilities for several hundred lines measured in that discharge.

2. Measurement of Lines from High Levels

The relative populations of Ar I levels in the Dieke-Crosswhite discharge were determined from gA values measured in a consistent set of high-current constricted arc experiments [2, 3]. Since these measurements included no lines with upper levels above 120000 cm^{-1}, more arc measurements of lines from high levels were undertaken to permit calculation of Dieke-Crosswhite relative populations at higher energy levels. These measurements were made side-on in a wall-stabilized arc operating in argon at 1 atm total pressure at currents of 30, 40, and 60 A. In each experiment the continuum intensity at 4315 Å was recorded during the usual side-on traverse of the arc. Then in a view only of the center, i.e., along an arc diameter, the spectral regions of interest were recorded. The intensity measurements were put on an absolute scale by recording the spectrum of a calibrated tungsten strip filament lamp placed in the arc position and with the arc window in the optical path. From an Abel inversion of the 4315 Å continuum intensity the radial temperature distribution in the arc was calculated using equilibrium argon composition tables [2] and the approximate continuum intensity expression [4]:

$$I = 1.63 \times 10^{-28} \gamma \xi(\lambda) N_e^2 / (T^{1/2} \lambda^2 Z_+)$$

erg cm^{-3} sr^{-1} s^{-1} $Å^{-1}$

where N_e is the electron number density, T is the temperature, Z_+ is the ion partition function, and $\gamma = 6$ for argon. In a separate set of experiments carried out by methods previously described [2] a value for the Gaunt factor ξ(4315 Å) of 2.3 was obtained in good agreement with the value 2.4 reported by Morris et al. [5], for similar experiments. From the radial temperature distribution the number of excited atoms along an arc diameter was computed as a function of upper energy level again using the equilibrium composition tables and integrating across the source. The gA values then follow directly by division of the measured line intensities by the number of emitters in the appropriate upper levels.

In order to minimize any systematic errors the 4300 Å Ar I transition probability was measured in each

[1] Figures in brackets indicate the literature references at the end of this paper.
[2] Editor's Note: 1 torr = 1/760 standard atmospheres = 133.322 N/m^2.

experiment along with the other lines and the scale factor required to produce $A_{4300}=4.11\times10^5$ s^{-1}, the value reported in [2], was then applied to all the other gA values. In every case the correction factor was within 11 percent of unity. The resulting arc measured transition probabilities are given in column 4 of table 1. Systematic errors arising, for example, from any inaccuracies involved in the integrations leading to the number of emitters along an arc diameter, or from the failure to record the spectrum exactly at the arc center, or from any uncertainty in ξ(4315 Å) are believed negligible. The fact that the transition probabilities proved to be independent of the arc current suggests that local thermodynamic equilibrium (L.T.E.) among the Ar I levels was maintained even at the low electron densities ($\sim 2\times10^{16}$) of the 30 A arc, although this test is obscured in the high energy lines by the uncertainty in the large line wing corrections that were required.

Quantitative line wing corrections were made wherever practical by assuming dispersion profile line shapes [6] and, in addition, allowing for overlapping with other highly Stark broadened neighboring lines. In the comparatively favorable case of the narrow 4300 Å line of Ar I which lies 30 Å from its nearest neighbor this intensity correction amounts to 3 percent even in the 30 A arc. At the higher currents with $N_e \simeq 10^{17}$ cm^{-3}, 10 to 15 percent of the line intensity lies beneath the apparent "continuum background" established by the intensities at 4285 and 4315 Å. The transition probabilities obtained from the 60 A arc required such large wing corrections (factors of 2) for the lines from high levels that their accuracy is doubtful and we have omitted them from the averages presented in table 1 although their mean deviation from these averages is only 7 percent.

A few transitions are included in which no resolution of the arc experimental intensities into individual lines was possible. In these cases either the upper energy levels were sufficiently close together (e.g., 5738–40 Å, 4334–5 Å) that the total gA value still has meaning, at least for most quasi-thermal sources, or, as in the case of the 6032 Å Ar I line, a reasonably unambiguous resolution could be effected by the use of tentative relative gA values from the Dieke and Crosswhite data. Since the Dieke-Crosswhite relative values in turn depended somewhat upon this resolution the procedure was necessarily an iterative one.

3. Level Populations and Intensities in the Microwave Discharge

With the aid of the transition probabilities of references [2] and [3] and the new measurements in table 1 we can examine the level populations in the discharges studied by Dieke and Crosswhite. We have chosen to work with the 6.5 torr microwave discharge for two reasons: the higher the pressure, the more nearly a discharge tends to exhibit an equilibrium population distribution and, furthermore, since the data are taken from tracings, it is possible to subtract the background radiation. It is evident by comparison with the tracings that their tabulated values have not been so corrected.

TABLE 1. *New values and published values of transition probabilities for* Ar I

Wavelength	Transition	g_u	$A\times10^{-5}$ (sec^{-1})		
			Arc	Avg. from literature	Dieke-Crosswhite disch.
Å					
3607	$1s_4-4p_5$	1	10.9	9.9±1.4	.....
3650	$1s_2-4p_1$	1	10.6	10.0±0.8	.....
3691	$1s_5-4Y$	.....	($gA=1.6$)	.....	.....
4159	$1s_5-3p_6$	5	15.9	15.5±1.4	13.5
4164	$1s_5-3p_7$	3	2.9	2.73±0.23	2.90
4182	$1s_3-3p_2$	3	.....	5.3± .8	5.8
4198	$1s_4-3p_5$	1	.....	31.0± .4	25.9
4201	$1s_5-3p_9$	7	.....	10.0± .5	9.7
4251	$1s_5-3p_{10}$	3	1.2	1.10± .14	1.32
4259	$1s_2-3p_1$	1	43.5	45. ±4.	45.
4266	$1s_4-3p_6$	5	3.6	3.3±0.2	3.6
4272	$1s_4-3p_7$	3	8.7	8.7± .4	9.0
4300	$1s_4-3p_8$	5	4.11	4.1± .2	4.2
4334	$1s_2-3p_3$	5	($gA=44.$)	6.2± .3	7.4
4335	$1s_2-3p_2$	3		4.3± .3	4.4
4345	$1s_2-3p_4$	3	3.5	3.5± .1	4.1
4364	$1s_4-3p_{10}$	3	0.2	.163± .004	0.196
4424	$1s_3-3p_7$	3	.1	.091± .009	.109
4511	$1s_2-3p_5$	1	12.6	12.2±1.1	9.4
4522	$1s_3-3p_{10}$	3	1.0	1.07±0.08	0.95
4589	$1s_2-3p_6$	5	0.04	.....	.047
4596	$1s_2-3p_7$	3	1.2	1.12± .05	1.19
4628	$1s_2-3p_8$	5	0.5	.46± .02	0.49
4702	$1s_2-3p_{10}$	3	1.21	1.19± .02	1.43
5188	$2p_{10}-5s_1''$	5	14.8	.....	15.3
5738	$2p_7-6d_6$	1	($gA=52.2$)	.....	.....
5740	$2p_7-5s_1''''$	5		.....	8.9
5834	$2p_6-5s_1''$	5	6.4	.....	6.7
5860	$2p_{10}-3s_2$	3	3.5	.....	3.7
5912	$2p_{10}-4s_1'$	3	11.7	.....	12.2
6032	$2p_9-5d_1'$	9	24.3	25.6±1.1	22.7
6059	$2p_{10}-4s_1''$	5	5.1	4.9±0.2	5.4

To determine the level populations from the data at hand, we note that the radiant power of a spectrum line emitted by N_u atoms in an excited state u is

$$I=N_u h\nu A_{ul}$$

where A_{ul} is Einstein's transition probability or rate (per second) from an upper state u to a lower state l. Since the number of magnetic sublevels in the upper state is $2J_u+1=g_u$, the actual sublevel population is

$$\frac{N_u}{g_u}=\frac{1}{hc}\cdot\frac{I\lambda}{g_u A_{ul}}.$$

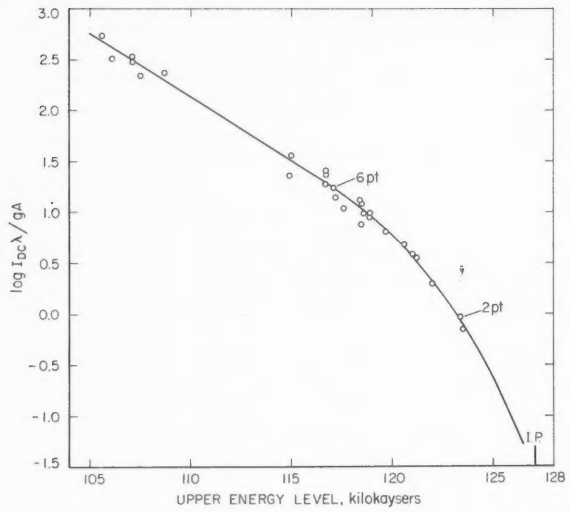

FIGURE 1. *Population distribution among levels of* Ar I *in a 6.5 torr microwave discharge*

In the expectation that the population of levels in the discharge will depend primarily upon the energy of the levels above the ground state we attempt to represent the population distribution among the levels of Ar I by plotting log $I\lambda/gA$ as a function of E, the energy of the upper level. Such a plot for the 6.5 torr microwave discharge in argon is shown in figure 1.

In a plot such as that in figure 1, a straight line would represent a thermal equilibrium population distribution. In this case the population of the lower levels is declining at a rate that would correspond to a temperature of 5000 °K. Above about 117000 cm^{-1} the slope gradually grows steeper. The important aspect of the plot from our standpoint is that, within the range of scatter of the points, it defines a relationship between population and energy level value that is sufficiently regular to be used as an interpolation curve from which transition probabilities can be derived for the lines measured in the microwave discharge.

Before we can be sure that the intensity data are suitable for reduction to transition probabilities, we must find out if there is any self-absorption affecting the stronger lines and we must be sure that the intensity scale is correct as a function of wavelength. In order to detect any self-absorption in the intensity data, we calculated from the transition probabilities of Shumaker and Popenoe [3] unabsorbed relative intensities for the strong $4s-4p$ transitions of Ar I as they would appear in Dieke and Crosswhite's discharge. The appropriate upper level populations are taken from figure 1. A plot of the ratio of Dieke and Crosswhite's intensities to the calculated ones versus the calculated (unabsorbed) intensities in figure 2 shows that about three-quarters of the lines are self-

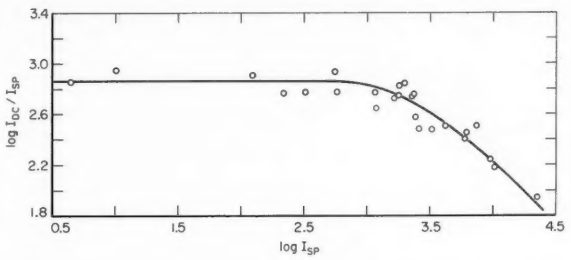

FIGURE 2. *A plot of the ratio of Dieke and Crosswhite's intensities to unabsorbed intensities derived from Shumaker and Popenoe's transition probabilities versus the unabsorbed intensity.*
All but seven of the lines in the $4s-4p$ transition array show some self-absorption.

absorbed in the microwave discharge. All values of log I_{DC} larger than 5.7 are so affected. Only lines fainter than this have been plotted in figure 1.

All of the lines from upper levels higher than the $4p$ levels are much fainter than the self-absorbed lines. The strongest of the high level lines is only 6 percent as intense as the weakest of the self absorbed lines. We have therefore assumed all of the lines from high levels to be free of self-absorption.

In discussing the accuracy of the intensity scale as a function of wavelength, we note, in the first place, that the scale of the tracings below 4000 Å is ten times that of those above 4000 Å. Furthermore, a plot of the ratio of A-values calculated from Dieke and Crosswhite's intensities to those of Malone and Corcoran [7], who measured about 20 A-values in this region, shows that Dieke and Crosswhite's intensity scale, after allowing for this scale shift, gradually declines below 4150 Å, until it is too small by about a factor of 10 at 3550 Å. For this reason we have not reported transition probabilities from their data below 4150 Å. Other comparisons (with data from table 1 and refs [2] and [3]) indicate that for the range 4150 to 8799 Å their relative scale of intensities is correctly calibrated.

4. Results From Dieke and Crosswhite's Measurements

The results of our derivation of transition probabilities as outlined above are presented in tables 2 and 3 for 240 lines of Ar I. The wavelengths and transition designations (in Paschen's notation) are taken from Dieke and Crosswhite's report. The energy levels in kaysers (cm^{-1}) are taken from Moore's Atomic Energy Levels [8]. The statistical weights ($g=2j+1$) are listed next for the lower and upper levels respectively. The values of log I are read from the tracings in the D.-C. report and corrected for the background intensity level. The transition probabilities in the last column are given in units of 10^5 per second. They are calculated with the formula

$$A=\frac{\lambda}{g}\,\text{antilog}\left[\log I_{DC}-\log\frac{I\lambda}{gA}\right]$$

TABLE 2. *Transition probabilities for lines of* Ar I *arising from levels below 124000 kaysers*

Wavelength	Transition	Energy Levels		g_l	g_u	Log I	A
Å		K					10^8/s
4158.591	$1s_5-3p_6$	93143.80	117183.65	5	5	4.43	13.5
4164.179	$1s_5-3p_7$	93143.80	117151.39	5	3	3.55	2.90
4181.883	$1s_3-3p_2$	94553.71	118459.66	1	3	3.66	5.8
4198.317	$1s_4-3p_5$	93750.64	117563.02	3	1	3.96	25.9
4200.674	$1s_5-3p_9$	93143.80	116942.82	5	7	4.48	9.7
4251.185	$1s_5-3p_{10}$	93143.80	116660.05	5	3	3.27	1.32
4259.362	$1s_2-3p_1$	95399.87	118870.98	3	1	4.00	45.
4266.286	$1s_4-3p_6$	93750.64	117183.65	3	5	3.85	3.6
4272.169	$1s_4-3p_7$	93750.64	117151.39	3	3	4.03	9.0
4300.100	$1s_4-3p_8$	93750.64	116999.39	3	5	3.95	4.2
4333.561	$1s_2-3p_3$	95399.87	118469.12	3	5	3.97	7.4
4335.337	$1s_2-3p_2$	95399.87	118459.66	3	3	3.52	4.4
4345.168	$1s_2-3p_4$	95399.87	118407.49	3	3	3.50	4.1
4363.794	$1s_4-3p_{10}$	93750.64	116660.05	3	3	2.43	0.196
4423.996	$1s_3-3p_7$	94553.71	117151.39	1	3	2.10	0.109
4510.733	$1s_2-3p_5$	95399.87	117563.02	3	1	3.49	9.4
4522.323	$1s_3-3p_{10}$	94553.71	116660.05	1	3	3.10	0.95
4589.288	$1s_2-3p_6$	95399.87	117183.65	3	5	1.93	0.047
4596.096	$1s_2-3p_7$	95399.87	117151.39	3	3	3.12	1.19
4628.441	$1s_2-3p_8$	95399.87	116999.39	3	5	2.98	0.49
4702.316	$1s_2-3p_{10}$	95399.87	116660.05	3	3	3.26	1.43
5048.813	$2p_{10}-5s_5$	104102.14	123903.30	3	5	2.10	2.11
5054.178	$2p_{10}-4s_2$	104102.14	123882.30	3	3	1.80	1.72
5056.53	$2p_{10}-4s_3$	104102.14	123873.07	3	1	1.30	1.64
5073.076	$2p_{10}-6d_3$	104102.14	123808.60	3	5	1.61	0.66
5151.394	$2p_{10}-6d_6$	104102.14	123508.96	3	1	2.56	23.5
5162.285	$2p_{10}-6d_5$	104102.14	123468.03	3	3	2.97	19.3
5187.747	$2p_{10}-5s_1''$	104102.14	123372.99	3	5	3.12	15.3
5421.349	$2p_9-5s_5$	105462.80	123903.30	7	5	2.57	6.7
5439.990	$2p_{10}-4s_4$	104102.14	122479.46	3	3	2.20	1.81
5442.237	$2p_9-6d_1'$	105462.80	123832.50	7	7	1.93	1.05
5451.651	$2p_{10}-4s_5$	104102.14	122440.11	3	5	2.91	5.5
5457.416	$2p_8-5s_4$	105617.32	123935.97	5	3	2.13	4.2
5459.648	$2p_9-6d_4$	105462.80	123773.92	7	7	1.20	0.171
5467.163	$2p_8-5s_5$	105617.32	123903.30	5	5	1.70	0.91
5473.455	$2p_8-4s_2$	105617.32	123882.30	5	3	2.01	3.0
5490.122	$2p_8-6d_1''$	105617.32	123826.85	5	5	1.74	0.96
5495.873	$2p_9-6d_4'$	105462.80	123653.24	7	9	3.26	15.3
5506.110	$2p_8-6d_4$	105617.32	123773.92	5	7	2.57	4.0
5524.958	$2p_9-5s_1'''$	105462.80	123557.46	7	7	2.22	1.69
5540.867	$2p_9-5s_1''''$	105462.80	123505.54	7	5	1.36	0.32
5558.702	$2p_{10}-5d_3$	104102.14	122086.97	3	5	3.27	9.7
5572.541	$2p_8-5s_1'''$	105617.32	123557.46	5	7	2.84	7.1
5581.869	$2p_9-5s_1''$	105462.80	123372.99	7	5	1.70	0.63
5588.721	$2p_8-5s_1''''$	105617.32	123505.54	5	5	2.13	1.90
5606.733	$2p_{10}-5d_5$	104102.14	121932.91	3	3	3.34	18.3
5618.010	$2p_7-4s_2$	106087.30	123882.30	3	3	1.85	2.15
5620.917	$2p_7-4s_3$	106087.30	123873.07	3	1	1.66	4.2
5635.575	$2p_7-6d_1''$	106087.30	123826.85	3	5	1.78	1.08
5641.385	$2p_7-6d_3$	106087.30	123808.60	3	5	1.74	0.98
5648.688	$2p_6-5s_4$	106237.60	123935.97	5	3	1.92	2.66
5650.704	$2p_{10}-5d_6$	104102.14	121794.15	3	1	3.09	29.0
5659.128	$2p_6-5s_5$	106237.60	123903.30	5	5	2.10	2.36
5681.898	$2p_6-6d_1'$	106237.60	123832.50	5	7	2.29	2.51
5683.731	$2p_6-6d_1''$	106237.60	123826.85	5	5	1.34	0.39
5700.874	$2p_6-6d_4$	106237.60	123773.92	5	7	1.60	0.45
5739.519	$2p_7-5s_1''''$	106087.30	123505.54	3	5	2.79	8.9
5772.114	$2p_6-5s_1'''$	106237.60	123557.46	5	7	2.35	2.38
5783.541	$2p_7-5s_1''$	106087.30	123372.99	3	5	1.60	0.52
5789.477	$2p_6-5s_1''''$	106237.60	123505.54	5	5	1.51	0.47
5802.080	$2p_6-6d_5$	106237.60	123468.03	5	3	2.34	5.1
5834.264	$2p_6-5s_1''$	106237.60	123372.99	5	5	2.71	6.7
5860.310	$2p_{10}-3s_2$	104102.14	121161.36	3	3	2.81	3.7
5882.624	$2p_{10}-3s_3$	104102.14	121096.67	3	1	2.98	15.8
5888.583	$2p_9-4s_5$	105462.80	122440.11	7	5	3.21	11.8
5912.085	$2p_{10}-4s_1'$	104102.14	121011.98	3	3	3.36	12.2
5916.58	$2p_8-5d_2$	105617.32	122514.29	5	3	1.64	0.54
5927.111	$2p_9-5d_1'$	105462.80	122329.72	7	7	2.06	0.56
5928.812	$2p_8-4s_4$	105617.32	122479.46	5	3	2.95	11.1
5940.86	$2p_5-4s_2$	107054.32	123882.30	1	3	1.70	1.61
5942.668	$2p_8-4s_5$	105617.32	122440.11	5	5	2.51	2.37
5949.260	$2p_4-5s_4$	107131.76	123935.97	3	3	1.68	1.61
5964.479	$2p_5-5s_1'$	107054.32	123815.53	1	3	1.60	1.25
5968.315	$2p_4-4s_2$	107131.76	123882.30	3	3	1.68	1.54
5971.604	$2p_4-4s_3$	107131.76	123873.07	3	1	2.17	14.3
5981.90	$2p_8-5d_1'$	105617.32	122329.72	5	7	1.36	0.113
5987.303	$2p_9-5d_4$	105462.80	122160.22	7	7	2.65	1.96
5994.66	$2p_4-6d_3$	107131.76	123808.60	3	5	1.18	0.288
5999.000	$2p_8-5d_1''$	105617.32	122282.13	5	5	2.43	1.78
6005.725	$2p_3-5s_4$	107289.75	123935.97	5	3	1.71	1.74
6013.679	$2p_9-5d_3$	105462.80	122086.97	7	5	2.36	1.29
6025.152	$2p_3-4s_2$	107289.75	123882.30	5	3	2.48	9.8
6032.127	$2p_9-5d_4'$	105462.80	122036.13	7	9	3.86	22.7
6043.223	$2p_8-5d_4$	105617.32	122160.22	5	7	3.48	13.4
6052.723	$2p_{10}-4s_1''''$	104102.14	120619.08	3	5	2.97	2.53
6059.372	$2p_{10}-4s_1''$	104102.14	120600.94	3	5	3.30	5.4
6064.758	$2p_3-6d_4$	107289.75	123773.92	5	7	1.84	0.83
6081.245	$2p_2-5s_4$	107496.46	123935.97	3	3	1.36	0.79
6085.86	$2p_7-5d_2$	106087.30	122514.29	3	3	0.90	0.102
6090.786	$2p_5-6d_5$	107054.32	123468.03	1	3	2.18	3.7
6098.805	$2p_7-4s_4$	106087.30	122479.46	3	3	2.63	5.5
6101.16	$2p_2-4s_2$	107496.46	123882.30	3	3	1.84	2.28
6113.463	$2p_7-4s_5$	106087.30	122440.11	3	5	1.84	0.52
6119.662	$2p_4-6d_5$	107131.76	123468.03	3	3	1.48	0.74
6121.86	$2p_2-6d_1''$	107496.46	123826.85	3	5	0.90	0.154
6127.416	$2p_8-5d_5$	105617.32	121932.91	5	3	2.18	1.38
6128.726	$2p_2-6d_3$	107496.46	123808.60	3	5	1.70	0.97
6145.441	$2p_3-5s_1'''$	107289.75	123557.46	5	7	2.82	7.5
6155.239	$2p_6-4s_4$	106237.60	122479.46	5	3	2.42	3.4
6165.123	$2p_3-5s_1''''$	107289.75	123505.54	5	5	1.78	0.94
6170.173	$2p_6-4s_5$	106237.60	122440.11	5	5	2.74	4.2
6173.095	$2p_7-5d_1''$	106087.30	122282.13	3	5	2.91	5.5
6179.41	$2p_3-6d_5$	107289.75	123468.03	5	3	1.23	0.42
6212.502	$2p_6-5d_1'$	106237.60	122329.72	5	7	2.89	4.0
6215.942	$2p_3-5s_1''$	107289.75	123372.99	5	5	2.58	5.3
6230.928	$2p_6-5d_1''$	106237.60	122282.13	5	5	1.30	0.137
6243.396	$2p_2-6d_6$	107496.46	123508.96	3	1	1.48	2.37
6248.406	$2p_7-5d_3$	106087.30	122086.97	3	5	2.10	0.74
6278.652	$2p_6-5d_4$	106237.60	122160.22	5	7	1.48	0.139
6296.874	$2p_2-5s_1''$	107496.46	123372.99	3	5	2.76	8.1

TABLE 2. *Transition probabilities for lines of* Ar I *arising from levels below 124000 kaysers*—Continued

Wavelength	Transition	Energy Levels		g_l	g_u	Log I	A
Å		K					10^8/s
6307.656	$2p_6-5d_3$	106237.60	122086.97	5	5	3.00	5.9
6309.14	$2p_7-5d_5$	106087.30	121932.91	3	3	1.84	0.65
6364.894	$2p_7-5d_6$	106087.30	121794.15	3	1	2.23	4.5
6369.576	$2p_6-5d_5$	106237.60	121932.91	5	3	2.66	4.3
6384.716	$2p_{10}-3s_4$	104102.14	119760.22	3	3	3.15	4.6
6416.306	$2p_{10}-3s_5$	104102.14	119683.11	3	5	3.83	12.8
6431.555	$2p_8-3s_2$	105617.32	121161.36	5	3	2.08	0.76
6466.550	$2p_5-5d_2$	107054.32	122514.29	1	3	2.15	1.92
6481.141	$2p_5-4s_4$	107054.32	122479.46	1	3	1.48	0.41
6493.971	$2p_8-4s_1'$	105617.32	121011.98	5	3	1.76	0.34
6513.848	$2p_4-4s_4$	107131.76	122479.46	3	3	1.65	0.61
6538.112	$2p_9-4s_1'''$	105462.80	120753.52	7	7	2.78	1.35
6596.116	$2p_9-4s_1''''$	105462.80	120619.08	7	5	1.95	0.263
6598.684	$2p_3-4s_5$	107289.75	122440.11	5	5	1.70	0.41
6604.854	$2p_8-4s_1'''$	105617.32	120753.52	5	7	3.07	2.66
6632.087	$2p_7-3s_2$	106087.30	121161.36	3	3	1.60	0.260
6656.88	$2p_5-5d_2$	107496.46	122514.29	3	3	1.40	0.35
6660.678	$2p_7-3s_3$	106087.30	121096.67	3	1	2.60	7.5
6664.053	$2p_8-4s_1''''$	105617.32	120619.08	5	5	2.76	1.72
6677.281	$1s_4-2p_1$	93750.64	108722.67	3	1	3.96	3.1
6684.73	$2p_4-5d_3$	107131.76	122086.97	3	5	1.78	0.38
6698.875	$2p_6-3s_2$	106237.60	121161.36	5	3	2.45	1.86
6719.219	$2p_5-5d_5$	107054.32	121932.91	1	3	2.48	3.0
6752.835	$2p_{10}-4d_3$	104102.14	118906.66	3	5	4.28	28.2
6756.10	$2p_3-5d_3$	107289.75	122086.97	5	5	2.68	3.0
6766.613	$2p_6-4s_3$	106237.60	121011.98	5	3	2.87	4.5
6779.933	$2p_1-6d_5$	108722.67	123468.03	1	3	1.70	1.36
6818.291	$2p_4-5d_6$	107131.76	121794.15	3	1	1.84	1.97
6827.253	$2p_3-5d_5$	107289.75	121932.91	5	3	2.34	2.22
6851.884	$2p_2-5d_3$	107496.46	122086.97	3	5	1.90	0.51
6871.290	$2p_{10}-4d_5$	104102.14	118651.45	3	3	4.23	38.
6879.59	$2p_7-4s_1''''$	106087.30	120619.08	3	5	2.86	2.23
6925.010	$2p_2-5d_5$	107496.46	121932.91	3	3	2.28	1.96
6937.666	$2p_{10}-4d_6$	104102.14	118512.17	3	1	3.90	51.
6951.46	$2p_6-4s_1''''$	106237.60	120619.08	5	5	3.06	3.6
6960.23	$2p_6-4s_1''$	106237.60	120600.94	5	5	3.08	3.7
6992.17	$2p_2-5d_6$	107496.46	121794.15	3	1	2.58	11.1
7030.252	$2p_9-3s_5$	105462.80	119683.11	7	5	4.26	38.
7086.70	$2p_5-3s_2$	107054.32	121161.36	1	3	2.40	1.75
7107.478	$2p_8-3s_5$	105617.32	119683.11	5	5	3.38	5.0
7125.825	$2p_4-3s_2$	107131.76	121161.36	3	3	3.06	8.0
7147.041	$1s_5-2p_4$	93143.80	107131.76	5	3	5.00	7.7
7158.83	$2p_4-3s_3$	107131.76	121096.67	3	1	3.11	26.0
7162.57	$2p_5-4s_1'$	107054.32	121011.98	1	3	2.11	0.83
7206.981	$2p_3-3s_2$	107289.75	121161.36	5	3	3.63	30.
7229.93	$2p_8-4d_1''$	105617.32	119444.88	5	5	2.45	0.55
7265.173	$2p_7-4d_2$	106087.30	119847.81	3	3	2.88	2.91
7270.66	$2p_9-4d_4$	105462.80	119212.93	7	7	3.04	1.37
7272.935	$1s_4-2p_2$	93750.64	107496.46	3	3	5.29	17.2
7285.44	$2p_3-4s_1'$	107289.75	121011.98	5	3	2.32	1.37
7311.724	$2p_7-3s_4$	106087.30	119760.22	3	3	3.49	11.4
7316.007	$2p_2-3s_2$	107496.46	121161.36	3	3	3.11	9.3
7350.78	$2p_2-3s_3$	107496.46	121096.67	3	1	2.78	12.5
7353.316	$2p_8-4d_4$	105617.32	119212.93	5	7	4.00	12.6
7372.119	$2p_9-4d_4'$	105462.80	119023.70	7	9	4.45	25.9
7392.97	$2p_6-3s_4$	106237.60	119760.22	5	3	3.38	8.9
7412.334	$2p_4-4s_1''''$	107131.76	120619.08	3	5	3.28	6.3
7425.290	$2p_3-4s_1'''$	107289.75	120753.52	5	7	3.23	4.3
7435.33	$2p_6-3s_5$	106237.60	119683.11	5	5	3.77	12.9
7471.168	$1s_4-2p_4$	93750.64	107131.76	3	3	3.51	0.261
7484.24	$2p_7-4d_1''$	106087.30	119444.88	3	5	3.43	5.4
7510.42	$2p_3-4s_1''$	107289.75	120600.94	5	5	3.18	5.1
7618.33	$2p_2-4s_1''''$	107496.46	120619.08	3	5	2.90	2.71
7628.86	$2p_2-4s_1''$	107496.46	120600.94	3	5	3.15	4.8
7670.04	$2p_8-4d_5$	105617.32	118651.45	5	3	2.90	1.98
7891.078	$2p_6-4d_3$	106237.60	118906.66	5	5	3.48	5.2
8053.305	$2p_6-4d_5'$	106237.60	118651.45	5	3	3.26	4.8
8605.779	$2p_3-4d_3$	107289.75	118906.66	5	5	3.40	4.7
8667.944	$1s_3-2p_7$	94553.71	106087.30	1	3	5.54	24.0
8761.691	$2p_2-4d_3$	107496.46	118906.66	3	5	3.54	6.7
9194.637	$2p_{10}-2s_2$	104102.14	114975.07	3	3	4.42	24.9
9291.58	$2p_{10}-2s_3$	104102.14	114861.67	3	1	4.04	31.
9354.218	$1s_2-2p_7$	95399.87	106087.30	3	3	5.11	9.6
9784.501	$1s_2-2p_8$	95399.87	105617.32	3	5	5.69	20.0

TABLE 3. *Transition probabilities for lines of* Ar I *with upper levels between 124500 and 126300 kaysers*

Wavelength	Transition	Energy Levels		g_l	g_u	Log I	A
Å		K					10^5/s
4544.746	$2p_{10}-11d_5$	104102.14	126099.49	3	3	0.70	0.93
4554.319	$2p_{10}-7s_1''$	104102.14	126053.21	3	5	0.60	0.43
4584.958	$2p_{10}-10d_3$	104102.14	125906.61	3	5	1.30	1.83
4586.610	$2p_{10}-10d_5$	104102.14	125898.64	3	3	1.23	2.60
4587.21	$2p_{10}-10d_6$	104102.14	125895.72	3	1	1.08	5.5
4642.148	$2p_{10}-9d_3$	104102.14	125637.93	3	5	1.18	1.09
4647.493	$2p_{10}-9d_5$	104102.14	125613.12	3	3	1.08	1.41
4746.823	$2p_{10}-8d_6$	104102.14	125163.00	3	1	1.23	4.0
4752.940	$2p_{10}-8d_5$	104102.14	125135.90	3	3	1.83	5.1
4768.675	$2p_{10}-6s_1''$	104102.14	125066.50	3	5	2.00	4.3
4798.742	$2p_9-12d_4'$	105462.80	126295.79	7	9	1.08	0.99
4835.97	$2p_9-11d_4'$	105462.80	126135.42	7	9	1.18	1.05
4836.697	$2p_{10}-6s_5$	104102.14	124771.67	3	5	1.54	1.14
4876.261	$2p_{10}-7d_3$	104102.14	124603.96	3	5	2.20	4.6
4886.29	$2p_9-10d_4'$	105462.80	125922.53	7	9	1.36	1.30
4887.948	$2p_{10}-7d_5$	104102.14	124554.94	3	3	2.18	7.0
4894.691	$2p_{10}-7d_6$	104102.14	124526.75	3	1	1.78	8.3
4921.042	$2p_8-10d_4$	105617.32	125932.59	5	7	0.95	0.66
4937.718	$2p_9-8s_5$	105462.80	125709.45	7	5	0.70	0.41
4956.750	$2p_9-9d_4'$	105462.80	125631.69	7	9	1.68	2.05
4989.948	$2p_8-9d_4$	105617.32	125652.04	5	7	1.32	1.16
5032.026	$2p_9-7s_5$	105462.80	125329.99	7	5	1.20	0.92
5060.079	$2p_9-8d_4'$	105462.80	125219.88	7	9	2.16	4.2
5070.99	$2p_8-7s_4$	105617.32	125331.93	5	3	1.48	2.94
5078.03	$2p_9-6s_1'''$	105462.80	125150.00	7	7	1.18	0.53
5087.085	$2p_8-8d_4$	105617.32	125269.52	5	7	1.68	1.87
5104.74	$2p_7-9d_1''$	106087.30	125671.53	3	5	1.08	0.98
5118.206	$2p_8-6s_1'''$	105617.32	125150.00	5	7	1.93	2.98
5127.802	$2p_8-6s_1''''$	105617.32	125113.48	5	5	1.30	0.94
5177.540	$2p_9-6s_5$	105462.80	124771.67	7	5	1.90	2.79
5210.492	$2p_9-7d_4$	105462.80	124649.55	7	7	1.72	1.21
5214.774	$2p_8-7d_2$	105617.32	124788.39	5	3	1.59	2.34
5216.28	$2p_8-6s_4$	105617.32	124782.77	5	3	1.40	1.51
5221.269	$2p_9-7d_4'$	105462.80	124609.92	7	9	2.76	9.9
5241.091	$2p_8-7d_1''$	105617.32	124692.02	5	5	1.65	1.48
5246.24	$2p_6-8d_1'$	106237.60	125293.65	5	7	1.48	1.24
5249.20	$2p_6-8d_3$	106237.60	125282.97	5	2	1.20	0.89
5252.786	$2p_8-7d_4$	105617.32	124649.55	5	7	2.42	6.1
5254.471	$2p_7-6s_1''''$	106087.30	125113.48	3	5	1.93	4.1
5286.071	$2p_6-6s_1'''$	106237.60	125150.00	5	7	1.48	1.09
5290.00	$2p_6-8d_5$	106237.60	125135.90	5	3	1.08	1.02
5309.517	$2p_6-6s_1''$	106237.60	125066.50	5	5	1.42	1.25
5317.726	$2p_3-7s_1'''$	107289.75	126089.56	5	7	1.51	2.96
5373.495	$2p_7-7d_1''$	106087.30	124692.02	3	5	1.95	3.0
5393.971	$2p_6-6s_5$	106237.60	124771.67	5	5	1.48	1.10
5410.475	$2p_6-7d_1'$	106237.60	124715.16	5	7	1.95	2.28
5492.086	$2p_4-5s_3$	107131.76	125334.75	3	1	1.30	6.3
5528.967	$2p_5-8d_5$	107054.32	125135.90	1	3	1.18	1.34
5534.490	$2p_3-5s_2$	107289.75	125353.31	5	3	1.40	2.7
5552.773	$2p_4-8d_5$	107131.76	125135.90	3	3	1.00	0.89
5597.478	$2p_3-6s_1'''$	107289.75	125150.00	5	7	2.10	4.8
5623.778	$2p_3-6s_1''$	107289.75	125066.50	5	5	1.64	2.19
5637.330	$2p_5-7d_2$	107054.32	124788.39	1	3	1.20	1.03
5639.123	$2p_5-6s_4$	107054.32	124782.77	1	3	1.56	2.37
5712.512	$2p_5-7d_5$	107054.32	124554.94	1	3	1.26	0.98
5773.994	$2p_3-7d_3$	107289.75	124603.96	5	5	1.65	1.52

where λ, g, and log I_{DC} are the values in tables 2 and 3 and log $I\lambda/gA$ was read with a precision of 0.01 (3%) from the ordinate of a large scale plot of figure 1 for each upper energy level.

The 184 lines reported in table 2 arise from levels in Ar I below 124000 cm^{-1} where the population curve in figure 1 is well calibrated. The 56 lines in table 3 arise from levels in the range of energy from 124000 to 126300 cm^{-1} where the population curve is extrapolated. If we assume that the error arising from the extrapolation does not exceed the difference between the curve as shown in figure 1 and a tangent line drawn to the curve at 124000 cm^{-1} then we can say that the uncertainty of the values in table 3 will gradually increase with increasing upper energy level to a maximum value of 60 percent at 126300 cm^{-1}. Extrapolation is always an unsatisfactory procedure but the possibility of obtaining transition probabilities in this energy range is otherwise remote. In the high-current constricted arc experiments, for example, these energy levels are practically obliterated by level broadening and lowering of the ionization potential.

Some measure of the accuracy of the relative values of the Dieke-Crosswhite transition probabilities of table 2 can be obtained by comparison with mean relative values for those lines on which extensive reliable measurements have already been reported. For this purpose the arc transition probabilities reported above as well as those of Drawin [9], Gericke [10], Olsen [11], Popenoe and Shumaker [2], Bott [12], and Wiese [13] together with the shock tube values of Coates and Gaydon [14] and the RF heated plasma values of Malone and Corcoran [7] were averaged together as relative values and adjusted to the absolute transition probability scale used here. These mean values and the standard deviations of the individual determinations are shown in column 5 of table 1. The corresponding Dieke-Crosswhite derived values from table 2 are shown in column 6 for comparison. The deviations of column 6 from the mean values in column 5 average 11 percent compared to an average standard deviation in column 5 of 7 percent.

The status of the absolute transition probabilities is somewhat less satisfactory. The absolute scale used throughout this paper is that which, in arc measurements, is consistent with electron densities determined from the shape of the 4861 Å line of impurity hydrogen [2, 5, 13, 15]. This scale is in agreement with the small

number of direct lifetime measurements in Ar I [16] but leads to the conclusion that Ar II levels in the arc experiments are not in L.T.E. [5]. However, if in such arc experiments complete L.T.E. is assumed and the plasma diagnostics are based upon the Fowler-Milne method [11] or Richter's generalization of it [4] instead of upon electron density measurements, then an absolute scale for Ar I transition probabilities generally about 25 percent lower is indicated. This latter interpretation of the experiments produces Ar I transition probabilities in agreement with shock tube measurements [14] and also Ar II transition probabilities consistent with Ar II lifetime measurements [17, 18]. At the present it is not clear which interpretation, if either, is correct and the possibility that our results are systematically too high must be admitted.

5. References

[1] G. H. Dieke and H. M. Crosswhite, The Spectrum of Ar I, The Johns Hopkins University, Department of Physics, Baltimore (1954).

[2] C. H. Popenoe and J. B. Shumaker, Jr., J. Res. NBS **69A** (Phys. and Chem.) No. 6, 495 (1965).

[3] J. B. Shumaker, Jr. and C. H. Popenoe, J. Opt. Soc. Am. **57,** 8 (1967).

[4] J. Richter, Z. Astrophysik **61,** 57 (1965).

[5] J. C. Morris, R. L. Garrison, and R. U. Krey, private communication and Bull. Am. Phys. Soc. **12,** 811 (1967).

[6] W. L. Wiese and J. B. Shumaker, Jr., J. Opt. Soc. Am. **51,** 937 (1961).

[7] B. S. Malone and W. H. Corcoran, J. Quant. Spectrosc. Radiat. Transfer **6,** 443 (1966).

[8] C. E. Moore, Atomic Energy Levels, NBS Circ. 467, **I,** 211 (1949).

[9] H.-W. Drawin, Z. Phys. **146,** 295 (1956).

[10] W. E. Gericke, Z. Astrophysik **53,** 68 (1961).

[11] H. N. Olsen, J. Quant. Spectrosc. Radiat. Transfer **3,** 59 (1963).

[12] J. F. Bott, Physics of Fluids **9,** 1540 (1966).

[13] W. L. Wiese, Eighth Internat. Conf. Ion. Phenom. in Gases, Vienna (1967).

[14] P. B. Coates and A. G. Gaydon, Proc. Roy. Soc. (London) **A293,** 452 (1966).

[15] B. Wende, Z. Phys. **198,** 1 (1967).

[16] J. Z. Klose, J. Opt. Soc. Am. **57,** 1242 (1967).

[17] W. R. Bennett, Jr., P. J. Kindlmann, and G. N. Mercer, Appl. Opt. Suppl. **2,** 34 (1965).

[18] J. Bakos, J. Szigeti, and L. Varga, Physics Letters **20,** 503 (1966).

(Paper 71A6–473)

JOURNAL OF RESEARCH of the National Bureau of Standards—A. Physics and Chemistry
Vol. 71A, No. 6, November–December 1967

The Fifth Spectrum of Praseodymium

Victor Kaufman and Jack Sugar

Institute for Basic Standards, National Bureau of Standards, Washington, D.C. 20234

(June 5, 1967)

Twelve spectral lines of quadruply-ionized praseodymium in the region 840 to 2250 Å are reported. Five terms ($4f\ ^2F$, $5d\ ^2D$, $6s\ ^2S$, $6p\ ^2P$, and $7s\ ^2S$) and the hyperfine splitting of the $6s\ ^2S$ term are given. A calculation of the principal ionization energy ($Pr^{4+} \rightarrow Pr^{5+}$) leads to a value of 57.44 eV with an estimated uncertainty of ± 0.05 eV.

Key Words: Atomic energy levels, isoelectronic sequence, praseodymiun, rare earth, spectrum, sliding spark discharge lamp.

1. Introduction

The one-electron Cs I isoelectronic sequence has been observed through Ce IV. The present work extends this to Pr V. Several orbital properties such as quantum defect, doublet splitting, and term energy intervals were found to vary in a regular way through the Cs I sequence. These regularities have been used here to verify the analysis of Pr V.

This is the first example of the structure of the fifth spectrum of a rare earth. The regularities in the level structure of the $4f$ period of atoms in lower stages of ionization indicate that Pr V may serve as a guide to the interpretation of the more complex fifth spectra of the rare earths.

2. Experimental Procedure

The spectrum plates obtained in the investigation of Pr IV [1][1] were found to contain several very strong and fairly isolated lines in a 500-A spark exposure which showed no trace in the 50-A exposure. These could only be interpreted as high excitation Pr IV lines, which is unlikely because of their unusual strength, or Pr V lines. Unfortunately, the sliding-spark light source [2] used in this experiment does not suppress Pr IV relative to Pr V. Therefore, the assignment of these lines to Pr V could not be based exclusively on excitation separation.

Exposures were made in the first order of a 35-ft Eagle vacuum spectrograph at a reciprocal dispersion of 0.78 Å/mm. For further corroboration of the lines of the $6s-6p$ and $6p-7s$ transitions and for a better intensity relationship between these lines, exposures were also made in the first order of a 2.2-meter Eagle vacuum spectrograph at a reciprocal dispersion of 2.75 Å/mm. Calculated and measured wavelengths of C, N, O, Si, Ge, and Cu in various stages of ionization were used as standards of calibration [3–7]. The estimated wavelength uncertainty for all lines, except those at 1958 Å, is ± 0.005 Å. Those at 1958 Å have an estimated uncertainty of ± 0.003 Å.

[1] Figures in brackets indicate the literature references at the end of this paper.

3. Wavelengths and Energy Levels

A list of the classified lines of Pr V, including visual estimates of their relative intensities, wavenumbers, and classifications is given in table 1. The list of energy levels of Pr V derived therefrom is given in table 2. It includes the level designation, the observed position with estimated uncertainty, the fine structure splitting where appropriate, and the hyperfine structure splitting for the $6s\ ^2S$ term. The hyperfine splitting of the $7s$ level is calculated to be about 1. cm^{-1}. Because the width of the $6p-7s$ lines is about 2. cm^{-1}, this splitting could not be observed.

The interpretation of the observed spectral lines was begun with an accurate estimate of ζ_{4f} obtained from the $4f6s$ configuration of Pr^{3+}. This value allowed an unambiguous interpretation of the intense $4f-5d$ lines. Using this $5d$ doublet splitting, we were

TABLE 1. *Observed spectral lines of* Pr V

Wavelength (Å)	Intensity	Wavenumber (cm^{-1})	Classification
843.783	200	118 513.9	$4f\ ^2F^o_{5/2}-5d\ ^2D_{5/2}$
865.902	7000	115 486.5	$4f\ ^2F^o_{7/2}-5d\ ^2D_{5/2}$
869.170	5000	115 052.3	$4f\ ^2F^o_{5/2}-5d\ ^2D_{3/2}$
869.662	80	114 987.2	$5d\ ^2D_{3/2}-6p\ ^2P^o_{3/2}$
896.654	1000	111 525.7	$5d\ ^2D_{5/2}-6p\ ^2P^o_{3/2}$
922.290	750	108 425.8	$5d\ ^2D_{3/2}-6p\ ^2P^o_{1/2}$
1234.070	250	81 032.7	$6p\ ^2P^o_{1/2}-7s\ ^2S_{1/2}$
1342.775	250	74 472.6	$6p\ ^2P^o_{3/2}-7s\ ^2S_{1/2}$
1958.088	200	51 070.23	$6s\ ^2S_{1/2}\ (F=2)-6p\ ^2P^o_{3/2}$
1958.201	400	51 067.28	$6s\ ^2S_{1/2}\ (F=3)-6p\ ^2P^o_{3/2}$
2246.759	300	44 508.56	$6s\ ^2S_{1/2}\ (F=2)-6p\ ^2P^o_{1/2}$
2246.900	300	44 505.76	$6s\ ^2S_{1/2}\ (F=3)-6p\ ^2P^o_{1/2}$

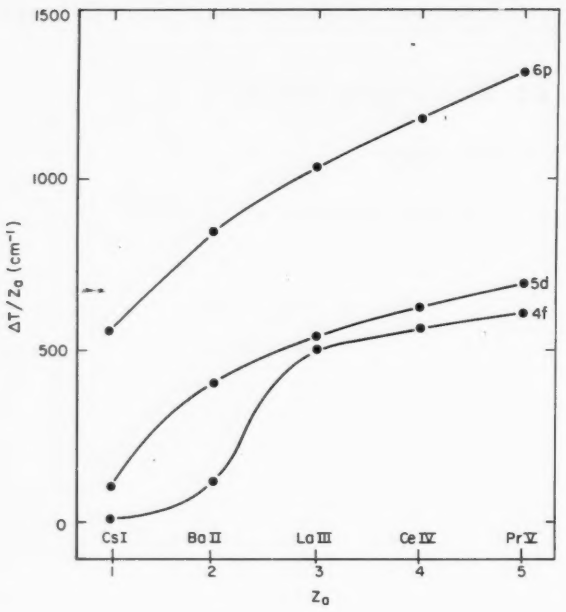

FIGURE 1. *Variation of* $\frac{\Delta T}{Z_a}$ *along the* Cs I *isoelectronic sequence* where ΔT *equals spin-orbit splittings of the* $4f\,^2F$, $5d\,^2D$, *and* $6p\,^2P$ *terms.*

Note the anomalous position of the Ba II $4f\,^2F$ point. References for the plotted values are Cs I: H. Kleiman, J. Opt. Soc. Am. **52**, 441 (1962), Ba II: E. Rasmussen, Zeit. f. Phys. **83**, 404 (1933), La III: see ref. [10], Ce IV: see ref. [8].

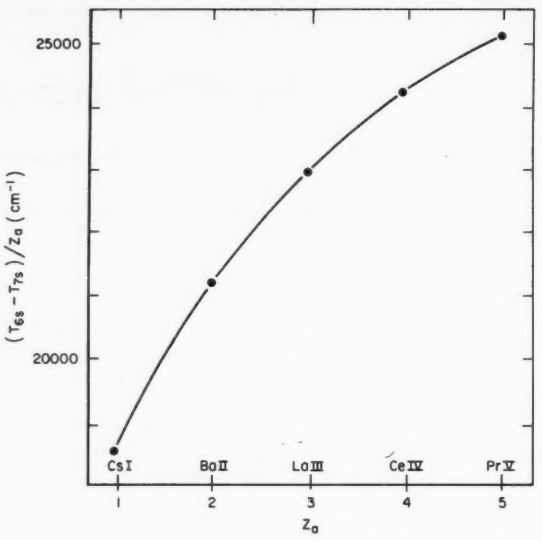

FIGURE 2. *Variation of the ratio of separation of the* 6s ^{2}S *and* 7s ^{2}S *terms to* Z_a *along the isoelectronic sequence.*

For references for the plotted values see the caption of figure 1.

able to interpret the almost-equally prominent $5d-6p$ lines. In figure 1, the ratios of the spin-orbit splitting, ΔT to Z_a are plotted against Z_a in the Cs I isoelectronic sequence. The spin-orbit splittings are those of the $4f\,^2F$, $5d\,^2D$, and $6p\,^2P$ terms, and Z_a is the positive charge on the ion remaining after the removal of the outer electron. The values for Pr V provide smooth extensions of the curves drawn through the previously known points.

The combinations of the $6p\,^2P$ term with the 6s and $7s\,^2S$ levels were not so easily distinguished because of the comparable strength of numerous Pr IV lines in the same spectral region. Evidence for our interpretation of these lines in terms of the behavior of the $6s-7s$ energy interval is presented in figure 2 where the observed value for Pr V follows the smooth variation of this interval in the Cs I isoelectronic sequence.

In figure 3 we present the sequential behavior of the quantum defect, $n-n_a$, for each of the observed terms. These points are interrelated since the quantum defects depend on the positions of the terms relative to the ionization limit which in turn is determined by the positions of the $ns\,^2S$ terms. Therefore the agreement of the Pr V experimental values with the isoelectronic sequence is a strong confirmation of the analysis of this spectrum.

Because of the noticeable departure of the Ba II $4f\,^2F$ points in figures 1 and 3, we have examined the nf series of Ba II in detail and found that the behavior of $(n-n_a)$ versus $1/n_a^2$ is quite different from that of the same series in Cs I and La III. It is our impression that this part of the Ba II analysis bears reexamination.

The value of the spin-orbit parameter, ζ_{4f}, derived from the $4f\,^2F$ term of Pr V equals 865.0 ± 0.3 cm^{-1}. From the $4f6s$ configuration of Pr IV, one finds [1] $\zeta_{4f}=860.8\pm0.2$ cm^{-1}. The difference is due to a slight shielding of the $4f$ electron by the 6s electron in Pr IV. The same order of magnitude of this effect can be found in the comparison of the same configurations of Ce IV and Ce III [8, 9]. However, the value of ζ_{4f} from La III [10] is slightly smaller than that obtained from $4f6s$ of La II [11]. This is probably due to a small perturbation in La II where configurations of the same parity are very close.

TABLE 2. *Energy levels of* Pr V

Designation	J	Energy (cm^{-1})	Uncertainty (cm^{-1})	Splitting (cm^{-1})
$4f\,^2F^\circ$	2½	0.0		3027.4
	3½	3 027.4	±1.0	
$5d\ ^2D$	1½	115 052.3	1.0	3461.5
	2½	118 513.8	1.0	
$6s\ ^2S$ (F = 2)	½	178 969.4	1.5	2.95
(F = 3)	½	178 972.3	1.5	
$6p\ ^2P^\circ$	½	223 478.1	1.5	6561.4
	1½	230 039.5	1.5	
$7s\ ^2S$	½	304 511.5	2.0	

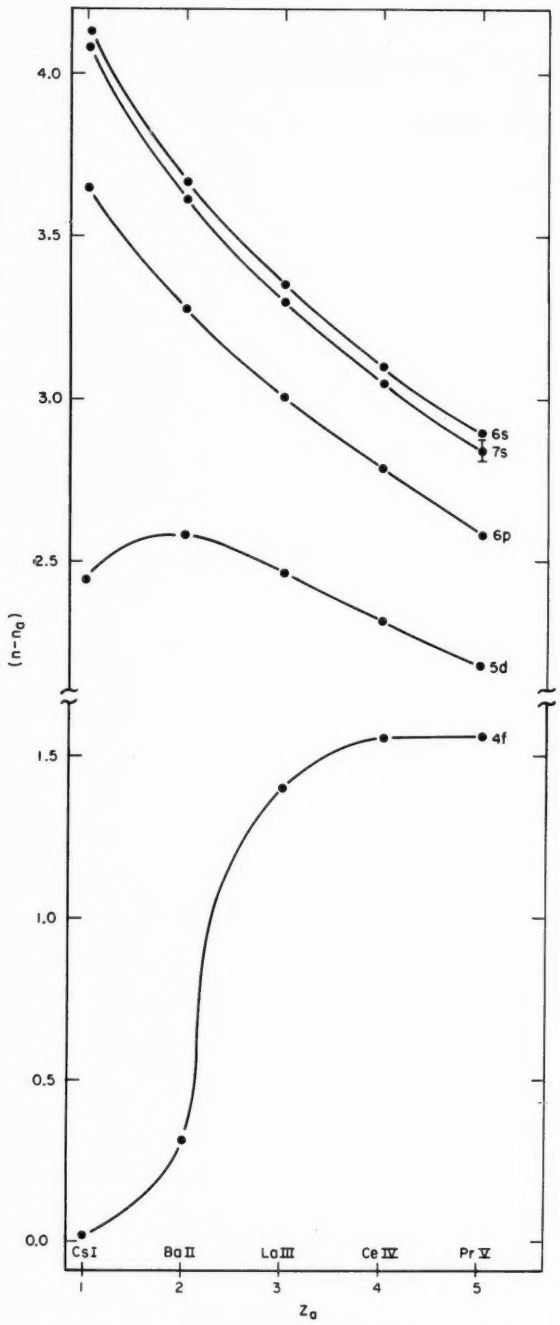

FIGURE 3. *Variation of quantum defect of the center of gravity of the* 4f, 5d, 6p, 6s, *and* 7s *terms along the* Cs I *isoelectronic sequence.*

Note the anomalous position of the Ba II 4*f* point. The error bar on the 7*s* ^{2}S Pr V point indicates the variation in the quantum defect for a change in the ionization energy of ± 400 cm^{-1}. For references for the plotted values see the caption of figure 1.

4. Ionization Potential

In table 2 of the recent paper of Sugar and Reader [12] values of $\Delta n_a = n_a(7s) - n_a(6s)$ derived from several $4f^N ns$ series in the region of the rare earths are given which show that a value of $\Delta n_a = 1.050 \pm 0.005$ cm^{-1} can be used with confidence to compute the ionization energies of rare earths. The values listed are for singly, doubly and triply ionized species. With this value and the experimentally determined value of $\Delta T = E(7s) - E(6s) = 125540.4$ cm^{-1}, the equation

$$\Delta T = \frac{Z_a^2 R}{[n_a(6s)]^2} - \frac{Z_a^2 R}{[n_a(6s) + \Delta n_a]^2},$$

where $Z_a = 5$, was solved for $n_a(6s)$. The corresponding value of $T(6s) = Z_n^2 R/[n_a(6s)]^2$, when added to the level value of 6*s* ^{2}S gives the ionization potential as 463 350 cm^{-1}. On the basis of the uncertainty in the value of Δn_a, the value of the ionization potential is given as 463 400 $\pm$ 400 *cm*$^{-1}$ (57.44 $\pm$ 0.05 eV).

In figure 3, the error bar on the 7*s* ^{2}S, Pr V point shows the extent of the possible change in the position of that point for a change in the ionization energy of the stated uncertainty. This gives us confidence that the value of Δn_a used is valid for highly ionized rare earths.

5. Hyperfine Splitting of the 6*s* Term

The hyperfine splitting of the 6*s* ^{2}S term of 2.95 $\pm$ 0.05 cm^{-1} leads to a value for the splitting factor of the 6*s* electron (a_{6s}) of $0.98_3 \pm 0.01_7$ cm^{-1}. It is of interest to compare this value with $a_{6s} = 0.639 \pm 0.007$ cm^{-1} for Pr III given by Reader and Sugar [13]. Relating these splittings according to the Goudsmit-Fermi-Segré formula, we get

$$\left[\frac{a_{6s}}{Z_a^2} \cdot \frac{n_a^3}{dn_a/dn}\right]_{\text{Pr V}} = \left[\frac{a_{6s}}{Z_a^2} \cdot \frac{n_a^3}{dn_a/dn}\right]_{\text{Pr III}}$$

Insertion of the experimental values in the above equation gives a_{6s} (Pr V) $= 1.03_8 \pm 0.03_2$ cm^{-1}, which leads to an expected splitting of 3.11 ± 0.10 cm^{-1}. This compares quite well with the experimentally determined value listed above.

6. References

[1] J. Sugar, J. Opt. Soc. Am. **55,** 1058 (1965).
[2] J. Sugar, J. Opt. Soc. Am. **53,** 831 (1963).
[3] V. Kaufman and K. L. Andrew, J. Opt. Soc. Am. **52,** 1223 (1962).
[4] V. Kaufman, L. J. Radziemski, Jr., and K. L. Andrew, J. Opt. Soc. Am. **56,** 911 (1966).
[5] V. Kaufman and J. F. Ward, J. Opt. Soc. Am. **56,** 1591 (1966).
[6] V. Kaufman and J. F. Ward, Appl. Opt. **6,** 43 (1967).
[7] B. Edlén, Rep. Prog. Phys. **26,** 181 (1963).
[8] R. J. Lang, Can. J. Res. **14A,** 127 (1936).
[9] N. Spector, J. Opt. Soc. Am. **55,** 492 (1965).
[10] J. Sugar and V. Kaufman, J. Opt. Soc. Am. **55,** 1283 (1965).
[11] H. N. Russell and W. F. Meggers, BS J. Res. **9,** 625 (1932) RP497.
[12] J. Sugar and J. Reader, J. Opt. Soc. Am. **55,** 1286 (1965).
[13] J. Reader and J. Sugar, Phys. Rev. **137,** B784 (1965).

(Paper 71A6-474)

277-259 O - 68 - 13

JOURNAL OF RESEARCH of the National Bureau of Standards—A. Physics and Chemistry
Vol. 71A, No. 6, November–December 1967

Fundamental Energy Levels of Neutral Promethium (Pm I)*

Joseph Reader and Sumner P. Davis**

Institute for Basic Standards, National Bureau of Standards, Washington, D.C. 20234

(August 21, 1967)

The spectrum of atomic promethium has been observed with a variety of light sources and spectrographs. The Zeeman effect has also been recorded. Analysis of the spectrum shows that the ground configuration of the neutral promethium atom is $4f^5 6s^2$. The relative positions (in cm^{-1}) of the low levels of this configuration are:

$^6H^\circ_{5/2}$	0.00	$^6H^\circ_{13/2}$	3919.03	$^6F^\circ_{5/2}$	5872.84
$^6H^\circ_{7/2}$	803.82	$^6H^\circ_{15/2}$	5089.79	$^6F^\circ_{7/2}$	6562.86
$^6H^\circ_{9/2}$	1748.78	$^6F^\circ_{1/2}$	5249.48	$^6F^\circ_{9/2}$	7497.99
$^6H^\circ_{11/2}$	2797.10	$^6F^\circ_{3/2}$	5460.50	$^6F^\circ_{11/2}$	8609.21

This group represents all levels of $4f^5 6s^2$ expected below 14,000 cm^{-1}. From these results the following values of interaction parameters and their estimated uncertainties have been inferred:

$$\zeta_{4f} = 925 \pm 20 \text{ cm}^{-1} \qquad E^3 = 510 \pm 20 \text{ cm}^{-1}$$

Data on 209 upper levels of even parity and 714 classified lines are given.

Key Words: Atomic spectroscopy, electronic energy levels, neutral atom, promethium, rare earth.

1. Introduction

In this paper we present the first results of our investigation to determine the electronic structure of neutral promethium.

Promethium was the last lanthanon element to be discovered. Since the early 1900's it was known that an element lying between neodymium and samarium with atomic number 61 remained to be discovered. A large number of attempts were made to find this element in nature without success. Two false claims of discovery resulted in the early names of illinium and florentium for element 61. The long sought-for element was finally identified in 1947, when Marinsky, Glendenin, and Coryell made a chemical separation of a new element from among the fission products of uranium. They chose the name *promethium* for element 61 ". . . after Prometheus, the Titan in Greek mythology who stole fire from heaven for the use of mankind." This name was chosen not only to symbolize the dramatic way in which the element could be produced in quantity as a result of man's harnessing of the energy of nuclear fission, but also to ". . . warn man of the impending danger of punishment by the vulture of war," [1].[1]

The first extensive work on the spectrum of Pm was carried out at the National Bureau of Standards by Meggers, Scribner, and Bozman [2], who published a list of 2249 Pm lines excited in arcs and sparks. Their attempts to separate the lines according to ionization state and to find spectral regularities were not successful. Their paper gives many of the details of the history of the discovery of Pm and of earlier spectroscopic studies.

Promethium is an entirely artificial element. All of its isotopes are radioactive, and none has ever been found in nature. In the several investigations of the promethium spectrum to date, including the present one, the samples have consisted of monoisotopic Pm^{147}. This is the only readily available form of Pm. It is produced in nuclear reactors as 2.6 percent of the fission products of uranium. Pm^{147} decays by β^- emission (0.22 MeV) into Sm^{147} with a half-life of 2.6 years.

The original paper of Meggers, Scribner, and Bozman suggested the existence of appreciable hyperfine structure in a number of Pm^{147} spectrum lines. This hfs was investigated by Klinkenberg and Tomkins [3] with a 9-meter grating spectrograph and later by Reader and Davis [4, 5] with Fabry-Perot interferometers. As a result of these investigations and others by the methods of paramagnetic resonance [6] and atomic beam resonance [7], it is known that the Pm^{147} nucleus has a spin $I = 7/2$, a magnetic dipole moment $\mu_I = 2.6$ nm, and an electric quadrupole moment

*Part of this work was supported by a grant from the National Science Foundation and an optical research equipment grant from the Advanced Research Projects Agency to one of the authors (SPD).

**University of California, Berkeley 94720.

[1] Figures in brackets indicate literature references at the end of this paper.

$Q \sim 0.7$ barn. These nuclear moments cause many Pm lines to appear with very broad and complex hyperfine structure which impedes attempts to describe the spectrum.

The ionization energy of the neutral promethium atom has been estimated [8] by an interpolation method to be 5.55 ± 0.02 eV.

2. Experimental Procedure

2.1. Light Sources

The construction of light sources was undertaken with the greatest care, because Pm, being radioactive, cannot be handled in the ordinary way. The first light source was a cooled hollow cathode, made for the investigation of hyperfine structure. Its use was essential for that work [4], but it was not used extensively in the present investigation.

The more useful sources were electrodeless discharge tubes, constructed especially for us by Earl Worden at the Lawrence Radiation Laboratory, Livermore. The promethium was obtained from Oak Ridge National Laboratory, and purified either there or at the Lawrence Radiation Laboratory, Berkeley. A spectrographic analysis was made prior to its use. A typical tube was constructed of a section of fused silica tubing 2 cm long with 7 mm o.d. and 5 mm i.d., containing 200 μg of PmI_3. A long handle was attached. No filling gas was admitted, since an initial heating of the tube released enough iodine to make subsequent starting of the discharge relatively easy.

Altogether, six of these tubes were used. Each tube was operated inside a microwave cavity, supplied with rf power by a magnetron at a frequency of 2450 MHz. The temperature of the tube (and hence intensity of the spectrum) was regulated by adjustment of power to the cavity and the amount of air-cooling. During operation, the discharge was a brilliant blue color.

2.2. Spectrographs

Our experimental investigation of the spectrum of promethium has extended over several years, and has included the taking of hundreds of spectrograms on several instruments, under many different conditions. As we gained experience and familiarity with the spectrum, each set of spectrograms was taken to provide specific information.

The 6.4-meter concave grating at Berkeley was used for preliminary testing of the light sources and identification of spectrum lines. The instrument has a plate factor of 1.25 Å/mm at 5000 Å in the first order.

The 3-meter Czerny-Turner plane-grating spectrograph at Berkeley was used for accurate wavelength measurements. This instrument has a grating of width 12.5 cm, ruled with 300 grooves/mm. It is used at angles of incidence and diffraction of approximately 64 deg. At 5000 Å the instrument is used in the 12th order, and the plate factor is 0.36 Å/mm.

A 3.4-meter Ebert plane-grating spectrograph at the Lawrence Radiation Laboratory, Berkeley, was used for some of the Zeeman spectrograms. The angles of use, orders, and plate factor of this instrument are about the same as for the 3-meter Czerny-Turner spectrograph just described.

The 9-meter concave grating spectrograph at the Argonne National Laboratory [9, 10] was used for the early spectrograms taken for wavelength measurements, temperature classification, and Zeeman effects. Spectrum lines were observed in orders as high as the eighth, although we generally confined our measurements to the third and fourth, in order to avoid overlapping orders. At these lower orders, overlapping could be prevented through the use of filters. The plate factor is about 0.45 Å/mm at 4000 Å in the fourth order.

2.3. Exposures

Three different magnets were used for the Zeeman spectrograms. Most of them were taken at Argonne, by using an electromagnet with iron pole-pieces, producing a field of 24,000 G. The discharge tube was excited in the cavity placed between the poles, perpendicular to the field.

The electromagnet used at the Radiation Laboratory produced a field of 29,000 G. A second magnet used there was a superconducting solenoid [11] operated at a field of 41,000 G. In this case, the source was operated in the cavity, but alined parallel to the magnetic field. A more stable operation of the discharge resulted with this orientation. A small mirror placed inside the solenoid permitted observation of the light emitted in a direction perpendicular to the field.

2.4. Exposures

The exposures made at Argonne were taken on 5×45 cm plates, with nine separate tracks on each plate. Thorium standard lines were placed on the top and bottom, with seven promethium exposures in-between. Each Pm exposure was taken at a different lamp temperature to help separate the spectra [12]. The intensities differed by as much as a factor of 80 from the weakest to the strongest exposures. These plates proved to be very valuable for spectrum separation, but the presence of small unexplained shifts made them less useful for absolute wavelength measurements. Since the wavelengths of most of the classified lines given in this paper are based on these exposures, it is possible that the present wavelengths may eventually have to be revised by a few thousandths of an angstrom. The Zeeman exposures included pi, sigma, and no-field lines. The field was calibrated by means of patterns belonging to several lines of Ca, Ag, and Cu which appeared on the plates.

The spectrograms taken at Berkeley for wavelength measurements were made on 10×25 cm plates, with the thorium and promethium lines overlapping, to eliminate any errors of measurement. A samarium spectrum was also included on these plates to identify impurity lines due to small amounts of Sm formed by the decay of Pm. Overlapping grating orders were

TABLE 1. *Theoretical predictions for the low-lying levels of the* $4f^5 6s^2$ *configuration of* Pm I.[a]

Level	Calculated energy (cm^{-1})	Interval (cm^{-1})	Calculated g-value	Percentage composition
$^6H^\circ_{5/2}$	0		0.297	96% ^6H
		816		
$^6H^\circ_{7/2}$	816		0.829	97% ^6H
		953		
$^6H^\circ_{9/2}$	1769		1.071	98% ^6H
		1046		
$^6H^\circ_{11/2}$	2815		1.201	99% ^6H
		1109		
$^6H^\circ_{13/2}$	3924		1.278	99% ^6H
		1146		
$^6H^\circ_{15/2}$	5070		1.327	95% ^6H
$^6F^\circ_{1/2}$	4915		−0.649	98% ^6F
		182		
$^6F^\circ_{3/2}$	5097		1.057	
		381		
$^6F^\circ_{5/2}$	5478		1.303	
		675		
$^6F^\circ_{7/2}$	6153		1.389	
		924		
$^6F^\circ_{9/2}$	7077		1.429	
		1094		
$^6F^\circ_{11/2}$	8171		1.451	

[a] J. G. Conway and B. C. Wybourne, Phys. Rev. **130**, 2325 (1963).

separated by use of an external prism predisperser [13], which prevented light from the unwanted orders from entering the spectrograph. Each grating order was photographed separately.

Eastman Kodak spectroscopic plates were used for all exposures, processed in the recommended manner. Types 103a–O, 103a–F, 103–O, 103–F, and I–N were utilized. All but the first two were prefogged by exposures to weak light, prior to loading in the spectrograph.

2.5. Measurements

The plates were measured on two semiautomatic scanning comparators, one at the University of California and one at the National Bureau of Standards. Wavelengths for the thorium standards were taken from the work of Meggers and Stanley [14]. The estimated uncertainty of the wavelength measurements is about ±0.005 Å. At the present time some of our plates from Argonne and most of the plane-grating plates remain to be measured. When these measurements are complete, we expect to provide a full description of the Pm spectrum.

3. Analysis

In the neutral rare earths the ground configurations are generally of the type $4f^N 6s^2$ or $4f^{N-1}5d6s^2$. Since the ground configurations in Nd I and Sm I are $4f^4 6s^2$ and $4f^6 6s^2$, respectively, it was expected that the ground configuration in neutral Pm would be $4f^5 6s^2$. The lowest level of $4f^4 5d6s^2$ was not expected to be less than 10,000 cm^{-1} above the lowest level of $4f^5 6s^2$. The levels of $4f^5 5d6s$ were expected to start at about 8500 cm^{-1} above the lowest level of $4f^5 6s^2$. Prior to out beginning the Pm I analysis, Conway and Wybourne [15] had published theoretical predictions for the relative energies and g-values of the low levels of $4f^5 6s^2$ by using hydrogenic ratios for the Slater parameters and interpolating values of ζ/F_2. These predictions proved to be very useful to us in carrying out the analysis. Their results for Pm I are summarized in table 1.

The first part of the analysis was carried out through the use of the Zeeman data. A large number of self-reversed lines showed resolved patterns involving levels having $J = 5/2$ and $7/2$ and g-values of about 0.30 and 0.83, respectively. It was clear that these lines were transitions to the $4f^5 6s^2\ ^6H^\circ_{5/2}$ and $^6H^\circ_{7/2}$ levels. After a certain amount of trial and error in searching for repeating differences involving these lines, the $^6H^\circ_{5/2} - {}^6H^\circ_{7/2}$ interval was found to be 803.82 cm^{-1}. About 15 upper even levels were established in this process. The good agreement between this result and the prediction of Conway and Wybourne showed that the predictions would be useful in extending the analysis.

By continuing to use the Zeeman data and by using an electronic computer to search for constant differences between groups of strong lines, two sets of classified lines were built up. One group represented transitions to the $4f^5 6s^2\ ^6H^\circ_{5/2-13/2}$ group of levels; the other represented transitions to the $4f^5 6s^2\ ^6F^\circ_{1/2-7/2}$ levels. However the connection between these two groups was not known. After a considerable amount of searching for this connection, a few weak, resolved

TABLE 2. *Low levels of the* $4f^5 6s^2$ *configuration of* Pm I

Level	Energy (cm^{-1})	Interval (cm^{-1})	g-value
$^6H^\circ_{5/2}$	0.00		0.305
		803.82	
$^6H^\circ_{7/2}$	803.82		0.831
		944.96	
$^6H^\circ_{9/2}$	1748.78		1.079
		1048.32	
$^6H^\circ_{11/2}$	2797.10		1.205
		1121.93	
$^6H^\circ_{13/2}$	3919.03		1.307
		1170.76	
$^6H^\circ_{15/2}$	5089.79		1.33
$^6F^\circ_{1/2}$	5249.48		−0.68
		211.02	
$^6F^\circ_{3/2}$	5460.50		1.051
		412.34	
$^6F^\circ_{5/2}$	5872.84		1.293
		690.02	
$^6F^\circ_{7/2}$	6562.86		1.385
		935.13	
$^6F^\circ_{9/2}$	7497.99		1.440
		1111.22	
$^6F^\circ_{11/2}$	8609.21		1.458

Zeeman patterns were found in the ultraviolet which proved to be transitions from upper levels known from combinations with $^6F^\circ$ levels down to the low $^6H^\circ$ levels. This established the energies of the $^6F^\circ$ levels relative to the ground state. The $^6H^\circ_{15/2}$, $^6F^\circ_{9/2}$, and $^6F^\circ_{11/2}$ levels were later established, thus bringing our knowledge of the low levels to its present state. According to a recent diagonalization by Conway [16] this group represents all levels of $4f^5 6s^2$ expected below 14000 cm^{-1}.

The results are given in tables 2, 3, and 4. Table 2 gives the energies and g-values of the odd levels. Table 3 gives the energies, J-values and g-values for the even levels. The classified lines are given in table 4. The estimated uncertainty in the values of the low levels given in table 2 is ± 0.01 cm^{-1}. The estimated uncertainty in the values of the high levels given in table 3 is about ± 0.03 cm^{-1}.

4. Discussion

The total number of self-reversed lines in Pm I is 122. Of these 120 have been classified as transitions to $4f^5 6s^2$. This makes it certain that the ground configuration of Pm I is $4f^5 6s^2$.

The eigenvectors given by Conway and Wybourne as a result of their diagonalization of $4f^5$ show the $^6H^\circ$ and $^6F^\circ$ terms to be nearly pure in LS coupling. We therefore would have expected a somewhat regular variation in intensity of the lines making transitions from a single upper level to several lower levels. However, according to our observations this is not the case. Figure 1 gives some of the more striking examples of the irregular intensities. Of special note are the lines from 26725.52(3/2). In this case the transition to $^6F^\circ_{3/2}$ is just barely visible on the plates. The complete absence of the line from 28186.31(7/2) to $^6H^\circ_{7/2}$ is also very striking. A similar set of puzzling intensities has been observed by Shenstone [17] in the $3d^6 4s - 4p$ transitions of Co III. Here the anomalous intensities were found in groups of lines connecting terms of different multiplicity. In this connection Shenstone noted "Especially difficult to understand is the not uncommon habit of intersystem combinations of missing the central of three levels of successive J." Although this phenomenon has not yet been investigated theoretically, it is clear that it stems from the lack of pure LS coupling in the upper configurations. It is likely that a theoretical study of the transition probabilities for the $3d^6 4s - 3d^6 4p$ array in Co III would shed more light on this problem.

ODD / EVEN	$^6H^\circ$ 5/2	7/2	9/2	11/2	13/2	15/2	$^6F^\circ$ 1/2	3/2	5/2	7/2	9/2
21 348.22 (7/2)	700	100	400								
22 294.96 (9/2)		x	500	400							
26 181.98 (13/2)				3	300	200					
26 725.52 (3/2)	300						500	1	50		
28 169.71 (7/2)	x	300	100						x	x	x
28 186.31 (7/2)	200	x	200						x	500	50
29 002.94 (3/2)	x						35	8	150		

FIGURE 1. *Anomalous intensities in* Pm I.
No observed transition = X.

No real effort has been made yet to understand the origin of the known upper levels in Pm I. However we note the following points. There are only two configurations which can make transitions to $4f^5 6s^2$ with appreciable intensity, namely $4f^5 6s6p$ and $4f^4 5d6s^2$. For the $4f^5 6s6p$ configuration, the strongest transitions to the $4f^5 6s^2$ $^6H^\circ$ and $^6F^\circ$ levels will originate from levels of the type $4f^5(^6H)6s6p$ and $4f^5(^6F)6s6p$. If we consider the levels of the type $4f^5(^6H)6s6p(J=5/2)$, we would expect them to fall into two groups: six of the type $4f^5(^6H)+6s6p(^3P)$ and two of the type $4f^5(^6H)+6s6p(^1P)$. This type of coupling (first described by Shenstone [18] in the case of the $3d^9 4s4p$ configuration of Cu I) will hold approximately here because the parameter which determines the $^1P - ^3P$ splitting, $G_1(sp)$, is expected by interpolation from other rare earths to be about 2640 cm^{-1}, whereas ζ_p and ζ_f are only about 1000 cm^{-1}. The f-s and f-p interactions are much smaller (see Smith and Wybourne's treatment of the $4f^7(^8S)6s6p$ configuration in Eu I [19]) and for our purpose may be neglected. If one interpolates a value for the $4f^5(^6H)6s^2 - 4f^5(^6H)6s6p$ energy difference and uses the above parameters to estimate the level positions, one finds that the six ^3P type levels with $J=5/2$ will lie in the region 14000–16000 cm^{-1} and the two ^1P type levels with $J=5/2$ will lie at about 20000–21000 cm^{-1} [20]. Of the 27 observed upper levels with $J=5/2$, 22 make strong transitions to the ^6H group of lower levels. These 22 levels are distributed as follows: 14 between 20250 and 23550 cm^{-1}, 8 between 26600 and 28350 cm^{-1}. Thus of the observed levels with $J=5/2$, only 2 would be expected to belong to $4f^5(^6H)6s6p$. It should also be noted that none of the lines classified so far in Pm I shows the appreciable hyperfine structure which would be expected if one of the configurations contained a single 6s electron. Judd [21] has shown that it is possible for lines from certain levels of $4f^N 6s6p$ configurations to $4f^N 6s^2$ to show no hyperfine structure. However, there are too many levels here whose transitions show no hfs to believe that the theory is applicable here. The absence of hfs in these lines more likely is evidence of a closed 6s shell in both upper and lower configurations. In this case the hyperfine structures due to the 4f electron in the upper and lower levels have the same sign and about the same magnitude, so that the observed line shows no resolved structure. For these reasons we believe that most of the known upper levels belong to the $4f^4 5d6s^2$ configuration.

Comparison of the observed positions of the $4f^5 6s^2$ $^6H^\circ$ and $^6F^\circ$ levels with the calculations of Conway and Wybourne shows that their predictions for the intervals within each term are very good, generally within ± 30 cm^{-1} of the observed levels. However, the predicted positions of the $^6F^\circ$ levels are too low

by nearly 7 percent in every case. This discrepancy results from the fact that the calculated intervals within the individual terms are very sensitive to the value of the spin-orbit parameter, but rather insensitive to the electrostatic parameters. On the other hand the separation between the barycenters of terms is governed primarily by the electrostatic parameters. At the time of Conway and Wybourne's work there was no neutral rare earth with more than one known term of $4f^N6s^2$. Therefore, information about the electrostatic parameters could be inferred from the known levels only through second order effects. Thus, a difference of only 7 percent between the predicted and observed $^6H°-{}^6F°$ separation in Pm I can be considered to be fairly good agreement.

It is not possible to obtain reliable values for the electrostatic parameters E^1, E^2, and E^3 from the known levels, because only one term separation is available. However, we note that since the $^6H°$ and $^6F°$ terms are nearly pure in LS coupling, to a first approximation the energy difference between the $^6H°$ and $^6F°$ barycenters $\Delta E(^6F, {}^6H)$ will be equal to $9E^3$ [22]. If we include the Trees $\alpha L(L+1)$ correction [23], to a very good first approximation we then have:

$$\Delta E(^6F, {}^6H) = 9E^3 - 18\alpha.$$

If we use the known positions of the $^6F°$ and $^6H°$ levels to determine $\Delta E(^6F, {}^6H)$, we find $\Delta E(^6F, {}^6H) = 4167.92$ cm^{-1}. If we set $\alpha = 30$ cm^{-1} as indicated by the theoretical interpretation of the spectra of Ce III [24] and Pr III [25] we find $E^3 \sim 520$ cm^{-1}.

A preliminary value of ζ_{4f} can be obtained by considering the total widths of the $^6H°$ and $^6F°$ terms. To a first approximation the sum of these two widths is $91\zeta_{4f}$, which gives $\zeta_{4f} \sim 930$ cm^{-1}.

Crosswhite [26] has made a least squares fit of the $^6F°$ and $^6H°$ levels to the theoretical energy formulas by using hydrogenic ratios for the electrostatic parameters and a fixed value of 20 cm^{-1} for α. The parameters E^3 and ζ_{4f} were allowed to vary. A diagonalization with $E^3 = 510$ cm^{-1} and $\zeta_{4f} = 914$ cm^{-1} gave a mean error of 25 cm^{-1}. This could be reduced to about 8 cm^{-1} if slightly different values of ζ_{4f} were used for the two terms: 912 cm^{-1} for ^6H and 938 cm^{-1} for ^6F. Crosswhite notes that this is probably caused by a spin-other-orbit interaction. The J-dependence of this interaction is the same as that of the spin-orbit interaction. However, the spin-other-orbit interaction constant varies from term to term. Thus, this interaction will cause the spin-orbit constants derived from different terms of a configuration to appear to be slightly different. This effect was first treated for l^N configurations by Horie [27]; the principal aspects of the theory have been summarized by Wybourne [28]. Since spin-other-orbit effects cannot be observed by studying only one term of a configuration, the present results for Pm I provide a first opportunity to view their magnitude for the neutral rare earths.

The residual errors in the above calculation have a form very close to that expected from neglect of a spin-spin interaction. If an estimate of the spin-spin interaction energy is made by using Judd's [29] matrix elements and interpolated values of the radial integrals from the calculations of Blume, Freeman, and Watson [30], the mean error can be further reduced to about 2 cm^{-1}. When this is done the values of ζ_{4f} are changed to 910 cm^{-1} for $^6H°$ and 940 cm^{-1} for $^6F°$ [26].

In view of the uncertainties in the ratios of the electrostatic parameters, the value to be used for α, and the Hamiltonian needed to describe the levels, we give the values of E^3 and ζ_{4f} for the $4f^56s^2$ configuration of Pm I as:

$$\zeta_{4f} = 925 \pm 20 \text{ cm}^{-1}$$

$$E^3 = 510 \pm 20 \text{ cm}^{-1}$$

That this value of ζ_{4f} fits in well with other values of ζ_{4f} in the rare earths is shown by the plot in figure 2.

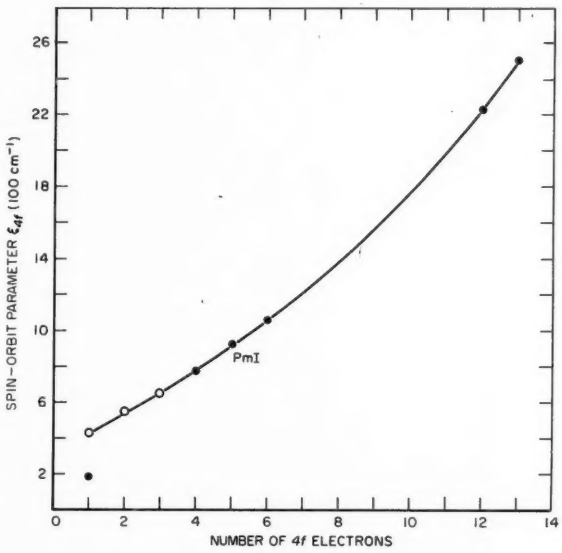

FIGURE 2. *Values of ζ_{4f} in the rare earths.*

The solid circles represent values derived from $4f^N6s^2$ configurations of neutral atoms; the open circles are derived from $4f^N$ configurations of doubly ionized atoms. References: $N=1$, La I, H. N. Russell and W. F. Meggers, J. Res. NBS **9,** 625 (1932); $N=1$, La III, J. Sugar and V. Kaufman, J. Opt. Soc. Am. **55,** 1283 (1965); $N=2$, Ce III, N. Spector, J. Opt. Soc. Am. **55,** 492 (1965); $N=3$, Pr III, R. Trees, J. Opt. Soc. Am. **54,** 651 (1964); $N=4$, Nd I, J. G. Conway and B. G. Wybourne, Phys. Rev. **130,** 2325 (1963); $N=5$, Pm I, this paper; $N=6$, Sm I, J. G. Conway and B. G. Wybourne, Phys. Rev. **130,** 2325 (1963); $N=12$, Er I, J. Reader, unpublished calculations based on data of L. C. Marquet and S. P. Davis, J. Opt. Soc. Am. **55,** 471 (1965). This value of ζ_{4f} of 2237 cm^{-1} is nearly identical to the 2236 cm^{-1} value of ζ_{4f} derived from the $4f^{12}6s$ configuration of Er II by Z. Goldschmidt, J. Opt. Soc. Am. **53,** 594 (1963); $N=13$, Tm I, W. F. Meggers, Rev. Mod. Phys. **14,** 96 (1942). For simplicity, several values of ζ which have been published for $4f^N6s$ configurations of singly ionized rare earths have not been included.

TABLE 3. *Even levels of* Pm I. *Levels with asterisk are uncertain.*

Energy (cm^{-1})	J	g	Energy (cm^{-1})	J	g	Energy (cm^{-1})	J	g	Energy (cm^{-1})	J	g
17104.72	7/2	0.885	23443.79	5/2	0.784	26065.63	1/2	−0.36	28169.71	7/2	0.9
20006.04	3/2	0.068	23480.63	9/2	1.16	26080.99	17/2	1.29	28186.31	7/2	1.98
20157.85	7/2	0.503	23501.57	11/2	1.283	26096.75	17/2	1.25	28196.56	1/2	2.44
20265.98	5/2	0.527	23538.86	5/2	0.780	26101.28	13/2		28273.52	7/2	0.764
20517.96	5/2	0.659	23550.60	11/2	1.170	26103.56	11/2	1.2	28274.21	9/2	1.055
20567.76	5/2	0.910	23571.27	9/2	1.26	26181.98	13/2	1.55	28325.13	7/2	1.38
20660.00	7/2	1.114	23584.31	7/2	1.123	26211.44	7/2	0.715	28338.98	5/2	0.963
20675.81	5/2	1.075	23629.06	13/2	1.09	26237.84	9/2	1.43	28467.52	7/2	0.87
20909.00	7/2	0.929	23712.56	7/2	1.181	26282.20	13/2	0.95	28490.35	9/2	1.123
21100.10	7/2	1.319	23732.57	1/2	3.24	26285.02	7/2	0.877	28565.66	9/2	1.0
21143.06	7/2	0.977	23740.42	13/2		26300.30	1/2	0.955	28607.33	9/2	1.079
21237.49	9/2	0.841	23743.96	7/2	1.111	26456.26	13/2		28608.57	3/2	1.740
21348.22	7/2	0.815	23760.57	11/2		26468.80	1/2	−0.45	28657.02	1/2	0.29
21371.95	7/2	0.927	23926.91	3/2	1.754	26479.61	3/2	0.731	28680.26	7/2	0.88
21590.60	3/2	0.135	23938.76	13/2	1.044	26522.35	3/2	1.135	28994.90	11/2	1.30
21625.45	9/2	1.117	24013.29*	13/2	1.29	26545.85	17/2	1.14	29002.94	3/2	0.99
21657.89*	5/2	1.01	24038.82	11/2	1.08	26555.44	13/2	1.07	29074.03	9/2	
21666.80	7/2	0.696	24071.03	9/2	1.12	26591.40	13/2	1.10	29129.60	9/2	1.162
21732.93	9/2	1.137	24091.39	3/2	1.395	26609.39	5/2	0.56	29161.96	9/2	1.0
21920.49	9/2	0.986	24122.41	13/2		26630.56	5/2	0.32	29242.64	11/2	1.259
21946.12	3/2	−0.01	24180.80	13/2	1.28	26694.38	11/2	1.095	29585.21	11/2	1.2
21976.26	7/2	1.218	24204.37	7/2	0.670	26695.79	5/2		29595.58	9/2	1.04
22013.40	3/2	0.887	24234.42	9/2		26703.97	13/2	1.30	29648.42*	9/2	
22080.08	5/2	0.571	24245.66	13/2	1.14	26725.52	3/2	0.65	29705.77	11/2	
22084.65	7/2	0.858	24338.33	9/2	1.17	26830.74	3/2	0.794	29757.69	11/2	
22205.44	9/2	0.974	24418.44	7/2	1.124	26841.36	5/2	1.38	29784.08	9/2	
22259.21	1/2	−0.32	24443.15	13/2	1.17	26955.22	15/2		29856.72	11/2	1.10
22294.96	9/2	1.245	24443.57	9/2	1.037	27036.66	5/2	0.931	29883.87	7/2	1.199
22301.24	5/2	0.976	24471.10	7/2	0.83	27042.18	15/2		29908.90	9/2	
22309.94	7/2	0.850	24503.45	11/2	1.22	27109.75	15/2		29960.42*	11/2	1.18
22355.68	9/2	1.374	24520.23	13/2	1.34	27245.99	5/2	0.761	30008.40	11/2	1.28
22388.06	3/2	0.84	24533.27	11/2	1.183		7/2		30063.62	9/2	1.224
22414.17	11/2	1.12	24558.56	9/2	1.39	27272.46	9/2	0.8		11/2	
22425.58	5/2	0.83	24627.53	9/2	0.961	27304.15*	15/2	1.44	30251.50*	13/2	1.2
22446.20	11/2	1.531	24681.68	11/2	0.895	27319.28	7/2	1.274	30281.98	13/2	
22456.72	9/2	0.936	24705.25	15/2	1.102	27334.48	5/2	0.947	30374.95	11/2	1.226
22522.90	5/2	0.735	24754.58	9/2	0.888	27351.42	7/2	0.92	30457.44	13/2	1.226
22586.77	9/2	1.283	24770.04	13/2	1.17	27383.92	15/2		30541.28	11/2	
22654.34	7/2	0.84	24789.86	9/2	1.08	27468.45	3/2	0.21	30726.26	9/2	
22656.68	5/2	0.936	24884.90	11/2		27476.28	7/2	1.077	30785.03	9/2	
22761.33	11/2	1.296	24912.34	11/2	1.29	27512.95	5/2	0.913	31103.24	11/2	
22817.13	11/2	1.134	25104.27	11/2	1.15	27596.27	13/2	1.29	31846.70	11/2	
22905.24	5/2	1.16	25306.07	15/2	1.21	27621.74	7/2		32022.32	9/2	
22934.70	7/2	1.237	25351.46	3/2	0.58	27685.89*	3/2	2.049	32435.06	13/2	
23006.35	11/2		25357.24	11/2		27829.89	9/2	1.024	33180.50	15/2	1.285
23033.95	11/2	1.0	25402.61	11/2	1.211	27919.29	3/2	1.31	33246.65	9/2	
23178.13	7/2	1.150	25405.29	13/2	1.034	27923.37	5/2	0.869			
23188.54	5/2	1.48	25448.28	9/2	1.14	27939.87	9/2	1.025			
23198.33	11/2	1.12	25474.46	15/2		28008.09	7/2				
23276.10	9/2	0.83	25521.55*	9/2	0.910	28030.99	13/2	1.39			
23278.90	7/2	1.0	25537.36	13/2	1.39	28075.94	9/2	1.155			
23334.10	5/2	0.571	25618.77	15/2	1.13	28084.28	5/2	0.904			
23337.53	7/2	1.257	25755.17	11/2	1.016	28086.21	11/2	1.150			
23345.07	11/2	1.323	25919.50	13/2	1.26	28150.73	7/2	1.071			
23435.40	9/2	1.00	26015.94	11/2		28153.69	5/2	0.632			

TABLE 4. *Classified lines of* Pm I

The wavelengths are in air. Even levels are designated by the energy in cm^{-1} followed by the J-value in parenthesis. Intensities are visual estimates on a scale of 1 to 1000.

C – complex
L – shaded to longer wavelengths
S – shaded to shorter wavelengths
W – wide
P – perturbed by close line, but resolved
U – perturbed by close line, but unresolved
D – double
B – blend
H – hazy
R1 – very widely reversed
R2 – widely reversed
R3 – moderately reversed
R4 – slightly reversed
R5 – barely detectably reversed
* – classification in doubt

λ (A)	*I*	σ (cm^{-1})	Classification
6420.171	10	15571.61	$^6F^\circ_{11/2} - 24180.80$ (13/2)*
6355.910	100*P*	15729.04	$^6F^\circ_{11/2} - 24338.33$ (9/2)
6348.654	8	15747.02	$^6F^\circ_{7/2} - 22309.94$ (7/2)
6335.048	100	15780.84	$^6F^\circ_{9/2} - 23278.90$ (7/2)
6313.796	15	15833.95	$^6F^\circ_{11/2} - 24443.15$ (13/2)*
6313.663	10	15834.29	$^6F^\circ_{11/2} - 24443.57$ (9/2)
6311.586	85	15839.50	$^6F^\circ_{9/2} - 23337.53$ (7/2)
6308.577	20	15847.05	$^6F^\circ_{9/2} - 23345.07$ (11/2)
6302.377	60	15862.64	$^6F^\circ_{7/2} - 22425.58$ (5/2)
6283.239	70	15910.96	$^6F_{11/2} - 24520.23$ (13/2)
6278.104	2	15923.97	$^6F^\circ_{11/2} - 24533.27$ (11/2)
6268.138	150	15949.29	$^6F^\circ_{11/2} - 24558.56$ (9/2)
6263.942	10	15959.97	$^6F^\circ_{7/2} - 22522.90$ (5/2)
6255.078	10	15982.59	$^6F^\circ_{9/2} - 23480.63$ (9/2)
6246.909	50	16003.49	$^6F^\circ_{9/2} - 23501.57$ (11/2)
6220.118	10	16072.42	$^6F^\circ_{11/2} - 24681.68$ (11/2)
6219.809	50	16073.22	$^6F^\circ_{9/2} - 23571.27$ (9/2)
6214.768	75	16086.25	$^6F^\circ_{9/2} - 23584.31$ (7/2)
6208.146	80	16103.41	$^6F^\circ_{5/2} - 21976.26$ (7/2)
6193.898	200	16140.46	$^6F^\circ_{5/2} - 22013.40$ (3/2)
6186.089	2	16160.83	$^6F^\circ_{11/2} - 24770.04$ (13/2)
6168.403	5	16207.17	$^6F^\circ_{5/2} - 22080.08$ (5/2)
6165.603	70	16214.53	$^6F^\circ_{9/2} - 23712.56$ (7/2)
6153.685	80	16245.93	$^6F^\circ_{9/2} - 23743.96$ (7/2)
6142.459	100	16275.62	$^6F^\circ_{11/2} - 24884.90$ (11/2)
6132.934	40	16300.90	$^6H^\circ_{7/2} - 17104.72$ (7/2)
6132.125	200	16303.05	$^6F^\circ_{11/2} - 24912.34$ (11/2)
6117.382	100	16342.34	$^6F^\circ_{7/2} - 22905.24$ (5/2)
6085.359	150*P*	16428.34	$^6F^\circ_{5/2} - 22301.24$ (5/2)
6082.102	30*S*	16437.13	$^6F^\circ_{5/2} - 22309.94$ (7/2)
6053.356	150	16515.19	$^6F^\circ_{5/2} - 22388.06$ (3/2)
6039.646	30	16552.68	$^6F^\circ_{5/2} - 22425.58$ (5/2)
6032.252	90	16572.97	$^6F^\circ_{9/2} - 24071.03$ (9/2)
6015.361	5	16619.50	$^6F^\circ_{5/2} - 22080.08$ (5/2)
6013.146	40	16625.63	$^6F^\circ_{7/2} - 23188.54$ (5/2)
5980.648	100*D*	16715.97	$^6F^\circ_{7/2} - 23278.90$ (7/2)
5973.373	10	16736.32	$^6F^\circ_{9/2} - 24234.42$ (9/2)
5969.214	20	16747.98	$^6F^\circ_{11/2} - 25357.24$ (11/2)
5960.957	3	16771.18	$^6F^\circ_{7/2} - 23334.10$ (5/2)
5959.738	125	16774.61	$^6F^\circ_{7/2} - 23337.53$ (7/2)
5953.095	100	16793.33	$^6F^\circ_{11/2} - 25402.61$ (11/2)
5951.191	100	16798.71	$^6F^\circ_{3/2} - 22259.21$ (1/2)
5936.504	200	16840.26	$^6F^\circ_{9/2} - 24338.33$ (9/2)
5922.221	3	16880.88	$^6F^\circ_{7/2} - 23443.79$ (5/2)
5909.318	5	16917.74	$^6F^\circ_{7/2} - 23480.63$ (9/2)
5905.899	100	16927.53	$^6F^\circ_{3/2} - 22388.06$ (3/2)
5899.630	20	16945.52	$^6F^\circ_{9/2} - 24443.57$ (9/2)
5892.838	10*P*	16965.05	$^6F^\circ_{3/2} - 22425.58$ (5/2)
5877.354	30*C*	17009.74	$^6F^\circ_{1/2} - 22259.21$ (1/2)
5878.337	50	17021.38	$^6F^\circ_{7/2} - 23584.31$ (7/2)
5869.549	30	17032.36	$^6F^\circ_{5/2} - 22905.24$ (5/2)
5859.865	50	17060.51	$^6F^\circ_{9/2} - 24558.56$ (9/2)
5844.718	200*L*	17104.72	$^6F^\circ_{5/2} - 17104.72$ (7/2)
5833.183	125	17138.55	$^6F^\circ_{1/2} - 22388.06$ (3/2)
5829.407	50	17149.65	$^6F^\circ_{7/2} - 23712.56$ (7/2)
5818.750	3*P*	17181.06	$^6F^\circ_{7/2} - 23743.96$ (7/2)
5776.992	200	17305.25	$^6F^\circ_{5/2} - 23178.13$ (7/2)
5730.809	200	17444.70	$^6F^\circ_{3/2} - 22905.24$ (5/2)
5724.260	60	17464.66	$^6F^\circ_{5/2} - 23337.53$ (7/2)
5710.075	20	17508.05	$^6F^\circ_{7/2} - 24071.03$ (9/2)*
5671.018	500	17628.62	$^6F^\circ_{11/2} - 26237.84$ (9/2)
5657.260	300	17671.50	$^6F^\circ_{7/2} - 24234.42$ (9/2)
5644.515	10	17711.40	$^6F^\circ_{5/2} - 23584.31$ (7/2)
5639.234	50	17727.98	$^6F^\circ_{3/2} - 23188.54$ (5/2)
5624.182	20	17775.43	$^6F^\circ_{7/2} - 24338.33$ (9/2)
5603.922	125*L*	17839.69	$^6F^\circ_{5/2} - 23712.56$ (7/2)
5598.944	2	17855.55	$^6F^\circ_{7/2} - 24418.44$ (7/2)
5597.807	10*H*	17859.18	$^6F^\circ_{9/2} - 25357.24$ (11/2)
5594.077	100	17871.09	$^6F^\circ_{5/2} - 23743.96$ (7/2)
5591.080	35*C*	17880.67	$^6F^\circ_{7/2} - 24443.57$ (9/2)*
5583.619	15	17904.56	$^6F^\circ_{9/2} - 25402.61$ (11/2)*
5559.525	150*L*	17982.15	$^6F^\circ_{11/2} - 26591.40$ (13/2)
5559.188	5	17983.24	$^6F^\circ_{3/2} - 23443.79$ (5/2)
5555.354	100	17995.66	$^6F^\circ_{7/2} - 24558.56$ (9/2)
5546.769	10*U*	18023.51	$^6F^\circ_{9/2} - 25521.55$ (9/2)
5537.379	200*C*	18054.07	$^6F^\circ_{3/2} - 23926.91$ (3/2)
5529.938	3	18078.36	$^6F^\circ_{3/2} - 23538.86$ (5/2)
5527.883	5	18085.09	$^6F^\circ_{11/2} - 26694.38$ (11/2)*
5524.945	150	18094.70	$^6F^\circ_{11/2} - 26703.97$ (13/2)
5487.381	20	18218.57	$^6F^\circ_{5/2} - 24091.39$ (3/2)
5484.872	10*U*	18226.90	$^6F^\circ_{7/2} - 24789.86$ (9/2)*
5471.313	150*C*	18272.07	$^6F^\circ_{3/2} - 23732.57$ (1/2)
5430.600	25	18409.06	$^6H^\circ_{9/2} - 20157.85$ (7/2)
5421.374	10	18440.38	$^6H^\circ_{11/2} - 21237.49$ (9/2)
5413.736	100*C*	18466.40	$^6F^\circ_{3/2} - 23926.91$ (3/2)
5408.846	100*C*	18483.09	$^6F^\circ_{1/2} - 23732.57$ (1/2)
5405.328	2	18495.12	$^6H^\circ_{13/2} - 22414.17$ (11/2)
5392.454	10	18539.28	$^6H^\circ_{15/2} - 23629.06$ (13/2)
5390.622	20	18545.58	$^6F^\circ_{5/2} - 24418.44$ (7/2)
5365.939	50	18630.89	$^6F^\circ_{3/2} - 24091.39$ (3/2)
5352.567	25*C*	18677.43	$^6F^\circ_{1/2} - 23926.91$ (3/2)
5334.737	200	18739.85	$^6F^\circ_{9/2} - 26237.84$ (9/2)
5305.840	75*S*	18841.91	$^6F^\circ_{7/2} - 24091.39$ (3/2)
5305.732	50*B*	18842.30	$^6H^\circ_{13/2} - 22761.33$ (11/2)
5303.854	7	18848.97	$^6H^\circ_{15/2} - 23938.76$ (13/2)
5290.064	15	18898.10	$^6H^\circ_{13/2} - 22817.13$ (11/2)
5286.398	2	18911.21	$^6H^\circ_{9/2} - 20660.00$ (7/2)
5252.679	25	19032.61	$^6H^\circ_{15/2} - 24122.41$ (13/2)
5230.058	10	19114.93	$^6H^\circ_{13/2} - 23033.95$ (11/2)
5227.747	20	19123.38	$^6H^\circ_{11/2} - 21920.49$ (9/2)
5218.879	100	19155.87	$^6H^\circ_{15/2} - 24245.66$ (13/2)
5217.699	30*P*	19160.20	$^6H^\circ_{9/2} - 20909.00$ (7/2)
5185.467	100	19279.30	$^6H^\circ_{13/2} - 23198.33$ (11/2)
5171.689	10	19330.66	$^6F^\circ_{11/2} - 27939.87$ (9/2)
5166.176	10*P*	19351.29	$^6H^\circ_{9/2} - 21100.10$ (7/2)
5165.623	150	19353.36	$^6H^\circ_{15/2} - 24443.15$ (13/2)
5165.443	100	19354.03	$^6H^\circ_{7/2} - 20157.85$ (7/2)
5150.995	150	19408.32	$^6H^\circ_{11/2} - 22205.44$ (9/2)
5146.298	500R3	19426.03	$^6H^\circ_{13/2} - 23345.07$ (11/2)
5145.126	400R4	19430.46	$^6H^\circ_{15/2} - 24520.23$ (13/2)

TABLE 4. *Classified lines of* Pm I—Continued

λ (A)	*I*	σ (cm^{-1})	Classification
5136.752	5	19462.13	$^6H^\circ_{7/2}$ −20265.98 (5/2)
5132.836	10*C*	19476.98	$^6F^\circ_{11/2}$ −28086.21 (11/2)
5129.749	200	19488.70	$^6H^\circ_{9/2}$ −21237.49 (9/2)
5127.342	400R3	19497.85	$^6H^\circ_{11/2}$ −22294.96 (9/2)
5111.431	40	19558.54	$^6H^\circ_{11/2}$ −22355.68 (9/2)
5105.170	50	19582.53	$^6H^\circ_{13/2}$ −23501.57 (11/2)
5100.766	400R3	19599.44	$^6H^\circ_{9/2}$ −21348.22 (7/2)
5096.601	50	19615.45	$^6H^\circ_{15/2}$ −24705.25 (15/2)
5096.181	200	19617.07	$^6H^\circ_{11/2}$ −22414.17 (11/2)
5094.831	400R3	19622.27	$^6H^\circ_{9/2}$ −21371.05 (7/2)
5092.418	200	19631.56	$^6H^\circ_{13/2}$ −23550.60 (11/2)
5087.872	10*C*	19649.10	$^6H^\circ_{11/2}$ −22446.20 (11/2)
5085.154	25	19659.61	$^6H^\circ_{11/2}$ −22456.72 (9/2)
5081.182	50	19674.98	$^6F^\circ_{7/2}$ −26237.84 (9/2)
5079.822	100	19680.24	$^6H^\circ_{15/2}$ −24770.04 (13/2)
5072.149	150	19710.02	$^6H^\circ_{13/2}$ −23629.06 (13/2)
5071.094	25	19714.12	$^6H^\circ_{7/2}$ −20517.96 (5/2)
5058.311	300R2	19763.93	$^6H^\circ_{7/2}$ −20567.76 (5/2)
5051.739	60	19789.65	$^6H^\circ_{11/2}$ −22586.77 (9/2)
5043.672	15	19821.30	$^6F^\circ_{9/2}$ −27319.28 (7/2)
5034.813	50L	19856.18	$^6H^\circ_{7/2}$ −20660.00 (7/2)
5030.805	200R3	19871.99	$^6H^\circ_{7/2}$ −20675.81 (5/2)
5029.624	50*C*	19876.66	$^6H^\circ_{9/2}$ −21625.45 (9/2)
5026.019	30	19890.91	$^6F^\circ_{3/2}$ −25351.46 (3/2)
5019.185	100	19918.00	$^6H^\circ_{9/2}$ −21666.80 (7/2)
5007.559	15	19964.24	$^6H^\circ_{11/2}$ −22761.33 (11/2)
5002.571	10	19984.15	$^6H^\circ_{9/2}$ −21732.93 (9/2)
4997.095	500R1	20006.04	$^6H^\circ_{5/2}$ −20006.04 (3/2)
4993.676	50	20019.74	$^6H^\circ_{13/2}$ −23938.76 (13/2)
4993.601	75	20020.04	$^6H^\circ_{11/2}$ −22817.13 (11/2)
4981.727	5*L*	20067.76	$^6F^\circ_{7/2}$ −26630.56 (5/2)
4975.162	5	20094.24	$^6H^\circ_{13/2}$ −24013.29 (13/2)*
4973.250	25	20101.97	$^6F^\circ_{1/2}$ −25351.46 (3/2)
4972.448	150R5	20105.21	$^6H^\circ_{7/2}$ −20909.00 (7/2)
4968.843	35*S*	20119.79	$^6H^\circ_{13/2}$ −24038.82 (11/2)
4965.600	5	20132.94	$^6F^\circ_{7/2}$ −26695.79 (5/2)
4959.461	700R1	20157.86	$^6H^\circ_{5/2}$ −20157.85 (7/2)
4956.053	100	20171.72	$^6H^\circ_{9/2}$ −21920.49 (9/2)
4948.286	125	20203.38	$^6H^\circ_{13/2}$ −24122.41 (13/2)
4946.851	100	20209.24	$^6H^\circ_{11/2}$ −23006.35 (11/2)
4945.127	125	20216.28	$^6H^\circ_{15/2}$ −25306.07 (15/2)
4942.390	40*S*	20227.48	$^6H^\circ_{9/2}$ −21976.26 (7/2)
4940.101	30	20236.85	$^6H^\circ_{11/2}$ −23033.95 (11/2)
4934.027	50	20261.77	$^6H^\circ_{13/2}$ −24180.80 (13/2)
4932.994	600R1	20266.01	$^6H^\circ_{5/2}$ −20265.98 (5/2)
4929.960	3	20278.48	$^6F^\circ_{7/2}$ −26841.36 (5/2)
4925.637	10*C*	20296.28	$^6H^\circ_{7/2}$ −21100.10 (7/2)
4918.283	400R4	20326.62	$^6H^\circ_{13/2}$ −24245.66 (13/2)
4917.008	2*C*	20331.90	$^6F^\circ_{9/2}$ −27829.89 (9/2)
4916.047	3*C*	20335.87	$^6H^\circ_{9/2}$ −22084.65 (7/2)
4915.234	125	20339.23	$^6H^\circ_{7/2}$ −21143.06 (7/2)
4904.278	300R4	20384.67	$^6H^\circ_{15/2}$ −25474.46 (15/2)*
4904.035	15*S*	20385.68	$^6F^\circ_{11/2}$ −28994.90 (11/2)
4900.296	400R3	20401.23	$^6H^\circ_{11/2}$ −23198.33 (11/2)
4897.663	3*P*	20412.20	$^6F^\circ_{5/2}$ −26285.02 (7/2)*
4892.516	700R2	20433.68	$^6H^\circ_{7/2}$ −21237.49 (9/2)
4890.549	10	20441.89	$^6F^\circ_{9/2}$ −27939.87 (9/2)*
4889.191	50*C*	20447.57	$^6H^\circ_{15/2}$ −25537.36 (13/2)
4887.018	500R3	20456.66	$^6H^\circ_{9/2}$ −22205.44 (9/2)
4885.070	25	20464.82	$^6F^\circ_{11/2}$ −29074.03 (9/2)
4882.946	1	20473.72	$^6F^\circ_{7/2}$ −27036.66 (5/2)
4881.674	2*C*	20479.06	$^6H^\circ_{11/2}$ −23276.10 (9/2)*
4872.416	700R2	20517.97	$^6H^\circ_{5/2}$ −20517.96 (5/2)
4871.845	30	20520.37	$^6F^\circ_{11/2}$ −29129.60 (9/2)
4870.957	50	20524.11	$^6H^\circ_{13/2}$ −24443.15 (13/2)
4869.801	400R4	20528.98	$^6H^\circ_{15/2}$ −25618.77 (15/2)
4866.147	100	20544.40	$^6H^\circ_{7/2}$ −21348.22 (7/2)
4865.724	500R2	20546.19	$^6H^\circ_{9/2}$ −22294.96 (9/2)
4865.302	300R3	20547.97	$^6H^\circ_{11/2}$ −23345.07 (11/2)
4862.183	100	20561.15	$^6H^\circ_{9/2}$ −22309.94 (7/2)
4860.745	700R1	20567.23	$^6H^\circ_{7/2}$ −21371.05 (7/2)
4860.619	400R3	20567.77	$^6H^\circ_{5/2}$ −20567.76 (5/2)
4858.210	25	20577.97	$^6F^\circ_{9/2}$ −28075.94 (9/2)
4856.687	100	20584.42	$^6H^\circ_{13/2}$ −24503.45 (11/2)
4855.787	75	20588.23	$^6F^\circ_{9/2}$ −28086.21 (11/2)
4852.727	350R3	20601.21	$^6H^\circ_{13/2}$ −24520.23 (13/2)
4851.808	50	20605.12	$^6F^\circ_{3/2}$ −26065.63 (1/2)
4851.379	35	20606.94	$^6H^\circ_{9/2}$ −22355.68 (9/2)
4849.663	20	20614.23	$^6H^\circ_{13/2}$ −24533.27 (11/2)
4844.012	200	20638.28	$^6H^\circ_{11/2}$ −23435.40 (9/2)
4841.379	15	20649.50	$^6F^\circ_{5/2}$ −26522.35 (3/2)
4840.626	100	20652.71	$^6F^\circ_{9/2}$ −28150.73 (7/2)
4838.919	400R4	20660.00	$^6H^\circ_{5/2}$ −20660.00 (7/2)
4837.655	800R1	20665.40	$^6H^\circ_{9/2}$ −22414.17 (11/2)
4835.220	10*S*	20675.80	$^6H^\circ_{5/2}$ −20675.81 (5/2)
4833.506	50	20683.14	$^6F^\circ_{7/2}$ −27245.99 (5/2)
4833.417	75	20683.52	$^6H^\circ_{11/2}$ −23480.63 (9/2)
4832.297	50	20688.31	$^6F^\circ_{9/2}$ −28186.31 (7/2)
4830.170	125*C*	20697.42	$^6H^\circ_{9/2}$ −22446.20 (11/2)
4828.524	20	20704.47	$^6H^\circ_{11/2}$ −23501.57 (11/2)
4827.716	400R3	20707.94	$^6H^\circ_{9/2}$ −22456.72 (9/2)
4821.054	40	20736.56	$^6F^\circ_{5/2}$ −26609.39 (5/2)
4817.116	400R4	20753.51	$^6H^\circ_{11/2}$ −23550.60 (11/2)
4816.438	75	20756.43	$^6F^\circ_{7/2}$ −27319.28 (7/2)
4816.131	7*P*	20757.75	$^6F^\circ_{5/2}$ −26630.56 (5/2)
4815.000	50*C*	20762.63	$^6H^\circ_{13/2}$ −24681.68 (11/2)
4812.914	100	20771.63	$^6F^\circ_{7/2}$ −27334.48 (5/2)
4812.323	100	20774.18	$^6H^\circ_{11/2}$ −23571.27 (9/2)
4811.850	50*P*	20776.22	$^6F^\circ_{9/2}$ −28274.21 (9/2)
4809.536	700R2	20786.22	$^6H^\circ_{13/2}$ −24705.25 (15/2)
4808.994	30	20788.56	$^6F^\circ_{7/2}$ −27351.42 (7/2)
4802.618	30*C*	20816.16	$^6F^\circ_{1/2}$ −26065.63 (1/2)
4801.356	900R1	20821.63	$^6H^\circ_{7/2}$ −21625.45 (9/2)
4801.051	100	20822.95	$^6F^\circ_{3/2}$ −26695.79 (5/2)
4800.083	3	20827.15	$^6F^\circ_{9/2}$ −28325.13 (7/2)
4799.491	150	20829.72	$^6H^\circ_{15/2}$ −25919.50 (13/2)
4798.977	700R1	20831.95	$^6H^\circ_{11/2}$ −23629.06 (13/2)
4797.586	100	20837.99	$^6H^\circ_{9/2}$ −22586.77 (9/2)
4797.171	15	20839.79	$^6F^\circ_{3/2}$ −26300.30 (1/2)
4794.588	250	20851.02	$^6H^\circ_{13/2}$ −24770.04 (13/2)

TABLE 4. *Classified lines of* Pm I—Continued

λ (A)	*I*	σ (cm⁻¹)	Classification
4794.207	50	20852.68	$^6F^\circ_{5/2}$ −26725.52 (3/2)
4791.840	35*C*	20862.98	$^6H^\circ_{7/2}$ −21666.80 (7/2)
4782.081	150R4	20905.55	$^6H^\circ_{9/2}$ −22654.34 (7/2)
4781.292	900R1	20909.00	$^6H^\circ_{5/2}$ −20909.00 (7/2)
4780.285	150	20913.41	$^6F^\circ_{7/2}$ −27476.28 (7/2)
4776.699	100R5	20929.11	$^6H^\circ_{7/2}$ −21732.93 (9/2)
4773.458	700R1	20943.32	$^6H^\circ_{11/2}$−23740.42 (13/2)*
4771.916	150	20950.09	$^6F^\circ_{7/2}$ −27512.95 (5/2)
4770.142	150	20957.88	$^6F^\circ_{5/2}$ −26830.74 (3/2)
4768.866	25	20963.48	$^6H^\circ_{11/2}$−23760.57 (11/2)
4767.719	60	20968.53	$^6F^\circ_{3/2}$ −26841.36 (5/2)
4766.024	5*C*	20975.99	$^6F^\circ_{11/2}$−29585.21 (11/2)
4763.670	2	20986.35	$^6F^\circ_{11/2}$−29595.58 (9/2)
4762.569	700R1	20991.20	$^6H^\circ_{15/2}$−26080.99 (17/2)
4762.309	5*C*	20992.35	$^6F^\circ_{9/2}$ −28490.35 (9/2)
4762.095	75U	20993.29	$^6H^\circ_{13/2}$−24912.34 (11/2)
4758.996	800R1	21006.96	$^6H^\circ_{15/2}$−26096.75 (17/2)
4758.694	150	21008.29	$^6F^\circ_{3/2}$ −26468.80 (1/2)
4757.968	5	21011.50	$^6H^\circ_{13/2}$−26101.28 (13/2)
4757.732	500R2	21012.54	$^6H^\circ_{11/2}$−22761.33 (9/2)
4756.247	90D	21019.10	$^6F^\circ_{3/2}$ −26479.61 (3/2)
4751.701	20	21039.21	$^6F^\circ_{11/2}$−29648.42 (9/2)*
4749.076	70D	21050.84	$^6F^\circ_{1/2}$ −26300.30 (1/2)
4747.268	3*C*	21058.86	$^6F^\circ_{7/2}$ −27621.74 (7/2)
4746.595	30	21061.84	$^6F^\circ_{3/2}$ −26522.35 (3/2)
4745.282	10*P*	21067.67	$^6F^\circ_{9/2}$ −28565.66 (9/2)
4745.128	350R2	21068.35	$^6H^\circ_{9/2}$ −22817.13 (11/2)
4739.776	200*C*	21092.15	$^6H^\circ_{15/2}$−26181.98 (13/2)
4738.779	2	21096.58	$^6F^\circ_{11/2}$−29705.77 (11/2)
4737.987	500R2	21100.11	$^6H^\circ_{5/2}$ −21100.10 (7/2)
4735.915	75*C*	21109.34	$^6F^\circ_{9/2}$ −28607.33 (9/2)
4734.274	800R1	21116.66	$^6H^\circ_{7/2}$ −21920.49 (9/2)
4728.678	400R3	21141.65	$^6H^\circ_{11/2}$−23938.76 (13/2)
4728.361	700R1	21143.06	$^6H^\circ_{5/2}$ −21143.06 (7/2)
4727.144	10	21148.50	$^6F^\circ_{11/2}$−29757.69 (11/2)
4727.062	300	21148.87	$^6F^\circ_{3/2}$ −26609.39 (5/2)
4723.722	125	21163.83	$^6F^\circ_{5/2}$ −27036.66 (5/2)
4722.332	40*D*	21170.06	$^6F^\circ_{3/2}$ −26630.56 (5/2)
4721.752	30*B*	21172.66	$^6H^\circ_{7/2}$ −21976.26 (7/2)
4719.607	2	21182.28	$^6F^\circ_{9/2}$ −28680.26 (7/2)
4718.800	100	21185.90	$^6H^\circ_{9/2}$ −22934.70 (7/2)
4717.351	75	21192.41	$^6H^\circ_{15/2}$−26282.20 (13/2)
4712.058	50	21216.21	$^6H^\circ_{11/2}$−24013.29 (13/2)*
4711.368	125*C*	21219.32	$^6F^\circ_{1/2}$ −26468.80 (1/2)
4708.968	150	21230.14	$^6F^\circ_{1/2}$ −26479.61 (3/2)
4706.401	100	21241.72	$^6H^\circ_{11/2}$−24038.82 (11/2)
4705.114	100	21247.52	$^6F^\circ_{11/2}$−29856.72 (11/2)
4702.886	10*W*	21257.59	$^6H^\circ_{9/2}$ −23006.35 (11/2)
4701.242	1	21265.03	$^6F^\circ_{3/2}$ −26725.52 (3/2)
4700.803	100*C*	21267.01	$^6F^\circ_{7/2}$ −27829.89 (9/2)
4699.508	200	21272.87	$^6F^\circ_{1/2}$ −26522.35 (3/2)
4699.276	150	21273.92	$^6H^\circ_{11/2}$−24071.03 (9/2)
4698.761	150	21276.25	$^6H^\circ_{7/2}$ −22080.08 (5/2)
4697.749	30*C*	21280.83	$^6H^\circ_{7/2}$ −22084.65 (7/2)
4696.796	500R2	21285.16	$^6H^\circ_{9/2}$ −23033.95 (11/2)
4693.589	40*L*	21299.70	$^6F^\circ_{11/2}$−29908.90 (9/2)
4687.952	20	21325.31	$^6H^\circ_{11/2}$−24122.41 (13/2)
4682.920	700R1	21348.22	$^6H^\circ_{5/2}$ −21348.22 (7/2)
4682.266	150	21351.20	$^6F^\circ_{11/2}$−29960.42 (11/2)*
4680.223	2	21360.52	$^6F^\circ_{7/2}$ −27923.37 (5/2)
4678.918	60	21366.48	$^6H^\circ_{15/2}$−26456.26 (13/2)
4678.093	400R5	21370.25	$^6F^\circ_{3/2}$ −26830.74 (3/2)
4677.916	500R2	21371.06	$^6H^\circ_{5/2}$ −21371.05 (7/2)
4677.456	200	21373.16	$^6F^\circ_{5/2}$ −27245.99 (5/2)
4675.764	5*C*	21380.89	$^6F^\circ_{3/2}$ −26841.36 (5/2)
4675.148	35	21383.71	$^6H^\circ_{11/2}$−24180.80 (13/2)
4674.420	500R4	21387.04	$^6H^\circ_{13/2}$−25306.07 (15/2)
4671.759	400	21399.22	$^6F^\circ_{11/2}$−30008.40 (11/2)
4671.234	500R2	21401.63	$^6H^\circ_{7/2}$ −22205.44 (9/2)
4665.188	400R2	21429.36	$^6H^\circ_{9/2}$ −23178.13 (7/2)
4663.455	600R2	21437.33	$^6H^\circ_{11/2}$−24234.42 (9/2)
4663.261	300R4	21438.22	$^6H^\circ_{13/2}$−25357.24 (11/2)
4661.729	25*U*	21445.26	$^6F^\circ_{7/2}$ −28008.09 (7/2)*
4661.476	40*C*	21446.43	$^6F^\circ_{5/2}$ −27319.28 (7/2)
4661.012	60	21448.56	$^6H^\circ_{11/2}$−24245.66 (13/2)
4660.794	500R3	21449.56	$^6H^\circ_{9/2}$ −23198.33 (11/2)
4659.745	2	21454.40	$^6F^\circ_{11/2}$−30063.62 (9/2)
4659.383	300	21456.06	$^6H^\circ_{15/2}$−26545.85 (17/2)
4658.169	75	21461.65	$^6F^\circ_{5/2}$ −27334.48 (5/2)
4657.301	50	21465.66	$^6H^\circ_{15/2}$−26555.44 (13/2)
4655.046	500R5	21476.05	$^6F^\circ_{1/2}$ −26725.52 (3/2)
4654.496	400	21478.59	$^6F^\circ_{5/2}$ −27351.42 (7/2)
4653.413	400R3	21483.59	$^6H^\circ_{13/2}$−25402.61 (11/2)
4652.834	5	21486.26	$^6H^\circ_{13/2}$−25405.29 (13/2)
4650.525	500	21496.93	$^6F^\circ_{9/2}$ −28994.90 (11/2)
4650.421	600R5	21497.41	$^6H^\circ_{7/2}$ −22301.24 (5/2)
4649.508	600	21501.63	$^6H^\circ_{13/2}$−26591.40 (13/2)
4648.537	50	21506.12	$^6H^\circ_{7/2}$ −22309.94 (7/2)
4647.028	600R3	21513.11	$^6F^\circ_{7/2}$ −28075.94 (9/2)
4645.234	40	21521.41	$^6F^\circ_{7/2}$ −28084.28 (5/2)
4643.959	200	21527.32	$^6H^\circ_{9/2}$ −23276.10 (9/2)
4643.355	700R2	21530.13	$^6H^\circ_{9/2}$ −23278.90 (7/2)
4640.961	400R3	21541.23	$^6H^\circ_{11/2}$−24338.33 (9/2)
4638.672	100	21551.86	$^6H^\circ_{7/2}$ −22355.68 (9/2)
4633.473	300*B*	21576.04	$^6F^\circ_{9/2}$ −29074.03 (9/2)
4633.452	600R3	21576.14	$^6F^\circ_{3/2}$ −27036.66 (5/2)
4632.353	10*P*	21581.26	$^6F^\circ_{9/2}$ −26830.74 (3/2)
4630.930	200	21587.89	$^6F^\circ_{7/2}$ −28150.73 (7/2)
4630.742	15	21588.77	$^6H^\circ_{9/2}$ −23337.53 (7/2)
4630.349	125	21590.60	$^6H^\circ_{5/2}$ −21590.60 (3/2)
4629.127	150	21596.30	$^6H^\circ_{9/2}$ −23345.07 (11/2)
4627.595	400R3	21603.45	$^6F^\circ_{5/2}$ −27476.28 (7/2)
4625.289	500R2	21614.22	$^6H^\circ_{15/2}$−26703.97 (13/2)
4624.409	900*W*	21618.33	$^6H^\circ_{13/2}$−25537.36 (13/2)
4623.675	700R1	21621.76	$^6H^\circ_{7/2}$ −22425.58 (5/2)
4623.310	500	21623.47	$^6F^\circ_{7/2}$ −28186.31 (7/2)
4621.571	500	21631.61	$^6F^\circ_{9/2}$ −29129.60 (9/2)
4619.750	500R4	21640.13	$^6F^\circ_{5/2}$ −27512.95 (5/2)
4618.487	400R4	21646.05	$^6H^\circ_{11/2}$−24443.15 (13/2)
4618.398	200	21646.47	$^6H^\circ_{11/2}$−24443.57 (9/2)
4617.023	600R1	21652.91	$^6H^\circ_{7/2}$ −22456.72 (9/2)
4615.961	50*SP*	21657.89	$^6H^\circ_{5/2}$ −21657.89 (5/2)
4614.670	2	21663.96	$^6F^\circ_{9/2}$ −29161.96 (9/2)
4614.059	150	21666.82	$^6H^\circ_{5/2}$ −21666.80 (7/2)
4612.787	10	21672.80	$^6F^\circ_{11/2}$−30281.98 (13/2)
4609.846	500R3	21686.62	$^6H^\circ_{9/2}$ −23435.40 (9/2)
4607.062	150	21699.73	$^6H^\circ_{13/2}$−25618.77 (15/2)
4605.657	600R2	21706.35	$^6H^\circ_{11/2}$−24503.45 (11/2)
4604.739	400*C*	21710.67	$^6F^\circ_{7/2}$ −28273.52 (7/2)
4604.593	400	21711.36	$^6F^\circ_{7/2}$ −28274.21 (9/2)

TABLE 4. *Classified lines of* Pm I—Continued

λ (A)	I	σ (cm⁻¹)	Classification
4602.957	400R3	21719.08	$^6H^\circ_{7/2}$ −22522.90 (5/2)
4602.105	15*W*	21723.10	$^6H^\circ_{11/2}$−24520.23 (13/2)
4600.250	500R3	21731.86	$^6H^\circ_{9/2}$ −23480.63 (9/2)
4599.338	35	21736.17	$^6H^\circ_{11/2}$−24533.27 (11/2)
4597.546	800R5	21744.64	$^6F^\circ_{9/2}$ −29242.64 (11/2)
4596.646	400*C*	21748.90	$^6F^\circ_{5/2}$ −27621.74 (7/2)
4595.822	400R4	21752.80	$^6H^\circ_{9/2}$ −23501.57 (11/2)
4593.991	50	21761.47	$^6H^\circ_{11/2}$−24558.56 (9/2)
4593.817	200	21762.29	$^6F^\circ_{7/2}$ −28325.13 (7/2)
4593.086	75	21765.76	$^6F^\circ_{11/2}$−30374.95 (11/2)
4589.456	125	21782.97	$^6H^\circ_{7/2}$ −22586.77 (9/2)
4588.921	35	21785.51	$^6F^\circ_{3/2}$ −27245.99 (5/2)
4585.487	300R3	21801.82	$^6H^\circ_{9/2}$ −23550.60 (11/2)
4583.131	125	21813.03	$^6F^\circ_{3/2}$ −27685.89 (3/2)*
4581.145	300	21822.49	$^6H^\circ_{9/2}$ −23571.27 (9/2)
4579.478	300R3	21830.43	$^6H^\circ_{11/2}$−24627.53 (9/2)
4578.411	200R5	21835.52	$^6H^\circ_{9/2}$ −23584.31 (7/2)
4578.285	300	21836.12	$^6H^\circ_{13/2}$−25755.17 (11/2)
4575.752	200	21848.21	$^6F^\circ_{11/2}$−30457.44 (13/2)
4575.267	400R1	21850.52	$^6H^\circ_{7/2}$ −22654.34 (7/2)
4574.781	60	21852.85	$^6H^\circ_{7/2}$ −22656.68 (5/2)
4572.148	300R5	21865.43	$^6H^\circ_{15/2}$−26955.22 (15/2)
4570.367	200*P*	21873.95	$^6F^\circ_{3/2}$ −27334.48 (5/2)
4568.145	300R4	21884.59	$^6H^\circ_{11/2}$−24681.68 (11/2)
4563.960	50	21904.66	$^6F^\circ_{7/2}$ −28467.52 (7/2)
4559.206	300R5	21927.50	$^6F^\circ_{7/2}$ −28490.35 (9/2)
4558.253	50	21932.08	$^6F^\circ_{11/2}$−30541.28 (11/2)
4555.338	500R1	21946.12	$^6H^\circ_{5/2}$ −21946.12 (3/2)
4554.034	300R3	21952.40	$^6H^\circ_{15/2}$−27042.18 (15/2)
4552.979	3	21957.48	$^6H^\circ_{11/2}$−24754.58 (9/2)
4551.672	60	21963.79	$^6H^\circ_{9/2}$ −23712.56 (7/2)
4549.775	400R2	21972.95	$^6H^\circ_{11/2}$−24770.04 (13/2)
4549.088	175*D*	21976.27	$^6H^\circ_{5/2}$ −21976.26 (7/2)
4545.173	200	21995.20	$^6H^\circ_{9/2}$ −23743.96 (7/2)
4544.083	500R2	22000.47	$^6H^\circ_{13/2}$−25919.50 (13/2)
4543.598	20*C*	22002.82	$^6F^\circ_{7/2}$ −28565.66 (9/2)
4542.539	75	22007.95	$^6F^\circ_{3/2}$ −27468.45 (3/2)
4541.746	450R4	22011.79	$^6H^\circ_{9/2}$ −23760.57 (11/2)
4541.415	300R5	22013.40	$^6H^\circ_{5/2}$ −22013.40 (3/2)
4540.062	300*H*	22019.96	$^6H^\circ_{13/2}$−27109.75 (15/2)
4535.008	45*D*	22044.50	$^6F^\circ_{7/2}$ −28607.33 (9/2)
4534.608	100	22046.44	$^6F^\circ_{5/2}$ −27919.29 (3/2)
4533.759	25*U*	22050.57	$^6F^\circ_{5/2}$ −27923.37 (5/2)
4533.378	50	22052.42	$^6F^\circ_{3/2}$ −27512.95 (5/2)
4527.700	400R1	22080.08	$^6H^\circ_{5/2}$ −22080.07 (5/2)
4526.762	250R5	22084.65	$^6H^\circ_{5/2}$ −22084.65 (7/2)
4526.231	2	22087.24	$^6F^\circ_{9/2}$ −29585.21 (11/2)
4526.116	250R4	22087.80	$^6H^\circ_{11/2}$−24884.90 (11/2)
4524.250	65	22096.91	$^6H^\circ_{13/2}$−26015.94 (11/2)
4524.115	50	22097.57	$^6F^\circ_{9/2}$ −29595.58 (9/2)
4523.323	200	22101.44	$^6H^\circ_{7/2}$ −22905.24 (5/2)
4520.502	100	22115.24	$^6H^\circ_{11/2}$−24912.34 (11/2)
4520.128	40	22117.06	$^6F^\circ_{11/2}$−30726.26 (9/2)
4520.052	5	22117.44	$^6F^\circ_{7/2}$ −28680.26 (7/2)
4517.306	200	22130.88	$^6H^\circ_{7/2}$ −22934.70 (7/2)
4516.418	20*CP*	22135.23	$^6F^\circ_{5/2}$ −28008.09 (7/2)*
4513.313	25	22150.46	$^6F^\circ_{9/2}$ −29648.42 (9/2)*
4508.148	1	22175.84	$^6F^\circ_{11/2}$−30785.03 (9/2)
4506.843	250	22182.26	$^6H^\circ_{13/2}$−26101.28 (13/2)
4506.379	60	22184.54	$^6H^\circ_{13/2}$−26103.56 (11/2)
4501.666	20*C*	22207.77	$^6F^\circ_{9/2}$ −29705.77 (11/2)
4500.925	40	22211.42	$^6F^\circ_{5/2}$ −28084.28 (5/2)
4500.330	350R2	22214.36	$^6H^\circ_{13/2}$−27304.15 (15/2)*
4499.398	150	22218.96	$^6F^\circ_{1/2}$ −27468.45 (3/2)
4498.090	3	22225.42	$^6F^\circ_{3/2}$ −27685.89 (3/2)*
4490.504	300R4	22262.97	$^6H^\circ_{13/2}$−26181.98 (13/2)
4487.493	20	22277.91	$^6F^\circ_{5/2}$ −28150.73 (7/2)
4485.842	25	22286.11	$^6F^\circ_{9/2}$ −29784.08 (9/2)
4485.052	300R3	22290.03	$^6H^\circ_{9/2}$ −24038.82 (11/2)
4482.792	75*U*	22301.27	$^6H^\circ_{5/2}$ −22301.24 (5/2)
4481.603	300R1	22307.19	$^6H^\circ_{11/2}$−25104.27 (11/2)
4481.047	15	22309.95	$^6H^\circ_{5/2}$ −22309.94 (7/2)
4478.577	350R1	22322.26	$^6H^\circ_{9/2}$ −24071.03 (9/2)
4471.271	15*D*	22358.73	$^6F^\circ_{9/2}$ −29856.72 (11/2)
4470.382	25*P*	22363.18	$^6H^\circ_{13/2}$−26282.20 (13/2)
4468.155	250R2	22374.32	$^6H^\circ_{7/2}$ −23178.13 (7/2)
4466.077	8*C*	22384.73	$^6H^\circ_{7/2}$ −23188.54 (5/2)
4465.838	125*P*	22385.93	$^6F^\circ_{9/2}$ −29883.87 (7/2)
4465.408	100*C*	22388.09	$^6H^\circ_{5/2}$ −22388.06 (3/2)
4462.895	20*S*	22400.69	$^6F^\circ_{5/2}$ −28273.52 (7/2)
4460.859	10	22410.92	$^6F^\circ_{9/2}$ −29908.90 (9/2)
4457.945	30	22425.57	$^6H^\circ_{5/2}$ −22425.58 (5/2)
4452.638	25	22452.30	$^6F^\circ_{5/2}$ −28325.13 (7/2)
4451.985	100	22455.59	$^6H^\circ_{9/2}$ −24204.37 (7/2)
4451.350	5	22458.79	$^6F^\circ_{3/2}$ −27919.29 (3/2)
4450.628	10	22462.43	$^6F^\circ_{9/2}$ −29960.42 (11/2)*
4450.544	50	22462.86	$^6F^\circ_{3/2}$ −27923.37 (5/2)
4448.677	30	22472.28	$^6H^\circ_{7/2}$ −23276.10 (9/2)
4448.126	75	22475.07	$^6H^\circ_{7/2}$ −23278.90 (7/2)
4446.038	35	22485.62	$^6H^\circ_{9/2}$ −24234.42 (9/2)
4444.376	75	22494.03	$^6F^\circ_{11/2}$−31103.24 (11/2)
4441.911	15	22506.51	$^6H^\circ_{15/2}$−27596.27 (13/2)
4441.136	3*L*	22510.44	$^6F^\circ_{9/2}$ −30008.40 (11/2)
4440.995	3*L*	22511.16	$^6F^\circ_{7/2}$ −29074.03 (9/2)
4438.682	300R2	22522.89	$^6H^\circ_{5/2}$ −22522.90 (5/2)
4437.224	125	22530.29	$^6H^\circ_{7/2}$ −23334.10 (5/2)
4436.546	300R3	22533.73	$^6H^\circ_{7/2}$ −23337.53 (7/2)
4435.859	250R4	22537.22	$^6H^\circ_{13/2}$−26456.26 (13/2)
4431.354	100	22560.13	$^6H^\circ_{11/2}$−25357.24 (11/2)
4430.275	100	22565.63	$^6F^\circ_{9/2}$ −30063.62 (9/2)
4430.054	10	22566.75	$^6F^\circ_{7/2}$ −29129.60 (9/2)
4425.584	35	22589.54	$^6H^\circ_{9/2}$ −24338.33 (9/2)
4424.577	25	22594.69	$^6F^\circ_{5/2}$ −28467.52 (7/2)
4422.459	10	22605.51	$^6H^\circ_{11/2}$−25402.61 (11/2)
4421.935	75	22608.19	$^6H^\circ_{11/2}$−25405.29 (13/2)
4418.871	50	22623.86	$^6F^\circ_{3/2}$ −28084.28 (5/2)*
4417.361	5*H*	22631.60	$^6H^\circ_{7/2}$ −23435.40 (9/2)
4416.422	150	22636.40	$^6H^\circ_{13/2}$−26555.44 (13/2)
4415.724	150	22639.99	$^6H^\circ_{7/2}$ −23443.79 (5/2)
4413.540	125	22651.19	$^6H^\circ_{11/2}$−25448.28 (9/2)
4412.924	75	22654.35	$^6H^\circ_{5/2}$ −22654.34 (7/2)
4412.470	500R2	22656.68	$^6H^\circ_{5/2}$ −22656.68 (5/2)
4409.938	125*S*	22669.69	$^6H^\circ_{9/2}$ −24418.44 (7/2)
4409.416	400R4	22672.37	$^6H^\circ_{13/2}$−26591.40 (13/2)
4408.552	35	22676.82	$^6H^\circ_{7/2}$ −23480.63 (9/2)
4405.370	10	22693.20	$^6F^\circ_{3/2}$ −28153.69 (5/2)
4405.063	60	22694.78	$^6H^\circ_{9/2}$ −24443.57 (9/2)
4399.722	50	22722.33	$^6H^\circ_{9/2}$ −24471.10 (7/2)
4399.305	75	22724.48	$^6H^\circ_{11/2}$−25521.55 (9/2)
4397.262	150	22735.04	$^6H^\circ_{7/2}$ −23538.86 (5/2)

TABLE 4. *Classified lines of* Pm I – Continued

λ (A)	I	σ (cm⁻¹)	Classification
4397.124	150	22735.75	$^6F^\circ_{3/2}$ – 28608.57 (3/2)
4397.066	70*D*	22736.05	$^6F^\circ_{5/2}$ – 28196.56 (1/2)
4396.252	50*U*	22740.26	$^6H^\circ_{11/2}$ – 25537.36 (13/2)
4393.466	2*W*	22754.68	$^6H^\circ_{9/2}$ – 24503.45 (11/2)
4391.001	75	22767.45	$^6H^\circ_{7/2}$ – 23571.27 (9/2)
4389.473	75	22775.38	$^6H^\circ_{13/2}$ – 26694.38 (11/2)
4388.489	400R3	22780.49	$^6H^\circ_{7/2}$ – 23584.31 (7/2)
4387.718	35	22784.49	$^6H^\circ_{9/2}$ – 24533.27 (11/2)
4387.630	100	22784.94	$^6H^\circ_{13/2}$ – 26703.97 (13/2)
4383.305	100	22807.43	$^6F^\circ_{5/2}$ – 28680.26 (7/2)
4382.852	50	22809.78	$^6H^\circ_{9/2}$ – 24558.56 (9/2)
4369.700	25*U*	22878.44	$^6F^\circ_{3/2}$ – 28338.98 (5/2)*
4369.640	300R2	22878.75	$^6H^\circ_{9/2}$ – 24627.53 (9/2)
4364.583	100	22905.26	$^6H^\circ_{5/2}$ – 22905.24 (5/2)
4363.917	350R2	22908.76	$^6H^\circ_{7/2}$ – 23712.56 (7/2)
4359.322	80	22932.90	$^6H^\circ_{9/2}$ – 24681.68 (11/2)
4358.975	5	22934.73	$^6H^\circ_{5/2}$ – 22934.70 (7/2)
4357.943	100*S*	22940.16	$^6H^\circ_{7/2}$ – 23743.96 (7/2)
4357.745	75	22941.20	$^6H^\circ_{15/2}$ – 28030.99 (13/2)
4356.625	125*D*	22947.10	$^6F^\circ_{1/2}$ – 28196.56 (1/2)
4354.545	100*B*	22958.06	$^6H^\circ_{11/2}$ – 25755.17 (11/2)
4347.715	200	22994.12	$^6H^\circ_{15/2}$ – 27383.92 (15/2)
4345.510	50	23005.79	$^6H^\circ_{9/2}$ – 24754.58 (9/2)
4339.778	80	23036.18	$^6H^\circ_{13/2}$ – 26955.22 (15/2)
4338.856	60	23041.07	$^6H^\circ_{9/2}$ – 24789.86 (9/2)
4323.458	75	23123.13	$^6H^\circ_{13/2}$ – 27042.18 (15/2)
4322.156	150	23130.09	$^6F^\circ_{3/2}$ – 29002.94 (3/2)
4321.030	20	23136.12	$^6H^\circ_{9/2}$ – 24884.90 (11/2)
4318.797	400	23148.09	$^6F^\circ_{3/2}$ – 28608.57 (3/2)
4315.905	1*W*	23163.60	$^6H^\circ_{9/2}$ – 24912.34 (11/2)
4313.197	50	23178.14	$^6H^\circ_{5/2}$ – 23178.13 (7/2)
4311.255	40*P*	23188.58	$^6H^\circ_{5/2}$ – 23188.54 (5/2)
4310.858	2	23190.72	$^6H^\circ_{13/2}$ – 27109.75 (15/2)
4309.779	15	23196.52	$^6F^\circ_{3/2}$ – 28657.02 (1/2)
4305.638	200R5	23218.83	$^6H^\circ_{11/2}$ – 26015.94 (11/2)
4305.192	35	23221.24	$^6F^\circ_{7/2}$ – 29784.08 (9/2)
4303.889	200*C*	23228.27	$^6F^\circ_{9/2}$ – 30726.26 (9/2)
4298.848	40	23255.50	$^6F^\circ_{11/2}$ – 31846.70 (11/2)
4296.687	50	23267.20	$^6H^\circ_{7/2}$ – 24071.03 (9/2)
4294.529	20	23278.89	$^6H^\circ_{5/2}$ – 23278.90 (7/2)
4293.026	10	23287.04	$^6F^\circ_{9/2}$ – 30785.03 (9/2)
4289.872	4*P*	23304.16	$^6H^\circ_{11/2}$ – 26101.28 (13/2)
4289.448	100	23306.46	$^6H^\circ_{11/2}$ – 26103.56 (11/2)
4286.776	125	23320.99	$^6F^\circ_{7/2}$ – 29883.87 (7/2)
4284.368	300R5	23334.10	$^6H^\circ_{5/2}$ – 23334.10 (5/2)
4283.751	40*P*	23337.46	$^6H^\circ_{5/2}$ – 23337.53 (7/2)
4280.448	75	23355.47	$^6H^\circ_{9/2}$ – 25104.27 (11/2)
4279.787	50*U*	23359.07	$^6F^\circ_{3/2}$ – 28608.57 (3/2)
4275.061	3	23384.90	$^6H^\circ_{11/2}$ – 26181.98 (13/2)
4272.179	100*C*	23400.67	$^6H^\circ_{7/2}$ – 24204.37 (7/2)
4270.924	50*C*	23407.55	$^6F^\circ_{1/2}$ – 28657.02 (1/2)
4269.908	10	23413.12	$^6F^\circ_{11/2}$ – 32022.32 (9/2)
4264.321	300R3	23443.79	$^6H^\circ_{5/2}$ – 23443.79 (5/2)
4247.098	150R3	23538.86	$^6H^\circ_{5/2}$ – 23538.86 (5/2)
4246.451	8	23542.45	$^6F^\circ_{3/2}$ – 29002.94 (3/2)
4238.912	60	23584.32	$^6H^\circ_{7/2}$ – 23584.31 (7/2)
4235.147	15*S*	23605.28	$^6F^\circ_{9/2}$ – 31103.24 (11/2)
4233.467	50	23614.65	$^6H^\circ_{7/2}$ – 24418.44 (7/2)
4226.453	5	23653.84	$^6H^\circ_{9/2}$ – 25402.61 (11/2)
4225.504	60	23659.15	$^6H^\circ_{11/2}$ – 26456.26 (13/2)
4224.049	75R4	23667.30	$^6H^\circ_{7/2}$ – 24471.10 (7/2)
4222.272	200	23677.26	$^6H^\circ_{13/2}$ – 27596.27 (13/2)
4218.308	50R4	23699.51	$^6H^\circ_{9/2}$ – 25448.28 (9/2)
4215.984	60	23712.58	$^6H^\circ_{5/2}$ – 23712.56 (7/2)
4210.411	15	23743.96	$^6H^\circ_{5/2}$ – 23743.96 (7/2)
4208.727	35	23753.46	$^6F^\circ_{1/2}$ – 29002.94 (3/2)
4207.865	3	23758.33	$^6H^\circ_{11/2}$ – 26555.44 (13/2)
4205.303	125	23772.80	$^6H^\circ_{9/2}$ – 25521.55 (9/2)
4201.505	15*P*	23794.29	$^6H^\circ_{11/2}$ – 26591.40 (13/2)
4196.315	85	23823.72	$^6H^\circ_{7/2}$ – 24627.53 (9/2)
4183.396	150	23897.29	$^6H^\circ_{11/2}$ – 26694.38 (11/2)
4181.722	5	23906.85	$^6H^\circ_{11/2}$ – 26703.97 (13/2)
4174.056	50	23950.76	$^6H^\circ_{7/2}$ – 24754.58 (9/2)
4167.915	50	23986.05	$^6H^\circ_{7/2}$ – 24789.86 (9/2)
4164.379	10	24006.42	$^6H^\circ_{9/2}$ – 25755.17 (11/2)
4163.572	5	24011.07	$^6F^\circ_{5/2}$ – 29883.87 (7/2)
4149.687	20*CP*	24091.41	$^6H^\circ_{5/2}$ – 24091.39 (3/2)
4146.151	150R5	24111.96	$^6H^\circ_{13/2}$ – 28030.99 (13/2)
4137.064	2	24164.91	$^6H^\circ_{13/2}$ – 27383.92 (15/2)
4136.673	15	24167.20	$^6H^\circ_{13/2}$ – 28086.21 (11/2)
4130.322	2	24204.36	$^6H^\circ_{5/2}$ – 24204.37 (7/2)
4119.631	10	24267.17	$^6H^\circ_{9/2}$ – 26015.94 (11/2)
4104.818	5*P*	24354.74	$^6H^\circ_{9/2}$ – 26103.56 (11/2)
4102.807	2	24366.68	$^6F^\circ_{9/2}$ – 31846.70 (11/2)
4094.117	75	24418.40	$^6H^\circ_{5/2}$ – 24418.44 (7/2)
4085.306	200R5	24471.07	$^6H^\circ_{5/2}$ – 24471.10 (7/2)
4076.425	2	24524.37	$^6F^\circ_{9/2}$ – 32022.32 (9/2)
4074.455	100	24536.23	$^6H^\circ_{9/2}$ – 26285.02 (7/2)
4057.716	5	24637.45	$^6F^\circ_{11/2}$ – 33246.65 (9/2)
4056.565	200R3	24644.44	$^6H^\circ_{7/2}$ – 25448.28 (9/2)
4044.537	125	24717.72	$^6H^\circ_{7/2}$ – 25521.55 (9/2)
4031.260	100	24799.13	$^6H^\circ_{11/2}$ – 27596.27 (13/2)
4007.594	150	24945.57	$^6H^\circ_{9/2}$ – 26694.38 (11/2)
3986.768	200	25075.88	$^6H^\circ_{13/2}$ – 28994.90 (11/2)
3976.162	100	25142.77	$^6H^\circ_{11/2}$ – 27939.87 (9/2)
3968.364	100	25192.17	$^6H^\circ_{15/2}$ – 30281.98 (13/2)
3961.816	300	25233.81	$^6H^\circ_{11/2}$ – 28030.99 (13/2)
3954.759	300R5	25278.84	$^6H^\circ_{11/2}$ – 28075.94 (9/2)
3953.158	50	25289.08	$^6H^\circ_{11/2}$ – 28086.21 (11/2)
3947.771	300R5	25323.59	$^6H^\circ_{13/2}$ – 29242.64 (11/2)
3943.420	25	25351.52	$^6H^\circ_{5/2}$ – 25351.46 (3/2)*
3940.912	200	25367.66	$^6H^\circ_{15/2}$ – 30457.44 (13/2)
3934.714	20	25407.61	$^6H^\circ_{7/2}$ – 26211.44 (7/2)
3930.629	15	25434.02	$^6H^\circ_{7/2}$ – 26237.84 (9/2)
3926.704	75	25459.44	$^6F^\circ_{7/2}$ – 32022.32 (9/2)
3923.982	300	25477.10	$^6H^\circ_{11/2}$ – 28274.21 (9/2)
3923.352	400	25481.20	$^6H^\circ_{7/2}$ – 26285.02 (7/2)
3916.820	200	25523.69	$^6H^\circ_{9/2}$ – 27272.46
3904.745	75	25602.62	$^6H^\circ_{9/2}$ – 27351.42 (7/2)
3895.073	200	25666.19	$^6H^\circ_{13/2}$ – 29585.21 (11/2)
3890.971	250	25693.25	$^6H^\circ_{11/2}$ – 28490.35 (9/2)
3885.792	300R3	25727.49	$^6H^\circ_{9/2}$ – 27476.28 (7/2)
3882.598	35	25748.66	$^6F^\circ_{9/2}$ – 33246.65 (9/2)
3879.598	50	25768.56	$^6H^\circ_{11/2}$ – 28565.66 (9/2)
3876.863	200	25786.74	$^6H^\circ_{13/2}$ – 29705.77 (11/2)
3874.034	300	25805.57	$^6H^\circ_{7/2}$ – 26609.39 (5/2)
3873.336	300	25810.22	$^6H^\circ_{11/2}$ – 28607.33 (9/2)
3870.862	35	25826.72	$^6H^\circ_{7/2}$ – 26630.56 (5/2)
3869.073	75	25838.66	$^6H^\circ_{13/2}$ – 29757.69 (11/2)
3854.297	75	25937.71	$^6H^\circ_{13/2}$ – 29856.72 (11/2)

TABLE 4. *Classified lines of* Pm I—Continued

λ (A)	I	σ (cm⁻¹)	Classification
3839.519	300	26037.54	$^6H^\circ_{7/2} - 26841.36$ (5/2)
3838.951	250W	26041.39	$^6H^\circ_{13/2} - 29960.42$ (11/2)*
3833.101	500R5	26081.14	$^6H^\circ_{9/2} - 27829.89$ (9/2)
3831.891	150	26089.37	$^6H^\circ_{13/2} - 30008.40$ (11/2)
3817.009	300	26191.09	$^6H^\circ_{9/2} - 27939.87$ (9/2)
3816.033	75	26197.79	$^6H^\circ_{11/2} - 28994.90$ (11/2)
3814.046	50	26211.44	$^6H^\circ_{5/2} - 26211.44$ (7/2)
3810.932	400	26232.85	$^6H^\circ_{7/2} - 27036.66$ (5/2)
3807.093	25	26259.30	$^6H^\circ_{9/2} - 28008.09$ (7/2)
3804.538	75	26276.94	$^6H^\circ_{11/2} - 29074.03$ (9/2)
3803.370	400	26285.01	$^6H^\circ_{5/2} - 26285.02$ (7/2)
3797.292	75	26327.08	$^6H^\circ_{9/2} - 28075.94$ (9/2)*
3796.513	300	26332.48	$^6H^\circ_{13/2} - 30251.50$ *
3795.800	500	26337.43	$^6H^\circ_{9/2} - 28086.21$ (11/2)
3792.125	100	26362.95	$^6H^\circ_{13/2} - 30281.98$ (13/2)
3791.842	50	26364.92	$^6H^\circ_{11/2} - 29161.96$ (9/2)
3783.806	100	26420.92	$^6H^\circ_{9/2} - 28169.71$ (7/2)
3781.429	200	26437.52	$^6H^\circ_{7/2} - 28186.31$ (7/2)
3780.768	300	26442.14	$^6H^\circ_{7/2} - 27245.99$ (5/2)
3780.284	150	26445.53	$^6H^\circ_{11/2} - 29242.64$ (11/2)
3776.986	250R4	26468.62	$^6H^\circ_{7/2} - 27272.46$
3775.419	300P	26479.61	$^6H^\circ_{5/2} - 26479.61$ (3/2)
3770.312	100P	26515.47	$^6H^\circ_{7/2} - 27319.28$ (7/2)
3769.334	75S	26522.35	$^6H^\circ_{5/2} - 26522.35$ (3/2)
3768.994	200P	26524.74	$^6H^\circ_{9/2} - 28273.52$ (7/2)
3768.895	150	26525.44	$^6H^\circ_{9/2} - 28274.21$ (9/2)
3767.052	40	26538.42	$^6H^\circ_{13/2} - 30457.44$ (13/2)
3765.747	300	26547.61	$^6H^\circ_{7/2} - 27351.42$ (7/2)
3761.678	200	26576.33	$^6H^\circ_{9/2} - 28325.13$ (7/2)
3757.007	75	26609.37	$^6H^\circ_{5/2} - 26609.39$ (5/2)
3755.190	50	26622.24	$^6H^\circ_{13/2} - 30541.28$ (11/2)
3754.020	5	26630.54	$^6H^\circ_{5/2} - 26630.56$ (5/2)
3748.122	150	26672.45	$^6H^\circ_{7/2} - 27476.28$ (7/2)
3746.530	25	26683.78	$^6F^\circ_{7/2} - 33246.65$ (9/2)
3744.846	35	26695.78	$^6H^\circ_{5/2} - 26695.79$ (5/2)
3742.973	300R4	26709.14	$^6H^\circ_{7/2} - 27512.95$ (5/2)
3741.629	150	26718.73	$^6H^\circ_{9/2} - 28467.52$ (7/2)
3740.679	300	26725.51	$^6H^\circ_{5/2} - 26725.52$ (3/2)
3738.433	200	26741.58	$^6H^\circ_{9/2} - 28490.35$ (9/2)
3731.939	200	26788.10	$^6H^\circ_{11/2} - 29585.21$ (11/2)
3727.938	300	26816.86	$^6H^\circ_{9/2} - 28565.66$ (9/2)
3726.009	500	26830.74	$^6H^\circ_{5/2} - 26830.74$ (3/2)
3724.534	100	26841.36	$^6H^\circ_{5/2} - 26841.36$ (5/2)
3722.153	400	26858.53	$^6H^\circ_{9/2} - 28607.33$ (9/2)
3715.219	200	26908.66	$^6H^\circ_{11/2} - 29705.77$ (11/2)
3712.074	35	26931.46	$^6H^\circ_{9/2} - 28680.26$ (7/2)
3708.064	75	26960.58	$^6H^\circ_{11/2} - 29757.69$ (11/2)
3704.436	200	26986.99	$^6H^\circ_{11/2} - 29784.08$ (9/2)
3699.079	75	27026.06	$^6H^\circ_{7/2} - 27829.89$ (9/2)
3697.626	300R5	27036.68	$^6H^\circ_{5/2} - 27036.66$ (5/2)
3687.381	200	27111.80	$^6H^\circ_{11/2} - 29908.90$ (9/2)
3686.328	250	27119.54	$^6H^\circ_{7/2} - 27923.37$ (5/2)
3684.088	25	27136.03	$^6H^\circ_{7/2} - 27939.87$ (9/2)
3677.558	10	27184.21	$^6H^\circ_{13/2} - 31103.24$ (11/2)
3674.848	200	27204.26	$^6H^\circ_{7/2} - 28008.09$ (7/2)
3673.896	250	27211.31	$^6H^\circ_{13/2} - 30008.40$ (11/2)
3669.218	300R5	27246.00	$^6H^\circ_{5/2} - 27245.99$ (5/2)
3666.455	15	27266.54	$^6H^\circ_{11/2} - 30063.62$ (9/2)
3665.702	20	27272.14	$^6H^\circ_{7/2} - 28075.94$ (9/2)
3664.588	25	27280.43	$^6H^\circ_{7/2} - 28084.28$ (5/2)
3658.578	75	27325.24	$^6H^\circ_{9/2} - 29074.03$ (9/2)
3655.898	100	27345.27	$^6H^\circ_{13/2} - 32435.06$ (13/2)
3655.678	50	27346.91	$^6H^\circ_{7/2} - 28150.73$ (7/2)
3655.284	50	27349.86	$^6H^\circ_{7/2} - 28153.69$ (5/2)
3655.077	20	27351.41	$^6H^\circ_{5/2} - 27351.42$ (7/2)
3653.144	300	27365.89	$^6H^\circ_{7/2} - 28169.71$ (7/2)
3646.844	300	27413.16	$^6H^\circ_{9/2} - 29161.96$ (9/2)
3641.368	100	27454.39	$^6H^\circ_{11/2} - 30251.50$ *
3639.503	300	27468.45	$^6H^\circ_{5/2} - 27468.45$ (3/2)
3639.338	350	27469.70	$^6H^\circ_{7/2} - 28273.52$ (7/2)
3639.249	150	27470.37	$^6H^\circ_{7/2} - 28274.21$ (9/2)
3637.328	35	27484.88	$^6H^\circ_{11/2} - 30281.98$ (13/2)
3636.136	20	27493.89	$^6H^\circ_{9/2} - 29242.64$ (11/2)
3633.617	25	27512.95	$^6H^\circ_{5/2} - 27512.95$ (5/2)
3632.512	3	27521.31	$^6H^\circ_{7/2} - 28325.13$ (7/2)
3630.678	50	27535.21	$^6H^\circ_{7/2} - 28338.98$ (5/2)*
3625.065	200	27577.85	$^6H^\circ_{11/2} - 30374.95$ (11/2)
3619.304	5	27621.74	$^6H^\circ_{5/2} - 27621.74$ (7/2)
3613.816	400R5	27663.69	$^6H^\circ_{7/2} - 28467.52$ (7/2)
3610.835	75	27686.53	$^6H^\circ_{7/2} - 28490.35$ (9/2)
3603.332	15	27744.18	$^6H^\circ_{11/2} - 30541.28$ (11/2)
3601.038	100	27761.85	$^6H^\circ_{7/2} - 28565.66$ (9/2)
3595.645	100	27803.49	$^6H^\circ_{7/2} - 28607.33$ (9/2)
3591.392	75	27836.41	$^6H^\circ_{9/2} - 29585.21$ (11/2)
3590.049	250	27846.82	$^6H^\circ_{9/2} - 29595.58$ (9/2)
3586.236	50	27876.43	$^6H^\circ_{7/2} - 28680.26$ (7/2)
3583.252	50	27899.64	$^6H^\circ_{9/2} - 29648.42$ (9/2)*
3580.731	20	27919.29	$^6H^\circ_{5/2} - 27919.29$ (3/2)
3580.209	100	27923.36	$^6H^\circ_{5/2} - 27923.37$ (5/2)
3579.465	100	27929.16	$^6H^\circ_{11/2} - 30726.26$ (9/2)
3577.348	25	27945.69	$^6H^\circ_{13/2} - 31846.70$ (11/2)
3575.902	100	27956.99	$^6H^\circ_{9/2} - 29705.77$ (11/2)
3571.949	100	27987.93	$^6H^\circ_{11/2} - 30785.03$ (9/2)
3569.377	50	28008.10	$^6H^\circ_{5/2} - 28008.09$ (7/2)
3569.271	100	28008.92	$^6H^\circ_{9/2} - 29757.69$ (11/2)
3565.911	40	28035.32	$^6H^\circ_{9/2} - 29784.08$ (9/2)
3559.695	500R5	28084.27	$^6H^\circ_{5/2} - 28084.28$ (5/2)
3558.878	100	28090.72	$^6H^\circ_{15/2} - 33180.50$ (15/2)
3553.264	300	28135.10	$^6H^\circ_{9/2} - 29883.87$ (7/2)
3550.916	300	28153.70	$^6H^\circ_{5/2} - 28153.69$ (5/2)
3550.109	35	28160.10	$^6H^\circ_{9/2} - 29908.90$ (9/2)
3546.808	200	28186.31	$^6H^\circ_{7/2} - 28186.31$ (7/2)
3543.627	50	28211.61	$^6H^\circ_{9/2} - 29960.42$ (11/2)*
3536.282	50	28270.21	$^6H^\circ_{7/2} - 29074.03$ (9/2)
3535.869	300	28273.51	$^6H^\circ_{5/2} - 28273.52$ (7/2)
3531.795	75	28306.12	$^6H^\circ_{11/2} - 31103.24$ (11/2)
3530.711	200	28314.82	$^6H^\circ_{9/2} - 30063.62$ (9/2)
3529.426	2	28325.12	$^6H^\circ_{5/2} - 28325.13$ (7/2)
3527.701	250	28338.97	$^6H^\circ_{5/2} - 28338.98$ (5/2)*
3525.319	75	28358.12	$^6H^\circ_{7/2} - 29161.96$ (9/2)
3511.772	20	28467.51	$^6H^\circ_{5/2} - 28467.52$ (7/2)
3505.794	100	28516.05	$^6H^\circ_{13/2} - 32435.06$ (13/2)
3494.457	5	28608.56	$^6H^\circ_{5/2} - 28608.57$ (3/2)
3492.308	15	28626.16	$^6H^\circ_{9/2} - 30374.95$ (11/2)
3485.722	50	28680.25	$^6H^\circ_{5/2} - 28680.26$ (7/2)
3472.223	10	28791.75	$^6H^\circ_{7/2} - 29595.58$ (9/2)
3472.132	25	28792.50	$^6H^\circ_{9/2} - 30541.28$ (11/2)
3465.864	35	28844.58	$^6H^\circ_{7/2} - 29648.42$ (9/2)*
3449.970	50	28977.46	$^6H^\circ_{9/2} - 30726.26$ (9/2)
3449.639	25	28980.24	$^6H^\circ_{7/2} - 29784.08$ (9/2)

TABLE 4. *Classified lines of* Pm I—Continued

λ (A)	*I*	σ (cm^{-1})	Classification	λ (A)	*I*	σ (cm^{-1})	Classification
3442.984	50	29036.25	$^6H^\circ_{9/2}$ −30785.03 (9/2)	3345.327	20	29883.85	$^6H^\circ_{5/2}$ −29883.87 (7/2)
3437.803	15	29080.01	$^6H^\circ_{7/2}$ −29883.87 (7/2)	3341.011	50	29922.46	$^6H^\circ_{7/2}$ −30726.26 (9/2)
3420.721	75	29225.22	$^6H^\circ_{11/2}$−32022.32 (9/2)	3334.464	75	29981.21	$^6H^\circ_{7/2}$ −30785.03 (9/2)
3416.680	40	29259.79	$^6H^\circ_{7/2}$ −30063.62 (9/2)				
3416.484	50	29261.47	$^6H^\circ_{13/2}$−33180.50 (15/2)	3319.548	25	30115.92	$^6H^\circ_{9/2}$ −31846.70 (11/2)
				3302.264	25	30273.53	$^6H^\circ_{9/2}$ −32022.32 (9/2)
3405.661	3	29354.45	$^6H^\circ_{9/2}$ −31103.24 (11/2)	3283.174	25	30449.56	$^6H^\circ_{11/2}$−33246.65 (9/2)
3373.083	75	29637.95	$^6H^\circ_{11/2}$−32435.06 (13/2)	3202.305	25	31218.48	$^6H^\circ_{7/2}$ −32022.32 (9/2)

We acknowledge the very generous assistance of John Conway and Earl Worden of the Lawrence Radiation Laboratory in preparing the electrodeless lamps and in other phases of our experiment. We also thank Mark Fred and Frank Tomkins of the Argonne National Laboratory for their help in photographing the first set of wavelength and Zeeman effect plates, and Henry Crosswhite of the Johns Hopkins University for his suggestions concerning the calculation of the parameters. Our success in making the recent plane-grating spectrograms is due in large measure to the efforts of Richard J. Wolff. Some of the Zeeman plates were measured and reduced at the Argonne National Laboratory by Thomas Dickinson. The Zeeman plates taken at M.I.T. by L. Johnson were made available to us by Lee C. Bradley, III.

5. References

[1] J. A. Marinsky and L. E. Glendenin, Chem. Eng. News **26**, 2346 (1948).
[2] W. F. Meggers, B. F. Scribner, and W. R. Bozman, J. Res. NBS **46**, 85 (1951) RP2179.
[3] P. F. A. Klinkenberg and F. S. Tomkins, Physica **26**, 103 (1960).
[4] J. Reader and S. P. Davis, J. Opt. Soc. Am. **53**, 431 (1963).
[5] J. Reader, Phys. Rev. **141**, 1123 (1966).
[6] H. J. Stapleton, C. D. Jeffries, and D. A. Shirley, Phys. Rev. **124**, 1455 (1961).
[7] B. Budick and R. Marrus, Phys. Rev. **132**, 723 (1963).
[8] J. Reader and J. Sugar, J. Opt. Soc. Am. **56**, 1189 (1966).
[9] F. S. Tomkins and M. Fred, Spectrochimica Acta **6**, 139 (1954).
[10] F. S. Tomkins and M. Fred, Applied Optics **2**, 715 (1963).
[11] J. G. Conway, S. P. Davis, and R. J. Wolff, J. Opt. Soc. Am. **57**, 583 (1967).
[12] E. F. Worden, R. G. Gutmacher, and J. G. Conway, Applied Optics **2**, 707 (1963).
[13] J. Reader, L. C. Marquet, and S. P. Davis, Applied Optics **2**, 963 (1963).
[14] W. F. Meggers and R. W. Stanley, J. Res. NBS **69A** (Phys. and Chem.) No. 2, 109 (1965).
[15] J. G. Conway and B. G. Wybourne, Phys. Rev. **130**, 2325 (1963).
[16] J. G. Conway, private communication (1966).
[17] A. G. Shenstone, Can. J. Phys. **38**, 677 (1960).
[18] A. G. Shenstone, Phil. Trans. Roy. Soc. London **241**, 297 (1948).
[19] G. Smith and B. G. Wybourne, J. Opt. Soc. Am. **55**, 121 (1965).
[20] J. Sugar, private communication (1967).
[21] B. R. Judd, Seventh Brookhaven Conference on Molecular Beams and Atomic Resonance, Uppsala, Sweden (1964)—unpublished.
[22] C. W. Nielson and G. F. Koster, Spectroscopic Coefficients for the p^n, d^n, and f^n Configurations (The MIT Press, Cambridge, Mass., 1963).
[23] R. Trees, Phys. Rev. **83**, 756 (1951); **84**, 1089 (1951).
[24] N. Spector, J. Opt. Soc. Am. **55**, 192 (1965).
[25] R. Trees, J. Opt. Soc. Am. **54**, 651 (1964).
[26] H. M. Crosswhite, private communication (1967).
[27] H. Horie, Progr. Theoret. Phys. (Kyoto) **10**, 296 (1953).
[28] B. G. Wybourne, Spectroscopic Properties of Rare Earths, pp. 78–82 (Interscience Publishers, New York, 1965).
[29] B. R. Judd, Proc. Phys. Soc. (London) **A69**, 157 (1956).
[30] M. Blume, A. J. Freeman, and R. E. Watson, Phys. Rev. **134**, A320 (1964).

(Paper 71A6–475)

JOURNAL OF RESEARCH of the National Bureau of Standards—C. Physics and Chemistry
Vol. 71A, No. 6, November–December 1967

Publications of the National Bureau of Standards*

Selected Abstracts

Effects of finite lattice heat capacity on spin-lattice relaxation theory and numerical analysis, R. L. Peterson, *Mono. 102 (Aug. 1, 1967)*

The transient magnetic behavior of a paramagnetic substance, after an initial disturbance, is considered theoretically for a variety of situations in which the lattice temperature rises as a result of energy flow from the magnetic (electron spin) system. The relaxation mechanisms considered are the direct process, involving interaction between spins and the resonant-phonon modes, and a T^9 Raman process, involving the remaining phonon modes. It is first assumed that the resonant and remaining modes are strongly coupled to each other, and that the helium bath has been removed (helium temperatures are assumed). The resulting transient behavior typically does not differ much from exponential relaxation (the rate increases somewhat during the relaxation), but the difference should be experimentally observable, particularly if the resonance line is inverted initially.

Next, the opposite extreme is considered—that in which the resonant and remaining modes are totally uncoupled; the helium bath is again assumed to have been removed. Two dramatic effects can then occur, depending upon initial conditions. One is the rapid decay to saturation from initial inversion, due to an avalanching creation of resonant phonons by the spins. The second is the pronounced inhibition of the subsequent decay, with the spins remaining near saturation. This decay rate is typically very much slower than the Raman rate, and is due to the flow of the resonant-phonon energy back into the spin system as the spin energy flows into the remaining lattice. Eventually the rate increases to the Raman rate characteristic of the final lattice temperature. Because of inelastic phonon scattering at crystal boundaries, which couples the phonon modes together, this effect of inhibited decay may be difficult to observe. Finally, we consider the case of spins coupled only to the resonant phonons, which in turn are coupled to a constant temperature bath, whether this be the helium or the remaining modes. Recent phonon avalanche experiments are discussed in this context. It is pointed out that such experiments, performed in the absence of a bath, may provide a reliable measurement of inelastic phonon-boundary scattering.

Key Words: Spin-lattice relaxation, phonon bottleneck, phonon-boundary scattering, spin-phonon interactions.

NBS standard frequency and time services, radio stations WWV, WWVH, WWVB, WWVL, *Misc. Publ. 236, 1967 Edition (1967).*

Detailed descriptions are given of eight technical services provided by the National Bureau of Standards radio stations WWV, WWVH, WWVB, and WWVL. These services are: 1. Standard radio frequencies; 2. Standard audio frequencies; 3. Standard musical pitch; 4. Standard time intervals; 5. Time signals; 6. UT2 corrections; 7. Radio propagation forecasts; and 8. Geophysical alerts. In order to provide users with the best possible services, occasional changes in the broadcasting schedules are required. This publication shows the schedules in effect on June 1, 1967. Annual revisions will be made. Advance notices of changes occurring between revisions will be sent to regular users of these services upon request.[1] Current data relating to standard frequencies and time signals are also available monthly in the Time and Frequency Services Bulletin.[2]

Key Words: Broadcast of standard frequencies, high frequency, low frequency, standard frequencies, time signals, very low frequency.

Standard Reference Materials: Recommended method of use of standard light-sensitive paper for calibrating carbon arcs used in testing textiles for color-fastness to light, E. Passaglia and P. J. Shouse, *Misc. Publ. 260–15 (July 21, 1967).*

The use of NBS Light-Sensitive Paper and NBS Booklets of Standard Faded Strips in the standardization of fading lamps is described. These lamps are used to determine the fading characteristics of textiles, and the light-sensitive paper is thus useful in standardizing this procedure.

Key Words: Light-sensitive paper; booklets of faded strips; fading characteristics; textiles; fading standardization.

Determination of trace elements in standard reference materials by neutron activation analysis, G. W. Smith, D. A. Becker, G. J. Lutz, L. A. Currie, and J. R. DeVoe, *Anal. Chem. Acta* **38,** *333–340 (1967).*

Neutron activation analysis with its high sensitivity and accuracy in trace analysis, is being used at the NBS for analysis of Standard Reference Materials. Problems affecting precision and accuracy have been encountered and solutions to four problems are discussed. First, the positive bias introduced by induced radioactivity of similar gamma-ray energy was found in the determination of interstitial argon in ultra-pure silicon. A decay curve resolution technique was used to compensate for the error. Secondly, errors due to differences in geometrical location between sample and standard during irradiation were observed. Flux gradients were determined by copper foil flux monitoring to give necessary means of correction. Thirdly, errors are caused by differences in neutron self-shielding between sample and standard during irradiation. An empirical correction method was used and computer program written for calculation. Examples are given. Finally, the problem of gamma-ray attenuation during counting of sample and standard has been explored. A theoretical and experimental study gives the necessary corrections. It is concluded that careful study is vital to assure accurate analyses by neutron activation analysis on trace elements in complex matrices such as many Standard Reference Materials.

Key Words: Neutron, activation, analysis, trace, Standard Reference Materials, accuracy, precision, similar gamma-ray energy, decay curve resolution, geometrical location, neutron self-shielding, gamma-ray attenuation.

Distillation as a tool for purification of research quantities of material, R. T. Leslie, *Ann. N. Y. Acad. Sci.* **137,** *19–29 (1966).*

Distillation can increase the purity of nearly any real vaporizable mixture if sufficient effort is made. The method is invaluable for purifying relatively small quantities of material for research purposes. The selection of the proper still column for a particular problem can be based on a knowledge of the characteristics of a few basic types of columns. Some operating procedures which favor good results can be outlined in a general way, but testing of stills by the operator using mixtures whose behaviors can be predicted under various conditions is recommended.

Some possibilities for the improvement of still columns is suggested.

Gas phase radiolysis of cyclobutane, R. D. Doepker and P. Ausloos, *J. Chem. Phys.* **44,** *1641–1647 (Feb. 1966).*

The gas phase radiolysis of cyclo-C_4H_8 and cyclo-C_4D_8 has been investigated in the presence of O_2, NO, H_2S, NH_3, and several or-

277-259 O - 68 - 14

ganic compounds. From the products formed, it could be inferred that the following fragmentation processes occur:

$$C_4H_8^+ - C_3H_5^+ + CH_3$$

$$C_4H_8^+ - C_2H_4^+ + C_2H_4$$

$$C_4H_8^+ - C_2H_5^+ + C_2H_3$$

$$C_4H_8^+ - C_3H_4^+ + CH_4$$

At 20 torr, the ion pair yields which can be ascribed to some of these processes are lower than the corresponding ion pair yields observed in the mass spectrometer at a pressure of 10^{-5} torr.

When compounds such as NO (I.E = 9.25 eV) or $(CH_3)_3N$ (I.E = 7.8 eV) are added to cyclobutane, butene (I.E = 9.13 − 9.58 eV) is a major product. On the other hand, when organic or inorganic compounds whose ionization energy is higher than that of butene are added to cyclobutane, the yield of butene is, in most cases, negligibly small. The formation of butene can be tentatively accounted for by a ring opening of the parent ion followed by charge transfer. On the basis of this mechanism, a minimum value of 0.42 with an estimated possible deviation of 0.02 can be ascribed to $M(C_4H_8^+)/N$. When an electrical field is applied in the saturation current region, during radiolysis of cyclobutane-NO mixtures, the yields of methane, ethane and butene which have the parent ion or fragments thereof as precursors, remain unchanged. On the other hand, the yields of products such as ethylene, allene, acetylene, and 1,3-butadiene whose formation is, in part, attributed to the decomposition of neutral excited molecules, are seen to increase due to increased excitation by electron impact. In the absence of an electrical field, the number of neutral excited molecule decompositions per ion pair is estimated to be $\leq 0.65 \pm 0.05$.

Key Words: Cycloalkanes, ion-molecule reactions, ion-pair yields, radiolysis unimolecular decomposition.

Investigating ion-molecule reactions by analyzing neutral products formed in the radiolysis and photoionization of hydrocarbons, P. Ausloos, S. G. Lias, and A. A. Scala, *Adv. Chem. Ser.* **58,** *264–277 (1966).*

The analysis of neutral products produced in the radiolysis and photoionization of suitable deuterium labled hydrocarbons or hydrocarbon mixtures provides information concerning: (a) the relative rates of H^+, H^-, H_2^+, and H_2-transfer reactions; and (b) the structure of the reacting ion or reaction complex. The reaction cross section of a given ion with various alkanes is generally seen to increase with increasing polarizability of the neutral molecule. The actual increase in rate is, however, faster than that of the collision cross section given by the expression: $2\pi e(\alpha/\mu)^{1/2}$. Good quantitative and qualitative correspondence is seen between the information on reactions of parent ions obtained from gas phase radiolysis studies and that derived from photoionization experiments carried out at wavelengths slightly above the ionization energy of the molecule.

Mass spectrometric study of the photoionization of small molecules, V. H. Dibeler, R. M. Reese, and M. Krauss, *(Proc. 3d Intern. Conf. Mass Spectrometry, Paris, France, Sept. 1964), Book, Advances in Mass Spectrometry* **3,** *471–488 (Institute of Petroleum, London, England, 1966).*

A windowless vacuum untraviolet monochromator and mass spectrometer are combined for the study of photoionization processes in the energy range 2000 to 600A. The apparatus and techniques of measurement are described briefly and photoionization curves are given for the molecules: argon, krypton, xenon, hydrogen, deuterium, acetylene, acetylene-d_2, benzene, and benzene-d_6. The ionization energies of the $^2P_{3/2}$ and $^2P_{1/2}$ states of the rare gases are measured and autoionized levels are observed between the doublets of krypton and xenon. The first ionization energies of H_2 and D_2 are measured and autoionization ascribed to the D and D', $^1\pi_u$ state is observed. First ionization energies of C_2H_2, C_2D_2, C_6H_6 and C_6D_6 are measured and vibrational levels of the ground state of the ions are detected. No electronically excited state is observed in acetylene at energies below 14 eV. In benzene, autoionized Rydbergs are observed leading to a second onset of ionization about 2.2 eV above the first ionization threshold. The shape of the curve above the first onset suggests similar energies for the lowest bonding π and σ orbitals.

Microwave spectrum of excited vibrational states of FCN, W. J. Lafferty, and D. R. Lide, Jr., *J. Mol. Spectry.* **23,** *No. 1, 94–96 (May 1967).*

The microwave and infrared spectra of FCN are reported. The band centers of ν_2^1 and ν_1 have been obtained from resolved infrared bands. The band center for $2\nu_2^0$ has been obtained both from a "hot band" Q branch and, less accurately, by direct observation of the unresolved band. The rotational constants of all Σ vibrational states up to *ca.* 2100 cm^{-1}, and several π and Δ states have been obtained from the microwave spectrum. Combination of the microwave and infrared work permits correction for the Fermi resonance between ν_1 and $2\nu_2^0$. Unperturbed vibrational frequencies for $2\nu_2^0$ and ν_1 are reported. The value of the Fermi resonance matrix element is $35.2_8 \pm .4$ cm^{-1}.

Key Words: Fermi resonance, infrared spectrum, microwave spectrum, rotational constants, unperturbed vibrational frequencies, vibrational spectrum.

Microwave spectrum, structure, dipole moment, and barrier to internal rotation of phosphorus trifluoride-borane, R. L. Kuczkowski and D. R. Lide, Jr., *J. Chem. Phys.* **46,** *No. 1, 357–365 (Jan. 1967).*

The microwave spectrum of several isotopic species of phosphorus trifluoride borane ($F_3P^{11}BH_3$) has been measured and the following structural parameters determined: $d(BH) = 1.207 \pm 0.006$ Å; $d(PF) = 1.538 \pm 0.008$ Å; $d(PB) = 1.836 \pm 0.012$ Å; $\angle HBH = 115°04' \pm 1°$; $\angle FPF = 99°50' \pm 1°$. The dipole moment was evaluated from Stark splitting as 1.64 ± 0.02 D.

The vibrational satellite spectrum associated with the excited ν_{12} (E) and ν_6 (A_2) states for $F_3P^{11}BH_3$ was found to be strongly perturbed and was fitted to the theory for a first order Coriolis interaction. The analysis of this perturbation and the measurement of the ν_{12} fundamental in the infrared spectrum permitted the inactive torsional fundamental ν_6 to be determined as 197 ± 5 cm^{-1}. This leads to a potential barrier to internal rotation of 3240 ± 150 cal/mol.

The enthalpy of dissociation for the reaction $2F_3PBH_3 \rightleftharpoons 2PF_3 + B_2H_6$ (298°) was determined as 10.99 kcal/mol. The experimental results are compared to those found for other related compounds.

The indicated uncertainties represent maximum error believed to be possible.

Key Words: Barrier, Coriolis, dipole moment, microwave spectrum, phosphorus trifluoride-borane.

Microwave studies of rotational isomerism, D. R. Lide, Jr., *Trans. Am. Cryst. Assoc.* **2,** *106–116 (1966).*

The application of microwave spectroscopy to the study of rotational isomerism is reviewed. Molecules of the butadiene type are found to exist predominantly in the planar *trans* form; no spectra from other isomers have been detected. Normal propyl compounds show both *trans* and *gaucha* isomers at room temperature. Two isomers are also found in propionaldehyde and related compounds. Conclusions regarding structure and stability of rotational isomers are discussed.

Key Words: Butadiene, isomerism, microwave spectroscopy, propionaldehyde, rotational, structure.

Monomer-polymer equilibria of deuterated alpha-methylstyrenes, L. J. Fetters, W. J. Pummer, and L. A. Wall, *J. Polymer Sci.* **4,** *Part A-1, 3003–3011 (1966).*

The equilibria between α-trideuteromethyl-β,β-dideuterostyrene, α-methyl-2,3,4,5,6-pentadeuterostyrene and perdeutero-α-methylstyrene and their respective polymeric anion in tetrahydrofuran has been investigated between 253° and 308 °K. The heat and entropy changes were both increased by deuteration of the alkyl group. Qualitatively the effect observed appears best explained by the premise that a lowering of steric repulsions occurs with deuterium; and hence the effective volume for deuterium is less than that for hydrogen.

Key Words: Anionic polymerization, heats and entropies of the polymerizations of deuterated α-methylstyrenes.

Mössbauer spectroscopy: applications to aerospace, J. R. DeVoe and J. J. Spijkerman, *Book, Radioisotopes for Aerospace, Part 2, Systems and Applications, pp. 254–269 (Plenum Press, Inc., New York, N.Y., 1966).*

The principle of the Mössbauer Effect will be discussed. A few possible applications of the technique with respect to physics and engineering in aerospace will be outlined. Of greater interest are the possible applications of the technique for determining chemical structure and solid state properties of materials. Solid phase transitions of materials subjected to severe conditions similar to that existing in space can be measured by Mössbauer Effect.

The National Bureau of Standards' Mössbauer spectrometer will be discussed and some data taken on a number of materials (such as tecktites, steels, glasses, and metal alloys) will be presented.

Key Words: Aerospace, applications, materials structure analysis, Mössbauer Effect, spectrometer, standards.

Needs of American Chemical Society members for property data, H. M. Weisman, *J. Chem. Doc.* **7,** *No. 1, 10–14 (Feb. 1967).*

In August of 1965 the American Chemical Society, on behalf of the NBS Office of Standard Reference Data, sent a questionnaire to its membership asking for information on their needs for compilations of critically evaluated data. Through this questionnaire, the Office of Standard Reference Data obtained information on the preferences and needs of the chemical profession for data compilations, and equally importantly, located a substantial number of compilation activities of which it was not aware. Further, the Office of Standard Reference Data identified dozens of individuals who are both interested and competent to undertake additional projects. Approximately 16,000 replies were received. Overwhelmingly, response was that present compilations of data satisfy poorly or at best only moderately the requirements of the membership of ACS. The survey identified the properties which ACS Workers most often sought in the literature as well as those data compilations most often consulted by respondents. Many worthwhile comments and suggestions were contributed as to approaches taken, compilation priorities and techniques of format and presentation.

Key Words: American Chemical Society, Chemical and Physical Properties, compilation, data, NSRDS, Office of Standard Reference Data, questionnaire, survey, users.

Photolysis of cyclopentane at 1470, 1236, and 1048–67 A, R. D. Doepker, S. G. Lias, and P. Ausloos, *J. Chem. Phys.* **46,** *No. 11, 4340–4346 (June 1, 1967).*

The photolysis of cyclopentane has been investigated at 1470, 1236 and 1048–67 Å. The primary process, cyclo-$C_5H_{10} + h\nu \rightarrow C_5H_8 + H_2$ is of major importance at 1470 Å, but its quantum yield diminishes at shorter wavelengths where processes involving C–C cleavage become more predominant. The products formed in the gas phase photolysis of cyclo-C_5D_{10}–H_2S mixtures and in the solid phase phopropane formed in the photoionization of $C_5D_{10} - C_5H_{10} - O_2$ mixtures it is shown that the parent ion dissociates as follows: $C_5H^+_{10} \rightarrow$ phase, the internally excited 1-pentene decomposes entirely to form methyl and ethyl radicals. Evidence is also obtained for the occurrence of the dissociative process: $C_5H^+_{10} \rightarrow C_2H_4 + C_3H_6$ where C_3H_6 consists of cyclopropane and propylene. At 1048–67 Å (11.6–11.8 eV) ionization is extensive (ionization potential of cyclo-C_5H_{10} = 10.5 V). Saturation current measurements yielded a value of 0.68 for $\eta_{C_5H_{10}}/\eta_{N_2O}$. On the basis of an isotopic analysis of the propane formed in the photoionization of $C_5D_{10} - C_5H_{10} - O_2$ mixtures it is shown that the parent ion dissociates as follows: $C_5H_{10} \rightarrow C_3H_6 + C_2H_4$ and that the $C_3H_6^+$ ions participate in an H_2^- transfer reaction: $C_3H^+_6 + C_5H_{10} \rightarrow C_3H_8 + C_5H^+_8$ Fragmentation of the parent ion diminishes with an increase in pressure. The collisonal deactivation process is more pronounced for the perdeuterated than for the perprotonated cyclopentane ion. The data also indicate that a fraction of the parent ions undergoes ring opening to form cis or trans 2-pentene as a final product.

Key Words: Photolysis, photoionization, cycloalkanes, ion molecule reactions, free radical reactions, cyclopentane.

Simultaneous determination of copper and zinc in human lung tissue by neutron activation analysis. R. G. Keenan, J. H. Marcus, and J. R. DeVoe, *Am. Ind. Hygiene Assoc. J.* **27,** *128–134 (Mar.–Apr. 1966).*

Certain trace elements including copper and zinc are constituents of numerous enzymes and function as essential catalysts in biosyntheses. The expanded interest in these substances has supplied a demand for microanalytical techniques of increased sensitivity, accuracy and precision if meaningful conclusions are to be derived from the analytical data. This paper shows that good precision may be realized in the activation analysis of complex biological specimens with only a few one-step chemical separations.

The nuclear reactions Cu^{63} (n, γ) Cu^{64} (12.8h) and Zn^{68} (n, γ) Zn^{69m} (13.8h) were used for the analysis. The samples were irradiated in a thermal neutron flux of 10^{13} n/cm^2/sec. The copper was extracted as the acetylacetonate into chloroform from an acetate system buffered at a *p*H of 4.75. The remaining aqueous phase was extracted with chloroform to remove most of the acetylacetone dissolved in the aqueous phase. The zinc was extracted as the dithizonate into chloroform and was back-extracted into 1% HCl for counting. Careful internal standardization was used for correction of results for variation in chemical yields.

Applications of the method to the simultaneous determination of copper and zinc in lung samples provided values of the same order of magnitude as those reported by Tipton and Cook for U.S. adults using emission-spectrographic procedures which were between 7 and 10 ppm for copper and 40 and 70 ppm for zinc. Comparison of the precision of this method with that of emission spectroscopy indicates that this activation technique has at least three times better precision.

The crystal structure of sodium tetraborate, A. Hyman, A. Perloff, F. Mauer, and S. Block, *Acta Cryst.* **22,** *No. 6, 815–821 (June 1967).*

Single crystals of sodium tetraborate, $Na_2O \cdot 4B_2O_3$, have been synthesized and studied. The structure has been determined using the method of symbolic addition. The space group is $P2_1/a$ with unit cell dimensions: $a = 6.507 \pm 0.001$, $b = 17.796 \pm 0.002$, $c = 8.377 \pm 0.001$, and $\beta = 96°34' \pm 2'$; $Z = 4$. The structure consists of two infinite, independent, and interlinking boron-oxygen networks, each containing alternating single and double rings. The sodium atoms serve to hold the networks together through coordination with oxygen atoms.

Key Words: Crystal structure, x-ray, sodium tetraborate, symbolic addition.

The determination of bound styrene soluble high styrene-butadiene resins, M. A. Post, *J. Paint Technol.* **38,** *No. 497, 336–342 (June 1966).*

Bound styrene is determined in insoluble emulsion polymerized styrene-butadiene copolymers by measurement of the 10.3μm/13.2μm absorbance ratio using the baseline method. This ratio is obtained from the infrared spectrogram of the copolymer and the styrene content is determined from a standard curve. The standard curve is constructed from absorbance ratios of 10.3μm/13.2μm derived from the infrared spectrograms of cast films of styrene-butadiene latexes over a range of percentage compositions. Bound styrene is determined in these latexes by nitration of the isolated and extracted copolymers. Styrene content based on nitration is determined from standard curves relating styrene concentration to spectrophotometric absorbance measurements at wavelengths of 285.0, 273.8, and 265.0 nm. The source of the styrene for these curves is NBS standard rubber #1500.

Key Words: Absorbance ratio method, bound styrene, infrared, insoluble styrene-butadiene copolymers, masonry paints.

The microwave spectrum and dipole moment of pyrazole, W. H. Kirchhoff, *J. Am. Chem. Soc.* **89,** *No. 7, 1312–1316 (Mar. 1967).*

The microwave spectrum of pyrazole in the region 8000 Mc/s to 35000 Mc/s has been assigned. The rotational constants are $a = 9618.92 \pm 0.14$ Mc/s, $B = 9412.59 \pm 0.13$ Mc/s and $C = 4755.88 \pm 0.11$ Mc/s. The dipole moment $\mu = 2.214 \pm 0.015$ D, was calculated from the Stark effect of the $0_{0,0} \rightarrow 1_{0,1}$ and $0_{0,0} \rightarrow 1_{1,1}$ transitions but only after the perturbation treatment had been extended to fourth order. The indicated uncertainties are three times the standard errors

obtained from the least squares fit. The interpretation of the data shows that in the gas phase pyrazole is a planar molecule with no in-plane symmetry axis.

Thermal decomposition of 4,4-dimethylpentene-1 in a single-pulse shock tube, W. Tsang, *J. Chem. Phys.* **46,** *No. 7, 2817–2822 (Apr. 1, 1967).*
4,4-Dimethylpentene-1 has been pyrolyzed in a single pulse shock tube. The initial process is apparently the breaking of the allylic carbon-carbon bond. The rate expression for the reaction,

$$C_4H_9-C_3H_5 \xrightarrow{k} t-C_4H_9\cdot + C_3H_5.$$

has been found to be

$$k = 10^{15.8} \exp(-65{,}500/RT)\ \text{sec}^{-1}.$$

Assuming no activation energy for the recombination process this leads to a value of 12 kcal for the allylic resonance energy.

Key Words: 4,4-Dimethylpentene-1, allyl radicals, *t*-butyl radicals, thermal decomposition, bond energy, allylic resonance energy, single pulse shock tube, 1-butene, 4-methylpentene-1, 1,5 hexadiene.

Two National Bureau of Standards data centers: chemical kinetics and mass spectrometry, D. Garvin and H. M. Rosenstock, *J. Chem. Doc.* **7,** *No. 1, 31–34 (Feb. 1967).*
Two current information retrieval centers, one for chemical kinetics, the other for mass spectrometry are described. The methods and philosophies of operation of these programs are compared. The role of specialized information systems in promoting data evaluation, the evaluation of their usefulness as sources for reference material, the choice of techniques and possibilities for inter-center coordination are discussed.

Key Words: Chemical kinetics, mass spectrometry, information retrieval.

Vapor deposition of tungsten by hydrogen reduction hexafluoride process variables and properties of the deposit, J. F. Berkeley, A. Brenner, and W. E. Reid, Jr., *J. Electrochem. Soc.* **114,** *No. 6, 561–568 (June 1967).*
An investigation of the variables involved in the deposition of tungsten from a mixture of tungsten hexafluoride and hydrogen has shown that the fastest rate of deposition (about 5 mils thickness in 2 min) was obtained at atmospheric pressure with a hydrogen/tungsten hexafluoride ratio of 1.5 (by volume) at a temperature of 800°–850 °C. The presence of hydrogen fluoride or chloride in the reacting gases diminished the rate of deposition. The deposits had about the same hardness, electrical conductivity, and density as commercial wrought tungsten. The tensile strength of the deposits was about 30,000 lb/in.^{2}. The internal stress within the deposits was also about 30,000 lb/in.^{2}. Codeposition of carbon, from carbon monoxide, greatly increased the hardness of the deposits.

The Bi I–II transition pressure measured with a dead-weight piston guage, P. L. M. Heydemann, *J. Appl. Phys.* **38,** *No. 6, 2640–2644 (May 1967).*
A dead weight piston gage was used to determine the Bismuth I–II transition pressure and the volume change at the transition. The transition pressure for one sample, believed to contain less than .001% impurities, was found to be 25,306 ± 60 bars. With another sample, of substantially less purity and of larger grain size, a transition pressure of 25,500 ± 60 bars was measured. The average relative volume change was .035.

Key Words: Free piston gage, bismuth, polymorphic phase transition, transition pressure, volume change, high pressure.

Calibration of germanium thermometers from 2° to 20 °K, G. Cataland and H. H. Plumb, *(Proc. Intern. Inst. Refrigeration, Commission 1, Boulder, Colorado, 1966, Annexe 1966–5), Suppl. Bull. Inst. Intern. Froid, pp. 153–163 (Louvain, Belgium, 1966).*
SUMMARY: The National Bureau of Standards Provisional Temperature Scale 2–20 (1965) has been established for calibrating thermometers between 2° and 20 °K. The scale is the result of measurements with the National Bureau of Standards Acoustical Thermometer which determined isotherms of the speed of sound in helium-4 gas as a function of pressure. The isotherms were extrapolated to zero pressure, to approximate an "ideal gas," and from the intercepts values of temperature on the Thermodynamic Temperature Scale have been calculated. A group of reproducible germanium thermometers, calibrated at the isotherm temperatures, maintain the scale [NBS P 2–20 (1965)] against which submitted thermometers are calibrated.
To perform calibrations of submitted thermometers, a comparator was constructed. The temperature of the comparator can be maintained constant within 0.005 °K for extended periods of time an any desired temperature within the calibration range. Calibrations of submitted thermometers consist of resistance determinations at approximately each degree from 2° to 20 °K. We attempt to fit a polynomial of the form

$$\log_{10} R = \sum_{n=0}^{m} A_n (\log_{10} T)^n,$$

—where the upper limit of m is varied in individual functional fittings from 3 to 8—to the individual resistor's calibration. For some types of resistors reasonable fittings (± .005 °K) of the calibration data are achieved.

Key Words: Calibration at low temperature, germanium resistors, low temperature thermometry.

Computer aided typesetting, W. R. Bozman, *Book, Advances in Computers,* **7,** *Chapt. 4, 195–207 (Academic Press, Inc., New York, N.Y., 1966).*
Several examples are given of typesetting prepared by a computer.

Key Words: Photocomposition, typesetting, computers, printing, automation, publication.

Invariance of the homology of a lattice, J. Mather, *Proc. Am. Math. Soc.* **17,** *No. 5, 1120–1124 (Oct. 1966).*
Rota, Kan, Peterson and Whitehead have developed a homology theory for finite lattices which *a priori* depends upon the choice of a cross-cut of the lattice. It is shown here that the different cross-cuts of a lattice lead to simplicial complexes which have the same homotopy type and are therefore homology equivalent.

Key Words: Homology, lattice, combinatorics.

A comparator for thermal AC-DC transfer standards, R. S. Turgel, *Proc. 21st Annual ISA Conference and Exhibit, New York, N.Y., Oct. 24–27, 1966, ISA Preprint 12.3–1–66 (Oct. 1966).*
Thermal transfer standards play an important role in precision a-c measurements. They are calibrated by intercomparison with standards of known ac-dc differences. A comparator is described that simplifies such routine calibrations. A sequence of null balances in the measuring circuit operates a simple analog computer which indicates the result of the intercomparison directly in parts per million of ac-dc difference.

Key Words: A-C, D-C, calibration, transfer standard, thermoelement, intercomparison.

Calibration of the NBS photoelectric pyrometer of 1961, R. D. Lee, *Proc. 7th session, Comite Con. de Thermometrie, Paris, France, pp. 74–78 (Sept. 24, 1964).*
Factors affecting the reproducibility of the NBS Photoelectric Pyrometer are listed, and progress in reducing these factors are described. A calibration to realize the International Practical Temperature Scale (IPTS) above 1063 °C to 1256 °C is described. At present, the estimated uncertainty in realizing the IPTS is about 0.1 °C at 1063 °C, 0.2 °C at 1256 °C, and is predicted to be 0.8 °C at 2400 °C.

Cyrogenic thermocouple thermometry, L. L. Sparks and R. L. Powell, *Meas. Data,* **1,** *No. 2, 82–90 (Mar.–Apr. 1967).*
Commercially available low-temperature thermocouple wire from all major U.S. manufacturers has been exhaustively tested to determine the inhomogeneity and interchangeability characteristics of the wire. Spot calibrations between liquid-helium and liquid-nitrogen temperatures, and between liquid-nitrogen and ice temperatures,

show that the NBS interim low-temperature tables are sufficient for most engineering and scientific requirements. Preliminary work on several gold-iron alloys indicates that these alloys will allow more accurate thermoelectric temperature measurement in the liquid-helium/liquid-hydrogen temperature range. Research, now well underway, will lead to establishment of standard thermocouple tables for temperatures from liquid helium up to 0 °C for all of the cryogenically useful commercial thermocouple alloys.

Key Words: Thermometry, thermocouples, cryogenics.

On long-term stability of Zener reference diodes, W. G. Eicke, Jr., and H. H. Ellis, *Proc. 11e Session, Comite Conf. D'Electricite, May 10–12, 1965, pp. E–73–E–77 (May 1965).*
This paper gives a summary of a three year study of the stability of Zener Diodes either when operated intermittently or continuously. The diodes that were studied under intermittent use were in use for periods of 5 to 10 minutes with periods of two to four weeks between measurements. The diodes studied had normal voltage ranging from 8.1 to 9.2. The studies were conducted at 25.00 ± .02 °C. The studies indicated that the Zener diodes gave stable output voltage to within 3 to 10 ppm over a three year period.

Potential applications of the x-ray/density method for the comparison of atomic-weight values, R. D. Deslattes, H. S. Peiser, J. A. Bearden, and J. S. Thomsen, *Metrologia* **2,** *No. 3, 103–111 (July 1966).*
Without presenting experimental details, this report outlines and reappraises the principles involved in measurement of crystal lattice parameters and density for the determinations of atomic-weight values.
Attention is drawn to the advantages to be derived from a comparison of densities and lattice spacings with those of a crystal of mononuclidic elements, rather than from absolute measurements of x-ray spacings and density.
Errors arising from physical and chemical imperfections are discussed as are the general techniques of adequate precision for density and lattice spacings measurements.
Recent literature data is used by way of illustration to derive the effective atomic weight of calcium appertaining to a group of calcite samples from that of a group of silicon crystals (really an unsuitable "standard"). The calcium value obtained is 40.0795 ± 0.0019 (probable error); it compares with IUPAC's adopted 40.08 and a "physical value" of 40.078 from nuclidic masses and isotopic abundance measurements. There are several elements for which the x-ray/density method is judged to be potentially the most promising for atomic-weight re-determinations in the foreseeable future.

Key Words: Atomic weights, crystal densities, crystal perfection, experimental methods, lattice parameters.

Statistical concepts in metrology, H. H. Ku, *Book, Handbook of Industrial Metrology, Chapt. 2, pp. 20–54 (Prentice-Hall, Inc., Englewood Cliffs, N.J., 1967).*
These two chapters, statistical concepts of a measurement process and statistical analysis of measurement data, are part of the textbook, *Industrial Metrology* sponsored by the American Society of Tool and Manufacturing Engineers.
Beginning with the differentiation between arithmetic and measurement numbers, the properties of the latter are developed and described, leading to a discussion of precision and accuracy at the end of the first chapter.
A basic kit of tools for the comparison and manipulation of means and variances are given in the second chapter, including a collection of propagation of error formulas. The use of control chart techniques for monitoring stability is emphasized. Examples are given using actual calibration data of NBS.
Selected references are given for topics introduced but not treated in detail.

Thermal converters used as transfer standards for the measurement of alternating current and voltage, F. L. Hermach, *Proc. 11e Session, Comite Con. D'Electricite, May 10–12, 1965, pp. E–83–E–88 (May 1965).*
This report to the Advisory Committee outlines recent progress at NBS in the development of ac-dc transfer standards (comparators) for measurements of alternating current and voltage with 20 ppm accuracy or better at audio frequencies. Electrothermic transfer standards of the thermocouple type offer good prospects of meeting this goal. Their ac-dc differences appear to be very stable. The standards can be read with high precision and are rugged and portable. Furthermore, they can readily be intercompared for ac-dc difference, to step up and down the current and voltage scale with a precision of a few ppm. They are thus worthy of consideration for international comparisons of the accuracy of alternating current and voltage measurements.

Use of a laser for length measurement by fringe counting, *Metrologia* **2,** *No. 3, 95–98 (July 1966).*
The use of a 633-nm He-Ne laser of normal neon isotopic abundance as a light source for an automatic fringe counting interferometer was found to improve the counting precision and extend the usefulness of the interferometer to the full one meter limit of its carriage travel.
A 91-mm length was measured in terms of Hg^{198} and laser fringes. From the fringe counts obtained and the wavelength of the Hg^{198} line, the laser vacuum wavelength was measured to be 632.991 46 nm with a standard error of 1.1×10^{-7}. With the laser wavelength so determined, each decimeter interval of a one meter line standard was measured by counting laser fringes. All measured decimeter interval lengths agreed with the assigned values within the mutual limits of uncertainty, the largest discrepancy being less than 0.5 μm. The result obtained for the total length of the line standard agreed with the assigned length of the line standard to 7 parts in 10^8, which is well within the mutual limits of uncertainty.
This method is being applied to routine calibration of line standards using a stabilized isotopic He-Ne laser.

Annual report on spectroscopy, C. E. Moore, *Astron. J.* **71,** *No. 9, 796–797 (Nov. 1966).*
This report is furnished annually to the Astronomical Journal in order to present to astrophysicists the spectroscopic work that they are particularly interested in. It is published with the Observatory Reports and provides a brief summary of activity at the National Bureau of Standards.

Key Words: Atomic spectra, rare-earth spectra, transition probabilities, solar spectrum.

Approximate eigenfunctions of the Liouville operator in classical many-body systems. II. Hydrodynamic variables, R. J. Nossal and R. Zwanzig, *Phys. Rev.* **157,** *No. 1, 120–126 (May 5, 1967).*
A variational solution of the Liouville Equation is used to obtain collective coordinates for simple classical fluids. Comparison is made with macroscopic analogs determined from relevant hydrodynamic equations. Approximate eigenfunctions of the Liouville operator, when constructed from linear combinations of the spatial fourier transforms (fluctuations) of the mass, momentum, and energy density operators for the fluid, are found appropriate to low frequency disturbances. When time derivatives of fluctuations are included among trial functions the variational procedure provides fluid state counterparts of usual solid state phonons.

Key Words: Eigenfunctions, Liouville operator, many-body systems, hydrodynamic variables, irreversible processes.

Autoionizing D states in He below the *n*-2 level of He, J. W. Cooper, S. Ormonde, C. H. Humphrey, and P. G. Burke, *Proc. Phys. Soc.* **91,** *285–287 (1967).*
Positions and widths of the autoionizing ^1D and ^3D levels lying below the *n*-2 level of He^+ are calculated by close coupling methods and compared with experiment and previous calculations.

Key Words: Autoionizing series, calculation, close coupling, level width, resonance.

Certificates of radioactivity standards, S. B. Garfinkel, A. P. Baerg, and P. E. Zigman, *Report of the Subcommittee on the Use of Radioactivity Standards, Natl. Acad. Sci.-Natl. Res. Council, pp. 1–11 (Washington, D.C., Dec. 1966).*

Recommendations for certificates of standards of radioactivity are presented. It is hoped that commercial producers of such standards in the United States of America will use these recommendations in the preparation of certificates which they supply with their standards.

Key Words: Certificates, commercial standards, radioactivity standards, standards accuracy, combination of errors, precision, measurements.

Conformation of adsorbed polystyrene measured by attenuated total reflection in the ultraviolet region, P. Peyser and R. R. Stromberg, *J. Phys. Chem.* **71,** *No. 7, 2066–2074 (June 1967).*
Attenuated total reflection (ATR) in the ultraviolet region was used to measure the extension and concentration of an adsorbed layer of polystyrene. The polystrene was adsorbed on a quartz surface from cyclohexane solution at the theta temperature. The ATR prism, which allowed 15 to 16 reflections, was constructed from synthetic crystalline quartz. It was designed to be placed in a spectrophotometer without the need of additional optical components. the measured adsorbed polymer "extension" agreed reasonably well with similar ellipsometric measurements on nearly the same system. The study reported here was restricted to the use of an adsorbed layer that could be treated as a homogeneous film. The possible use of the method to determine the concentration distribution of adsorbed segments normal to the surface is discussed. Measurements in the ultraviolet region of the refractive indexes of the polymer solutions and of the benzene-methanol and toulene-methanol solutions that were used to test the method are also described.

Key Words: Attenuated total reflection, ultraviolet spectrophotometry, adsorption of polymers, polymer adsorption, conformation of adsorbed polymer molecules, refractive index in ultraviolet region, index of refraction in ultraviolet region, total reflection, frustrated total reflection.

Deformation twinning in Ni and F.C.C. Fe-Ni alloys, R. P. Reed, *Phil. Mag.* **15,** *No. 137, 1051–1055 (May 1967).*
Using electron and optical microscopy techniques, deformation twinning has been found in Ni and f.c.c. Fe-Ni alloys at low temperatures (76–4 °K).

Key Words: Nickel, Fe-Ni alloys, deformation twinning, low temperature.

Dependence of 50 and 100 keV bremsstrahlung on target thickness, atomic number, and geometric factors, R. C. Placious, *J. Appl. Phys.* **38,** *No. 5, 2030–2038 (Apr. 1967).*
Experimental data have been obtained for the bremsstrahlung spectra produced with 50 and 100 keV electrons incident on different targets. The spectrum per unit solid angle per incident electron is measured for photon emission angles of 30, 70, and 110 degrees, for normal and oblique incidence of the electrons on the targets having atomic numbers of 13, 50, and 79, and for four target thicknesses equal to different fractions of the electron range in the given material. Also, results are given for the bremsstrahlung production efficiencies per unit solid angle at a given emission angle. The experimental results show good agreement with the theoretical predictions of Berger and Seltzer, which are based on thin target bremsstrahlung cross sections and which employ Monte Carlo calculations to account for multiple scattering and energy loss effects.

Key Words: Thick target bremsstrahlung, low energy, photon emission angles, efficiencies, Monte Carlo predictions.

Development of the engineering method and some simplified methods of structure shielding analysis, C. Eisenhauer, *(Lecture Notes, OCD Summer Inst., Kansas State Univ., Manhattan, Kansas, 1962–1963, 1965), TR–40, Radiation Shielding—Analysis and Design Principles as Applied to Nuclear Defense Planning, V–1—V–iv (Supt. Docs., Govt. Printing Office, Washington, D.C. 20402, Nov. 1966).*
These lecture notes describe the technical basis for the procedures currently being used by the Office of Civil Defense to evaluate fallout protection in structures. The notes describe in detail how the equations and charts used in these procedures were derived from fundamental calculations of radiation shielding. Examples are given for simple structures.

Dielectric constants of $PbWO_4$ and $CaWO_4$, W. S. Brower and P. H. Fang, *J. Appl. Phys.* **38,** *No. 5, 2391 (Apr. 1967).*
The dielectric constants (ϵ') $PbWO_4$ and $CaWO_4$ were measured at 24.5 °C in air. Two specimens of each orientation were measured. The averages and deviations therefore of the two measured values of the reflective dielectric constants are as follows:

$$PbWO_4\ \epsilon' \parallel a\ 23.6 \pm 0.3;\ \epsilon' \parallel c\ 31.0 \pm 0.4;$$
$$CaWO_4\ \epsilon' \parallel a\ 11.7 \pm 0.1;\ \epsilon' \parallel c\ \ 9.5 \pm 0.2.$$

Key Words: Dielectric constant, single crystal, calcium tungstate, lead tungstate.

Effects of environment on the fracture glass, S. M. Wiederhorn, *Proc. RIAS Conf., Baltimore, Md., June 7–8, 1965, pp. 293–317 (Gordon and Breach, New York, N.Y., 1966).*
This paper briefly reviews previous work on the topic of delayed fracture of glass, and then presents the results of a new experimental approach to the subject. Using the double-cantilever cleavage technique, it was possible to observe crack motion and to accurately measure crack velocities in glass. The temperature and stress dependence of the crack velocity indicates that the observed fracture is an activated process with an activation energy of 19,500 calories/mole. The existence of a static fatigue limit is inferred from the experimental data. Experimental results will be discussed with reference to current theories of static fatigue.

Key Words: Glass, fracture, crack propagation, static fatigue, corrosion, cleavage.

Internal friction in rutile containing Ni or Cr, J. B. Wachtman, Jr., S. Spinner, W. S. Brower, T. Fridinger, and R. W. Dickson, *Phys. Rev.,* **148,** *No. 2, 811–816 (Aug. 1966).*
Rutile containing Ni gives an internal friction peak centered near 50 °C at 2 kHz characterized by $H = 15.3 \pm 2.4$ kcal/mole and $\tau_0 = 3 \times 10^{-15 \times 1.7}$ sec; this peak occurs for tensile stress along [100] or [110]. A peak centered near 200 °C with $H = 21.4 \pm 2.1$ kcal/mole and $\tau_0 = 8 \times 10^{-15 \pm 1.0}$ sec occurs for stress along [100] but not for stress along [110]. Rutile containing Cr gives similar peaks characterized by $H = 13.5 \pm 2.4$ kcal/mole and $\tau_0 = 2 \times 10^{-14 \pm 1.6}$ sec and by $H = 22.2 \pm 1.5$ kcal/mole and $\tau_0 = 4 \times 10^{-15 \pm 0.2}$ sec. Light reduction in vacuum decreases the amplitude of the low temperature peak and enhances the high temperature peak in both cases. Heavy reduction of rutile containing Cr removes both peaks but they reappear upon subsequent reoxidation. The evidence suggests that the motion of interstitial cations is involved and that reduction causes the formation of a compound defect. A tentative interpretation is given in terms of unpaired Ni^{3+} interstitials for the low temperature peak and of interstitial pairs composed of $Ni^{3+} - Ti^{3+}$ for the high temperature peak in Ni-doped specimens; the corresponding peaks in Cr-doped rutile are tentatively interpreted in terms of Ti^{4+} interstitials and of interstitial pairs consisting of $Ti^{4+} - Ti^{3+}$. It is possible to have two charge-compensating Cr^{3+} on adjacent substitutional sites and preserve the last two models.

Key Words: Activation energy, internal friction, point defect, reduction, rutile, symmetry conditions.

Irradiation-induced color centers in magnesium fluoride, R. F. Blunt and M. I. Cohen, *Phys. Rev.* **153,** *1031–1038 (Jan. 1967).*
Color centers, produced by 50 kV x-rays, have been studied in the rutile-structured MgF_2, largely at room temperature. An initial, slightly anisotropic, absorption band near 260 nm is tentatively identified as an F-center. Subsequent optical bleaching results in the formation of a strong band at 370 nm and several weak bands including one at 320 nm. Both of these appear only for $E \perp c$ and are believed to be due to *M*-centers. The choice of models is dictated in part by the observation of typical trapped electron ESR spectra in irradiated samples. Bleaching studies show that the 320 nm band arises from centers lying along the [110] directions, while the 370 nm band seems to be cylindrically symmetric about the *c*-axis. Furthermore, the 320 nm band is reversibly converted into the 370 nm band. Selection rules have been derived for $(1s)^2 \rightarrow (1s2p)$ transitions in each of the four possible *M*-center configurations permitted in the rutile structure. It is found that of the two types having F − F bonds in the (001) plane, one identifies rather well with the 370 nm band and the other with the 320 nm band.

Key Words: Color centers, magnesium fluoride, radiation damage.

Low temperature heat capacity of NdCl and PrCl, J. H. Colwell and B. W. Mangum, *J. Appl. Phys.* **38,** *No. 3, 1478–1469 (Mar. 1, 1967).*
Heat capacities of $PrCl_3$ and $NdCl_3$ have been measured between 0.3 and 4 °K. The dominant feature of the heat capacity curves is a broad anomaly indicating a region of extensive short-range magnetic ordering. The anomaly in $NdCl_3$ has a maximum at 0.47 °K and fits closely that of a linear Ising chain model. In addition, two small peaks appear at the same temperatures as the sharp spikes found in the magnetic susceptibility. $PrCl_3$ has a sharp peak in the heat capacity at 0.4 °K which is presumably associated with long-range ordering. The broad anomaly in $PrCl_3$ has a maximum at 0.8 °K. The magnetic entropy change for the temperature region of the measurements is approximately 80% of the R $\log_e 2$ for both salts.

Key Words: Heat capacity, magnetic entropy, magnetic susceptibility, $NdCl_3$ (neodymium trichloride), $PrCl_3$ (praeseodymium trichloride, temperature measurement.

Molecules in the sun, C. E. Moore-Sitterly, *Proc. Symp. "Sun Spots" honoring Galileo, Florence, Italy, Sept. 9–12, 1964, Ed. G. Righini, pp. 181–185 (G. Barbera, Editore, Florence, Italy, 1966).*
Paper to be presented at a symposium September 9–12 in Florence, Italy, honoring Galileo.

Multichannel photo-ionization of atomic systems, R. J. W. Henry and L. Lipsky, *Phys. Rev.* **153,** *No. 1, 51–56 (Jan. 1967).*
Expressions for multi-channel photoionization are obtained with the dipole approximation assuming *LS* coupling, which, while including the effects of coupling between channels, give separate contributions for each channel. The explicit form of the cross sections for atomic systems with configurations $1s^22s^22pq$ is obtained assuming superpositions of determinantal wave functions (Hartree-Fock) for initial and final states. The effects of core relaxation are considered. The formalism is applied to the photoionization of neon with the result that coupling between channels and core relation have a larger effect on the individual channel cross sections than on the total cross section. Both effects tend to bring the dipole velocity and length forms of the cross section into closer agreement with each other, but the improvement is appreciable only near threshold.

Key Words: Close-coupling, core relaxation, multi-channel, neon, photoionization, standing waves, $2p$ shell.

Multichannel resonances in the inelastic scattering of electrons by helium, G. E. Chamberlain, *Phys. Rev.* **155,** *No. 1, 46–51 (Mar. 5, 1967).*
Resonance structure due to intermediate negative-ion states has been observed in the differential cross section for inelastic scattering of electrons at zero angle in helium. Resonances were observed in all four of the $1s \rightarrow 2s$, $2p$ channels within the incident-energy range of 19.5 to 24 eV.

Key Words: Cross section, electron, excitation threshold, helium, inelastic scattering, negative ion, resonance.

Newly measured and calculated wavelengths in the vacuum ultraviolet spectrum of neutral nitrogen, V. Kaufman and J. F. Ward, *Appl. Opt.* **6,** *No. 1, 43–46 (Jan. 1967).*
The NBS 10.7-meter vacuum spectrograph was used in second order to obtain precision measurements of three N I lines at 1492–1495 Å ($2p^3\ ^2D^\circ - 2p^23s\ ^2P$) and four at 1742–1745 Å ($2p^3\ ^2P^\circ - 2p^23s\ ^2P$). By combining these values with other available information on the energy levels of the neutral nitrogen atom, 78 calculated wavelengths of N I from 908 to 1745 Å are given with uncertainties of +0.001 Å or less.

Nuclear magnetic resonance of nitrogen-14 in potassium azide, R. A. Forman, *J. Chem. Phys.* **45,** *No. 4, 118–1123 (Aug. 1966).*
The nuclear magnetic resonance of ^{14}N, split by large quadrupole interactions, has been observed in single crystals of potassium azide (KN_3). The observed spectrum at arbitrary orientation consists of eight resonance lines, which can be decomposed into two groups of four lines each. The resonances in each group are of the same apparent intensity, and one group is twice as intense as the other. The quadrupole coupling constants and asymmetry parameters of the two inequivalent nitrogens have been obtained from a rotation study. For the end nitrogen $e^2qQ/h = 1.79 \pm 0.03$ MHz with $\eta = 0.04 \pm 0.02$. For the central nitrogen $e^2qQ/h = 1.028 \pm 0.03$ MHz with $\eta = 0.03 \pm 0.02$. Unsuccessful attempts were also made to observe the pure quadrupole resonance of the end nitrogens.

Key Words: Azides, nitrogen, nuclear magnetic resonance, nuclear quadrupole.

Nuclear magnetic resonance of ^{7}Li and ^{1}H in solid lithium imide, lithium amide, and lithium nitried, P. J. Haigh, R. A. Forman, and R. C. Frisch, *J. Chem. Phys.* **45,** *No. 3, 812–816 (1966).*
Nuclear magnetic resonance lines of ^{7}Li nuclei have been observed in solid polycrystalline samples of $LiNH_2$, Li_2NH, and Li_2N. Proton resonance lines have also been observed in the first two samples. In $LiNH_2$ there is a splitting of the resonance line due to first order quadrupole effects which indicates a coupling constant of 119 ± 2 kHz (estimated limit to maximum error) at room temperature. In Li_2NH no quadrupole effects are seen which is in agreement with the fact that the lithium nuclei in this compound are situated in sites of cubic symmetry. In Li_3N both first and second order quadrupole effects have been observed simultaneously. From these data coupling constants for Li_3N have been found to be 296 ± 4 kHz and 200 ± 10 kHz at room temperature. An unexplained line was also observed at low magnetic fields for this compound. These effects were found to vary with temperature and with the purity of the sample.
Key Words: Ammonia analogues, hydrogen, lithium, nuclear magnetic resonance, resonance.

Nuclear-resonance spin-echo study of ^{61}Ni hyperfine fields in ferromagnetic Ni-Al, Ni-V, and Ni-Cr systems, R. L. Streever and G. A. Uriano, *Phys. Rev.* **149,** *No. 1, 295–301 (Sept. 9, 1967).*
The nuclear-magnetic-resonance line shapes of ^{61}Ni have been studied in ferromagnetic Ni rich Ni-Al, Ni-V and Ni-Cr powders by plotting the spin-echo amplitude as a function of frequency across the inhomogeneously broadened resonance lines. The measurements were made at 4.2 °K in alloys containing concentrations of up to 12.3 at.% Al, 5.5% V and 5.3% Cr. In all three systems, the average hyperfine fields decreased approximately linearly with increasing solute concentration. A general discussion of the relationship between the average hyperfine field and the atomic moments is presented. The major contribution to the hyperfine field is believed due to the moment on the parent atom with a smaller contribution from moments on neighboring atoms via conduction electron polarization. The detailed structure of the resonance spectra is analyzed. It is found that the magnetic disturbances are spatially more widespread in the Ni-Al and Ni-V systems than in the Ni-Cr system. The Ni-Cr system in turn has a more delocalized behavior than the Ni-Co system previously studied. The results in the Ni-V and Ni-Cr system are consistent with results obtained by Collins and Low using neutron scattering techniques.

Optical properties of $SrTiO_3$ under applied stress and electric field, R. C. Casella, *Phys. Rev.* **154,** *No. 3, 743–749 (Feb. 1967).*
Motivated by recent experiments on the effects of uniaxial stress on the superconducting transition and normal-state transport properties of $SrTiO_3$, we have carried out a symmetry analysis, obtaining the perturbed band structure and optical selection rules for the cases of uniaxial stress along the (111) and (001) axes and of static electric field along (001). A comparison of the last case with $BaTiO_3$ in the C_{4v} ferroelectric phase suggests a model with a reversal in the order of the valence bands in $SrTiO_3$ relative to that proposed earlier. Selection rules for polarized light are obtained for both models and criteria for deciding experimentally which is correct are stated. An example is given of how the sign of the relative energy shift of the conduction valleys with stress may be determined optically.

Key Words: Electro-optical effects, energy bands, selection rules, stress-optical effects, strontium titanate.

Oscillatory photoconductivity and luminescence in $SrTiO_3$, L. H. Grabner, *Proc. Cairo Solid State Conf., Cairo, Egypt, Sept. 3–8, 1966, ed. A. Bishay, pp. 155–170 (Plenum Press, Inc., New York, N.Y., 1967).*
Photocurrents and luminescence in $SrTiO_3$ oscillate at low temperatures (~ 4 °K) at a threshold of about 100 volts/cm. Voltage-current

curves show negative differential resistance in the region of oscillation. We suggest that these effects are due to the field ionization, into the valence band, of a hole trapped 1 eV from the valence band. The hole is ionized by the local field ($\sim 10^6$ V/cm) which differs from the externally applied field of 10^2 V/cm because of the high dielectric constant of $SrTiO_3$ ($\sim 10^4$) at low temperatures.
Key Words: Electric field quenching, luminescence, negative resistivity, photoconductivity, strontium titanate.

Photographic and spectroscopic studies of exploding wires in a sealed vessel, E. C. Cassidy and K. K. Neumann *(Proc. 7th Intern. Cong. High-Speed Photography, Zurich, Switzerland, Sept. 12–18, 1965), Book, Kurzzeitphotographie, ed. O Helwich, pp. 178–185 (Verlag Dr. Othmar Helwich, Dramstadt, West Germany, 1967).*
Investigations of the mixing process between exploding wires and a confined air environment are described. The various high-speed framing camera, combined framing camera and drum camera, periodic still, and ultraviolet photographic techniques employed for time resolution of the explosion are described and illustrated. The photographic results are correlated with time-resolved (by photographic techniques) spectroscopic observations. Results have suggested a method and suitable intervals (during the explosion) for estimating the average temperature of the exploding vapor column. A phenomenon apparently due to reflecting shock waves was observed at a later stage of the explosion.

Key Words: High-speed, photographic, time-resolved, spectrographic, exploding wires, electrical discharge.

Resonances in the photo-ionization continuum of Ne I (20–150 eV), K. Codling, R. P. Madden, and D. L. Ederer, *Phys. Rev.* **155,** *No. 1, 26–37 (Mar. 5, 1967).*
The absorption spectrum of neon in the region 20–150 eV has been studied photographically and photoelectrically, using synchrotron light as a background source. Discrete structure has been observed in three distinct energy ranges. The first is between the $^2P_{1/2, 3/2}$ limit near 22 eV, involving resonances analogous to those observed by Beutler in Ar, Kr and Xe; the second is the region between 44 and 60 eV, the structure here being classified as due to two types of excitation: (i) the excitation of a subshell s electron, (ii) the simultaneous excitation of two outer p electrons; the third region is near 80 eV, where two weak resonances are observed, due presumably to the simultaneous excitation of a sub-shell s and an outer p electron. The resonance profiles of the states $2s2p^6\ np\ ^1P_1^o$, where $n = 3$, 4 and 5, and the two-electron excitation state $2p^3\ (^3P_{hcsp}\ ^1P_1^o$ have been studied quantitatively and values of q, Γ and ρ determined for each.

Key Words: Absorption spectrum, Ne I, synchrotron light, 20–150 eV, analysis, resonances.

Spectral distribution of scattered light in a simple fluid, R. D. Mountain, *Rev. Mod. Phys.* **38,** *No. 1, 205–214 (Jan. 1966).*
The spectral distribution of light scattered by density fluctuations in a dense, monatomic, one component fluid is calculated from the time dependence of the density fluctuations predicted by the linearized hydrodynamic equations of irreversible thermodynamics. The results of Landau and Placzek are verified and a procedure for deriving correction terms is discussed with the dispersion in the velocity of thermal sound waves obtained as an illustration. Particular attention is paid to the critical region. The properties of carbon dioxide are used to estimate the spectral distribution of critical opalescence. A comparison is made between light scattering and sound propagation experiments. Space dispersion near the critical point in the pressure and the thermal conductivity is examined briefly. Finally, some of the experimental problems involved in measuring the spectral distribution of the scattered light are discussed.

Status of the National Standards for physical measurement, R. D. Huntoon, *Science* **150,** *No. 3693, 169–178 (Oct. 8, 1965).*
This article outlines various stages of sophistication in the development of a measurement system, from a "unit-standard" system to a consistent system in which standards are tied to atomic and molecular properties in an independently reproducible way. The present stage of development of our measurement system is discussed in this context, and predictions are made regarding its future development.

Key Words: Ampere, candela, current, degree Kelvin, International System of Units, kilogram, length, luminous intensity, mass, meter, metric system, second, standards for physical measurement, temperature, time.

Structure of the alkali hydroxides. I. Microwave spectrum of gaseous CsOH, D. R. Lide and R. L. Kuczkowski, *J. Chem. Phys. (June, 1967).*
The microwave spectra of gaseous CsOH and CsOD have been studied in a high-temperature spectrometer. The spectrum indicates a linear or near-linear molecule with a large-amplitude, low-frequency bending vibration. A large number of excited states involving the bending mode and the Cs-O stretching mode have been identified. The rotational constant B_v shows an unusual variation as the bending mode is excited; the cause is not yet understood. The Cs-O bond length is found to be 2.40 ± 0.01 Å and the O-H distance is probably about 0.97 Å. The electric dipole moment is 7.1 ± 0.5 D. Relative intensity measurements indicate a Cs-O stretching frequency of about 400 cm^{-1} and a bending frequency in the neighborhood of 300 cm^{-1}. All of the evidence supports a highly ionic cesium-oxygen bond.

Key Words: Cesium hydroxide, dipole moment, high-temperature, microwave, molecular structure, spectrum, vibration.

The basis of our measurement system, R. D. Huntoon, *Phys. Teacher* **4,** *No. 3, 113–120 (Mar. 1966).*
This article outlines various stages of sophistication in the development of a measurement system, from a "unit-standard" system to a consistent system in which standards are tied to atomic and molecular properties in an independently reproducible way. The present stage of development of our measurement system is discussed in this context, and predictions are made regarding its future development.

Key Words: Degree Kelvin, kilogram, measurement system, meter, physical constant, second, standard, unit.

The elastic energies of non-regular hexagonal dislocation loops, R. DeWit and A. W. Ruff, Jr., *Phil. Mag.* **15,** *No. 137, 1065–1069 (May 1967).*
The elastic energies of dislocation loops have been calculated as a continuous function of shape from equilateral triangle to hexagon. A smooth decrease in energy is found in this sequence; a relatively rapid change is associated with truncation of the triangle corners. The results are compared with previous calculations for other geometric shapes. The effect of a stacking fault in the loop plane is also considered.

Key Words: Dislocation, elastic energy, loops, stacking fault.

The photonuclear effect in heavy deformed nuclei, H. Arenhovel, W. Greiner and M. Danos, *Phys. Rev.* **157,** *No. 4, 1109–1125 (May 1967).*
The theory of Raman scattering is extended to include electric quadrupole radiation. The results obtained are used to compute the elastic and Raman scattering cross sections of heavy deformed nuclei. The dipole and quadrupole resonances are described by a previously developed theory which includes surface vibrations and rotations. The computed cross sections are compared with experimental data for all those nuclei where both absorption and scattering cross sections are available. Some discrepancies still exist in certain details; however, the overall agreement between theory and experiment is very good.

Key Words: Photon scattering, nuclear Raman effect, nuclear structure, photonuclear effect, photon absorption cross sections, collective model.

Temperature dependence of the high-frequency moduli of vitreous B_2O_3, W. Capps, P. B. Macedo, B. O'Meara, and T. A. Litovitz, *J. Chem. Phys.* **45,** *No. 9, 3431–3438 (Nov. 1, 1966).*
Measurements of ultrasonic velocity allowed the calculation of the high frequency shear and bulk moduli of B_2O_3 from 80 °C below to 300 °C above the glass transition. The temperature dependences of these moduli were found to be consistent with a semi-empirical extension of the theory of Zwanzig and Mountain.
Key Words: B_2O_3, high frequency moduli, ultrasonic velocity.

Vacuum ultraviolet wavelength standards and improved energy levels in the first spectrum of silicon, L. J. Radziemski, Jr., K. L. Andrew, V. Kaufman, and U. Litzen, *J. Opt. Soc. Am.* **57,** *No. 3, 336–340 (Mar. 1967).*

The photolysis of $CD_3CH_2CD_3$, $CH_3CD_2CH_3$ and C_3H_8-C_3D_8 mixtures has been investigated at 1470 Å (8.4 eV), 1236 Å (10 eV) and 1048–67 Å (11.6 – 11.8 eV) both at 20° and 77 °K. On the basis of the isotopic analysis of the products it is concluded that the following primary fragmentation processes occur:

$$\begin{aligned} C_3H_8 + h\nu &\rightarrow C_3H_7 + H & a \\ &\rightarrow C_3H_6 + H_2 & b \\ &\rightarrow C_2H_6 + CH_2 & c \\ &\rightarrow C_2H_5 + CH_3 & d \\ &\rightarrow C_2H_4 + CH_4 & e \end{aligned}$$

Hydrogen, methane, and ethane are mainly formed by elimination processes from a single carbon atom which results in the simultaneous formation of a carbene in each case. In this respect the primary processes occurring in the solid phase are the same as those reported to occur in the gas phase. The elucidation of the primary processes in the condensed phase is facilitated because of the inhibition of secondary decomposition of the internally excited fragments formed in processes *a* to *e*. On the other hand, the occurrence of geminate disproportionation and combination leads to difficulties in determining the relative quantum yields of the primary processes *a* and *d*. It is noted that the C-H and C-C cleavage reactions *a* and *d* increase in importance when the energy of the incident photon is augmented.

Although propane ions, which have an ionization energy of 11.07 eV in the gas phase must be produced at 1048–67 Å, no concrete information could be obtained as to the fate of these ions in the solid phase. The data, however, show that decomposition of the super-excited molecules is of major importance at these wavelengths.

Key Words: Photolysis, propane, solid phase, free radicals, primary dissociations.

W spin for any spin, H. Harari, D. Horn, M. Kugler, H. J. Lipkin, and S. Meshkov, *Phys. Rev.* **146,** *No. 4, 1052–1057 (June 24, 1966).*

The general "W-spin" properties of an arbitrary spin state constructed from any number of basic spin 1/2 objects are discussed in detail. Explicit formulae for expressing the eigenstates of W^{-2} as linear combinations of ordinary spin states are given and some properties of the transformation matrices are discussed.

Density and vapor pressure of nitromethane 26° to 200 °C, H. A. Berman and E. D. West, *J. Chem. Eng. Data* **12,** *No. 2, 197–199 (Apr. 1967).*

The density of nitromethane between 25° and 200 °C and its vapor pressure between 130 and 200° have been determined experimentally. Within these limits, the density is represented by the equation

$$d = 1.1615 - 1.1952 \times 10^{-3}t - 1.553 \times 10^{-6}t^2$$

and the vapor pressure by the equation

$$\log_e P = 10.8210 - 3905.39/(t + 260)$$

where d is in g/cm³, P in atm, and t in °C.

Key Words: Nitromethane density, nitromethane vapor pressure.

Geometry and vibrational spectra of the alkaline-earth dihalides. I. MgF_2, D. E. Mann, G. V. Calder, K. S. Seshadri, D. White, and M. J. Linevsky, *J. Chem. Phys.* **46,** *No. 3, 1138–1143 (Feb. 1, 1967).*

The infrared spectra of vaporized MgF_2 isolated at liquid hydrogen temperatures in both argon and krypton matrices are reported. Six major regions of absorption have been found vis. 240, 450, 477, 483, 740 and 840 cm^{-1}. On the basis of corresponding matrix spectra of Mg^nF_2, $Mg^{26}F_2$ and a 1 : 1 mixture of $Mg^nF_2 - Mg^{26}F_2$, it is possible to demonstrate unequivocally that the 240, 477, 740 and 840 cm^{-1} absorptions are due to molecular species containing one magnesium atom. The 450 and 483 cm^{-1} features are clearly attributable to polymeric species. From the magnitude of the measured isotope shifts the 740 cm^{-1} and 477, 240 and 840 cm^{-1} absorptions have been assigned to MgF and ν_1, ν_2, ν_3 of MgF_2 respectively. The observation of ν_1 shows that MgF_2 is bent. The higher resolution and precise frequency measurement employed in this work have been used to calculate the apex angle. This lies in the range 145 to 160° the most probable value being 150°.

Key Words: Assignment, frequency, geometry, infrared, matrix, MgF, $Mg^{24}F_2$, $Mg^{26}F_2$.

Infrared and raman spectra of some trihalide ions: IC1-, IBr-, I-, I Br-, and BrIC1-, A. G. Maki and R. Froneris, *Spectrochim. Acta* **23A,** *867–880 (1967).*

The Raman spectrum and infrared absorption spectrum have been studied for a number of trihalide compounds. All three fundamental vibrations were located for each trihalide ion and the force constants are given. Differences in the spectra as the cation is changed are attributed to differences in the anion structures and/or differences in the crystal lattice which result in differing selection rules and force constants. The force constants are interpreted as indicating that the bottom of the potential well for the central atom of the trihalide ions is unusually flat. In agreement with previous observations the stretching force constants were found to have a value about half that of the corresponding halogen or interhalogen molecules.

Key Words: Force constants, infrared spectrum, Raman, Trihalide ions.

Measurements on the molecular nitrogen pulsed laser, T. Kasuya and D. R. Lide, Jr., *Appl. Opt.* **6,** *No. 1, 69–80 (Jan. 1967).*

Accurate wavelength measurements of the pulsed laser emission from the nitrogen molecule have been made. About one hundred new stimulated emission lines which belong to the first and second positive systems were obtained and identified as to rotational quantum number. The relative intensities of the laser lines in the rotational band spectrum are analyzed. Some characteristics of the oscillations, including the recovery time after the laser pulse, are discussed.

Molecular and ionic interactions in dielectrics, W. S. Lovell, *Book, 1965 Digest of Literature on Dielectrics* **29,** *Chapt. III, pp. 81–198 (National Academy of Sciences, National Research Council, Wash., D.C., 1967).*

A survey is given of the 1965 literature treating molecular interactions, pressure broadening, dielectric polarization and refraction, dielectric constant, dipole moments, dielectric relaxation, internal rotation, and electrical conductance of liquids and solutions.

Key Words: Molecular interactions, pressure broadening, dielectric polarization and refraction, dielectric constant, dipole moments, dielectric relaxation, internal rotation, and electrical conductance of liquids and solutions.

Collective treatment of the giant resonances in spherical nuclei, M. G. Huber, M. Danos, H. J. Weber, and W. Greiner, *Phys. Rev.* **155,** *No. 4, 1073–1084 (Mar. 20, 1967).*

In a collective treatment the energies of the giant resonances are given by the boundary conditions at the nuclear surface which is subject to vibration in spherical nuclei. Therefore a coupling between these two collective motions is consistently present. Its general form is given by angular momentum and parity conservation, the coupling constants being completely determined within the hydrodynamical model.

In the present treatment the influence of the surface vibrations on the total photon absorption cross section has been calculated. It turned out that in most of the spherical nuclei this interaction leads to a pronounced structure in the cross section. The agreement with the experiments in medium heavy nuclei is striking; many of the experimental characteristics are reproduced by the present calculations. In some nuclei, however, there are indications of single particle excitations which are not yet contained in this work.

Key Words: Giant resonances, dipole-quadrupole interaction, cross section.

Instrumentation and measurements, J. E. Gray and H. E. Bussey, *Book, 1965 Digest of Literature on Dielectrics* **29,** *Chapt. I, pp. 1–25 (National Academy of Sciences, National Research Council, Wash., D.C., 1967).*

A classified bibliography of abstracts from the literature of instrumentation and measurement applicable to the study of dielectric materials has been prepared for publication as the first chapter of the Digest of Literature on Dielectrics for 1965.

Key Words: Instrumentation, measurement, dielectric standards, electrical insulation, permittivity, dielectric constant, dielectric breakdown.

Optical heterodyne measurement of neon laser's millimeter wave difference frequency, J. L. Hall and W. W. Morey, *Appl. Phys. Letters* **10,** *No. 5, 152–155 (Mar. 1, 1967).*
We report detection and measurement of the millimeter wave difference frequency between two near laser lines at 1.152μ. The two spectral transitions, separated by 2.26Å, oscillate in pure neon in a single laser device, producing about 150μW total power in several longitudinal modes. The many resulting 51.3-kmc beat frequencies have been studied by optical heterodyne techniques. A type of diode has been found which has enough microwave sensitivity *and* enough optical sensitivity to combine the optical detector and the microwave heterodyne functions in a single element. The preliminary value for the difference in frequency between the $2S_2 \rightarrow 2P_4$ and $2S_4 \rightarrow 2P_7$ transitions in neon at 150 mtorr is (51,360 ±150) Mc. This value is not in agreement with the value calculated from Vol. I of Sitterly's *Atomic Energy Levels* (ref. 12).

Key Words: Neon, laser, optical heterodyne techniques, wave difference frequency.

Theory of the magnetic torque anisotropy of the samarium iron garnet, J. A. White, *Proc. Phys. Soc.* **90,** *1095–1109 (1967).*
It is observed that the anisotropy measured by Pearson above 80 °K varies nearly as T^{-3}. This is the temperature dependence to be expected if the samarium ions in the garnet are subjected to an isotropic exchange field and a crystal Stark field of predominantly cubic symmetry. The magnitude of the anisotropy corresponds to an exchange field $\beta H_{ex}/k = 29$ °K. This is considerably less than the 55 °K which, for an isolated cubic quartet, produces the splittings in Sm^{3+} observed calorimetrically. It is suggested that the exceptionally large exchange splittings at T = 0 and apparently large exchange field can be understood as the result of an exchange field of 29 °K combined with 1) partial decoupling of the spin and orbital angular momenta by the Stark and exchange fields, 2) restoration by the exchange field of some of the angular momentum quenched by the crystal field, and 3) rhombic anisotropy of the exchange field and crystal field.

Widths of Kikuchi lines in germanium, H. A. Fowler and L. Marton, *J. Appl. Phys.* **38,** *No. 4, 1735–1738 (Mar. 15, 1967).*
Transmission Kikuchi patterns at 80 keV from wedges of germanium have been measured with high angular resolution. Linewidths are compared with the Fourier potential calculated from a simple coherent-elastic-amplitude model. Germanium shows a higher experimental curve of scattering amplitude per unit cell volume than silicon, as may be expected from its greater atomic scattering potential. Suppressed contrast is found for the (111) reflection; this is interpreted as an overlap between the halves of the line-pair or band.

Key Words: Germanium, electron diffraction, Kikuchi lines, cross section, electron scattering.

Other NBS Publications

Bibliography and index on vacuum and low pressure measurement. January 1960 to December 1965, W. G. Brombacher, Mono. 35 Supplement 1 (May 31, 1967), 65 cents.
Nuclear science and technology for ceramists, Proceedings of the American Ceramic Society Symposium, Washington, D.C., April 7–12, 1966, Misc. Publ. 285 (May 26, 1967), $1.75.
Proceedings of the 1966 Standards Laboratory Conference, Misc. Publ. 291 (July 13, 1967), $1.00.
Hardboard, CS251–63, reprinted April 1967 with amendments (Nov. 15, 1966), 10 cents.
Grading of abrasive grain on coated abrasive products, PS8–67 (Jan. 9, 1967), 15 cents. (Supercedes CS217–59).
Calorimetry, G. T. Armstrong, 1967 McGraw-Hill Yearbook of Science and Technology, pp. 124–127 (1967).
Charge-transfer spectrum of the tetrachlorocuprate ion, M. Sharnoff and C. W. Reimann, J. Chem. Phys. **46,** No. 7, 2634–2640 (Apr. 1, 1967).
Correlation of some Precambrian rocks and metamorphic events in parts of Wyoming and Montana, E. J. Catazaro, Mt. Geol. **4,** No. 1, 9–21 (1967).
Erratum: Mass-spectrometric study of the reactions of O atoms with NO and NO_2, F. S. Klein and J. T. Herron, J. Chem. Phys. **44,** No. 9, 3645–3646 (May 1, 1966).
Magnetic and optical spectra of two dimeric copper-chloride pyridine-N-oxide complexes, G. F. Kokoszka, H. C. Allen, Jr., and G. Gordon, J. Chem. Phys. **46,** 3020 (Apr. 1967).
Measurement of the direct *l*-doublet transitions in carbonyl sulfide, A. G. Maki, J. Mol. Spectry. **23,** No. 1, 110–111 (May 1967).
Microtexture and composition of reaction products in the system kaoline-lime-water, W. C. Ormsby and L. A. Bolz, J. Am. Ceram. Soc. **49,** No. 7, 364–366 (July 1966).
Microwave spectroscopy, D. R. Lide, Jr., Encyclopedia of Industrial Analysis **2,** 600–611 (John Wiley and Sons, Inc., New York, N.Y., 1966).
Nuclear magnetic relaxation studies of $(CD_3O)_2^{11}BH$, N. Boden, H. S. Gutowsky, J. R. Hansen, and T. C. Farrar, J. Chem. Phys. **46,** 2849 (1967).
Radiation and photochemistry, P. Ausloos, Ann. Rev. Phys. Chem. **17,** 205–236 (1966).
Sublimation, E. C. Kuehner and R. T. Leslie, Encyclopedia of Industrial Chemical Analysis **3,** 573–584 (1966).
Symposium on problems of small information groups. Introductory remarks, M. B. Henderson (Div. Chem. Lit. Symp. Problems of Small Information Groups, 151st Natl. Meeting Am. Chem. Soc., Pittsburgh, Pa., Mar. 25, 1966), J. Chem. Doc. **6,** 143 (Aug. 1966).
Systematic errors in "recovery" and "detection" efficiency as related to radiochemical analysis, L. A. Currie, Proc. 11th Annual Bio-Assay and Analytical Chemistry Meeting, Albuquerque, N. Mex., Oct. 7–8, 1965, AEC No. 651008, p. 35 (Clearinghouse for Federal Scientific and Technical Information, Springfield, Va., 1967).
The chain decomposition of propane initiated by vacuum ultraviolet photolysis, A. H. Laufer and J. R. McNesby, J. Phys. Chem. **70,** 4094–4096 (1966).
The microwave spectrum, structure, dipole moment, and quadrupole coupling constants of *trans*-nitrous acid, A. P. Cox and R. L. Kuczkowski, J. Am. Chem. Soc. **88,** No. 22, 5071–5074 (Nov. 1966).
Vacuum-ultraviolet photolysis of solid propane at 20° and 77 °K, R. E. Rebbert and P. Ausloos, J. Chem. Phys. **46,** No. 11, 4333–4339 (June 1967).
A new ultra-low-frequency bridge for dielectric measurements, W. P. Harris, 1966 Annual Report, Conf. Electrical Insulation and Dielectric Phenomena, National Academy of Sciences – National Research Council, Mount Pocono, Pennsylvania, 1966, pp. 72–74 (1967).
A 100 Mc/s 2 out of 3 gate, J. K. Whittaker, Nucl. Instr. Methods **45,** No. 1, 138–140 (Nov. 1966).
A single axis, two crystal x-ray instrument, R. D. Deslattes, Rev. Sci. Instr. **38,** No. 6, 815–820 (June 1967).
A testing and rating method for refrigerated trucks with respect to cooling load, P. R. Achenbach, C. W. Phillips, and R. W. Penny Annex to Proc. Intern. Inst. Refrigeration, Comm. VII, pp. 29–35 (London, England, Sept. 1966).
Two-crystal, vacuum monochromator, R. D. Deslattes, Rev. Sci. Instr. **38,** No. 5, 616–620 (May 1967).
Air-to-air heat pumps for military housing, Military Engr. **384,** 270 (July–Aug. 1966).
An improved transportable 10 picofarad capacitor, R. D. Cutkosky and L. H. Lee, Proc. 11th Session, Comité Con. D'Eléctricité, May 10–12, 1965, pp. 65–66 (May 1965).
Comparison of the Hall-Petch parameters of zone-refined iron determined by the grain size and extrapolation methods, B. W. Christ and G. V. Smith, Acta Met. **15,** 809–816 (May 1967).
Discussion of the paper "flow in culverts and related design philosophies," J. L. French, J. Hydraulics Div. Am. Soc. Civil Eng. **93,** No. HY1, 85–91 (Jan. 1967).
Five years of VLF worldwide comparison of atomic frequency standards, B. E. Blair, E. L. Crow, and A. H. Morgan, Radio Sci. **2,** No. 6, 627–636 (June 1967).

Performance criteria for building components and systems, P. R. Achenbach, Proc. Porcelain Enamel Institute Forum, University of Illinois, Urbana, Ill., Sept. 28–30, 1966, **28,** 176–195 (1966).

Transistorized current stabilizer for x-ray tubes with directly heated cathodes, K. W. Yee and R. D. Deslattes, Rev. Sci. Instr. **38,** No. 5, 637–638 (May 1967).

Anniversaries in 1966–67 of interest to statisticians. Part II: Tercentennials of Arbuthnot and De Moivre, C. Eisenhart and A. Birnbaum, Am. Stat. **21,** No. 3, 22–29 (June 1967).

Comparison of three spin algebras employed in SU(6) theories, R. C. Casella, Phys. Rev. **147,** No. 4, 962–964 (July 1966).

Fundamental polygons for Fuchsian groups, L. Greenberg, J. Anal. Math. **18,** 99–105 (1967).

Fundamental polyhedra for kleinian groups, L. Greenberg, Ann. Math. **84,** No. 3, 433–441 (Nov. 1966).

On a theorem of Ahlfors and conjugate subgroups of L. Greenberg, Am. J. Math. **LXXXIX,** No. 1, 56–68 (Jan. 1967).

International standardization and expanded world trade, A. V. Astin, Mag. Std. **37,** No. 7, 191–194 (July 1966).

Review of elementary theory of the photometry of projection apparatus, C. S. Douglas, Illum. Eng. **62,** No. 4, 246–253 (Apr. 1967).

The photometry of colored light, A. C. Wall, Illum. Engr. **62,** No. 4, 239–242 (Apr. 1967).

A note on thermal expansion coefficients of rare gas solids, R. D. Mountain, J. Phys. Chem. Solids **28,** 1071–1073 (Dec. 29, 1966).

A simple and accurate method of calibration by photopeak efficiencies, J. M. R. Hutchinson and D. H. Walker, Intern. J. Appl. Radiation Isotopes **18,** No. 1, 86–89 (Jan. 1967).

Additional stopping power and range tables for protons, mesons and electrons, M. J. Berger and S. M. Seltzer, NASA–SP–3036, (1966).

Alpha gamma angular correlations in three heavy odd-A nuclides, J. M. R. Hutchinson, Phys. Rev. **157,** No. 4, 1093–1098 (May 1967).

Cold-neutron study of hindered rotations in solids and liquid methyl chloroform, neopentane and ethane, J. J. Rush, J. Chem. Phys. **46,** No. 6, 2285–2291 (Mar. 1967).

Correction of some erroneous calculations of the Einstein A coefficient for the 18 cm transition of OH, D. R. Lide, Jr., Nature **213,** No. 5077, 694–695 (Feb. 18, 1967).

Effect of oxygen on the photoelectron yield from tungsten in the vacuum ultraviolet, B. J. Waclawski, L. R. Hughey, and R. P. Madden, Appl. Phys. Letters **10,** 305 (1967).

Eigenchannel theory of nuclear reactions, M. Danos and W. Greiner, Phys. Rev. **146,** No. 3, 708–712 (June 1966).

Electron beams: National Bureau of Standards and the new technology, H. W. Koch, Science **156,** No. 3773, 321–328 (Apr. 21, 1967).

Experimental evidence concerning the conduction band of $SrTiO_3$, H. P. R. Frederiske, W. R. Hosler, and W. R. Thurber (Proc. Intern. Conf. Physics of Semiconductors, Kyoto, Japan, 1966), J. Phys. Soc. **21,** Suppl., 32–36 (1966).

Exposure rate measurements of x- and gamma-rays with silicon radiation detectors, K. Scharf, Health Phys. **13,** No. 6, 575–586 (June 1967).

Ferromagnetic iron alloys lacking a hyperfine field at the iron site, L. H. Bennett and L. J. Swartzendruber, Physics Letters **24A,** No. 7, 359–360 (Mar. 27, 1967).

Future spectroscopy for late-type stars, C. E. Moore, Proc. Colloquim on Late-Type Stars, Trieste, Italy, June 13–17, 1966, pp. 15–24, (Stampato Presso, Trieste, Italy, 1967).

High purity powdered CsI as a high reflectance infrared diffuser, J. Geist, G. J. Kneissl, and V. R. Weidner, Appl. Opt. **6,** No. 7, 1280–1281 (July 1967).

Report on international conference on spectroscopy, Bombay, 9–18 January 1967, C. E. Moore (Intern. Conf. Spectroscopy, Bombay, India, Jan. 9–18, 1967), Appl. Opt. **6,** No. 5, 836 (May 1967)

Interpretation of the far infrared laser oscillation in ammonia, D. R. Lide, Jr., Physics Letters **24A,** No. 11, 599–600 (May 1967).

Lineshapes due to anistropic interactions in magnetic resonance experiments, R. A. Forman and A. H. Kahn, J. Chem. Phys. **45,** No. 12, 4586–4588 (Dec. 1966).

Mean lives of atomic levels excited by electron impulse, J. Z. Klose, Proc. Intern. Conf. Electronic Excitation of an Atomic Vapor—Application to Spectroscopy, Grenoble, France, May 23–26, 1966, pp. 191–192 (Centre Natl. de la Recherche Scientifique, Paris, France, 1967).

Microwave line shape and the inversion spectrum of ND_3 and ND_3—argon mixtures, A. A. Maryott and S. J. Kryder, J. Chem. Phys. **46,** No. 7, 2856–2857 (Apr. 1967).

Modulus of rupture of glass below room temperature, M. J. Kerper T. G. Scuderi, Am. Ceramic Soc. Bull. **45,** No. 9, 782–783 (Sept. 1966).

On the diffraction profiles of spectrograph slits of finite width, K. D. Mielenz, Optik **25,** No. 3, 138–139 (May 17, 1967).

Piezo-optical effects in solids by sample rotation, A. Feldman, Physics Letters **23,** No. 11, 627–628 (Dec. 1966).

Radioactivity criteria for radiation processing of foods, H. W. Koch and E. H. Eisenhower, Book, Radiation Preservation of Foods, Advances in Chemistry Series 65, Chapt. 7, pp. 87–108 (American Chemical Society, Washington, D.C., 1967).

Reactor physics in the resonance and thermal regions, D. T. Goldman, J. Franklin Inst. **283,** No. 5, 437–438 (May 1967).

Reflective scattering from substrates and evaporated films in the far ultraviolet, R. G. Johnston, L. R. Canfield, and R. P. Madden, Appl. Opt. **6,** 719 (Apr. 1967).

Scattering of cold neutrons in ammonium carbonate, ammonium citrate, and ammonium acetate, V. Myers, J. Chem. Phys. **46,** No. 10, 4034–4035 (May 1967).

Spectroscope slit images in partially coherent light, K. D. Mielenz, J. Opt. Soc. Am. **57,** No. 1, 66–74 (Jan. 1967).

Stretch scheme, a microscopic description of rotations in nuclei, M. Danos and V. Gillet, Phys. Rev. Letters **17,** No. 13, 703–705 (Sept. 26, 1966).

SU(3) reaction inequalities at high energies, S. Meshkov and G. B. Yodh, Phys. Rev. Letters **18,** No. 12, 474–481 (Mar. 1967).

The standardization of cobalt-57, S. B. Garfinkel and J. N. R. Hutchinson, Intern. J. Appl. Radiation Isotopes **17,** No. 10, 587–593 (Oct. 1966).

Transactions of the triple commission for spectroscopy, Subcommittee D-Atomic Spectra, C. E. Moore, J. Opt. Soc. Am. **55,** No. 6, 745 (1965).

Treatment of nuclear reactions above the two-particle threshold, M. Danos and W. Greiner, Z. Phys. **202,** 125 (1967).

Triple-filament method for solid-sample lead isotope analysis, E. J. Catanzaro, J. Geophys. Res. **72,** No. 4, 1325–1327 (Feb. 15, 1967).

Electrolysis of nonaqueous systems, A. Brenner, Book, Advances in Electrochemistry and Electrochemical Engineering, Ed. C. W. Tobias, Chapt. V, pp. 205–248 (John Wiley & Sons, Inc., New York, N.Y., 1967).

Galvanostalametry: A technique for chemical analysis, A. Brenner and J. L. Sligh, J. Electrochem. Soc. **114,** No. 5, 461–465 (May 1967).

Novel aromatization of inositols in dimethyl sulphoxide-acetic anhydride, A. J. Fatiadi, Chem. Commun. **9,** 441 (May 10, 1967).

Generalized integrating-sphere theory, D. G. Goebel, Appl. Opt. **6,** No. 1, 125–128 (Jan. 1967).

High order correlations in a turbulent field, F. N. Frenkiel and P. S. Klebanoff, Phys. Fluids **10,** No. 3, 507–520 (Mar. 1967).

Space-time correlations in turbulence, F. N. Frenkiel and P. S. Klebanoff (Proc. Symp. Dynamics of Fluids and Plasma, University of Maryland, Oct. 7–9, 1965), Book, Dynamics of Fluids and Plasmas, pp. 257–274 (Academic Press Inc., New York, N.Y., 1966).

Terms, definitions, and symbols in reflectrometry, D. B. Judd, J. Opt. Soc. Am. **57,** No. 4, 445–452 (Apr. 1967).

Polarization of cosmic OH 18-cm radiation, P. L. Bender, Phys. Rev Letters **18,** No. 14, 562–564 (Apr. 3, 1967).

Progress in electron physics during the last 20 years, L. Marton, Third Czechoslovak Conf. Electronics and Vacuum Physics, Prague, Czechoslovakia, Sept. 23–28, 1965, pp. 17–25 (Czechoslovak Academy of Sciences, Prague, Czechoslovakia, 1967).

Random walk with an excluded origin, R. J. Rubin, J. Math. Phys. **8,** No. 3, 576–581 (Mar. 1967).

**Publications for which a price is indicated are available by purchase from the Superintendent of Documents, U.S. Government Printing Office, Washington, D.C. 20402 (foreign postage, one-fourth additional). The NBS non-periodical series are also available from the Clearinghouse for Federal Scientific and Technical Information, Springfield, Va. 22151. Reprints from outside journals and the NBS Journal of Research may often be obtained directly from the authors.*

JOURNAL OF RESEARCH of the National Bureau of Standards—A. Physics and Chemistry
Vol. 71A, No. 6, November–December 1967

Index to Volume 71A

January to December 1967

A

Absorption spectra 53, 277
Accelerators 19
Acid base catalysis in D_2O 137
Acyclic sugars 53
Aldopyranoid sugars 53
Allyl and propenylbenzoic acids 379
Aluminum borides 307
α-AlB_{12} 307
Aluminum fluoride 105, 307
Al_2O_3 317
Aluminum trifluoride 185
Analysis of Yb II 397
Aniostropic crystal 363
Annealed glass 287
Annealing 231
Annihalation radiation 347
Antonucci, J. M., L. A. Wall, Synthesis of poly-*p*-oxyperfluorobenzylene and related polymers. A novel synthesis of the monomer 2,3,5,6-tetrafluoro-4-trifluoromethylphenol 33
Aqueous solution 25
Argentar, H., G. M. Brauer, G. Durany, Ionization constants of substituted benzoic acids in ethanol-water 379
Argon 575
Armstrong, G. T., E. S. Domalski, The heat of formation of boron trifluoride by direct combination of the elements 195
—, —, The heats of combustion of polytetrafluoroethylene (Teflon) and graphite in elemental fluorine 105
—, —, The heats of formation of aluminum diboride and α-aluminum dodecarbide 307
Ash content 43
Atomic energy levels 583
Atomic energy levels of Yb II 396
Atomic spectra 567, 575
Atomic spectroscopy 587
Atomic term values 163
Au III 149

B

Bates, R. G., B. J. Steel, R. A. Robinson, Dissociation constant of *m*-nitrophenol in 50 wt percent methanol-water solvent from 25 to 40 °C and related medium effects 9
Beryllium aluminate (1 : 1) 89
Beryllium 1 : 3-aluminate 3, 97
Bestul, A. B., S. S. Chang, J. A. Horman, Heat capacities and related thermal data for diethyl phthalate crystal, glass, and liquid to 360 °K 293
Billick, I. H., M. Schulz, G. H. Weiss, On the calculation of moments of molecular weight distribution from sedimentation equilibrium data 13
Bomb calorimeter 307
Bomb calorimetry 195
Boron 195
Boron fluoride 307
Boron trifluoride 195
Borosilicate crown glass 231
Bozman, W. R., W. F. Meggers, C. H. Corliss, An improved description of technetium spectra (Tc I and Tc II), 2000 to 9000 Å 547
Brauer, G. M., G. Durany, H. Argentar, Ionization constants of substituted benzoic acids in ethanol-water 379
1-*t*-Butoxy-2,3,5,6-tetrafluoro-4-trifluoromethylbenzene 33

C

CaF_2 1
CaF_2 crystals 355
Calculated transition strengths between the configurations $5d^n6s$ and $5d^n6p$ in Au III 153
Calculation of moments of molecular weight distribution from sedimentation equilibrium data 13
Carbon-14-labeled L-fucose 133
Carbon tetrafluoride 105
Cerezo, A. S., R. S. Tipson, V. Deulofeu, A. Cohen, Infrared absorption spectra of some aldofuranoid, aldopyranoid, and acyclic 1-acylamido derivatives of sugars 53
Chain-folded crystals 261
Chang, S. S., J. A. Horman, A. B. Bestul, Heat capacities and related thermal data for diethyl phthalate crystal, glass, and liquid to 360 °K 293
Change of pK with dielectric constant 379
Chemical association 219
Chromatography on seed-test paper 49
Chrysoberyl 89
Classified lines of Yb II 396
Clausius-Mossotti function 287
Cohen, A., R. S. Tipson, A. S. Cerezo, V. Deulofeu, Infrared absorption spectra of some aldofuranoid, aldopyranoid, and acyclic 1-acylamido derivatives of sugars 53
Compton wavelength of the electron 347
Conductivity 355
Configurations $5d^n6s$ 149
Corliss, C. H., W. R. Bozman, W. F. Meggers, An improved description of technetium (Tc I and Tc II), 2000 to 9000 Å 547
—, J. B. Shumaker, Jr., Transition probabilities in argon I 575
—, J. L. Tech, Lifetimes of energy levels in neutral iron 567
Cross-linking 25
Crystal 293
Crystal growth 127, 245, 261
Crystal size 225
Crystallized rubber 225
CsCl 1
Cyclohexane 169

D

Davis, S. P., J. Reader, Fundamental energy levels of neutral promethium (Pm I) 587
Defect pairs 355
Density 287
Derivatives of sugars, aldofuranoid, aldopyranoid, and acyclic 1-acylamido, infrared absorption spectra 53
Deslattes, R. D., W. C. Sauder, Zeeman effect in positronium annihilation at low temperatures 347
Deulofeu, V., R. S. Tipson, A. S. Cerezo, A. Cohen, Infrared absorption spectra of some aldofuranoid, aldopyranoid, and acyclic 1-acylamido derivatives of sugars 53
Deuterium isotope effects 137
Dexiran 25
Dextran triacetate 25
D-fructose 137
D-glucose 137
Dibeler, V. H., J. A. Walker, S. K. Liston, Mass spectrometric study of photoionization. VII. Nitrogen dioxide and nitrous oxide 371
Dielectric constant 287
Dielectric constant of *n*-hexane as a function of temperature, pressure, and density 287
Dielectric relaxation 355
Diethyl phthalate 293
Dilatometer 287
Dimarzio, E. A., J. I. Lauritzen, Jr., E. Passaglia, Kinetics of crystallization in multicomponent systems. I. Binary mixtures of *n*-paraffins 245
Dissociation 9, 119, 317, 371
Dissociation constant 213, 385
Dissociation constant of *m*-nitrophenol in 50 wt percent methanol-water solvent from 25 to 40 °C and related medium effects 9
Dissociation constants of some disubstituted anilines and phenols in aqueous solution at 25 °C 213
Dissociation constants of some substituted nitrophenols in aqueous solution at 25 °C 385
Ditmars, D. A., T. B. Douglas, Measured relative enthalpy of anhydrous crystalline aluminum trifluoride, AlF_3, from 273 to 1173 °K and derived thermodynamic properties from 273 to 1600 °K 185
—, —, Relative enthalpy of berrylium 1 : 1-aluminate, $BeO \cdot Al_2O_3$, from 273 to 1173 °K. Thermodynamic properties from 273 to 2150 °K 89
—, —, Relative enthalpy of beryllium 1 : 3-aluminate, $BeO \cdot 3Al_2O_3$, from 273 to 1173 °K. Thermodynamic properties from 273 to 2150 °K 97
Domalski, E. S., G. T. Armstrong, The heat of formation of boron trifluoride by direct combination of the elements 195
—, —, The heats of combustion of polytetrafluoroethylene (Teflon) and graphite in elemental fluorine 105
—, —, The heats of formation of aluminum diboride and α-aluminum dodecaboride 307
Douglas, T. B., D. A. Ditmars, Measured relative enthalpy of anhydrous crystalline aluminum trifluoride, AlF_3, from 273 to 1173 °K and derived thermodynamic properties from 273 to 1600 °K 185
—, —, Relative enthalpy of beryllium 1 : 1-aluminate, $BeO \cdot Al_2O_3$, from 273 to 1173 °K. Thermodynamic properties from 273 to 2150 °K 89
—, —, Relative enthalpy of beryllium 1 : 3-aluminate, $BeO \cdot 3Al_2O_3$, from 273 to 1173 °K. Thermodynamic properties from 273 to 2150 °K 97
Drop calorimetry 89, 97, 185
Durany, G., G. M. Brauer, H. Argentar, Ionization constants of substituted benzoic acids in ethanol-water 379

E

Effect of environment upon the melting point of Al_2O_3 317
Effects of a distribution of volume relaxation times in the annealing of BSC glass 231
Electric fields 1
Electric fields produced in cubic crystals by point defects 1
Electrode capacitance 355
Electrolytes 9
Electronic 587
Elemental analysis 43
Energy levels 567, 587
Enthalpy 3
Enthalpy measurements 89, 97, 185

Page

Entropy ... 3
Environmental effects ... 317
Equation of state ... 203
Equation of state for fluid parahydrogen from the triple-point to 100 °K at pressures to 350 atmospheres ... 203
Ethylbenzene ... 169
Extinction coefficient ... 169

F

Far infrared spectrum of vulcanized natural rubber ... 19
Fatiadi, A. J., Infrared absorption spectra of 2-oxo-1,3-bis(phenylhydrazono) derivatives and related bis-, and tris-phenylhydrazones ... 277
Fermi surface ... 127
Fifth spectrum of praseodymium ... 583
Fluorine ... 105, 195, 307
Fluorine bomb calorimetry ... 105
Flynn, J. H., L. A. Wall, W. L. Morrow, Irradiation of dextran and its aqueous solutions with cobalt-60 gamma rays ... 25
Foster, H. J., P. H. E. Meijer, Techniques for the growth of large single crystals of potassium of high purity ... 127
Fragment ions ... 371
Franklin, A. D., S. Marzullo, J. B. Wachtman, Jr., Surface-layer relaxation in dielectric spectrum of CaF_2 doped with GdF_3 ... 355
—, *D. J. Sparks*, Electric fields produced in cubic crystals by point defects ... 1
Frush, H. L., Large-scale, preparative paper chromatography ... 49
—, *H. S. Isbell, N. B. Holt*, Synthesis of α-L-fucose-*l*-^{14}C (6-deoxy-L-galactose-*l*-^{14}C) ... 133
Fundamental energy levels of neutral promethium (Pm I) ... 587
Furukawa, G. T., W. G. Saba, Heat capacity and thermodynamic properties of beryllium 1 : 3-aluminate, $BeO \cdot 3Al_2O_3$, from 15 to 390 °K ... 3

G

Gamma irradiation ... 25
Gibbs energy ... 3
Glass ... 231
Glass transformation ... 293
Goodwin, R. D., An equation of the state for fluid parahydrogen from the triple-point to 100 °K at pressures to 350 atmospheres ... 203
Graphite ... 105
Gruneisen's constant ... 363

H

Hammett sigma constants ... 379
Hartree-Fock multiplet strengths for K I, Ca II, and Sc III ... 157
Heat capacities and related thermal data for diethyl phthalate crystal, glass, and liquid to 360 °K ... 293
Heat capacity ... 3
Heat capacity and thermodynamic properties of beryllium 1 : 3-aluminate, $BeO \cdot 3Al_2O_3$, from 15 to 390 °K ... 3
Heat capacity calorimetry ... 293
Heat of combustion ... 105, 307
Heat of formation ... 105, 307
Heat of formation of boron trifluoride by direct combination of the elements ... 195
Heating rate ... 225
Heats of combustion of polytetrafluoroethylene (Teflon) and graphite in elemental fluorine ... 105
Heat of formation of aluminum diboride and α-aluminum dodecaboride ... 307
High pressure ... 287
High-temperature calorimetry ... 89, 97, 185
Holt, N. B., H. S. Isbell, H. L. Frush, Synthesis of α-L-fucose-*l*-^{14}C (6-deoxy-L-galactose-*l*-^{14}C) ... 133
Homogeneity ... 43
Horman, J. A., S. S. Chang, A. B. Bestul, Heat capacities and related thermal data for diethyl phthalate crystal, glass, and liquid to 360 °K ... 293
Hydrogen ... 203
Hydrogen, fluoride—aqueous ... 203
Hyland, R. W., E. A. Mason, Third virial coefficient for air-water vapor mixtures ... 219

I

Index of refraction ... 231
Improved description of technetium spectra (Tc I and Tc II), 2000 to 9000 Å ... 547
Infrared absorption spectra of some aldofuranoid, aldopyranoid, and acyclic 1-acylamido derivatives of sugars ... 53
Infrared absorption spectra of 2-oxo-1, 3-bis(phenylhydrazono) derivatives and related bis- and tris-phenylhydrazones ... 277
Infrared spectra ... 53, 277
Interconversions ... 137
Interferometer ... 363
Ionic crystals ... 1
Ionization ... 371
Ionization constants ... 379
Ionization constants of substituted benzoic acids in ethanol-water ... 379
Iron ... 567
Iron, lifetimes in ... 567
Irradiation of dextran and its aqueous solutions with cobalt-60 gamma rays ... 25
Isbell, H. S., H. L. Frush, N. B. Holt, Synthesis of α-L-fucose-*l*-^{14}C (6-deoxy-L-galactose-*l*-^{14}C) ... 133
—, *C. W. R. Wade*, Deuterium isotope effects in α-β pyranose and in pyranose-furanose interconversions ... 137
Isoelectronic sequence ... 583
Isotope effects ... 137

K

Kaufman, V., J. Sugar, The fifth spectrum of praseodymium ... 583
Kinetics ... 245, 261

Page

Kinetics of crystallization in multicomponent systems. I. Binary mixtures of *n*-paraffins ... 245
Kinetics of crystallization in multicomponent systems. II. Chain-folded polymer crystals ... 261
Kirby, R. K., Thermal expansions of rutile from 100 to 700 °K ... 363

L

Large-scale paper chromatography ... 49
Large-scale, preparative paper chromatography ... 49
Lattice sums ... 1
Lauritzen, J. I., Jr., E. Passaglia, Kinetics of crystallization in multicomponent systems. II. Chain-folded polymer crystals ... 261
—, —, *E. A. Marzio*, Kinetics of crystallization in multicomponent systems. I. Binary mixtures of *n*-paraffins ... 245
Lennard-Jones potential parameters ... 219
L-fucose-*l*-^{14}C ... 133
L-fuconic acid-*l*-^{14}C ... 133
Lifetimes in Fe I ... 567
Lifetimes of energy levels in neutral iron ... 567
Linning, F. J., J. E. Stewart, The far infrared spectrum of vulcanized natural rubber ... 19
Liston, S. K., V. H. Dibeler, J. A. Walker, Mass spectrometric study of photoionization. VII. Nitrogen dioxide and nitrous oxide ... 371
Lithium content ... 43
Low temperature calorimetry ... 3

M

Macedo, P. B., A. Napolitano, Effects of a distribution of volume relaxation times in the annealing of BSC glass ... 231
Marzullo, S., A. D. Franklin, J. B. Wachtman, Jr., Surface-layer relaxation in the dielectric spectrum of CaF_2 doped with GdF_3 ... 355
Mason, E. A., R. W. Hyland, Third virial coefficient for air-water vapor mixtures ... 219
Mass spectrometer ... 371
McDaniel, C. L., S. J. Schneider, Effect of environment upon the melting point of Al_2O_3 ... 317
—, —, Phase relations in the systems TiO_2-IrO_2 and SnO_2-IrO_2 in air ... 119
McIntyre, D., Preparation, purity, and homogeneity of NBS standard samples 705 and 706, polystyrene ... 43
—, *V. M. Story, J. H. O'Mara*, Solvent effects on the ultraviolet absorption of polystyrene ... 169
Measured relative enthalpy of anhydrous crystalline aluminum trifluoride, AlF_3, from 273 to 1173 °K and derived thermodynamic properties from 273 to 1600 °K ... 185
Measurement at 0 °C ... 125
Mechanism of mutarotation ... 137
Meggers, W. F., The second spectrum of ytterbium (Yb II) ... 396
—, *W. R. Bozman, C. H. Corliss*, An improved description of technetium spectra (Tc I and Tc II) 2000 to 9000 Å ... 547
Meijer, P. H. E., H. J. Foster, Techniques for the growth of large single crystals of potassium of high quality ... 127
Melting and recrystallization of partially melted stark rubber ... 225
Melting point ... 317
Melting range ... 225
Melting temperature ... 225
Mendlowitz, H., Calculated transition strengths between the configurations $5d^n 6s$ and $5d^n 6p$ in Au III ... 149
Methanol ... 9
Mixed oxides ... 89, 97
Molecular configurational state ... 293
Molecular weight average ... 13
Molecular weight distribution ... 13
Molecular weights ... 43
Molecule ... 371
Moments ... 13
Mono-, bis-, and tris-(phenylhydrazones) ... 277
Mopsik, F. I., The dielectric constant of *n*-hexane as a function of temperature, pressure, and density ... 287
Morrow, W. L., J. H. Flynn, L. A. Wall, Irradiation of dextran and its aqueous solutions with cobalt-60 gamma rays ... 25
Multicomponent systems ... 245, 261
Multiplet strength ... 157
Mutarotation ... 137

N

NaCl ... 1
Napolitano, A., P. B. Macedo, Effects of a distribution of volume relaxation times in the annealing of BSC glass ... 231
Natural rubber ... 19
n-Hexane ... 287
Neutral atom ... 587
Nitrophenols ... 385
NO_2, NO_2^+, N_2O, N_2O^+ ... 371
Nonaqueous solvents ... 9
Normal and supercooled liquid ... 293
n-Paraffins ... 245
Nuclear quadrupole ... 125

O

O'Mara, J. H., D. McIntyre, V. M. Story, Solvent effects on the ultraviolet absorption of polystrene ... 169
Orientation ... 127
Oriented ... 225
Oscillator strengths for the helium isoelectronic sequence ... 163

P

Page

Paper chromatography of radioactive carbohydrates ... 49
Parahydrogen ... 203
Partial melting ... 225
Passaglia, E., J. I. Lauritzen, Jr., Kinetics of crystallization in multicomponent systems. II. Chain-folded polymer crystals ... 261
—, —, *E. A. Dimarzio*, Kinetics of crystallization in multicomponent systems. I. Binary mixtures of *n*-paraffins ... 245
Perfluoro-*p*-quinonemethide ... 33
Phase diagrams pair distributions ... 245
Phase relations ... 119
Phase relations in the systems TiO_2-IrO_2 and SnO_2-IrO_2 in air ... 119
Phase transition ... 185
Phenols ... 9
Phenylazo compounds ... 277
Photoionization ... 371
pK values in ethanol water ... 379
Point defects ... 1
Polarization ... 1
Polydispersity ... 13
Polymer ... 43, 169, 261
Polymer degradation ... 25
Polymerization ... 33
Polynomial representation ... 13
Poly-*p*-oxyperfluorobenzylene ... 33
Polystyrene ... 43, 173
Polystyrene, NBS standard samples 705 and 706, preparation, purity and homogeneity ... 43
Positronium ... 347
Postirradiative decay ... 25
Potassium ... 127
Potassium chlorate ... 125
Potassium of high purity, techniques for the growth of large single crystals ... 127
Praseodymium ... 583
Premelting ... 317
Preparation ... 43
Preparation, purity, and homogeneity of NBS standard samples 705 and 706, polystyrene ... 43
Pressure ... 287
Pretransition phenomena ... 185
Promethium ... 587
Purity ... 43, 125
PVT-relations ... 203
Pyranose-furanose ... 137
Pyranose-furanose interconversions ... 137
Pyrolysis ... 33

Q

Quenched glass ... 293
Quenching ... 347

R

Radiation lifetimes ... 567
Radioactive carbohydrates ... 133
Rare earth ... 583, 587
Reader, J., S. P. Davis, Fundamental energy levels of neutral promethium (Pm I) ... 587
Recrystallization ... 225
Recrystallization and melting of partially melted stark rubber ... 225
Relative enthalpy of beryllium 1 : 1-aluminate, $BeO \cdot Al_2O_3$, from 273 to 1173 °K. Thermodynamic properties from 273 to 2150 °K ... 89
Relative enthalpy of beryllium 1 : 3-aluminate, $BeO \cdot 3Al_2O_3$, from 273 to 1173 °K. Thermodynamic properties from 273 to 2150 °K ... 97
Relaxation times ... 231
Residual (configuration) entropy ... 293
Resonance thermometry ... 125
Roberts, D. E., Recrystallization and melting of partially melted stark rubber ... 225
Robinson, R. A., Dissociation constants of some disubstituted anilines and phenols in aqueous solution at 25 °K ... 213
—, Dissociation constants of some substituted nitrophenols in aqueous solutions at 25 °C ... 385
—, *B. J. Steel, R. G. Bates*, Dissociation constant of *m*-nitrophenol in 50 wt percent methanol-water solvent from 25 to 40 °C and related medium effects ... 9
Rubber ... 225
Rutile ... 363

S

Saba, W. G., G. T. Furukawa, Heat capacity and thermodynamic properties of beryllium 1 : 3-aluminate, $BeO \cdot 3\,Al_2O_3$, from 15 to 390 °K ... 3
Sample purity and N.Q.R. of Cl^{35} in $KClO_3$ at 0 °C ... 125
Sampling ... 43
Sauder, W. C., R. D. Deslattes, Zeeman effect in positronium annihilation at low temperatures ... 347
Schneider, S. J., C. L. McDaniel, Effect of environment upon the melting point of Al_2O_3 ... 317
—, —, Phase relations in the systems TiO_2-IrO_2 and SnO_2-IrO_2 in air ... 119
Schulz, M., I. H. Billick, G. H. Weiss, On the calculation of moments of molecular weight distribution from sedimentation equilibrium data ... 13
Second spectrum of ytterbium (Yb II) ... 396
Sedimentation equilibrium ... 13
Self-consistent field ... 157
Shumaker, J. B., Jr., C. H. Corliss, Transition probabilities in argon I ... 575
Sigma constants in ethanol-water ... 379
Sliding spark discharge lamp ... 583
Slow melting ... 225
SnO_2-IrO_2 system ... 119
Solid solution ... 119
Solvent effects ... 169
Solvent effects on the ultraviolet absorption of polystrene ... 169
Spark cutting ... 127
Sparks, D. J., A. D. Franklin, Electric fields produced in cubic crystals by point defects ... 1
Specific heat ... 89, 97, 185
Spectra of technetium ... 547
Spectroscopy ... 567
Spectrum ... 583
Spectrum, Yb II ... 396
Standard sample ... 43
Stark rubber ... 225
Steel, B. J., R. A. Robinson, R. G. Bates, Dissociation constant of *m*-nitrophenol in 50 wt percent methanol-water solvent from 25 to 40 °C and related medium effects ... 9
Stewart, J. E., F. J. Linnig, The far infrared spectrum of vulcanized natural rubber ... 19
Story, V. M., D. McLatyre, Solvent effects on the ultraviolet absorption of polystyrene ... 169
Substituted anilines ... 213
Substituted benzoic acids ... 379
Substituted phenols ... 213, 385
Sugar, J., V. Kaufman, The fifth spectrum of praseodymium ... 583
Sugars in solution ... 137
Sulfur ... 19
Surface energy ... 261
Surface-layer relaxation in dielectric spectrum of CaF_2 doped with GdF_3 ... 355
Surface layers ... 355
Synthesis of α-L-fucose-*1*-^{14}C (6-deoxy-L-galactose-*1*-^{14}C) ... 133
Synthesis of poly-p-oxyperfluorobenzylene and related polymers. A novel synthesis of the monomer 2,3,5,6-tetrafluoro-4-trifluoromethylphenol ... 33
Synthesis of radioactive sugar ... 133

T

Tech, J. L., C. H. Corliss, Lifetimes of energy levels in neutral iron ... 567
Techniques for the growth of large single crystals of potassium of high purity ... 127
Technetium, spectra ... 547
Teflon ... 105, 195, 307
Term values ... 157
2,3,5,6-Tetrafluoro-4-trifluoromethylphenol ... 33
Tetramethylthiuram disulfide ... 19
Thermal expansion ... 363
Thermal expansions of rutile from 100 to 700 °K ... 363
Thermodynamic properties ... 3, 89, 97, 185, 203, 293
Thermodynamics ... 9
Third virial coefficient for air-water vapor mixture ... 219
Three terminal electrode set ... 287
Threshold ... 371
TiO_2-IrO_2 System ... 119
Tipson, R. S., A. S. Cerezo, V. Deulofeu, A. Cohen, Infrared absorption spectra of some aldofuranoid, aldopyranoid, and acyclic 1-acylamido derivatives of sugars ... 53
Transition probabilities ... 575
Transition probabilities in argon I ... 575
Two relaxation time model ... 231

U

Ultraviolet absorption ... 173
Use of heavy paper in preparative chromatography ... 49
Utton, D. B., Sample purity and the N.Q.R. of Cl^{35} in $KClO_3$ at 0 °C ... 125

V

Vacuum ultraviolet ... 371
Virial coefficients ... 219
Volatile content ... 43
Volume relaxation ... 231
Vulcanization ... 19

W

Wachtman, J. B., Jr., A. D. Franklin, S. Marzullo, Surface-layer relaxation in the dielectric spectrum of CaF_2 doped with GdF_3 ... 355
Wade, C. W. R., H. S. Isbell, Deuterium isotope effects in α-β pyranose and in pyranose-furanose interconversions ... 137
Walker, J. A., V. H. Dibeler, S. K. Liston, Mass spectrometric study of photoionization. VII. Nitrogen dioxide and nitrous oxide ... 371
Wall, L. A., J. M. Antonucci, Synthesis of poly-*p*-oxyperfluorobenzylene and related polymers. A novel synthesis of the monomer 2,3,5,6-tetrafluoro-4-trifluoromethylphenol ... 33
—, *J. H. Flynn, W. L. Morrow*, Irradiation of dextran and its aqueous solutions with cobalt-60 gamma rays ... 25
Water vapor-air mixtures ... 219
Wavefunctions ... 157, 163
Wavelengths of technetium ... 547
Weiss, A. W., Hartree-Fock multiplet strengths for K I, Ca II, and Sc III ... 157
—, Oscillator strengths for helium isoelectronic sequence ... 163
—, *I. H. Billick, M. Schulz*, On the calculation of moments of molecular weight distribution from sedimentation equilibrium data ... 13

Y

Ytterbium, second spectrum ... 396

Z

Zeeman, effect in Yb II ... 396
Zeeman effect on positronium annihilation at low temperature ... 347
Zinc dibutyldithiocarbomate ... 19
Zinc dimethyldithiocarbomate ... 19
ZnS ... 1
Zone refining ... 127

U.S. GOVERNMENT PRINTING OFFICE : 1968 O - 277-259

Selected Publications of the National Bureau of Standards

Atomic Energy Levels, C. E. Moore:

Circular 467, Volume I. H to V (Z=1 to 23) 206 spectra. 309 p. (1949) $5. 50
Circular 467, Volume II. Cr to Nb (Z=24 to 41) 152 spectra. 227 p. (1952) $4. 00
Circular 467, Volume III. {Mo to La (Z=42 to 57) / Hf to Ac (Z=72 to 89)} 124 spectra. 245 p. (1958) $3. 00

An Ultraviolet Multiplet Table, C. E. Moore:

Circular 488, Section 1. H to V (Z=1 to 23); Selected Multiplets of 79 Spectra. 78 p. (1950) and Section 2. Cr to Nb (Z=24 to 41); Selected Multiplets of 46 Spectra. 115 p. (1952). $1. 25

Circular 488, Section 3. {Mo to La (Z=42 to 57) / Hf to Ra (Z=72 to 88)} Selected Multiplets of 78 Spectra. 94 p. (1961). $0. 60

Circular 488, Section 4. H to Nb (Z=1 to 41); Finding List for Sections 1 and 2 of the Table. 65 p. (1961). $0. 45

Circular 488, Section 5. {Mo to La (Z=42 to 57) / Hf to Ra (Z=72 to 88)} Finding List for Section 3 of the Table. 30 p. (1961). $0. 30

Selected Tables of Atomic Spectra—Atomic Energy Levels and Multiplet Tables Si II, Si III, Si IV. Charlotte E. Moore.

National Standard Reference Data Series–NBS 3, Section 1. 33 p. (1965) $0. 35

Table of Wavenumbers, C. D. Coleman, W. R. Bozman, and W. F. Meggers:

Monograph 3, Volume I. 2000 A to 7000 A. 508 p. (1960) $6. 00
Monograph 3, Volume II. 7000 A to 1000 μ. 542 p. (1960) $6. 00
Monograph 32, Part I. Arranged by Elements. 474 p. (1961) $4. 00
Monograph 32, Part II. Arranged by Wavelengths. 272 p. (1961) $3. 00
Monograph 32 Supplement. Revision of the NBS Tables Below 2450 Å. 36 p. (1967) $0. 30

New Description of Thorium Spectra, Romuald Zalubas:

Monograph 17, 106 p. (1960) $0. 65

Tables of Spectral-Line Intensities, W. F. Meggers, C. H. Corliss, and B. F. Scribner:

The above publications may be purchased from the Superintendent of Documents, U.S. Government Printing Office, Washington, D.C. 20402. (Add one-fourth additional for foreign mailing.)

A Multiplet Table of Astrophysical Interest, C. E. Moore. A Reprinting of the 1945 Multiplet Table (Princeton Univ., Obs. Contr. No. 20):

Technical Note 36 (PB151395), Part I Table of Multiplets, and Part II Finding List, λλ2951Å–13164Å. 242 p. (1959). $3. 00

The above Technical Note may be purchased by the PB number from the Clearinghouse for Federal Scientific and Technical Information, National Bureau of Standards, Springfield, Virginia 22151.

UNITED STATES
GOVERNMENT PRINTING OFFICE
DIVISION OF PUBLIC DOCUMENTS
WASHINGTON, D.C. 20402

OFFICIAL BUSINESS

POSTAGE AND FEES PAID
U.S GOVERNMENT PRINTING OFFICE

JOURNAL OF RESEARCH of the National Bureau of Standards Vol. 71A, No. 6 November–December 1967
A. Physics and Chemistry

Contents

Guest Editor: CHARLES H. CORLISS

	Page
William Frederick Meggers, A Tribute. Karl G. Kessler.	II
The second spectrum of ytterbium (Yb II). W. F. Meggers. (Edited by Charlotte E. Moore.)	396
An improved description of technetium spectra (Tc I and Tc II), 2000 to 9000 Å. W. R. Bozman, W. F. Meggers, and C. H. Corliss.	547
Lifetimes of energy levels in neutral iron. C. H. Corliss and J. L. Tech.	567
Transition probabilities in argon I. C. H. Corliss and J. B. Shumaker, Jr.	575
The fifth spectrum of praseodymium. Victor Kaufman and Jack Sugar.	583
Fundamental energy levels of neutral promethium (Pm I). Joseph Reader and Sumner P. Davis.	587
Publications of the National Bureau of Standards.	601
Index to volume 71A, January to December 1967.	613

Library of Congress Catalog Card Number: 62–37059

For sale by the Superintendent of Documents, U.S. Government Printing Office, Washington, D.C. 20402. Price $1 (single copy).
Subscription price: $5 a year; $1 additional for foreign mailing.
UNITED STATES GOVERNMENT PRINTING OFFICE, WASHINGTON : 1967